DEPARTMENT OF ARCHITECTURE

University of Strathclyde Engineering

Exploring the use of seaweed biopolymers in composite construction products

by Cassandra Dove

A thesis presented in fulfilment of the requirements for the degree of Doctor of Philosophy.

Department of Architecture
James Weir Building
University of Strathclyde
75 Montrose Street
Glasgow G1 1XJ
Scotland, UK

May 2017

This thesis is the result of the author's original research. It has been composed by the author and has not been previously submitted for examination which has led to the award of a degree.

Signed: ______________________ Date: ________________________

Acknowledgements

I would like to thank my supervisors Ms Fiona Bradley and Dr Siddharth Patwardhan for the guidance provided through-out the course of the project. I would also like to thank Dougie MacInnes and David Mackie from Marine Biopolymers, and their associates, for providing financial support and sharing their insightful knowledge on the topic. Invaluable assistance was also provided by various technicians at the University of Strathclyde including Dr Fiona Sillars, Stuart Adams and James Gillespie. I would also like to acknowledge Donald Booth (Energy Technology Partnership) for his assistance during the early stages of the project. Further thanks are also made to Michael Thomson at Ibstock for the provision of materials and to Dr. Mike Jarvis from the University of Glasgow and Prof. Carmen Galán-Marín and Prof. Carlos Rivera-Gómez from the University of Seville for their technical advice and expertise. Finally I would like to thank my family, friends and colleagues for providing continual support and encouragement.

Abstract

The ambition of this research was to develop composite building products which utilise a locally sourced, natural material in the form of alginate - a biopolymer derived from macro-algae. Two case study materials were included as part of the project: unfired clay bricks, where the alginate was used as a stabilising additive, and an alginate-based insulation, which was proposed as an alternative to petrochemical-based foams or silica aerogels. For both materials, a series of prototypes were produced and characterised in order to investigate the role of the alginate source and chemical composition on the properties of the final material.

The results demonstrated that the source and composition of the alginate can have an important influence on the properties of the two proposed products. For the clay bricks, improvements in mechanical strength were found to be dependent upon the alginate source and the composition of the soil. The greatest increase in compressive strength equated to 2.5 times that of the equivalent control specimen and was achieved using an alginate sourced from the *Laminaria Hyperborea* seaweed. Increases in the alginate dosage did not necessarily lead to an increase in strength suggesting that there is an optimum concentration at which strength improvement is most effective. For the aerogel product, whilst all of the biopolymers tested offered an improvement over the control sample, again the results confirmed that the type of alginate used has a significant influence on the physical properties of the composites. Although alginate variables are not typically considered in the existing literature, this study has demonstrated that there may be significant variations in the quality of specimens produced using alginate from different sources. It was also concluded that, for both of the proposed products, larger prototypes should be analysed in order to facilitate direct comparison with other buildings materials.

Table of Contents

Table of Tables

Appendix Tables

Table of Figures

Appendix Figures

List of Abbreviations

^{1}H-NMR	Proton nuclear magnetic resonance
AAC	Autoclaved Aerated Concrete
AB	Acid bentonite
ADP	Abiotic Depletion Potential (ADP)
AI	Alginate Industries
AN	Ascophyllum Nodosum
ANOVA	Analysis of Variance
B	Bentonite
BET	Brunauer–Emmett–Teller
BRE	Building Research Establishment
BS	British Standards
CB	Calcium bentonite
CEB	Compressed Earth Block
CEC	Cation Exchange Capacity
CFC	Chlorofluorocarbon
CIP	Combined Impregnation Processes
CMC	Carboxymethyl Cellulose
CO_2	Carbon Dioxide
CSEB	Compressed stabilised earth blocks
DECC	Department of Energy & Climate Change
DI	De-ionised
DLS	Dynamic Light Scattering
DSC	Differential Scanning Calorimetery
DVLO	Derjaguin, Verwey, Landau and Overbeek
EC	Embodied Carbon
EDL	Electric double layer
EDS	Energy Dispersive Spectroscopy
EDTA	Ethylenediaminetetraacetic acid
EE	Embodied Energy
EG	Ethyl Glycol
EMC	Equilibrium Moisture Content
EMC	Equilibrium Moisture Content
EPCs	Energy Performance Certificates
EPS	Expanded Polystyrene
EU	European Union
FAAS	Flame atomic absorption spectrometry
G	Guluronic acid
GDL	D-glucono-δ-lactone
GFP	Gas-filled panels
GGBS	Ground Granulated Blast-furnace Slag
GHG	Greenhouse Gas
GWP	Global Warming Potential
HFC	Hydrofluorocarbons

HIPE	High internal phase emulsion
HIPF	High internal phase foam
HTSCD	High temperature supercritical drying
I	Illite
IAQ	Indoor Air Quality
ICE	Inventory of Carbon & Energy
ICP	Inductively Coupled Plasma
K	Kaolinite
LCA	Life Cycle Analysis
LCI	Life Cycle Inventory
LCIA	Life Cycle Impact Analysis
LH	Laminaria Hyperborea
LL	Liquid Limit
LOD	Loss on Drying
LOI	Loss on Ignition
LS	Linear shrinkage
LTSCD	Low temperature supercritical drying
M	Mannuronic acid
MB	Methylene Blue
MBA	N,N'-methylenebisacrylamide
MBL	Marine Biopolymers Ltd.
MBV	Moisture Buffer Value
MDD	Maximum Dry Density
MMC	Monopolies and Mergers Commission
MMT	Montmorillonite
NASA	National Aeronautics and Space Administration
OMC	Optimum Moisture Content
ONS	Office for National Statistics
OPC	Ordinary Portland Cement
OSB	Oriented Strand Board
PAM	Polyacrylamide
PFA	Pulverised Fuel Ash
pH	Potential of Hydrogen
pKa	Acid dissociation constant
PI	Plasticity Index
PIR	Polyisocyanurate
PL	Plastic Limit
PLA	Poly-lactic acid
PPM	Parts per million
PSD	Particle Size Distribution
PUR	Polyurethane
PVA	Poly(vinyl acetate)
PVOH	Polyvinyl Alcohol
PVP	Polyvinyl Pyrolidone
PZC	Point of zero charge
RH	Relative Humidity

RPM	Revolutions per minute
RSC	Royal Society of Chemistry
SEM	Scanning Electron Microscope/Microscopy
SIP	Structurally Insulated Panels
SRI	Sound Reduction Index
SSA	Specific Surface Area
TEOS	Tetraethoxylane
TMOS	Tetramethoxysilane
UF	Urea-formaldehyde
UK	United Kingdom
USA	United States of America
V	Vermiculite
VIP	Vacuum Insulation Panels
XRD	X-Ray Diffraction
XPS	Extruded Polystyrene

List of Symbols

A	Area
A_v	Avogadro's number (6.02 x 10^{23}/mol)
a	Thermal Diffusivity
b	Width
c	Concentration
C	Consistency Index
C_a	Abrasive Strength Coefficient
C_m	Meniscus Correction
C_p	Specific Heat
C_U	Coefficient of Uniformity
C_{wi}	Initial Rate of Absorption
C_Z	Coefficient of Curvature
d	Depth or Thickness
D	Diameter
E	Young's Modulus of Elasticity
f	Flexural Strength (Modulus of Rupture)
F	Load
F_m	Maximum Load
g	Acceleration Due to Gravity
H	Height
H_o	Original Height
H_p	Unit Moisture Content in Ambient Conditions
k	Thermal Conductivity
K	Kappa Value
l	Length
l_o	Original Length
m	Mass
M	Mass per Unit Area
M_b	Mass of a Masonry Unit
n	Flow Index
N_{MB}	Normality of Methylene Blue
p	Calculated Probability
R	Radius
R_h	True Hydrometer Reading
R_h'	Observed Hydrometer Reading
s	Seconds
t	Time
T	Temperature
T	Thickness of a Masonry Unit
t	Time
$t_{0.5}$	Transient Half-time
U	Overall Heat Transfer Coefficient

$\boldsymbol{V}$	Volume
$\boldsymbol{\upsilon}$	Velocity
$\boldsymbol{W}$	Weight
$\boldsymbol{w}$	Moisture Content
$\boldsymbol{w_{opt}}$	Optimum Moisture Content
$\boldsymbol{w_{m}}$	Moulding Moisture Content
$\boldsymbol{\Delta H}$	Change in Height
$\boldsymbol{\zeta}$	Zeta Potential
$\boldsymbol{\eta}$	Viscosity
$[\boldsymbol{\eta}]$	Intrinsic Viscosity
$\dot{\boldsymbol{\gamma}}$	Shear Rate
$\boldsymbol{\eta_{r}}$	Relative Viscosity
$\boldsymbol{\tau_{o}}$	Yield Shear Stress
$\boldsymbol{\lambda}$	Wavelength
$\boldsymbol{\rho}$	Bulk Density
$\boldsymbol{\sigma}$	Compressive Strength
$\boldsymbol{\mathcal{E}}$	Compressive strain
$\boldsymbol{\tau}$	Shear Stress

1. INTRODUCTION

1.1. Sustainability in the Construction Industry

Buildings play a significant part in global society, providing shelter and comfort for the occupants as well as providing a physical representation of the technological development of mankind. In a growing population where an estimated 8.5 billion people will be living on the planet by 2030 (DESA, 2015), the demand for new buildings is set to increase. However, in recent decades, the construction industry has been at the forefront of scrutiny regarding not only the large quantities of natural resources which it is responsible for consuming but also the way in which theses resources are utilised. The act of building directly intervenes in natural systems and can have a detrimental effect upon the global biosphere by affecting hydrological cycles, exhausting finite materials, destroying habitats and generating tonnes of solid waste which cannot easily be returned to the ecosystem (Wernick and Ausubel, 1995). At present, the building industry is responsible for extracting vast amounts of the Earth‘s natural capital in a manner which is not only energy intensive but often involves re-manipulating raw materials into new static forms which break the otherwise naturally occurring cycles of energy and resources. Construction and civil infrastructure in fact account for 60% of all raw materials consumed on the planet (Bribián et al., 2011) while buildings specifically use approximately 40% of global energy as well as contributing to around a third of Greenhouse Gas (GHG) emissions (Costa et al., 2013). The cement industry in isolation has been reported to account for 5 to 7% of total CO_2 emissions (Benhelal et al., 2013). At a national level, the UK has also identified the construction industry as the largest consumer of resources (Howard, 2000). This includes the annual consumption of over 420 Mt of materials and the emission of 29 Mt of CO_2 (Hammond and Jones, 2008). Additionally, during both their construction and use, buildings account for approximately 50% of national energy use and water consumption as well as generating a third of landfill waste (DBERR, 2008).

Following the outcomes of the *Kyoto Proctocol* (UN, 1997), legally binding targets to reduce GHG emissions have been established. The European Union (EU) for example has made commitments to increase overall energy efficiency by 20% as well as reduce GHG emissions by 20% compared to 1990 levels by 2020 (European Commission, 2010) with a longer term goal of a reducing GHG emissions by at least 80% by 2050. This will have a significant impact on the way that buildings of the future will be designed, requiring new considerations of how energy and resources are utilised across all stages of the building life cycle.

In addition to these energy and CO_2 based targets, it is also important to ensure that buildings of the future provide safe, healthy and cost-effective habitats. There have therefore been increasing efforts to align the construction industry with broader sustainable development goals. Today the most commonly cited definition of sustainability, as described in Brundtland Commission Report, proposes that sustainability can only be achieved by acknowledging the complex relationships between environmental, social and economic factors and by considering both our current needs and the needs of future generations (Brundtland, 1985). This philosophy therefore extends beyond the reduction of CO_2 emissions and improved energy efficiency. Kibert (1994) defines sustainable construction as the creation of a healthy built environment using *“resource-efficient, ecologically based principles”*. Hill and Bowen (1997) further outline the ‘four pillars’ of sustainable construction which include social, economic, biophysical and technical sustainability, all of which need to be considered throughout the building’s life-cycle. In other definitions, specific criteria such as reducing energy consumption, minimising the use of non-renewable resources and conservation of the natural environment are also described (CIB, 1999). Despite these variations in the definition of sustainable construction, there is agreement on the fundamental aim of reducing the detrimental environmental impacts of the construction industry.

1.1.1. The Role of Building Materials

Materials form the physical fabric of a given structure and consequently play an important role in the structural performance and durability of any building. There is also an associated energy and resource footprint for all materials which can vary drastically depending on the raw materials consumed as well as the processing methods and transportation required. Material selection also has an impact on operational aspects such as indoor air quality, thermal comfort, acoustic buffering and fire protection. In recognition of the importance of material selection on the overall environmental performance of a building, more recently focus has been placed on whole life-cycle design which considers the impacts of the materials used over the entire life span of the building. This has been facilitated by the introduction of standardised Life Cycle Assessment (LCA) through ISO 14040: 2006. This ‘cradle to grave’ approach in building design requires consideration of the operational phase as well as the embodied energy required to manufacture, transport, maintain and dispose of all the components. It should be noted that an interesting shift is also occurring regarding the balance between operational and embodied energy in buildings. While in recent decades operational energy consumption, including heating, cooling, lighting, and appliances has accounted for up to 90% of a building’s energy consumption over its lifespan (Boyle, 2005), as efforts to improve energy-efficiency and operational performance increase in line with legislative targets (European Commission, 2010), the role of the embodied energy is likely to become much more significant (Thormark, 2002; Sartori and Hestnes, 2007; Fouquet et al., 2015). In this sense, those involved in the design process have an important role to play in selecting appropriate materials and understanding their whole-life cycle impacts.

As further evidence of the increasing importance of material selection, environmental policies and regulations for construction products are also continually being developed. For example the *Construction Products Regulation* (Official Journal of the European Union, 2011) published in 2011 to replace the previous *Construction Products Directive* (Official Journal of the European Union, 1989), aims to harmonise the assessment methods used to determine environmental performance. This allows for easier comparison between similar products on the European market as well as requiring manufacturers to declare the known environmental impacts. A series of technical standards (CEN TC 350) are also being developed for both individual products and whole buildings. This includes *Environmental Product Declarations* (BSI, 2012a) which require an assessment of Global Warming Potential (GWP) and Abiotic Depletion Potential (ADP), including assessments of energy resources used, water consumption and options for waste disposal and recycling. These declarations are valid for 5 years and are intended to make the environment impacts of building materials more apparent as well as helping manufacturers to identify elements of the production process which can be improved upon. The Building Research Establishment (BRE) has also developed an assessment methodology for building materials (BRE, 2008), again based on LCA, and has incorporated this into the *Green Guide to Specification* which allows designers to make comparison between similar materials or systems. In this case the materials are categorised based on function (walls, floor, roof etc.) and then rated from A+ to E. Overall these assessment tools are helping to increase the level of consideration given to the environmental performance of construction materials. On the producers' side, this evaluation process can also identify the parts of the production process which are most harmful and facilitate further improvements. It can also potentially give products which are less harmful to the environment a competitive advantage. For the consumer, this increased transparency and availability of comparable data can also assist in decision making, allowing for more informed choices to be made whilst also helping designers to meet the increasingly stringent environmental targets required for buildings.

1.1.2. The Use of Biopolymers in Construction

Biopolymers are polymeric substances which are derived from natural sources, the majority being carbohydrates from plant and algal feedstocks. Carbohydrates, which are molecules consisting of carbon, oxygen and hydrogen, represent half of all the organic carbon in the world and polysaccharides (polymeric carbohydrates) constitute over 90% of these compounds (BeMiller, 2000). As such, polysaccharides are readily available materials which can be obtained from renewable sources and have been adopted by humans in a wide range of applications including agriculture, the food industry, textile and paper manufacturing as well as more recent developments like biomedical materials and bio-plastics (Nussinovitch, 1997). The use of biopolymers specifically in building materials is not a new concept and in fact such organic materials were used widely during the Roman era where locally available natural products would be used to enhance the properties of concrete and masonry materials (Plank, 2005;Quagliarini and Lenci, 2010). Even today biopolymers like lignosulphonate and derivatives of starch and cellulose are used in concrete admixtures, mortars and grouts, paints and oil well drilling fluids (Plank, 2005; Vieira et al., 2005). However, with increasing efforts to improve the environmental impacts of building materials and reduce the consumption of finite resources, the idea of utilising renewable bio-based components in buildings is now being revisited (Christian and Billington, 2009; Francese et al., 2013). Insights into biology and examinations of materials in the natural world are also inspiring the development of novel building products (Pacheco-Torgal and Labrincha, 2014).

Biopolymers in particular have a number of potential advantages which make them attractive as components in composite materials. This includes the fact that they are mainly sourced from renewable plant-based resources, many of which can be viewed as CO_2 stores and, when sourced from non-terrestrial sources such as algae, they do not compete with arable land for food production. Furthermore, biopolymers are usually non-toxic and have more desirable ‘end-of-life’ disposal options than conventional fossil fuel derived polymers (Vilaplana et al., 2010). All of these properties are highly beneficial in considering whole-life cycle design and the drive to develop low carbon, healthy buildings.

1.2. Research Motivations

In addition to the more general incentives within the construction industry to improve the environmental performance of buildings and building materials, a more specific driving force for the project stemmed from the project’s industrial partner, Marine Biopolymer's Ltd (MBL). The company are currently developing an innovative alginate processing technique and aiming to reintroduce alginate production to the west coast of Scotland. An initial pilot plant has been established in Ayr, ahead of a full scale processing factory which will be located in the Barcaldine, near Oban (D. MacInnes, July 2015, *pers. comm.*). MBL were therefore keen to consider alternative output markets for their evolving product range and became interested in a study conducted jointly between the University of Strathclyde in Glasgow and the University of Seville in Spain involving the use of alginate as a binder in clay bricks (Galán-Marín et al., 2010). These initial experiments showed some promising results however there were still some unanswered questions regarding the importance of any alginate variables. MBL therefore wanted to investigate the role of the alginate, not only within a masonry product but also in other contemporary construction applications.

Although the majority of research regarding applications for alginates relates to pharmaceutical, medical and food-based industries, there are some examples of alginate compounds being utilised within the field of construction. A review of these potential uses can be found in an unpublished Master's thesis (Dove, 2012) where they are broadly divided into 5 categories: i. masonry products, ii. timber products, iii. plastics and composites, iv. fibres and textiles and v. paints and coatings. A summary of theses existing studies is provided in Table 1-1.

In reviewing the possible uses for alginate in construction applications, it became evident that this particular biopolymer is highly versatile and the potential applications are numerous. Given the limited timescale of this project, it was however deduced that only 2 products would be investigated in order to focus the investigation.

Table 1-1: Use of Alginate in Construction

	Product	Function	Ref.
Masonry	Concrete	Metal-alginate colloid coating which is used to make the concrete resistant to alkali and magnesium sulphates	(Erdahl, 1922)
	Concrete (lightweight)	Alginate spheres are uniformly dispersed through the concrete mixture to create a porous structure. Alternative to air-entrainment agents or lightweight aggregates	(Merton, 1964) (Glenn et al., 1998).
	Concrete	Alginate is used as an admixture which controls the viscosity of the concrete	(Chan et al., 1999)
	Unfired Clay Bricks	Alginate, in combination within lignin and natural or synthetic fibres is used as a binder to improve the strength of the bricks.	(Galan-Marin et al., 2012; 2013; Rivera-Gómez et al., 2014)
Timber	Timber Preservative	Sodium-alginate coatings are used to improve the durability by reducing moisture loss and prevent surface checking	(Wallis, 1970) (Harrison, 1968) (Rice et al., 1988)
	Timber Preservative	Uses alginate compounds in a Combined Impregnation Processes wood preservative	(Liibert et al., 2011)
	Timber Preservative	Uses a 'nano-zinc' preservative as a means of protecting timber from fungal decay, using a solution of zinc acetate, NaOH and alginic acid	(Bak et al., 2012)
	Fire protection coating	Describes a process for treating wood lumber with sodium alginate in order to improve heat and flame resistance	(DeBrouse, 2013)
Plastics & Composites	Transparent Plastic	Describes a solid, transparent material produced by heating a metal-alginate compound	(Edwin, 1949).
	Insulation Foam	Describes grains of alginate foam combined with a binding matrix which can be moulded into a lightweight composite.	(Appleton et al., 1946) (Plesch and Cefoil Ltd., 1947)
	Insulation Foam	Uses alginate in combination with clay minerals to produce a composite aerogel foam	(Ohta and Nakazawa, 1995) (Chen et al., 2012)
	Wood composites	Describes a wood-fibre pressed board, utilising either sawdust, wood chips or strands, combined with an alginate-based binder	(DeBrouse, 2013
Fibres & Textiles	Insulation Batts	Describes alginate and cotton or lace yarns where the alginate acts as a temporary scaffold which could be used to for insulation batts	(John and Norman, 1946) (Garner, 1945)
	Fire Retardant Textiles	Describes textiles which are impregnated with alginic compounds or utilising calcium alginate fibres which are inherently flame retardant	(Genevieve and Francois, 1959) (Kong et al., 2009).
Paints & Coatings	Paint Additive	Uses a sodium-alginate compound as an additive in both water and oil based paints as a means of improving fire resistant	(DeBrouse, 2013)
	Sheathing Board Coating	Describes a fibreboard with a protective film of asphalt emulsion, rubber latex and alginate	(Roux, 1958)
	Emulsion Coating	Describes an alginate and bitumen emulsion which can be applied to roofing felts or flooring.	(Clark et al., 1946)

In order to ensure that the study would generate a unique contribution to knowledge and add to the existing evidence base, whilst also addressing the earlier discussions regarding the impact of the construction industry and the role of building materials, selection was based on the following criteria:

- The proposed material should be one for which there is a current demand within the construction industry
- Existing evidence should suggests that the addition of alginate will have a functional role in the proposed product
- Prototypes for the proposed material should be technically feasible to produce with the available equipment
- The proposed material should be one which is not yet commercially developed
- Prototypes for the proposed material should be financially feasible to produce with available equipment
- The proposed material should potentially offer a more environmentally friendly alternative to an existing product and/or;
- The proposed material should potentially help to minimise the overall energy consumption of a given building

On this basis, two of the potential applications which were found to meet all of these criteria and therefore selected for further investigation were: **i. Unfired Clay Bricks** and **ii. Aerogel Insulation.** These two applications are discussed in more detail in Part I and Part II of the thesis, respectively.

1.3. Research Objectives

The overall aim of the study was to investigate the use of Scottish sourced alginate products, supplied by the project's industrial partner (MBL), in construction applications and establish whether MBLs products would be suitable in the development of new composite building materials. In response to this primary research question, the following objectives were established:

- A literature review regarding the use of alginate in the two proposed applications – unfired clay masonry and insulation
- Characterisation of a range of seaweed and alginate products supplied by MBL
- Characterisation of the soil and clay products to be used in the proposed composites
- Production of prototype unfired clay bricks using alginates provided by MBL and other commercial alginate products
    - Characterisation of the brick prototypes through a series of physical tests including rheology observations, mechanical testing and microstructural analysis
    - Analysis of the impact of composition variables on the physical properties of the brick prototypes including a comparison of different alginate types, different soil types and mix ratios
- Production of prototype areogel insulation materials using alginates provided by MBL and other commercial alginate products
    - Characterisation of the insulation prototypes through a series of physical tests including rheology observations, mechanical testing and microstructural analysis
    - Analysis of the impact of composition variables on the physical properties of the insulation prototypes including a comparison of different alginate types, different clay types and mix ratios
- Assessment of the commercial feasibility of the proposed materials including comparison with other existing products on the market

1.4. Thesis Structure

The first section of the thesis includes the general introduction (Chapter 1) and background information relating to seaweeds and seaweed biopolymers (Chapter 2). An overview of the materials used throughout the study is also provided in Chapter 3. The rest of the thesis is then divided into two distinct parts with Part I being dedicated to the first case study material (unfired clay bricks) and Part II to the second material of interest (aerogel insulation).

Part I consequently begins with a literature review of earth masonry (Chapter 4), including its main advantages and disadvantages in construction as well as a summary of additives which are typically used to modify the properties of earth. This is followed by Chapter 5 which discusses the methods used to prepare and characterise the prototype brick specimens. The results and discussion for Part I are then provided in Chapter 6 while the overall conclusions are presented in Chapter 7.

The structure of Part II then mirrors that of Part I, with a literature review of building insulation and aerogel products included in Chapter 8 and an outline of the methodology provided in Chapter 9. Chapter 10 then discusses the results from tests performed on the aerogels and the differences observed for the variables included within the testing programme. Chapter 11 then summarises the conclusions for Part II. The Appendices include some more detailed information regarding the alginate products supplied by MBL (Appendix A) and the characterisation tests performed on the soils and clay (Appendix B & D). Other supplementary data for Part I and Part II are provided in the remaining appendices.

1.5. Publications Arising from Thesis

As part of the ongoing development of this thesis, the following **journal publications** have been produced:

Dove, C. 2014. “The Development of Unfired Earth Bricks Using Seaweed Biopolymers.” *WIT Transactions on The Built Environment* 142: 219–30.

Dove, Cassandra A, Fiona F Bradley, and Siddharth V Patwardhan. 2016. “Seaweed Biopolymers as Additives for Unfired Clay Bricks.” *Materials and Structures*, 1–20.

In addition, the following **conference presentations** have been produced:

Dove, C. 2014. “Exploring the use of seaweed biopolymers in construction materials” *3rd Annual Conference of the Energy Technology Partnership, Dundee, Scotland, 23 - 24 April 2014*

Dove, C. 2014. “The Development of Unfired Earth Bricks Using Seaweed Biopolymers.”
5th International Conference on Harmonisation between Architecture and Nature, Siena, Italy, 24 - 26 September 2014

Dove, C. 2015. “Exploring the use of seaweed biopolymers in construction materials” *University of Strathclyde Research Presentation Day, Glasgow, Scotland, 24 June 2015*

The following **poster presentations**:

Dove, C. 2013. “Exploring the use of seaweed biopolymers in construction materials” *2nd Annual Conference of the Energy Technology Partnership, Edinburgh, Scotland, 16 – 17 April 2013 [1st Prize]*

Dove, C. 2013. “Exploring the use of seaweed biopolymers in composite construction products” *University of Strathclyde Research Presentation Day, Glasgow, Scotland, 27 June 2013*

Dove, C. 2014. “Exploring the use of seaweed biopolymers in construction materials” *8th Annual Environmental and Clean Technology Conference, Glasgow, UK, 26th June 2014*

Dove, C. 2014. “Exploring the use of seaweed biopolymers in composite construction products” *SEDA Research Conference 2014, Edinburgh, UK, 25th April, 2014*

2. BACKGROUND

2.1. Seaweeds

Algae are a group of autotrophic organisms known to be one of the oldest life-forms on Earth, with evidence of their existence dating back to the early Cambrian era (Gensel, 2008). Algal species are also incredibly diverse with estimates of the number of different species ranging from 40,000 to 140,000 (Chapman, 2009). They exist as two main groups; micro-algae and macro-algae. Whilst micro-algae species are minute organisms, visible only with the aid of a microscope, macro-algae exist as the large plant-like species which we more commonly refer to as seaweed. Seaweeds can be further divided into three main categories based on pigmentation; *Phaeophyta* (brown algae), *Rhodophyta* (red algae) and *Chlorophyta* (green algae). While these macro-algae are a form of perennial vegetation, they differ from more complex land plants in that they have no leaves, stems or any of the other organs found within vascular plants and are dependent on water as their source of nutrients (Walker, 1947). Despite their relatively simple structures, in comparison to their land based counter-parts algal life-forms are vital to the biosphere since they perform around half of all global photosynthesis and therefore contribute greatly to the world's oxygen levels (Field et al., 1998). Since seaweeds require access to sunlight, as well as a substrate to which the holdfast element of the algae can attach, they are restricted to tidal and benthic photic zones but still contribute to approximately 10% of all marine productivity (Israel et al., 2010).

Historically macro-algae has been utilised in numerous applications with the earliest evidence of seaweed being harvested by humans dating back to the fourth century in China (Kenicer et al., 2000; McHugh, 2003). Today seaweed is harvested on a global scale with an annual consumption rate of approximately 14.7 million metric tonnes (Buchholz et al., 2012). However it is important to note that there has been a significant shift towards farmed seaweeds which now contribute to around 94% of the world's annual seaweed supplies compared to around 50% in the mid-1990s (Lindsey Zemke-White and Ohno, 1999). The majority of seaweeds are therefore cultivated in near-shore plantations rather than harvested from wild stocks which form the remaining 6% of seaweeds produced for commercial purposes (Lindsey Zemke-White and Ohno, 1999). Whilst consumer demand had previously been satisfied by natural supplies, by the 1950s cultivated seaweeds were developed in order to accommodate the growing popularity of seaweed products, particular for human consumption (Bixler and Porse, 2011). Worldwide, the farming of aquatic plants has grown steadily since the 1970s with an average yearly increase of 7.7% (FAO, 2011).

Seaweed production is currently dominated by countries in East and Southeast Asia where the domestic food market is the principal output, with species such as *Laminaria Japonica* (more commonly known as Kombu) and *Porphyra Yezoensis* (also known as Nori) being the most popular edible seaweeds. These regions therefore produce approximately 99.8% of cultivated macro-algae supplies (FAO, 2011), with China alone responsible for over half of this production (Buchholz et al., 2012). Other key producers include Indonesia (20%) and the Philippines (12%) followed by the Republic of Korea and Japan (FAO, 2011). It is important to note that whilst Japan contributes a relatively small proportion of seaweed production by weight, the high market value of Japanese products means that it is still regarded as the second most important producer. Outwith Asia, the next largest producer is Chile followed by Africa, particularly Tanzania and Madagascar (FAO, 2011). In a

European context, the principal producers are Spain, France, Italy, and Russia (Buchholz et al., 2012).

2.1.1. The Seaweeds of Scotland

Despite the dominance of other regions in the global seaweed market, the sheltered waters of the Scottish coastline harbour a rich and abundant supply of wild seaweeds, with the most recent studies revealing that Scotland's macro-algae community consists of over 600 different species (Kenicer et al., 2000). Scotland possesses a particularly rich heritage of seaweed harvesting, including a variety of industrial applications which were unique to the UK. The earliest evidence of their use in Scotland dates back to 563 AD when Saint Columba and his monks reportedly gathered seaweeds cast on coastal rocks as a source of food for the poor (Indergaard and Minsaas, 1991). Since then, the use of seaweed has played an integral part in both the social and economic development of the country, particularly for west coast communities where seaweed supplies are most abundant (Kenicer et al., 2000). Generally however the industry has witnessed a cyclical pattern of boom and bust, with innovative uses for seaweeds often being quickly superseded by cheaper alternatives (Kenicer et al., 2000).

Phaeophytes are the most dominant type of macro-algae in Scotland and these species can typically grow at considerable depths since their pigments are more effective at absorbing the light wavelengths which reach these deeper waters (Rothe et al., 2012). Macro-algae can be found in most coastal environments around Scotland however the most abundant supplies are concentrated around the Outer Hebrides, the Orkneys and other peripheral areas of the Scottish coastline. The two most commonly found species Scotland are part of brown algae family (Figure 2-1).

This includes *Ascophyllum nodosum,* also known as knotted wrack, and *Laminaria,* also known as kelp, of which there are various types including *Laminaria saccharina, Laminaria hyperborea* and *Laminaria digitata* (Burrows et al., 2010). A number of *Fucus* species are also reasonably abundant in Scotland. Whilst other variations are also found in Scottish waters, including *Chondrus crispus* and *Mastocarpus stellatus* (red algae) and *Trentepohlia* (green algae), these exist in much smaller quantities and commercial harvesting is usually concentrated on the *phaeophytes* (Milliken and Bridgewater, 2001).

Figure 2-1: Types of Phaophytes

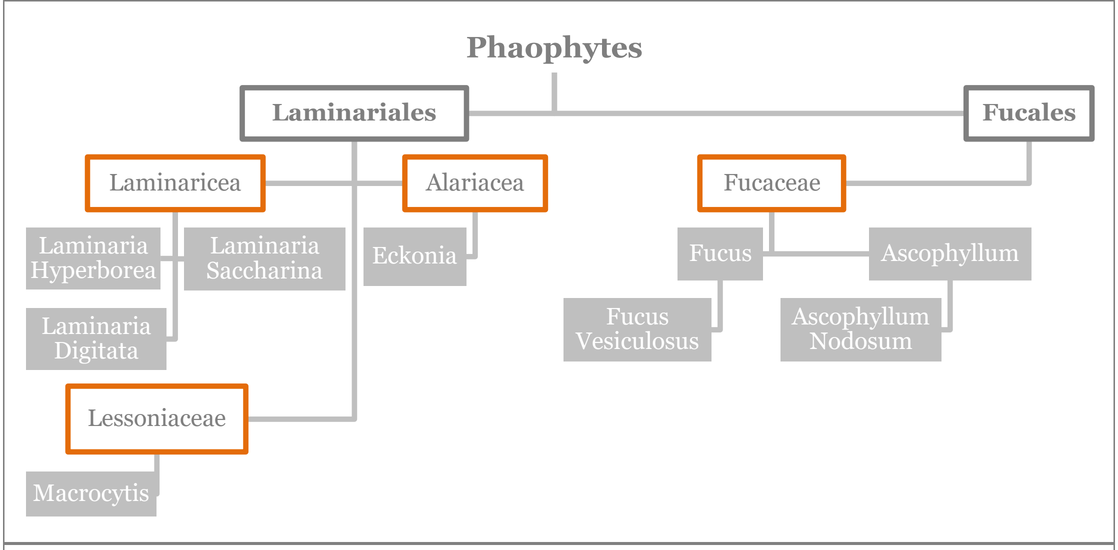

Author's own image

2.1.2. Seaweed Harvesting

Traditionally seaweeds would have been harvested by hand and gathered from the coastline during low tide. At the peak of kelp industry in the Western Isles, over 40,000 people may have been involved in this harvesting process (BioMara, 2014). During stormy seasons, *Laminaria* would often be cast on the rock, eliminating the need for the weeds to be removed from their holdfasts. For *Ascophyllum* species, a sickle or other scythe-like tool would be used to cut the seaweed, leaving a stub around 15cm in length (Kelly et al., 2001). This would commonly take place between the months of June and October. Today, however, mechanical harvesting techniques are more likely to be adopted. These methods take place during high tide using specially designed barges which utilise a water-jet rather than rotating blades to assist movement (McHugh, 2003). However some countries like Norway, Ireland and France have now imposed regulations regarding the intensity of harvesting including restrictions on machinery use (Scottish Government, 2013).

There have also been a number of investigations regarding the optimal harvesting and regrowth cycles for seaweeds (Walker, 1947; Lehre Seip, 1980; Sharp, 1987; Tyler, 1994; Kelly et al., 2001). Most studies recommended a harvest interval of 3 to 6 years although this is dependent on factors which affect the capacity for regrowth such as the quantity harvested, the expanse of the harvest area, the types of equipment and machinery employed, grazing by other animals and the particular characteristics of the bed location (Burrows et al., 2010). For example, in locations with particularly high wave exposure, regeneration is often impeded as a result of the harsh conditions of the habitat (Petraitis and Dudgeon, 2004) . The quantity of the seaweed left after cutting also influences the speed of regeneration. For example, for *Ascophyllum* species, if 0.5% of the original seaweed was left after harvesting then approximately 23% of the weed would return after 3 years. However if a 12% mass is left, then the seaweed can grow to 70% of the original size within the same time frame (Burrows et al., 2010). If these responsible harvesting practices are adopted, seaweed may be viewed as renewable and sustainable resource.

2.1.3. Principal Uses

Today the main markets for seaweed are either as a food source or as a source of chemicals. Globally, the majority of seaweeds (76%) are currently harvested for human consumption, with the biggest markets being Japan, China and Korea (Chopin, 2012). It should be noted however that the seaweeds which are indigenous to Scotland (i.e. *Ascophyllum* and *Laminaria*) generally have a lower nutritional values than the red and green algae (Fleurence, 1999). There is therefore a limited market for edible seaweeds in Scotland, although some local producers do harvest small quantities for use in food products (Milliken and Bridgewater, 2001). Aside from human consumption, historically seaweeds were also used as animal fodder in Scotland (Kenicer et al., 2000). As another indirect role in food production, seaweeds were also often used as a form of fertilizer or soil conditioner due to their high nitrogen and potassium contents (Kenicer et al., 2000).

Aside from the direct use of raw seaweed, the majority of other applications involve the extraction of useful components from the organism. Historically, one of the first industrial uses for seaweed was in the production of potash (sodium salts) and soda (sodium carbonate) which could be obtained by burning the seaweed in a kiln (Forsythe, 2006). These chemicals became particularly valuable in industries such as glass making, soap production, textile dyeing and gunpowder production (Forsythe, 2006). However by the late 1800s, alternative and more economical methods for producing these materials had emerged and the demand for seaweed ash had diminished (Barker et al., 1956). Other developments included the production of seaweed-derived iodine (Woodward, 1951), although again this was short lived due to the discovery of alternative iodine sources (Kenicer et al., 2000).

Today the most common and most profitable non-food use of seaweed is the phycocolloid market (Bixler and Porse, 2011). Whilst the term ‘phycocolloid’ refers specifically to algal sources of colloids, these belong to the larger group of ‘hydrocolloids’. These are substances which are soluble in water but mix with the water molecules to form a gel-like material (Burey et al., 2008). The three principal seaweed hydrocolloids which are used in commercial applications are agar and carrageenan, derived from red algae, and alginates, derived from brown algae (Bixler and Porse, 2011). Whilst the use of these substances dates back to the mid-1600s, phycocolloids were not produced on a commercial scale until after the Second World War (McHugh, 2003) when they became useful stabilising and gelling agents within the processed food and textile industries. Even today the demand for phycocolloids increases by 8-10% on an annual basis (Dhargalkar & Verlecar, 2009) with alginates and carrageenans forming the largest part of the market. In the context of Scotland, given the dominance of brown algae, alginates are currently the principal form hydrocolloid available.

More recently, the possibility of using macro-algae sources as a method of energy production has also been explored (John et al., 2011). Although this research was initially developed in the late 1960s (Wilcox, 1975), the interest in algae-based energy has resurfaced in recent years as a result of rising oil prices. The research includes both the production of methane based biogas through anaerobic digestion and the production of bioethanol through fermentation (Milledge et al., 2014). The main driver behind the development of these technologies is that fact that algal resources do not compete with food crops in terms of requirements for land, irrigation and fertilisers (Rothe et al., 2012). Whilst these techniques are still in their infancy, it should be noted that one of the main challenges in utilising brown algae in energy production is that the alginate component of the biomass cannot be easily broken down by microbes during the fermentation process and therefore does not convert as easily as the other sugars found within seaweed. Consequently some investigations have explored the potential of integrating both alginate extraction and energy production (Langlois et al., 2012) which could be particularly advantageous in improving the commercial viability of such processes.

2.1.4. Seaweed Biopolymers in Scotland

Following the collapse of Scotland's seaweed industry during the 19th century, chemist E.C.C. Stanford began exploring alternative uses for macro-algae, using *Laminaria* seaweeds harvested from Scotland. After establishing a small-scale plant on the Isle of Tiree in the Inner Hebrides Stanford had major breakthrough during the late 1800s when he discovered a colloidal substance, similar to cellulose, which could be extracted from these brown seaweeds (Woodward, 1951). Stanford went on to submit a patent for the process involved in obtaining this new substance which he named as 'alginic acid' (Stanford, 1886).

Further investigations into alginic acid slowed over the following decades and the seaweed industry continued to decline (Kenicer et al., 2000). Almost 50 years after Stanford's original discovery, the properties of alginic acid were revisited by C.W. Bonnikson who along with a team of colleagues investigated the production of cellophane-like films produced from the acid (BioMara, 2014). In 1934, the team formed a new company named Cefoil Ltd, setting up a small factory in Campeltown (Bailey, 1998) with the objective of investigating the properties of alginic acid and alginates (MMC, 1979). Following the Second World War, further research into alginates took place with the Ministry of Supply funding the construction of additional factories in Scotland, including one in Girvan (Ayrshire) and another in

Barcaldine (Argyllshire). As well as these key processing facilities, collection bases and drying stations were also created in North Uist, South Uist and Lewis, thereby generating an efficient network of seaweed processing activities (MMC, 1979). During this period, the company began investigating more experimental applications such as the production of calcium-alginate fibres and yarns for use in camouflage textiles (Woodward, 1951). Other investigations included the production of lightweight materials which could be used in aircraft. An example of this includes the De Havilland Mosquito, which incorporated solid calcium alginate foam within the wing design (RSC, 2014). Since common aircraft materials such as aluminium and balsa wood had to be imported during the war, a shortage of lightweight components for aircraft emerged and so other locally sourced alternatives had to be found (BioMara, 2014). However by 1944 German blockades were withdrawn and there was no further need for such a product (RSC, 2014).

When the war concluded, the Ministry of Supply withdrew from the research (BioMara, 2014). By 1945 Cefoil Ltd began to focus on other commercial developments and was renamed as Alginate Industries Ltd (AI Ltd). After investing in further research work, securing an economic supply of raw materials and setting up an export strategy, AI Ltd began generating substantial profits during the 1950s. The success continued over the following decades, assisted by developments in the textile industry which became one of the major output markets and by 1973 the company became a listed public company (MMC, 1979). In 1979, AI Ltd was sold to a Californian alginate manufacturer named Kelco and the Scottish operations were therefore rebranded under Kelco/AI Ltd (MMC, 1979). Despite the efforts of the new management, production began to decline throughout the 1980s and subsequent acquisitions took place. By 1996, Scottish activities were operating under Monsanto, with only the Girvan factory remaining in operation. During this period most of the raw materials were still sourced from the peripheral regions of Scotland but the lack of adequate drying facilities in these areas meant that the wet seaweeds would be have to be transported to Girvan (Kenicer et al., 2000). This was not only highly inefficient in terms of transportation costs, but the raw material was often of a poorer quality since the seaweeds would begin to rot before reaching the factory. As a result, the company began importing cheaper foreign seaweeds, particularly from Iceland and Tasmania, although more local supplies from the Irish coast were also utilised (Milliken and Bridgewater, 2001). Later developments also failed to revive the industry, and despite the Norwegian company FMC Biopolymer taking over the business in 2008, alginate production at the remaining factory ceased in 2009.

In more recent developments, MBL are hoping to reintroduce sustainable alginate production to Scotland within the next few years. They have established an initial pilot plant in order to conduct initial research and development work and are currently seeking investment to develop a full-scale production factory. It is proposed that their new patented production process will be more cost effective and more energy efficient than the previous practices in Scotland due to the innovative ‘wet’ processing methods adopted. Furthermore, based on surveys of existing seaweed stocks, an estimate of 3,868,000 tonnes has been provided for *Laminaria* species in Scotland (Walker, 1954). Following a more up to date survey of the available intertidal seaweeds around the Western Isles, it has also been estimated that the total available biomass of the *Ascophyllum* species alone equates to approximately 170, 500 tonnes (Burrows et al., 2010). After considering the proportion of these resources which are easily accessible and accounting for the 4 year recovery period required to achieve sustainable harvesting, is estimated that the annual yield in this area alone could reach 15,000 tonnes. It is also noted that if additional landing sites were to be developed, the yield could increase to 25,000 tonnes (Burrows et al., 2010). There is therefore considerable scope for large scale production and a long-term business model given the quantities of natural seaweed stocks available.

It should also be noted that there is a major advantage to using natural seaweeds stocks since the alginate producing phaophytes, which are abundant in Scotland, are not commonly cultivated since the farming of these species is relatively expensive (McHugh, 2003). Even though the alginate yielding *Laminaria Japonica* is farmed extensively in Asia, this is produced principally for human consumption rather than alginate production. Additionally, alginates produced from this specific species tend to produce lower gelling strengths than Scotland's native *Laminaria* types and other forms alginophytes such as *Ascophyllum*. This is due to the fact that the alginate contributes to the flexibility and mechanical strength of algal plants and can therefore be compared to the cellulose components of land based plants (Andresen et al., 1977; Donati and Paoletti, 2009). Species which inhabit turbulent waters, such as those in Scotland, therefore tend to have a higher alginate content (McHugh, 2003). Scotland is therefore well placed within the market given the abundance of natural stocks which can be used to produce high quality alginate products.

2.1.5. The Current Market for Alginates

Global production of alginate is approximately 30,000 tonnes per year with *Laminaria* and *Lessonia* being the most commonly harvested species (Bixler and Porse, 2011). The majority of actual alginate production takes place in the Asian-Pacific region while in Europe approximately two thirds of the production takes place in Norway (Bixler and Porse, 2011). One of the main barriers to alginate production is the decreasing accessibility and increasing cost of harvesting brown seaweeds. Nonetheless, current production represents only 10% of the available natural alginate within living organisms (Donati and Paoletti, 2009). It should be noted that aside from seaweeds, other bacterial sources of alginates are also emerging such as *Azotobacter* and *Pseudomonas* although these are not yet used commonly in industry (Gacesa, 1998; Hoefer et al., 2015).

Alginates have variety of potential industrial applications. The most common output for alginate, in quantitative terms, is within textile printing where it is utilised in creating dye pastes which are applied to fabrics during the screen printing process (McHugh, 2003). In paper production, alginates are also used to create surface coatings (Joyce et al., 1996) and in the fabrication of welding rods the polymer is used as a form of binding agent (McHugh, 2003). These technical grades of alginate form around 42% of the market, by volume, while most of the remaining production involves food and pharmaceutical grade products (Bixler and Porse, 2011). Alginates are in fact commonly used as a thickening and emulsifying agents in processed foods like ice cream and other dairy products, as well as in restructured foods (Nussinovitch, 1997). In terms of biomedical uses, alginates are primarily used in wound dressings, anti-reflux suspensions and controlled release medications (Draget and Taylor, 2011). The gel forming properties of alginates are also advantageous in the dental industry where they are used as moulds for dental impressions (Cook, 1986a). In cost terms, industrial grades alginates such as those used in the industries are typically sold for a minimum of ~£3/kg while higher grade products with tailored molecular weights and M/G compositions can cost over £70/kg (Hay et al., 2013).

3. MATERIALS

3.1. Alginate

As discussed in Chapter 2, alginate is a biopolymer obtained from brown seaweeds. More specifically, alginate is the collective term for the salts of alginic acid which are obtained from the cell walls of the macro-algae. These salts, usually in the form of sodium or potassium, contribute to 20-60% of the dry matter of the algae (Rehm, 2009). Figure 3-1 shows the structure for sodium alginate $(C_6H_7NaO_6)_n$ which is a block co-polymer consisting of (1-4)-linked β-D-mannuronic acid and α-L-guluronic acid residues. The ratio and sequence of these components, otherwise known as M and G blocks, vary within the polymer chain depending on factors such as the type and age of the algal species from which the alginate is sourced, the season during which it is harvested and the general growing conditions (Rehm, 2009). Variations in the alginate composition can also be found in different parts of the same organism. For example, in the *Laminaria Hyperborea*, it has been shown that the stem will have a much higher G content than the frond, the leaf like component, due to the fact that the st em part requires a stronger structure (Draget et al., 2009).

Figure 3-1: Alginate Chemical Structure

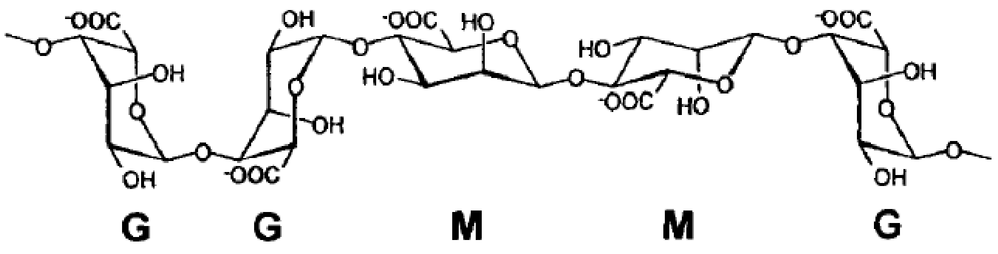

Source: Adapted from Draget et al. (2005)

One of the most useful properties of alginates is their ability to form cross-linked gels through iontropic gelation. Unlike some other hydrocolloids, alginate does not depend on temperature induced gelation (Lencina et al., 2013) and is therefore currently used in numerous stabilising, binding and gel-forming applications. This includes many commercial products ranging from processed foods and textile dyes to dental impression materials and pharmaceutical products (Draget et al., 2009). Gelation occurs when a soluble form of alginate, usually sodium alginate, is converted to an insoluble gel through the introduction of divalent metal cations such as Ca^{2+}. For alginates, this gel-forming mechanism is commonly described by the 'egg-box model' (Grant et al., 1973) as illustrated in Figure 3-2.

Figure 3-2: Egg-box model

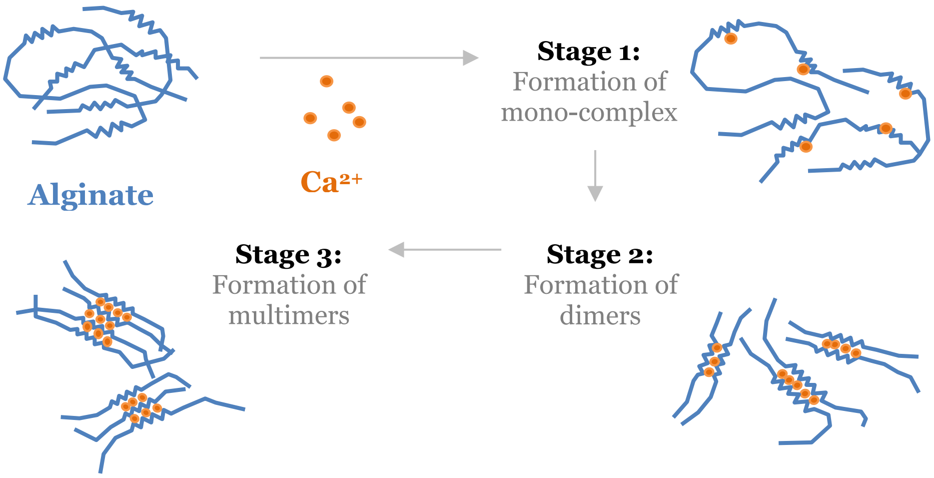

Source: Adapted from Funami et al. (2009)

This process involves co-operative binding in water where interactions between the G blocks of the negatively charged alginate polymer and the positively charged cations create chain to chain associations. This is due to the formation of junction zones between two or more chains where the cations sit within the buckled parts of the molecule, like eggs in an egg box. During the gelation process, the number of chain to chain associations increases, eventually leading to the formation of a continuous network (Rees and Welsh, 1977). Consequently, the gelation process can be influenced by factors such as the M/G ratio and sequencing of the alginate, the cation type and dosage, the alginate molecular weight and the molecular weight distribution (Funami et al., 2009).

3.1.1. Sources

A total of 14 different seaweed products were used throughout the study. These are summarised in Table 3-1 with images of the samples provided in Figure 3-3. The majority of materials used in this study were sourced directly from MBL and are labelled using acronyms provided by the company (PR = Production Run). Two commercially available products were also studied.

Table 3-1: Seaweed Products – Sources

	Seaweed Source	Type	Supplier
LH	*Laminaria hyperborean – frond & stem*	Milled Seaweed	MBL
AN	*Ascophyllum nodosum*	Milled Seaweed	MBL
PR22	*Laminaria hyperborean- stem*	Dried Sodium Alginate	MBL
PR24	*Laminaria hyperborean – stem*	Dried Sodium Alginate	MBL
PR25	*Laminaria 27hyperborean- stem*	Dried Sodium Alginate	MBL
PR29	*Laminaria hyperborean – stem*	Dried Sodium Alginate	MBL
PR30	*Laminaria 27hyperborean- frond*	Dried Sodium Alginate	MBL
PR32	*Laminaria 27hyperborean- frond*	Dried Sodium Alginate	MBL
PR52	*Ascophyllum nodosum*	Dried Sodium Alginate	MBL
PR14	*Laminaria 27hyperborean – frond & stem*	Residue	MBL
PR38	*Laminaria 27hyperborean – frond & stem*	Residue	MBL
PR17	*Ascophyllum nodosum*	Residue	MBL
DA	Mixed	Powder (Chromatic Alginate)	PSP Dental
AC	Mixed	Powder (Na-Alginate)	Acros Organics

Figure 3-3: Product Types

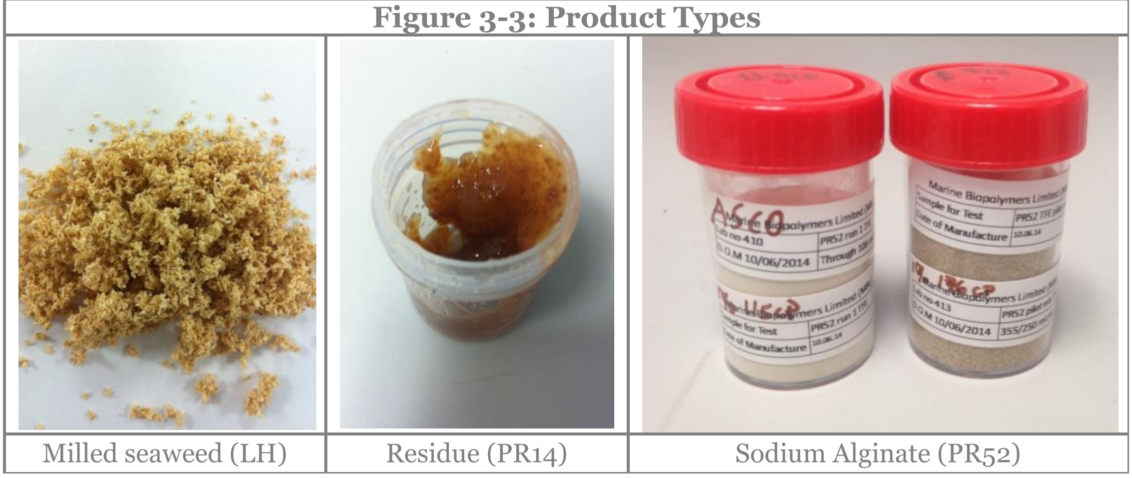

Milled seaweed (LH) | Residue (PR14) | Sodium Alginate (PR52)

Figure 3-4: Alginate Production Process

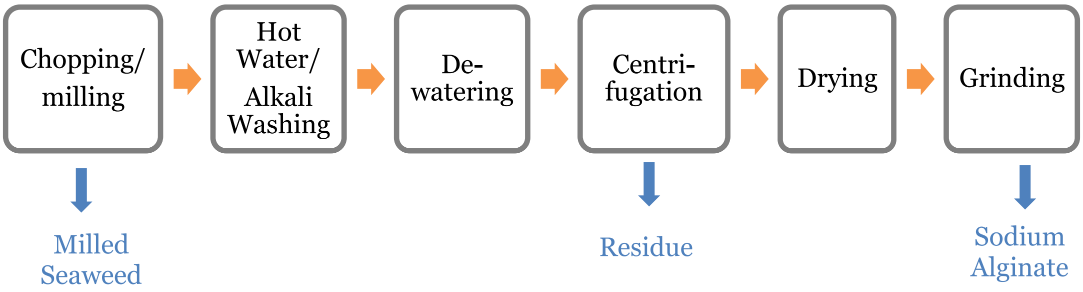

Author's own image

MBL Products

The MBL products tested can be grouped into 3 main categories relating to different stages of the production process shown in Figure 3-4. This includes milled seaweed products, residue products and dried alginate products. All of the MBL products were derived from natural species of brown macro-algae found in Scotland's coastal environment, the most common of which are *Ascophyllum nodosum* and *Laminaria hyperborea* (Burrows et al., 2010).

Milled seaweed

In firstly considering the milled seaweed products, this material has undergone minimal processing and simply been harvested, washed, chopped and milled – a process which is a precursor to alginate extraction. The milled seaweed is a fibrous material with a moisture content of between 70-90%. The alginate content will vary depending on the type of seaweed and for the products used here was expected to be between 4-6% by weight of the wet product (D. Mackie, personal communication, Mar 2013). Other components include cellulose, laminarins and fucoidans (polysaccharides), mannitol, amino acids, polyphenols, lipids and iodine (metabolites). In this case 2 milled seaweed products were considered including milled *Laminaria hyperborean* (LH) and *Ascophyllum nodosum* (AN).

Dried Sodium Alginate

This material represents the end product of the alginate extraction process. The aim of the extraction is to transform all of the alginate salts present within the algae into sodium alginate salts as this can be more easily separated from the other solid components of the seaweed. The milled seaweed is firstly washed with acid in order to eradicate the cross-linking ions which cause the alginate salts to become insoluble (McHugh, 2003). The seaweed is then broken down and mixed in an alkali solution. After approximately two hours, the alginate salts will dissolve, leaving a resulting mixture or slurry which can be filtered to separate the solid cell wall debris and cellulose residue from the alginate solution (McHugh, 2003). Water is also added at this stage in order to dilute the viscous mixture and facilitate the filtration process. If desired, bleaching may also take place to remove the pigmentation of the seaweed. The sodium alginate will be in the form of a dilute, aqueous solution and will then need to be transformed into a solid salt. MBL achieve this by casting a thin-film of the material onto a flat surface. This film is then dried and pulverised to produce a sodium alginate powder. A total of 8 different MBL products, produced using this method were studied including 5 LH stem, 2 LH frond and 1 AN product.

Residues

During the centrifugation process required to extract the solubilised sodium alginate, various by-products consisting of the remaining parts of the seaweed and water are generated. These so-called '*residue*' products are sludge-like materials with moisture contents of approximately 90%. As well as containing the cellulose and proteins which are removed from the seaweed during the extraction process, these materials will also contain residual amounts of alginate which have not been fully separated during the centrifugation process. MBL provided two batches of this material (PR14 and PR38) sourced from LH residues. These products have an approximate alginate content of 0.5 to 0.7%.

Commercial Products

Other commercially available products were also studied including a dental impression powder (DA) produced by PSP Dental Co Ltd (Kent, UK). According to the manufacturer this product had an alginate content of 15-30%. The other commercial product (AC) was a technical grade sodium alginate powder from Acros Organics™ (Geel, Belgium). These products are typically produced using a mix of seaweed sources.

3.1.2. Properties

The different alginate or seaweed types were characterised in order to identify any important differences between the products. A summary of these properties is provided in Table 3-2. Chemical composition was analysed by investigating the M/G ratios. This data was provided by MBL and obtained using ^{1}H-NMR spectroscopy as per the methods of Grasdalen et al. (1979) and Davis et al. (2003). The pH of alginate was also determined from triplicate measurements of 1%wt solutions in deionised (DI) water using a Mettler-Toledo benchtop pH meter. Cost data was provided by MBL or obtained from the relevant suppliers for the commercial products. Embodied energy values for the alginate were also estimated from energy data supplied by MBL. Further details of the estimated energy consumption can be found in Appendix A.

Table 3-2: Seaweed Products - Properties

	M/G ratio	pH	Cost (£/kg)	Intrinsic Viscosity [η] (dL/g)
LH	-	-	0.04	-
AN	-	-	0.04	-
PR22	1.04	8.20 (±0.49)	11.00	0.26
PR24	0.23	6.71 (±0.01)	11.00	0.48
PR25	0.56	9.28 (±0.01)	11.00	0.65
PR29	0.19	6.40 (±0.31)	11.00	0.57
PR30	0.78	6.90 (±0.05)	11.00	0.21
PR32	0.72	5.44 (±0.06)	11.00	0.20
PR52	0.77	6.30 (±0.04)	8.50	0.20
PR17	-	9.70 (±0.01)	0.20	-
PR38	-	7.50 (±0.02)	0.20	-
DA	-	9.10 (±0.06)	8.00	-
AC	0.83	6.84 (±0.03)	80.00	0.63

M/G ratio and cost data supplied by MBL. Other properties determined as part of characterisation tests.

Viscosity measurements were conducted using a Brookfield R/S Rheometer (CC45) with attached water bath to maintain a temperature of 25°C. Newton-Stokes Law relates viscosity (η), shear rate ($\dot{\gamma}$) and shear stress (τ) as shown in Equation 1. The shear rate is defined as the change of shear strain per second while shear stress is the tangential force applied over a given area (Luckham and Rossi, 1999).

$$\boldsymbol{\eta = \frac{\tau}{\dot{\gamma}}}$$

Equation 1

Since alginates are non-Newtonian fluids meaning that their viscosity varies depending on the level of shear which they are exposed to, viscosity was measured over a range of shear rates rather than a single point viscosity measurement. Solutions of 1.0% (w/v) alginate in 0.1 M NaCl were therefore used to obtain comparable flow curves which plot shear rate ($\dot{\gamma}$) against shear stress (τ) for each of the alginate types. As shown in Figure 3-5, all of the alginate types were found to exhibit 'shear-thinning' or 'pseudo-plastic' behaviour whereby the viscosity decreases with an increasing shear rate. As per the methods of Haug and Smidsrod, (1962), additional viscosity measurements were also made for alginate concentrations of 0.05% to 1.0% (w/v) and converted to an intrinsic viscosity $[\boldsymbol{\eta}]$ using Equation 2, where η_r is the relative viscosity and c is the concentration.

$$[\boldsymbol{\eta}] = \lim_{c\to 0}\left(\frac{\boldsymbol{\eta_r} - \mathbf{1}}{\boldsymbol{c}}\right)$$

Equation 2

Figure 3-5: Alginate Flow Curves

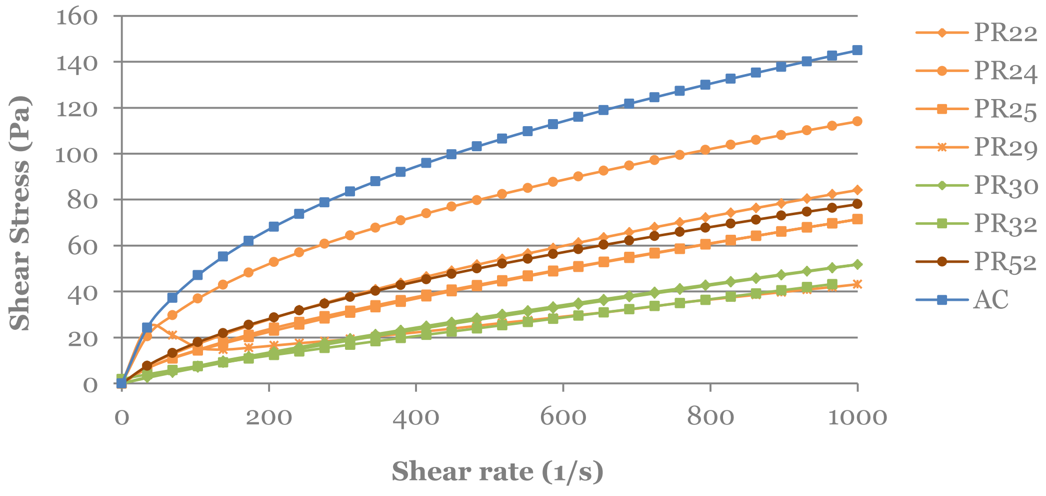

Flow curves showing the dependence of shear stress over a shear rate ramp of 0 – 1000/s. All tests performed on 1.0% alginate solutions in 0.1 M NaCl at a temperature of 25°C.

3.2. Soil and Clay

Soil is a mixture of clay, silt, sand and sometimes other larger particles such as gravel. These constituents are the products of rock erosion and are therefore created as a result of natural weathering processes (Minke, 2006). The relative proportions of these different particle sizes impact on various soil properties which are important for brickmaking including cohesiveness, workability and forming characteristics, drying behaviour and shrinkage (Craig, 2004). As a natural material, the properties of soils will vary depending on geographic location and consequently variations in particle size grading and composition are vast. Soil texture classification is normally determined using the particle sizing method with clay particles defined as those with a metric size of less than 0.002mm whilst silt, sand and gravel particles are within the ranges of 0.002–0.06mm, 0.06-2mm and 2–60mm, respectively (Minke, 2006). Typically soils will consist of a mix of granular materials such as quartz and feldspars and clay minerals. Other minerals such as carbonates, phosphates and sulphates are also present in small quantities.

The clay fraction influences the physical properties of a given soil, including its compressive strength, shrinkage behaviour and cation exchange capacity (CEC). Therefore understanding the properties and composition of the clay minerals present is highly important in assessing the soil’s suitability for building applications. Clay minerals are essentially layered crystalline structures based on tetrahedral silicate sheets, formed from SiO_4 tetrahedra and octahedral hydroxide sheets, which consist of an aluminium core surrounded by hydroxyl groups (-OH). Depending on the structural arrangement, these clay minerals can then be classified as 1:1 phyllosilicates or 2:1 phyllosilicates, as illustrated in Figure 3-6. For example a 1:1 clay type would contain one tetrahedral sheet and one octahedral sheet whereas a

2:1 clay type would consist of one octahedral sheet between two tetrahedral sheets. The clay minerals are further classified into groups depending on their specific composition and how these semi-basic 1:1 or 2:1 units are stacked, with most common groups being the kaolins such as kaolinite and halloysite, the smectities such as montmorillonite and the micas such as illite and muscovite.

Figure 3-6: Structure of Clay Minerals

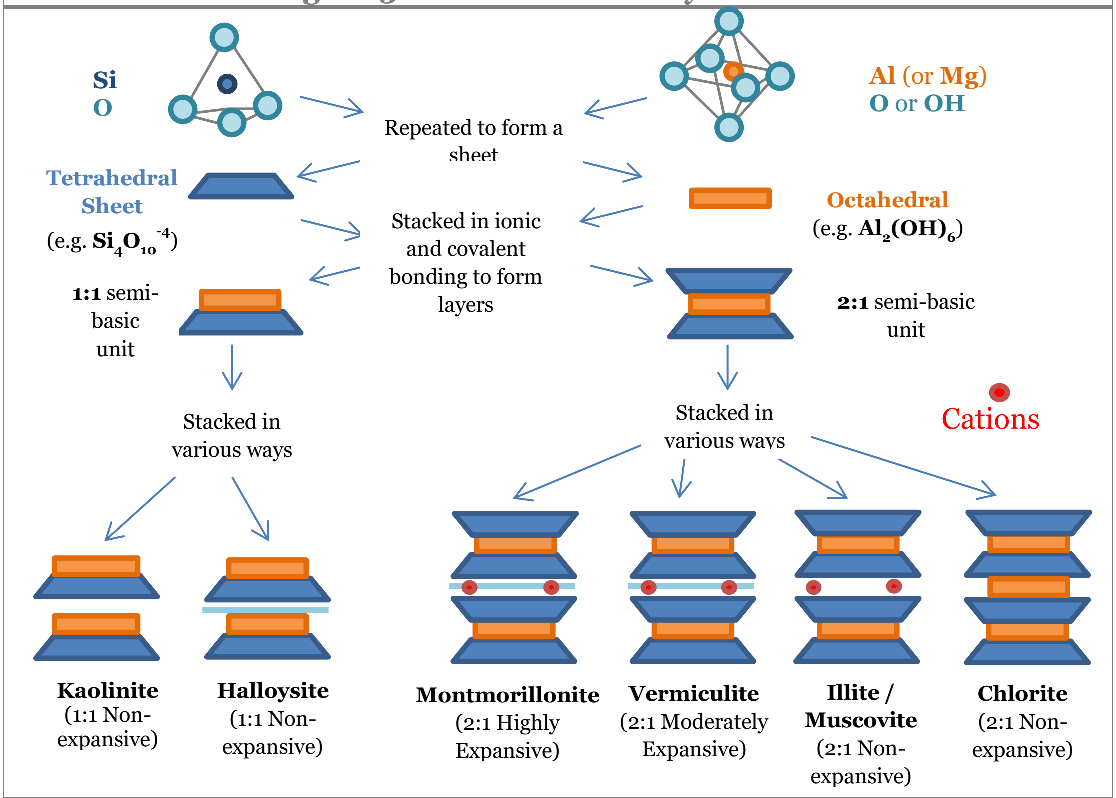

Source: Adapted from Mitchell and Soga (2005)

Clay minerals belonging to the 2:1 group are generally more expansive in nature than the 1:1 group since water molecules can penetrate the interlayers more easily, meaning that the clay has the tendency to swell upon the addition of water. Furthermore, since the tetrahedral sheets display the greatest negative charge, they also induce strong interlamellar binding (Minke, 2006). Depending on the composition of the sheets, the layer will have with an overall neutral charge or a negative charge. In the kaolinite group, the stability of the double layered structure results in a neutral charge. However the smectite group which displays a sandwich structure with two tetrahedral sheets is negatively charged and has to be balanced by positively charged ions between layers. These exchangeable metallic cations are usually in the form of calcium (Ca^{2+}), magnesium (Mg^{2+}), potassium (K^{+}), sodium (Na^{+}) or, in some cases, aluminium (Al^{3+}).

3.2.1. Sources

The soils used in the study were supplied by Ibstock Ltd and sourced from UK clay quarries. A summary of the quarry locations and soil sources is provided Appendix B. Due to limitations in current quarry operations, it was not possible to source Scottish clays and so the soils were obtained from quarries located in England. Two additional clay products were also purchased from Acros Organics™ (Geel, Belgium). This included a bentonite clay (B) which is a 2:1 smectite type clay consisting primarily of montmorillonite and a kaolinite (K) which is a 1:1 type.

3.2.2. Properties

All soils were characterised using standard procedures and their properties are summarised in Table 3-3. Loss on Drying (LOD) and Loss on Ignition (LOI) were calculated using the methods outlined in BS EN 15935 (BSI, 2012b). Soil pH was measured using a 1:5 volume ratio of dry soil and a 0.01 mol/L $CaCl_2$ solution (BSI, 2012c). Particle size distributions (PSD) were obtained using the sedimentation method described in BS 1377-2 (BSI, 1990a). Atterberg limits were calculated using the soil thread method for plastic limit (PL) and the cone penetrometer method for the liquid limit (LL) as also described in BS 1377-2. The maximum dry density (MDD) and optimum moisture contents (OMC) were determined using an adapted version of the procedure outlined in BS 1377-4 (BSI, 1990b). In this case, rather than adopting the standard Proctor method which uses a 1L cylindrical mould and either a 2.5 or 4.5kg rammer, and consequently uses a greater level of compaction than typical used in earth block production (Mesbah et al., 1999; Kouakou and Morel, 2009), the adapted method involved using the same rectangular moulds and hand compaction technique as used to produce the final blocks in this study. Cation exchange capacity (CEC) and specific surface area (SSA) were calculated from the Methylene Blue test (BSI, 2013a) and calcium (Ca) contents were obtained by inductively coupled plasma (ICP) measurements on soil extracts using the aqua-regia method for 'Total Elemental Ca' and a DI water extract for the 'Available Ca'.

Table 3-3: Soil Properties

		U	**V**	**W**
pH ($CaCl_2$)		4.78 (±0.01)	6.75 (±0.01)	6.90 (±0.00)
LOD at 105°C (%)		2.9 (±0.3)	3.9 (±0.5)	2.3 (±0.3)
LOI at 550°C (%)		7.5 (±0.5)	8.2 (±0.6)	6.5 (±0.4)
Soil Colour (Munsell, 2000)		7.5YR 4/2	5Y 4/1	5YR 5/2
PSD				
Sand and Gravel (%)	60µm >	24	29	23
Silt (%)	2 - 60µm	45	44	61
Clay (%)	< 2µm	31	27	16
Soil Classification		Clay Loam	Loam	Silt Loam
Atterberg Limits				
PL (%)		16.0	14.6	15.3
LL (%)		27.3	27.9	25.4
PI (%)		11.3	13.3	10.1
Plasticity Classification		CL lean clay with sand	CL lean clay with sand	CL lean clay with sand
Activity		0.36	0.49	0.62
Compaction Behaviour				
Maximum Dry Density (kg/m^3)		1820	1980	1920
OMC (%)		16	18	14
Chemical properties				
Electrical Conductivity (µS/cm)		640(±2)	115(±3)	169(±2)
CEC (meq/100g)		4	5	5
SSA (m^2/g)		6.1	9.8	8.6
Total Elemental Ca (ppm)		1670	3910	3460
Available Ca (ppm)		750	2330	1730
Mineralogy: XRD				
Clay type		Kaolinite dominant	Kaolinite, Illite, Vermiculite	Kaolinite dominant

Analysis of the overall chemical composition was obtained by Scanning Electron Microscopy-Energy Dispersive Spectroscopy (SEM-EDS). X-ray diffraction (XRD) was performed on the fine fraction (<2 μm) of the soils using the oriented aggregate mount method (Moore and Reynolds Jr, 1989) using a Bruker D8 Advance Diffractometer with a Cu Kα anode at an angle a range of 3° to 40°. The resulting diffractograms and elemental compositions can be found in Appendix B along with further details of the characterisation tests. The results showed that this fine fraction of the soils is predominantly kaolinite and illite. Although kaolinite is dominant in soils U and W, soil V has a higher proportion of illite as well as containing vermiculite.

Tests which were also suitable for the bentonite and kaolinite samples were also performed as summarised in Table 3-4. As expected, the bentonite clay was found to have higher PI, CEC and SSA values compared to the kaolinite due to the presence of 2:1 layered silicates (i.e. montmorillonite) in the bentonite sample.

Table 3-4: Clay Properties

	B	K
pH	8.60 (±0.01)	7.02 (±0.05)
LOD at 105°C (%)	7.2 (±0.7)	1.8 (±0.2)
Atterberg Limits		
PL (%)	34.2%	23.2%
LL (%)	76.7%	34.0%
PI (%)	42.5%	10.8%
Plasticity Classification	OH	CL
Activity	0.4	0.1
Chemical properties		
Electrical Conductivity (μS/cm)	1943 (±15)	495 (±14)
CEC (meq/100g)	65	4
SSA (m^2/g)	26	9
Mineralogy: XRD		
Clay type	Montmorillonite dominant	Kaolinite dominant

PART I: ALGINATE AS AN ADDITIVE FOR EARTH MASONRY

Part I focusses on the use of alginate products as additives in earth-based building materials. The aim is to use the biopolymer as a means of providing the raw earth with sufficient compressive strength for use in internal and low load bearing applications, therefore negating the need for the energy intensive firing processes normally associated with clay bricks. As discussed in Chapter 2, while some previous studies have investigated the use of alginate in this capacity, there are still unanswered questions regarding the specific role of the alginate and the properties which affect its success as an additive for masonry. Part I will therefore investigate a range of alginate products and produce prototype brick products which can be characterised and compared.

4. LITERATURE REVIEW

4.1. Masonry Construction

Masonry construction is one of the oldest and most commonly adopted building techniques with surviving buildings from the Neolithic period still visible throughout the world (Smith and Austin, 1989). The term ‘masonry’ is used to describe any form of construction which involves stacked units or blocks which are laid in a mortar. Traditional forms of masonry, such as adobe and natural stone, would have been constructed using locally available raw materials helping regional identities to develop, with the materiality of the built environment often reflecting the geology below. However, technological developments such as improvements in transportation systems, the development of fossil fuel powered kilns and advances in cement technology during the industrial revolution facilitated the development of contemporary masonry materials such as concrete blocks and ceramics (Smith et al., 2009).

One of the main advantages of masonry as a construction method is its inherent flexibility, both in design and construction. Masonry materials are available in various geometries, sizes, colours and textures and hence allow for great versatility in their application. In addition, masonry can be used to fulfill multiple functions simultaneously by providing structure, a thermal envelope, acoustic insulation and an aesthetic finish (Hendry, 2001). Other attractive properties include its durability, relatively low maintenance and inherent fire resistant. It is also well-established method of building meaning that there are recognised technical standards and an existing workforce who are familiar with the construction techniques. Indeed, from a funding point of view, investors and mortgage lenders view masonry as a relatively reliable build technique (Barker, 2004). Masonry also has a high aesthetic appeal and remains a popular choice of construction for most domestic dwellings.

There are however disadvantages to masonry construction. One of the major drawbacks is that it requires on-site construction and wet trades meaning that it can often be labour intensive, time consuming and delayed by external factors such as weather. Whilst there have been developments in prefabricated masonry units which negate some of these issues, these off-site manufacturing techniques are not yet commonplace in the UK (Rogatzki, 2015). In this sense, masonry has been described as relatively outdated and inefficient with some suggesting that its popularity is due only to a lack of innovation within the construction industry (Lovell and Smith, 2010; Barker, 2004; Ross, 2002). Furthermore, the low tensile strength of most masonry products means that its use is often restricted to medium and low rise buildings unless reinforced or supported by an additional load bearing structure (Hendry, 2001). Nonetheless, traditional masonry still remains a popular choice for domestic scale buildings where its inherent strength is still sufficient.

4.1.1. UK Context & Market Trends

The construction industry is particularly sensitive to national economic trends. This is particularly evident for masonry products given their high dependence on the rate of house building. Over the past three decades whilst there have been some fluctuations in demand, production levels peaked during housing boom in the late 1980s. Since then production has generally been on the decline, with an annual figure of 2000 million in 2014 (ONS, 2015). As shown in Figure 4-1, in more recent years, the economic recession in 2008 had a direct impact on the use of the industry demand for masonry products. This led to the downsizing and closure of several manufacturing facilities across the UK (Carbon Trust, 2010).

Figure 4-1: Masonry Production in the UK

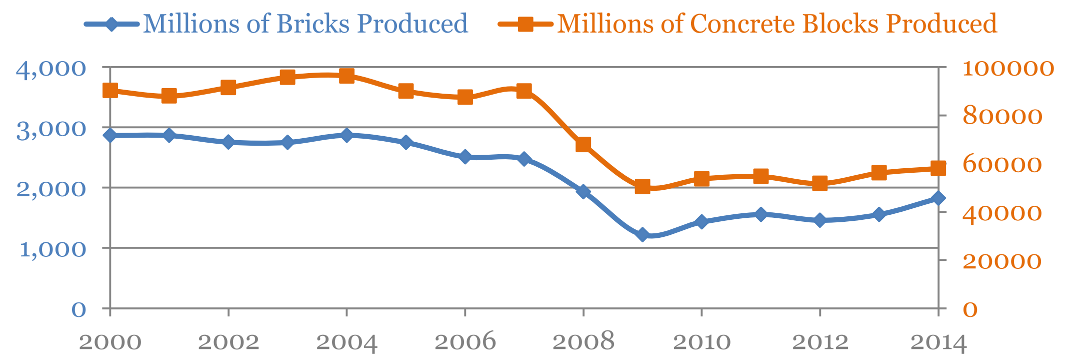

Source: ONS (2015)

However since the economy has started to recover, this has led to new problems, particularly for the brick industry. At present the UK has an urgent need to provide more housing to meet the demands of population growth and as such there has been an increased requirement for both new build properties and the refurbishment of existing stock. Within Scotland alone, it is estimated that 500,000 new homes will be needed by 2035 (National Records of Scotland, 2012). As a consequence of this renewed demand, between 2014 and 2015 there has in fact been a shortage of bricks in the UK, with the mothballing of factories during the recession meaning that the national production capacity has been unable to meet industry requirements. This is particularly apparent in Scotland which is heavily reliant on imports due to the closure of several winning operations and brickworks. Even before the recession, Scotland accounted for only 4% of bricks made in the UK (British Geological Survey, 2007). By 2014, only one brick producer, Raeburn Brick Limited, remained in operation in Scotland (Smith, n.d.).

In addition to changing supply-demand relationships, wider economic issues such as fluctuating energy prices have also remained a threat to the financial viability of brick production (Competition Commission, 2007). Decreased production output has also resulted in kilns being operated at reduced capacities leading to inefficiencies and higher production costs meaning that smaller producers have struggled to compete with the economies of scale offered by the larger companies (Competition Commission, 2007). In the case of concrete blocks, as shown in Figure 4-1, production figures have followed a similar trend to ceramic bricks, albeit with much greater production volumes. Indeed the production capacity for concrete blocks in the UK is much greater than for bricks with around 90 different production plants run by 30 different manufacturers (CBA, 2014).

There has also been a general decline in the demand for the common brick which has gradually been displaced by other materials (Bloodworth et al., 2001). Given the drive to minimise build costs and increase productivity on site, larger units have become the preferred option since these are both faster and easier to lay. For example the dimensions of a typical concrete block (440 x 100 x 215 mm) are equivalent to the volume of six standard bricks meaning that, not only is the laying process accelerated, but less mortar can be used. Similarly, new systems for internal partitions such a frame and panel/board systems are commonly being specified as alternatives to masonry systems in an effort to minimise the presence of 'wet' trades on site. While brick and block cavity wall construction has historically been the most common construction technique for low-rise, domestic dwellings (Pan et al., 2007), this picture is beginning to change. This is primarily due to increasing competition with timber frame systems where the inner concrete leaf is replaced with structural timber members. Although recent figures show that timber frame forms only 13% of the overall market in the UK, in Scotland the figure is over 60% (CBA, 2014). In general offsite manufacture, the development of prefabricated systems and the introduction of alternative cladding systems in recent decades has further diminished the role of masonry (Competition Commission, 2007). Other factors contributing to the drop in the demand for masonry products include the decreasing footprint of domestic dwellings (Robert-Hughes et al., 2011) which consequently consume less material. Additionally, the increasing urban density of population centres has resulted in a decrease in the number of detached properties as well as an increasing number of flats and multi-storey buildings which are typically built using steel and reinforced concrete (British Geological Survey, 2007).

A number of environmental issues, some of which are closely related to the financial concerns surrounding masonry construction, have also been identified. This applies not only to the raw material extraction phase but also to processing operations and the utilisation of the final products. For example, the *Climate Change Levy* (Parliament of the United Kingdom, 2000) which came into effect in 2001, commits energy-intensive industries, which includes the production of ceramics, cement and lime, to making significant reductions in CO_2 emissions. This is supplemented by the *EU Emissions Trading Scheme* which allows trade emission allowances to be bought and sold and provides further financial incentives for companies to meet their targets (POST, 2012). The shared objectives of these policies are to reduce the energy consumption and GHG emissions associated with such processes and encourage the efficient use of resources. One of the biggest concerns for the brick industry in particular, is energy consumed during the firing process which can be up to 83% of the total fuel consumption of the brickmaking process as illustrated in Figure 4-2 (Carbon Trust, 2010).

Figure 4-2: Energy use in the Brickmaking Process

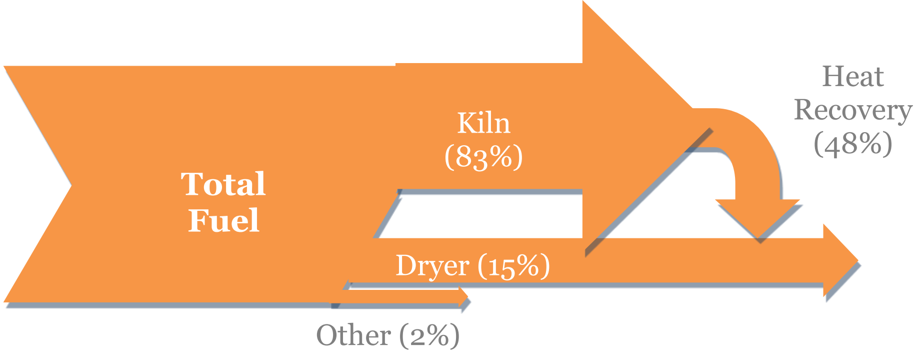

Source: Adapted from Carbon Trust (2010)

Whilst there are increasing efforts to increase the efficiency of the kiln-firing process, through methods such as heat recovery, it is estimated that increases in process efficiencies will only amount to a maximum energy reduction of 20% (Carbon Trust, 2010). Indeed reports from the brick industry indicate that over a ten year period, the overall energy production per tonne of material produced had been reduced by only 6% (Brick Development Association, 2012). In the case of concrete products, the biggest issue is the significant volumes of Ordinary Portland Cement (OPC) utilised since this requires high production temperatures and significant energy inputs (Habert et al., 2011).

The *EU Integrated Pollution and Prevention Control Directive* (Official Journal of the European Union, 1996) also places restrictions on raw material extraction, operations and atmospheric emissions with limits on the permitted levels of emissions likely to become more stringent in the future (Bloodworth et al., 2001). Therefore in addition to energy-efficiency targets, there are also limits being placed on the emission of pollutants such as carbon dioxide, hydrogen fluoride and particulates (Carbon Trust, 2010). Water consumption is also an important factor with manufacturers being driven to minimise the use of fresh waste and re-use secondary sources wherever possible. In manufactured masonry products, water is added to the dry materials in order to produce a workable mix which can then be moulded into the desired shape. The addition of additives such as plasticisers reduces the requirement for water and this technique is being used in some cases to improve the plasticity of the material. In some cases however the additives can be costly and may therefore not prove worthwhile. Cheaper alternatives for improving workability include products such as industrial sludges and natural products such as food starches (Brick Development Association, 2001). Other efforts to improve the resource efficiency include responsible sourcing of raw materials, minimising waste and the increased use of recycled and secondary aggregates. For example, additives such as pulverised fuel ash (PFA) which is a by-product of the coal industry is often incorporated as a partial cement substitute (Man and Yeung, 1997) while alternative aggregates such as recycled construction and demolition wastes (Poon et al., 2002) can be used in concrete block production to reduce the consumption of primary aggregates. Clay brick manufacturers are also being encouraged to incorporate recycled materials contents of above 10% while also reducing the amount of waste sent to landfill (Brick Development Association, 2012). Overall, there are therefore existing pressures for both brick and block manufacturers to reduce the environmental impacts of their products.

In summarising the future market for masonry within the UK, despite current challenges, since traditional brick and block construction is a tried a tested method it is likely to remain popular with house-builders provided that it can be shown to be more economical than other modern methods of construction (Barker, 2004). A recent study also demonstrated that consumers reportedly still favour brick/block construction over other methods (Brick Development Association, 2012). Given that the present market for masonry is focused primarily on domestic dwellings, the need for new homes will also help to support the future demand for masonry products. However, whilst there will be a continued demand in the near future, the replacement of fired clay bricks and concrete blocks with alternatives like timber and other pre-fabricated systems may also increase unless the industry is able to diversify and create new products which offer additional benefits. Although there are some new innovations in masonry which have become available commercially in the UK, such as the development of honeycomb ‘Ziegel’ blocks (GreenSpec, 2015a) or materials incorporating alternative materials such ‘Hemcrete®’ (Lime Technology, 2015), in general product innovation has remained relatively static in recent years (Competition Commission, 2007) with countries like Germany taking the lead in research and development activities. There is therefore further potential for new masonry products which offer compatibility with existing build methods but also respond to the need to reduce environmental impact and improve costs.

4.2. Earth Masonry Construction

Earth masonry materials are those which are manufactured using unfired clay soils. Therefore unlike conventional ceramic bricks, the clay material is simply dried or ‘baked’ rather than being fired at a high temperature. Earth is an ubiquitous material, contributing to over 70% of the global landmass (Borer and Harris, 1998). Due to this abundance and availability, raw earth has played a vital role in the development of mankind. This is primarily due to unique properties of the clay minerals contained within the soil which, when combined with water, act as a binding matrix with the other courser particles. Upon drying, this creates a solid material from which basic shelters can be constructed. Unfired earth has hence been utilised as a building material for thousands of years, with examples of sun-dried bricks dating back to 7000 BC having been found in Mesopotamia, Egypt and India (Smith and Austin, 1989). Minke (2006) also reports that adobe houses found in Turkmenistan were constructed as far back as 8000 -6000 BC. As a vernacular technique, building with earth often relies on the traditions and skills of local cultures passed down through generations, and therefore the vast regional variations exist. The basic types of earth construction are presented Figure 4-3.

Figure 4-3: Summary of Unfired Earth Systems

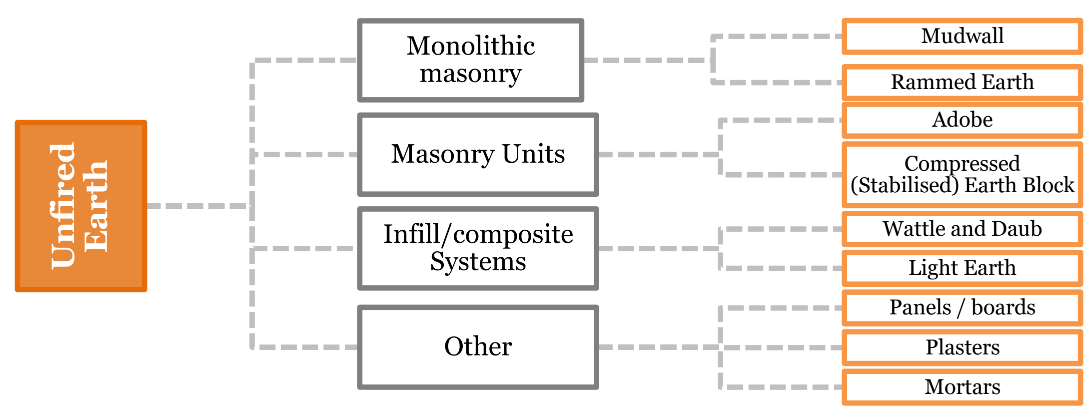

Author’s own image

In considering the current global context, an estimated one third of the worldwide population still inhabiting buildings made from earth (Houben and Guillaud, 1994). Whilst these various building methods have been used extensively in construction for centuries (Williams et al., 2010), in Western societies most of these materials have been replaced by contemporary ceramics such as fired bricks and concrete. In comparison to such materials, earth is considered to have a number of disadvantages such a relatively low strength and poor durability (Ruskulis, 2002a). However raw earth still remains as a cheap, abundant and eco-friendly material and when detailed appropriately can be used to create versatile architectural forms.

4.2.1. Earth Construction in the UK

Earth based construction was commonplace in the UK and in Scotland until the 18th century (Little et al., 2001). However traditional earth building techniques were considered to be labour intensive and experienced a decline as a result of the growing popularity of stone and timber. Although the majority of earth based buildings in existence today are located in developing countries, a resurgence in more traditional earth building techniques has been witnesses recent years, particularly within Europe, the USA, Australia and New Zealand (Pacheco-Torgal and Jalali, 2012), and there are an increasing number of studies which discuss the potential of unfired earth as a contemporary building material. This is mainly a result of the growing recognition of earth's environmental credentials as well as the associated hygro-thermal and acoustic benefits.

In the context of the UK, it is estimated that there are currently around 500,000 earth buildings in existence (Little et al., 2001). This includes traditional constructions such as cob and rammed earth construction as well as contemporary methods such as the Compressed Earth Block (CEB), a descendent of traditional adobe blocks, which has become particularly popular. As discussed by Heath et al. (2012a), industrially produced CEBs are more aligned with modern methods of construction since their improved strength can allow comparable wall thicknesses to conventional brick/block constructions. They also required similar skills to standard bricklaying and are therefore more likely to enter the mainstream market (Morton, 2008).

4.2.2. Properties of Earth as a Construction Material

As a natural material, the properties of earthen materials and their performance is dependent upon a number of factors including both material and production variables. The importance of these variables, as well as the general properties of earth including physical characteristics, aesthetics and cost, will therefore be discussed.

Soil Properties

Firstly, the composition of the soil used has an important influence on the final properties of the bricks or blocks being produced. Since the fine clay particles act as the main cohesive element in a soil, the PSD will affect the overall strength of the soil matrix. As discussed by Delgado and Guerrero (2007), the clay content can have a particularly significant effect on the compressive strength of unstabilised materials. There is however wide variation within existing technical guidance regarding optimum PSDs, with recommended clay proportions ranging from 5 to 40% (Delgado and Guerrero, 2007). In relation to plasticity, several authors also suggested the optimum range of Atterberg limits for soils which are to be used for building purposes. Houben and Guillaud (1994) for example suggest a LL of 25-51% and a PI of 2-31% for compressed earth blocks, with corresponding values for adobe materials of 31-50% and 16-33%. The role of the clay mineralogy is also discussed by Minke (2006) who describes how the ion binding capacity, including the quantity and type of ions present on the clay surface, is dictated by the mineral structure. This can in turn affect the overall compressive strength of the soil. In general, 1:1 minerals like kaolinite which have a low specific surface area and relatively low charge characteristics, are weaker binding agents than 2:1 minerals like montmorillonite (Röhlen and Ziegert, 2011). Given the wide range of soil types available globally, an understanding of the raw materials is critical in assessing it suitability for earth masonry products as well as facilitating comparisons between the results of physical tests, where different soil types have been used.

Mechanical Properties

The mechanical properties of earthen materials are commonly tested as measure of their anticipated structural performance and as an indicator of specimen quality. However at present there is a general lack of standardisation regarding testing procedures and the most appropriate methods for predicting the structural performance of earthen materials (Morton, 2008). Procedures are therefore often based on those used for mortars, concrete, blocks and fired bricks such as *BS EN 772-1* (BSI, 2011a), *BS EN 1351* (BSI, 1997a) and *BS EN 1015-11* (BSI, 2002). The compressive strength and flexural strength (modulus of rupture) are the two main tests conducted on masonry units as well as additional tests on the complete masonry systems such as the bond strength test and the RILEM test (Olivier et al., 1997).

The compressive strength is the most commonly cited mechanical property for earthen materials. In reviewing existing studies relating to earth brick and blocks (Table 4-1), without the use of additives, compressive strength values are found to vary between approximately 1 and 8 N/mm^2. Whilst most studies are based on similar testing principles, there is still variation between studies due to a lack of standardised procedures. For example some studies tested only the unit compressive strength (Kouakou and Morel, 2009; Heath et al., 2009) whilst others provide values for the characteristic strength, including the contribution of the mortar (Bei and Papayianni, 2003; Williams et al., 2011).

Table 4-1: Mechanical Properties - Literature Values

	Preparation Method	Approx. Dimensions (mm)	Bulk Density (kg/m^3)	Unit Comp. Strength (N/mm^2)	Reference
Unfired Earth Units – without cement/lime stabilisation	Compressed	145 × 145 × 90	2000	0.9 – 4.6	(Hansen and Hansen, 2002)
		145 × 145 × 90	2100	2.4 – 7.8	
	Mechanical Compaction	250 x 120 x 80	1975 – 2380	4.3 – 4.9	(Bei and Papayianni, 2003)
	Extruded (includes straw)	440 x 220 x 100	1674	0.6	(Williams et al., 2011)
	Hand compacted	450 x 185 x 140	1757	1.0	
	Hand compacted (straw)	200 x 85 x 90	1836	1.6	
		200 x 90 x 100	1816	1.5	
		210 x 90 x 95	1872	1.8	
	Adobe	70 x 60 x 140	1910 – 1990	1.8 – 3.1	(Kouakou and Morel, 2009)
	Mechanical Compaction	70 x 60 x 140	1940 – 2090	2.5 – 4.8	
	Extrusion	220 x 100 x 70	1597 – 2063	2-2 – 5.6	(Heath et al., 2009)
	Manual Compaction (with straw)	31 x 46 x 13	-	5.2 – 8.3	(Piattoni et al., 2011)
		15 x 23 x13	-	2.1 – 2.9	
	General	-	1700–2200	1 – 4	(Sutton et al., 2011)

In terms of the actual units being tests, variations in specimen production must also be considered. In addition to the previously discussed importance of soil selection, the method of manufacture can also influence the compressive strength. In traditional methods, such as adobes, the soil is mixed at a relatively high moisture content and is simply hand compacted into a mould and then left to dry in the sun. In more advanced systems, the material has a much drier consistency so that it can be compacted mechanically using either a manual or hydraulic press, or in some cases using an extruder. A typical mechanical press for example will compact the material at a pressure of 2 N/mm^2 (Walker and Stace, 1997). These different production methods, and resulting levels of compaction applied to the material, lead to different dry densities and mechanical properties. For example, as shown by Kouakou and Morel (2009), preparing blocks from the same soil using two different production methods led to significantly different strength characteristics. In this case the traditional adobe method was found to produce block of lower density and compressive strength than a pressed block produced at a lower moisture content. Some compaction techniques can also lead to a density gradient in the material which can again affect the strength results depending on the direction in which the specimen tested relative to the direction of compaction (Mesbah et al., 1999; Morel and Pkla, 2002). It is therefore unwise to directly compare materials which have been produced using different methods.

Furthermore, the geometry of the specimens being tested also has an important correlation with compressive strength. As discussed by various authors (Walker, 2004; Morel et al., 2007; Aubert et al., 2013; Aubert et al., 2015) this is due to the platen restraint effect (Figure 4-4) which results in confinement of the specimens due to friction against the platens and consequently increases the apparent compressive strength. This effect is enhanced with smaller distances between the platens meaning that the aspect ratio of the unit being tested has an important influence on the strength values achieved. In conventional masonry systems this variation can be accounted for using correction factors however there is still debate as to which values should be used (Heathcote and Jankulovski, 1992) and whether correction factors are even appropriate for earthen materials (Morel et al., 2007; Aubert et al., 2013). In some studies it is unclear whether correction factors have been applied and so again this may account for the wide variation of results.

Figure 4-4: Platen Restraint Effect

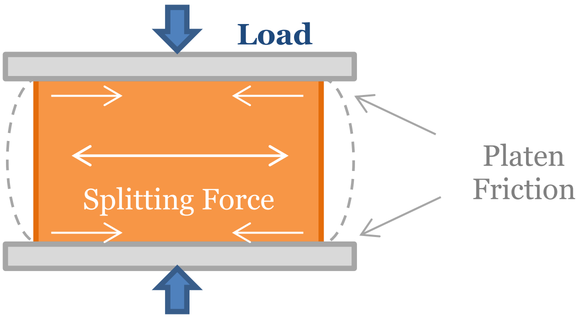

Source: Adapted from Lawrence et al. (2013)

Another factor which can affect the compressive strength of earthen materials is the moisture content of the unit at the time of testing. As shown by Heath et al. (2009), compressive strength can decrease by 30% upon an increase of 2% compared to the equilibrium moisture content. Hansen and Hansen (2002) also demonstrated a decreasing compressive strength with increasing moisture content. Differences may therefore be observed between samples which have been exposed to different environmental conditons.

In considering other mechanical tests, the flexural strength (modulus of rupture test) is also discussed within the existing literature, albeit less frequently than compressive strength. This property can be measured using the 3 point bending test which due to the simpler test procedure is more commonly used in field testing as an indicator of specimen quality (Rigassi, 1995; Morel and Pkla, 2002). Although the strength characteristics have less relevance in terms of the loading experienced in-situ as part of masonry construction, this test method is still useful in comparing the strength characteristics of the individual specimens and can be seen as an indirect method of measuring compressive strength. Another test method which assesses the behaviour of the full masonry system, including the mortar, is the RILEM test which measures the compressive strength of two half units stacked on top of each other with an earth mortar in between (Morel et al., 2007). This creates a greater aspect ratio to minimise the impact of confinement as well as taking into account the strength of the mortar layer.

Overall, the mechanical strength of unstablised earth is considered to be relatively low although in some cases it can be considered comparable to low grade concrete. As discussed by Houben and Guillaud (1994), in low rise buildings a downward load of 0.1 – 0.2 N/mm^2 is typical for a single storey and so when taking into account safety factors a design value of 2 – 2.5 N/mm^2 is considered sufficient for earthen walls. Indeed values of 1 – 1.5 N/mm^2 are noted as the minimum required for specimens with sufficient integrity while specimens with higher strengths (e.g. above 10 N/mm^2) may be considered unnecessary for low-loadbearing applications. Therefore while some unstablised specimens may pass this minimum criteria, the introduction of additives may help to further enhance strength.

Durability

Closely related to mechanical strength, durability is also an important characteristic for any building material and is particularly important for unfired earth products where the perceived poor water resisitance and weatherability is one of the biggest barriers to its use in modern construction (Morton, 2008). Concerns regarding the deterioration of the mechanical properties of earthen materials due to exposure to moisture or surface abrasion/impact must therefore be considered. A number of authors have attempted to quantify the durability of earthen materials through tests which mimic the impacts of weathering and erosion. Tests developed to date are based on applications where the material is to be used as external walling. Heathcote (1995;2002), Ogunye and Boussabaine (2002) and Walker (2004) describe a number of possible erosion and accelerated weathering tests which are suitable for earth masonry, the main objective of which is to measure the bond-holding capacity of the material. Procedures include the drip test, spray testing and the the accelerated erosion test. In both the drip and spray tests, the specimen is subjected to a pressurised water spray or controlled water droplets, either for a given time or until a given penetration depth with the material is reached. For the accelerated erosion test, the specimen is subjected to repeated cycles of wetting and drying as well as controlled abrasion using a wire brush. As discussed by Cid-Falceto et al. (2012a), these durability tests are also referred to in international guidance documents for earth building but there is again disparity regarding the specific procedures. There is also some criticism of these types of tests in that they are often much more severe than natural weathering conditions. Guettala et al. (2006) for example argues that whilst theses test are quick to perform, they are very aggressive and not representative of the likely conditions which the material will be exposed to, such as full submersion in water. Ogunye and Boussabaine (2002) further argue that inconsistencies emerge when laboratory tests are compared with long term in-situ studies. Indeed traditional adobe materials, which perform poorly in simulated erosion tests, have been used successfully in buildings around the world which are still standing today (Houben and Guillaud, 1994). In alternative durability studies, Adam and Agib (2001) studied the surface properties through repeated abrasion tests whilst Lenci et al. (2011) investigated damage evolution on dry units through cyclic loading tests, providing a profile of the mechanical behaviour.

Overall, most existing durability tests are designed for stabilised earthen materials which are to be used in external applications. These tests may therefore be too severe for lower-grade materials which are to be used in protected, internal applications. There is also a lack of standardisation among existing test procedures although given that weathering conditions are specific to different climatic regions, durability must also be considered in relation to the proposed building location. As discussed by Morton (2008), in the context of the UK which has a temperate, maritime climate, the use of unfired clay externally is not recommended. However in internal applications, provided that the earth masonry is constructed at least 75mm above ground level and protected with a damp proof course and local protection in areas such as behind sinks, the durability of the material should be adequate.

Hygroscopic Properties

Although the moisture sensitivity of unfired earth is regarded as one of its major weaknesses with regards to long term durability, its hygroscopicity may also be viewed as one of its key benefits in comparison with other building materials. An unfired brick can absorb up to 30 times more moisture comparison than a fired brick (Minke, 2006). As discussed in several studies, this behaviour can be highly beneficial in alleviating problems associated with moisture in buildings (Padfield, 1998; Osanyintola and Simonson, 2006). For instance, it has been estimated that human activities such as washing and cooking within a typical household can generate over 14 litres of water vapour on a daily basis (TenWolde and Pilon, 2007). If incorrectly ventilated, this can lead to serious problems such as condensation, dampness, mould growth and the on-set of so called ‘Sick Building Syndrome’. Hygroscopic materials can however help to regulate the indoor relative humidity (RH) levels by absorbing moisture from the air during periods of high humidity and storing this moisture until the room humidity decreases. This results in improved indoor air quality (IAQ) and consequently creates a healthier indoor environment for the occupants. In climates such as the UK, where occupants can spend up to 90% of their time in indoors, the quality of this environment is of vital importance (Minke, 2006). Secondary effects such as the reduced the requirement for mechanical ventilation, and therefore energy use, may also be experienced (Padfield, 1998). Osanyintola and Simonson (2006) for example have argued that in moderate climates the use of hygroscopic materials can reduce the energy required for heating by 7-8% as well as a 10-30% reduction in the cooling energy.

Unfired clay can offer such moisture buffering effects when exposed to the internal environment and this makes it an ideal product for interior applications (Morton, 2008). For example, a post-occupancy study of a house constructed using clay masonry demonstrated that the optimum RH range of 40-60% was maintained due to the regulating properties of the clay (Morton, 2005). Another study conducted in Germany also showed that the use of unfired masonry in new build housing could successfully normalise humidity levels, with tests conducted over an 8 year period demonstrating that RH remained at approximately 50%, creating a comfortable and healthy environment for the inhabitants (Minke, 2006). Aside from in-situ studies, tests for determining the moisture buffering potential of earthen materials are the same as those used for other building materials. For instance, *ASTM C1498 – 04a* (ASTM, 2010a) or *BS EN ISO 12571* (BSI, 2014) can be used to calculate the moisture absorbed by the material over a range of relative humidity (RH) levels. Padfield and Jensen (2011) demonstrated that unfired clay could absorb approximately 0.8 – 1.3% moisture over a RH range of 40-60% compared to >0.3% for standard fired bricks. Nordby and Shea (2013), in comparing work by Rode et al. (2005) and Padfield and Jensen (2011) also illustrated that unfired earth has a moisture buffer value (MBV) of 1.49 g/m^2 %RH. This is much greater than the equivalent value for concrete (0.38g/m^2 %RH). High humidity buffering values for unfired bricks in comparison to other ceramic products were also found by Hansen and Hansen (2002).

Overall, the moisture regulating behaviour of unfired earth is one of its major advantages over fired brick, concrete blocks and lightweight constructions such as stud walls. In addition to improved IAQ this can also lead to savings in energy due the reduced need for mechanical ventilation as well as minimising the need for heating and cooling due to latent heat exchange (Nordby and Shea, 2013). If this property can be exploited effectively, it could offer a major opportunity for the future utilisation and marketing of unfired materials. However, consideration must also be given to the impacts of any additives used in earthen materials upon their moisture buffering potential. For instance, the addition of stabilisers like cement and lime have been shown to reduce the vapour permeability of unfired earth (McGregor et al., 2014a).

Thermal Properties

In terms of thermal performance, earth masonry is considered to be a relatively poor insulator (Minke, 2006; Morton, 2008). This is primarily due to the high density of the material which can range from 1500 to 2000 kg/m^3 (Riza et al., 2010), giving corresponding thermal conductivity values of 0.7 to 1.2 W/m·K (Morton, 2008). Ibstocks's *Ecoterre* brick for example offers a thermal conductivity of approximately 1.0 W/m·K based on a material density of 1900 kg/m^3. According to Minke (2006), the thermal properties of earth can be improved through the inclusion of porous additives such as natural fibres, cork, pumice, foamed glass and expanded clay as well as waste products such as sawdust and crop husks. For example, Goodhew and Griffiths (2005) achieved a value as low as 0.18 W/m·K for a low density clay-straw mix. Commercially available products such as Claytec's *Light Earth Blocks* also offer a thermal conductivity of around 0.2 W/m·K. Whilst some systems such as light-earth construction and loam infill do offer much better thermal properties due to the inclusion of fibres, these are typically used as non-loadbearing in-fill materials in framed constructions rather than being considered as a form of masonry construction (Morton, 2008). Indeed the inclusion of fibres and pore forming additives which reduce the overall density often correlates with a reduction in compressive strength (Demir, 2008).

Other factors such as the moisture content can also affect thermal properties. The thermal conductivity of earthen materials can reportedly double when the moisture content is raised from 1% to 7% (Houben and Guillaud, 1994). This must be considered during testing and when calculating the expected performance of the material once installed. Nonetheless, existing studies have demonstrated that unfired clay bricks can still offer better thermal properties than conventional fired masonry. For instance, Oti et al. (2010a) measured the thermal conductivity and thermal resistance of unfired clay bricks stabilised either with lime or Ordinary Portland Cement (OPC) and activated Ground Granulated Blast-furnace Slag (GGBS), using a specialist thermal conductivity meter. The average values for thermal conductivity were given as 0.25 W/m·K and 0.26 W/m·K respectively which is lower than the equivalent value for a fired clay brick (0.40 W/m·K). Goodhew and Griffiths (2005) also demonstrated that an external cavity wall construction containing unfired clay bricks and sufficient insulation could achieve the minimum U-value (thermal transmittance value) required by UK building regulations. According to their results, achieving todays more stringent requirements for external walls in Scotland would require a 240mm clay brick outer leaf, a 150mm insulated cavity and a 110mm inner leaf.

Aside from thermal conductivity, another factor to consider is that the use of materials with high specific heat capacity and high density, like earth masonry, can provide thermal mass within the building. Lawrence et al. (2008) argue that this contribution to thermal mass can to a degree compensate for its poor performance as an insulator. This is due to the fact that a material like earth masonry allows heat to be stored and released as needed, providing a thermal lag and reducing variations in temperature as well as reducing the overall energy requirements for heating and cooling. The specific heat of unfired earth reportedly varies between 800 and 1000 J/(kg ·°K) (Houben and Guillaud, 1994) which is comparable to other masonry materials like fired brick and concrete. A study by Morton (2005) demonstrated that the thermal mass of earth bricks was beneficial in regulating the thermal fluctuations within a house where the energy consumption and steady-state heat flows were observed over a 12 month period. A more recent study conducted by Liuzzi et al. (2013) in Central West Africa also demonstrated through computer modelling that the use of unfired earth in the walls, floors slabs and roof led to the creation of desirable levels of thermal comfort. These combined hygro-thermal characteristics also mean that the moisture absorption of unfired clay creates further thermal inertia (Houben and Guillaud, 1994).

In summary, although earth may be considered as a poor insulator, particularly when compacted, it can still be used to meet the required U-values of UK building regulations if combined with appropriate insulation and detailed correctly. It can also be used effectively as part of a passive design strategy and exploited for its thermal storage properties if exposed internally. It should however be noted, factors such as the inclusion of voids or perforations, the moisture content, the specific material density and the composition of the clay and any additives will all have an influence on the specific thermal properties achieved.

Acoustic Properties

Noise travels through buildings by means of either airborne or impact sound, and can be generated from a variety of sources (McMullan, 2007). Sound insulation is becoming an increasingly important factor in the design of buildings, particularly between attached dwellings which share separating walls and floors (Smith et al., 2006). Most authors agree that earth masonry is regarded as a sufficient acoustic insulator (Walker and Stace, 1997; Morton et al., 2005; Hall and Swaney, 2005) although its specific properties will be dependent on the particular wall construction. For example, Houben and Guillaud (1994) give estimated Coefficients of Acoustic Attenuation (500 Hz) of 30 – 60 Db for a 400mm wall while Delgado and Guerrero (2006) also gives a general value of 58 dB (500 Hz) for 500mm earth walling. For more slender constructions, Morton (2008) states that a 130mm unfired masonry wall at a density of 1500 kg/m^3 would also be expected to achieve a

Sound Reduction Index (SRI) of 46 dB, with an equivalent value of 53 dB for a 240mm wall. Both of these wall types would therefore meet the minimum requirement of UK building regulations (HM Government, 2010; Scottish Government, 2015). As discussed by Binici et al. (2009), the acoustic performance of earthen materials can also be improved by incorporating high-porosity additives, such as basaltic pumice.

Fire resistance

Earthen materials are combustible only at very high temperatures and they are therefore considered to be relatively fire resistant (Röhlen and Ziegert, 2011). However the specific fire performance of a wall construction may be dependent on factors such as the composition, density and geometry of the masonry unit, the type of mortar used and the wall thickness. One major concern is that if a fire were to occur in an unfired earth building, the use of water as a fire fighting tool could also induce failure due to the poor water resistance of unfired materials (Morton, 2008). Therefore vulnerable areas would have to be sufficiently protected. The other main factor which can make unfired earth materials more vulnerable in fire situations is the inclusion of combustible materials such as natural fibres (Little et al., 2001). Some building standards, such as the UK, give a limiting value of 1% by weight for the quantity of combustible organic material whereas the German standard states that as long as the material achieves a minimum density of 1700 kg/m^3, it can be considered as incombustible (DIN, 1998). However Morton et al. (2005) demonstrated that an unfired earth product containing 50% organic fibres and with a density below the required German standard was able to pass the fire resistance requirements of *BS 476-20* (BSI, 1987). Buson et al. (2012) has also conducted fire testing on walls constructed from soil cement bricks and *'Kraftterra'* CEBs containing recycled paper fibres, with both types of materials demonstrating adequate fire resistance. The fire performance was also shown to improve with the inclusion of appropriate plasters. In general, Morton (2008) recommends that in cases where an earth masonry wall is required to be fire resistance, if the material does not have a density of over 1700 kg/m^2 or an organic content of less than 1%, the physical fire testing should be conducted to provide evidence of performance.

Mortar Compatibility

When designing earth masonry systems, the appropriate choice of mortar must also be considered. Even though the mortar component may account for less than 10% of the overall masonry system, its importance in relation to the performance of the overall construction can still be significant (Hendry, 2001). In general conventional cement based mortars are unsuitable for use with unfired earth units since they often have superior mechanical properties to the units themselves. For example Williams et al. (2011) studied the influence of mortar type on bond strength, characteristic compressive strength and flexural strength highlighting that cement mortars which are much stronger than the bricks can lead to considerable cracking. However earth slurry mortars, created using the same base material as the units, showed relatively good results. Overall, the most appropriate mortar may differ depending on the specific properties of the unit and therefore must be considered on an individual basis. Commercially available unfired brick products recommended using a light clay (>1400kg/m^3) or moderately hydraulic lime mortar (IBSTOCK, 2014). Some manufacturers even suggest that the units themselves may be rewetted and remixed to create a suitable mortar (Construction Resources, 2015).

In investigating alternative mortars for unfired earth systems, the most relevant study is that conducted by Lawrence et al. (2008). This explored the use of various mortar mixes including three sand/clay mortars, one of which also contained 5% lignosulfonate, a sand/cement mortar, a lime mortar and a sodium silicate mortar. The results showed that the sodium silicate mortars performed particularly well with the unfired units and achieved high bond strengths. This is an important factor to consider since a higher bond strength between the unit and the mortar will create a more stable structure. Lawrence et al. (2008) argue that this could therefore allow the standard 300mm wall thickness usually associated with earthen walls to be reduced to a thickness of 100mm, enabling more direct competition with other partition systems such as concrete blocks.

Later work on the sodium silicate mortar also tested characteristic compressive strength, flexural strength and initial shear strength of the masonry system demonstrating that in this case the weakest part of the construction was the bricks themselves rather than the mortar (Lawrence et al., 2010). However, given that sodium silicate has a relatively low carbon footprint as well as superior technical performance in comparison to the other mortars tested, it has been argued that this may be a promising avenue for the future development of unfired masonry.

Aesthetics

The aesthetic properties of any building material are of course highly subjective however the appearance of a particular finish can have an important impact on decisions surrounding material specification. Morton (2008) argues that the main advantage of earth masonry is that it is a highly versatile material and hence properties such as colour and texture can be modified to create the desired effect. Furthermore, unfired earth masonry can be left exposed or can be plastered, painted or lime washed to create an even wider range of finishes. Other techniques such as sandblasting and burnishing can also be adopted and ceramic tiling can also be incorporated in areas which may be particularly susceptible to water damage (Morton, 2008). A clay plaster, usually with added pigments, tends to be the most common approach as this provides an even finish whilst also protecting the masonry and still allowing a 'breathable' wall system. However some authors have noted that the application of wet plaster and renders to earth masonry can also have detrimental effects due to the moisture sensitivity of unfired materials, particularly when thick coatings are used on relatively slender walls (Heath et al., 2012b). This will therefore have to be considered when selecting the desired aesthetic finish.

4.2.3. Environmental Impact

There are a limited number of studies which discuss the environmental impact of unfired earth materials. In reference to unfired clay bricks (without stabilisers), Morton et al. (2005) provides embodied energy (EE) and embodied CO_2 (EC) values of 146 kWh/t and 44.6 $kgCO_2/t$, respectively. As shown in Figure 4-5, these values are considerably lower than for comparable ceramic products. This is due to the fact that the environmental impact of unfired materials includes only the excavation and transportation of the soil and processing factors such as mixing, forming and low temperature drying, thereby eliminating the need for energy-intensive kiln firing. Some authors even argue that where soil is excavated directly from the site, the embodied energy may be negligible (Shukla et al., 2009).

In considering stabilised materials, Venkatarama Reddy and Jagadish (2003) highlight that even cement stabilised blocks, with a 6% cement content use less than a quarter of the energy required to manufacture an equivalent fired brick product whilst steam cured bricks with 10% lime are also shown to require only 60% of this energy. However the contribution of the stabilisers is noted to be significant to the overall embodied energy of the brick. Furthermore, the authors also point out the importance of the mortar used in earth masonry systems which can also make a significant contribution to the overall embodied energy of the walling system. Whilst cement based mortars are shown to have the highest EE, the introduction of pozzolans into the mortar mix or the use of lime can lead to a reduction in the embodied energy (Venkatarama Reddy and Jagadish, 2003). Reddy and Kumar (2010) have also shown that systems such as rammed earth also offer a much lower embodied energy that typical fired brick systems but highlight the fact that the addition of stabilisers can effect properties such as the maximum dry density and optimum moisture content. This in turn will alter the energy required for key processes such as compaction.

Figure 4-5: Embodied Energy and CO_2 of Masonry Products

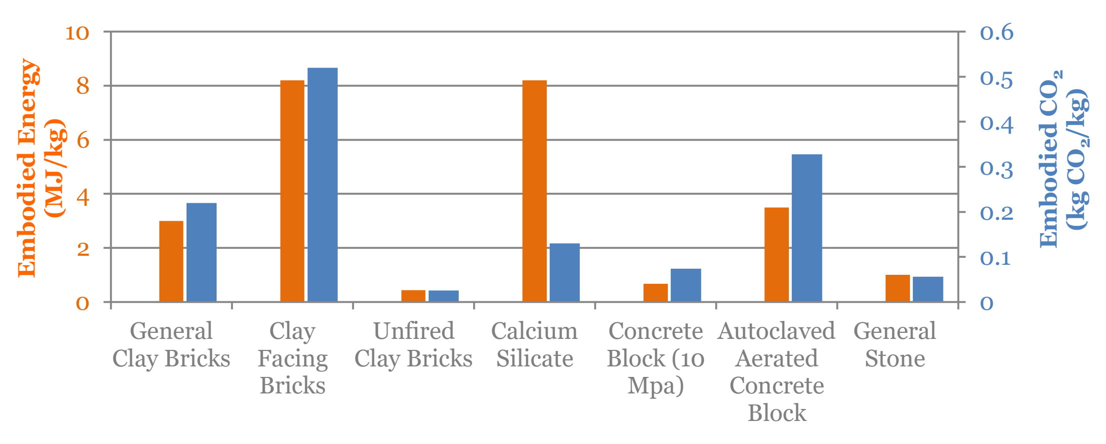

Source: Hammond and Jones (2011) and Morton et al. (2005)

In addition to these relatively low EE and EC figures, earthen materials also have other additional ecological benefits. According to Morton (2008), provided that the soil used is from a non-contaminated source, earth masonry materials are also nonpolluting and have a benign impact on biodiversity. This means that at the end of their useful life they can be broken down and recycled (WRAP, 2013). They are therefore reportedly easier to recycle that fired bricks or concrete (Heath, 2015). Another environmental benefit of earthen materials is that they are inherently inert and non-toxic, unlike many contemporary products and finishes used in buildings (Moquin, 1996). It has even been argued that the use of clay materials could help to absorb toxins from the indoor environment (Darling et al., 2012; Magwood, 2014).

4.2.4. Cost

Since unfired earth bricks make use of a ubiquitous and readily available raw material, the input costs are generally low which explains its frequent use in developing countries (Agarwal, 1981). The economic benefits of earth as a construction material have been reviewed by Zami and Lee (2010) with the general conclusion that although earth is a relatively cost-effective technique in comparison to other build methods, this can be dependent on factors other than the price of the soil. For example, the cost of labour, which can vary on a regional basis, will have an important influence on the overall build cost (Adam and Agib, 2001). The cost effectiveness is also dependent on whether the appropriate type of soil is available locally, otherwise the bulk material may have to be transported from other locations which adds to the material cost and the carbon footprint. Furthermore, locally available soil may require the use of additives to modify its properties and although this can be achieved through the use of small quantities of stabilisers, these can be relatively expensive (Adam and Agib, 2001). Other factors such as the type of manufacturing process adopted will also be important. For example, in developing countries where labour costs are low it is likely that manual processing will be used rather than the use of expensive equipment.

In the context of the UK, Morton (2008) gives cost estimates for different types of masonry units (Table 4-2 and Table 4-3). It should be noted that these costs per unit are based on 2006 prices, excluding VAT and transport costs. However they still highlight the relative differences in the m^2 rate for the different production methods. More recent figures (CES Edupack Database) give a cost of £0.39 – £1.04 per kg for a common clay brick (density range of 1980 - 2070 kg/m^3) and £0.03 – £0.05 per kg for concrete blocks (density range of 400 – 1400 kg/m^3). Overall the economic viability of earth construction will have to be assessed on a project by project basis and in the context of the UK, a cost comparison against other contemporary building materials will be required in order to justify its appropriateness.

Table 4-2: Estimated Costs for Earth Masonry (Bricks)

	Unit Type	**Unit Cost (£)**	**Equivalent cost per m^2** (100mm thick wall)
Bricks	Common Fired Clay Brick	0.17	12.17
	UK Industrial Mass-Produced Bricks	0.16-0.17	11.04-11.40
	UK Small-scale Mass-Produced Bricks	0.40-0.85	29.20-62.50
	Imported Mass Produced Earth Bricks	0.81-0.94	44.55-51.70
	One-off Commercial Hand-made Earth Bricks	2.00-3.00	114.00-171.00

Source: Morton (2008)

Table 4-3: Estimated Costs for Earth Masonry (Blocks)

	Unit Type	**Unit Cost (£)**	**Equivalent cost per m^2** (100mm thick wall)
Blocks	Lightweight Concrete Block	£0.70	16.10
	Imported Mass Produced Earth Blocks	£6.25	125.00
	UK Small-scale mass-produced Blocks	£1.60-3.00	44.80-84.00
	UK Large-scale mass-produced Blocks	£0.28	9.92
	One-off, Volunteer Made Earth Blocks	£3.00	0-72.00
	One-off, Commercially Hand Moulded Earth Blocks	£10.00-15.00	240.00-360.00

Source: Morton (2008)

4.2.5. Required Skills and workmanship

Although there are an estimated 500,000 existing earth buildings in the UK (Little et al., 2001), at present the required experience and technical skills associated with this material and similar unfired earth systems is limited. Little et al. (2001) argue that although the basic principles and techniques behind earth construction are relatively simple and have been used for centuries, earth masonry is now considered as a fairly niche method of construction and only a small number of specialist contractors have direct experience in working with this kind of system. Whilst some traditional techniques such as cob and mudwall are more labour intensive and perhaps more suited to the self -build market, other unfired products such as brick, blocks and panels are in fact highly compatible with conventional construction methods and the required skills are very similar to those required for known trades like bricklaying (Röhlen and Ziegert, 2011).

4.2.6. Standards and Regulations

In the UK there are existing technical standards for masonry products, covering common masonry units including clay, concrete bricks and blocks, calcium silicate and stone (BSI, 2011b). *Eurocode 6: Design of masonry structures* (BSI, 2012d), was introduced in in 2006 to create more harmonised technical standards for building materials across Europe although at present this design code does not cover unfired earth materials. There are however some existing guidance documents for earthen materials in countries such as Germany (Lehm, 2002), New Zealand (Standards New Zealand, 1998), Australia (Walker, 2002) and New Mexico (Government of New Mexico, 2009). More recently, the USA have also published a standard guide for the "*Design of Earthen Wall Building Systems*" (ASTM, 2010b).

Whilst these provide useful guidance regarding the design of earthen building, many of the recommendations are specific to the region in which they are produced and often the information relates to cement stabilised materials. There is therefore limited validity in transferring these standards to non-cement materials for use in the UK. As discussed by Maskell et al. (2015), the development of official compliance standards would increase the level of quality control and potentially encourage future use of the material.

4.3. Stabilisation of Earth Masonry

Whilst clay alone can act as a binding matrix within soils, and this property is exploited in many existing earth based building techniques, the inclusion of other additives can further enhance the ability of the soil particles to form a cohesive structure as well as reducing shrinkage and swelling (Ruskulis, 2002a). This is commonly referred to as soil stabilisation and can be achieved through a variety of methods including process-based methods such as heat treatments and mechanical compaction. Other methods typically rely on the use of additives which can be either inert substances (e.g. aggregates or fibres), which help to improve the mechanical properties of the material, or chemical additives (e.g. cement or lime) which react with or alter the properties of the soil through the formation of new minerals and cementation (Brandon et al., 2009). In some cases the stabiliser simply enhances the existing clay matrix by facilitating ion exchange and bonding (Houben and Guillaud, 1994). The most effective stabiliser will be dependent upon the soil type and therefore properties such as the PSD and PI should first be established in order to make sure that the soil is first of all a good candidate for stabilisation and that the most appropriate stabiliser is used (Burroughs, 2008).

4.3.1. Conventional Stabilisers

Stabilisation of soils through the use of additives is a common technique and a wide range of products can be used for this purpose. Additives can be organic or inorganic with dosage rates varying depending on the type of stabiliser and the type of soil on which it is being used. The use of the conventional additives can substantially improve the properties of raw earth when used appropriately. For instance there is a general consensus that the addition of fibres helps to increase the tensile strength of unfired masonry units as well decreasing the density and reducing shrinkage/cracking during drying (Houben and Guillaud, 1994; Ruskulis, 2002b). Natural fibres are particularly common adobe and cob building techniques and are usually used in proportion of 1 – 4 wt% (Ruskulis, 2002b). Aggregates such as sand and gravel are also frequently added to earthen materials to improve the soil grading and make the material more suitable for building applications (Houben and Guillaud, 1994;Röhlen and Ziegert, 2011).

More dramatic modifications can be achieved using chemical stabilisers. The use of cement, for example, can impart significant improvements in compressive strength and moisture resistance (Walker, 1995; Gooding and Thomas, 1995; Walker and Stace, 1997;Guettala et al., 2006; Morel et al., 2007). This not only facilitates the use of poorer quality soils, which in some cases allows for more local raw material sources to be employed, but the improvements in strength also mean that structurally sound walls can be achieved using a reduced wall thickness compared to non-stabilised materials. According to Walker (1999), dosage rates of 5-10 wt% cement are usually sufficient to produce CSEBs with compressive strengths exceeding 2 N/mm^2. Similar improvements in strength can also be achieved with lime, although this can be dependent upon the clay content of the soil, the curing time and temperature and the stabiliser dose. Lime is more effective in soils with a higher clay content (Osula, 1996) and dosage rates of 2-8 wt% are typically required to achieve full stabilisation (Oti et al., 2008). Significant strength improvements have also been demonstrated using blends of lime and cement, or mixtures containing GGBS and other pozzolans (Reddy and Lokras, 1998; Kumar et al., 2007;Oti et al., 2009; Oti et al., 2010b; Billong et al., 2009). Hydrocarbon products, like bitumen, asphalt and paraffin can also be used as soil stabilisers (Houben and Guillaud, 1994). These are particularly effective on granular soils but may be unsuitable for soils with a high moisture content (Houben and Guillaud, 1994; Hall et al., 2012).

On the other hand, there are also several disadvantages to conventional stabilisers. First of all the inclusion of a stabiliser, even at relatively low dosages, can lead to significant increases in cost. It also generates more complexity within the production process as well as, in some cases creating health and safety issues due to the use of hazardous materials (Hall et al., 2012). Furthermore it has been disputed that the use of additives like bitumen, cement and lime, when used in sufficient quantities, generally replaces the cohesive properties of the clay and therefore fundamentally alter the natural properties of the material (Morton, 2008). Arguably, these stabilised composites cannot therefore be considered as true 'unfired earth'. Indeed, in such cases it could be argued that the earth is simply acting as an aggregate in a cement bound composite (Röhlen and Ziegert, 2011). Another major issue is the increased environmental impact which results from the inclusion of stabilisers with high embodied energy and embodied CO_2. This is particularly true of cement due to the CO_2 emissions associated with the kilning of limestone and the calcination process involved in producing the clinker (Worrell et al., 2001; Huntzinger and Eatmon, 2009; Pacheco-Torgal and Jalali, 2012; Turgut, 2012; Hasanbeigi, 2013).

Although several authors have recommended lime as a potential alternative to cement due to its perceived lower environmental impact (Davis, 1994), according to Hammond and Jones (2008) the overall embodied energy of lime was actually shown to be greater than that of cement. Larger dosages of lime are also required to achieve the results seen with smaller quantities of cement which further diminishes its ecological benefits.

A summary of the most commonly used stabilisers and their function is shown in Table 4-4. Overall, although most studies have shown that earth–based walling systems typically have more desirable embodied energy values than traditional fired bricks and some concrete systems, there is recognition that the use of cement or lime based products has negative effect on the overall environmental impact.

Table 4-4: Summary of Conventional Stabilisers

Additive	Example	Function	Cost	Environmental Impact
Fibres	Straw	Reinforcement: Can improve tensile strength and reduces drying shrinkage	Low	Low – depending on source
Aggregates	Sand or gravel	Grading: Improves PSD	Low	Low – especially if recycled
Cement	OPC	Cementation: Creates inert, three-dimensional matrix. Can improve mechanical strength.	High	High
Lime	Hydrated lime	Linkage: Forms inert, three-dimensional matrix with clay. Can improve mechanical strength.	High	High
Hydro-carbons	Bitumen	Imperviousness: Can improve water resistant	High	High

Source: Adapted from Houben and Guillaud (1994)

4.3.2. Alternative Stabilisers

Although existing stabilisation methods like cement and lime have been proven to be effective in terms of strength improvements, their poor environmental credentials as well as issues associated with cost and material compatibility are still a concern. As a result, there are increasing efforts to find alternative methods of stabilisation which offer more environmentally friendly solutions to improving the properties of unfired earth (Browne, 2009).

There are various alternatives to conventional stabilisers which effectively modify soil properties, usually in less dramatic fashion than the likes of cement and lime, whilst still retaining the fundamental characteristics of the material. Although previous authors have discussed the use of non-traditional stabilisers in geotechnical applications (Emerson, 1956; Oldham et al., 1977; Scholen, 1992; Tingle et al., 2007; Orts et al., 2007;Brandon et al., 2009) including various synthetic and natural polymers, enzymes and emulsions, there is a growing body of research relating to the use of alternative stabilisers in masonry products. Some of these hark back to traditional building techniques by making use of locally available natural materials (Ruskulis, 2002b). This includes natural gums, resins and oils (Beas, 1991; Camões et al., 2012; Ruskulis, 2002b), lignin (Houben and Guillaud, 1994) and various animal derived products such as excrement, urine, blood, milk and animal glues (Houben et al., 1994;Ruskulis, 2002b). Even products such as whey, casein and cheese have reportedly been used (Minke, 2006).

Given that some of these techniques date back to the Roman era, robust experimental data if often lacking. However the principle behind the use of locally sourced, renewable additives has been receiving renewed attention in an effort to find alternatives to cement based systems. Recent studies have therefore investigated products such as tannins (Bishop et al., 2000; Sorgho et al., 2014) and various vegetable oils (Ogacho et al. ,2003; Forth and Zoorob ,2006; Vu and Forth, 2014; Balo et al., 2010; Balo and Yucel ,2013; Heaton et al., 2014). There have also been investigations into the use of polysaccharides obtained from biological sources as additives for soil based materials. This includes the likes of glucan (Chang and Cho, 2012), xanthan gum (Nugent et al.2009; Taytak et al. 2012; Chang et al., 2015) and guar gum (Nugent et al., 2009) as well as cellulose and starch (Röhlen and Ziegert, 2011).

Other recent studies have also explored the use of by-products and waste streams of industrial processes. Indeed various inorganic wastes such as pulverized fuel ash (PFA) and ground granulated blast-furnace slag (GGBS) have also been investigated as alternative additives for earth masonry (Malhotra and Tehri, 1996; Chindaprasirt and Pimraksa, 2008; Oti et al., 2008; Deboucha and Hashim, 2011). Sodium silicate has also been used as an alternative additive owing to its ability to increase plasticity and reduce the amount of water required when forming the clay body (Houben and Guillaud, 1994). It can also be used to improve resistance to chemical attack (Broderick and Daniel, 1990) and increase compressive strength (Panda et al., 2012). Sodium silicate can also be used in combination with geo-polymers (Zhang, 2013).Whilst these systems are still relatively new and require further development before being introduced on a wide scale, they have been proposed as a potential alternative to OPC. However Habert et al. (2011) has shown that although geo-polymers offer slight decreases in CO_2 emissions, there are concerns regarding their other environmental impacts.

Some examples of these non-traditional stabilisers and their proposed functions are provided in Table 4-5 and Table 4-6, showing studies relating to inorganic and organic substances respectively.

Table 4-5: Summary of Inorganic Stabilisers

Additive	Example(s)	Function	Ref.
Pozzolans	PFA, Silica fume, Rice Husk Ash, GGBS	Improves PSD Creates inert, 3D matrix (in combination with cement or lime). Can improve mechanical strength.	Chindaprasirt and Pimraksa (2008) Deboucha and Hashim (2011), Oti et al. (2008), Miqueleiz et al. (2013), Khater (2011), Muntohar (2011)
Sodium compounds	Sodium Silicate	Creates inert, 3D matrix (in combination with cement or lime). Can improve mechanical strength. Reduces water requirement	Broderick and Daniel (1990) Panda et al. (2012) Mukhopadhyay et al. (2005) Moayedi et al. (2011)
Geo-polymers	Slag/Rock/ Fly Ash based geopolymer	Creates inert, 3D matrix (in combination with cement or lime).	Zhang (2013) Habert et al. (2011)
Clay minerals	Bentonite	Can improve water resistance	Anifowose (2000), Hughes and Maul (1979)
Sulphate Minerals	Gypsum	Increase plasticity and reduces drying shrinkage. Can improve mechanical strength.	Vroomen (2007) Degirmenci (2008) Pekmezci et al. (2012)
Lightweight aggregates	Pumice, vermiculite	Improves PSD. Reduces Density	Mueller et al. (2008) Minke (2006)

Source: Adapted from Houben and Guillaud (1994)

Table 4-6: Summary Organic Stabilisers

Additive	Example(s)	Function(s)	Ref.
Plant derivatives	Fibres	Can improve tensile strength and reduces drying shrinkage	Minke (2006), Mesbah et al. (2004), Lertwattanaruk and Choksiriwanna (2011), Enokela and Alada (2012), Arumala and Gondal (2007), Bal et al. (2012), Murillo et al. (2005), Chan (2011)
	Oils, gums, resins, polysaccharides	Forms inert, 3D matrix with clay. Can improve mechanical strength.	Beas (1991), Camões et al. (2012), Ruskulis (2002b), Houben and Guillaud (1994), Bishop et al. (2000), Sorgho et al. (2014), Ogacho et al. (2003), Forth & Zoorob (2006), Vu and Forth (2014), Balo et al. (2010) Balo and Yucel (2013) Heaton et al. (2014) Nugent et al.(2009) Taytak et al. (2012) Chang et al. (2015) Röhlen & Ziegert (2011) Chang and Cho (2012)

Animal derivatives	Blood, urine, excrement, hair	Can improve tensile strength and reduce drying shrinkage Forms inert, 3D matrix with clay. Can improve mechanical strength. Can improve water resistance.	Jubran et al. (1988) Houben et al. (1994), Olaoye and Anigbogu (2000), Ruskulis(2002b), Minke (2006), Vilane (2010), Röhlen and Ziegert (2011), Silva et al. (2010) Galán-Marín et al. (2010), Cotter (2012), Aymerich et al. (2012), Taytak et al. (2012)
Agri-cultural Wastes	Fibres, husks, grains, sludges, residues	Can improve tensile strength and reduce drying shrinkage	Knirsch et al. (1998), Achenza and Fenu (2006), Pappu et al. (2007), Demir (2006; 2008), Muntohar (2011)
Industrial wastes	Lignosulphonate	Forms inert, 3D matrix with clay. Can improve mechanical strength.	Santoni et al. (2002) Tingle et al. (2007) Vinod et al. (2010) Maskell et al. (2012)
Synthetic polymers	PVA, PAM, PP	Forms inert, 3D matrix with clay. Can improve mechanical strength.	Green and Stott (1999) Murray et al. (2000) Binici et al. (2005), Orts et al. (2007), Kumar et al. (2007), Atzeni et al. (2008), Park (2009) Lenci et al. (2011) Naeini et al. (2012)

Source: Adapted from Houben and Guillaud (1994)

4.3.3. Alginate as an Additive for Unfired Earth

Given the wide range of examples of renewable materials sourced from nature which can potentially be used to modify the properties of earth, and the need to develop more environmentally alternatives to cement and lime based stabilisers, there would appear to be value in further investigating the potential for readily available and sustainably sourced biopolymers to be used in this capacity. Given that the objective of this study was to investigate the use of alginate in construction applications, previous studies involving the use of alginate as an additive for earthen materials were consequently reviewed in more detail.

Polysaccharides exist naturally in soils where they play an important role as a binding agent and contribute to soil stability (Theng, 2012a). Substances like alginate have consequently been used as additives in various soil engineering applications including ground-works and agricultural applications. For example, Quastel and Webley (1947) have investigated the use of sodium alginate as a soil modifier with the aim of improving soil fertility and the respiratory activity of micro-organisms. In this work the authors mixed a clay loam material with water and sodium alginate at dosages of 0.1- 1 wt%. It was found that the addition of alginate increased the oxygen uptake of the soils by increasing their water holding capacity as well as increasing the stability of the soil crumbs. These property changes were assumed to be a result of the alginate molecules exchanging with hydroxyl ions at the soil particle surface. This creates hydrophilic surfaces and facilitates bridging between the individual soil particles through calcium or aluminium cations. Calcium alginate was also investigated as part of the study but was found to be less effective than the sodium form due to its insolubility. Emerson (1956) further investigated the use of alginic acid, amongst a number of other synthetics polymers, as potential soil conditioners. The stability of the treated soil crumbs was found to be most effective when a high molecular weight sodium alginate polymer was used. However, no improvement in cohesion was found for acidic soils and the sodium alginate was also only effective when the crumbs were first sodium saturated in order to prevent calcium precipitation. In this case it is argued that the sodium ions can help to create bridges between the clay particles and so the binding mechanism is not necessarily dependent on the previously described egg-box model (Chapter 3). Schneider (1977) has also investigated the use of sodium alginate for stabilisation of fine or granular soils in preparation for road building. This stabiliser composition consisted of alginate or a similar swelling gum, water, a monohydric alcohol and a separately prepared calcium-based hardener such as calcium chloride. This is based on the principle that the alginate reacts with the calcium source and sets whilst binding the soil particles although it is noted that the speed of this reaction will depend on the specific calcium source used. In this case the calcium solution content is equivalent to 10-25% of the alginate content by weight, and overall stabiliser concentrations of 2.5% (volume), were applied to a given soil at a rate of ~2 L per m^2 . These quantities are reportedly sufficient to promote full cementation and eliminate water penetration. More recently, Bernu et al. (2010) has also described a soil stabilisation composition comprised of alginate , other hydrocolloids and a 'mulch' material such as shredded paper or wood fibre. According to the author, this mixture can then be applied to ground soils in order to prevent soil erosion and aid re-vegetation. Overall, it can be concluded that although not used extensively, there is evidence to support the use of alginate in soil stabilisation applications.

Whilst existing studies have primarily focussed on geotechnical applications, there is the potential for the same alginate-clay bonding mechanisms to be used in improving the structural performance of earthen construction materials. In referring specifically to the use of alginate within earthen building products, existing research has been limited to a few studies. The most detailed investigations to date are those conducted by Galán-Marín et al. (2010) and subsequent studies (Galan-Marin et al., 2012; Galán-Marín et al., 2013; Rivera-Gómez et al., 2014) which discuss the use of alginate, in combination within lignin and natural or synthetic fibres, as additives for unfired clay bricks. Maximum compressive strengths of over 4 N/mm^2 are reported and it is claimed that this material could offer a suitable replacement for alternative internal walling systems. A LCA study has also shown that these bricks may have a lower embodied energy than fired materials and a lower GWP than both fired bricks and reinforced concrete (Galán-Marín et al., 2015). Although the authors observed compressive strength improvements upon the addition of the alginate and lignin alone, the main focus of those studies was on the role of the fibrous components. Furthermore, more recent studies showed variable results when the same alginate was used with alternative soils and different fibres (Galán-Marín et al., 2013). The type of alginate products used in the studies also varied from liquid 'seaweed extracts' (Galán-Marín et al., 2010) to dried alginate powders (Rivera-Gómez et al., 2014), although limited details of these products are provided. With the 'seaweed extract' product, this dosage rate also included most of the required water content of mixture and would therefore contain only a small percentage of dry matter (ie <2%) which is mixture of sodium alginate, sodium carbonate and inorganic salts. Similarly, with the dental impression powder, this type of material often contains a sodium alginate of around 15% and is mainly composed of diatomaceous earth fillers as well as various other additives including a calcium salt, setting retarders (e.g. tetra sodium pyrophosate), setting aids (e.g. sodium fluorosilicate), pH modifiers (e.g. magnesium oxide) and flavourings (Cook, 1986; Craig, 1988). Therefore at a dosage rate of 1.2%, the specimens prepared using this powdered material will have an overall alginate content of ~0.2%. It was acknowledged that the test results could have been affected by the presence of other components within these products. Furthermore, all of the samples included 0.5% of lignin meaning that no tests consider the effect of adding alginate in isolation. Variations in dosage rates, increased alginate concentrations and different alginate sources have yet to be fully studied and there is therefore a general gap in research involving the role of the alginate polymer in relation to the strength improvements witnessed in the brick prototypes. Additionally, the alginate brick prototypes produced to date have been tested only in relation to structural performance and would require further development before being introduced commercially. For example investigations into other properties of the product such as thermal performance, moisture absorption, vapour permeability and long term durability still need to be conducted in order to evaluate the potential for wide scale use, particularly within the UK climate.

4.4. Summary

In considering the outlook for masonry products, with increasingly stringent technical standards and environmental legislation it is anticipated that continual improvement in the manufacturing processes associated with masonry units will be required. Given the scale of use associated with these types of materials, there is an incentive for alternative forms of masonry with lower environmental impacts to be developed. In addition to increasing the efficiency of the equipment used, alterations to existing products or the creation of new materials with improved environmental impacts would be welcomed (Carbon Trust, 2010). Recent research efforts have been guided either towards finding alternatives to cement (i.e. the use of waste residues, industrial by-products and renewable additives) or learning from traditional, vernacular techniques where the energy-intensive firing process is eliminated. The latter category has received particular attention in recent decades due to the perceived benefits of unfired clay in terms of hygro-thermal performance, low embodied energy and low cost. Although traditional uses of unfired earth such as rammed earth have regained popularity and are likely to have continued success in self-build and bespoke projects, a much bigger impact would be achieved in mainstream architecture through the development of contemporary unfired masonry units which are more suited to modern methods of construction. Whilst it is acknowledged that existing materials such as concrete blocks and fired bricks are superior in terms of their loadbearing capacities and durability, there are some applications in which the use of a lower strength product may be sufficient (Heath et al., 2012b). In particular, in the case of internal wall partitions where humidity buffering and thermal mass storage properties can be exploited, and demands on loadbearing capacity and exposure to extreme levels of moisture is minimised, unfired clay masonry may be the preferred material.

However as a natural material with significant variations in properties depending on the source used many earthen materials may be considered unsuitable for building purposes without some form of modification. Even soils with appropriate particle grading and plasticity may fall short of the minimum strength requirements for some applications and therefore must be improved through modification or stabilisation. While the commonly used methods of stabilisation (e.g. cement and lime) may offer significant improvements in compressive strength and durability, they also present some major disadvantages, particularly in terms of embodied energy, embodied CO_2 and cost. Furthermore, it may be argued that a ‘cement stabilised’ product cannot truly be considered as unfired earth since the cement component fundamentally alters the properties of the base material, and in some cases may diminish the initial advantages of using such a material.

In considering alternative stabilisation methods, there are increasing efforts to incorporate additives from more sustainable sources which help to improve the properties of earth masonry without sacrificing their ecological benefits. Biopolymers are a group of materials which may offer a potential solution to this problem in that they are not only natural, renewable and relatively abundant, but they have also been used historically to modify the properties of earth based materials. Alginate is one such biopolymer of which there is recent evidence to suggest potential as a strength improving additive for unfired earth. However, to date there is limited information regarding the specific properties of the alginate which influence interactions with the soil and the exact mechanisms behind any property changes observed in the final brick products. Furthermore, there has been no detailed investigation which compares alginates from different sources or with different chemical compositions. The effect of the alginate on properties other than mechanical strength has also yet to be explored.

5. EXPERIMENTAL METHODS (PART I)

Based on the identified gaps in the literature, the specific goal of Part I was to identify whether alginate, as a renewable biopolymer, would be a suitable additive for unfired earth masonry products. As discussed described in Chapter 1, the main objectives therefore included investigating the variable properties of alginate and their contribution towards any property changes observed when added to a soil. This was achieved by testing a range of alginate products, including some commercial alginate products and a range of MBL products in order to identify the optimum types and most appropriate mix ratios. The prototypes were then characterised in order to compare the effectiveness of the alginate as a natural stabiliser with other additives. A study of different soil types was also included to determine their impact on the properties of the composite. Finally, the commercially feasibility of the prototypes was also analysed by comparing aspects like cost and environmental impact with other available products.

Key questions

Q1: What impact do alginate variables (e.g. concentration, viscosity, composition) have upon the physical properties of a composite alginate-clay brick?
Q2: What impact do other variables (e.g. clay type, pH) have on the physical properties of a composite alginate-clay brick?
Q3: How suitable are the specimens for use as a contemporary masonry material?

Scope and Limitations

Samples were produced using only products supplied by MBL and 2 commercial products. While this excludes other alginate sources, the sample range still provided reasonable variations in alginate compositions. Similarly, the soil types studied were supplied from one manufacturer albeit from different quarries. Since the focus of Part I was on the effect of the alginate on the final brick properties, a standard production procedure was adopted throughout. This however results in the exclusion of potential process variables (e.g. the use of different moulding or drying procedures) and other material variables such as the use of additional additives (e.g. fibres). Given that the objective was to consider the influence of composition on the properties of the bricks, the testing was also limited to individual units only and did not consider a full masonry system nor investigate compatible mortar types.

5.1. Materials

The specific alginate and soil products used in the Part I study, and the corresponding acronyms for each specimen produced, are presented in Table 5-1.

Table 5-1: Specimens Produced

	Soil U	**Soil V**	**Soil W**
LH	LHU	LHV	LHW
AN	ANU	-	-
PR22	PR22U	PR22V	PR22W
PR24	PR24U	PR24V	PR24W
PR25	PR25U	-	-
PR29	PR29U	-	-
PR30	PR30U	-	-
PR32	PR32U	PR32V	PR32W
PR52	PR52U	PR52V	PR52W
PR14	PR14U	-	-
PR38	PR38U	-	-
DA	DAU	DAV	DAW
AC	ACU	ACV	ACW

5.2. Testing Programme

The testing programme for Part I is shown in Figure 5-1. Phase 1 consisted of rheology tests which were used to make initial observations regarding the interactions between the alginate and soil. For Phase 2, prototype brick specimens were produced and assessed based on their basic physical properties. Further studies on selected samples were then taken forward for further characterisation tests in Phase 3. Finally, Phase 4 consisted of an assessment of the commercial feasibility of the brick products, including an environmental and cost assessment.

Figure 5-1: PART I Testing Programme

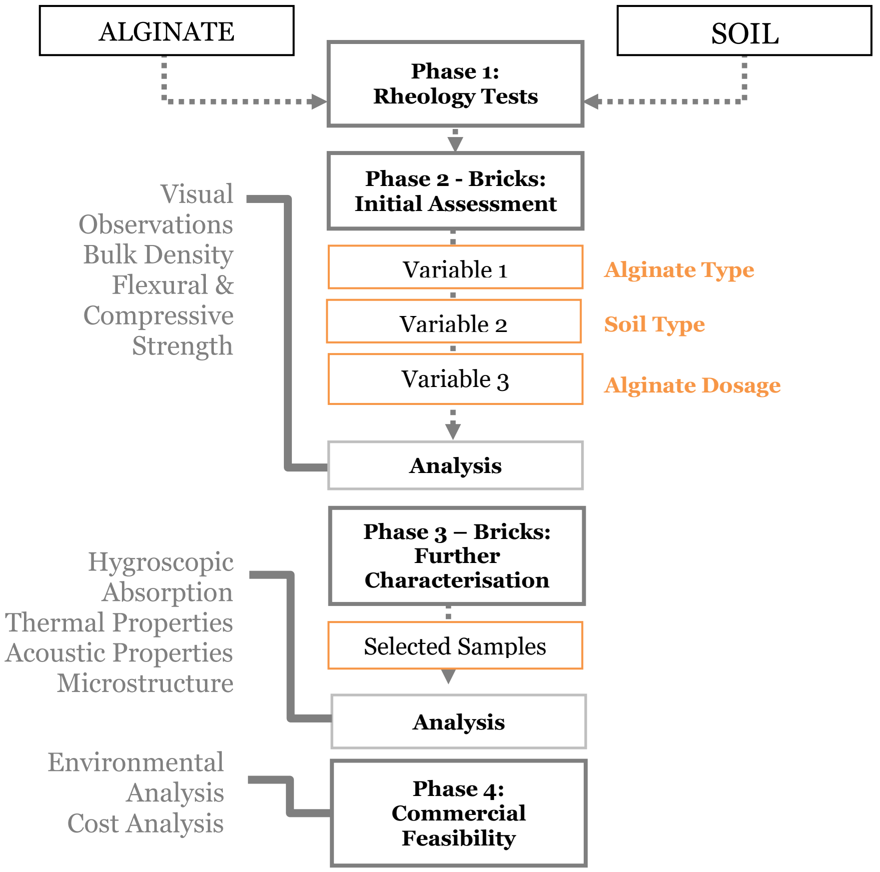

5.2.1. Phase 1 – Rheology Tests

Interactions between clay particles and polymers in a hydrated system can be studied through rheology. Rheology is a measure of the deformation and flow behaviour of materials and can be performed on various materials ranging from dilute suspensions to semi-solid materials, providing useful information on stress-strain relationships and the viscoelastic behaviour of materials. As part of Phase 1, some preliminary tests relating to the molecular scale interactions between the alginate and soil were conducted by observing changes in the plasticity and sedimentation behaviour of the hydrated soil upon the addition of different alginate polymers. The role of other potential variables such as the pH, calcium content and polymer dosage were also investigated.

5.2.1.1. Atterberg Limits

At high solid contents, the deformation or flow behaviour of a soil is linked to its plasticity. As discussed in Chapter 3, the Atterberg Limits are series of tests commonly performed on hydrated soils in order to characterise their plasticity at different moisture contents. In this sense, the liquid limit (LL) is effectively a rheological parameter which measures the shear strength of the material at its boundary between the plastic and liquid state. The undrained shear strength of a soil at the LL is typically between 1.7 and 2 kPa (Sharma and Bora, 2003). Although the liquid limit is a macro-scale property, it is closely related to the properties of the clay fabric (Mitchell, 1993) and has been used by various authors as a means of explaining nano-scale interactions within a soil matrix (Nugent et al., 2009). Typically a high liquid limit suggests that a flocculated soil fabric structure exists compared to a dispersed structure which has a lower resistance to shear (Nugent et al., 2009). Variables affecting the plasticity of a soil include moisture content, clay mineralogy, the particle size distribution and exchangeable cations as well as the presence of additives.

In this case, the objective was to identify any changes in soil plasticity upon the addition of alginate. The procedure described in Chapter 3 for determining the Atterberg limits was again used to obtain LL, PL and PI values for a range of alginate and soil mixtures. The process was similar to the methods described in BS 1924-2:1990 (BSI, 1990c) for cement and lime stablised soils, whereby the cation exchange mechanisms induced by theses additivies are measured through changes in the plasticity of the soil. Other studies by Rauch et al. (2002), Palomino and Santamarina (2005), Sung Ho Kim(2008) and Nugent et al. (2009) also use Atterberg limit tests to observed property changes in clay based systems upon the addition of various polymers. For this study, the soil samples were initially mixed with a known concentration of alginate solution to investigate the role of both alginate type and dosage. Further tests to explore the impact of soil pH and calcium content were also conducted.

5.2.1.2. Sedimentation

The sedimentation behaviour of a soil can be used to give an indication of particle size and electrokinetic properties. Various studies have therefore used changes in sedimentation behaviour to explain molecular scale interactions between soils or clays and other additives, including electrolytes and polymers (Michaels and Bolger, 1962; Clark et al., 1990; Rauch et al., 2002; Mpofu et al., 2004; Palomino and Santamarina, 2005; McFarlane et al., 2006; Akther et al., 2008; Chukwudi et al., 2008; Mekhamer et al., 2009; Zhang et al., 2013). Typically a faster settling rate is indicative of flocculation whereby the primary particles form larger units known as flocs (Michaels and Bolger, 1962). Where the particle associate in an face-to-face manner rather than edge-to-face, the larger units are referred to as aggregates (Palomino and Santamarina, 2005). If the particles remain dispersed, a slower settling rate and smaller sediment volume should be observed. In a stable colloidal system, the individual colloidal particles remain suspended in the solvent as the magnitude of the electrostatic repulsion between the particles is sufficient enough to keep them apart. A schematic of this process is illustrated in Figure 5-2. High molecular weight polymers are often used as flocculants in colloidal clay systems in order to increase these settling rates by inducing particle flocculation or aggregation through polymer bridging (McFarlane et al., 2006).

Figure 5-2: Sedimentation Behaviour

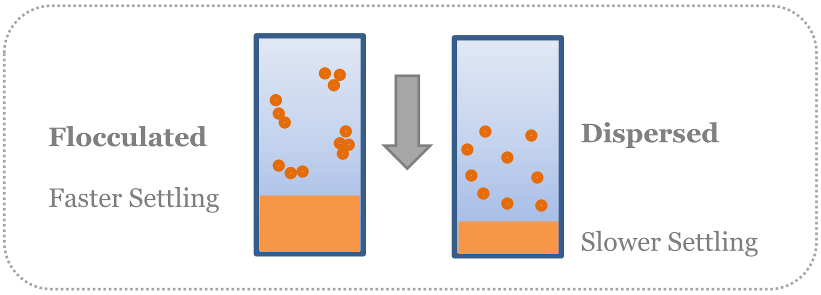

Author's own image

In this study, analysis of the sedimentation behaviour was similar to methods described by Mekhamer et al. (2009) whereby known concentrations of an alginate solution (0.1, 0.25 and 0.5 w/v%) were added to the soil to produce soil slurries (5 w/v%). Initial observations were also made regarding the influence of pH and calcium content on the settling behaviour of the alginate-soil mixtures. Each test mixture was placed in a 50ml graduated cylinder, sealed with a rubber stoppper and then inverted, end over end, 30 times over a period of 30s prior to measurement. The position of solid-liquid interface was then recorded at specified time intervals ranging from 30s to 24 hours. Trial studies indicated that the final bed height did not change signficantly after the 24 hour measurements and so this reading was taken as the final bed volume. The readings taken from the cylinder in ml were then converted to cm allowing values for the settling rate (cm/min) to be determined. The final bed volume was also converted to cm^3. The procedure was repeated 3 times for each mixture and the results were plotted as an average of these meaurements.

5.2.2. Phase 2 – Brick Prototypes: Initial Assessment

The objective of Phase 2 was to build upon the initial findings of Phase 1 by producing small scale brick prototypes. The brick specimens were produced using the methods of Galán-Marín et al., (2010) whereby soil, deionised water and the desired sodium alginate product were mixed together in a 5L mechanical mortar mixer. The amount of water for each mixture was calculated based on the plastic limit of the relevant soil (Table 5-2).

Table 5-2: Mix compositions (per brick specimen)

	Soil U	**Soil V**	**Soil W**
Soil (g)	500	500	500
Alginate (g)	0.5	0.5, 1.25, 2.5	0.5
Water content (%)	16	15	15

An alginate dosage of 0.1% by weight of the dry soil was tested initially and was dissolved in the required amount of water under magnetic stirring for 4 hours before being added to the soil. The soil and alginate mixture was then homogenised for a period of approximately 3 minutes in the mixer before being compacted into a steel mould (16 x 4 x 4cm). The moulds were filled in two layers with each layer being compacted using 25 strokes of a tamper. The filled moulds were then oven dried at

50°C(±5°C) for 24 hours. After oven-drying, all samples were stored in the laboratory at ambient temperature and relative humidity for a minimum of 14 days before testing. The same procedure was used for each batch with 3 specimens being produced for each batch. Images from the different stages of production are shown in Figure 5-3 alongside a schematic of the process (Figure 5-4).

Figure 5-3: Production Images

Figure 5-4: Lab Scale Process – Unfired Bricks

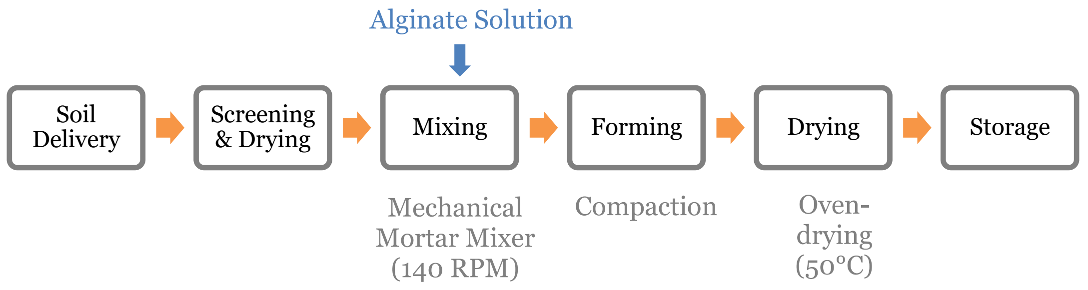

5.2.2.1. Visual Observations

General observations were made regarding the workability of the mixture during preparation as well as the quality of the final specimens. Samples which were relatively homogenous were labelled ‘*good*’ whilst those with some visible defects were labelled as ‘*moderate*’. ‘*Poor*’ samples were those where several defects and macroscopic voids were apparent in all specimens.

5.2.2.2. Dimensions, Mass & Density

Each brick was weighed using a digital balance to the nearest 0.1 g and measured using digital calipers to the nearest 0.1 mm. The unit mass (m) in kg and unit volume (v) in m^3 were then used to calculate the bulk density (ρ) using Equation 3.

$$\boldsymbol{\rho = \frac{m}{v}}$$

Equation 3

5.2.2.3. Linear Shrinkage

Linear drying shrinkage (LS) was also compared using the length of the dry specimen (l) and the initial mould dimensions (l_o) in Equation 4.

$$\boldsymbol{LS}(\%) = \boldsymbol{\frac{l_o - l}{l_o} x \, 100}$$

Equation 4

5.2.2.4. Mechanical Properties

Both the compressive strength and flexural strength of the specimens were measured based on the methods of Galán-Marín et al. (2010) and *BS EN 1015-11* (BSI, 1999) which are designed to measure the flexural and compressive strength of hardened mortars. Although these methods are not ideal, particularly where different geometries are being compared (Aubert et al., 2013; 2015), for the purposes of this study where the objective was to evaluate bricks of the same size and compare with previous research using similar materials, the procedure adopted by Galán-Marín et al. (2010) was deemed adequate. Since the focus at this stage was to compare only composistional differences in the individual units, testing of mortars and masonry prisms was not inlcuded in the mechanical testing.

A 3-point bending test was firstly performed on each of the full specimens (160 x 40 x 40mm) in order to determine flexural strength. The bending test set-up is illustrated in Figure 5-5. A load was applied gradually to a roller resting on top of the specimen, using an Instron 5969 universal testing machine at a rate of 1 mm/min. The maximum load (*F*), width (*b*) and depth (*d*) were recorded for each specimen and used to calculate the flexural strength using Equation 5.

$$f = 1.5\frac{Fl}{bd^2}$$

Equation 5

Results were calculated to the nearest 0.01 N/mm^2 as an average of three specimens. Specimens which offered a statistically significant change in strength compared to the control specimen at the $p<0.05$ level were denoted by an asterix (*).

Figure 5-5: 3-point Bending Test Set-Up

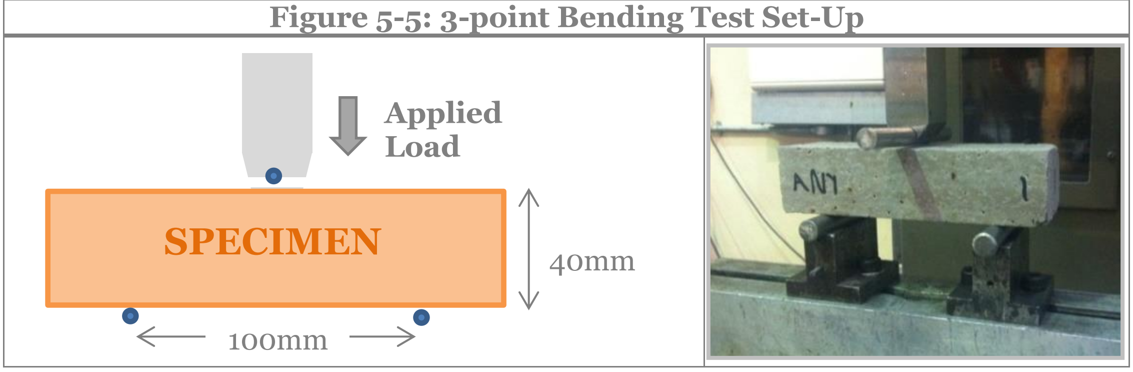

The 3 point bending test was then followed by compressive strength tests on the resulting half-brick specimens. An Instron 5969 universal testing machine was again used although this time two steel bearing plates were fitted (Figure 5-6). The specimens were also capped using 3mm plywood as recommended by Walker (2004). The aim of this was to create an even surface on the bedding plane to allow for a uniforn distribution of the load. This method was selected over alternative capping methods such as cement-based mortars or gypsum plasters which were deemed unsuitable due to the moisture sensitivity of the bricks. Applying a level layer or plaster can also be somewhat difficult and requires additional preparation time for each sample. The plywood method therefore offered a simple method of reducing the possibility of local failure due to concentrations of stress on the brick surface. However this method also has limitations in that the plywood itself may have contributed to the apparent strength of the specimens. While Maskell et al. (2013) found that that there were no significant differences in the compressive strength of unfired bricks capped with either plywood or plaster in comparison to uncapped specimens, it was also acknowledged that the use of plywood lead to increased variability in the compressive strength values.

The load was applied steadily at a rate of 2.5 mm/min until failure occurred and the maximum load (F_m) recorded. The compressive strength (σ) value for the specimens was then derived from F_m and the cross sectional area (A) of the specimen using Equation 6. A minimum of three specimens were tested for each batch and results again analysed in order to identify statistically significant results.

$$\boldsymbol{\sigma = \frac{F_m}{A_o}}$$

Equation 6

Compressive strain ($\mathcal{E}$) was also calculated from the change in platen position (ΔH) and the original position (H_O).

$$\mathcal{E} = \boldsymbol{\frac{\Delta H}{H_O}}$$

Equation 7

Figure 5-6: Compressive Strength Test Set-Up

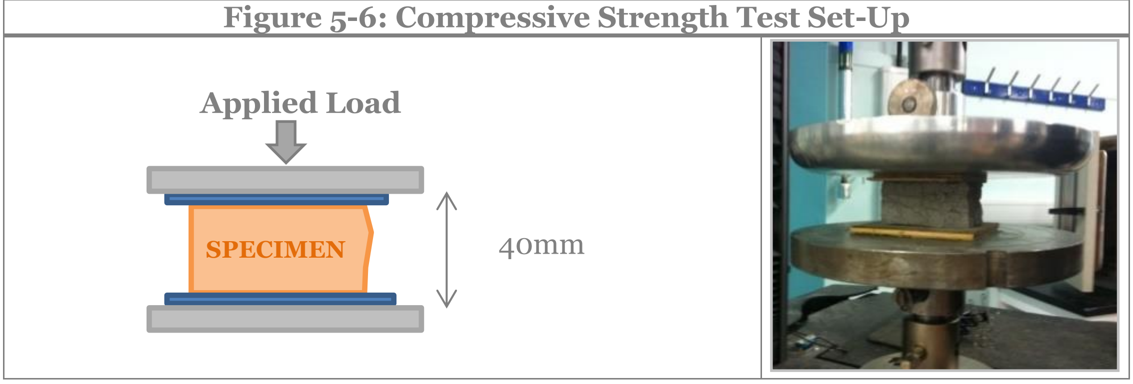

Platen restraint effects were also considered by using a correction factor which accounts for variations in specimen geometries (Morel et al., 2007). Since the height:width ratio of the specimens in this case is 1 (40:40), in this case a correction factor of 0.58 (Heathcote and Jankulovski, 1992; Aubert et al., 2015) was used and multiplied by F_{max} to give the unconfined compressive strength value.

The moisture content of the specimens at the time of testing was also determined by calculating the difference in mass after drying in an oven at 105°C for triplicate sub-samples of each brick specimen.

5.2.3. Phase 3 – Brick Prototypes: Further Characterisation

5.2.3.1. Hygroscopic Absorption

The procedure for this test was based on *ASTM C1498 – 04a* (ASTM, 2010a) and *BS EN ISO 12571:2014* (BSI, 2014) and involved placing the test material in environments of varying RH and measuring the amount of moisture absorbed in each condition. The samples were oven-dried to constant mass (m_1) before being placed in a non-absorbent container with a tight fitting lid. A desiccator with an appropriate saturated salt solution was also prepared and allowed to equilibrate to the required RH. The specific salt solutions used were Potassium Acetate (CH_3COOK), Magnesium Nitrate ($Mg(NO_3)_2 \cdot 6H_2O$), Sodium Chloride (NaCl) and Potassium Chloride (KCl), giving corresponding RH values of 23%, 54%, 75% and 85% as determined from BSI (2014). The samples were then placed inside the desiccator with the lids removed. After 24 hours, the samples were removed from the desiccator and weighed immediately. This process of daily weighing was repeated until 3 successive mass readings (m_2) showed a change in mass of less than 0.1%. The equilibrium moisture content (*EMC*) at the given RH was then calculated:

$$EMC\ (\%) = \frac{m_2 - m_1}{m_1} \text{ x } 100$$

Equation 8

This process was repeated for a minimum of 4 different RH values, working from low humidity to high humidity allowing isotherms showing the relationship between EMC and RH to be plotted.

Figure 5-7: Hygroscopic Absorption Test

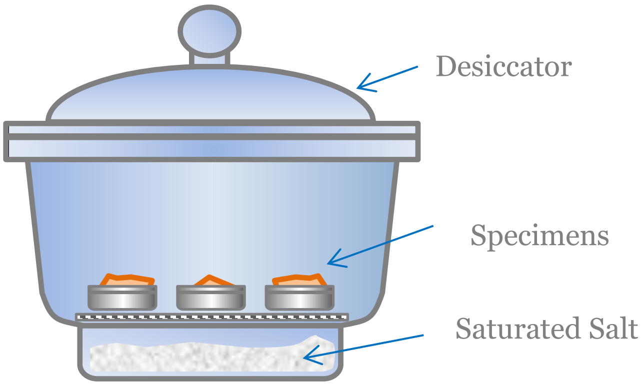

Author's own image

5.2.3.2. Thermal Properties

In considering both the thermal conductivity and heat storage properties of the specimens, both physical measurements and estimation models were used to assess the thermal behaviour of selected samples. In considering firstly the physical measurement, the specific heat capacity (J/(kg·°K)) of selected samples, defined as the amount of heat per unit mass needed to increase the temperature by 1 °K, was analysed using a Differential Scanning Calorimeter (DSC). In this case a Netzsch STA 449 C Jupiter DSC was used to provide combined thermogravimetric and DSC curves. The analysis was conducted using a sample of approximately 20 mg which was placed into a platinum crucible and heated from ambient temperature to 100°C using a measurement rate of 10°C/min. Sapphire was selected as the reference material with a known specific heat capacity. A correction run using only the empty crucibles was also conducted.

With regards to thermal conductivity which is measured in W/(m·°K) and quantifies how easily heat is transmitted through material, a number of different methods can be used. For building materials, measurement of the steady state heat transfer properties is typically achieved guarded hot plate method and the heat flow meter method as outlined in *BS EN 12664* (BSI, 2001a)**.** These methods aim to generate a temperature gradient over a specified sample thickness by controlling the heat flow from one side to the other (Yesilata and Turgut, 2007). More recently developed methods, such as the laser or light flash method, rely on transient dynamic techniques by measuring the thermal diffusivity as a function of time and temperature. These techniques are becoming more popular due to their ability to quickly and simultaneously measure various thermal properties of relatively small samples (Yesilata and Turgut, 2007).

Given the limited size of the prototypes used in this study, the laser flash method was adopted to provide some preliminary thermal data on a selected range of samples. In this case a Nettszch LFA 427 Laser Flash Apparatus (LFA) was used to determine the thermal conductivity based on the methods outlined in *BS EN 821-2* (BSI, 1997b) or *ASTM E1461 – 13* (ASTM, 2013). Small disc samples were prepared and then coated with a high emissivity graphite coating to improve the sample's ability to absorb energy. The LFA then applies a high intensity heat pulse to one side of the disc and measures the temperature rise at the opposite face as a function of time (Figure 5-8).

Figure 5-8: Laser Flash Method

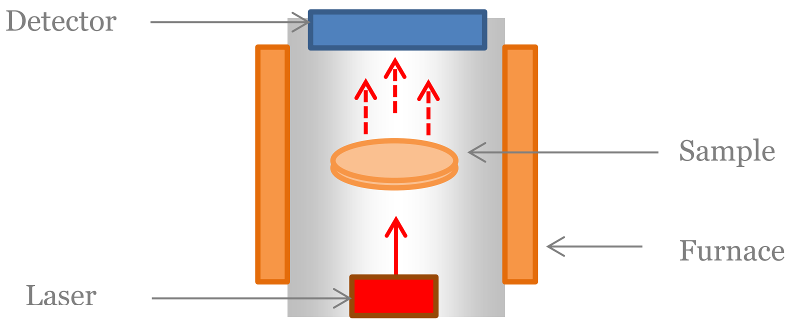

Author's own image

This change in temperature combined with the transient half time ($t_{0.5}$) is then used to calculate the thermal diffusivity (a) of the material in (m^2/s). This is essentially a measure of the rate at which heat flows through a material and is calculated using Equation 9, where d is the test piece thickness in mm, t_x is the time for the test piece rear face to reach a fraction of the maximum temperature in seconds and W_x is a constant relating to d and t_x.

$$a = \frac{W_x d^2}{\pi^2 t_x}$$

Equation 9

Based on the obtained thermal diffusivity values, the thermal conductivity can then be calculated using Equation 10, where C_p is the specific heat in J/(kg ·°K)), k is the thermal conductivity (W/(m ·°K)) and ρ is the apparent density in kg/m³.

$$\boldsymbol{k = \alpha C_p \rho}$$

Equation 10

For samples which were not physically tested, an estimation model proposed by Mosquera et al. (2014) for calculating the thermal conductivity of adobe materials was also adopted. This is based on Equation 11 where ρ is the apparent brick density (kg/m³) and H_p is the brick moisture content at ambient conditions.

$$\boldsymbol{\lambda_E} = \mathbf{0.11e^{(1.6\rho-0.75)}} + \boldsymbol{0.07H_p}; 1.5 < \rho < 2.0$$

Equation 11

In addition to thermal conductivity, the thermal storage properties of the samples were also calculated. The kappa (K) value for example can be used to give an estimate of thermal mass based on the heat capacity per unit area, measured in kJ/m²·K, of the thermally active part of a wall. This is calculated using Equation 12 where d_i is the layer thickness in mm, ρ_i is the density of the layer in kg/m³ and C_{pi} is the specific heat capacity of the layer in J/(kg ·°K).

$$\boldsymbol{K = 10^{-6}\ x\ \Sigma\,(d_i\ x\ \rho_i\ x\ C_{pi})}$$

Equation 12

In this case the thickness of the thermally active materials to be included in the calculation was limited to the point where the wall either reached a layer of insulation, the midpoint of the construction or the maximum thickness of a 100mm.

5.2.3.3. Acoustic Properties

The materials used in a building's construction have an impact of the levels of sound transmitted between adjoining spaces. In domestic dwellings, depending on the building category, a Sound Reduction Index (SRI of 43 – 56Db) for airborne sound is required for all separating walls (HM Government, 2010; Scottish Government, 2015). The SRI can be investigated either using physical testing techniques or calculated based on other material properties such as density and wall thickness. In the case of physical testing, this can be conducted on small samples via the impedance tube method as described in *ASTM E1050 – 12* (ASTM, 2012) or *BS EN ISO 10534-2* (BSI, 2001b), or using a larger test sample which is fitted within a partition between two rooms in a specialised laboratory as per *BS EN ISO 10140-2* (BSI, 2010). In both of these cases, sound waves are transmitted through the sample and then measured using specialised and relatively expensive equipment.

Alternatively, the *Mass law* can also be used to relate a single skin wall's density and thickness to its airborne sound transmission loss. For the purposes of this study, the objective was to obtain an estimation of the bricks' resistance to the passage of sound and investigate whether this would meet the minimum standards required by current building regulations. The *Mass law* method was therefore adopted in order to provide an initial comparison of the airborne sound insulation behaviour of different wall thicknesses up to the region of the critical frequency. This law firstly requires the calculation of the mass per unit area of the wall construction (M) in kg/m^2. This can be calculated using Equation 13 where M_b is the mass of the block (kg), ρ_M is density of the mortar (kg/m^3), T is the block thickness (m), d is the mortar thickness (m), l is the co-ordinating length, h is the co-ordinating height and V is the volume of any frogs or voids.

$$M = \frac{M_b + \rho_M [Td\,(l + h - d) + V]}{LH}$$

Equation 13

Once this figure has been calculated, it can then be incorporated into the mass law represented in Equation 14 where M is the mass per unit area in kg/m^2 and f is the frequency of the sound wave in Hz (Watson and Downey, 2008). Essentially this law states that doubling the mass of a single leaf wall will result in sound reduction of 6 dB, although 5 dB is often used as a more realistic estimate (McMullan, 2007). Doubling the frequency of the sound wave would also have the same effect.

$$SRI = 20\,log_{10}\,(M\,f) - 50$$

Equation 14

Although the numerical correction used can vary between sources, a value of 50 was used in this equation as advised by Watson and Downey (2008). Calculations were based on a standard brick dimension (215 x 102.5 x 65 mm) and an assumed mortar density of 1400 kg/m^3 with 10mm bed joints.

5.2.3.4. Microstructure

SEM can be used to generate 2D images of the surfaces of solid specimens. This is achieved by directing a beam of high-energy electrons towards the surface of the material. This returns signals, primarily in the form of secondary and backscattered electrons with information regarding the surface morphology and composition. A schematic diagram of the SEM system is illustrated in Figure 5-9. In this case, a HITACHI S-3700 SW scanning electron microscope (SEM) was used to generate detailed images of the fracture surface of each specimen. The images were then analysed by comparing the observed morphologies. Energy Dispersive Spectroscopy

(EDS) data was also obtained and used to quantify the elemental composition of the given samples. All of the samples were first cut to a size of approximately 2 x 2 x 2cm and then sputter coated in gold to create a conducting surface before being placed in the SEM chamber. The samples were then analysed under vacuum and images at magnifications ranging from x40 to x1000 were then generated for each sample.

Figure 5-9: Scanning Electron Microscope

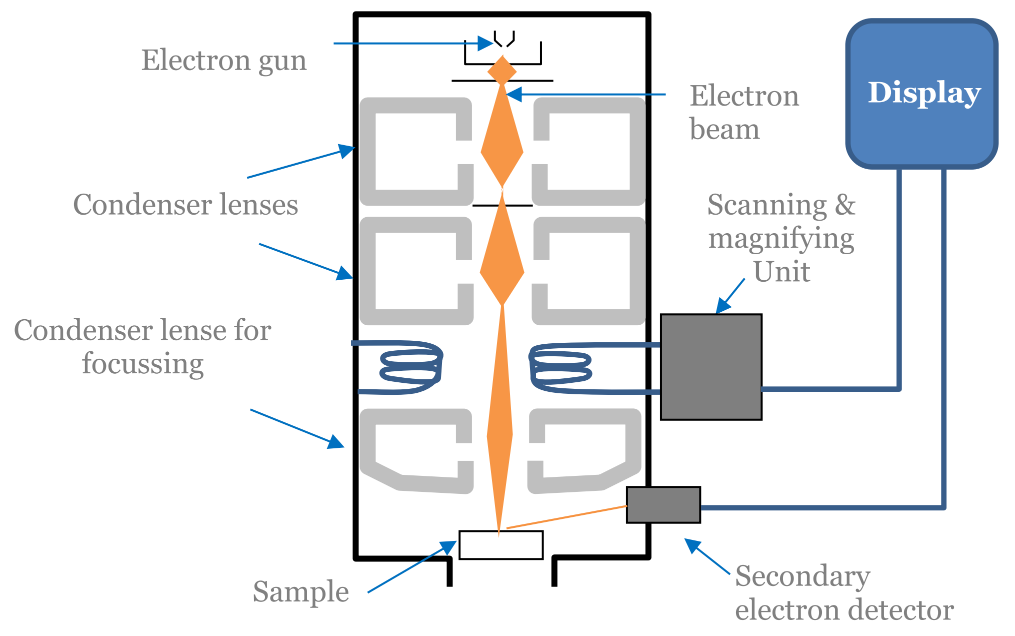

Source: Adapted from Ni (2013)

5.2.4. Phase 4 - Commercial Feasibility

5.2.4.1. Economic Potential

Qualitative cost modelling techniques, based on comparison with similar existing products, can be used to provide cost estimates of products during the early feasibility stage (Niazi et al., 2005). A case-based reasoning approach was selected and cost analysis performed based on financial data supplied by MBL and existing data for unfired clay bricks. Calculations were initially based on a 0.1% dosage of alginate, as per the specimens produced during the initial testing phase. A sensitivity analysis was then performed to assess the implications on the overall brick cost for increased dosages of up to 1%. Cost were also normalised to a £/m^2 rate in order to allow comparison with other systems.

5.2.4.2. Environmental Analysis

Typically environmental analysis is achieved using the LCA framework described in *ISO 14040: 2006*. This consists of 4 main stages. Stage 1 includes goal and scope definition whereby system boundaries, data sources and functional units are identified. In Stage 2, a Life Cycle Inventory (LCI) is compiled gathering the appropriate data which is then used in Stage 3, the Life Cycle Impact Analysis (LCIA) which evaluates the data in relation to different impact categories. The Interpretation phase then allows the most harmful inputs, outputs or processes to be identified so that recommendations for improvement can be made.

As discussed in the literature review, studies calculating the environmental impacts of earth masonry are relatively limited. As discussed by Maskell et al. (2015), this is partly due to the fact that data for commercially available products is often not publicly available. However those which do exist discuss properties such as EE and GWP and typically adopt the LCA methodology described in *ISO 14042* (Venkatarama Reddy and Jagadish, 2003; Reddy and Kumar, 2010; Maskell, 2013). As discussed by Maskell (2013), stabilisation techniques may have a negative on the overall environmental impact of unfired earth materials. It was therefore considered useful to investigate the influence of the alginate component and assess whether any significant increases in EE and GWP occurred. The only similar study conducted to date is that by Galán-Marín et al. (2015) where the environmental impacts of alginate-clay composites were investigated and compared with three other wall types including fired clay, concrete block and reinforced concrete.

In order to make an initial assessment of the environmental impact of the product prototypes, a comparative LCA was conducted using existing datasets for masonry products in combination with production data provided by MBL. In this case, the aim was to consider the impact of the MBL alginates as a stabiliser in earth masonry units in comparison to other stabilisers as well as other conventional masonry units. While advanced LCA can be used to provide a detailed environmental profile for the whole-life cycle of a product, this would involve more extensive calculations and require data not yet available at the prototype stage. Therefore in this case only estimations of EE and EC were considered at this stage. The total EE of a product is calculated by summing all of the energy and resources required to produce the product. In a 'cradle to gate' analysis for construction materials, this involves calculating all processes prior to delivery to the building site. In the case of unfired clay bricks, this covers the production process outlined in Figure 5-10. The main inputs required therefore include the soil, water and alginate as well as any electricity and fuel required during transporting, mixing, forming and drying.

Figure 5-10: Industrial Scale Process – Unfired Bricks

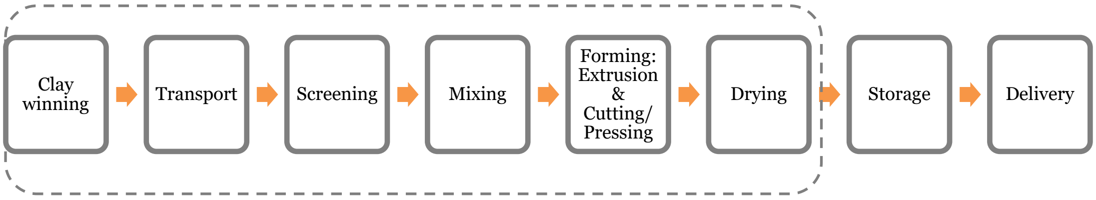

Author's own image

As per the study by Maskell (2013), existing data was obtained Hammond and Jones (2011). This dataset provided cradle-to-gate EE and GWP data from a wide range of secondary sources. This was compiled with data gathered during the literature review and normalised to a standard functional unit. As discussed in Chapter 3, primary data regarding the EE and EC of the alginate products produced by MBL was calculated based on data provided by MBL. The EE and EC of the brick prototypes were then calculated by adding the data for the alginate component to known baseline level values for pressed unfired earth units.

5.2.4.3. Market Comparison

Finally, in order to compare the overall properties of the alginate brick prototypes with existing products currently available in the UK, a market comparison was conducted based on data collected from manufacturers. As previously discussed, fired clay and concrete materials currently dominate the masonry market. In fact, only a small number of unfired systems are commercially available in the UK including IBSTOCK's Ecoterre® and Claytec's non-loadbearing unfired earth units. Therefore, while the literature there discusses various other unfired earth products which have been produced at a laboratory scale, at this stage only commercially available product were included in the comparison. Other masonry products such as fired clays and concrete block were also assessed. Properties considered were those considered most critical for use in internal walling including compressive strength, bulk density, acoustic performance, thermal conductivity and fire performance. Cost data and environmental impact data were also included where available. Data was based on a 100mm wall with no additional finishes.

5.3. Statistical Significance

Where necessary, the statistical significance of the experimental results was analysed using Origin 9.0. Analysis of Variance (ANOVA) was performed in order to compare differences between group means. Post-hoc Tukey tests were also conducted in order to determine which samples offered a statistically significant difference the $p<0.05$ level, compared to the relevant control sample. These statistical tests assume that there is a normal distribution of data and equal variance within groups. The Shapiro-Wilk test for normality and Levene's test for homogeneity of variances have also been performed to investigate these assumptions however it should be acknowledged that these tests can be unreliable for small sample sizes, such as those used in this study. However given that the aim of the project was to perform an initial scoping exercise comparing the different products, the statistical analysis was used in order to provide preliminary data on sample variability and identify if there were any particularly successful products. It would be anticipated that the statistical power and reliability of these tests could subsequently be improved by increasing the number of repeat samples.

6. RESULTS AND DISCUSSION

6.1. Phase 1 – Rheology Tests

6.1.1. Atterberg Limits (Variable 1: Alginate Type and dosage)

In order to firstly investigate the role of the alginate type and dosage, for the Atterberg limits test, a 200g sample of soil (soil V) was mixed with a 0.5 w/v% solution of 5 different alginate types. Additional concentrations (0, 0.1, 0.25, 0.5, 1.0 and 2.0 w/v%) were also studied for the commercial alginate. A control sample containing only DI water was also included for comparison.

A summary of the LL, PL and PI for each sample is provided in Table 6-1. The different alginate types were found to display similar behaviours with LL values of between 27 and 29%. All of these values are slightly higher than the control sample with no alginate (LL = 25%). For the dosage study with AC, while there is no difference in LL for the 0.1% and 0.25% samples, increasing the quantity of alginate to 0.5% leads to a small increase in LL of 2.7%. A similar effect is observed for the 1.0% dosage with an increase of 3.8%. As discussed by Rauch et al. (2002), where variations of a similar magnitude were found for a 4 different stabilising additives, it is estimated that a confidence interval of at least ±2.5% should be assumed in order to account for variations been different observers. Differences between the alginate products are therefore found to be insignificant. When the quantity of AC is increased to 2.0%, a much more dramatic increase in LL of 19.9% is observed (LL = 45. 3%) demonstrating that at this dosage the effect of the alginate is much more pronounced.

Table 6-1: Variable 1 – Atterberg Limits

	LL%	PL%	PI%
Soil V (Control)	25.4%	18.0%	7.4%
Soil V + PR22 (0.5%)	27.8%	15.9%	11.9%
Soil V + PR24 (0.5%)	28.1%	16.2%	11.9%
Soil V + PR32 (0.5%)	27.4%	16.2%	11.2%
Soil V + PR52 (0.5%)	28.1%	15.7%	12.4%
Soil V + AC (0.1%)	25.9%	17.3%	8.5%
Soil V + AC (0.25%)	25.9%	17.3%	8.5%
Soil V + AC (0.5%)	28.6%	15.3%	13.3%
Soil V + AC (1.0%)	29.7%	15.6%	14.0%
Soil V + AC (2.0%)	45.3%	24%	21.0%

Comparing to observations by Nugent et al. (2009) for Xanthan gum (molecular weight of 1.25 × 10^6), which like alginate is an anionic polysaccharide, the behaviour was more complex. Increases in LL were observed with increasing polymer dosage up to 0.5%, followed by a decreasing trend at dosages of 1% to 4%. The 2% dosage of Xanthan therefore resulted in a LL which was similar to the control sample. For dosages above 5%, much more dramatic increases in LL were then observed for Xanthan with the 10% dosage offering an increase of approximately 5 to 7 times that of the control. While dosages above 2% were deemed impractical for this study given the quantity of material available, it would be interesting to see if similar patterns would be observed for alginate. In Nugent et al's (2009) study, the observed behaviour is attributed to competing interactions at the nano-scale. For example, processes such at biopolymer crosslinking with divalent cations and H-bonding or cation bridging between the clay and biopolymer can help to form a polymer-clay network. These types of changes increase the overall strength. Other changes such as biopolymer induced aggregation, reduction in double layer thickness and the adsorption of monovalent cations to the clay surface, can all lead to a decrease in the strength of the soil structure and therefore counteract any strengthening impacts. It is possible that these competing interactions are taking place in the alginate-soil mixes and may explain why the observed increases are minor.

6.1.2. Atterberg Limits (Variable 2: pH)

In order to investiate variables other than the alginate dosage and type, the properties of the soil were also modified to give variations in pH. The original pH of the soil (6.8) was reduced to pH 5 and pH 3 using HCl. Only the AC sample was used in the pH study. A summary of the PL, LL and PI for each sample is provided in Table 6-2.

Table 6-2: Variable 2 – Atterberg Limits

	LL%	PL%	PI%
Soil V (Control) – pH 3	26.0%	15.4%	10.6%
Soil V (Control) – pH 5	25.4%	16.5%	8.9%
Soil V (Control) – pH 7	25.4%	18.0%	7.4%
Soil V + 0.5% AC – pH 3	27.2%	16%	11.2%
Soil V + 0.5% AC – pH 5	26.7%	15.9%	10.8%
Soil V + 0.5% AC – pH 7	28.6%	15.3%	13.3%

In the control samples, where no alginate is added, the reduction of the soil pH does not make a significant change to the LL. However when alginate is included, the acidic samples (pH 3 & 5) offer slight reductions in LL (1.4 and 1.9% respectively) compared to the neutral sample, giving a relative decreases of 4.9 and 6.6%. For the PL, reductions in pH also appear to have an effect on the alginate containing samples where reductions of 2.5 and 1.6% are shown for pH 3 and pH 5 compared to the neutral sample. Therefore although the PL values are slightly reduced at lower pH, the slight decrease in LL means that the PI values are only marginally increased.

For anionic polysaccharides, like alginate, although it would be expected that anionic polymers would not be adsorbed by the clay particles in the soil due to the repulsive forces between the two components, adsorption can occur in the form of anion exchange which takes place between the negatively charged polymer and the variable charge at the edges of the clay particles. This type of interaction is pH dependent since the edge charges can be positive, negative or neutral depending on the pH conditions. Furthermore the pH of the system also affects the magnitude of the charge on the ionic group of the polymer. Ligand exchange (where ligands are the molecules or ions surrounding a metal ion) can also occur between the acidic hydroxyl group of the polysaccharide, such as the carboxylic and phenolic groups, and hydroxyl groups of the clay surface (Theng, 2012b). In natural soils, most of the adsorption of organic and humic materials occurs in this way (Gu et al., 1994), particularly in acidic soils (Keil and Mayer, 2013). This adsorption mechanism is relatively strong and can reportedly last for over 100 years (Lützow et al., 2006).

It would therefore be expected that a low pH would help to reduce electrostatic repulsion between the two components and potentially promote adsorption. However, from the results presented here, this does not appear to be the case. Indeed for this particular alginate-soil mix reducing the soil pH does not lead to significant soil strength increases when this alginate type and dosage are used. This supports the findings of Emerson (1956) where sodium alginate was found to be a poor stabiliser for acidic soils. Investigation of a wider range of pH values would however be necessary in order provide further insights into the impacts of pH.

6.1.3. Atterberg Limits (Variable 3: Available cations)

In order to investigate the impact of increasing the quantity of available crosslinking ions present with the soil-alginate mixture, the calcium content of the soil was also modified. In this case Gypsum ($CaSO_4{\cdot}7H_2O$) from Acros Organics™ (Geel, Belgium) was used since this material will not affect the pH of soil. Again only the commercial alginate (AC) was used for Variable 3. A summary of the results is presented Table 6-3.

Table 6-3: Variable 3 – Atterberg Limits

	LL%	PL%	PI%
Soil V (Control) Natural Ca	25.4%	18.0%	7.4%
Soil V (Control) + 10g Gypsum	26.3%	14.9%	11.3%
Soil V (Control) + 20g Gypsum	26.8%	16.6%	10.2%
Soil V (0.5% AC) Natural Ca	28.6%	15.3%	13.3%
Soil V (0.5% AC) + 10g Gypsum	28.5%	13.8%	14.7%
Soil V (0.5% AC) + 20g Gypsum	23.1%	13.4%	9.6%

In reviewing the results from the calcium study, in the control samples which do not include alginate, the addition of the two different dosages of gypsum does not result in a significant change in LL but does cause a slight decrease in PL. In the case of the alginate containing samples, there is a significant change in LL observed when 20g of gypsum is added resulting in a reduction of 5.5% compared to the control sample giving a relative reduction of 19.2%. This change suggests that the addition of this quantity of calcium is in fact having a negative impact on the strength of the mix.

Typically the presence of polyvalent, exchangeable cations can help to promote cationic bridging between polysaccharides and clay, either directly or through a water bridge (Gu and Doner, 1992). For example, the presence of Ca^{2+} ions could help to create electrostatic bridges between the anionic part of the alginate ($COOH^-$) and the negative surface of the clay (Yalçın et al., 2002). While this bridging process would be expected to improve the overall strength of the clay-polymer matrix, the results here demonstrate the opposite trend. This supports the findings of Nugent et al. (2009) where the addition of a calcium salt ($Ca(NO_3)_2$) to the Xanthan-kaolinite mix also had negative impact on the LL at polymer dosages of up to 1%. This is explained by the fact that the addition of the calcium ions increases the ionic strength of the pore fluid and consequently reduces the size of the electric double layer (EDL) of the clay particles. Therefore even if biopolymer cross-linking is occurring, the impact on LL is counteracted by changes in the EDL. It should be noted that in the study by Nugent et al. (2009), at polymer dosages 2% and above, significant increases in LL are observed. For alginate it may also be possible that an increased polymer dosage would also lead to more pronounced cross-linking effects however this would need to be investigated further.

6.1.4. Atterberg Limits (Variable 4: Clay content)

The final variable to be studied as part of the plasticity tests was the clay content of the soil. Given that the natural soil already had a relatively high clay content (27%), the particle grading was modified by adding known quantities of sand in order to reduce the overall clay fraction by 25% and 50%. Again only the commercial alginate (AC) was used for Variable 4. A summary of the PL, LL and PI for each sample is also provided in Table 6-4.

Table 6-4: Variable 4 – Atterberg Limits

	LL%	PL%	PI%
Soil V (Control) – 27% clay	25.4%	18.0%	7.4%
Soil V (Control) – 20% clay	22.2%	12.5%	9.7%
Soil V (Control) – 14% clay	18.5%	11.7%	6.8%
Soil V + 0.5% AC – 27% clay	28.6%	15.3%	13.3%
Soil V + 0.5% AC – 20% clay	30.3%	14.5%	15.8%
Soil V + 0.5% AC – 14% clay	28.0%	15.4%	12.6%

In comparing these results for the three different clay contents, for the control samples with no alginate, reducing the clay fraction leads to a reduction in both LL and PL. This is expected given that replacing the finer clay particles with sand would inevitably reduce cohesion and plasticity within the soil as well as reducing the overall CEC. For the alginate containing samples, a different pattern is observed with all of the samples exhibiting relatively similar LL values (28 – 30%), regardless of clay content. This suggests that for sandy soils the inclusion of alginate, even at this low dosage, is sufficient to improve the shear strength of the soil. On the other hand, where there is already a sufficient quantity of clay present, the addition of alginate has a more limited effect as evidenced by the lower relative increase observed in the 27% clay sample. It should also be noted that the clay type, as well as the quantity of clay particles, will also have an impact on the interaction with the polymer. For example the study by Nugent et al. (2009) used a pure kaolinite while this study has investigated a natural soil which will contain a mix of clay minerals and larger particles. Since only one soil type has been used in these preliminary tests, variations in mineralogy will need to be investigated further in Phase 2.

6.1.5. Sedimentation behaviour (Variable 1: Alginate Type and dosage)

Examples of the soil slurries used in the sedimentation tests are shown in Figure 6-2. Three concentrations of each alginate solution (0.1, 0.25 and 0.5 w/v %) were compared against a control sample (soil and DI water). The results for Variable 1 are shown in Figure 6-2 and the final bed heights provided in Table 6-5.

Figure 6-1: Sedimentation Cylinders

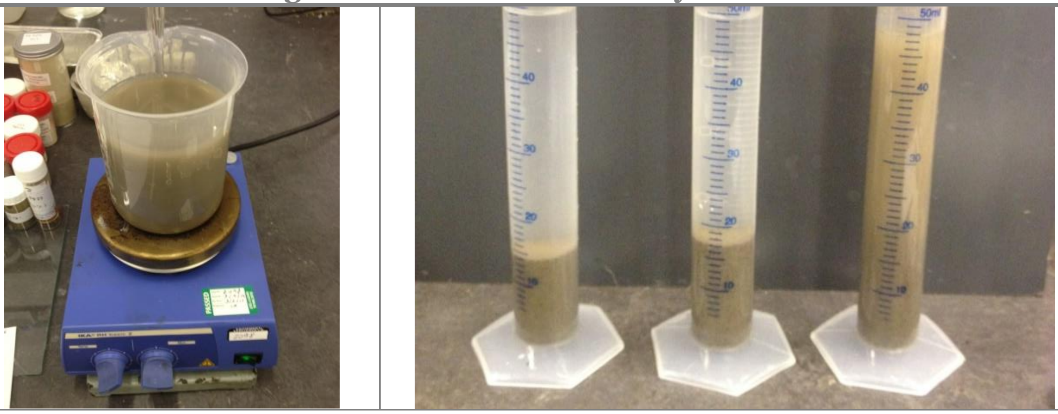

Samples (left to right) showing AC at dosage of 0.1%, 0.25% and 0.5% after 60s

Figure 6-2: Settling Rates – Variable 1: Alginate Type and Dosage

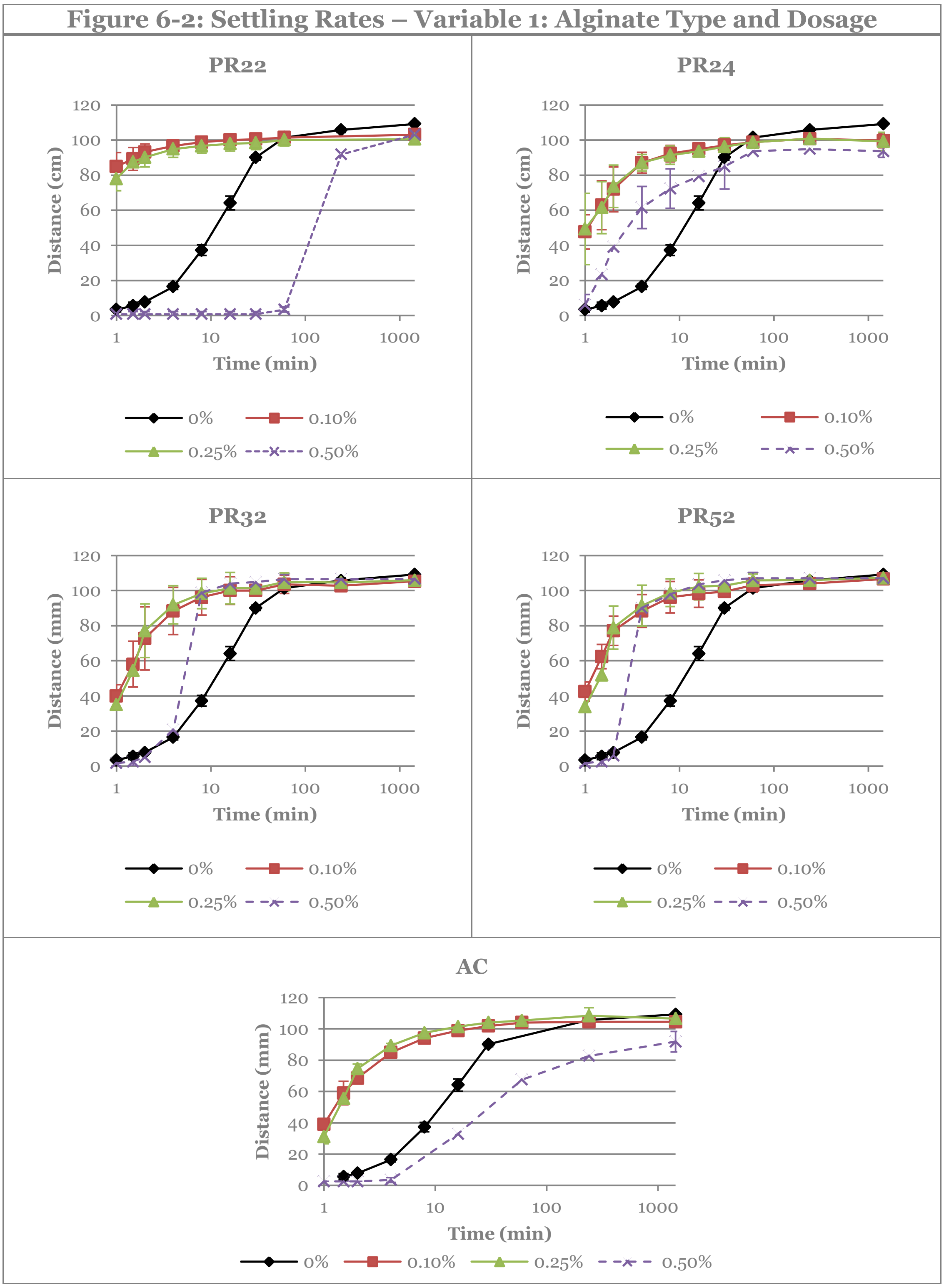

	Table 6-5: Variable 1 –Bed Heights after 24h (mm)			
	0%	**0.1%**	**0.25%**	**0.5%**
PR22	21(±0.0)	27(±3.0)	29(±3.0)	-
PR24	21(±0.0)	30(±4.0)	31(±5.3)	-
PR32	21(±0.0)	23(±2.6)	23(±2.7)	-
PR52	21(±0.0)	23(±2.6)	23(±0.8)	-
AC	21(±0.0)	26 (±0.8)	23(±0.0)	-

It should be noted that for the lower polymer dosages (0.1% and 0.25%) the flocculation effect is relatively rapid and a clear solid-liquid interface is formed. However for the control samples and the 0.5% polymer dosage the mixtures remained relatively turbid. Indeed the 0.5% polymer dosage demonstrated this type of behaviour even beyond the measurement at 2 minutes. In these cases the plots are therefore indicative of an apparent boundary (as shown by the dotted line) rather than a definitive interface. In all cases the settling profiles show that the addition of alginate at a dosage of 0.1% and 0.25% induces flocculation leading to a faster initial settling rate compared to the control sample. A difference was found between the sediment measurement at 1 minute for the control samples and those of the 0.1% and 0.25% samples, with the exception of PR32. In this case the difference was only significant for the 0.1% dosage. This effect is more pronounced for the PR22 sample given the greater differences in the 1 minute reading. There is also a statistically significant difference in final bed heights for PR22 (0.1% and 0.25%) and PR24 (0.25%) compared to the control samples. This is likely due to the formation of flocs in theses samples as these will be more loosely packed than individual particles.

For the higher polymer dosages (0.5%), the turbidity indicates that some particles remain dispersed in the liquid and an overall slower settling rate was observed compared to the control. This is similar to reports by Chukwudi et al. (2008) for kaolinite-starch mixtures where a decrease in the sedimentation rate was observed beyond an optimum dosage. Mpofu et al. (2004) also found that increasing the dosage of an anionic polyacrylamide (PAM) led to an increase in the settling rate of a smectite clay with a plateau reached at a dosage of 1000 g of the polymer per ton of clay. A similar plateau is described by Clark et al. (1990) for anionic PAM and kaolinite while Akther et al. (2008) also observe visible dispersion for a bentonite clay modified with anionic CMC. As discussed by Lee et al. (2012), this behaviour is attributed to the process of steric stabilisation which occurs once maximum polymer adsorption has been reached, resulting in the creation of a protective polymer coating which hinders further inter-particle bridging (Elimelech et al., 2013). This can result in simultaneous processes of flocculation and stabilisation within an aqueous clay/polymer system. These two types of interactions are illustrated in Figure 6-3. Where steric stabilisation occurs, the particles remain dispersed in the liquid phase. Given that an increase in polymer concentration is expected to increase the likelihood of stabilisation, this explains why an increased alginate dosage may in fact lead to a decrease in settling rates but greater sediment volumes. Again this can be attributed to the looser packing of the flocs and the increased volume of inter-floccule water trapped within the sediment (Mpofu et al., 2004). Overall, the variations in settling behaviour highlight that the molecular scale interactions are dependent upon both the polymer dosage and alginate source.

Figure 6-3: Flocculation and Stabilisation

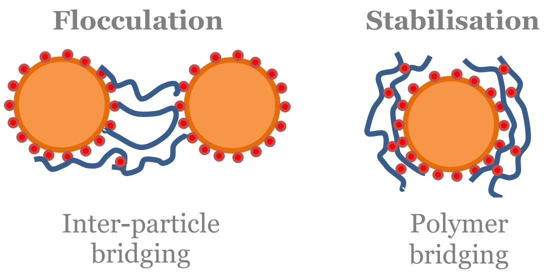

Source: Adapted from Lee et al. (2012)

6.1.6. Sedimentation behaviour (Variable 2: pH)

The results from the sedimentation tests for Variable 2 are shown in Figure 6-4 and Figure 6-5. In this case only the commercial alginate (AC) was studied. Again 3 concentrations of the alginate (0.1, 0.25 and 0.5 w/v%) were compared against a control sample containing only the soil and DI water. Prior to the experiment, pH modification was achieved using dilute HCl in order to obtain mildly acidic (pH 5) and strongly acidic (pH 3) samples which could be compared with the unmodified (neutral) sample from the previous round of tests (Variable 1).

Figure 6-4: Settling Rates – Variable 2: pH (Controls)

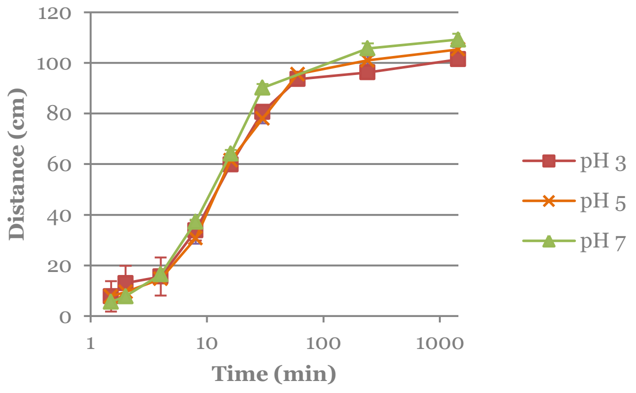

Figure 6-5: Settling Rates – Variable 2: pH (AC)

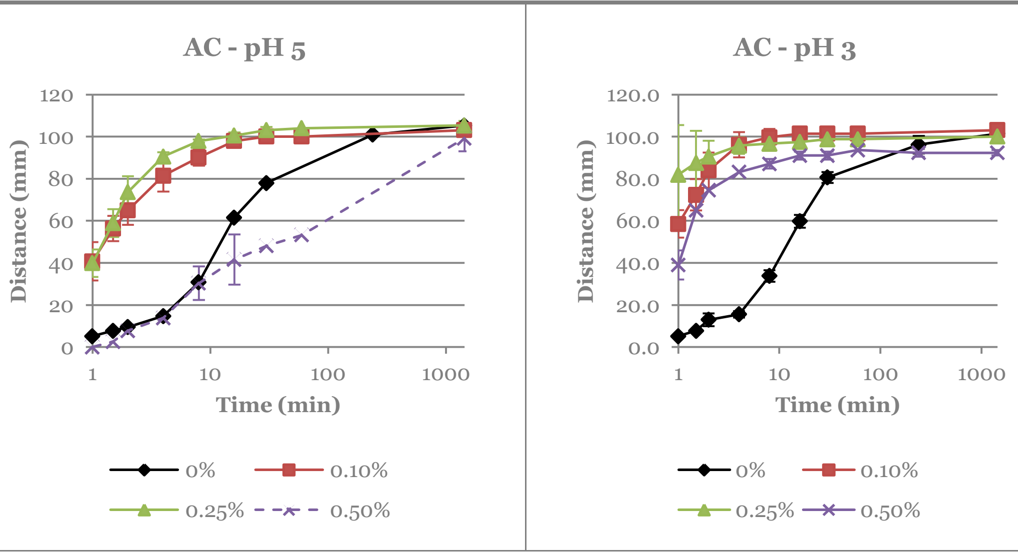

	Table 6-6: Variable 2 – Bed Heights after 24h (mm)			
	0%	**0.1%**	**0.25%**	**0.5%**
AC – pH 7	21(±0.0)	26 (±0.8)	23(±0.0)	-
AC – pH 5	25(±0.0)	27(±1.5)	25(±2.3)	31(±6.1)
AC – pH 3	25(±1.3)	27(±1.3)	26(±2.7)	38(±1.3)

In relation to sedimentation behaviour, in considering firstly the effect on the clay particles alone, the results from the control samples indicate that reducing the pH of the soil slurry increased the initial settling rate as evidenced by the different profiles of the curves in Figure 6-4. It would be expected that a low pH would increase the strength of edge-to-face bonding of the clay particles due to the increase in the positive charge density at the particle edge (Michaels and Bolger, 1962). As discussed by Palomino and Santamarina (2005), mildly acidic kaolinite suspensions (pH 5, low ionic strength) were found to exhibit mixed-mode sedimentation behaviour with a faster settling rate but similar final bed height to that of the neutral sample. In their study, a further reduction of pH (pH 3), resulted in an even faster settling rate and more compacted bed volume which is indicative of face to face aggregation. This behaviour was not apparent in the present study, with the all three samples exhibiting relatively similar settling behaviour. This is likely due to the fact that that these were natural soil samples and not pure clays and so the previously described impacts of pH modification will be applicable only to the clay fraction of the soil slurry. Despite the similar settling rates however, minor differences were found in the final bed heights with the neutral sample achieving a final sediment height of 8mm compared to 10 mm and 11 mm for the pH 5 and pH 7 samples respectively. This is perhaps indicative of larger flocs in the pH modified samples.

In considering the results of the alginate containing samples, as previously discussed a reduction in pH would theoretically lead to increased attraction between the polymer and the clay particles. At low polymer dosages (0.1% and 0.25%), pH modification did not have a major effect on the settling profiles given the relatively similar curves produced. For the higher polymer dosage (0.5%), a slight difference was found at pH 5 with an increased settling rate during the first hour however the mixture still remained relatively turbid indicating the presence of stabilised particles. A more visible increase in the settling rate was also found when the pH was further reduced to pH 3 and a clear solid-liquid interfaced could measure. This would suggest that for this higher polymer dosage, reducing the pH has a more dramatic effect on the polymer clay interaction with the faster settling rate and larger sediment volume indicating the that larger flocs are being formed. This is similar to observations by Akther et al. (2008) who also report on increased flocculation for acidic samples of bentonite and CMC compared to the neutral samples which remain dispersed. Whilst the results are limited in the fact that only 3 different pH levels have been compared, these initial findings indicate that increasing the acidity of the soil-alginate mix may result in changes in the interaction between the polymer chains and clay particles when sufficient quantities of the polymer are present.

6.1.7. Sedimentation behaviour (Variable 3: Available cations)

In order to investigate the influence of different cations, 3 concentrations of the commercial alginate (AC) were again tested using electrolyte solutions as an alternative to DI water. Not only does the presence of an electrolyte increase the ionic strength of the system, thereby leading to a compression of the EDL which would enhance particle to particle attraction (Mpofu et al., 2003; Orts et al., 2007; Chukwudi et al., 2008), but in the case of $CaCl_2$, the presence of Ca^{2+} also help to promote polymer induced flocculation through cationic bridging (Lee et al., 2012). In this case 0.1 M $CaCl_2$ was used as a source of divalent cations (Ca^{2+}) while 0.1 M NaCl was used to provide monovalent cations (Na^+). The settling curves produced for the two electrolytes are shown in Figure 6-6. The final bed heights are also shown in Table 6-7.

Figure 6-6: Settling Rates – Variable 3: Available Cations

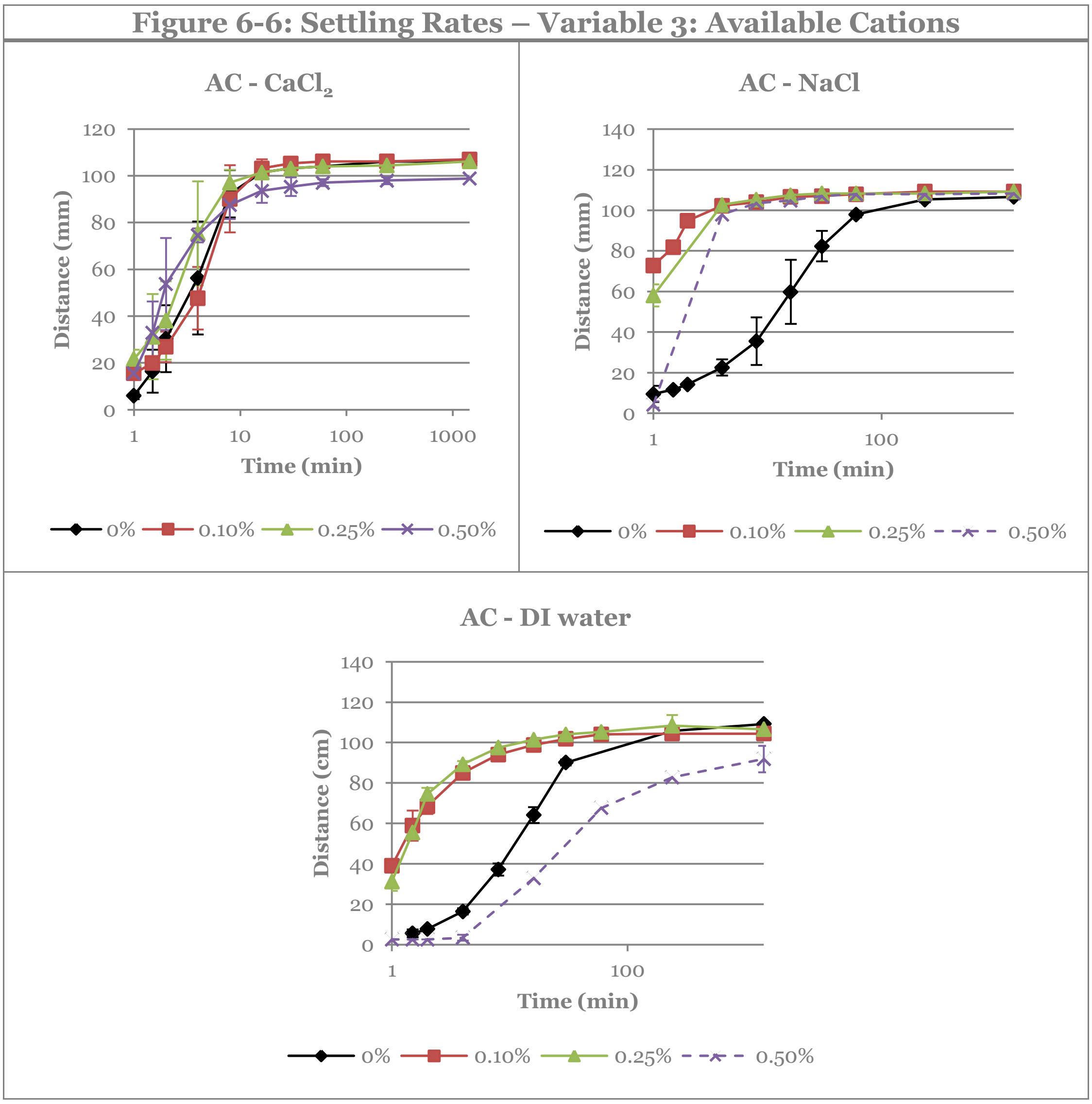

Table 6-7: Variable 3 – Bed Heights after 24h (mm)

	0%	0.1%	0.25%	0.5%
AC – DI Water	21 (±0.0)	26 (±0.8)	23(±0.0)	-
AC – $CaCl_2$	24(±0.8)	23(±0.8)	24(±0.8)	31
AC – NaCl	23(±0.0)	21(±0.0)	21(±0.0)	22(±0.8)

The differences observed between the DI and $CaCl_2$ samples where no alginate is included highlight the importance of electrostatic repulsion on the clay particles alone given the slightly steeper gradient observed for the first 10 minutes in the electrolyte sample. A small but significant increase in the final bed height was also observed, suggesting that the addition of Ca^{2+} leads to increased flocculation.
For the alginate samples, the curves produced for the $CaCl_2$ samples are relatively similar for all of the polymer dosages suggesting that the presence of Ca^{2+} outweighs more subtle influence of the different concentrations of alginate. Indeed there were no statistically significant differences found between any of the alginate containing samples at the 1 minute reading. For the low polymer dosages (0.1% and 0.25%), compared to the DI water samples, the $CaCl_2$ mixtures show an initially faster settling rate, again evidence by a statistically significant difference at the 1 minute reading. A significant decrease in the final bed height was also observed for the 0.1% sample upon the addition of $CaCl_2$. A more dramatic change is observed for the 0.5% sample with the appearance of a more visible mudline in the $CaCl_2$ sample at the 1 minute compared to the DI water where the particles remain dispersed. This supports the theory that the addition of Ca^{2+} helps to increase particle attraction, inducing flocculation amongst particles which would otherwise remain dispersed. The addition of Ca^{2+} also appears to help negate the effects of steric stabilisation for the higher polymer sample.

By comparison, for the NaCl samples the presence of Na^+ has no significant impact on the 1 minute reading for the control sample or the 0.5% sample, whilst an increase in the initial settling rate is observed for the lower polymer doses as shown by the difference in sediment heights achieved at the 1 minute reading. The effects are however less dramatic than the changes in sedimentation behaviour reported by Kaya et al. (2006) for pure kaolinite suspensions upon the addition of 0.1 M NaCl.

For the 0.5% sample, there is also a change in the settling profile with a much faster settling of the apparent sediment line within the first 4 minutes compared to the equivalent DI water sample. This is similar to reports by Ma and Bruckard (2010) for starch and kaolinite whereby the use of NaCl rather than DI water also enhances the adsorption of the polymer to the clay surface due to the reduced electrostatic repulsion. It should be noted that, unlike the $CaCl_2$ sample, for the high polymer dosage the NaCl mixture still remains turbid for the first 10 minutes indicating the presence of dispersed particles. In general, the comparison between the two electrolytes is in agreement with results by Mekhamer et al. (2009) which show that Ca^{2+} has a greater impact on flocculation that Na^{+} for kaolinite. The more pronounced effect observed for the $CaCl_2$ can be explained by the additional crosslinking mechanism of the divalent cations which would be expected to promote absorption between the alginate and the clay particles.

6.1.8. Phase 1 Summary

In concluding the results from the initial rheology tests, although these preliminary findings give some insight into the complexities of soil-alginate interactions and the impact of the polymer type and dosage as well as soil variables such as the pH, the type of crosslinking ions present and the particle size distribution, the next step is to investigate whether these variables have measurable impacts on larger scale specimens. In the case of the polymer type, while there were no major differences found between the five alginate products included as part of the LL tests, it is possible that this test method was not sensitive enough to demonstrate potential variations. More visible differences in the settling behaviour indicate that the alginate type may in fact have an important influence on the molecular scale interactions between the two components. It was therefore concluded that a wider range of alginate types should be included as part of Phase 2 in order to further explore the role of the alginate using large scale samples. Similarly, given the observed increases in LL for the AC product when higher polymer contents were used and the different curves produced for the highest dosage for most of the alginate types included in the sedimentation tests, the role of the polymer dosage in the larger scale brick samples is also considered worthy of further investigation. Finally, in considering the soil variables, the results from these initial tests were less definitive. There were no significant differences observed regarding pH and the Calcium modified soil only leaded to significant changes in behaviour when relatively large quantities of Ca^{2+} were added. The clay content did however appear to have an important influence on the interaction with the alginate with the greatest improvement in strength being observed for the mid-range clay content (~20%). In order to investigate all of these soil variables in more detail, and to reflect the complexities of real practice, it was deduced that a variety of natural soil types should be included in Phase 2. This would allow for a range of soil variables, typical of those used in brick manufacture, to be studied.

6.2. Phase 2 – Brick Prototypes: Initial Assessment

6.2.1. Variable 1: Alginate Type

In the first round of studies, the objective was to make an initial comparison of the different alginate types. A total of 15 different products were therefore tested including two residue products, two milled seaweed products, nine sodium alginate products (sourced from MBL) and two commercial products, including a dental alginate. A control batch, without the inclusion of any additives, was also included for comparison. All of the specimens were produced using Soil U and the alginate was incorporated at a dosage rate of 0.1% by weight of the dry soil. For the raw seaweed and residue products the quantity added was calculated based on the estimated alginate content to ensure that an approximate alginate content of 0.1% would still be achieved. The amount of water added was also adjusted to give an overall water content of 16%.

6.2.1.1. Visual Observations

The visual appearance of specimens produced with the different alginate products was found to vary, with some specimens displaying considerable voids and defects. A summary of the observations is presented in Table 6-8 and in Figure 6-7 to Figure 6-12. Visible drying cracks and damaged corners are observed in some samples. Specimen PR17U was found to be particularly poor, with the bottom face becoming very fragile upon removal from the mould (Figure 6-8). PR22U (Figure 6-10) and PR24U (Figure 6-11) were however much more homogenous with cleaner edges.

	Figure 6-7: U	**Figure 6-8: PR17U**	**Figure 6-9: ANU**
Photographs	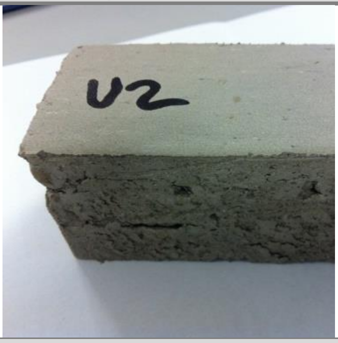	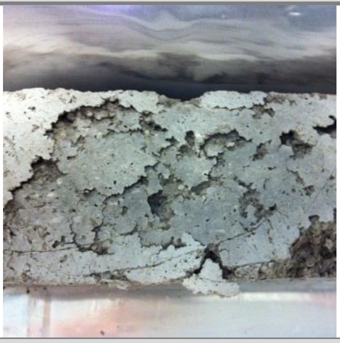	
	Figure 6-10: PR22U	**Figure 6-11: PR24U**	**Figure 6-12: PR29U**
	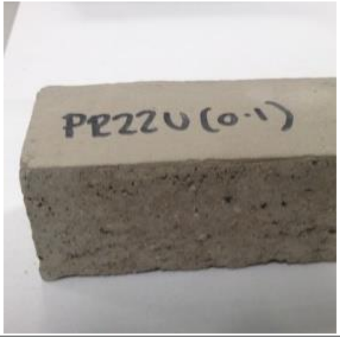		

Table 6-8: Variable 1 - Specimen Homogeneity

Specimen	Homogeneity	Specimen	Homogeneity
U	Moderate	**PR29U**	Moderate
PR17U	Poor	**PR30U**	Good
PR38U	Moderate	**PR32U**	Good
ANU	Poor	**PR44U**	Moderate
LHU	Good	**PR52U**	Moderate
PR22U	Good	**DAU**	Good
PR24U	Moderate	**ACU**	Moderate
PR25U	Good		

6.2.1.2. Dimensions, Mass & Density

The dry mass of the specimens was found to range between 364 and 445g with variations being attributed to a loss of materials during removal from the mould. All of the specimens experienced a degree of shrinkage during drying, ranging from approximately 3 to 8%. In terms of bulk density, the values obtained were relatively similar with all results falling within the 1800 and 2000 kg/m^3 range (Figure 6-13). This is comparable with other unfired brick products which typically offer dry densities of between 1700 and 2200 kg/m^3 (Sutton et al., 2011). The only significant difference compared to the control sample occurred for PR17U where a decrease was observed. This was likely due to the fact that PR17 is a residue product which will contain a significant proportion of cellulose.

Figure 6-13: Variable 1 – Bulk Density

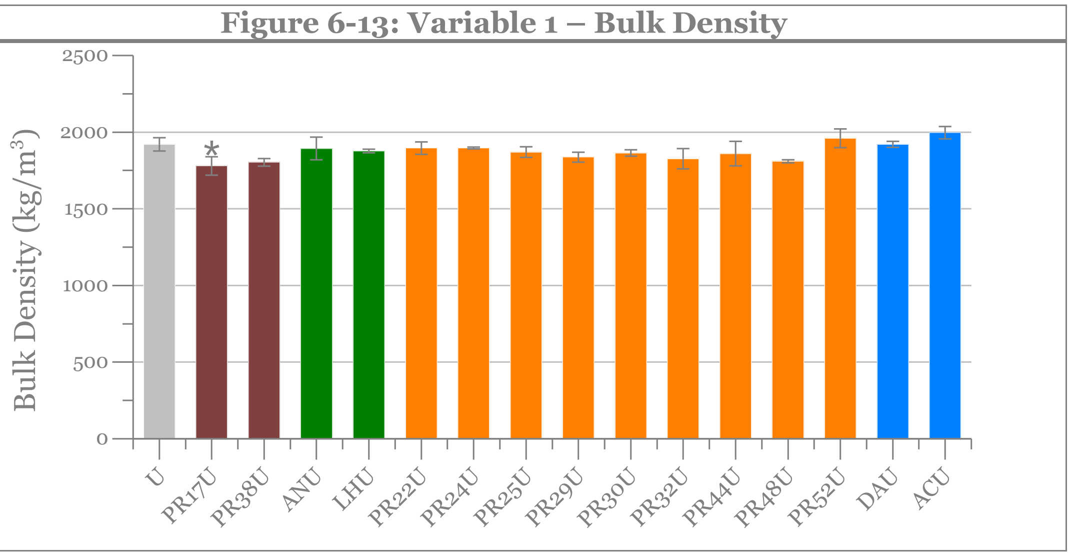

6.2.1.3. Mechanical Properties

The results for the flexural strength and compressive strength tests, comparing the different products are shown in Figure 6-14 and Figure 6-17 respectively. The average moisture contents of these specimens ranged between 1.3% and 2.5% at the time of testing.

Figure 6-14: Variable 1 – Flexural Strength Test Results

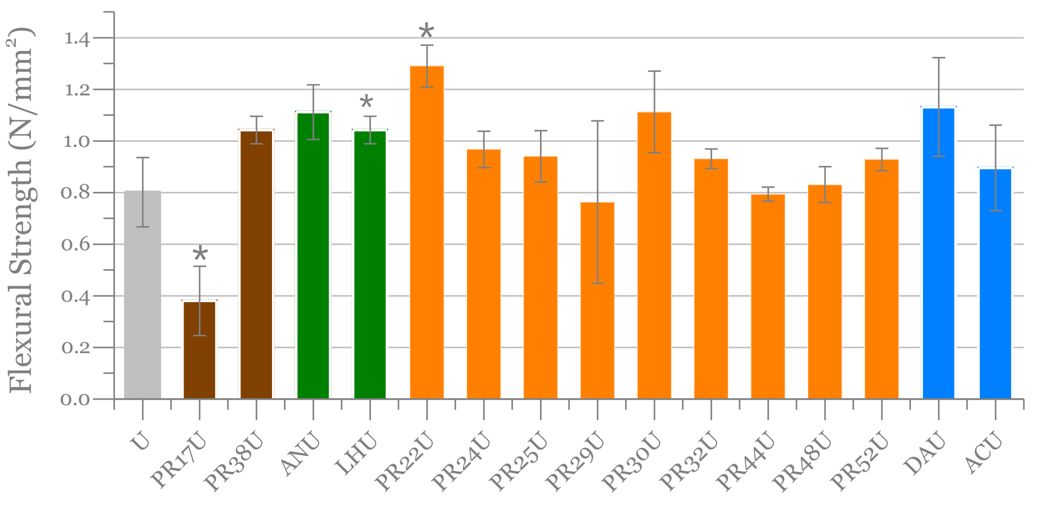

In the case of the 3 point bending tests, the only specimens which offered a statistically significant change in strength compared to the control specimen were PR17, which demonstrated a decrease in flexural strength, and PR22 and LHU which showed an increase in flexural strength of approximately 62%. High standard deviations were found for several samples indicating variations in quality between specimens within the same batch (Figure 6-14). Particularly high variation was observed in the case of PR29U. This specimen was noted to have visible cracks which likely affected the flexural strength. The poor performance of PR17U compared to the control sample is also likely due to the poor quality and homogeneity of this batch as noted in Table 6-8. As shown in the example stress-strain plots for the control batch (U) and PR22U (Figure 6-15), failure occurs relatively quickly and at low levels of strain. In all cases failure occurred at the mid-point of the specimen with the appearance of a visible fracture line as shown in Figure 6-16.

Figure 6-15: Stress-strain plot for U and PR22U (Flexural)

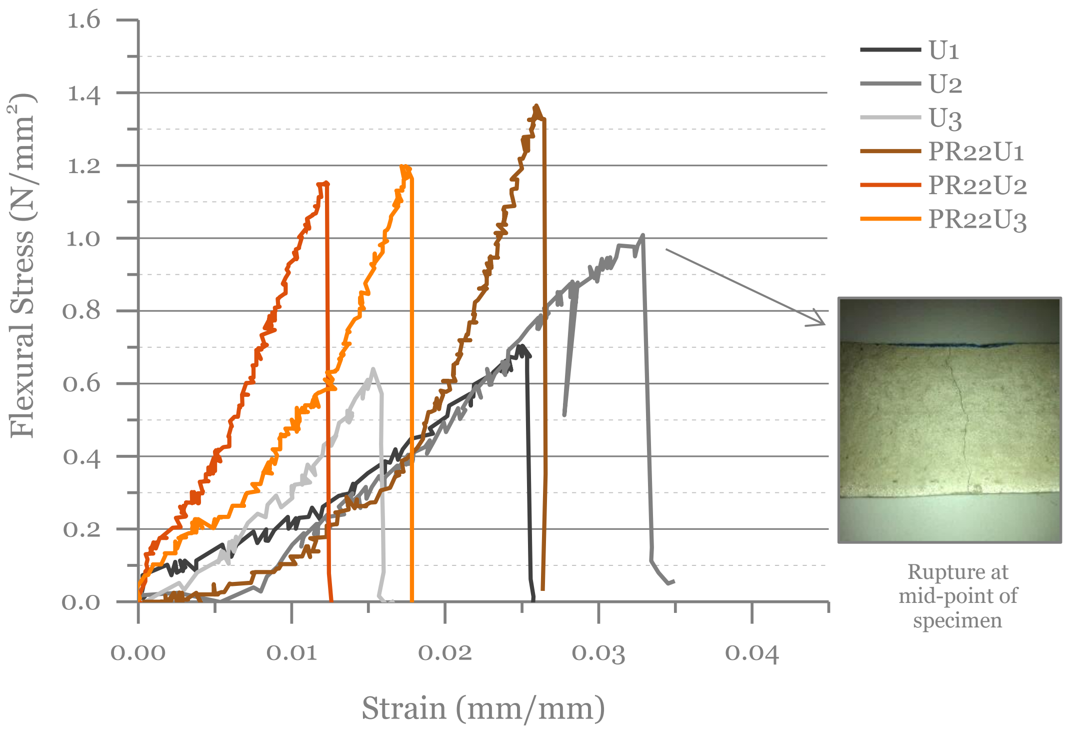

Figure 6-16: Example specimens after rupture

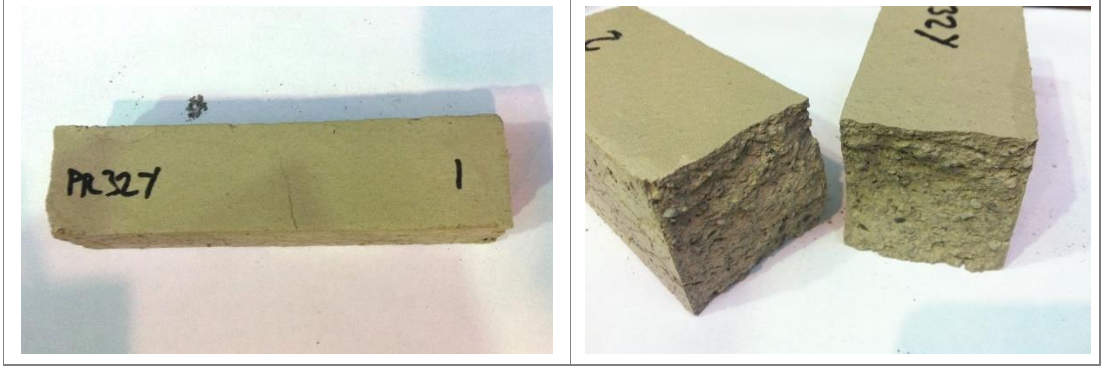

In the case of the compressive strength tests, Figure 6-17 illustrates the unconfined compressive strength results using a correction factor of 0.58 as recommended by Heathcote and Jankulovski (1992). The shaded grey bars indicate the compressive strength prior to any corrections. The statistically significant results are again denoted by an asterix. Only 3 of the specimens (LHU, PR22U and DAU), offered a statistically significant improvement over the control with an increase of 52% observed for both. The comparative compressive stress-strain plots for the control batch and one of the alginate containing samples is also shown in Figure 6-18. The specimens show an initial contact adjustment phase whereby the plywood is pushed down onto the sample, levelling any surface irregularities. This is followed by an apparent consolidation region whereby the soil particles are packed together leading to a reduction in voids in structure. This consolidation process appears to continue until the maximum stress is reached with a more linear stress-strain relationship observed in the alginate sample. In all cases failure was by crushing as illustrated in Figure 6-19. After the yield point, a softening regime can also be observed. It should be noted that while there is reasonable consistency for the PR22 samples with all of the stress-strain plots exhibiting a similar profile, there is much more variation for the control batch. High variability was also observed for PR52U and ACU, which again demonstrates differences in specimen quality.

Figure 6-17: Variable 1 – Unconfined Compressive Strength

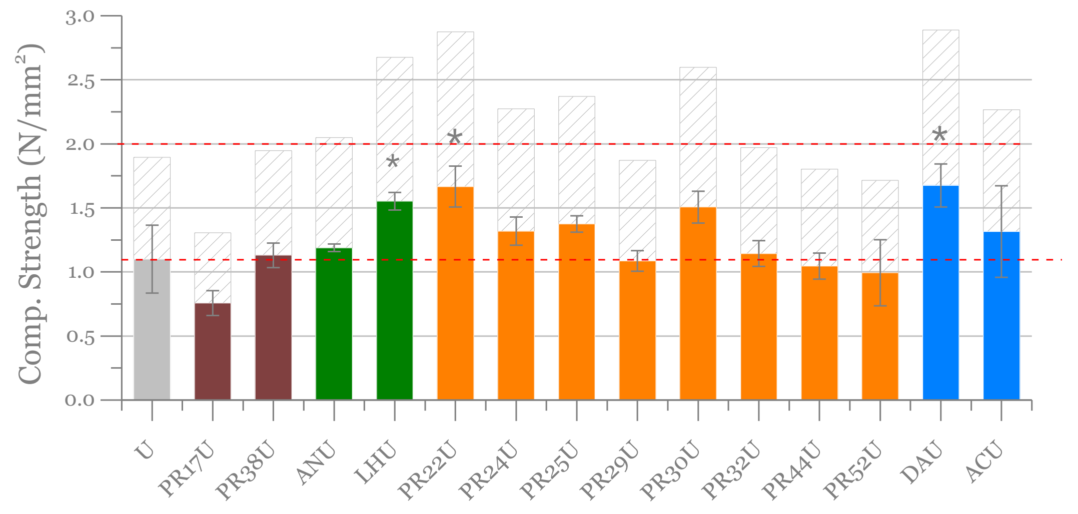

(Correction Factor = 0.58)

Figure 6-18: Stress-strain plot for U and PR22U (Compressive)

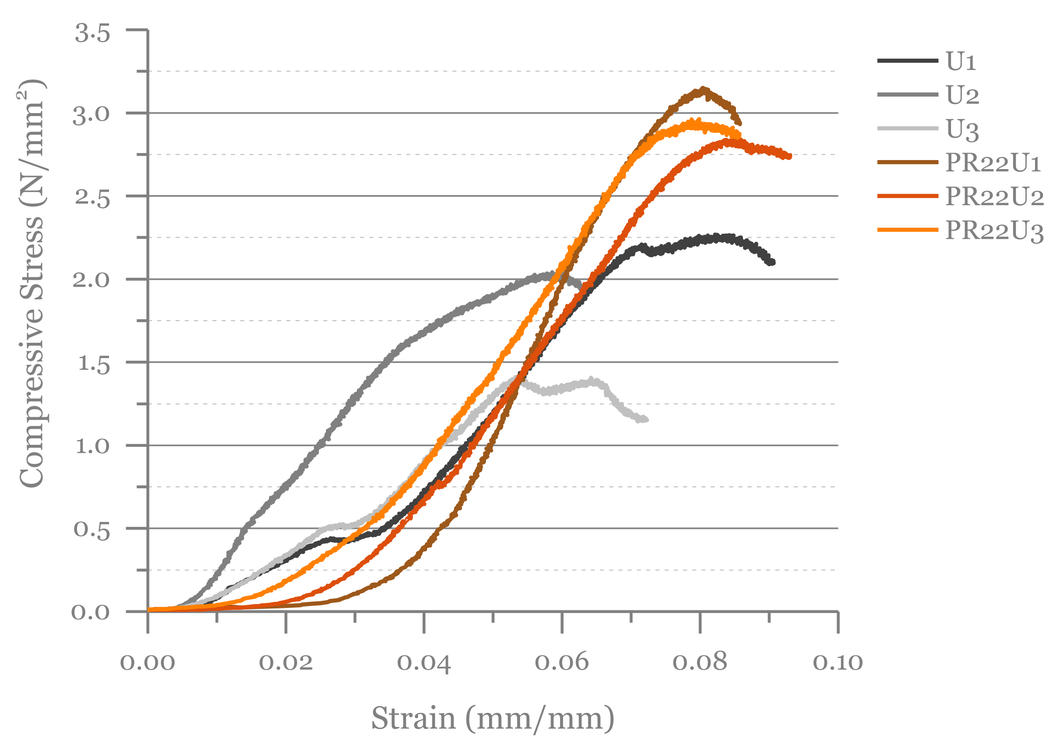

Figure 6-19: Example specimens (before and after compression test)

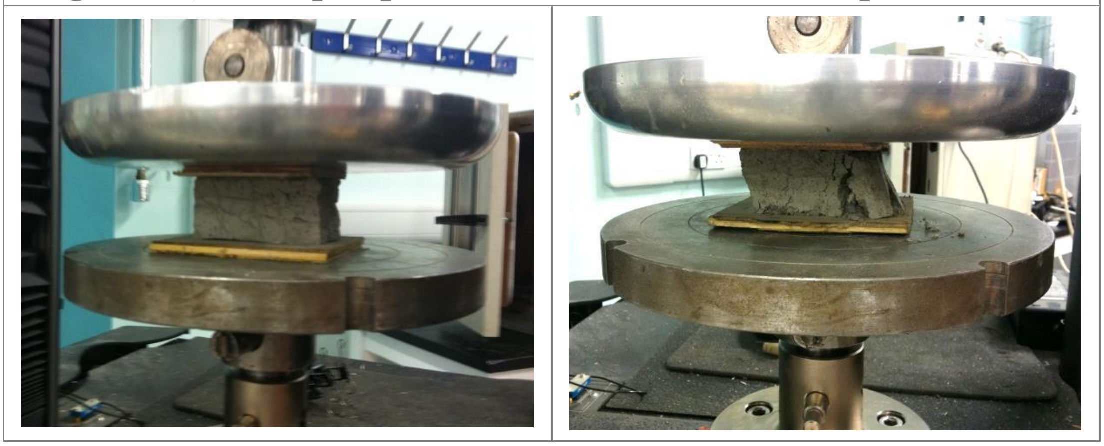

Overall, the results from Batch 1 suggest that while improvements in both flexural strength and compressive strength for Soil U can be achieved with a few of the alginate products at a 0.1% dosage, in most cases the results obtained are relatively similar to that of the control batch. The fact that PR22 for example offers a visible improvement in compressive strength while PR24, also sourced from the stem of the *LH* seaweed, suggests that other alginate properties such as the specific M/G ratio and viscosity may also play a role in the interaction between the alginate and the soil. In theory, a higher viscosity, high molecular weight alginate would provide longer polymer chains and hence lead to more crosslinking sites per chain. However, a high viscosity can also have a negative impact since the tortuous nature of the long polymer chains can inhibit potential interactions between the polymer and the clay by simply coating the clay particles but without creating sufficient inter-particle bridging to improve the overall strength of the structure. This is observed by Pongjanyakul and Puttipipatkhachorn (2007) in aqueous sodium alginate/smectite systems where stronger interactions were found between silicate particles and a low viscosity alginate compared to a high viscosity alginate of the same M:G composition. This may explain why PR24, which is a high viscosity product, has less of an impact than PR22 which is a medium viscosity product. This may also explain why the commercial alginate (AC), which has a similar M/G composition to PR22 but a much higher viscosity, produces inconsistent results. Furthermore in relating the viscosity of the different products to observations made during mixing, it was also noted during specimen production that the more viscous products, namely AC and PR24, inhibited mixing of the wet soil. This consequently led to less homogenous and poorer quality specimens and this may have contributed to the results. In the case of PR32 and PR52, although these alginates have similar M/G contents to PR22, they also have the lowest viscosities of all the products tested and it is therefore likely that the polymer chains are too small to impart significant improvements. This would suggest that there is an optimum viscosity range in which results are favourable in addition to their being sufficient G content on the polymer chain.

Overall the results support the conclusions of Nugent et al. (2009) that competing nano-scale interactions between polymers and clay particles contribute to overall strength changes. It is therefore likely that in cases where there is an improvement in strength, as per the PR22 specimens, interactions which improve the strength of the soil structure such as biopolymer cross-linking or clay-polymer interactions are more dominant. However, where no improvement is observed or indeed a reduction in strength occurs, this may be caused by the polymer having either an insufficient chain length or cross-linking capability, perhaps allowing other mechanisms which have been shown to reduce soil strength to occur. Such mechanisms include biopolymer induced aggregation or the adsorption of monovalent cations to the clay surface rather than the adsorption of the polymer (Nugent et al., 2009).

6.2.2. Variable 2: Soil Type

The second variable to be studied was the soil type and so in this case, in addition to Soil U, Soils W and V were also studied. A more limited range of alginate products were included: one milled seaweed products, four sodium alginate products (sourced from MBL) and two commercial products. A control batch, without the inclusion of any additives, was included for each of the different soil types and a dosage rate of 0.1% by weight of the dry soil was adopted for all of the polymers.

6.2.2.1. Visual Observations

A summary of the visual observations for Variable 2 is presented in Table 6-9. In general, the Soil W specimens were poorer in quality than the other types with several defects and damaged areas around the corners. This can be seen in Figure 6-20, Figure 6-21 and Figure 6-22. While some of the Soil V specimens displayed minor defects, the overall quality was superior to those of Soil W.

Table 6-9: Variable 2 – Specimen Homogeneity

Specimen	Homogeneity	Specimen	Homogeneity	Specimen	Homogeneity
U	Moderate	V	Moderate	W	Moderate
LHU	Good	LHV	Moderate	LHW	Moderate
PR22U	Good	PR22V	Good	PR22W	Moderate
PR24U	Moderate	PR24V	Good	PR24W	Moderate
PR32U	Good	PR32V	Good	PR32W	Moderate
PR52U	Moderate	PR52V	Moderate	PR52W	Poor?
DAU	Good	DAV	Good	DAW	Moderate
ACU	Moderate	ACV	Good	ACW	Moderate

Photographs

Figure 6-20:W

Figure 6-21: PR22W

Figure 6-22: PR52W

Figure 6-23: V

Figure 6-24: PR22V

Figure 6-25: PR52V

6.2.2.2. Dimensions, Mass & Density

The dry mass of the specimens was found to range between 379 and 453g with variations again being attributed to a loss of material during removal from the mould. All of the specimens experienced a degree of shrinkage during drying, ranging from approximately 3 to 7%. As shown in Figure 6-26, the bulk density values obtained were again relatively similar with all results falling within then 1800 and 2100 kg/m^3 range. However, significant differences in density were observed for several of the W specimens including PR22W, PR24W, PR32W and DAW indicating that the inclusion of theses additives did appear to affect the compaction behaviour for this particular soil type.

Figure 6-26 : Variable 2 – Bulk Density

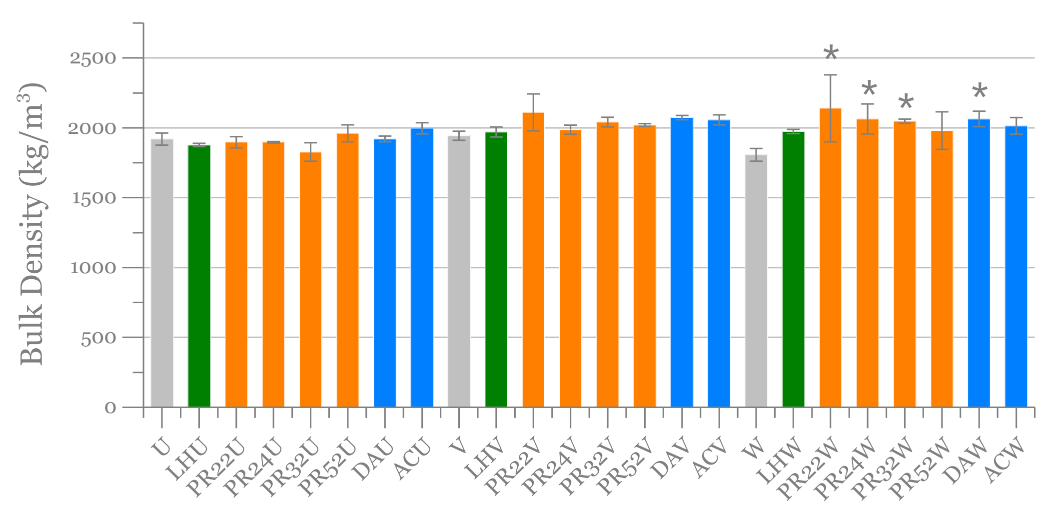

6.2.2.3. Mechanical Properties

The results for the flexural strength tests for Variable 2, comparing the 3 different soil types, are shown in Figure 6-27. Again the failure mode of all specimens was through the propagation of a mid-point fracture. Specimens which offer a statistically significant change in strength compared to the relevant control specimen, in addition to the already discussed U samples include ACV , PR22W and PR52W. Overall the soil W specimens demonstrate considerably lower values than soil U and V, both of which offer flexural strengths within the 0.8 – 1.3 N/mm² range. Overall this is comparable to the flexural results achieved by Galán-Marín et al. (2013) although those authors do not demonstrate any significant flexural strength increases compared to the control soils. In the case of soil W, it would therefore appear that the poorer homogeneity observed for the W specimens in Table 6-9 also translates to poorer flexural strength. However, the significant improvement in strength for PR22W (123% increase compared to the control) would suggest that this particular product helps to increase the soil cohesion. This also correlates with the increase in density observed for this sample.

Figure 6-27: Variable 2 – Flexural Strength Test Results

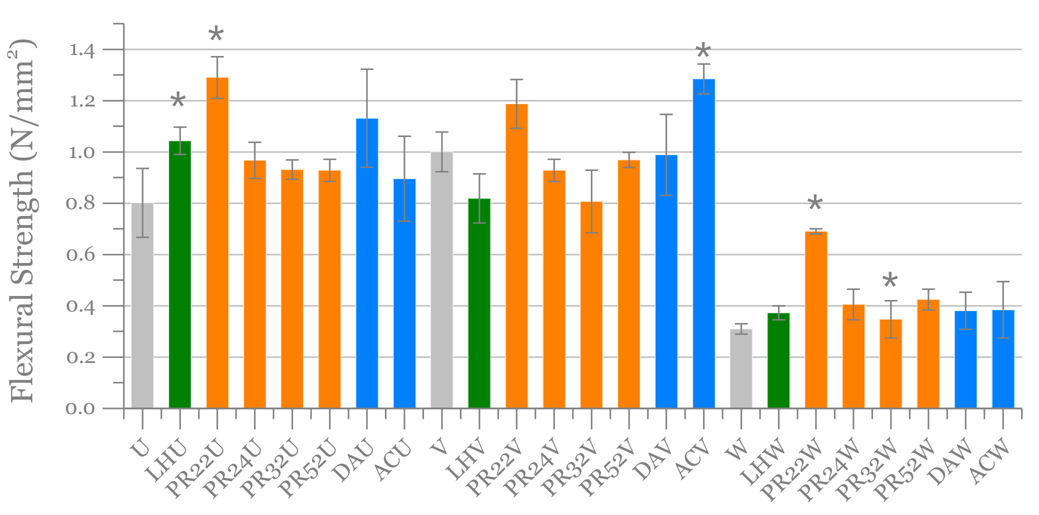

Figure 6-28: Stress-strain plot for W and PR22W (Flexural)

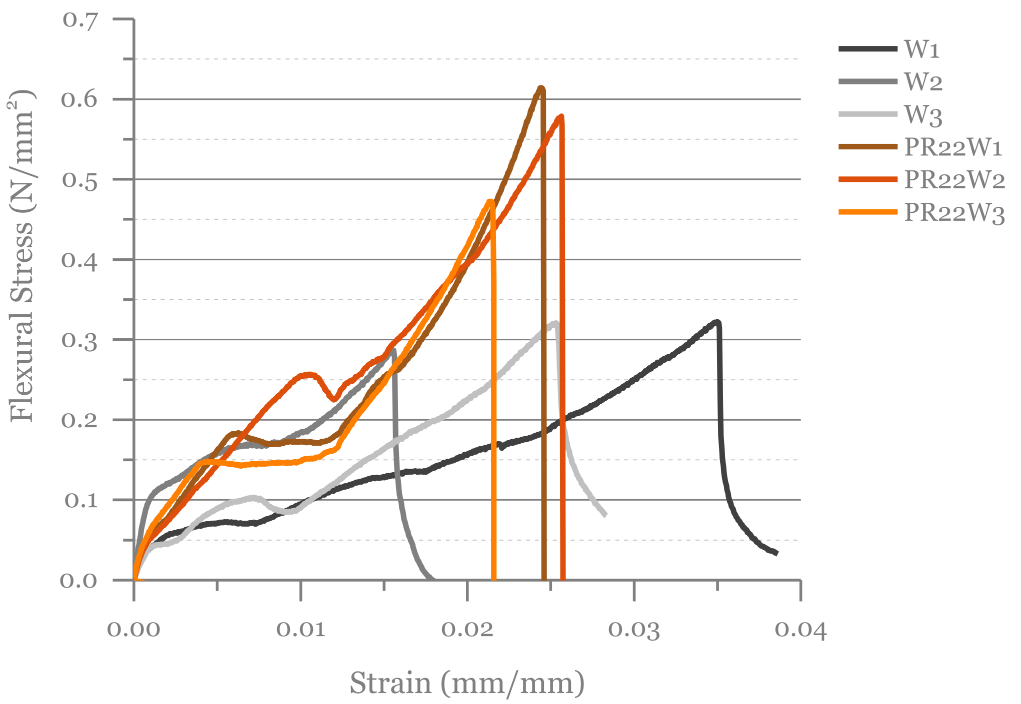

The unconfined compressive strength values achieved, using a correction factor of 0.58, were between 0.5 – 1.7 N/mm^2 (0.8 – 3 N/mm^2 without the correction factor). As shown in Figure 6-29, PR22 again appears to offer the greatest improvement for all soil types. A maximum increase of strength was witnessed for PR22W where an improvement of over 160% was achieved. This is highlighted in the difference between the stress-strain plots for these samples alongside the equivalent controls (Figure 6-30). As for the previous stress-strain plots for soil U (Figure 6-18), after the initial contact adjustment region, a more linear and steeper gradient is observed for the alginate sample suggesting a more even distribution of load and much higher yield stress.

The soil type was also clearly an important factor since all of the W specimens had the lowest values. While all of the alginate types led to a clear improvement in strength compared to the control sample for soil W, for soil V the control sample offered a relatively good compressive strength and apparent improvements were not found to be statistically significant with the exception of PR22. Since soil W has the lowest clay content (16%), this perhaps explains why this control sample has the lowest strength and particle cohesion. However the improvements witnessed upon the addition of alginate suggest that even the relatively small proportion of clay present in soil W is sufficient for interaction with the alginate to occur. Conversely, for soil U and V the higher clay contents of 31% and 27% respectively appear to provide a sufficient amount of cohesive strength between the soil particles meaning that only certain types of alginate offer any further improvement. It should also be noted that while the majority of specimens were found to have moisture contents of ~ 2% at the time of testing, specimens PR22V, PR52V and PR52W were found to have slightly higher values and this may have decreased the overall compressive strength.

Figure 6-29: Variable 2 – Unconfined Compressive Strength

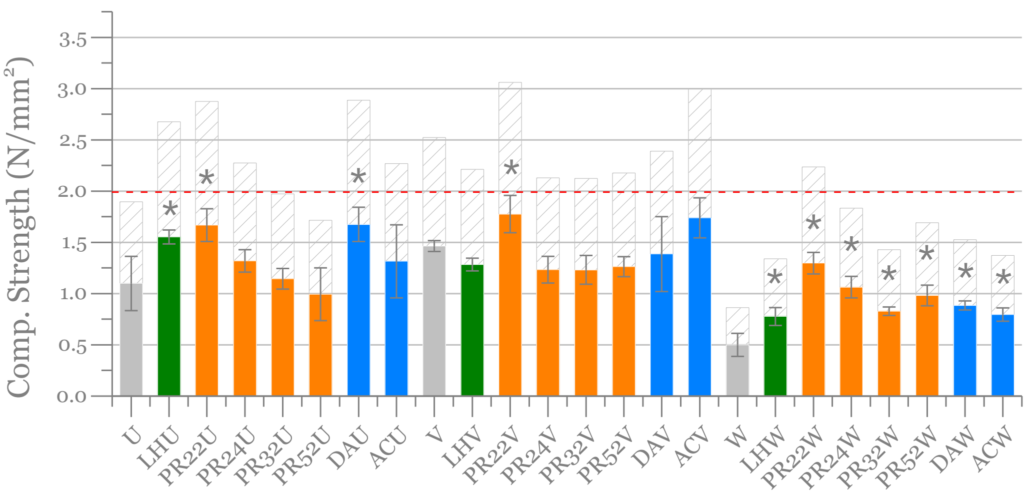

(Correction Factor = 0.58)

Figure 6-30: Stress-strain plot for W and PR22W (Compressive)

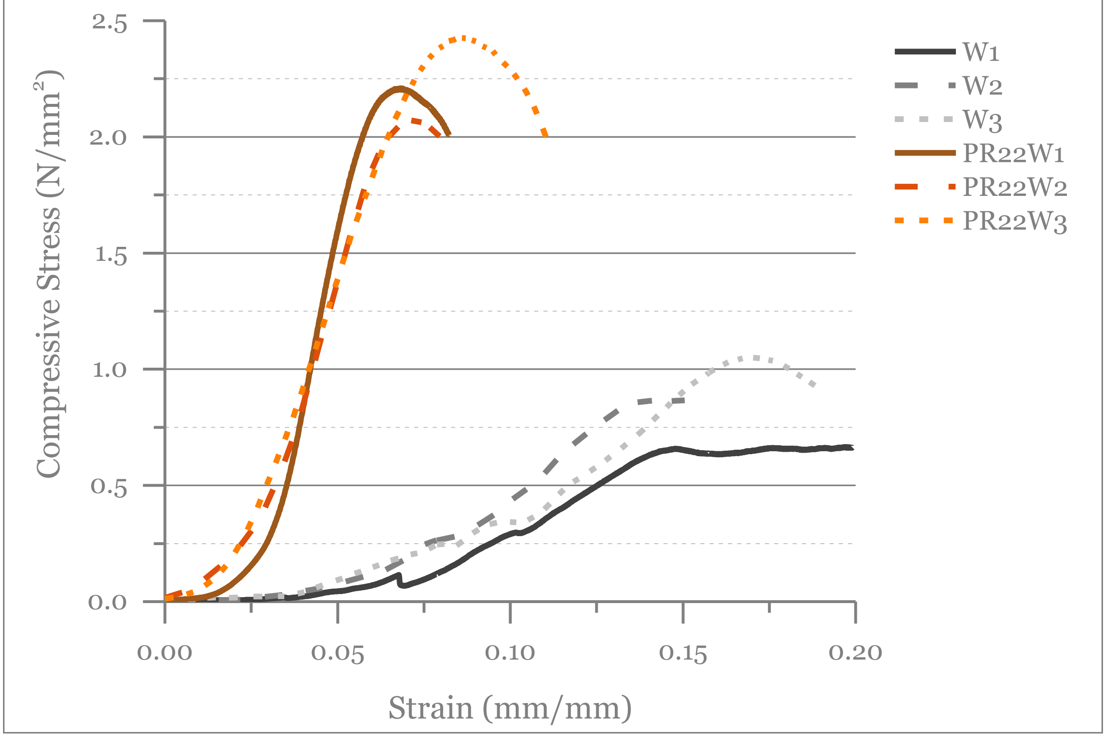

In considering the specific role of the soil, a number of differences in the three soils should be noted. Firstly, in comparing the chemical composition of the soils, soils W and V both have a higher calcium content than that of soil U (Table 3-3). This perhaps explains why soil W demonstrates significant improvements since there is more calcium available to crosslink with the polymer. Although soil V also contains a relatively high quantity of calcium, the crosslinking effects of the alginate appear to be overshadowed by the existing cohesive bonding imparted by the larger clay fraction as evidenced by the high strength values of the control specimen. Relating these findings to recommendations from other sources regarding optimum clay contents, Jiménez Delgado and Guerrero (2007) quote clay proportions ranging from 5 to 40% for adobe and compressed earth blocks. Walker (1995) on the other hand recommends a clay content of 20-35% for effective stabilisation of earthen materials with cement and also reports that increases in clay content can reduce the effectiveness of any stabilising additives due to the formation clay aggregates during mixing. This supports the findings in this study that the magnitudes of strength increases are lower for the high clay content soils however investigation into other clay contents within the 16-27% range would allow the role of the clay fraction to be explored further.

Several authors also give recommendations for the Atterberg limits of soils which are to be used for building purposes. Houben and Guillaud (1994) for example suggest a LL of 25-51% and a PI of 2-31% for compressed earth blocks – ranges which all of the soils within this study fall within. Burroughs (2008) also recommends a LL of ≤35% and a PI of <15%. The importance of PI is further highlighted in the conclusions of Galán-Marín et al. (2013) where it is proposed that success of the best performing soil is attributed to its high illite content (50%) and PI value (15.7%), even though this value is slightly higher than the recommendation by Burroughs (2008). In our study, the overall strength also appears to increase with increasing PI and illite content but this also has a negative impact on the percentage increase in strength when the alginate is added.

Finally, the three soils also have varying pH levels with soil U demonstrating a slightly acidic pH (4.8) while soil V (6.8) and soil W (6.9) are both neutral soils. However based on the mechanical tests alone it is difficult to determine the importance of pH due the complexity of other factors impacting the clay-polymer interactions. A further study where the soil pH could be modified as a controlled variable would therefore be required on order to determine whether the soil pH has a significant effect on any strength improvements.

6.2.3. Variable 3: Alginate Dosage

Given that all of the previous specimens were prepared using a standard quantity of alginate, as well as the indications from the rheology tests that increased polymer dosages would lead to increased strength of the alginate-soil structure, the third variable to be studied was the alginate dosage. Based on the trial studies, alginate dosages of above 1% were found to become unworkable, even with the aid of a mechanical mixer. Hence the dosage study was designed to include dosages of 0.1%, 0.25% and 0.5%. Only two soil types (Soil U and V) were used in this round of tests and a more limited range of alginates including the dental alginate (DA) and commercial alginate (AC), both of which had shown some positive results in the previous tests, and two of the MBL products. Due to issues regarding product availability from MBL, only PR24 and PR32 were used, representing one *LH Stem* and one *LH Frond* product. Although these materials did not display significant improvements for the 0.1% dosage, this provided an opportunity to investigate whether, for these particular products, interaction with the alginate could be improved simply by increasing the polymer dosage.

6.2.3.1. Visual Observations

A summary of the visual observations for the dosage study is presented in Table 6-10. Samples such as ACU (0.25%) offered relatively good homogeneity (Figure 6-32) whilst the same combination of alginate and soil produced at a higher dosage was poor in quality with considerable damage to the corner areas (Figure 6-33).

Table 6-10: Variable 3 – Specimen Homogeneity

Specimen	Homogeneity	Specimen	Homogeneity
U	Moderate	V	Moderate
PR24U (0.1%)	Moderate	**PR24V (0.1%)**	Good
PR24U (0.25%)	Good	**PR24V (0.25%)**	Good
PR24U (0.5%)	Moderate	**PR24V (0.5%)**	Poor
PR32U (0.1%)	Good	**PR32V (0.1%)**	Good
PR32U (0.25%)	Good	**PR32V (0.25%)**	Good
PR32U (0.5%)	Good	**PR32V (0.5%)**	Good
DAU (0.1%)	Good	**DAV (0.1%)**	Good
DAU (0.5%)	Good	**DAV (0.5%)**	Good
DAU (1.0%)	Poor	**DAV (1.0%)**	Moderate
ACU (0.1%)	Moderate	**ACV (0.1%)**	Good
ACU (0.25%)	Good	**ACV (0.25%)**	Good
ACU (0.5%)	Poor	**ACV (0.5%)**	Moderate

Photographs

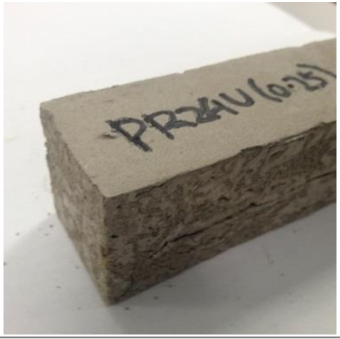
Figure 6-31: PR24U (0.25%)

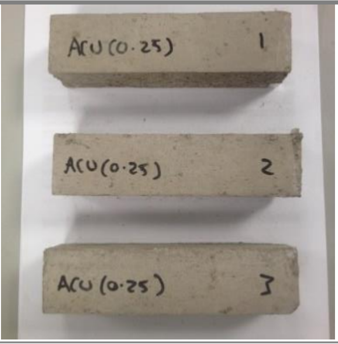
Figure 6-32: ACU (0.25%)


Figure 6-33: ACU (0.5%)


Figure 6-34: ACV (0.25%)


Figure 6-35: ACV (0.5%)


Figure 6-36: DAV (0.5%)

Similar defects were also noted for the ACV specimens as shown in Figure 6-34 and Figure 6-35. Generally speaking, increasing the alginate dosage resulted in an increased number of defects, most likely due to the increased viscosity of the initial mixture. For sample PR24V (0.5%), two of the samples were severely damaged upon removal from the mould meaning that only one specimen was available for testing.

6.2.3.2. Dimensions, Mass & Density

The dry mass of the specimens was found to range between 379 and 451 g and linear shrinkage ranged between 3 and 7%. The bulk density values obtained were again relatively similar with all results falling within the 1600 and 2100 kg/m^3 range (Figure 6-37). Only the 1.0% dosages of the DA product resulted in a statistically significant reduction compared to the control for each soil type.

Figure 6-37: Variable 3 – Bulk Density

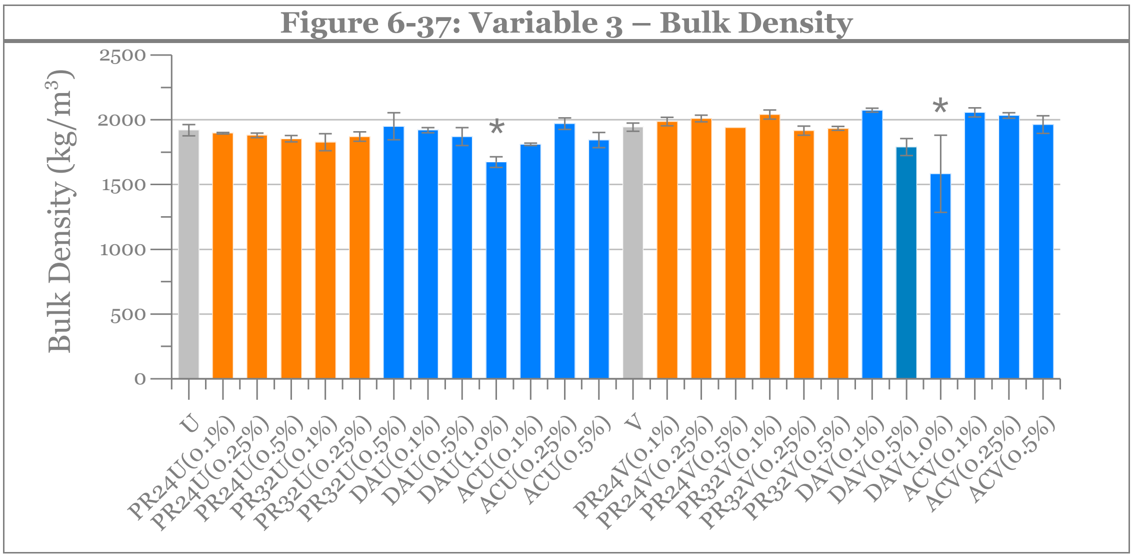

6.2.3.3. Mechanical Properties

The results for the flexural strength tests for Variable 3, comparing different dosages rate for a selected range of products, are shown in Figure 6-38. It should be noted that while the majority of specimens were found to have moisture contents of ~2% at the time of testing, specimens DAU(0.5%) and PR32V(0.5%) had slightly higher values and this may have decreased the overall compressive strength .

Figure 6-38: Variable 3 – Flexural Strength Test Results

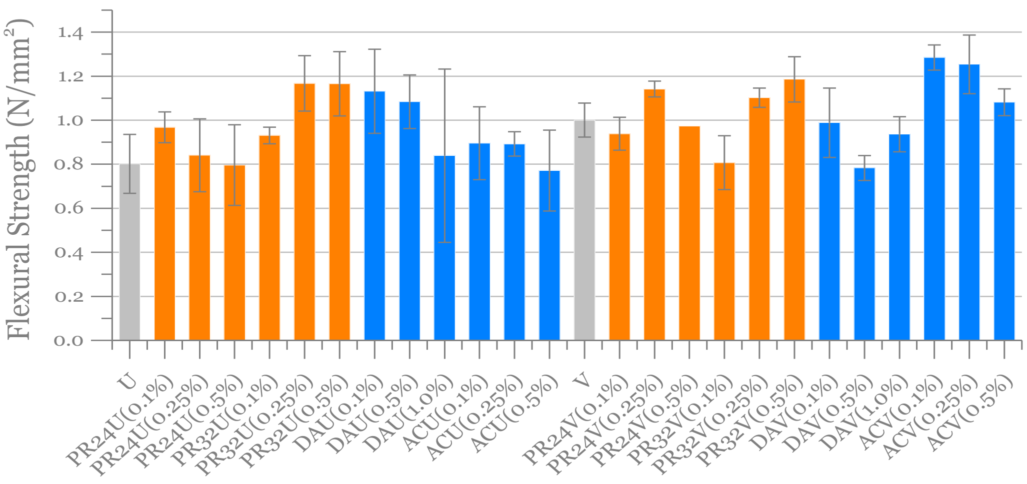

PR24V(0.5%) – Only one sample tested

Compared to the control samples, there were no apparent improvements in strength when the dosage was increased beyond 0.1%. For PR32 while there was an indication of increased strength at dosages of 0.25% and 0.5% compared to the 0.1% sample which performed relatively poorly, the differences were not found to be statistically significant. The flexural stress-strain plots for these particular samples are shown in Figure 6-39. Particularly varied results were found for batch DAU (1.0%), with one of the specimens having a flexural strength as low as 0.5 N/mm^2.

For the unconfined compressive strength, as shown in Figure 6-40, the values achieved using a correction factor of 0.58 were between 0.8 – 1.8 N/mm^2 (1.3 – 3.1 N/mm^2 without the correction factor). The results were inconsistent, with only the DAU (0.1% and 0.5%) and PR24V (0.25%) samples offering a statistically significant improvement over the control sample. While in some cases, such as PR32U, there was an indication of possible increasing strength with increasing alginate dosage, these increases were relatively small and not statistically significant. Overall the dosage study demonstrated that increasing the alginate dosage did not lead to significant increases in strength, with the exception of a few samples.

Figure 6-39: Stress-strain plot for PR32V 0.1 & 0.5% (Flexural)

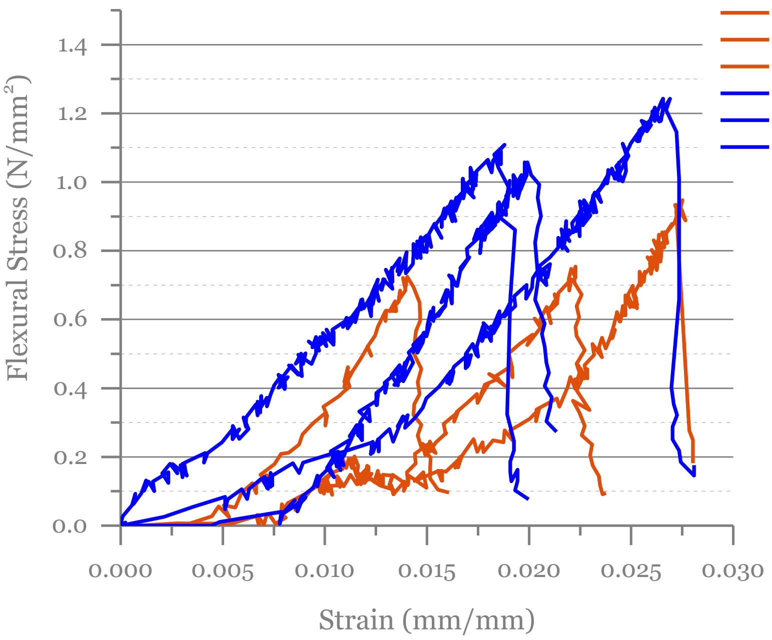

Figure 6-40: Variable 3 – Unconfined Compressive Strength

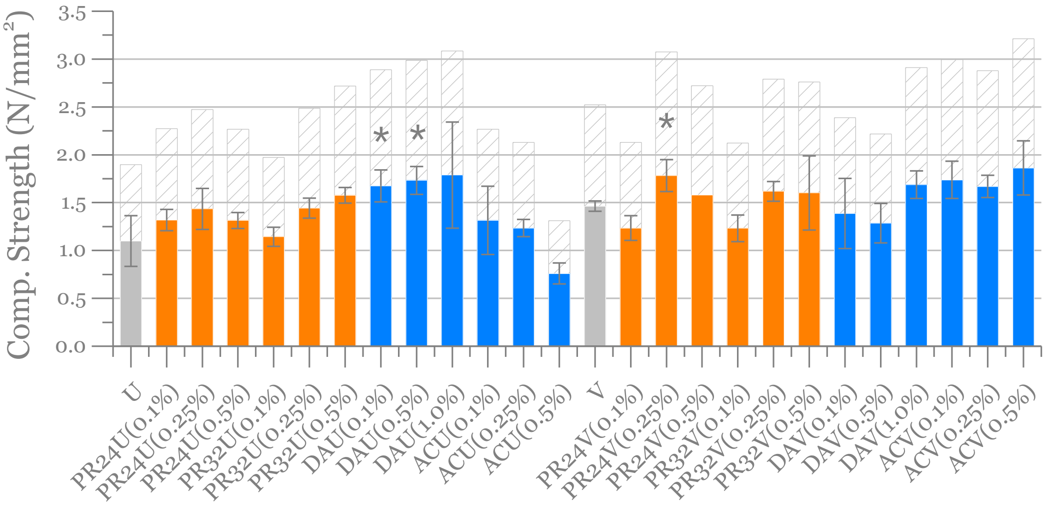

PR24V(0.5%) – Only one sample tested

(Correction Factor = 0.58)

6.2.4. Phase 2 Summary

In concluding the results of the Phase 2 tests, considerable differences in basic specimen properties were found in relation to variables of alginate type, soil type and alginate dosage. While the overall properties were largely related to those of the base material (i.e. soil type), particular alginate products (namely PR22) were able to improve mechanical properties at a dosage rate as low as 0.1%. For soil W, which had relatively poor cohesive and mechanical properties, all of the alginate products result in an increase in compressive strength compared to the control sample. The largest increase was observed for PR22W where both the flexural and compressive strength more than doubled.

Compared to other studies, these specific results are much greater than the maximum relative increases witnessed by Galán-Marín et al. (2010) upon the addition of alginate alone, with the best performing mixture offering an improvement of 69%. On the other hand, results by Chang et al. (2015) showed that addition of xanthan gum at a dosage of 1% increased the compressive strength of clay samples from 0.4 N/mm^2 to 2.5 N/mm^2. Furthermore for a natural soil material, a compressive strength of 3.7 N/mm^2 was achieved using the same dosage of xanthan although comparative data on the strength without the biopolymer is unavailable and so the percentage increase for this material is unclear. Other work by Chang and Cho (2012) demonstrated that the biopolymer glucan could either double or triple the compressive strength the soil studied at dosages of ~2.5% and ~5% respectively. As a further comparison, examples of other strength improvements achieved for earthen materials with other bio-based materials are shown in Table 6-11.

Table 6-11: Comparison to other Bio-based Additives

Additive	Dosage (%)	Soil Type	Max. Improvement (%)	Max. Comp. Strength (N/mm^2)	Ref.
Alginate	0.1% (PR22)	U	50%	1.7	This Study
		V	20%	1.8	
		W	160%	1.3	
Alginate + Lignin	<2%	Errol soil	69%	3.8	(Galán-Marín et al., 2013)
		Ibstock soil	20%	2.5	
		Raeburn soil	-9%	2.2	
Xanthan gum	1%	Clay (85%)	480%	2.5	(Chang et al., 2015)
		Natural Soil (~0% clay)	-	3.7	
		Natural soil (~0% clay)	-	4.8	
Glucan	2%	Hwangtoh (Korean soil)	110 – 140%	2.1 – 2.4	(Chang and Cho, 2012)
	5%	Hwangtoh (Korean soil)	140 – 330%	2.4 - 4.3	
Tannins	1.4%	18% Clay	8 – 19%	1.7 – 2.2	(Sorgho et al., 2014)
Seaweed glue	5%	Red Clay	15%	5.8	(Lee et al., 2008)
Cow Dung	20%	Natural Soil 11% Clay	25%	6.6	(Yalley and Manu, 2013)
Vegetable Residue	10%	Natural Soil >5% Clay	75%	4.4	(Achenza and Fenu, 2006)
Termite Mound Material	80%	Natural Soil	129%	2.2	(Olaoye and Anigbogu, 2000)
Earthworm Cast	8%	Natural Soil	178%	2.3	(Kamang, 1998)

While the results for PR22 are therefore relatively good given the low dosage required to give comparable strength increases compared to other natural materials, the overall compressive strength values are reasonably low. Although it is acknowledged that some of these studies do not discuss the use of correction factors and therefore may not be directly comparable, previous research indicates that unfired clay bricks generally achieve compressive strength values of 1 – 4 N/mm^2 depending on parameters such as moisture content and density (Andy Sutton et al., 2011). All of the alginate bricks therefore fall within the lower end of this range with a few samples achieving strengths of >1 N/mm^2. While this means that most of the samples are within the range of 1 – 1.5 N/mm^2 recommended by Houben and Guillaud (1994) for achieving units which are able to be easily handled on site, they fall below the target value of 2 N/mm^2 recommend by most international standards for compressed earth blocks (Cid-Falceto et al., 2012b). The results are also much lower than those obtained by Galán-Marín et al. (2010) as well as being much lower than values for other stabilised products such as cement and lime stabilised earth bricks. For example Millogo and Morel (2012) report values of 4.5 – 6.5 N/mm^2 for cement dosages of 4-12% while Oti et al. (2009) demonstrates values of 2.7–5 N/mm^2 for lime/GGBS and cement/GGBS stabilised bricks.

In considering UK regulations, minimum unit strength requirements for conventional masonry units to be used in domestic scale buildings are shown in Table 6-12 (Building Standards Division, 2010). While most cement and lime stabilised blocks achieve compressive strength comparable to the minimum requirement for concrete blocks (2.9 N/mm^2), the results achieved for the alginate bricks fall below this requirements. The values in this study are also considerably lower than the requirements of 5-9N/mm^2 for fired clay masonry.

Table 6-12: Required Strengths for Conventional Masonry Units

Masonry Unit	Clay Masonry Units		Calcium Silicate Masonry Units		Aggregate Concrete Masonry Units	AAC Masonry Units
Brick*	6	9	6	9	6	-
Block*	5	8	5	8	2.9	2.9

*for internal, protected wall which is less than 2.7 m in height

6.3. Phase 3 – Brick Prototypes: Further characterisation

Aside from the basic strength characteristics, a selected range of samples were tested regarding aspects such as microstructure, water stability, hygroscopic absorption, thermal behaviour and acoustic properties. The selected samples were those used for

'Variable 2' in Phase 1 as this allowed for the influence of both alginate type and soil type to be studied. Given the general lack of improvement observed for the increased dosages in Phase 1, only the 0.1% samples were included in Phase 3.

6.3.1. Hygroscopic Absorption

The samples used for the hygroscopic absorption tests and the dessicator set-up are illustrates are shown in Figure 6-41. The absorption isotherms for selected samples, illustrated in Figure 6-42 to Figure 6-44, show that the all of the specimens absorb approximately 1-2.5% moisture across a normal indoor RH range of 40-60%. These results were slightly higher than those of Padfield and Jensen (2011) for unfired clay which was shown to absorb around 0.8 – 1.3%. Nonetheless, the samples in this study appear to have better sorption properties than common fired bricks and concrete which absorb 0 – 0.6% across the same RH range (Padfield and Jensen, 2011). The addition of alginate does not appear to drastically affect the sorption properties since most of the results fall within ±0.5% of the equivalent control value sample. This finding is in agreement with other studies which argue that the hygroscopic behaviour is linked primarily to the properties of the soil and the type of clay minerals present (McGregor et al., 2014b). Further investigation regarding the water vapour permeability and moisture buffering values would however be required in order to fully characterise the humidity buffering behavior.

Figure 6-41: Absorption test set-up

Figure 6-42: Hygroscopic Absorption – Soil U

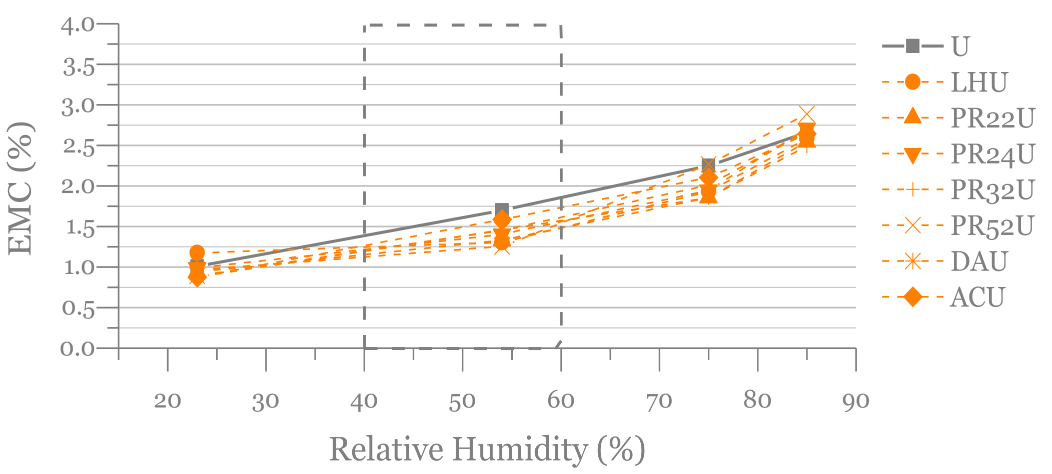

Figure 6-43: Hygroscopic Absorption – Soil V

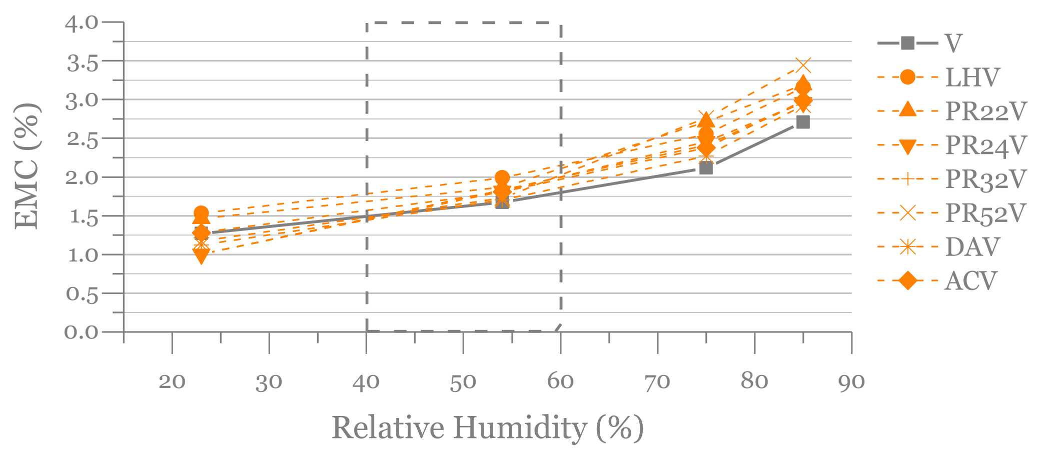

Figure 6-44: Hygroscopic Absorption – Soil W

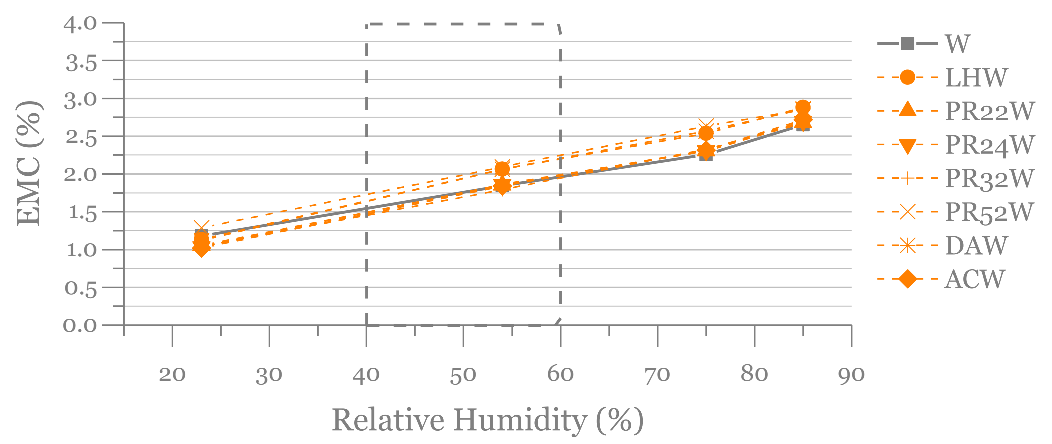

6.3.2. Thermal Properties

The measured values for specific heat (C_p), thermal diffusivity (α) and thermal conductivity (λ) are shown in Figure 6-45 and Table 6-13. Only the U soils were studied, with specimens PR22U and DAU selected based on the compressive strengths achieved in the previous mechanical tests. At a reference temperature of 23°C, all of the samples displayed relatively similar behaviour with thermal conductivity values falling within the 0.75 to 0.79 W/(m·K) range. At higher test temperatures, above the typical range likely to be experienced within a building, there were greater deviations between the specimens with the two alginate samples demonstrating slightly higher thermal conductivities than the control.

Figure 6-45: Measured Thermal Conductivity Values

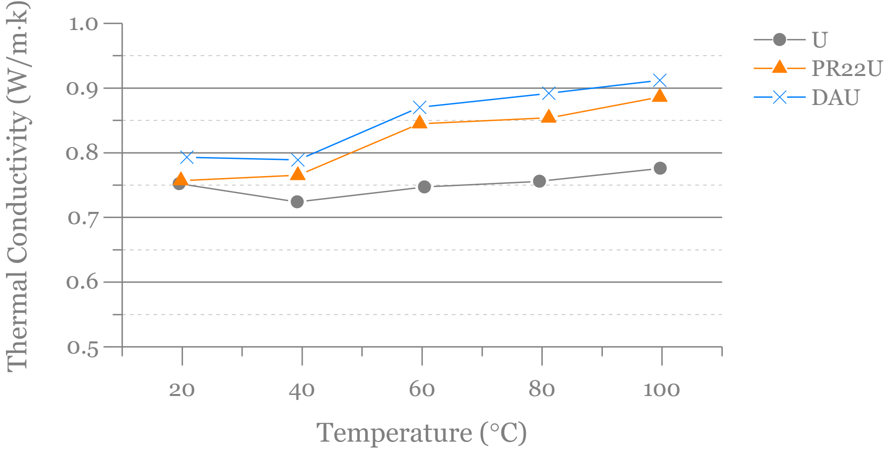

Table 6-13: Thermal Properties

Specimen	Bulk Density	Specific Heat (23°C)	Thermal Diffusivity (23°C)	Thermal Conductivity (23°C)
	(kg/m³)	J/(kg ·°K)	(mm)²/s	W/(m·K)
U	1600	870	0.54	0.75
PR22U (0.1%)	1590	900	0.53	0.76
DAU (0.1%)	1680	900	0.52	0.79

In considering the modelled values, the estimated thermal conductivities for a wider range of specimens, based on Equation 11, are illustrated in Figure 6-46. These results were based on the measured bulk densities of the specimens and assuming moisture contents of between 1-2.5% across the normal indoor humidity range as determined from the hygroscopic absorption tests. The variations in these results are therefore caused primarily by variations in material density. However, if the brick were to be industrially produced it would be assumed that more controlled compaction would allow for more similar densities to be obtained. Therefore based on an average density of 1900 kg/m^3, it would be expected that the bricks would achieve thermal conductivities of between 1.15 and 1.25 W/(m·K).

Figure 6-46: Estimated Thermal Conductivity Values

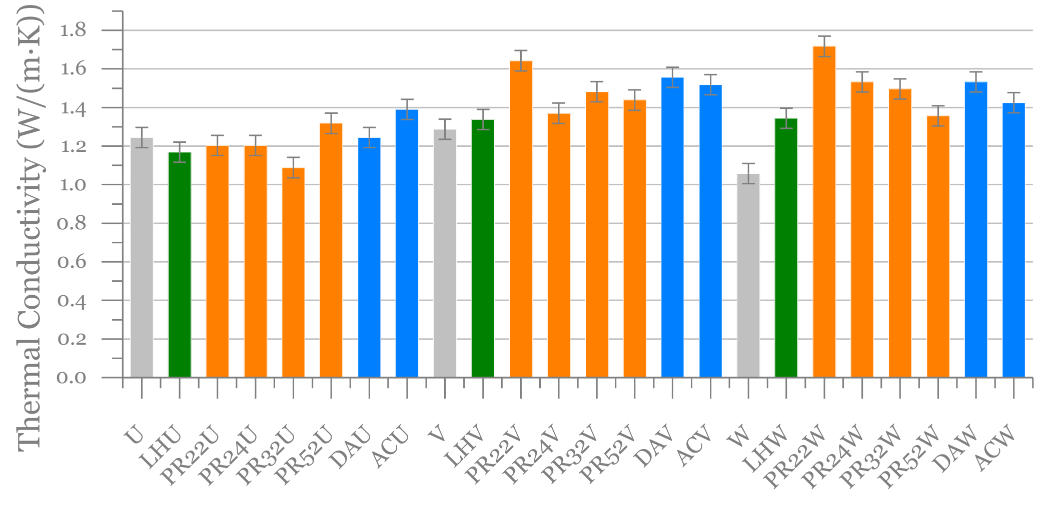

These results are higher than the measured values for specimens U, PR22 and DAU which is likely due to the lower density of the small scale disc samples. Indeed adjusting for density within the estimation model gives corresponding values of 0.78 – 0.87 W/(m·K) which are closer to the measured values. In comparing these measured and modelled results to other building materials, as show in Figure 6-47, the values for the alginate bricks are comparable with those for other high density earth masonry products, such as calcium silicate bricks and dense concrete materials, but greater than typical values for fired bricks and lightweight concrete.

Figure 6-47: Thermal Conductivity for Masonry Materials

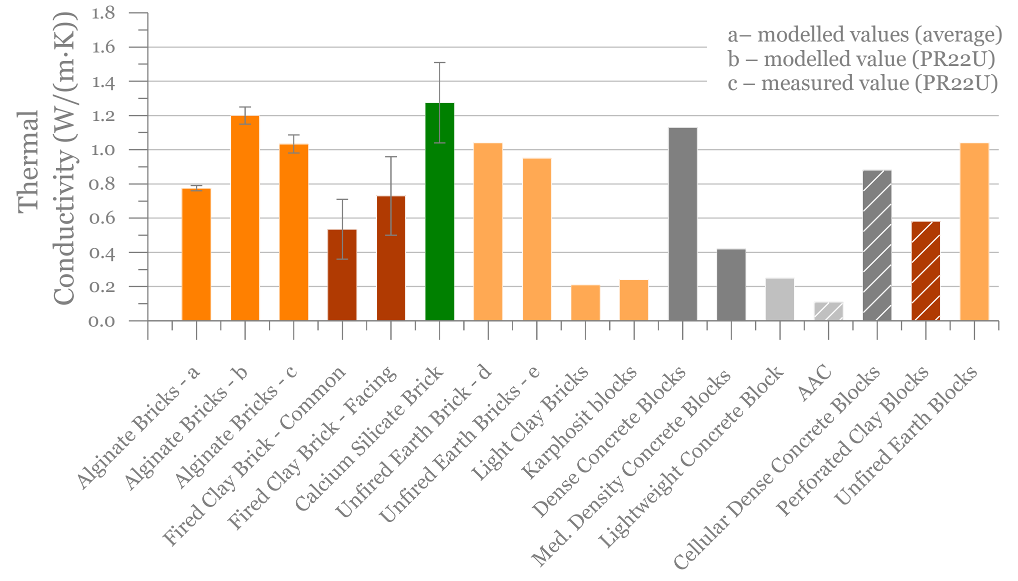

While this relatively high thermal conductivity, compared to conventional bricks or block-work, would perhaps be seen as a disadvantage for walls forming part of a building external envelope, for an internal partition this may be less of an issue. In fact in this scenario a greater heat storage capacity may be more advantageous than a low thermal conductivity. In this case the specific heat capacity of the alginate bricks (using the PR22U sample as an example) is ~900 J/(kg ·°K). This is within the range of 800 -1000 J/(kg ·°K) reported by Houben and Guillaud (1994) for unfired earth and similar other materials like brick and concrete. For a monolithic, unplastered wall with a thickness of 100m, the calculated '*K*' values for the alginate bricks, with a density of 1900 kg/m^3, are shown in Table 6-14 alongside values for other masonry materials. Assuming a thermally active thickness of 50mm, these estimations indicate that the alginate bricks would offer a greater heat storage capacity per unit area of wall than both fired bricks and lightweight concrete blocks while having a slightly lower value than dense concrete block-work.

Table 6-14: Thermal Mass Comparison (100mm thickness)

Specimen	**Alginate Bricks (0.1%)**	**Fired Brick**	**Dense Concrete**	**AAC**
Density (kg/m^3)	1900	1700	2300	600
Specific Heat (J/kg ·°K)	900	800	1000	1000
'K' value (kJ/m^2·°K)	**855**	**680**	**1150**	**300**

6.3.3. Acoustic Properties

The calculated SRI values for the specimens are summarised in Figure 6-48 showing the variation with frequency for the highest density and lowest density specimens. Based on a wall thickness of 100mm and an average density of 1900 kg/m^3, the SRI at 500 Hz is approximately 49 dB.

Figure 6-48: Summary of SRI values

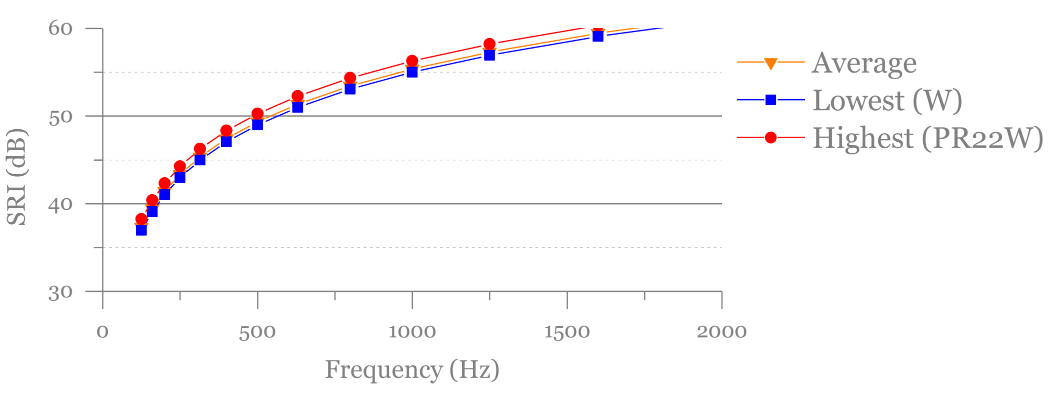

A comparison of the estimated SRI values for the alginate bricks and other walling systems, using manufacturer's data, is also shown in Figure 6-49. The values presented are for walls with an exposed finish however in practice it is possible that an unfired brick partition would also include a finishing material such as plaster. This can further improve the SRI value by reducing the number of gaps and increase the air tightness of the wall construction (McMullan, 2007).

Figure 6-49: Comparison of SRI values

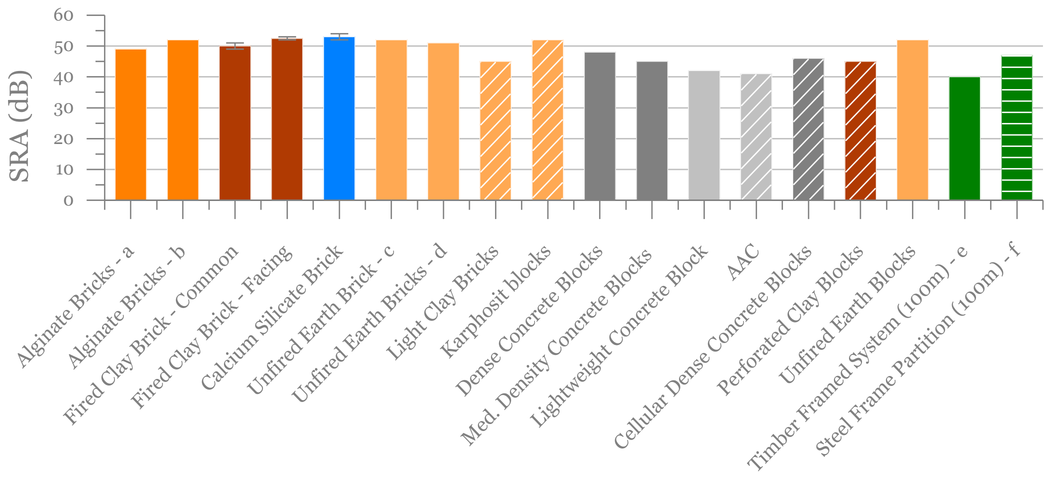

a – modelled values (this study)
b – modelled values (Galán-Marín et al., 2010)
c – modelled values (IBSTOCK 'Ecoterre')
d – modelled values (Claytec earth brick)
e & f – based on 100mm wall with 12.5mm Gyproc SoundBloc and 25mm insulation

Nonetheless, from these results the estimated sound reductions for the alginate brick are comparable with most other masonry systems, aside from lightweight concrete products which are typically poorer acoustic due to their lower density. The alginate bricks also offer superior values to framed systems of a comparable thickness, even with the inclusion of acoustic insulation. Based on the densities of the prototypes produced, the alginate stabilised brick would therefore provide sufficient airborne sound insulation to meet the 43dB requirement for internal partitions within a dwelling. However the acoustic insulation offered would be insufficient for separating walls between dwellings where a more stringent reduction of 56 dB is required (Scottish Government, 2015). As with a concrete block construction, an increased wall thickness, acoustic insulation and dry-lining or indeed a cavity wall construction would therefore be required in this scenario.

6.3.4. Microstructure

Prior to the microstructural analysis, fragments of the brick specimens were sputter coated in gold as shown in Figure 6-50. The resulting SEM micrographs for soils U, V and W are shown in Figure 6-51 to Figure 6-53. In the case of soil U, the control and alginate containing samples are relatively similar, showing an irregular fracture surface with aggregates of varying sizes. A mixture of both edge-to-edge and edge-to-face orientation of the clay particles can also be seen in all samples. This suggests that this dosage (0.1%), the polymer does not visibly affect the clay microstructure. For soil V, all of the samples again show agglomerates of varying sizes. Clay bridges around the larger silt and sand particles can even be seen in some areas as shown in Figure 6-52a. This is likely due to the higher clay content of soil V which facilitates cohesion between the silt and sand particles (Attou et al., 1998), even without the addition of the alginate. For soil W, the control sample appears to have a relatively flat fracture surface while the alginate containing samples show a more aggregated texture, particularly or samples PR22W, PR24W and ACW. This suggests that in these cases the inclusion of the alginate may be helping to promote particle linkages.

Figure 6-50: Gold coated specimens

Figure 6-51: SEM Images – U

		x50 -100	X1000-2000
U	U	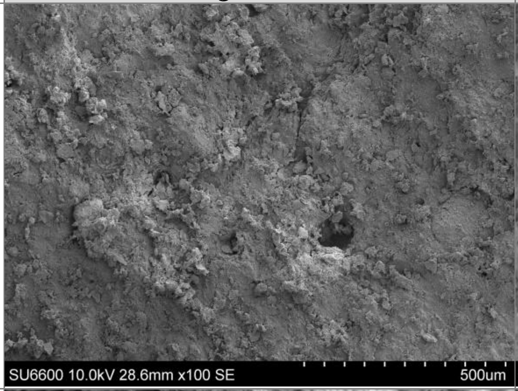	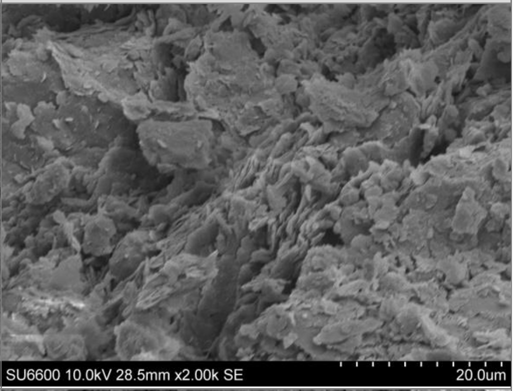
	LHU	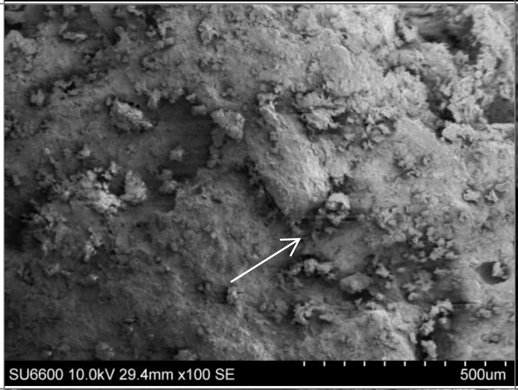	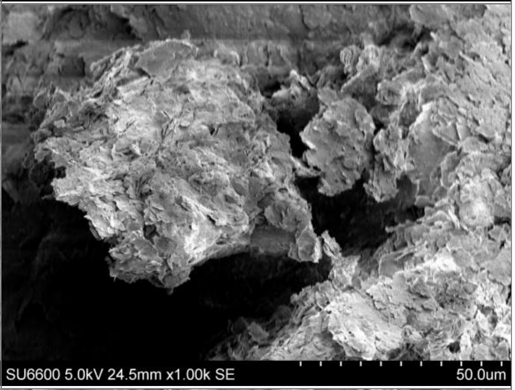
	PR22U	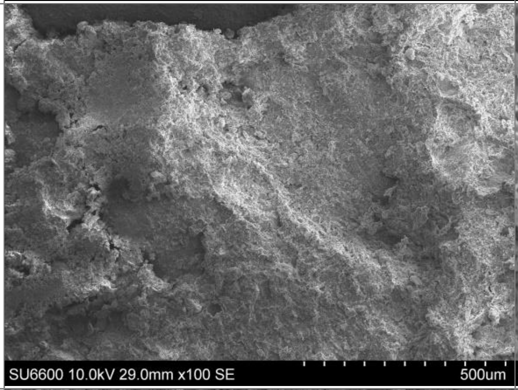	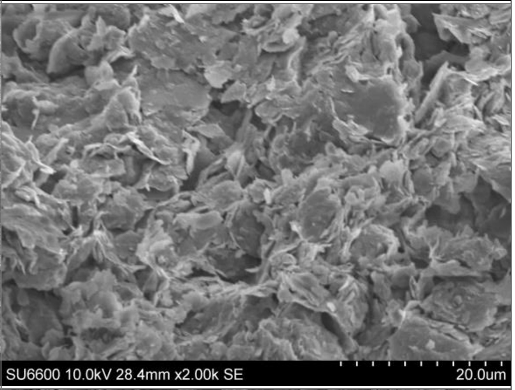
	PR24U	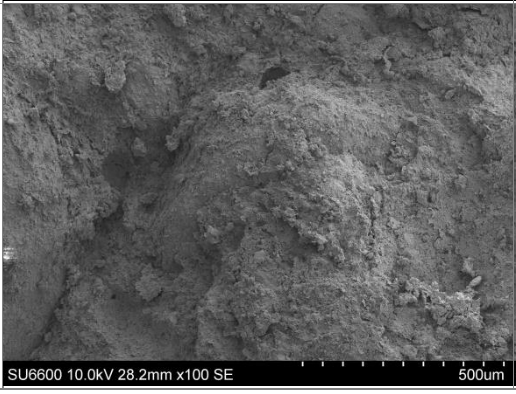	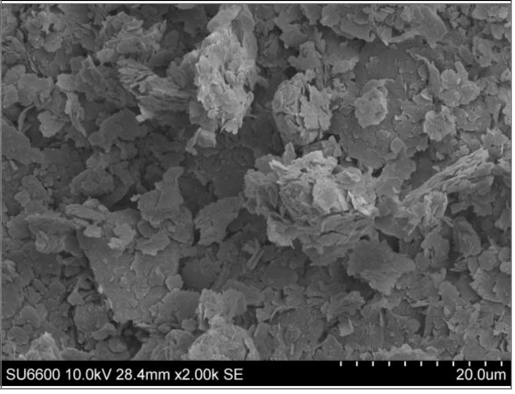

	PR32U	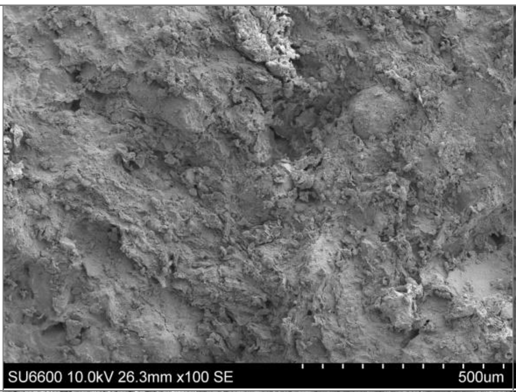	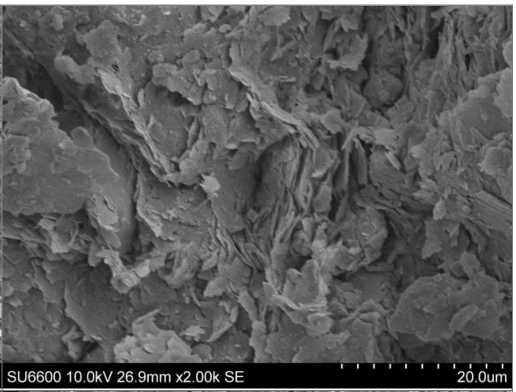
	PR52U	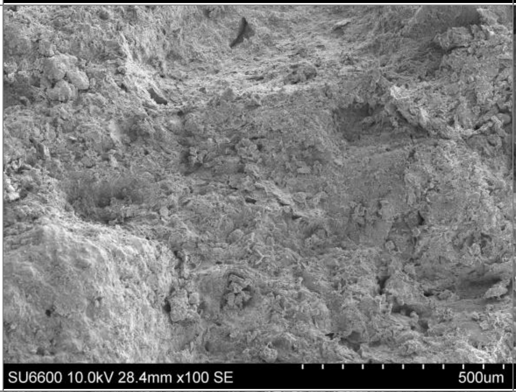	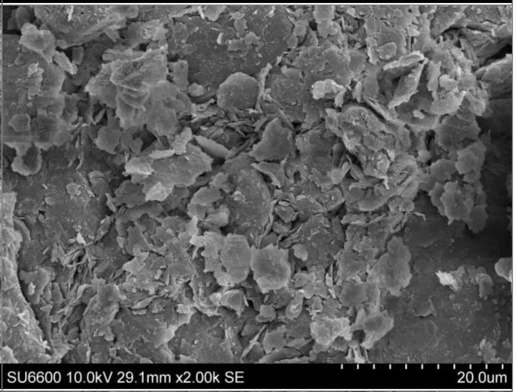
	DAU	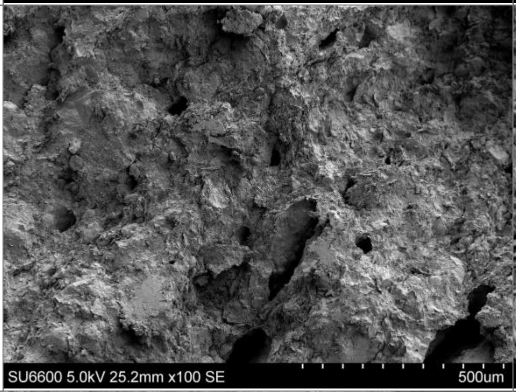	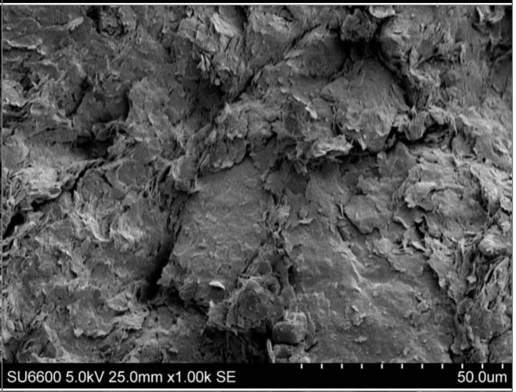
	ACU	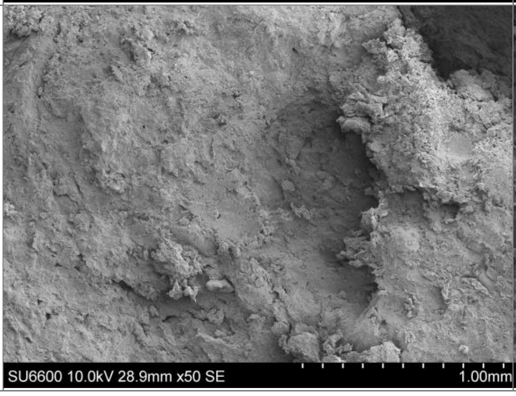	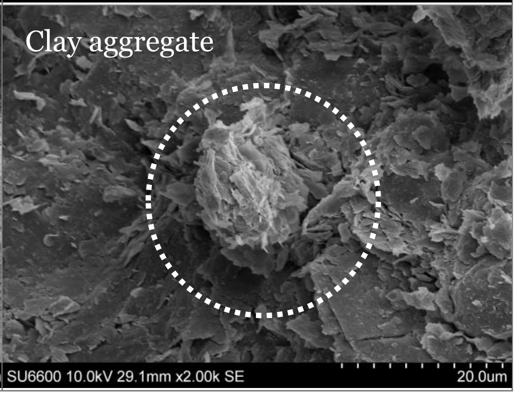

Figure 6-52: SEM Images – V

		x50 -100	X1000-2000
V	**V**	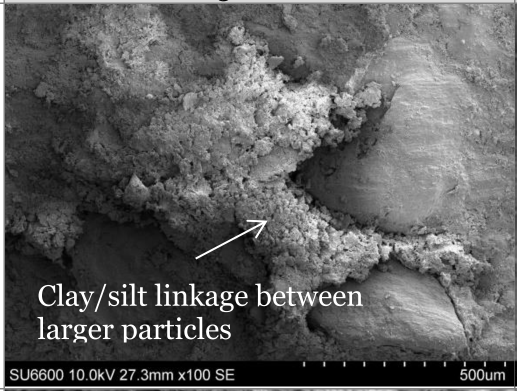	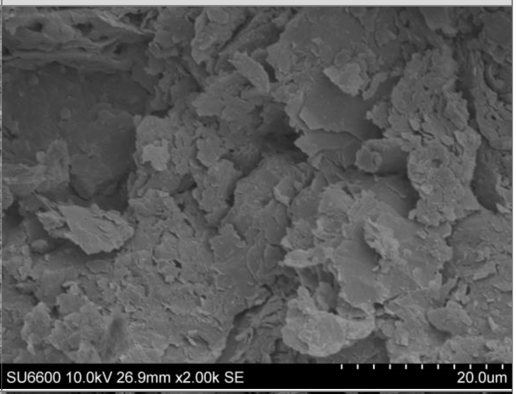
	LHV	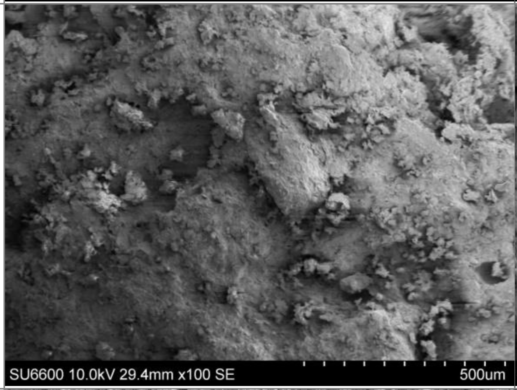	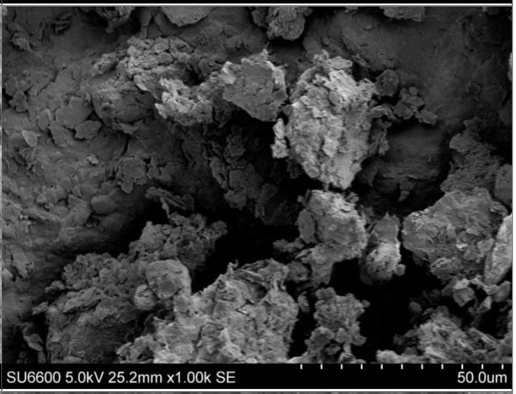
	PR22V	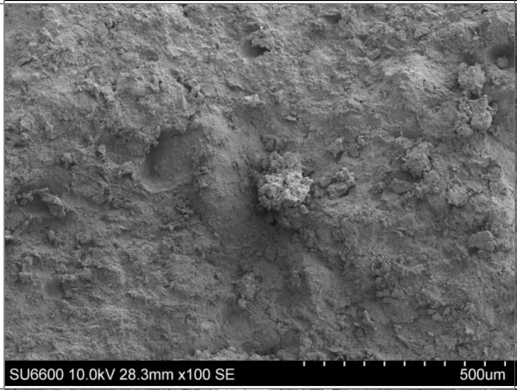	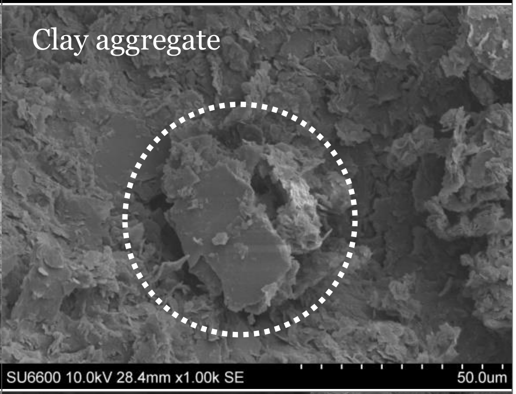
	PR24V	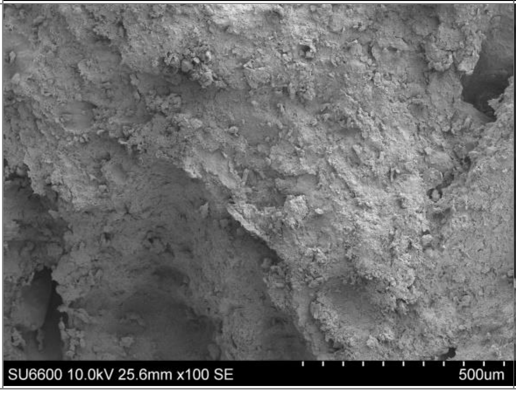	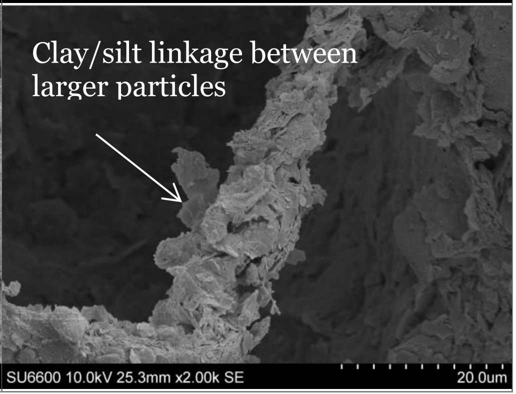

	PR32V	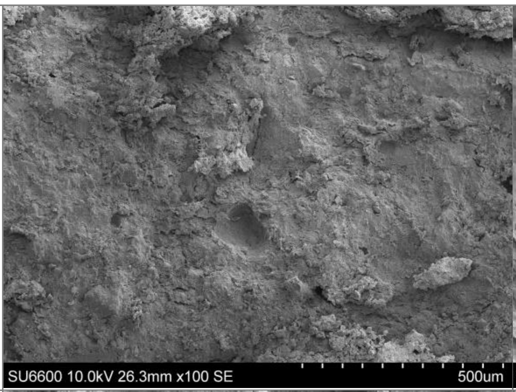	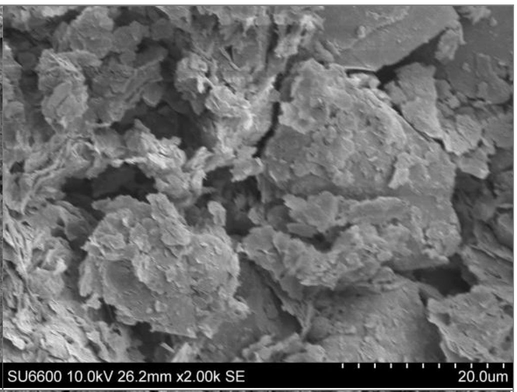
	PR52V	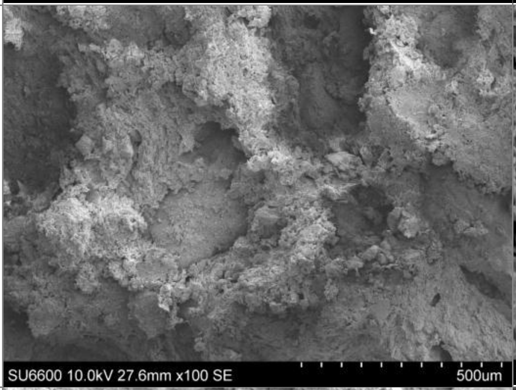	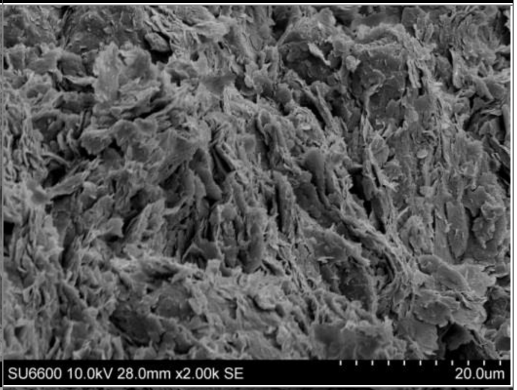
	DAV	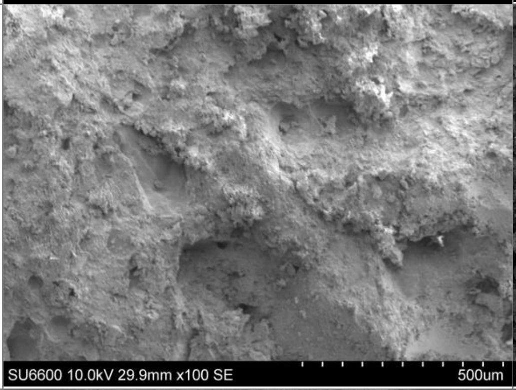	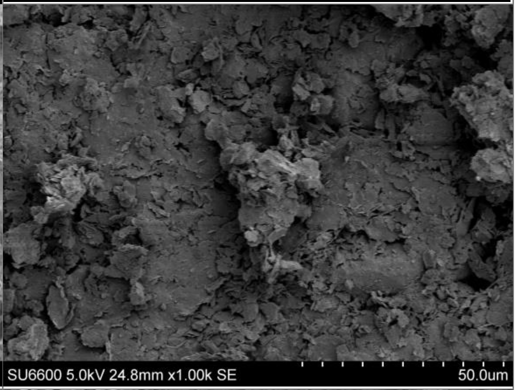
	ACV	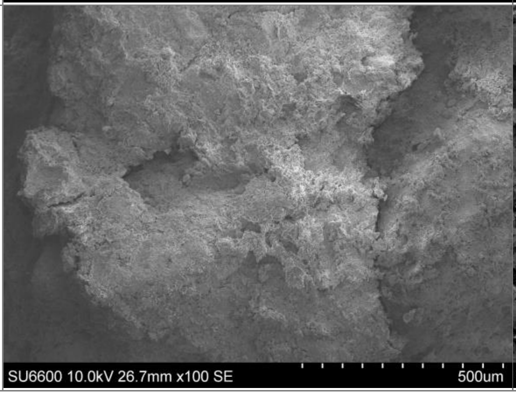	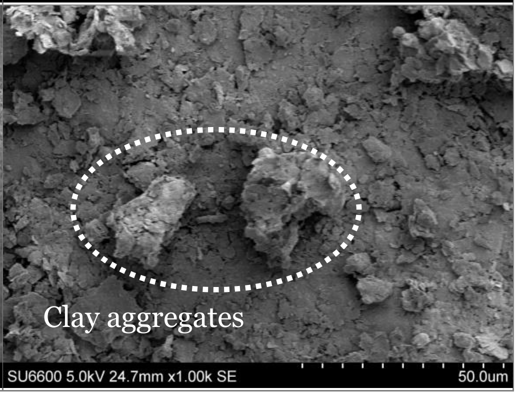

Figure 6-53: SEM Images – W

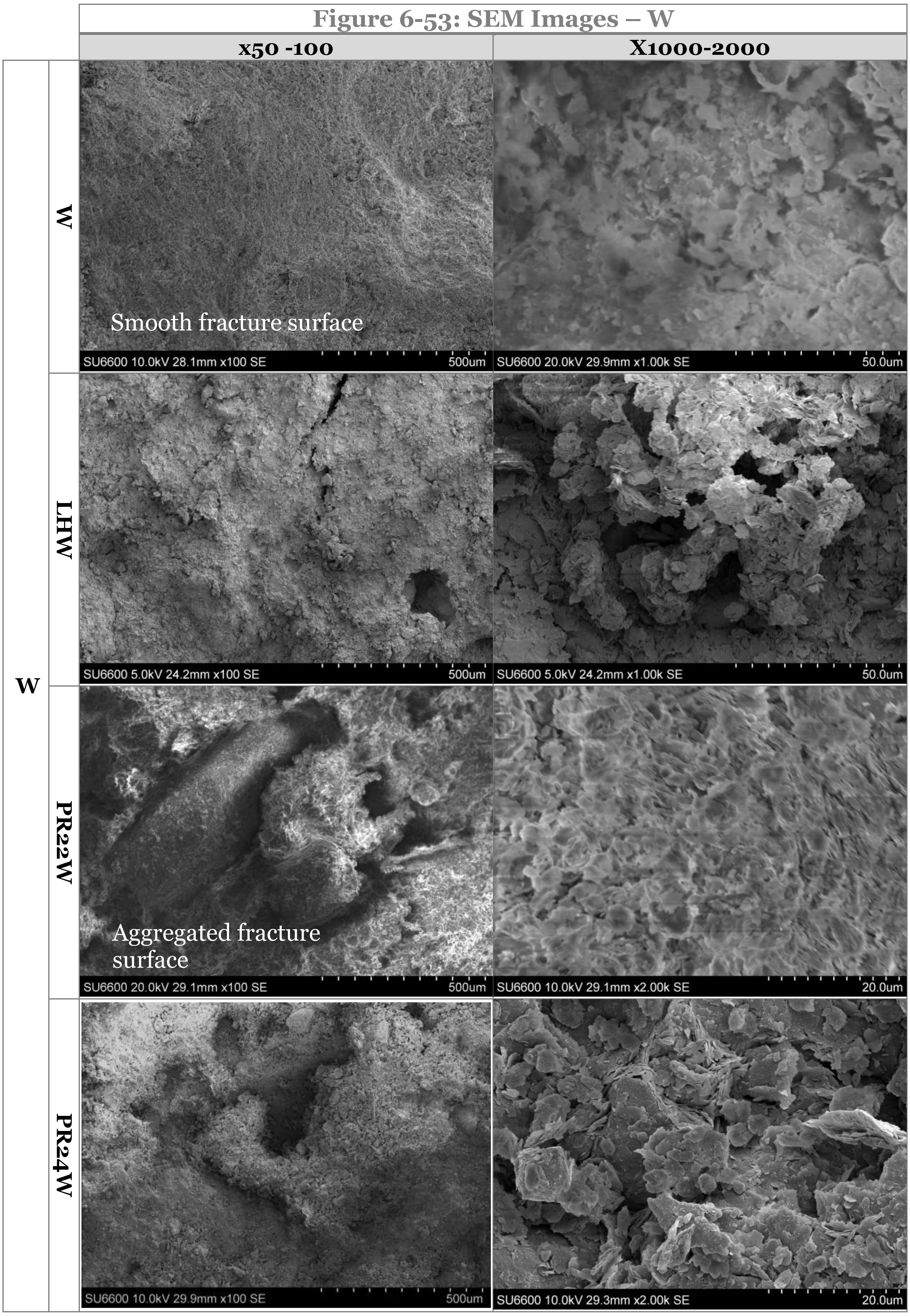

	PR32W	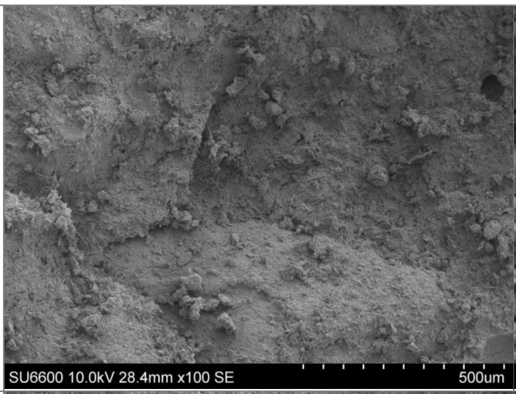	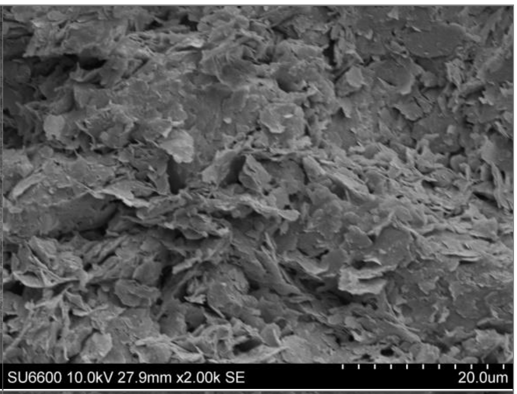
	PR52W	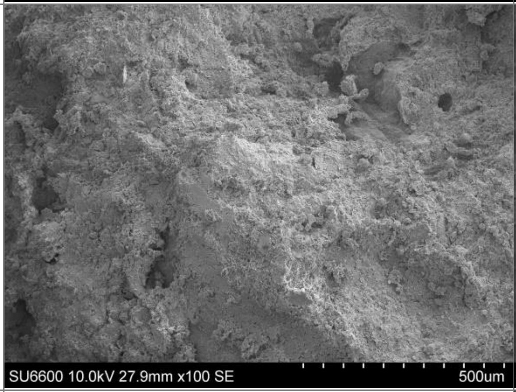	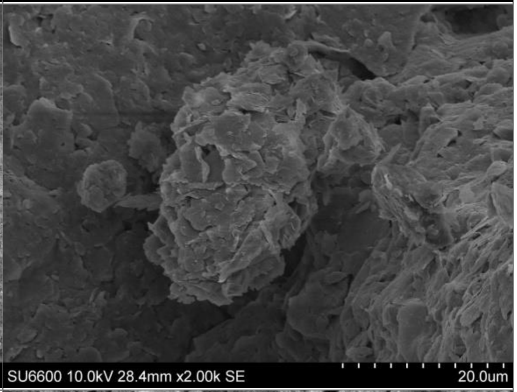
	DAW	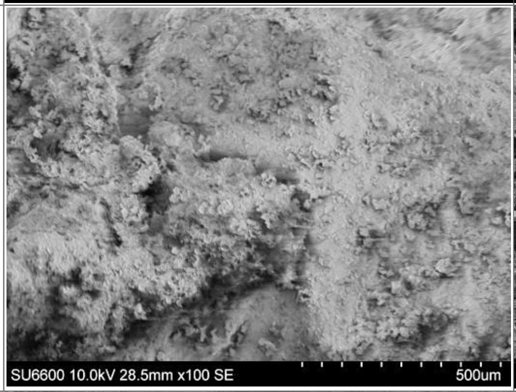	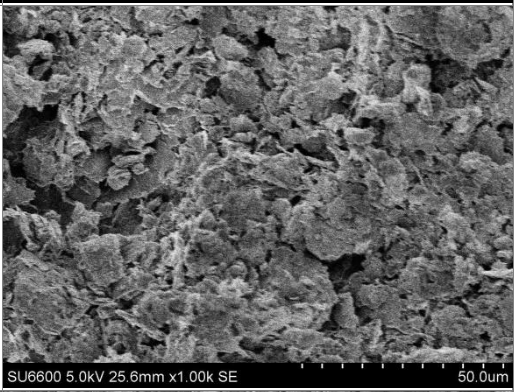
	ACW	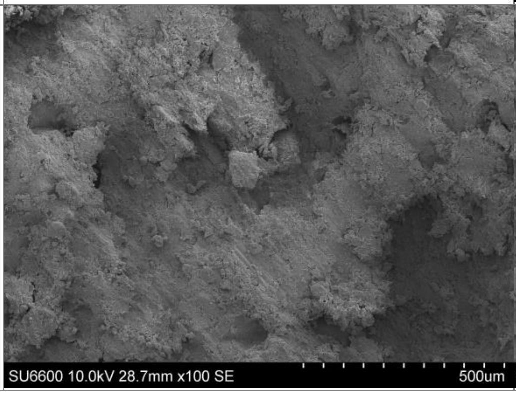	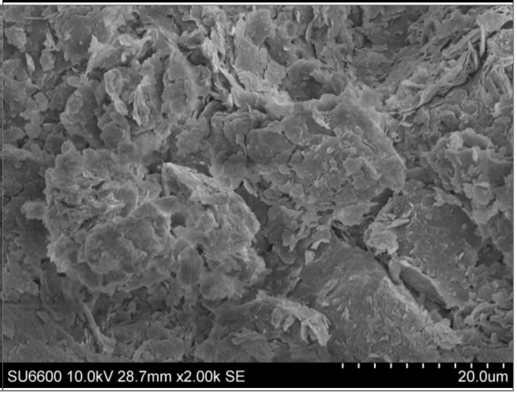

Overall the controls for soils U and V appear to have a coarser microstructure than soil W which shows a relatively flat surface indicating a clean break during fracture. Such observations can be linked due the higher clay content of soils U and V which promotes particle cohesion and aggregates the material. This perhaps explains why the increases in strength seen for soils U and V are relatively minor since there is already a relatively cohesive matrix formed by the existing clay fraction. On the other hand for soil W, where more dramatic increases in strength are observed, there is a more obvious change in microstructure supporting the fact that the addition of alginate leads to improved particle cohesion.

6.3.5. Phase 3 Summary

In summarising the outcomes of Phase 3, although not all of the samples were tested, some general conclusions can be made. Firstly, the results from this study support the findings from other investigations which show that unfired clay has superior hygroscopicity to conventional ceramics and concrete. Furthermore, unlike cement and lime stabilised soils where the moisture buffering properties can in fact be hindered due to the inclusion of the stabilisers, the use of the alginate at the 0.1% dosage did not appear to affect the moisture absorption behaviour of the bricks. In relation acoustic performance, since this is a property which is governed primarily by the density and thickness of the construction, the inclusion of alginate again did not affect the SRI. The SEM study also revealed some apparent changes microstructure, particularly for the W soils, where the most dramatic changes in strength during the Phase 2 tests were also observed. However a more detailed study of clay-biopolymer interactions would be required in order to assess structural changes in more quantifiable manner.

6.4. Phase 4 – Commercial Feasibility

6.4.1. Economic Potential

The results from the cost modelling calculations based on existing data by Morton (2008) and production cost information supplied by MBL are presented in Figure 6-17. Further details of the cost calculations are also provided in Appendix F. All results assume a unit density of 2000 kg/m^3.

Table 6-15: Cost Estimations – Bricks (LH)

	Unit Type (based on a 100mm thick wall)	**Standard Unit**	**Standard Unit + 0.1% alginate**	**Standard Unit + 0.5% alginate**	**Standard Unit + 1.0% alginate**
		(£/m^2)	(£/m^2)	(£/m^2)	(£/m^2)
Bricks	UK Industrial Mass-Produced Earth Bricks	10.40 - 11.05	10.61 – 11.26	11.50 – 12.15	12.60 – 13.25
	UK Small-scale Mass-Produced Earth Bricks	28.45 – 60.46	28.66 – 62.80	29.52 – 61.53	30.65 – 62.66
	One-off Hand-made Earth Bricks	108.23 – 162.34	108.44 – 162.55	109.33 - 163.44	110.43 – 164.54
Blocks	UK Large-scale mass-produced Earth Blocks	4.78	4.99	5.88	6.98
	UK Small-scale mass-produced Earth Blocks	22.14 - 41.51	22.35 – 41.72	23.24 – 42.61	24.34 – 43.71
	One-off Hand Moulded Earth Blocks	108.23 - 162.34	108.44 – 162.55	109.33 – 163.44	110.43 – 164.54

For industrially produced bricks, the inclusion of alginate based on an alginate cost of £11/kg (based on a *Laminaria Hyperborea* product) and a dosage 0.1% results in a cost increase of approximately £0.21 per m^2. This equates to a relative cost increase of around 2%. In the case of a smaller manufacturer, the lower economies of scale give rise to a higher initial cost per unit meaning the addition of alginate results in an overall increase of less than 1%. In considering higher alginate dosages, as expected, increasing the quantity of alginate added leads to increased costs. However even a dosage of 1%, there is a maximum increase of 17% based on an industrially produced brick. Substituting for a cheaper alginate product, such as an *Ascophyllum Nodosum* product (£8.50/kg) would also give a relative increase of between 1.5% and 14% at dosage rates of between 0.1 and 1% (Appendix F). In considering larger blocks, for the industrially produced scenario the relative increase per m^2 is 4.2% while for the small scale and hand-made units the cost increases by approximately 0.5-0.9% and 0.1-0.2%, respectively. Increasing the dosage by a factor of 10 (i.e. 1% dosage) would render the alginate product £2.20 pounds more expensive per m^2 than the non-stabilised product.

Figure 6-54 compares the proposed alginate earth bricks or blocks, normalised to a £/m^2 rate, to conventional masonry materials. Based on the industrially produced scenario (Table 6-15), using dosage rates of 0.1-1.0%, the bricks would be comparable to a standard fired brick while the blocks would less than half the cost of lightweight concrete blocks. It should be noted that costs are based only on the additional material costs associated with including alginate in the brick compositions. Costs for additional processes such as the storage and preparation of the alginate solution prior to mixing with the soil have not been included. However estimations indicate that the electricity required for such processes would equate to less than £0.01 per unit.

Figure 6-54: Comparison of Masonry Costs

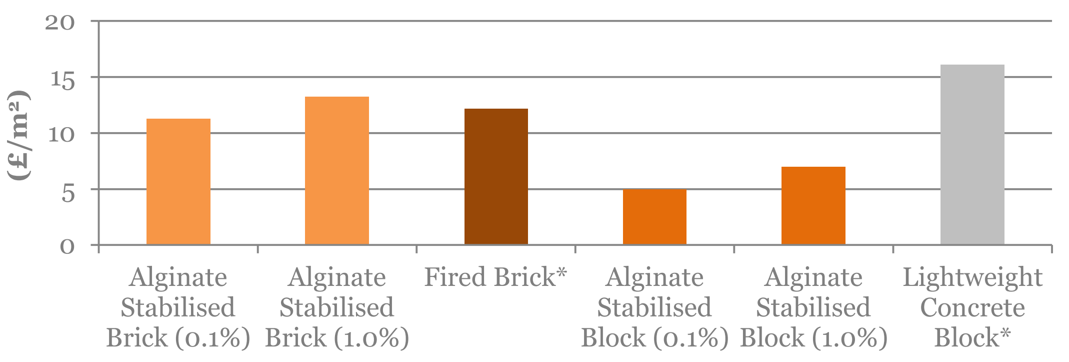

*Cost estimates from Morton (2008)

6.4.2. Environmental Analysis

In terms of the environmental analysis, the calculated embodied energy of the alginate, based the data supplied by MBL (Appendix A), equated to 8.5 and 6.7 MJ per kg of dry alginate product based on a sodium alginate produced from *LH* and *AN,* respectively (Table 6-16). Embodied CO_2 values have also been calculated using standard conversion factors (Hill et al., 2013; DECC, 2016). It should however be noted that the energy calculations for alginate do not take into account any heat recovery nor do they account for the production of any co-products, both of which could be included in a large scale alginate plant and would be expected to reduce the overall consumption.

Table 6-16: Estimated Energy Consumption

	Laminaria Hyperborea	**Ascophyllum Nodosum**
Embodied Energy (MJ/kg)	**8.47**	**6.65**
Embodied CO_2 (kg CO_2e/kg)	**0.51**	**0.38**

These estimated figures are slightly higher than the corresponding values for OPC and lime (4.6 and 5.3 MJ/kg). On the other hand, the values for alginate are significantly lower than other polymer stabilisers. For example, data compiled by Patel et al. (2005) showed that PVOH can reportedly have an embodied energy of approximately 50 – 100 MJ/kg whilst other biopolymers such as thermoplastic starch (TPS) and poly-lactic acid (PLA) have respective values of around 25 and 50 MJ/kg. It is also interesting that the embodied energy value calculated here is much lower that the value for ‘algae’ (20 MJ/kg) used by Galán-Marín et al. (2015). However this ‘algae’ data, sourced from Resurreccion et al. (2012), relates to cultivated micro-algae for biofuel production. Micro-algae requires very different energy and resource inputs to alginate produced from natural seaweed. This is therefore an inappropriate data source and it is therefore not surprising that there is a discrepancy with the estimates for alginate produced in the study .

Combining the values from Table 6-16 with existing data for industrially produced CEBs from Morton et al. (2005), an estimate of the total EE and EC for a standard unfired earth unit with alginate included was calculated (Appendix G). The EC values were not found to be significantly affected for the alginate dosage rage studied. The EE values are however presented in Figure 6-55 and Figure 6-56, alongside other masonry materials.

Figure 6-55: Embodied Energy Estimations – Earth Masonry

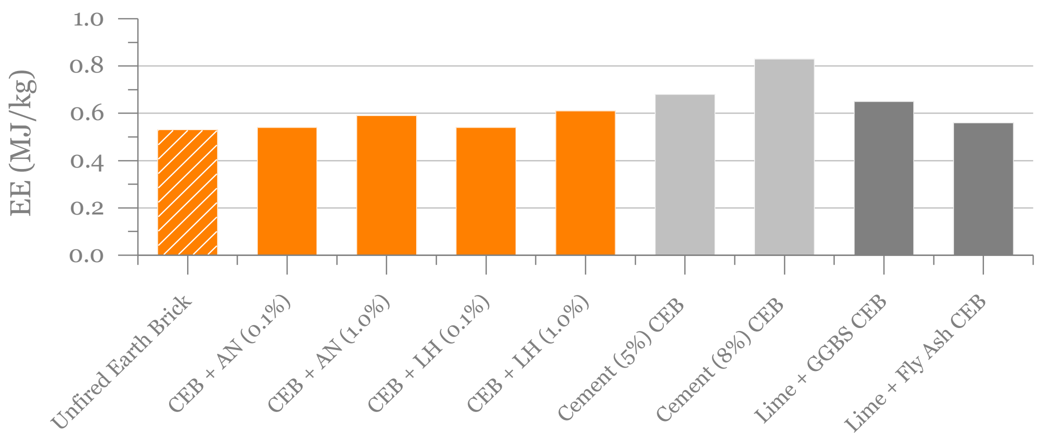

Figure 6-56: Embodied Energy Estimations – Other Masonry

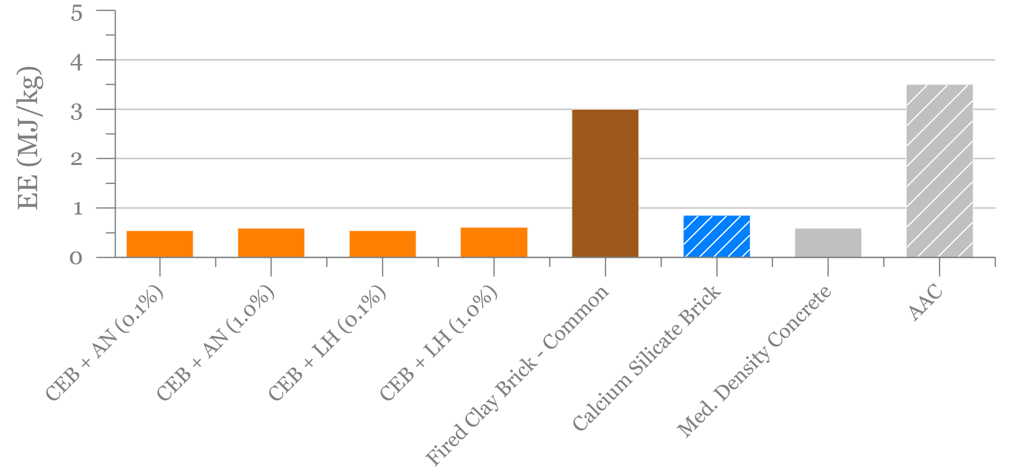

From these results, it was found that the addition of the 0.1% alginate to the soil mixture did not significantly increase the overall EE due to the low quantities used. Raising the alginate dosage up to 1% resulted in a maximum EE increase of 11%. In comparison to data for other products, the results for the alginate bricks are lower than for cement stabilised bricks and lime/GGBS bricks (Morton et al., 2005; Oti et al., 2009; Hammond and Jones, 2011). The estimated EEs for the alginate bricks are also slightly lower than for a calcium silicate brick and much lower than AAC units and fired bricks.

Two additional factors must be however be considered. First of all, the EE values are presented in relation to a mass based functional unit (kg) which does not account for differences in density. An AAC block for example may have a density as low as 500 kg/m^3 while a dense concrete block may have a density closer to 2000 kg/m^3. Therefore although the AAC blocks may have a higher EE per kg, less material may be need to produce a single unit. Several authors have therefore converted EE figures to an equivalent wall area based on a given wall thickness and the specific density of the material. Normalised values produced by Maskell (2013) from the data of Hammond and Jones (2011), and other sources where the material densities are known (Oti et al., 2009), are shown in Figure 6-57. The normalised value for the alginate product is based on an average density of 1900 kg/m^3.

In addition to different bulk densities, masonry systems will also offer varying structural capacities. Therefore although the values in Figure 6-57 have been normalised to a comparable thickness, this assumes that this thickness is sufficient to carry the required loads. Given that the alginate-stabilised prototypes produced in this study do not meet the required compressive strength values, the results are indicative only. Indeed a further study of the characteristic wall strength and the contribution on the mortar to the overall EE would also need to be included in order to calculate a more accurate EE value. For instance, Galán-Marín et al. (2015) have performed structural calculations as part of their LCA, based on the compressive strengths of the materials being compared and a given wall span, in order to calculated the exact wall thickness required. The EE of the entire wall is then determined based on the total mass of material needed. While this does give comparable figures for different wall constructions, it should be noted that for the alginate-stabilised brick included by Galán-Marín et al. (2015) the compressive strength (4.45 N/mm^2) is take from a previous publication which does not appear to take any correction factors into account. Furthermore their calculation does not account for the mortar component in either the structural calculations or in the LCA.

Figure 6-57: Normalised Embodied Energy

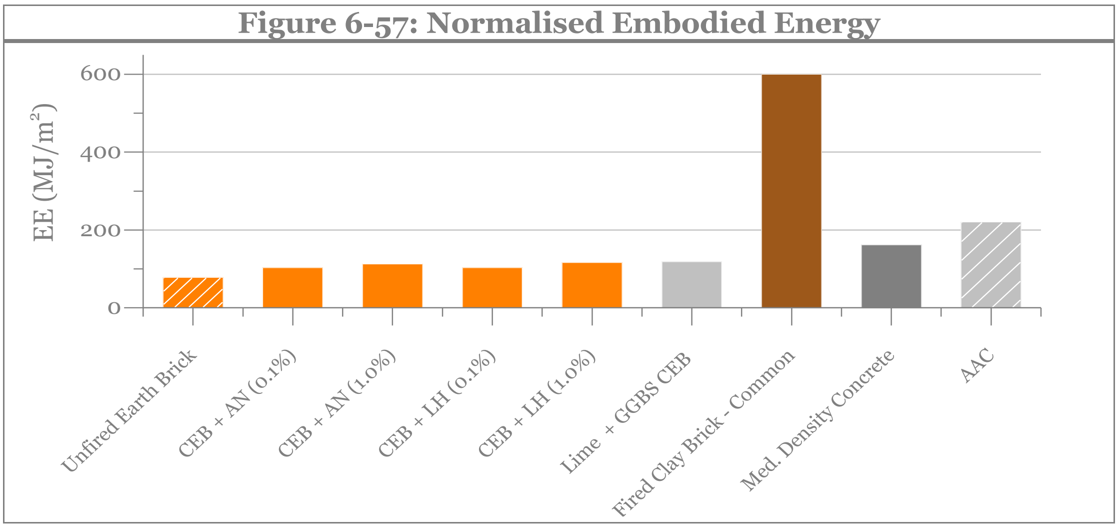

6.4.3. Market Comparison

In summarising all of the previously described results, in order to provide a comparison with commercially available products, generic data for similar products as obtained from the CES Database is shown in Table 6-17. Further details of commercially available unfired brick products can also be found in Appendix H.

Overall it would appear that the basic properties of the alginate bricks presented in Table 6-17 are similar to that of other unfired brick products in terms of their acoustic properties and cost but are disadvantaged in terms of their loadbearing capacities. Although the alginate bricks are estimated to have a slightly higher embodied energy than other unfired brick products, this is still considerably lower than for a comparable ceramic brick. This is offset by the fact that the fired brick achieves much greater compressive strength.

Table 6-17: Market Comparison

	Bulk Density	**Comp. Strength**	**SRI**	**Thermal Conductivity**	**Approx Cost**	**EE**
Units:	kg/m^3	N/mm^2	dB	W/mK	£/m^2	MJ/m$_2$
Alginate Bricks (0.1%)	1900	<2	49	1.15 – 1.25	13 – 14	100
Unfired Clay Brick	700 - 1940	<3.6	52	0.21 - 1.04	11	78 – 84
Fired Clay Brick	1980 – 2070	69-140	49-51	0.4 – 0.8	12	566 - 652
Lightweight Concrete Blocks	900 - 1400	0.5 – 8.2	42	0.07 – 0.7	16	70 - 121

7. PART I CONCLUSIONS

Part I of the thesis set out to explore the use alginate products as additives in earth-based building materials. A review of the literature in this field demonstrated that there is an incentive to develop additives for earth masonry which improve the compressive strength of raw earth without having a major detrimental effect on the environmental impacts. While some previous studies which investigated the use of alginate in masonry products were identified, details regarding the specific role of the alginate and the properties which affect its success as an additive for unfired bricks or blocks were somewhat limited. The goal was therefore to develop an experimental programme which would investigate a wider range of alginate variables. This began with an exploration of polymer-clay interactions through rheology observations which set out the context and parameters for the later investigations involving the brick prototypes.

In summarising the results of Part I, reference is made to the initial questions posed in the project objectives. Considering firstly the role of the alginate source and the variables affecting the properties of the brick prototypes, a number of conclusions can be made. First of all, it can be surmised from the range of specimens tested here that when used as an additive for earth masonry the type of alginate does have an important influence on the possible strength improvements. Indeed the results observed here for the brick specimens demonstrate that only some alginate types offer significant increases in strength when compared to the equivalent control specimen. The optimum strength improvement, for all soil types, was achieved using a *LH* stem product (PR22). However the other product sourced from the stem of this seaweed (PR24) was less successful. This observation highlights the importance of the specific composition of the alginate and not just the species of macro-algae from which it is sourced. PR22 for instance was noted to have a moderate viscosity and a fairly equal M/G ratio whereas PR24 had a high viscosity and high G content. In theory while a higher G content would increase the likelihood of cross-linking occurring with the calcium ions present in the soil, the longer and consequently more tortuous polymer chains of a higher viscosity product can also have a detrimental impact on potential bonding mechanisms. These results signal that, of the different polymers tested, PR22 offers the optimum conditions for facilitating binding with the soil given the aforementioned observations for PR24 and the lack of significant improvements in strength witness for products with a lower viscosity than PR22. A more detailed investigation of alginates with viscosities which are an intermediate of the PR22 and PR24 products would however be required in order to determine if other polymer chain lengths would give more favourable results. Furthermore, testing a range of products with similar viscosities but different M/G ratios would allow the contribution of the G content to be more clearly understood. The results from this study also indicate that, in most cases, increasing the dosage does not lead to significant strength improvements. While dosages above 1% were found to be impractical for laboratory scale production, this does not rule out industrial processing methods such as extrusion where higher alginate concentrations may be acceptable.

Secondly, in considering the role of the soil type, as expected the strength properties of the brick are closely linked with the base soil. However it can also be concluded from this study that the poorest soil in mechanical strength terms (soil W), appears to be most affected by the addition of alginate as evidenced by the comparative magnitude of strength increases. The greatest increase in compressive strength was therefore observed for soil W and the previously discussed PR22 product. In addition to having a low clay content, soil W was also characterised by a relatively high calcium content which may also have contributed to the increases in strength witnessed. However further investigation into the relative importance of the different soil properties (e.g. pH, calcium and clay type/quantity) using more sensitive tests parameters and a wider range of soils is desired to fully understand the role of the soil type.

In considering the final objective of Part I which concerns the suitability of the alginate bricks for use as building products, the main barrier to further development based on the results witnessed in this study is the relatively low strength of the material compared to results reported for earth blocks stabilised with conventional additives like cement and lime. Although some of the relative improvements observed compared to the control samples were encouraging and comparable to other stabilisers, none of alginate bricks passed the target compressive strength values for UK building standards. Therefore at this stage the material is not recommended for use in practice. However since the strength targets are based on a 100mm wall, it is possible that sufficient compressive strengths could be achieved using a greater wall thickness. On the other hand, this would require a greater mass of material and would therefore also increase the financial costs and environmental impacts, as well as being less suited to contemporary construction practices. It should also be acknowledged that the strength values achieved by the prototypes are somewhat limited by handmade nature of the bricks and it is anticipated that improved results could be achieved using alternative equipment. Indeed the final compressive strength values achieved by Galán-Marín et al. (2013) using similar materials, even for the control specimens, are greater than those observed in this study confirming that differences in the production process, particularly in the compaction technique, should be taken into account. An exploration of alternative compaction methods and different moulding water contents are also recommended in order to determine which variables have the most important influence on the strength characteristics.

Aside from mechanical strength, other properties such as moisture sensitivity are also a concern. Although it has been argued that this can be overcome through appropriate detailing and ensuring that the walls are sufficiently protected from moisture, it is likely to remain as a barrier to further commercial development. On the other hand, the hygro-thermal and acoustic properties of the prototypes were generally positive highlighting the benefits of earth masonry in comparison to conventional walling systems like fired bricks and concrete. Unlike some other stabilising additives, the use of alginate did not appear did not appear to be detrimental to theses beneficial properties. Similarly, due to the low quantities of alginate used, the impacts on the overall financial costs and embodied energy, in comparison to a standard unstabilised earth unit, were considered minimal.

7.1. Contribution to knowledge

In summarising the key **contributions to knowledge** contained within **Part I** of the thesis, a new empirical investigation into to the use of alginate biopolymers in an unfired clay brick product has been conducted. The work builds upon the existing academic literature by testing a wider range of alginate products than typically encountered in previous publications and consequently provides new evidence on the role of alginate variables. Chapter 6 in particular provides new information relating to the role of the alginate type in determining the magnitude of strength increase observed when the alginate is used as a binding additive for the bricks. Further new insights into the interactions between the alginate and different soil compositions are also provided thereby contributing to the wider field of polymer-clay complexes. As a further contribution, the work also presents a cost and environmental assessment of the proposed prototypes.

PART II: ALGINATE AS AN INSULATING MATERIAL

Part II focusses on the use of alginate as an additive in a composite aerogel product for use as an insulation material. This part of the thesis therefore includes a summary of conventional insulation materials as well as a review of existing research relating to the use of biopolymer/clay hybrids as insulation products. The development of prototype materials using a variety of alginate and clay products is then described followed by experimental work to determine and compare their basic properties. Finally, the prototypes are compared with existing products and evaluated in terms of their commercial feasibility.

8. LITERATURE REVIEW

8.1. Thermal Insulation in Buildings

8.1.1. Principles of Thermal Insulation

The purpose of thermal insulation materials in buildings is to reduce heat losses between internal heated spaces and adjacent unheated spaces (McMullan, 2007). Typical heat losses through the different elements of a domestic dwelling are shown Figure 8-1. Since up to two thirds of heat generated within a building can be lost through the building fabric (Carbon Trust, 2012), the appropriate specification of insulation materials can help to reduce the overall energy consumption. For example, improving the thermal performance of the building fabric can minimise the energy requirements of HVAC systems by reducing the need for heating, cooling and ventilation as well as extending the periods of indoor thermal comfort. This can in turn reduce the quantities of CO_2 produced per dwelling and reduce fuel costs.

Figure 8-1: Typical Heat Losses

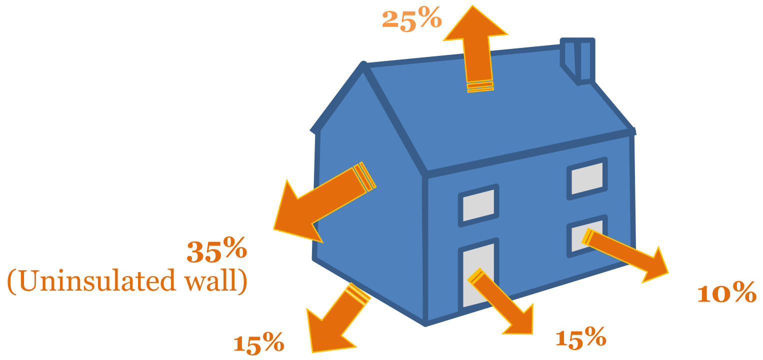

Source: Adapted from Virdi (2012)

Effective insulators should help to inhibit the various forms of heat transfer including conduction, convection and radiation (McMullan, 2007). In the case of conduction and convection, heat transfer can be minimised by the introduction of air voids and porous structures, whereas radial heat transfer can be counteracted by the use of reflective materials. Good insulation materials therefore include those with a cellular or porous structure with a layer of aluminium foil (Jelle, 2011) and are typically installed as batts or boards within the building structure. For instance, rectangular shaped panels can be fitted between or around posts or rafters within a timber or steel frame or within the air cavity in masonry wall construction. In refurbishment scenarios, insulation can be also fixed to the existing structure as external or internal layer. Spray foam and loose-fill insulation can also be retrofitted to cavity walls and lofts. The thermal performance of these insulation materials is dependent primarily on the density and thickness of material, although other factors such as temperature, moisture content and the quality of the installation can also affect the overall thermal transmittance (Jelle, 2011). Aside from minimising heat losses, insulation products can also provide acoustic and impact insulation or fire protection depending on the specific material utilised. Consideration must also be given to aspects like cost, ease of installation, potential health hazards, structural stability, durability, moisture absorption and vapour permeability (Al-Homoud, 2005).

8.1.2. Common Insulation Materials

Insulation products can generally be divided into four main types: polymer based materials, inorganic materials, materials produced from natural fibres and more recently developed high performance materials such as composite and vacuum sealed systems. A summary of these products is presented in Table 8-1.

Table 8-1: Summary of Insulation Materials

	Product	Example	Bulk Density (kg/m^3)	Thermal Conductivity (W/m-K)
Polymer Based	Expanded Polystyrene	Kingspan Aerobord ®	16–35	0.032–0.040
	Extruded Polystyrene	Kingspan Styrozone®	26–45	0.028 – 0.036
	Polyurethane/ Polyisocyanurate	Kingspan Thermawall ®	32	0.021 - 0.027
	Phenolic Foam	Kingspan Kooltherm ®	190 -210	0.05 – 0.54
In-organic	Rock Mineral Wool	Rockwool RW Slab ®	24 – 40	0.031 – 0.040
	Glass Mineral Wool	Knauf Earthwool ®	16 - 24	0.031 – 0.040
	Cellular Glass	Foamglas ®	100 - 165	0.038 – 0.050
Organic	Cellulose	Warmcel ®	32	0.038-0.04
	Wood Fibre (Rigid)	NaturePro ®	250	0.049
	Sheeps Wool	Thermafleece ®	25	0.039
	Cork	SecilVit® CORK	120	0.034 – 0.040
	Flax	Isolina ®	30 - 35	0.038
	Cotton	Inno-therm®/Metisse®	25	0.038
	Hemp	NatuHemp	30	0.039
High Performance	Vacuum Insulation Panels (VIP)	Kingspan OPTIM-R	180 – 210	0.007
	Transparent Aerogel Panels	Kalwall ® + Lumira	70 – 100	0.018
	Silica Aerogel Blanket	Spaceloft®	160	0.017

Polymer-based Insulation

Conventional polymer-based insulations include expanded polystyrene (EPS), extruded polystyrene (XPS), polyurethane (PUR), polyisocyanurate (PIR) and phenolic foams (Jelle, 2011; GreenSpec, 2015). Urea-formaldehyde (UF) products were also used commonly until the 1980s when it was discovered that these products could release airborne formaldehyde – a substance which has known detrimental health impacts (Harris et al., 1981). Most of these types of polymer foams are produced as a rigid board or batt, sometimes directly bonded to a dry-lining board or a reflective foil layer. Expanding foams can also be used in cavity wall insulation where they are blown through nozzles and then foamed in place. Polymer based foams are generally lightweight, cheap to produce and have good thermal properties and so currently form a large part of the market. EPS and XPS reportedly offer thermal conductivities of around 0.3 – 0.4 W/m-K (Jelle, 2011) whilst PUR has an even lower value of 0.2 – 0.3 W/m-K (Jelle, 2011), making it one of the best performing polymer-based products on the market. Phenolic foam based products, produced using phenol-formaldehyde, also offer excellent thermal properties with Cuce et al. (2014a) quoting a value of 0.18 W/m-K.

The main disadvantages of these materials is that their production involves the use petrochemical-based raw materials, fluorocarbon gases and other potentially hazardous substances, making them less attractive from an environmental perspective. EPS for example consists of small polystyrene beads which are expanded using a blowing agent to create an open pore structure (Cuce et al., 2014a). Previously CFC (chlorofluorocarbon) gases were used in this process but, due to their harmful effect on the ozone layer, pentane (C_6H_{12}) is now used as a less damaging alternative. Similarly, XPS is produced by melting polystyrene and adding expansion agentw such as HFCs (hydrofluorocarbons), CO_2 or C_6H_{12} (Jelle, 2011). Both EPS and XPS are also combustible and so hazardous materials such as Hexanbromcyclododecan are also often added to reduce their flammability (Papadopoulos, 2005). Products such as styrene and other hydrocarbons can also be emitted during the production process. PUR is formed by combining isocyanate with a polyol (an alcohol with more than one OH- group), using HFC, CO_2 or C_6H_{12} as an expansion gas. Again the major downside to PUR is its poor fire performance due to the emission of dangerous and toxic substances such as isocyanates and hydrogen cyanide (Stec and Hull, 2011). PIR offers a slight improvement on PUR as it uses alternative additives and catalysts to help improve fire performance. However both PUR and PIR products not only rely on the use on non-renewable resources, but they also have a high embodied energy and embodied CO_2. As reported by Hammond and Jones (2008), PUR/PIR foams in fact have one of the highest embodied energy values of all insulation materials (101.5 MJ/kg).

Overall, polymer based materials have the advantage of offering good thermal properties, being resistant to rot and vermin and being available at a relatively low cost. However their main disadvantages are the energy intensive production processes and hazardous materials involved in their production.

Inorganic Insulation

Mineral based insulations include rock wool, glass wool, perlite and vermiculite, amongst others. Rock wool and glass wool are long established products which reportedly account for around 60% of all insulation products in Europe (Kiss et al., 2013). They can be either formed into batts, rigid boards or be used as loose-fill materials. Rockwool is produced by extruding fibres from molten minerals or liquid iron slag whilst glass wool uses recycled glass to produce the fibres. In both cases the fibres are usually formed into a slab using resin binders (usually formaldehyde based), impregnation oils and heat treatments. The thermal conductivity of mineral wool materials is within the 0.3 – 0.4 W/m-K range (Cuce et al., 2014a) and they also have the advantage of being fire resistant or at least having limited combustibility depending on the binder content (Stec and Hull, 2011). Although they can be easily cut and adapted on site, this can result in dust formation and skin irritation during installation and so protective measures are often required (Al-Homoud, 2005). Perlite and vermiculite, both of which are natural minerals, are typically used as loosefill granules (Zukowski and Haese, 2010) or an expanded board (Law et al., 1998). More recently, other glass-based insulation materials such as cellular glass have also emerged on the market. In this case the glass is ground into a fine powder, heated and then foamed using a blowing agent in order to entrap gas bubbles within the material (Solomon and Rossetti, 1996). Again recycled glass can be used for this purpose and the final material has a good level of mechanical strength and dimensional stability compared to mineral and glass wool.

Overall mineral based insulations offer good durability, especially in terms of resistance to moisture and fungal degradation (Klamer et al., 2004). They also exhibit excellent fire performance and low thermal conductivities. Although inorganic insulations are produced from non-renewable materials, they are generally produced from abundant resources and in the case of products like slag wool and glass wool, recycled materials can be incorporated in order to minimise their environmental impact. In general, inorganic insulations therefore have lower embodied energy values than polymer based products.

Natural Fibre Insulation

The use of natural materials as insulation products is a well-known practice with wood fibres, plant fibres and even animal fibres having previously been used as insulators. Common examples include cellulose, cork, sheep's wool, straw, hemp, flax and cotton, all of which offer a renewable form of thermal insulation (A Sutton et al., 2011). Natural materials generally involve minimal processing and therefore have a lower embodied energy than polymer based products. Since the raw material generally comes from a plant-based resource, sequestered CO_2 can also be taken into account leading to low, and in some cases negative embodied CO_2. Densley-Tingley et al. (2015) for example showed that when sequestered CO_2 was included in a LCA study for wood fibre based insulation, an embodied carbon value of -142 $kgCO_2eq/m^3$ was achieved, offering a significantly lower value than other polymer and mineral based products. In some cases, waste resources are also used. For example, cellulose-based insulation can be manufactured using recycled newspapers while cotton-based products can be produced using recycled textiles. Most natural fibre insulations are produced as loose batts however products like cork can be used as fillers or board materials and cellulose is often used as a sprayed insulation (Jelle, 2011). Natural insulation materials are generally low-cost and easy to handle as well as being vapour permeable which makes them compatible with breathing constructions (Sutton et al., 2011). They also possess good hygro-thermal properties meaning that they are able to absorb and desorb moisture from the internal environment and therefore help to regulate indoor humidity levels (Korjenic et al., 2011). On the other hand, this sensitivity to moisture can also have detrimental effects since prolonged exposure to high levels of humidity or indeed direct contact with water can increase the thermal conductivity or lead to degradation of the material, including attacks by bacteria and fungi (Korjenic et al., 2011). The high organic content also means that natural fibre materials are combustible and require treatment with fire retardants, usually ammonium or borate based substances (Day and Wiles, 1978; Sutton et al., 2011; Lazko et al., 2013). Whilst natural fibres offer good thermal conductivities, usually within the 0.038–0.040 W/m-K range, the thicknesses required in order to achieve sufficient U-values are generally greater than for polymer based materials. Although there are some existing products on the market (e.g. Thermafleece ®), the costs are still relatively high in comparison to polymer or mineral based products and they therefore constitute less than 1% of the UK market (A Sutton et al., 2011). Overall natural fibre insulations offer the advantage of low embodied energy and the fact that they can be produced from renewable resources. They are however disadvantaged in terms of their poorer durability and moisture sensitivity.

High Performance Insulation

More recent innovations within the insulation market have included products such as Structurally Insulated Panels (SIP), Vacuum Insulation Panels (VIP), Gas-filled panels (GFP) and aerogels. SIPs usually consist of a core insulation material such as EPS or PIR sandwiched between two rigid boards, usually made from oriented strand board (OSB) or plywood (Yang et al., 2012). These prefabricated panels can be fitted together to form entire walls, floors and roofs thereby acting as both structural and insulating elements. The Kingspan TEK system for example uses an insulation core with a thermal conductivity value of 0.023 W/m-K, meaning that the whole system achieves an overall U-value of 0.16 W/m^2. K. SIPs also offer fast build times since the components can be prefabricated offsite (Hairstanes and Kermani, 2007).

VIPs are a composite system consisting of a cellular core such as fumed silica, glass fibre or polymer based foams, which is vacuum sealed within a layer of foil faced plastic (Alam et al., 2011). Although this type of system offers thermal conductivities below 0.004 W/m-K, demonstrating an dramatic improvement on conventional insulations, this value increases over time due to the deterioration of the vacuum and the thermal properties can also be compromised if the material is damaged or punctured (Jelle, 2011). Although VIPs have been used for decades in appliances such as refrigerators (Fricke et al., 2008), the use of VIPs in building elements is a much more recent concept. Nonetheless various demonstration projects have investigated the performance of VIPs in buildings, including external façade panels, internal wall insulation and prefabricated elements such as window and door frames (Binz et al., 2005). Kingspan also introduced a VIP product (Optim-R®) in 2012 which has been used in various new build and refurbishment projects in the UK. Other available products include Marley Eternit's SlimVac® and Vacupor® by Porextherm. However VIPs still have a relatively high cost and a longer payback period compared to conventional insulation materials (Alam et al., 2011). Furthermore, an LCA study of fumed silica VIPs has demonstrated the high levels of electricity consumption involved during manufacturing which contribute to the overall embodied energy of the product (Binz et al., 2005).

GFPs are similar to VIPs although in this case, rather than a vacuum, an inert gas with a lower conductivity than air such as argon (Ar) or krypton (Kr) is used and the inner core consists of a honeycomb-like structure with a low emissivity surface (Jelle, 2011). The thermal conductivities reported for GFPs are higher than for VIPs although both systems shares the major disadvantage that they cannot be cut to fit onsite (Baetens et al., 2010). Another alterative form of insulation is thin reflective multi-foil insulations which consist of several layers of reflecting film along with foam or wadding (Tenpierik and Hasselaar, 2013). The benefit of these materials is that a much thinner layer of material is required compared to conventional insulations like mineral wool and PUR.

Aerogels are another technology which has been explored for insulation purposes. An aerogel is a high porosity material usually formed by removing the liquid component from the gel. This material can be formed into sheets, embedded within fibres to form a blanket, used as an infill material in the form of granules or used to form the inner-core of VIPs. The use of aerogel materials, particularly silica aerogels, within building applications has increased in recent years and has consequently been the subject of several recent review papers (Berevoescu et al., 2009; Baetens et al., 2011; Riffat and Qiu, 2013; Cuce et al., 2014a). Due to their excellent thermal properties, aerogels can be used as 'super-insulators' in walls, roofs, floors and glazing. The most well-known products include the Spaceloft® and Spacetherm® products. These composite systems consist of a silica aerogel which is embedded within a fibrous reinforcement system. The resulting aerogel blanket can then be bonded to plywood or a fireproof board. This gives the otherwise fragile aerogel additional durability and flexibility (Riffat and Qiu, 2013). There is still ongoing research into other methods of encapsulating aerogel materials and strategies to address issues such as dimensional instability, hydrophobicity and dust generation during installation (Carty et al., 2013). According to the manufacturers, the Spaceloft® and Spacetherm® products offer thermal conductivities as low as 0.013 W/m-K. Compared to conventional insulations, the desired U-values can usually be achieved using a reduced thickness of material (Cuce et al., 2014a). Consequently, aerogels are particularly useful in applications where space is restricted and they have therefore been used in several UK refurbishment projects (Baker, 2011; Jenkins, 2012).

In addition, since aerogels can also be transparent, they can also be used as filler materials within a glazing, allowing the building to access natural light whilst minimising heat losses. For example Duer and Svendsen (1998), have studied the use of various monolithic silica aerogel materials sandwiched between glazing panels whilst Reim et al. (2002) proposed a similar system using aerogel granules, low-e coated glass and krypton gas, giving a heat transfer coefficient of below 0.4 W/m-K. Jensen et al. (2004) also demonstrated that glazing tiles produced from a monolithic aerogel (~15mm thickness) could achieve a centre U-value of less than 0.7 W/m-K whilst maintaining a solar transmittance of over 75%. These principles have since been developed into various commercial products, such as the Lumira® aerogel system developed by Cabot. Other experimental techniques also include the use of a silica-aerogel film as a coating on glazing (Kim and Hyun, 2003; Cha et al., 2008) or transparent aerogels used as part of a Trombe wall system (Dowson et al., 2014). The latter consists of a high thermal mass wall, orientated to absorb solar gains, combined with a cavity and a layer of translucent aerogel insulation. This design allows solar radiation to heat the solid wall which then transfers heat to the interior while simultaneously preventing the heat from escaping (Fricke and Tillotson, 1997). More recently, the use of aerogels in insulated plasters has also been developed. Stahl et al. (2012) for example describes material which incorporates silica aerogel granules and a cement-free binder. The product, which has since been developed commercially, is noted to achieve a thermal conductivity value of around 0.025 W/m-K, making it superior to existing insulated plaster systems on the market. Buratti et al. (2014) also describe a similar aerogel plaster where values as low as 0.018–0.020 W/m-K are achieved, depending on the volume of aerogel included. Other potential applications include the use of aerogel granules as lightweight aggregates in concrete. Gao et al. (2014) for example have shown that incorporating silica aerogel granules (60% volume) can create an insulating concrete with a compressive strength of approximately 8 N/mm^2 and a thermal conductivity of 0.26 W/m-K. Similar concrete materials have also been discussed by Ng et al. (2015) and Fickler et al. (2015).

It should be noted that there are a few other potential application for aerogels within buildings which can be found in the literature but are not related to thermal insulation. The first of these is air purification materials where the high porosity and specific surface area of aerogels can be used to remove contaminants such as VOCs, NO_x and SO_x from the internal environment (Khaleel et al., 1999;Riffat and Qiu, 2013). Other uses which have been studied to a lesser degree include acoustic insulation products which make use of the high sound absorption of aerogels (Gibiat et al., 1995) and fire retardant materials where the non-combustibility of silica aerogels is exploited (Riffat and Qiu, 2013).

Overall aerogels are therefore considered as promising materials for use in buildings and offer a wide range of possible applications. Similar to VIPs, although several commercial aerogel products now exist on the market, their relatively high cost compared to conventional insulations still limits their widespread use (Cuce et al., 2014a).

8.1.3. UK Context & Market Trends

Based on 2014 figures, the building insulation sector was estimated to have a market value of around £800 million in 2014 (AMA Research, 2015) and this figure is expected to increase in the future due to factors such as changes in building regulations, financial drivers and the increasing scrutiny of the whole lifecycle costs of buildings. Each of these topics are therefore discussed in more detail in the following sections, highlighting their likely influence on the future demand for insulation.

Regulatory Requirements

In considering firstly the influence of regulatory requirements, within the context of the UK, the appropriate selection of thermal insulation is necessary to meet the increasingly stringent regulations for new buildings. Indeed the maximum area weighted U-values required have been lowered with each revision of the building regulations. The values from the most recent building regulations for Scotland (Section 6) and England (Part L) are shown in Table 8-2, alongside the demands for the Passivhaus standard which the UK regulations are edging closer towards. Passivhaus is a technique developed in Germany in the 1990s which relies of high levels of superinsulation and air-tightness in order to minimise overall energy requirements (McLeod et al., 2011). In order to meet these standards, new buildings are required to either incorporate increased thicknesses of conventional insulations, which in turn has an effect on the amount of material required and the available floor space, or utilise high performance materials which can meet the required U-values.

In addition to the advancing standards for new buildings, it has been reported that 75% of the domestic buildings and 60% of the non-domestic buildings which will exist in the UK by 2050 will have been built prior 2010 (MacKenzie and Mackenzie, 2010). The building regulations have therefore also incorporated minimum U-values for refurbishment and conversion projects, as well as buildings other than dwellings (Table 8-3). Improving the energy-efficiency of an existing building can often be achieved through retrofitting cavity wall or loft insulation. However in so-called ‘hard to treat’ properties, such as solid wall constructions, buildings with no loft-space or listed buildings, alternative methods are required (Carty et al., 2013). A particular need has been identified for solid wall insulation since only 3% of these buildings have any form of insulation (DECC, 2013a). One option for these buildings is external wall insulation where the building is re-clad with a new material (Densley-Tingley et al., 2015). However in cases where it is necessary for the external appearance to be preserved, such as buildings with a listed status, this is not a viable option. While internal wall insulation offers an alternative solution, this technique also reduces the internal room dimensions, leading to a loss in floor space. It can also involve covering up existing decorative features. There is therefore a demand for products which can be fitted internally, with minimal impact, while also reducing the overall thermal conductivity of the building fabric.

Table 8-2: Area Weighted U-values for New Domestic Buildings

	Walls (W/m^{2}K)	**Floors** (W/m^{2}K)	**Roofs** (W/m^{2}K)
England (2013)	0.30	0.25	0.20
Scotland (2015)	0.22	0.18	0.15
Passivhaus	0.15	0.15	0.15

Table 8-3: Area Weighted U-values for Conversions and Non-domestic Buildings

	Walls* (W/m^{2}K)	**Floors*** (W/m^{2}K)	**Roofs*** (W/m^{2}K)
Domestic Conversions	0.30	0.25	0.25
Non-domestic (New Build)	0.27	0.22	0.20
Non-domestic (Conversions)	0.30	0.25	0.25
Non-domestic (Refurbishment and extensions)	0.25	0.20	0.15

*Figures for Scotland

Financial Incentives

Aside from regulatory requirements to increase the levels of insulation in buildings, there are also a number of financial incentives which are likely to increase the demand for insulation products. Although the initial cost of insulation generally comprises only 5% of the total build cost (Al-Homoud, 2005), savings in fuel costs are achieved over the full operational phase of the building. Improved thermal insulation can therefore help to reduce operational costs over the building's lifetime and provide the occupants with lower energy bills. Indeed, schemes like Passivhaus, where the reliance on mechanical heating systems is minimised, have been shown to offer significant fuel savings for the occupants (McLeod et al., 2012). Investment in appropriate design and specification of insulation materials can therefore be highly cost-efficient when considering whole life costs, especially when the predicted increases in domestic energy prices are also taken into account (DECC, 2013b).

Other financial drivers include funding schemes such as the Energy Company Obligation (ECO) which places a legal obligation on energy suppliers to make energy efficiency improvements to domestic buildings (Rosenow et al., 2013). Government funding schemes such as the *Warm Front* scheme in England (Critchley et al., 2007) and the *Home Energy Efficiency Programmes for Scotland* (Scottish Government, 2014) have also provided financial support for properties requiring energy efficiency upgrades. The introduction of Energy Performance Certificates (EPCs) provides a further motivation for ensuring good levels of insulation are installed within both new and existing buildings since prospective property buyers and tenants are presented with energy performance data when properties are first built, sold or rented (UK Government, 2007). Improving the energy efficiency may therefore also help to improve the overall value of the property (Fuerst et al., 2015).

Whole Life-Cycle Costs

Insulation materials have an important role to play in the lifecycle costs and environmental impacts of buildings since they contribute to both the operational energy requirements and overall embodied energy. Although energy will be saved by incorporating insulation due to the reduced heat losses, as demonstrated in a case study by Hammond and Jones (2008), insulation can still constitute contribute to around 20% of the overall embodied energy value for a house in the UK. In Europe the most commonly used materials are non-renewable materials such as glass and stone wool or petrochemical derived foams (Papadopoulos, 2005; Cuce et al., 2014a) and, as shown in Figure 8-2, polymer and mineral fibres in fact account for approximately 95% of the market in the UK.

Figure 8-2: Market Share of Insulation Products in the UK

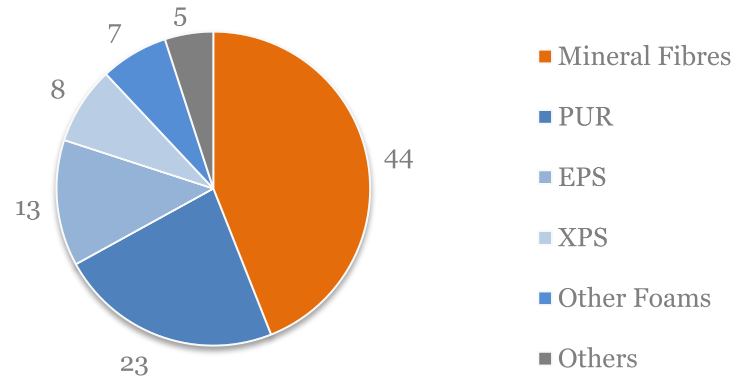

Source: Adapted from Cuce et al. (2014a)

Due to the increasing importance of LCA in buildings, it is crucial to obtain a balance between the energy used to produce the material and the potential energy savings resulting from reduced thermal losses during the operational phase. It is therefore likely that that demand for more ecological products will increase in the future (Van Wyk et al., 2012). For example, although natural fibre insulation products currently only form a small part of the UK insulation market (Sutton et al., 2011), they have been gaining popularity in recent years due to their low embodied energy and a growing desire for 'natural' materials within buildings. In terms of high performance insulations like VIPs and aerogels, although such products have witnessed positive trends in the last few years with major increases in the global market share (Cuce et al., 2014a), again in the UK these form only a minor part of the current market. Their high embodied energy and high capital costs also make them less favourable candidates when considering whole life cycle costs.

8.2. Aerogels

8.2.1. Early Studies and Development

Aerogels are a porous and lightweight solid where the dispersed phase consists of a gas (Alemán et al., 2007). They are derived from sol-gel technology, where by a colloidal solution known as a *sol* is formed into a semi-solid material or *gel* (Pierre and Pajonk, 2002). If this gel material is then dried in a manner whereby the solvent is removed whilst retaining the structure or network formed by the solid component, it becomes an *aerogel*. It is important to make a distinction between an *aerogel* and a *xerogel* which is dried through evaporation. Xerogels experience considerable shrinkage during drying and do not retain their network structure as shown in the schematic diagram in Figure 8-3.

Figure 8-3: Aerogel Production

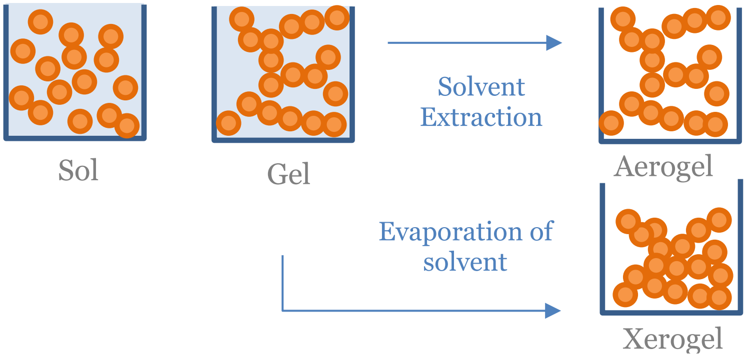

Author's own image

Kistler (1931; 1932; 1934) was one of the first researchers to experiment with aerogels in an effort to develop an understanding of gel structures by removing the solvent component. In recognising that simply drying gels through evaporation resulted in dramatic shrinkage and hence destruction of the gel network (i.e. the formation of a *xerogel*), Kistler began investigating alternative drying methods where the structure of the solid component could be preserved. Initial experiments were conducted with various metal oxides such silica and alumina as well as some organic gels, demonstrating that aerogels could be produced successfully using supercritical drying methods (Kistler, 1932).

The supercritical drying technique requires both the temperature and pressure to be controlled and raised above the critical temperature and pressure of the solvent used, allowing the liquid to vaporise without fully changing phase. While in this supercritical state, the solvent possesses properties of both the liquid and gas phases meaning that surface tension is removed and the solvent can be vented off without destroying the structure of the solid component. It was therefore concluded that aerogels could be formed from most gelling materials but that the final properties were found to vary widely depending on the starting material and its processing conditions. Kistler discussed the silica-based aerogels in the greatest detail as these were shown to exhibit relatively good mechanical properties. These particular aerogels were formed using sodium metasilicate (Na_2SiO_3) and hydrochloric acid (HCl). After being soaked in alcohol to form an ‘alcogel’, the material was then dried in an autoclave at 270°C and a pressure of 10 MPa. This allows the alcohol to vaporise and causes the pores to fill with air. The resulting silica aerogels were found to be transparent and could be produced using solids contents as low as 2%. Upon identifying silica aerogels as the cheapest and easiest to produce, further studies were conducted including an investigation of thermal properties (Kistler and Caldwell, 1934). Due to the limitations of the equipment used and the appearance of cracks and defects when preparing large monoliths, these studies were performed on granular forms of aerogel, with preliminary results showing that thermal conductivities below that of air could be achieved. It was therefore identified that silica aerogels could be a useful thermal insulator in appliances such as refrigerators or ovens. Some commercial applications were explored and ‘Santocel’, a milled aerogel product developed with Monsanto in 1950s, was used as both an insulation product and as a thickening agent in products such as paints and as components in cigarette filters (Monsanto, 1954; Zhang and Zhao, 2012). However the high production costs of silica aerogels in combination with the development of other competing materials, such as fumed silica, meant that this success was relatively short-lived (Fricke and Tillotson, 1997).

Further commercial development of aerogels did not take place until the 1980s when the properties of aerogels were revisited and it was discovered that the refractive index of silica aerogels made them suitable components for Cherenkov radiation counters (Bourdinaud et al., 1976). In the following years aerogels were explored further by the scientific community and the first international conference on the subject took place in 1985, highlighting the unique properties of aerogels such as the low density, low refractive index and low dielectric constant as well as high porosity and surface area (Fricke, 1985). More detailed studies regarding thermal transport properties, sound absorption and mechanical properties were also developed during this period (Fricke and Tillotson, 1997). Consequently, new applications for aerogels began to emerge including use in catalysts, filters, sensors, optics and capacitors as well as thermal and acoustic insulation (Hrubesh, 1998). One of the most publicised developments occurred during the 1990s when NASA began employing aerogel materials in the Stardust Missions where they were utilised for particle capture and the Mars Pathfinder rover where an aerogel was used as a high performance thermal insulator (Jones, 2006). An example of a commercially available silica aerogel and its properties is provided in Table 8-4.

Table 8-4: Silica Aerogel

Product	**Bulk Density** (kg/m^3)	**Thermal Conductivity** (W/m-K)	
Aerogel Technologies Classic Silica ™	20 - 100	0.01 -0.02	[This image has been removed by the author of this thesis for copyright reasons]

Source: http://www.buyaerogel.com/product/classic-silica-disc

Aside from developing new applications, other researchers began to focus on alternative manufacturing techniques with the aim of both reducing costs and improving safety. For example new silica precursors such as tetramethoxysilane (TMOS) or tetraethoxylane (TEOS) were investigated as alternatives to sodium silicate (Wagh et al., 1999). One of the most notable developments was the introduction of CO_2 supercritical drying as an alternative to Kistler's previous alcohol method (Tewari et al., 1985). Liquid CO_2 is not only non-flammable but also has a lower critical temperature and pressure than the alcohol. In this case, replacing the solvent reduces the risk of explosion associated with high temperatures and pressures as well as reducing the energy consumption during drying. Other supercritical drying methods for aerogels such as freeze-drying have also been investigated (Hyun et al., 2000). In this case, rather the solvent transforming into a gas from the supercritical phase, the solvent is first frozen and then dried below a critical temperature and pressure, so it can transition directly from the solid to gas phase. A summary of these different drying methods is shown in Figure 8-4.

Figure 8-4: Aerogel Drying

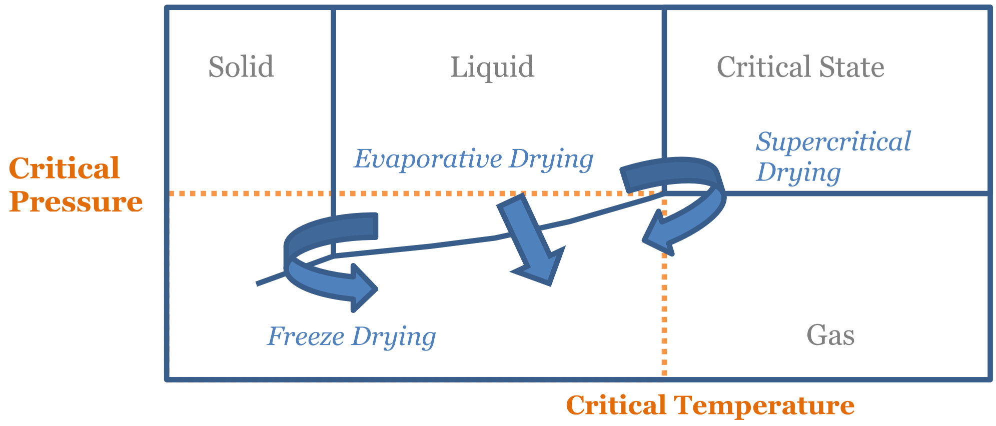

Source: Adapted from Bisson et al. (2003)

In addition to the development of new processing techniques, investigations into alternative types of aerogels have also been conducted. Although the majority of work since Kistler's first experiments has involved silica-based materials, other inorganic aerogels produced from clays (van Olphen, 1967) and transition metal alkoxides such as titania (Campbell et al., 1992) and zirconia (Ward and Ko, 1993) have also been developed but with more limited commercial applications. Aerogels prepared from organic substances such as resorcinol and formaldehyde (Pekala, 1989; Wu et al., 2005), phenolic-furfural (Pekala et al., 1995), melamine-formaldehyde (Nguyen and Dao, 1998) and polyurethanes (Rigacci et al., 2004) have also been studied. These organic aerogels can also be heated in an inert atmosphere in order to form carbon aerogels (Lu et al., 1993; Pekala et al., 1998). These materials have received much attention due to their electrokinetic properties which make them useful in applications such as supercapacitors (Pekala et al., 1998) and electro-sorption (Meena et al., 2005). Building on previous work by Kistler (1932) on the use of organic materials such as cellulose, nitrocellulose, gelatin, agar, egg albumin and rubber, various authors have also investing the use of aerogels produced from natural polymers. For example Quignard et al. (2008) have explored aerogels produced from marine-derived polysaccharides such as alginate, carrageenan and chitosan, while Aaltonen and Jauhiainen (2009) have investigated aerogels produced from wood-based materials including cellulose, lignin and xylan. As further discussed by García-González et al. (2011), various polysaccharide materials have been successfully used to create aerogels with potential uses in biomedical and drug delivery systems. Hatakeyama and Hatakeyama (2005) have also investigated a polyurethane based foam which incorporates polysaccharides and lignin as additives to minimise the negative environmental impacts of the material. The variety of materials which can potentially be used to form aerogels is therefore vast and the development of hybrid aerogels further increases the range of possible materials.

8.2.2. Clay-polymer Aerogels

Although having previously received less attention than silica aerogels, renewed interest in clay-based aerogels has occurred in recent years in an effort to counteract the high-cost and poor environmental performance of conventional silica aerogels.

Whilst the concept clay aerogels has been known for decades (Mackenzie, 1953; Call, 1953; Norrish and Rausell-Colom, 1962; van Olphen, 1967; Lincoln and Tettenhorst, 1971), reports regarding their brittle behaviour meant that they were initially considered as inferior to silica products. Early studies conducted by Van Olphen (1965;1967) described the production of aerogels from kaolinite, bentonite and illite clays using water as the solvent and freeze-drying as the method of sublimation. Although when used alone the kaolinite and illite clays were noted to exhibit poor gel forming capabilities and thus more fragile aerogels in comparison with the bentonite, the addition of a polyelectrolyte, in this case sodium-CMC, was found to substantially improve the strength characteristics of the aerogels as it acted as a binder for the clay particles. For the bentonite aerogels, which even without the addition of the polymer were found to produce relatively stable aerogels, the addition of CMC also helped to improve strength. Although only small scale specimens were produced, van Olphen (1967) highlighted the potential uses for this clay-polymer composite aerogel including thermal insulation, gas-diffusion membranes and various adsorbent materials. Several decades later, Ohta and Nakazawa (1995) also investigated the use of various organic polymers and their use as additives in clay based aerogels, in this case describing the materials as potential substitutes for polystyrene foams. Their studies focused particularly on agar and starch however other biopolymers including sodium alginate, CMC and gelatin were also discussed. Again the freeze-drying method was used to create aerogel monoliths, 19mm in diameter and 30mm in height. Characterisation tests of the resulting materials demonstrated that for clay:polymer ratios of 50:50, the agar and starch samples offered compressive strength values of 0.9 and 0.5 N/mm^2, respectively. The authors also highlighted that, where the agar component was above 20%, the resulting aerogel achieved compressive strengths similar to polystyrene foams (0.2 N/mm^2) but that increasing the polymer concentration also resulted in reduced pore sizes. In addition to improvements in mechanical strength, other studies also describe the improvements in thermal stability offered by including clay particulates (Alexandre and Dubois, 2000).

More recent investigations into organic-inorganic hybrid aerogels have also taken place and in the last 10 years there has been particular interest in clay-polymer aerogels as evidenced by the growing amount of literature in this area. This includes a series of studies involving clay aerogels that have been developed by Case Western Reserve University in Ohio by Schiraldi et al. (2006; 2010) and associated researchers (Bandi et al., 2005; Somlai et al., 2006; Arndt et al., 2007; Finlay et al., 2007; Gawryla et al., 2008; Hostler et al., 2009; Johnson III et al., 2009; Pojanavaraphan et al., 2010; Alhassan et al., 2010; Johnson and Schiraldi, 2012; Chen et al., 2013a; Chen et al., 2013b; Yuxin Wang et al., 2013; Wang et al., 2014). All of the studies conducted within this research group have adopted similar practices to those of van Olphen (1967) whereby the composite gels are prepared by mixing and then dried via the freeze-drying method. The work describes an array synthetic and natural polymers, as well as various surfactants, which have been combined with smectite clays in order to produce stable aerogels (Bandi and Schiraldi, 2006; Arndt et al., 2007). Clay concentrations in the initial hydrogel are typically between 1 – 10%wt whilst the polymer contents range from 0 – 15%wt.

The use of natural polymers in composite aerogels has received particular attention owing to efforts to reduce the consumption of fossil-fuel derived polymers and create biodegradable and non-toxic materials. Indeed studies have shown that coherent biopolymer-clay aerogels can be manufactured at a competitive price with a relatively simple production process, using more environmentally friendly methods than those of silica aerogels (Dalton et al., 2010; Schiraldi et al., 2010). For example, Gawryla et al. (2008) and Pojanavaraphan et al. (2010) describe the production of a biopolymer-clay aerogel utilising casein, a natural polymer derived from milk, and sodium montmorillonite clay. For these composite aerogels, density and compressive modulus increased with an increasing quantity of casein although a minimum polymer content 5% was required to produce a sufficiently stable structure. Thermal conductivity tests were also conducted on a single sample giving a value of 0.045 W/m-K, similar to the value for foamed polystyrene (0.03 W/m-K). Other biopolymer-clay hybrids studied to date include those containing alginate (Chen et al., 2012), chitosan (El Kadib and Bousmina, 2012), pectin (Chen et al., 2013a), whey/alginate (Chen et al., 2013b), xanthan gum/agar (Wang et al., 2014), lignin and lignin/alginate (Viggiano and Schiraldi, 2014). In addition to polymer based additives, a number of researchers have also investigated the use of bio-based fibres including silk, hemp, soy silk bamboo and ramie (Finlay et al., 2007) as well as cellulose whiskers (Gawryla et al., 2009) as another means of improving strength.

Aside from the polymer and/or fibres used, the type of clay and processing variables, such as the level of shear during mixing and freezing techniques, can result in varying structures. This can range from coherent aerogel monoliths to expanded powders and fragile foams or flakes (Somlai et al., 2006). The smectite clay types are noted to be the most successful since they do not phase separate during the freeze-drying process. This is due to the fact that the large negatively charged surface area of the smectite clays and the 2:1 structure facilitates exchange with cations and other polar molecules within the interlayer region (Somlai et al., 2006). Coherent aerogels using these smectite clays and PVOH polymers have since been patented (Schiraldi et al., 2007) and developed into a product known as AeroClay™ which is currently being marketed primarily as an environmentally friendly packaging material although other potential applications cited include pipework insulation, pollutant adsorbents and cat litter pellets are also cited. Some other developments in relation to clay-polymer based aerogels as potential insulation materials for buildings have also taken place. For example, Dalton et al. (2010) describe a system where a clay-PVOH aerogel, as developed by Schiraldi et al. (2007) is vacuum sealed within a polyester and foil coated material. Here it is argued that although the clay aerogel has slight reduced thermal resistivity compared to silica based systems, this is compensated by the significantly reduced cost and improved strength. Another similar European research project known as ICECLAY is also currently investigating the use of clay-polymer aerogels using PVA and cellulose for building applications (ICECLAY, 2014). In this case it is again argued that using this freeze-dried product can cut up to half of the costs usually associated with silica aerogels.

8.2.3. Alginate aerogels

As previously described, the gel-forming ability of alginate is one of its most useful and unique properties. Consequently, alginate based hydrogels have been studied rather extensively and developed for various applications including structural and texture modifiers for food products (Burey et al., 2008) and numerous biomedical uses such as gel capsules for drug delivery (Patil et al., 2012), dental impression materials (King et al., 2008), wound dressings (Balakrishnan et al., 2005; Oh et al., 2011), tissue engineering scaffolds (Rowley et al., 1999; Kuo and Ma, 2001; Rezende et al., 2007) and various forms of cell encapsulation (Lim and Sun, 1980; Thu et al., 1996; Ashton et al., 2007; Tan and Takeuchi, 2007). Studies include both acidic alginate gels, which are created by lowering the pH of the alginate solution, or iontropic gels which are formed using multi-valent ions (Draget et al., 2006). In the former method, lowering the pH of the alginate gel below the pKa value, which is usually between 3.4 and 3.7 (Draget et al., 2009), can create a stable gel if correctly controlled. However an abrupt decrease in pH can also result in precipitation. A slowly hydrolysing lactone such as D-glucono-δ-lactone (GDL) is therefore typically used during pH modification. For the iontropic gelation method, which is the more commonly used technique, most studies use Ca^{2+} as the crosslinking ion (Funami et al., 2009) but some authors have also successfully created gels using Ba^{2+} (Zimmermann et al., 2007), St^{2+} and Zn^{2+} (Place et al., 2011), Cu^{2+} (Lu et al., 2006), Al^{3}+ (Nokhodchi and Tailor, 2004) and Mg^{2+} (Donati et al., 2009; Topuz et al., 2012). Two main types of iontropic gelation are utilised: the diffusion method and the internal setting method. For the diffusion method, the alginate is added drop-wise into a multivalent crosslinking solution leading to the rapid formation of gel beads or microspheres (Martinsen et al., 1989; Ashton et al., 2007;Patil et al., 2012). For the internal setting method, the gelation process is more controlled and homogenous since the crosslinking cation is gradually released using a slowly soluble salt and a sequestering agent (Stokke et al., 2000; Yuguchi et al., 2000;Liu et al., 2003;Tan and Takeuchi, 2007). As reported by Kuo and Ma (2001), this method has been shown to create a more uniform gel with superior mechanical properties to the diffusion based methods. It should also be noted that for both methods of iontropic gelation, the pH can alter the electrostatic interactions between the polymer chains and thereby affect the gel structure (Draget et al., 2009).

In addition to the method of gel formation used, existing studies highlight the importance of the alginate variables in determining the properties of the final gel. For example Martinsen et al. (1989) studied alginate hydrogel beads created from the $CaCl_2$ diffusion method using alginates sourced from six different seaweed types and with varying molecular weights. The results showed that the strength of beads increased with increasing alginate concentration, increasing G content of the alginate chain and increasing molecular weight for molecular weights lower than 2.10 x 10^5 g/mol. Draget et al. (1998) also showed that the type of monovalent ion present in the initial alginate salt prior to gelation can also affect gelation kinetics with the potassium alginate product exhibiting a more rapid sol-gel transition and a higher elastic moduli than the sodium alginate. Straatmann and Borchard (2003) have also highlighted the importance of alginate concentration on gel strength, giving a minimum value of 0.5% for successful gel formation. Liu et al. (2003) in measuring the gel points of alginate hydrogels prepared using the internal setting method also demonstrated that factors such as molecular weight, molecular weight distribution, the M/G ratio of the alginate and the ratio of the crosslinking ion to the carboxyl groups on the alginate influence the gelation behaviour. Funami et al. (2009) further describe the importance of the feeding ratio of Ca^{2+} to the G blocks giving a critical value of 0.5 (Ca^{2+}/G) for the formation of an egg-box gel network to occur. Overall, the main factors affecting the gelation kinetics and properties of alginate hydrogels as discussed by Draget et al. (2009) include alginate variables such as the chemical composition and molecular weight as well as the type of calcium source and modulators used. This is illustrated Figure 8-5.

Figure 8-5: Variables Affecting Gelation

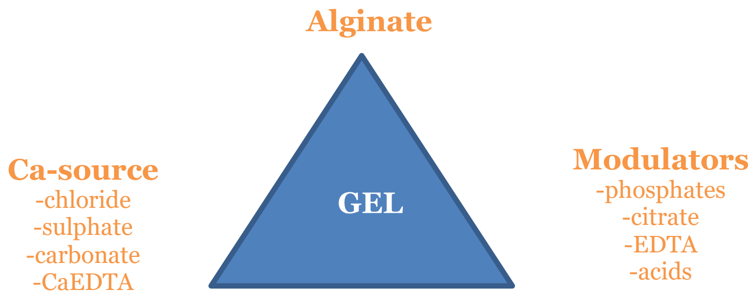

Source: Adapted from Draget et al. (2009)

Although the production of alginate based hydrogels has therefore been well studied, research into alginate based aerogels is much more limited. Contemporary research into the use of alginate-based aerogels, as per alginate hydrogels, is mainly limited to biomedical functions. For example Nussinovitch et al. (1993) discuss the potential use of agar and alginate aerogels as wound dressings whilst Mehling et al. (2009) considered drug delivery applications. In the former study the author concluded that the alginate aerogel exhibited superior mechanical properties than the agar based product whilst Mehling et al. (2009) showed that the alginate aerogels offered greater porosity, lower density and a greater surface area when compared to starch based aerogels. Other studies have also proposed using alginate aerogels as absorbents (Deze et al., 2012; Cheng et al., 2012).

In most studies the alginate gel is first synthesised through iontropic gelation in a similar manner to hydrogels. In the case of the diffusion method, gel spheres are formed and subsequently dried to produce a granular form of aerogel (Valentin et al., 2005; Trens et al., 2007; Quignard et al., 2008; Deze et al., 2012). For the internal setting method, larger aerogel monoliths can be created since the gel can be formed in any appropriate container or mould. For example Nussinovitch et al. (1993) used calcium hydrogen orthophosphate ($CaHPO^4$) and calcium carbonate ($CaCO^3$) as crosslinking agents in combination with GDL which slowed the gelation process by slowly hydrolysing and freeing calcium ions from the salts (Funami et al., 2009). Similar gelation methods were used by Mehling et al. (2009) and Cheng et al. (2012). After gelling, various drying methods can be implemented. For example Valentin et al. (2005), Quignard et al. (2008), Robitzer et al. (2008) and Mallepally et al. (2012) adopted a solvent exchange process with ethanol followed by supercritical drying with CO_2 whilst Nussinovitch et al. (1993) and Cheng et al. (2012) used water as a solvent and then used freeze-drying to remove the liquid.

A number of studies have also considered the use of alginate in composite aerogel products where the alginate is combined with another material. For example, Ohta and Nakazawa (1995) described the use of sodium alginate in combination with montmorillonite. In this case, 10% wt. solutions of the alginate and the clay were prepared separately before being mixed together at various ratios to form clay-alginate gels which are subsequently dried through freeze-drying. The reported results in this work are related to clay-agar aerogels and so limited details are given on the properties alginate product.

The most detailed studies of alginate being used within clay aerogels are those previously mentioned by Chen et al. (2012), where ammonium alginate is used in combination with montmorillonite, and Chen et al. (2013b) who described alginate and clay/whey protein isolate aerogels. In the former study the samples tested included alginate only aerogels and cross-linked alginate aerogel. In the latter case, both $CaCl_2$ and $CaCO_3$/GDL were used as a Ca^{2+} source. Alginate-clay aerogels with and without a calcium crosslinking source were also studied. The authors' concluded that the compressive modulus was found to increase with increasing alginate content and that the addition of clay led to further improvements in mechanical strength. The combined use of GDL with an additional calcium source was also found to increase the compressive modulus up to a certain concentration, beyond which entrapment of CO_2 bubbles caused structural imperfections within the aerogel. The microstructure of the aerogel, observed through SEM, was also found to be related to the viscosity of the initial solution. High molecular weight, high concentrations or increased levels of crosslinking were therefore found to increase the hydrogel viscosity resulting in a network like morphology rather than a lamellar structure in the final aerogel. Both the addition of clay and calcium were also found to improve the thermal stability and the clay-alginate aerogel also offered reduced flammability compared to the neat alginate material. Overall the authors compared the mechanical properties of the aerogels to those of rigid PUR and balsa and described positive effects when combining the properties of the alginate and clay. Aside from aerogels, other hybrid materials involving alginate and various clay types have also been investigated including composite hydrogels (Benli et al., 2011; Oh et al., 2011), films (Yang et al., 2009), sorption materials (Ely et al., 2011), nanocomposites (Bandeira et al., 2012;Yizhe Wang et al., 2013) and drug delivery materials (Kaygusuz et al., 2015).

Other non-clay based composite aerogels which incorporate alginate include silica-alginate (Shchipunov and Karpenko, 2004), lanthanide-alginate (F. Liu et al., 2008), starch-alginate (Martins et al., 2015) and lignin-alginate hybrids (Quraishi et al., 2015). Cheng et al. (2012) also illustrated that the addition of other reinforcing components such as CMC and N,N'-methylenebisacrylamide (MBA) could be used to further improve the strength of the aerogels, whilst a plasma surface modification technique could be used to make the material hydrophobic. Barbetta et al. (2009) have also investigated methods for controlling the porosity of alginate aerogels through either high internal phase emulsion (HIPE) or high internal phase foam (HIPF) templating. In other research, Horga et al. (2007) have also shown that alginate aerogels can be used as precursors for transition metal oxide nanoparticles.

It should be noted that in most of these studies regarding alginate aerogels, alginate variables are not considered in detail. For example Nussinovitch et al. (1993) use a 'low viscosity' alginate powder (Kelgin LV, Kelco) but do not discuss its chemical composition. Trens et al. (2007), Nussinovitch and Zvitov-Marabi (2008), Robitzer et al. (2008) and Deze et al. (2012) give details of the M/G ratio but these only range from 1.5 to 1.8, giving a relatively limited range of G contents (35-40%). Mallepally et al. (2012) mention the use of two different grades of alginate but then give no further details of their composition. The most detailed investigation regarding the influence of alginate variables on the final aerogel properties is that by Valentin et al. (2005) where three different types of alginate with varying G contents (20%, 45% and 76%) and viscosities (0.2, 2 and 2 Pa·s) are discussed. In this case the rich sample is noted to have a more compact structure, as revealed by SEM, however there is still limited investigation into the importance of the alginate variables in relation to the final properties of the aerogel. Although Chen et al. (2012) gives the most in-depth analysis regarding the characterisation of the aerogels, the main variables studied are the alginate concentration and the addition of other components such as montmorillonite and crosslinking agents.

Overall the production of aerogel materials using either alginate alone or in combination with other materials has received a reasonable amount of attention in recent years, with the majority of studies having been published in the past decade. Most of the materials are however at the prototype stage and have not yet been developed in to commercial products and there is still limited understanding of the role of alginate variables in determining the properties of such aerogels.

8.2.4. Environmental Impacts

As discussed by Dowson et al. (2012),where aerogels are to be used as a method of preventing heat loss in buildings, it is also important that the energy and GHG emissions involved in the production of aerogels do not outweigh the potential energy savings. Whilst some studies have calculated the operational energy and GHG emission reductions possible when using aerogels as insulators within buildings (Cuce et al., 2014b), few studies have investigated the environmental impacts of the material itself. Indeed Johansson (2012) highlighted the general lack of existing LCA studies for aerogel materials. Silica aerogels for example require various solvents like ethanol, methanol and acetone, in combination with energy intensive drying procedures which can significantly affect the overall environmental impact of the material. Typical embodied energy and embodied carbon values quoted for commercially available products like Spaceloft® are 53 MJ/kg and 4.2 kg of CO_2/kg respectively. In comparison to conventional insulation materials, silica aerogel blankets are therefore relatively high in embodied energy, albeit lower than some polymer based products as shown in Figure 8-6. They also have a greater embodied CO_2 value than most other insulation materials.

Figure 8-6: Embodied Energy of Insulation Products

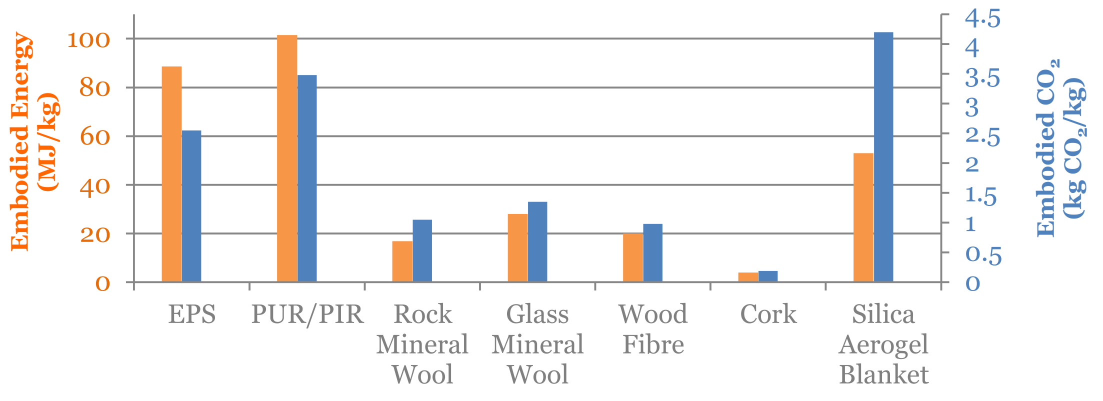

Source: G. Hammond and Jones (2008)

There have therefore increasing efforts to improve the environmental impact of silica aerogels. Green Earth Aerogels (GEAT, 2016), for example, have developed a method of using rice husk ash as an alternative raw material. Svenska Aerogel AB have also focussed on improving the efficiency of the processing methods and have reportedly reduced the production costs by 90% by developing an ambient pressure and drying methods (Business Innovation Observatory, 2015). Again there is however limited quantitative data on the environmental impacts. One study by

Dowson et al. (2012) describes a cradle to gate LCA, comparing two different processing methods for silica aerogels - high temperature supercritical drying method (HTSCD) and low temperature supercritical drying method (LTSCD). Both production methods reportedly offer payback periods of less than two years when considering their embodied energy values against their potential operational savings over a 15 year period, based on replacing a single –glazed window to a translucent aerogel panel. The HTSCD method demonstrated a lower overall production energy (1824 MJ/m^2) and CO_2 burden (23 kgCO_2/m^2) compared to the LTSCD method (2728 MJ/m^2 and 120 kgCO_2/m^2), mainly due to the fact that the LTSCD method required larger volumes of solvent. When these values are compared with the overall predicted energy savings of 1440 MJ per year, which are possible when these materials are used to improve the building fabric, it becomes apparent that the energy involved in manufacturing the materials outweighs the potential energy savings. It should be stated however that the processing data was based on a laboratory scale study which does not take into account the benefits of increased economies of scale involved in commercial production. Final estimates based on best practice gave overall embodied energy values similar to that of Spaceloft®.

Other studies regarding the use of aerogel materials for insulation purposes do not include embodied energy or embodied carbon values. While the likes of Dalton et al. (2010) and Schiraldi et al. (2007), claim that clay based aerogels have environmental advantages over silica products and make use of more benign production processes, to date there is no known comprehensive LCA study which compares the environmental impacts of these materials. Indeed, Gawryla et al. (2008) acknowledged the need to conduct a “full carbon-utilization cycle analysis” in order to confirm that the use of clay and natural polymers will have environmental benefits. As discussed by Cuce et al. (2014a), there are also various environmental hazards associated with aerogels mainly due to the production of airborne dusts during installation. Measures to protect from these potential hazards would also need to be considered if such materials were to be used in construction.

8.2.5. Costs

In considering the economic viability of aerogels, according to Riffat and Qiu (2013) the manufacturing costs of silica based aerogels are still relatively high in comparison to other insulation materials. Indeed, even for silica aerogel blankets which are relatively well established and available commercially, costs of £24 - 174/m^2, depending on product thickness, are reported. A recent study in the UK also quoted costs of around £50/m^2 for a 40mm Spacetherm® product (BRE, 2016). This is presented in Figure 8-7 along with some typical costs for other insulations. As illustrated, the cost of Spacetherm® is at least double the cost of any of the other insulation product discussed. This cost must however be weighed against the potential long term cost savings in relation to reduced heat losses, and the advantages of aerogels with regards to the minimised thicknesses required in achieving the desired U-values.

Figure 8-7: Typical Costs for Insulation Products

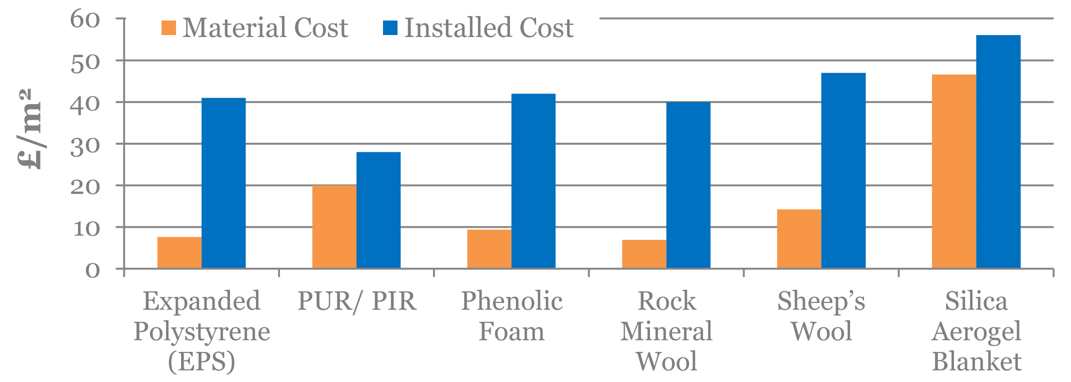

Source: BRE (2016)

One of the major contributors to the cost of aerogels relates to processing and the energy used during manufacture (Riffat and Qiu, 2013). Indeed the energy costs alone can reportedly contribute to around 30% of the total production costs (Carlson et al., 1995). For instance, the supercritical drying methods required, which typically involve long periods of high temperature and pressure drying, are both dangerous and expensive compared to the processing techniques involved for conventional insulation materials (Herrmann et al., 1995). It has therefore been argued that the development of drying techniques performed in ambient conditions may help to reduce costs and various studies have explored these cheaper and safer methods (Tewari et al., 1985; Smith et al., 1992; Wei et al., 2007). Supercritical drying through vacuum freeze-drying, as previously described, has also been proposed as another alternative, lower cost drying method (Schiraldi et al., 2007; Su et al., 2012). However, since aerogels are still a developing technology, many of these processing techniques are still being investigated and developed for larger scale production.

In addition to processing factors, the raw materials used in the product will also influence the total cost. According to Carlson et al. (1995), in silica based aerogels the sodium silicate precursor can form approximately 40% of the total aerogel production costs. In the case of alternative aerogel materials, such as clay-based products, Dalton et al. (2010) provided estimated production costs, reporting that the aforementioned “Aeroclay” product could be produced at a significantly lower cost than both a pure silica aerogel and a commercially available silica aerogel blanket. This would suggest that their proposed method of using clay and natural polymers, as an alternative to silica, as well as the use of freeze-drying as opposed to CO_2 supercritical helps to reduce costs. Therefore, although the high costs of aerogel insulations still hinder their widespread use, strategies to reduce their processing costs and make use of lower cost raw materials, will likely make aerogels more affordable in the future and hence increase the commercial viability of using such materials in bulk applications like building insulation.

Overall it has been reported that positive market trends and increased demand for aerogels will likely reduce future costs with Cuce et al. (2014a) suggesting that by 2050 the price of aerogel materials will be less than £500/m^3. It has also been predicted that a wider range of potential markets will emerge. The global aerogel market is currently around £200 million and an estimated 10,680 metric tons of aerogel was sold in 2014 alone, most of which was used in the oil and gas industry although other sectors such as aerospace, construction and healthcare are also included (Technavio, 2015). According to a recent report, building insulation applications in particular are noted to be important in the future for aerogel development (Business Innovation Observatory, 2015).

8.3. Summary

In summarising the findings of the Part II literature review, there is a market for new insulation products which offer good thermal performance, comparable to that of PUR/PIR and silica aerogels, but which are less damaging to the environment and efficient to produce in both cost and energy terms. Existing studies indicate that alginate-based aerogels are one such material that offers a high porosity and low bulk density as well as being produced from a renewable resource. It is therefore possible that if an economically viable form of production can be developed for manufacturing an alginate aerogel then this could be a viable option for developing alginate-based insulation products. In existing studies relating to alginate aerogels, the alginate is often combined with other materials such as clay minerals and calcium crosslinking agents in order to improve the mechanical properties and create coherent composite aerogels. The specific properties reported in existing studies however vary quite considerably depending on the preparation techniques used and the form of aerogel are being studied (i.e. bead vs monoliths of various sizes). The characterisation tests performed also differ with some authors focusing on porosity characteristics while others are more concerned with mechanical properties. Shrinkage, thermal decomposition, water absorption and flammability tests are only conducted in a few studies. BET surface areas range between 150 – 590 m^2/g whilst bulk density ranges from 40 – 170 kg/m^3 but direct comparison between the results of existing studies is difficult due to the different methodologies and materials being tested. Furthermore, although most studies involving alginate *hydrogels* discuss the importance of the type of alginate used on the gelation mechanisms and hence the gel structure and strength, few of the *aerogel* studies discuss the alginate properties in great detail. Indeed while most of the hydrogel studies include at least two different alginate types within the experimental methodology, most of the aerogel studies investigate only one alginate type and therefore do not consider potential alginate variables such as viscosity and M/G ratio. This again makes comparison between existing studies difficult. There has therefore been no comprehensive study to date which discusses the role of alginate variables (source, M/G ratio, viscosity and concentration) on the structural and mechanical properties of alginate-clay aerogels.

9. EXPERIMENTAL METHODS (PART II)

Following the findings of the literature review, the ambition of Part II was to identify whether aerogel specimens prepared using alginate and clay would be suitable as a building insulation product and whether they offer any advantages over existing materials such as a silica aerogels. As per Part I, one of the key objectives was to investigate the role of the alginate source and identify the optimum types of alginate and most appropriate mix ratios required to produce the final aerogel product. It was also proposed that different clay types would be studied in order to determine their impact on the properties of the composite and their interaction with the different alginate types. The final objective was to assess the commercial viability of the alginate aerogel in comparison with other similar products.

Key questions

Q1: What impact do alginate variables (e.g. concentration, viscosity, composition) have upon the physical properties of a composite alginate-clay aerogel?

Q2: What impact do other variables (e.g. clay type, pH) have upon the physical properties of a composite alginate-clay aerogel?

Q3: Are the specimens produced suitable for use as a building insulation material?

Scope and Limitations

The study was designed only to test 5 alginate products supplied by MBL and one commercial product. Other potential alginate sources were not investigated at this stage since these 6 products alone provided arrange of different polymer compositions. Given that the objective was to assess how these variations in composition influenced the aerogel properties, a standard preparation method was used meaning that process variables (e.g. freezing and drying methods) were not considered at this stage. In order to focus on interactions between the alginate and clay components, the use of other additives (e.g. fibres or sequestering agents) was also excluded. As initial prototypes, the samples were also produced as small-scale monoliths rather than large scale insulation panels which would require industrial scale equipment and greater quantities of alginate.

9.1. Materials

Alginate

The alginate products used in Part II were identical to those used in Part I including two *Laminaria Hyperborea* (LH) stem products (PR22 and PR24), one *LH* frond product (PR32) and one *Ascophyllum* (AN) product (PR52). The previously described commercial product (AC) was also used for comparison.

Clay

For the initial batches of aerogels, a bentonite clay (B) as described in Chapter 3 was used. In later studies, clay variables were investigated by modifying the bentonite, either through pH adjustment (AB) or by saturating with ionic solution to produce a homo-ionic calcium bentonite (CB). A kaolinite clay (K) was also used for comparison. The different clay types are summarised in Table 9-1.

Table 9-1: Summary of Clay Types

	Bentonite	**pH modified Bentonite**	**Calcium Bentonite**	**Kaolinite**
Preparation	Unmod.	pH adjusted with HCl	3 x washes with $CaCl_2$ Rinse with DI water Oven-drying	Unmod.
Abbreviation	**B**	**AB**	**CB**	**K**

9.2. Testing Programme

The testing programme for Part II is illustrated in Figure 9-1**.** As per Part I, the properties of the alginate and clay materials were firstly characterised through a series of rheology based tests. Aerogel prototypes were then prepared at a variety of mix ratios. Observations were made regarding the workability of the wet mixtures and the occurrence of any defects in the dry samples. The prototypes were then tested in relation to their compressive strength and microstructure. An assessment of the commercial feasibility of the aerogel products, including an environmental assessment and cost analysis, was also conducted.

Figure 9-1: PART II Testing Programme

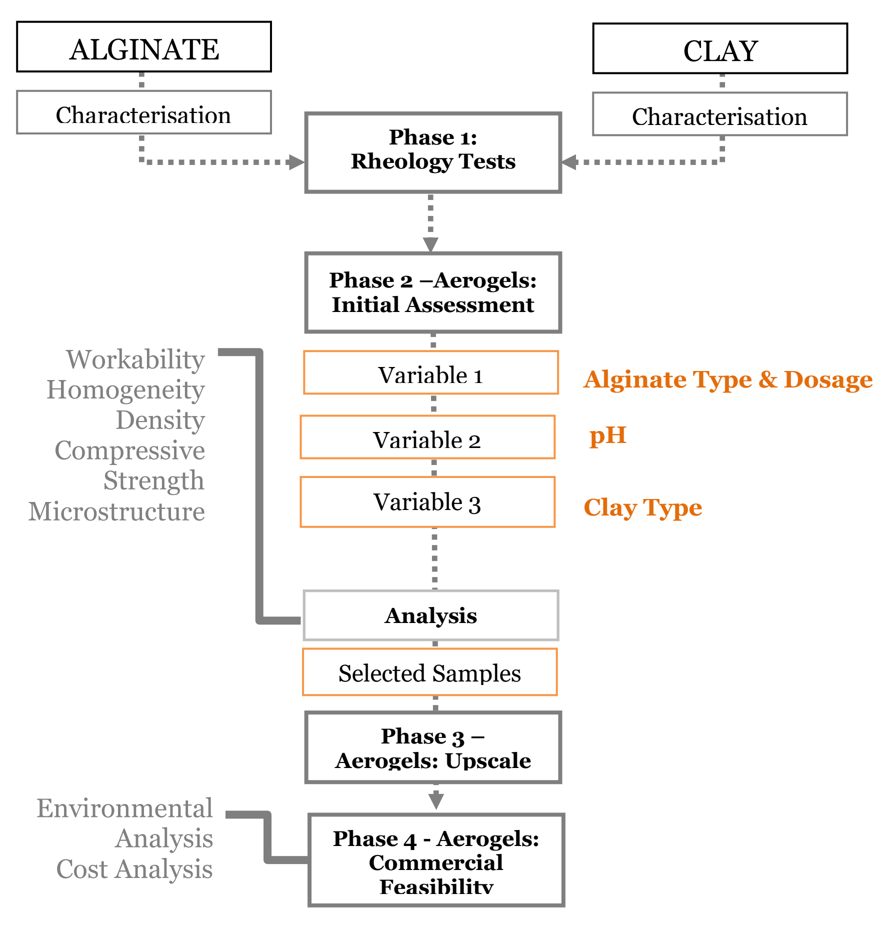

9.2.1. Phase 1 – Rheology Tests

As per Part I, rheology tests were performed as a preliminary investigation of the interactions between the clay and the different alginate products. Changes in the flow behaviour and viscoelastic properties of the clay-alginate mixtures were observed by comparing flow curves and creep deformation behaviour. Colloidal stability was also investigated by measuring the ζ-potential of each sample. Again the role of other potential variables such as the polymer dosage, pH and calcium content was also investigated. An additional XRD study was also included in order to further explore nano-scale interactions between the polymers and the clay.

9.2.1.1. Flow Behaviour

Viscosity is a measure of a fluid's resistance to flow. As discussed in Chapter 3, rheometers can be used to obtain flow curves which plot shear rate ($\dot{\gamma}$) against shear stress (τ). From this curve, it is also possible to determine other parameters by fitting the resulting plot to known rheological models. In this case, flow curves for the alginate-clay mixtures were obtained using a Brookfield R/S Rheometer (CC45) with an integrated water bath (25°C) as shown in Figure 9-2. The curves were then analysed in more detail and fitted to the Hershel-Bulkley model shown in Equation 15, allowing values for the consistency index (k), flow index (n) and yield stress (τ_o) to be determined.

$$\tau = \tau_o + C\gamma^n$$

Equation 15

The consistency index (C) represents the average viscosity of the fluid while the yield stress (τ_o) is the stress required to disrupt the materials internal structure and induce flow. The flow index (n) provides a measure of the degree of shear-thickening or thinning. The degree of thixotrophy, which is the decrease of viscosity caused by applying a shear stress or strain followed by a gradual recovery upon removal of the stress or strain (Barnes, 1997), was also determined by observing the hysteresis between the upward and downward shear rate ramp.

Figure 9-2: Rheometer Set-up

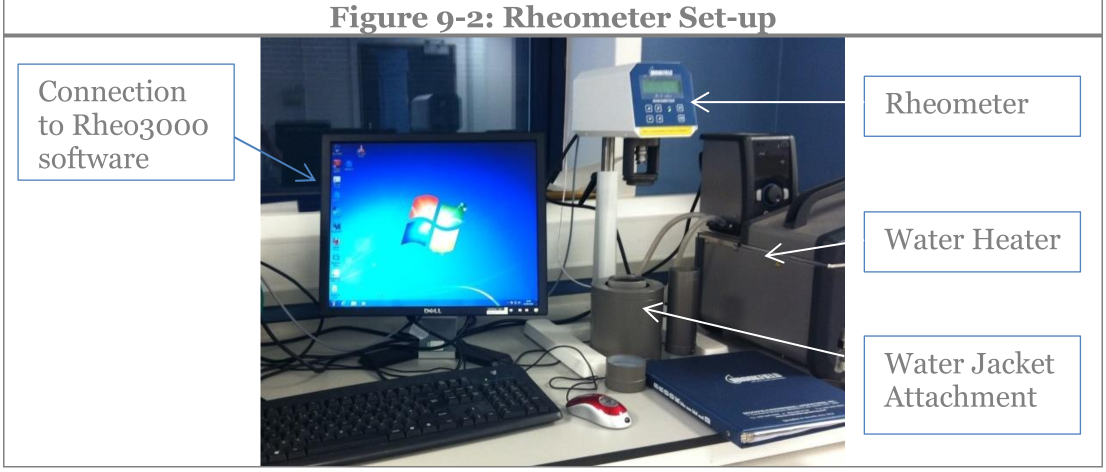

9.2.1.2. Viscoelastic Behaviour

In addition to viscosity and flow behaviour, dynamic measurements which record viscoelastic behaviour at low levels of stress can also be performed. One method of measuring this viscoelastic response is a creep recovery test which can be performed using a rotational rheometer. This involves measuring the time dependent deformation of the material at low shear stress, whereby the internal structure of the material is flexed without being completely destroyed. This technique has been used in other studies which analyse polymer-clay interactions (Durán et al., 2000; Benchabane and Bekkour, 2006). For this study a constant shear stress (τ) was applied to the material using a Brookfield R/S Rheometer for a given time (t). This was followed by a relaxation period where the load was removed. The shear creep compliance ($J(t)$) was then be derived from measured deformation (γ) using Equation 16 (Durán et al., 2000).

$$J(t) = \frac{\gamma(t)}{\tau}$$

Equation 16

Depending on the profile of the curve obtained, each sample was then categorised as either a linear elastic solid, a linear viscous fluid, a viscoelastic solid or a viscoelastic fluid. Depictions of these characteristic behaviours are illustrated in Figure 9-3.

Figure 9-3: Creep behaviour models

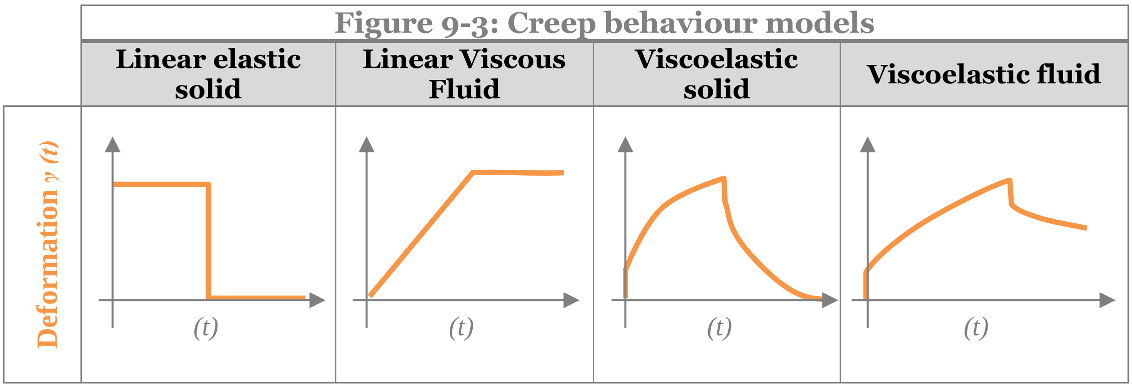

9.2.1.3. Colloidal Stability

The interaction between clays and polymers can be observed by measuring the stability and electro-kinetic properties of the particles within a liquid medium. However, unlike the soil slurries discussed in Part I where a wide range of particle sizes are present and the settling of the larger particles is usually visible to the naked eye, clay systems usually exhibit colloidal behaviour whereby the microscopic particles may remain suspended. A colloidal system is an intermediary of a solution and a suspension where the individual particles are larger than molecules but small enough to remain dispersed in the continuous phase. In a stable colloid the individual colloidal particles remain suspended in the solvent since the magnitude of the electrostatic repulsion between the particles is sufficient to keep them apart and well dispersed within the fluid. This is known as the DVLO theory as named after Derjaguin and Landau (1941) and Verwey and Overbeek (1955). This theory states that where there is a high ζ-potential, and therefore a high level of electrostatic repulsion, the particles will likely be repelled from each other. This creates a highly dispersed, stable suspension with a low viscosity. On the other hand, an unstable system is one where the electrostatic repulsion is lower than Van der Waals attractive forces meaning that the particles will aggregate to form larger particles or 'flocs'. In some cases these 'flocs' will settle creating a phase separated mixture with a clear solid-liquid interface. Where particles are strongly aggregated, forming a continuous network of particles (i.e. gel) rather than flocs, the system again becomes stable. A schematic of these different behaviours is illustrated in Figure 9-4.

Figure 9-4: Properties of colloidal suspensions

[This image has been removed by the author of this thesis for copyright reasons]

Source: Adapted from Fairhurst (2013)

As discussed in Part I, polymers can be added to clay systems in order to modify their electric-kinetic properties and induce either stabilisation, flocculation or aggregation (Tiraferri and Borkovec, 2015). Since ζ-potential values describe the magnitude of the electrostatic repulsion between particles, they provide an important measure of stability within a colloidal clay system. Existing studies therefore often correlate the electro-kinetic properties of clays with rheological observations (Van Olphen, 1964; Miano and Rabaioli, 1994; Durán et al., 2000). However, as discussed by Tiraferri and Borkovec (2015), there is general lack of studies regarding colloidal particles and polymers of the same charge, as is the case for clays and alginate. For this study dynamic light scattering (DLS) was used to provide information on the ζ -potential of the different clay-alginate mixtures. All measurements were made using a Malvern Zetasizer, ZSP (Malvern Instruments Limited, UK). A He-Laser with a wavelength of 633 nm and a detector angle of 173° was used for all experiments and a constant temperature of 25°C was adopted. All samples were prepared at the required clay: alginate ratio using Milli-Q ultrapure water and then centrifuged at 4500pm for 30 mins as per the methods of İşçi et al. (2006). The prepared samples were slightly turbid with no sign of sediment formation. Control samples of ultrapure water and various concentrations of clay and alginate were also prepared for comparison. Disposable capillary cuvettes were used for each sample and all results calculated as an average of 3 measurements.

9.2.1.4. X-ray Diffraction

In addition to clay mineral identification, as described in Chapter 3, XRD can also be used to investigate changes in the *d*-spacings of the crystal structure and provide useful information about interactions between clay and organic polymers. Polymer-clay adsorption can occur either as a separated phase, where adsorption take place only at the clay surface , or as an intercalated or exfoliated structure where the polymer is able to penetrate the galleries of the layered silicate. The two latter cases are referred to as 'nano-composites' rather than 'micro-composites' due to the nano-scale interactions taking place. A schematic of these structures is shown in Figure 9-5. For this study, in order to investigate any changes in the crystalline structure of clay minerals upon the addition of polymers, XRD of selected samples was performed using a the methods described in Chapter 3. In this case however, a known concentration of alginate was mixed with the clay prior to mounting.

Figure 9-5: Schematic of clay-polymer composites

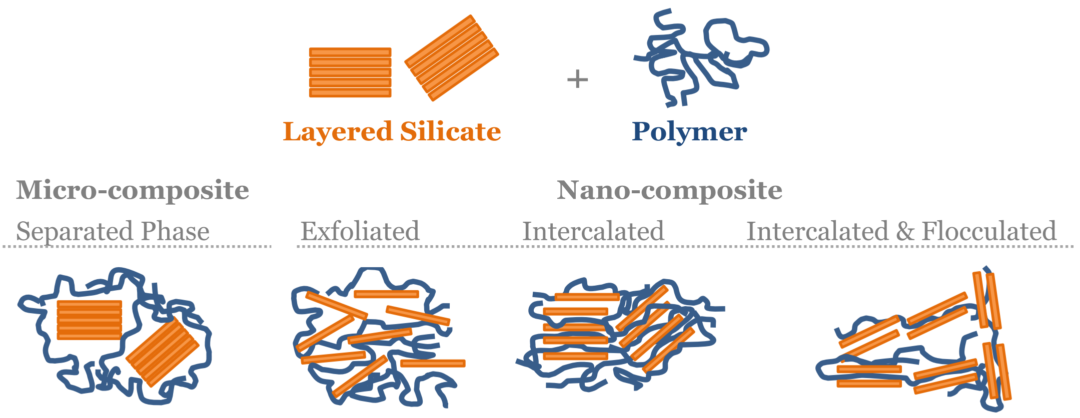

Source: Adapted from Galimberti (2012)

9.2.2. Phase 2 – Aerogel Specimens: Initial Assessment

Following the preliminary tests (Phase 1), the next stage was to produce prototype aerogel specimens. The clay-alginate aerogels were created using methods similar to that of Schiraldi et al. (2010) whereby separate 10 wt% solutions of the alginate and clay were firstly prepared with DI water. These were then mixed at the desired alginate: clay ratio using a handheld mixer, inserted into 2mL cryogenic vials and allowed to gel for 24 hours. Flash freezing was then conducted using iso-pentane and liquid nitrogen followed by a minimum of 24 hours drying in a Scanvac CoolSafe 110-4 PRO 4lt freeze dryer at a temperature of -80°C. After drying, the specimens were removed from the dryer, weighed and stored in sealed vials until further testing. Where required, the monoliths were trimmed with a scalpel and lightly sanded to produce cylindrical samples as shown in Figure 9-6.

Figure 9-6: Stages of the Aerogel Production Process

Hydrogels | **Aerogels** | **Cut Monoliths**

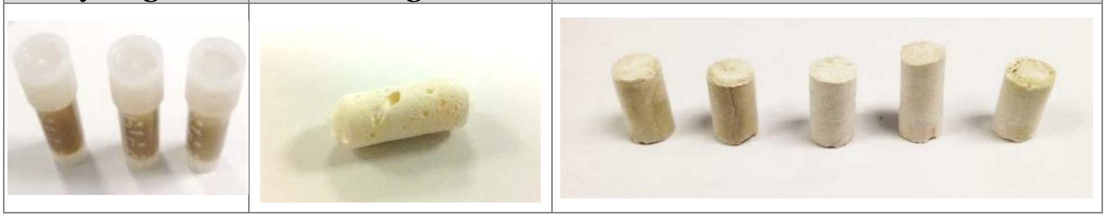

9.2.2.1. Visual Observations

Initial observations were made regarding the homogeneity of the prepared specimens based on the visibility of any cracks/defects or voids. Samples which appeared to be relatively homogenous were labelled ‘good’ whilst those with some visible voids and defects were labelled as ‘moderate’. ‘Poor’ samples were those where several defects and macroscopic voids were apparent in all specimens. The stability of the specimens was also assessed with samples which could easily be removed from the vial as one piece labelled as ‘monoliths’ whilst those samples which were unstable and collapsed upon removal were labelled as ‘powders’.

9.2.2.2. Dimensions, mass and bulk density

Once removed from the freeze-dryer each aerogel monolith was also weighed and its dimensions measured using digital calipers. The unit mass (m), recorded to 3 decimal places and unit volume (V), calculated from the measured dimensions, were then used to calculate the bulk density (ρ) in kg/m^3 using Equation 1 (Chapter 5). These measurements were then repeated following storage in ambient conditions for 72 hours and directly before compressive strength testing. Measurements were calculated as an average of 3-5 specimens.

9.2.2.3. Compressive Strength

The mechanical strength of the specimens was investigated based on the procedures outlined in BS EN 826(BSI, 2013b) and as described in other similar studies by Nussinovitch et al. (1993), Chen et al. (2012) and Martins et al. (2015). Testing was conducted on cylindrical specimens with a diameter of ~8mm and cut using a scalpel to a height of ~15mm. The surfaces of the two parallel faces were also gently sanded to create a smooth surface. An Instron 5969 universal testing machine was then used to apply a compressive force (F) to the material using a displacement rate of 5 mm/min (Figure 9-7).

Figure 9-7: Compressive Strength Test Set-Up

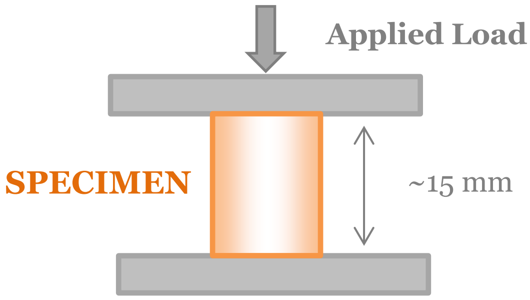

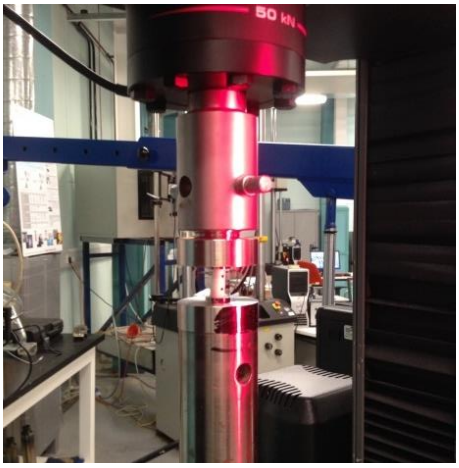

The compressive strength (σ) of the specimens was then calculated from the initial cross-sectional area of the specimen (*A)* and the maximum force (F_m) using Equation 6 (Chapter 5). In this case F_m was taken either as the yield point or at the 10% strain value for samples where no visible yield point was observed. Results were then calculated as the mean value of at least 3 test samples calculated to the nearest 0.1 N/mm^2. The compression modulus of elasticity (*E*) was also calculated from the initial linear gradient of the stress-strain plot.

9.2.2.4. Microstructure

SEM analysis was carried out in order to generate magnified images of the aerogel microstructures. The method was similar to that used in Part I although in this case much smaller samples were analysed (9mm diameter x 5mm height) and a higher resolution Field Emission SEM microscope (HITACHI SU-6600) was used. Cross-sections were cut from the bottom third of the cylindrical monoliths, in order to expose the internal part of the aerogel, and then sputter coated in gold. Similar techniques are used by Ohta and Nakazawa (1995) and Longo et al. (2013).

9.2.3. Phase 2 – Aerogel Specimens: Upscaling

In order to upscale from the prototype samples prepared using 2mL vials, a single large scale sample was also prepared using an 8 x 8 x 4cm steel mould. The initial gel material was prepared in the same manner as the small scale specimens. Flash freezing was performed in a large polystyrene container however the specimen was immersed in the liquid nitrogen for a longer duration than the previous samples (approximately 5 minutes). The specimen was then freeze-dried for 24 hours which was found to be a sufficient drying duration.

9.2.4. Phase 3 – Aerogel Specimens: Commercial Feasibility

In considering the commercial feasibility of using an alginate-clay aerogel as a building insulation material, aspects such as cost, environmental impact and market competition were investigated. The methods used were the same as those described in Part 1 (Chapter 5).

9.3. Statistical Significance

As discussed for Chapter 5, the statistical significance was investigated through ANOVA and Post-hoc Tukey tests. Again this was performed in order to compare the mean values for properties such as bulk density and compressive strength. In this case the aim was to determine any statistical significant differences in relation to variables like alginate type, alginate dosage or other clay variables.

10. RESULTS AND DISCUSSION

10.1. Phase 1 – Rheology Tests

10.1.1. Flow Behaviour - Variable 1: Alginate Type & Dosage

The flow curves generated for each of the alginates types at clay:alginate ratios of 5:0, 5:0.25, 5:0.5 and 5:1 are illustrated in Figure 10-1 to Figure 10-5. The samples are each labelled based on the mix ratio (e.g. C5A0.5 = 5% clay with a 0.5% dosage of the relevant alginate). As per results by Benli et al. (2011), the relationship between shear rate and shear stress showed non-linear behaviour. There was also a visible shift from near Newtonian behaviour, as observed for the clay only sample, to pseudo-plastic behaviour upon the addition of alginate. These results are similar those observed by Pongjanyakul and Puttipipatkhachorn (2007). In all cases the gradient of the curve, and hence viscosity, is increased with increasing quantity of alginate. This observed increase in viscosity can be caused by either by the increased polymer concentration or by interaction between the polymer and the clay particles (Tunç and Duman, 2008).

As shown in Figure 10-6 the type of alginate also has a visible influence on the rheological behaviour. Whilst PR24, PR52 and PR22 exhibit relatively similar behaviours at the 0.5% dosage, AC is much more viscous as evidenced by the steeper gradient of the flow curve. Indeed for AC the 5:1 is too viscous to be measured at shear rates above 500/s. On the other hand, PR32 is much less viscous and exhibits behaviour closer to that of a Newtonian fluid.

Figure 10-1: Flow Curve (AC)

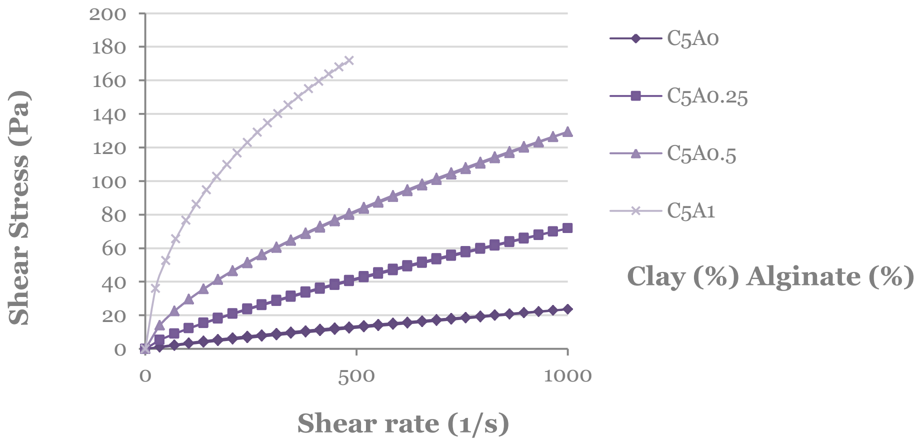

Figure 10-2: Flow Curve (PR22)

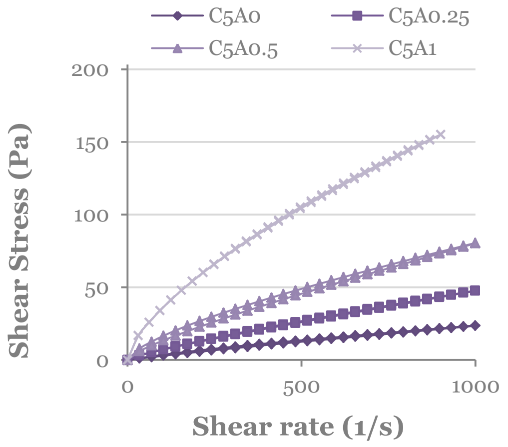

Figure 10-3: Flow Curve (PR24)

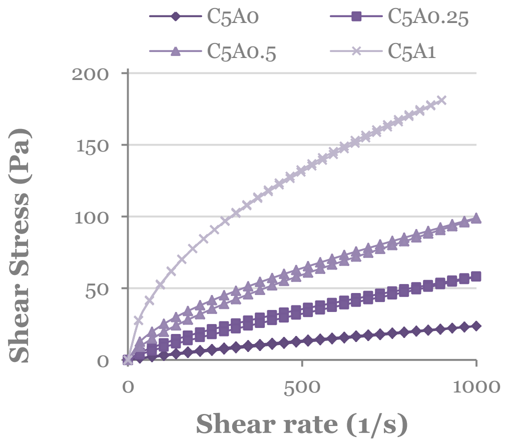

Figure 10-4: Flow Curve (PR32)

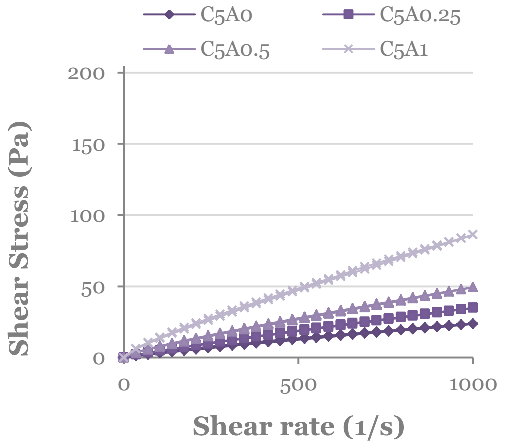

Figure 10-5: Flow Curve (PR52)

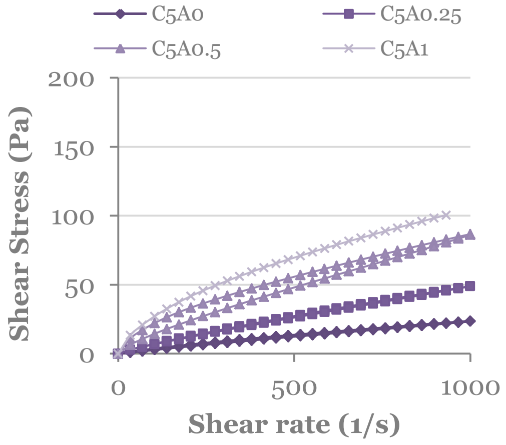

Although the highest viscosity alginate (AC) also has one of the lowest G contents, suggesting that the alginate composition is of less importance than the overall chain length in increasing the viscosity of the clay-alginate mixture, the high G content product (PR24) demonstrates a greater degree of thixotrophy than the other samples. This implies that this high G content sample takes longer to recover its initial viscosity after shearing. This is possibly due to the formation of cross-links at G sites which are broken up during shearing. PR24 (5:0.5) also exhibited the largest yield stress (5.8 Pa) while the majority of other samples had values of less than 1 Pa.

Figure 10-6: Variable 1 – Flow Curves

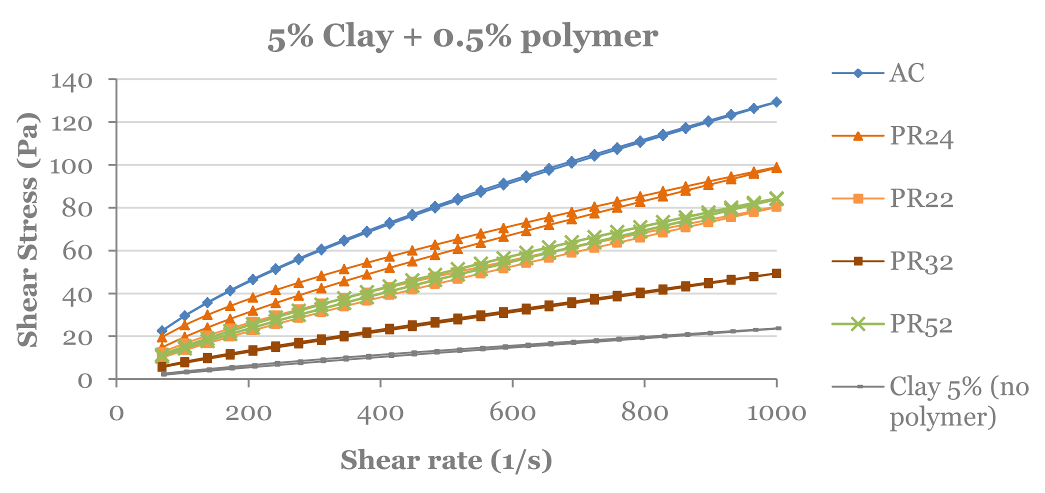

10.1.2. Flow Behaviour - Variable 2: pH

The flow curves for samples prepared at different pH levels, ranging from pH 3 to pH 9, are shown in Figure 10-7 to Figure 10-12. For the control samples (Figure 10-7), it would appear that pH only begins to affect the rheological behaviour below pH 4. This can be explained by the point of zero charge (PZC) which occurs at pH 2 – 3 for bentonite clay. This demonstrates that even without the alginate, the viscosity of the clay can be increased, albeit moderately, through pH modification.

Figure 10-7: Variable 2 - Flow Curves (Control– 5:0)

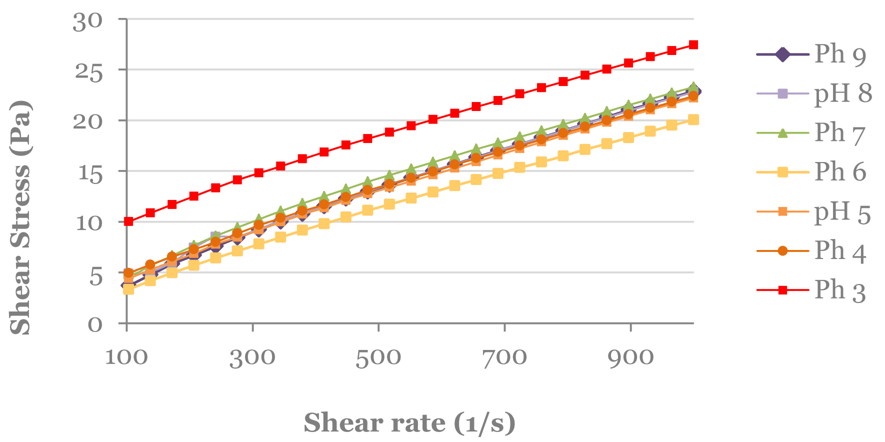

For AC, the flow curves for the 5:0.5 (clay: alginate) samples as shown in Figure 10-8 are fairly similar between pH 7 and 9 although at pH 8 the behaviour is more thixotropic. At pH 5, viscosity increases dramatically and the greatest degree of thixotrophy can also be observed as indicated by the difference between the upward and downward shear rate ramp (indicated by arrows). High yield stresses are also observed between pH 4 and 6. Indeed the pH 4 mix is too viscous to be studied at shear rates above 800/s. This increase in viscosity and shear strength is indicative of reduced electrostatic repulsion and increased bonding. However below pH 4, the flow curve changes rather dramatically resulting in a reduction in viscosity. This is likely due to the fact that in strongly acidic conditions, where the H^+ ions are added directly, the alginate may form a precipitate, thereby reducing viscosity.

For the MBL alginates, the flow curves generated for the 5:0.5 (clay: alginate) samples are shown in Figure 10-9 to Figure 10-12. In the case of PR22 (Figure 10-9), the flow curves for pH 8 and 9 are relatively similar but the gradient of the slope then increases with decreasing pH. Again the degree of thixotrophy also becomes greater in acidic conditions. This observation is particularly dramatic for pH 4 & 5 highlighting that, in these conditions, the intermolecular bonds are broken up at high shears and do not recover fully during the downward ramp. As per the observations for AC, at pH 3 the viscosity is dramatically reduced. For PR24 (Figure 10-10), again reducing the natural pH of the sample (pH 9) to pH 7-8 leads to an increase in viscosity. In acidic conditions the viscosity increases even further with pH 4 & 5 displaying the highest viscosities and greatest degree of thixotrophy. Yield stresses also appear to develop for PR24 when the pH is sufficiently acidic, with the greatest yield stress observed for pH 5. Below pH 4 there is again a dramatic decrease in viscosity. For samples PR32 and PR52, pH modification appears to have less of an effect since all samples exhibit similar behaviour.

According to McHugh (1987), alginate viscosity should not be dramatically affected over a pH range of 5 -11. The results from this study indeed show that the most dramatic changes occur at pH 4-5, similar to results by Auhim and Hassan (2013). Below pH 5, the increased concentration in H+ ions leads to protonation of the carboxyl groups (i.e. transformation from COO- to –COOH). This in turn reduces the negative charge of the alginate and reduces electrostatic repulsion between the polymer chains. A reduction in pH will also alter the surface charge of the clay particles where the pH is reduced below the PZC. In this case, the combined effects of the reduced negative charges on the anionic groups of the polymer and the surface of the clay particles would likely lead to increased attraction between the two components. This would result in an increased viscosity and the formation of a gel network, as observed for the samples in this study.

Figure 10-8: Flow Curves (AC – 5:0.5)

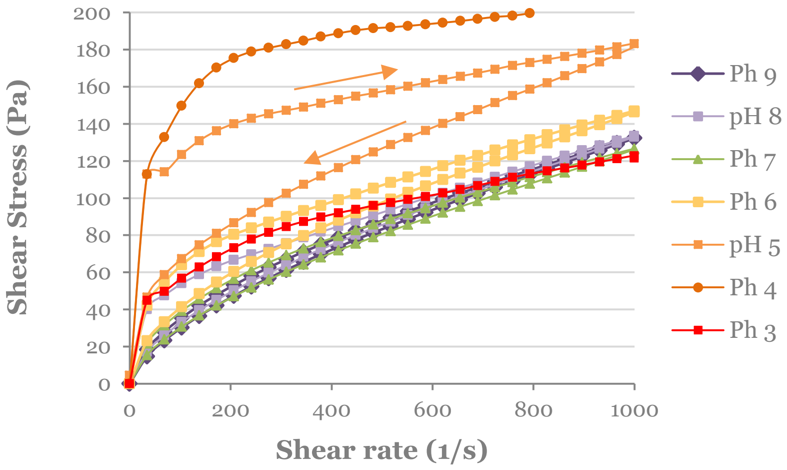

Figure 10-9: Flow Curves (PR22)

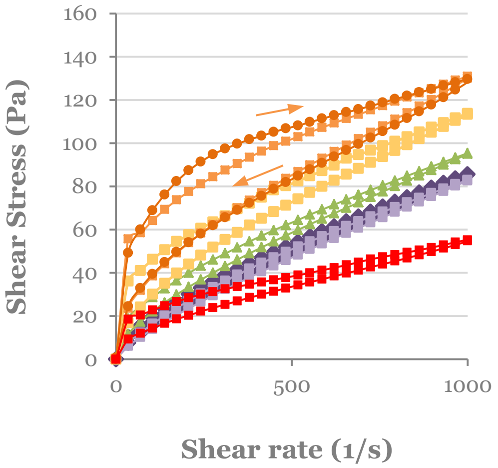

Figure 10-10: Flow Curves (PR24)

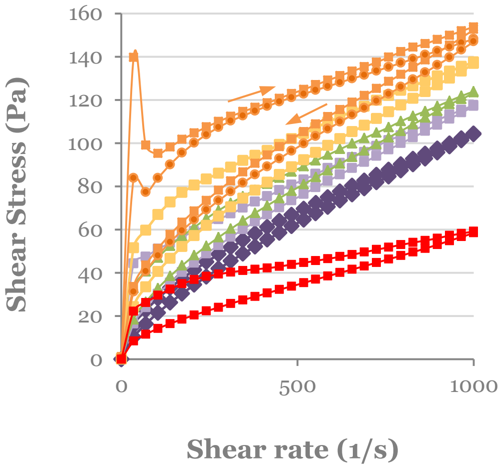

Figure 10-11: Flow Curves (PR32)

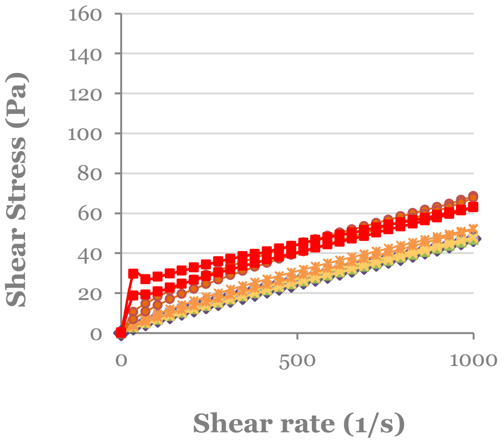

Figure 10-12: Flow Curves (PR52)

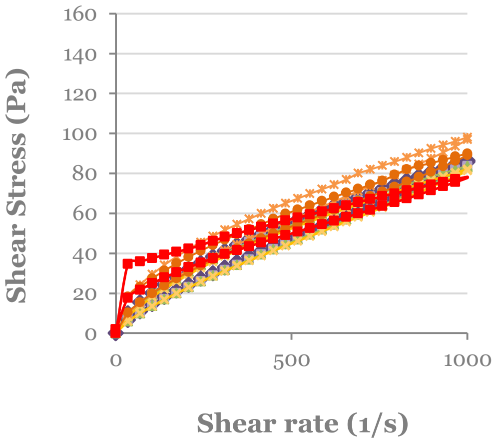

10.1.3. Flow Behaviour - Variable 3: Clay Type

For Variable 3, the flow behaviour of samples prepared using different clay types was also studied. Comparisons were made between a natural bentonite, as used for Variable 1 & 2, a calcium saturated bentonite and a kaolinite clay. Figure 10-13 illustrates the different flow curves produced for each of the clays, prior to the addition of any alginate. As shown, the kaolinite and Ca-bentonite samples exhibit similar rheological behaviours. Both of these clays are shear-thickening and they have a lower viscosity than the natural bentonite sample. This is consistent with results by Abu-Jdayil (2011) where a Ca-bentonite sample was found to be less viscous and less thixotropic than a Na-bentonite sample.

In comparing the different clays with each of the alginate types, for AC the highest viscosity is observed for the Ca-bentonite sample (Figure 10-14). Therefore although the addition of calcium ions reduces the viscosity of the clay only sample, when the alginate is included the addition of calcium leads to an increase in viscosity suggesting that Ca^{2+} crosslinking is taking place.

Figure 10-13: Flow Curves (Control Samples)

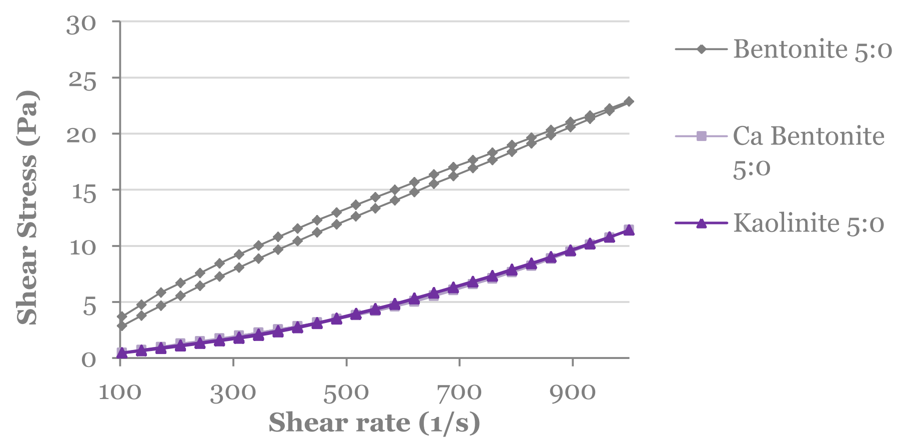

Figure 10-14: Flow Curves (AC – 5:0.5)

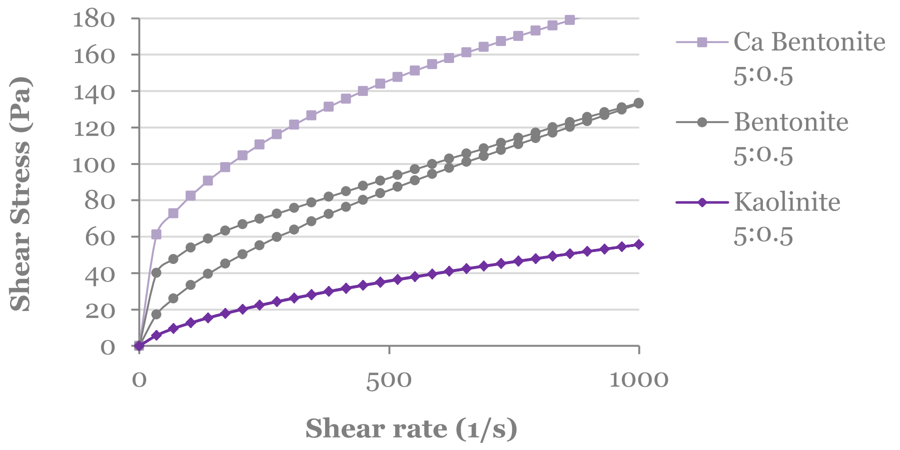

Similar behaviours are observed for PR22 and PR24 (Figure 10-15 and Figure 10-16) whereby increases in viscosity and thixotrophy are observed for the Ca-Bentonite samples. The increases are however less dramatic for PR32 and PR52 (Figure 10-17 and Figure 10-18). For the kaolinite sample, although the control sample exhibited similar flow behaviour to the Ca-B samples, the addition of all of the alginate types leads to a more modest increase in viscosity. This suggests that the more dramatic change in behaviour for the Ca-bentonite samples is likely due to clay-polymer interactions rather than polymer-polymer interactions.

Figure 10-15: Flow Curves (PR22)

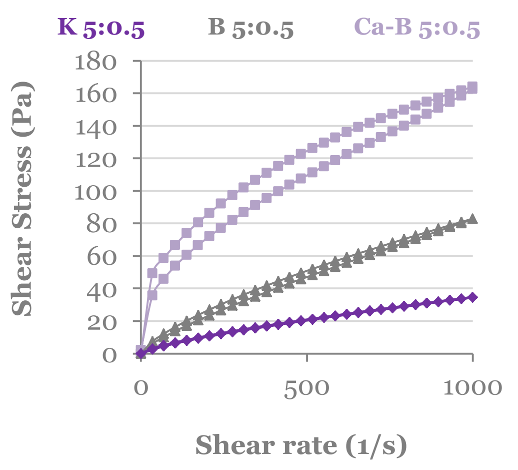

Figure 10-16: Flow Curves (PR24)

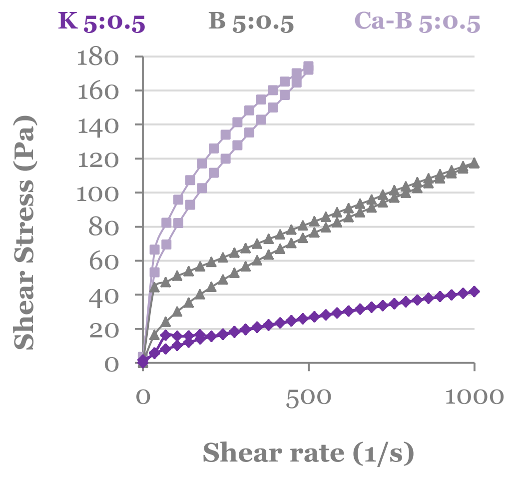

Figure 10-17: Flow Curves (PR32)

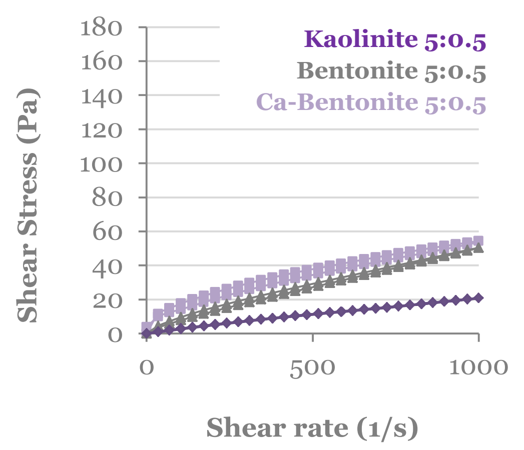

Figure 10-18: Flow Curves (PR52)

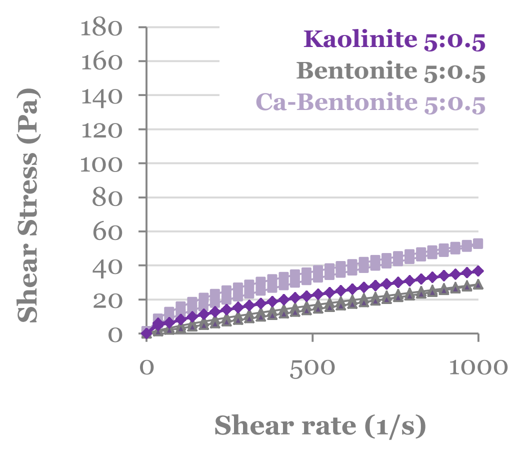

10.1.4. Viscoelastic Behaviour –Variable 1: Alginate Type & Dosage

The viscoelastic behaviours of the samples, prepared using different alginate types and different mix ratios, are illustrated in Figure 10-19 to Figure 10-23. The creep curves demonstrate that, for all samples, the magnitude of the measured deformation decreases upon the addition of alginate. In all cases the samples behave as linear viscous fluids but the decrease in the gradient during the first 60s is more dramatic for the high viscosity polymers (AC, PR24, PR22) compared to the clay only samples (C5A0).

Figure 10-19: Creep Curve (AC)

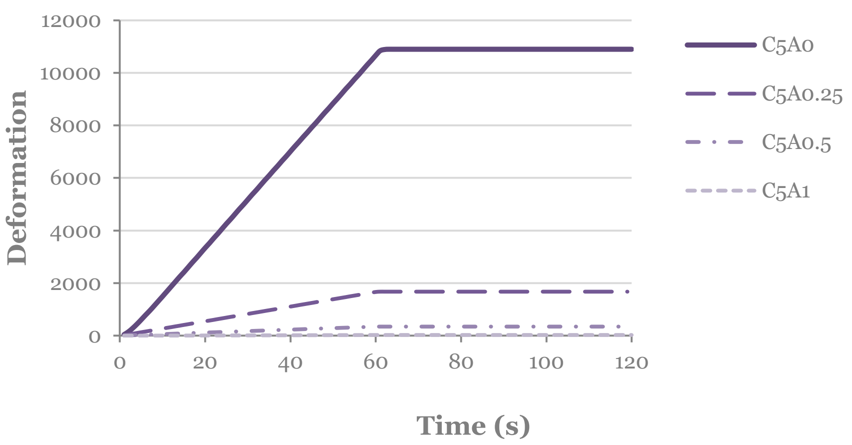

Figure 10-20: Creep Curves (PR22)

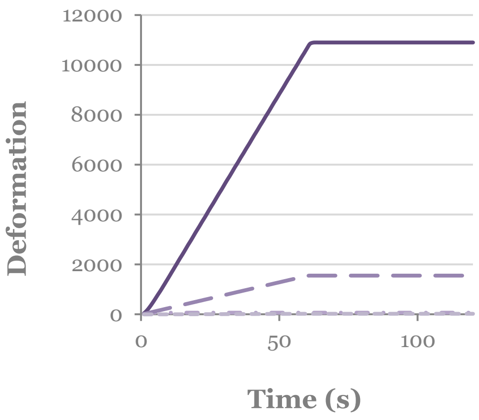

Figure 10-21: Creep Curves (PR24)

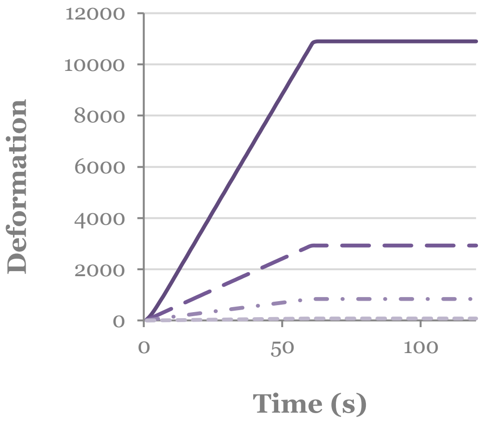

Figure 10-22: Creep Curves (PR32)

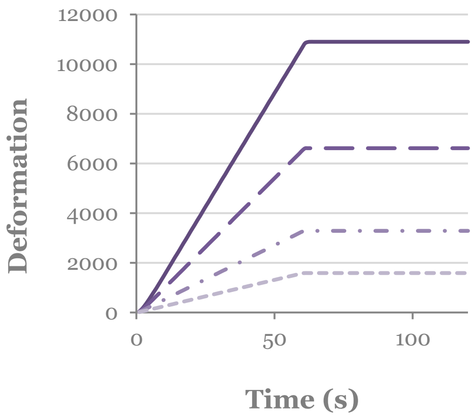

Figure 10-23: Creep Curves (PR52)

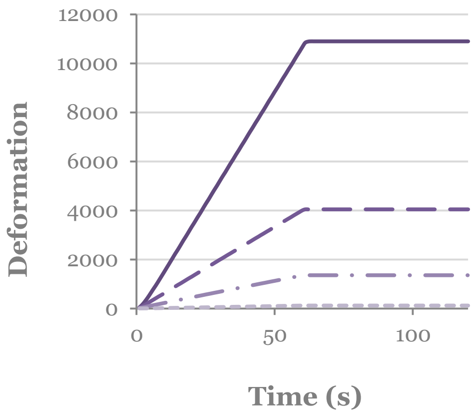

10.1.5. Viscoelastic Behaviour - Variable 2: pH

The creep curves for samples prepared at different pH levels are also shown in Figure 10-24 to Figure 10-28. In this case the results show that reducing the pH also increases the materials resistance to deformation. With the exception PR32, there is also a visible shift from linear viscous fluid behaviour to either a viscoelastic fluid or viscoelastic solid (AC – pH 5) upon the reduction of pH. This marks the transition to a gel-like structure. The increasing resistance to deformation with decreasing pH demonstrates that the strength of the structure is improved in acidic conditions due to increase interactions (either polymer-polymer or clay polymer).

Figure 10-24: Creep Curve (AC)

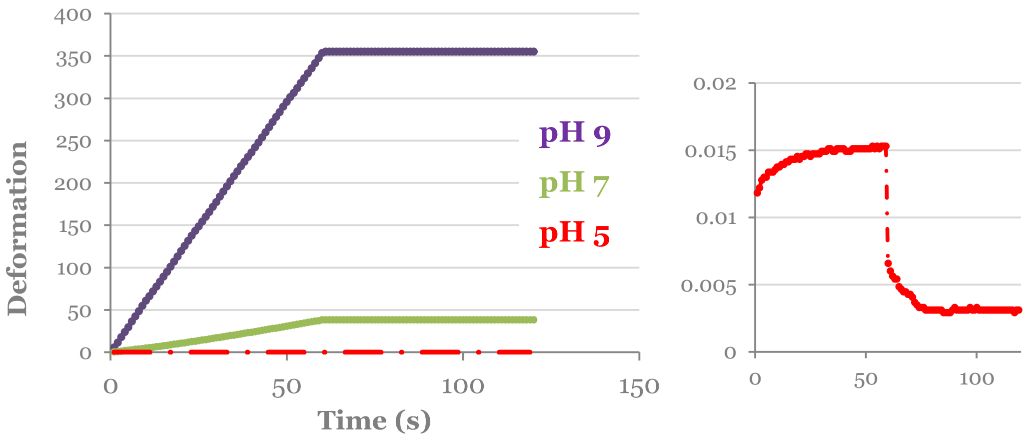

Figure 10-25: Creep Curves (PR22)

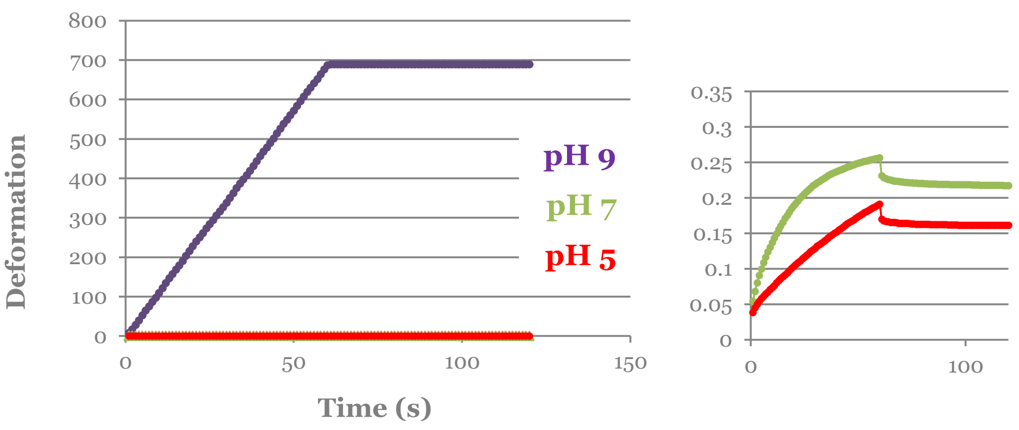

Figure 10-26: Creep Curves (PR24)

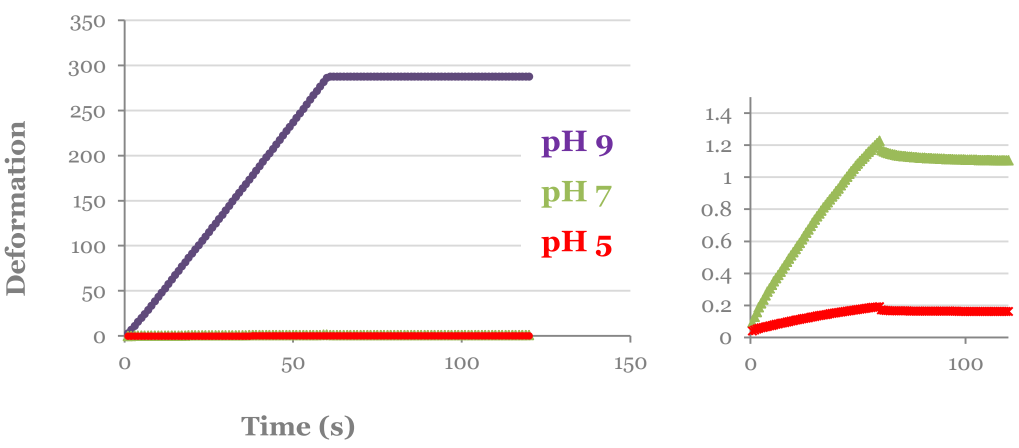

Figure 10-27: Creep Curves (PR32)

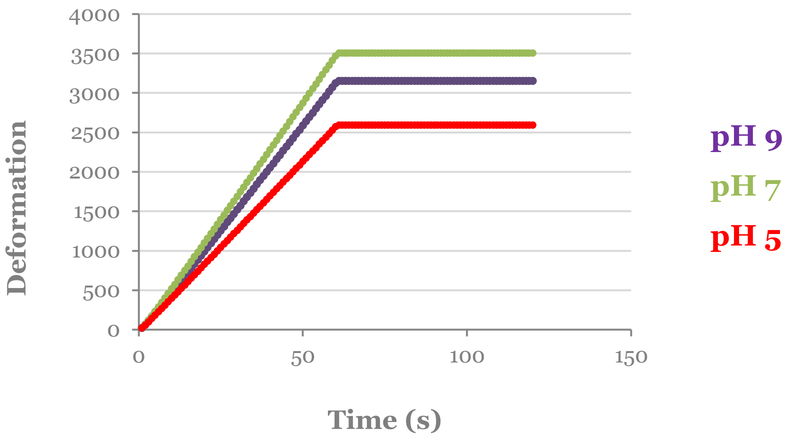

Figure 10-28: Creep Curves (PR52)

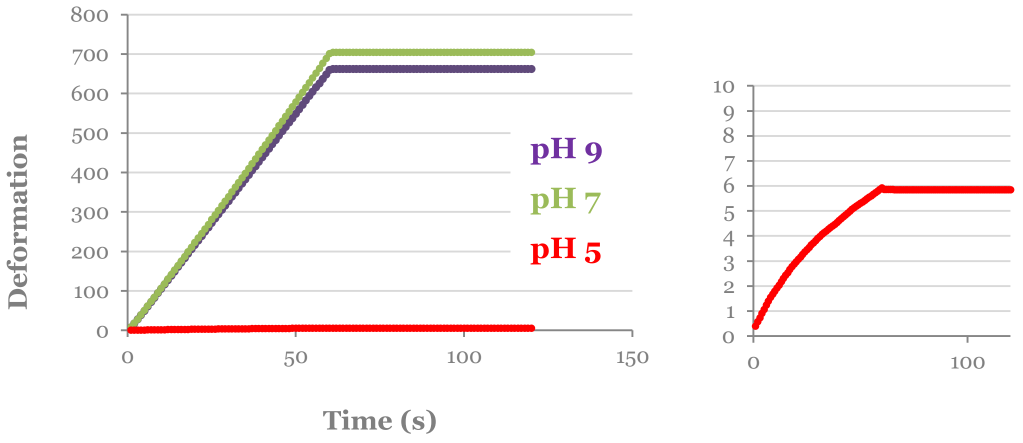

10.1.6. Viscoelastic Behaviour - Variable 3: Clay Type

Finally, in considering the impact of clay type upon the viscoelastic behaviour, the creep curves for Variable 3 are shown in Figure 10-29 to Figure 10-33. The calcium saturated samples had lower deformation values compared to the natural bentonite samples, highlighting the improved strength of the structure upon the addition of calcium ions. In some cases (PR22 & PR24) the addition of calcium causes a shift from linear viscous fluid behaviour to viscoelastic behaviour. This is consistent with the increase in viscosity observed through the flow curves and is likely due to Ca^{2+}

crosslinking, either between polymer molecules and the polymer and the clay particles. In the case of the kaolinite samples, all of the mixtures behave as linear viscous fluids with an increasing resistance to deformation upon increasing alginate content as per the unmodified bentonite. However the resistance to deformation is lower for kaolinite than for the bentonite samples suggesting that there is not the same level of interaction between the alginate and the kaolinite.

Figure 10-29: Creep Curve (AC)

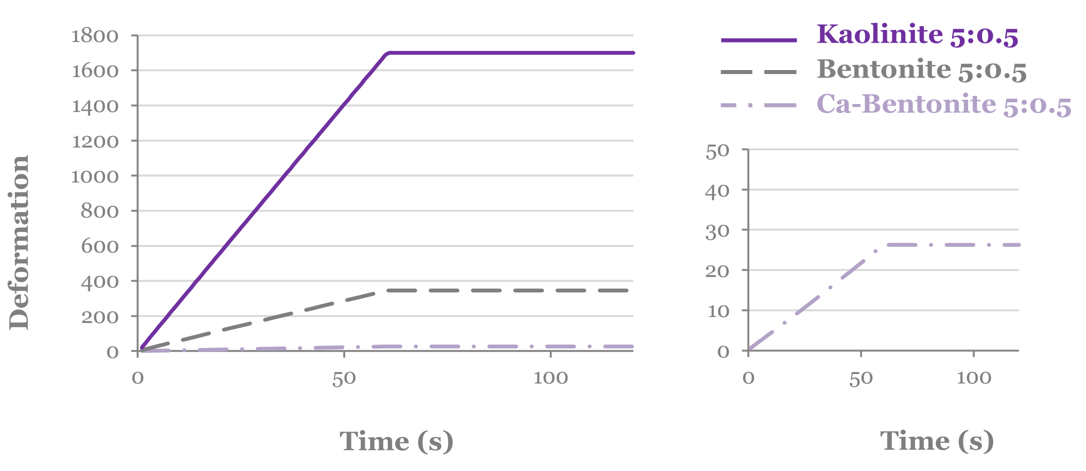

Figure 10-30: Creep Curves (PR22)

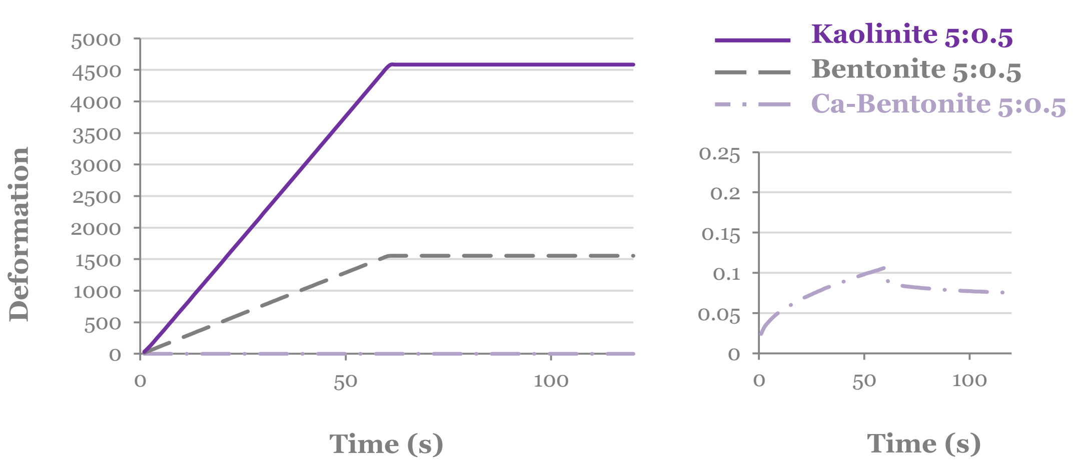

Figure 10-31: Creep Curves (PR24)

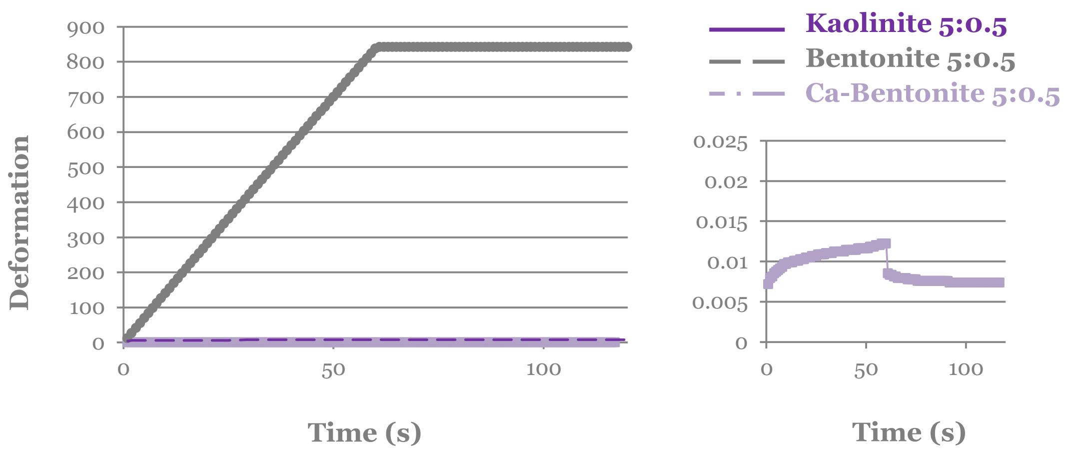

Figure 10-32: Creep Curves (PR32)

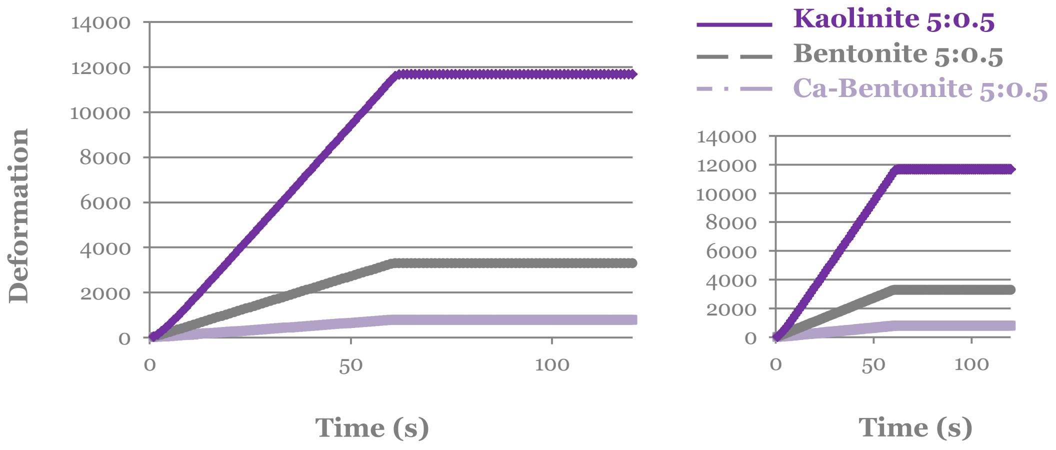

Figure 10-33: Creep Curves (PR52)

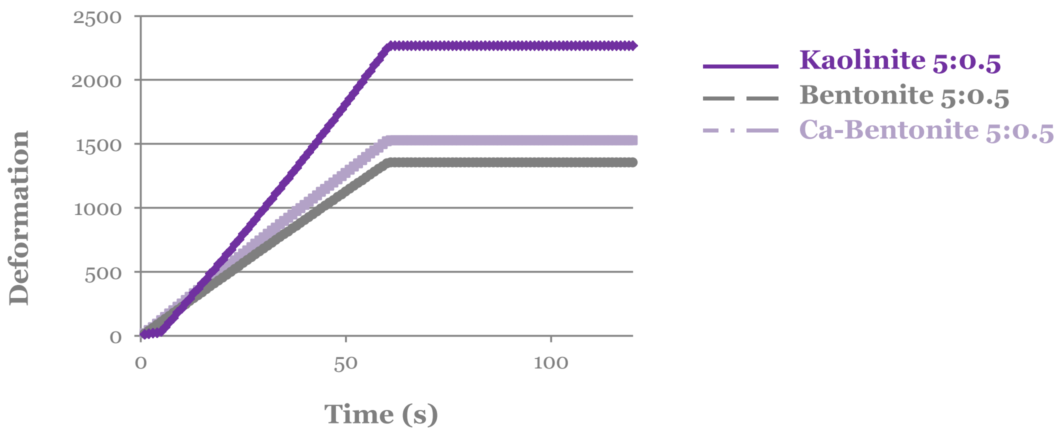

10.1.7. Colloidal Stability - Variable 1: Alginate Type & Dosage

The results from the ζ-potential analysis which was performed on the colloidal fraction of the samples is show in Table 10-1. Although these samples are much more dilute than those used in the previous rheology tests, or indeed the required solid concentrations for producing an aerogel material, the results give an indication of the nano-scale interactions between the two components. In comparing the ζ-potential values for the different alginate-bentonite mixtures, all mixes demonstrate an increase in the magnitude of the ζ-potential compared to the control. As expected, the ζ-potential of the clay therefore becomes increasingly negative upon the addition of alginate although the effect is more apparent for AC. This high ζ–potential is indicative of stabilisation for these samples.

Table 10-1: Variable 1 – Zeta potential

Sample	Zeta potential (mv)	SD
5% Clay + 0.5% AC - Centrifuged	-67.4	0.1
5% Clay + 0.5% PR22 - Centrifuged	-48.4	1.3
5% Clay + 0.5% PR24 - Centrifuged	-57.0	5.2
5% Clay + 0.5% PR32 - Centrifuged	-45.6	1.3
5% Clay + 0.5% PR52 - Centrifuged	-50.7	3.1
5% Clay - Centrifuged	-37.4	0.3

10.1.8. Colloidal Stability - Variable 2: pH

Further analysis of the impact of pH on ζ-potential is also provided in Table 10-2. In this case only the AC sample was studied and all samples were produced using a clay: alginate ratio of 5:0.5. For both the clay and clay-alginate samples, the lowest ζ-potential is observed at pH 4. In both cases this is therefore the pH at which there is the least repulsion between the particles and is consistent with the observations for the flow curves.

Table 10-2: Variable 2 – Zeta potential

Sample	Zeta potential (mv)	SD
5% Clay (pH 8)	-37.4	0.3
5% Clay (pH 7)	-33.1	1.4
5% Clay (pH 5)	-43.6	1.7
5% Clay (pH 4)	2.1	0.5
5% Clay + 0.5% AC (pH 8)	-65.1	1.3
5% Clay + 0.5% AC (pH 7)	-57.1	1.4
5% Clay + 0.5% AC (pH 5)	-57.1	1.7
5% Clay + 0.5% AC (pH 4)	-32.7	1.8

10.1.9. Colloidal Stability - Variable 3: Clay Type

Finally, in considering the influence of clay type upon the electro-kinetic properties of the clay-alginate mixtures, as per the observations for Variable 1 and 2, the addition of alginate led to a more negative ζ –potential. For both the clay control samples and the alginate containing samples the Ca-Bentonite had a slightly lower zeta potential than the kaolinite and bentonite. This is similar to other studies whereby the addition of Ca^{2+} was found to reduce the zeta potential of clay samples (Chorom and Rengasamy, 1995; Au and Leong, 2013). The reduction in electrostatic repulsion is also consistent with the findings from the rheological measurements.

Table 10-3: Variable 3 – Zeta potential

Sample	Zeta potential (mv)	SD
5% Clay (Kaolinite)	-41.0	4.5
5% Clay (Ca-Bentonite)	-20.1	1.2
5% Clay (Bentonite)	-37.4	0.3
5% Clay + 0.5% AC (Kaolinite)	-66.1	2.5
5% Clay + 0.5% AC (Ca-Bentonite)	56.4	1.2
5% Clay + 0.5% AC (Bentonite)	-65.1	1.3

10.1.10. X-ray Diffraction

The diffractograms produced for the alginate and clay mixes are shown in Figure 10-34 to Figure 10-37. In firstly considering the impact of the alginate type (Figure 10-34), analysis of the 0.5% polymer dosage for the commercial alginate and the

MBL products (PR22 and PR24) did not reveal any significant differences in terms of the patterns produced (Figure 10-34) thereby confirming that *d*-spacings are unaltered. A further comparison of samples prepared with 0.25%, 0.5% and 1.0% of the commercial alginate (AC) is shown in Figure 10-35. None of the peaks presented in neat clay disappeared upon the addition of the polymer, again ruling out the possibility of an exfoliated structure. There is also no visible shift in the locations of the peaks upon the addition of the alginate confirming that a phase separated rather than intercalated composite structure is present. The peaks do however appear to become more intense which is indicative of increased crystallinity. This is similar to observations by Pongjanyakul (2009) and Bandeira et al. (2012) for alginate-clay systems where the increased peak intensity is attributed to the flocculating behaviour of the alginate.

Figure 10-34: XRD – Alginate Type

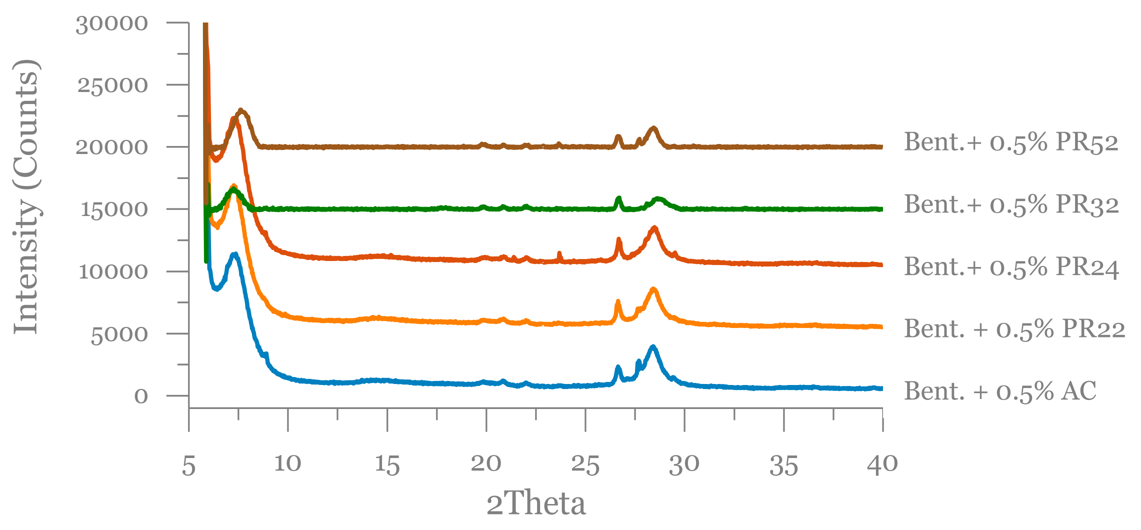

Figure 10-35: XRD – Bentonite & AC

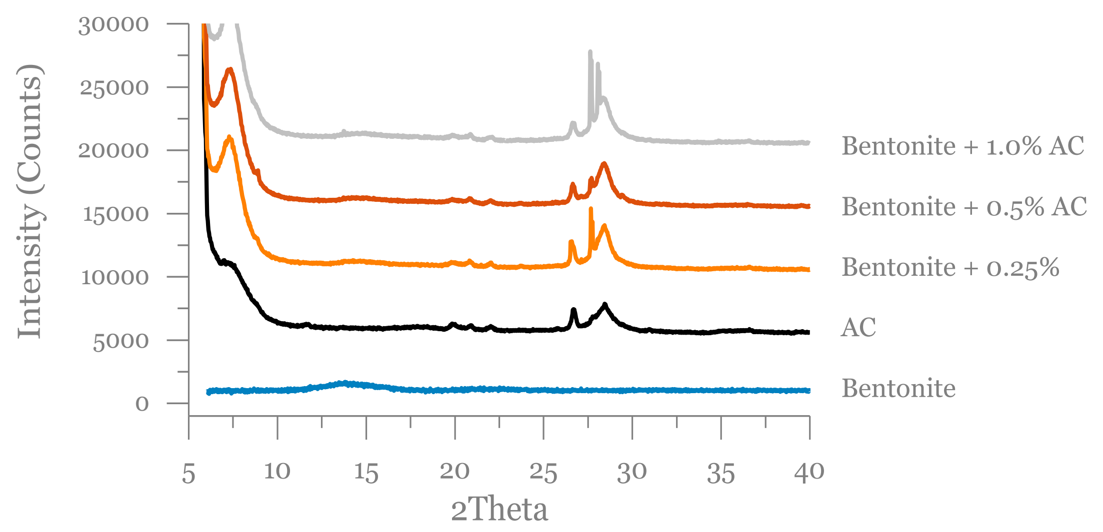

In terms of the influence of pH, again as shown in Figure 10-36 for the AC samples, there were no noticeable differences between samples prepared at different pH levels. Finally, in comparing the different clay types, as shown in Figure 10-37, as per the bentonite samples, there are no significant differences observed for the Ca-Bentonite or Kaolinite samples upon the addition of alginate.

Figure 10-36: XRD – Bentonite & AC (pH study)

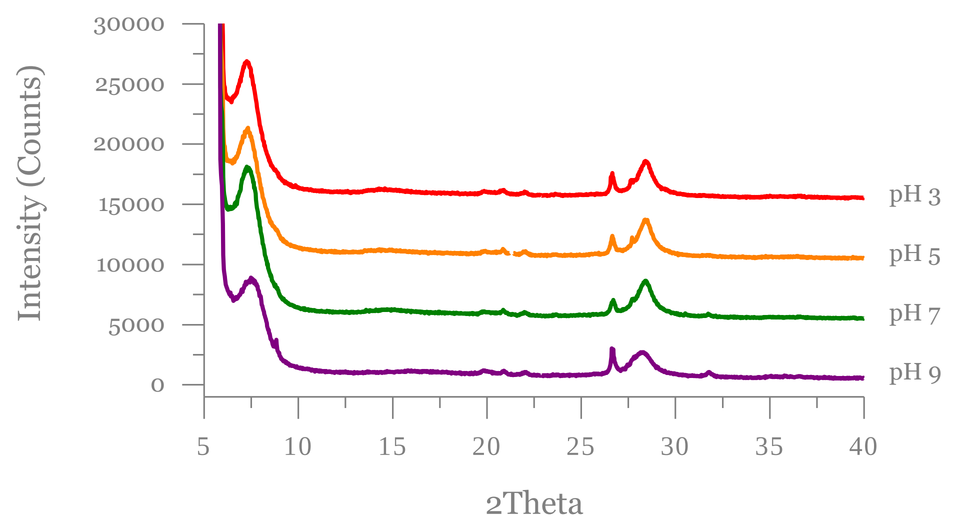

Figure 10-37: XRD –AC (Clay Study)

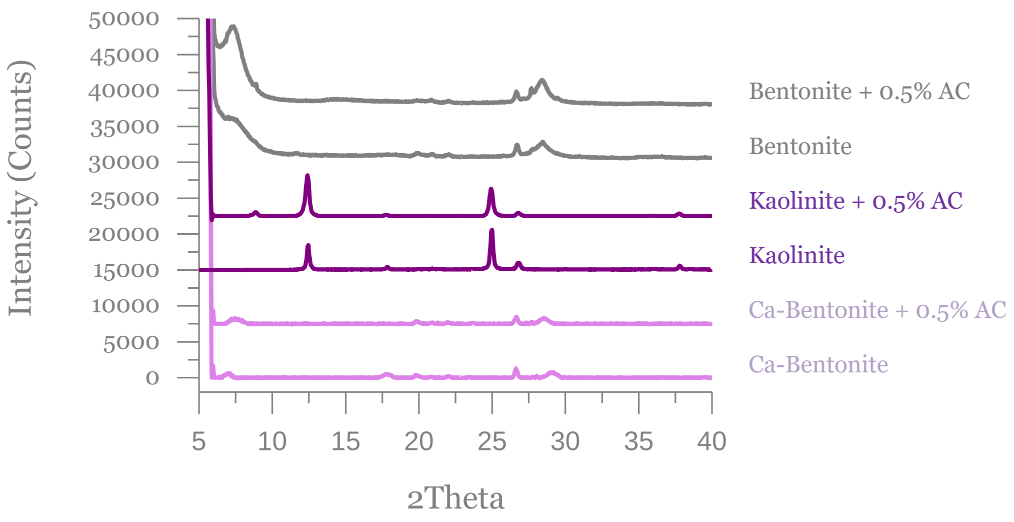

Overall the XRD study confirms that the samples appear to retain the crystal structure of the clay upon mixing with the different alginate types suggesting interaction at the surface level. This is in agreement with other studies by Pongjanyakul (2009), Tezcan et al. (2012) and Bandeira et al. (2012) where no changes in basal spacings are observed for clays upon the addition of alginate.

10.1.11. Phase 1 – Summary

From the Phase 1 results, the alginate type appears to have an important influence on the flow behaviour of the samples, with the highest G content sample exhibiting the greatest degree of thixotrophy. It can also be concluded that the commercial alginate (AC) had a more visible effect on the viscosity and resistance to deformation than the MBL products. Furthermore while the flow curves produced for the two *LH stem* products (PR22 & PR24) and the *AN* product (PR52) were relatively similar, the lowest viscosity product which was sourced from the *LH* frond (PR32) displays flow behavior much closer to that of the control clay sample. Maximum viscosities and yield stresses are also observed in mildly acidic conditions, although again the effects of this are less pronounced for PR32 and PR52. A reduction in pH also induces a shift from a linear viscous fluid to a viscoelastic solid for AC, PR22 & PR24. This is indicative of the formation of a three-dimensional network and is supported by the reduction in ζ -potential at pH 4. An increase in viscosity, thixotrophy and resistance to deformation as well as an associated reduction in electrostatic repulsion is also observed upon calcium saturation of the bentonite clay. This increase in viscosity is particularly apparent for the high G sample (PR24) highlighting the importance of Ca^{2+} crosslinking. This confirms that interaction between clay and the alginate could be enhanced by increasing the G content of polymer, reducing the pH or increasing the content of Ca^{2+}. These variables were therefore taken forward into the Phase 2 tests.

10.2. Phase 2 – Aerogel Specimens: Initial Assessment

10.2.1. Aerogel Specimens - Variable 1: Alginate Type and dosage

For the aerogel specimens, the first variables to be tested were the alginate type and dosage. A total of 5 different alginates were assessed using 5 different mix ratios (alginate: clay = 100:0, 75:25, 50:50. 25:75 and 0:100) as summarised in Table 10-4.

Table 10-4: Variable 1 - Specimens Tested

	100:0	**75:25**	**50:50**	**25:75**	**0:100**
AC	AC-A	AC-B	AC-C	AC-D	E
PR22	PR22-A	PR22-B	PR22-C	PR22-D	E
PR24	PR24-A	PR24-B	PR24-C	PR24-D	E
PR32	PR32-A	PR32-B	PR32-C	PR32-D	E
PR52	PR52-A	PR52-B	PR52-C	PR52-D	E

10.2.1.1. Visual Observations

The initial visual observations revealed that the homogeneity and stability of the specimens varied depending on the mix ratio used. Some of the samples (AC-B, AC-C, PR22-A and PR22-B) had visible voids as shown in Figure 10-38. This was more apparent in specimens with greater polymer contents due to the high viscosity of the hydrogel mixes which were more prone to the creation of air bubbles. PR52 was also found to be particularly poor in quality. Images of all the specimens can be found in Appendix E. It should also be noted that the clay only samples (E) were very friable and fell apart upon removal from the vial meaning that suitable monoliths for further tests could not be produced.

Figure 10-38: Variable 1 - Specimen Images

	AC-B	PR22-A	PR22-B	PR52-C
A - C				
E				

As shown in Table 10-5, the homogeneity and stability of the samples was generally found to be improved by the addition of alginate, although high polymer contents or high viscosity products did increase the chances of defects being formed. Similar observations were made by Gawryla et al. (2008) for casein-clay composites where high polymer contents were also found to increase the likelihood of defects.

Table 10-5: Variable 1 - Specimens Homogeneity

	100:0	75:25	50:50	25:75	0:100
AC	Mod.	Mod.	Mod.	Mod.	Poor
PR22	Poor	Mod.	Good	Good	Poor
PR24	Poor	Poor	Mod.	Good	Poor
PR32	Mod.	Mod.	Mod.	Mod.	Poor
PR52	Mod.	Good	Poor	Poor	Poor

10.2.1.2. Dimensions, mass and bulk density

The bulk density values for all of the samples were found to be within 90 – 150 kg/m^3 range (Figure 10-39). This is within the range of medium density rigid polymer foams (80 -170 kg/m^3) as described by Ashby et al. (2013) but slightly higher than results fromo Chen et al. (2012) who report densities of 85 kg/m^3 for a clay-alginate aerogel with a 50:50 mix ratio. The alginate only samples (A) are comparable to results by Mehling et al. (2009) which report average density values of 130 (±30) kg/m^3. The high variability in density, particularly for AC-A, is most likely due to defects in the specimens as shown in Figure 10-38. A comparison between the results observed here and those in other similar studies is shown in Table 10-6.

Figure 10-39: Variable 1 - Bulk Density

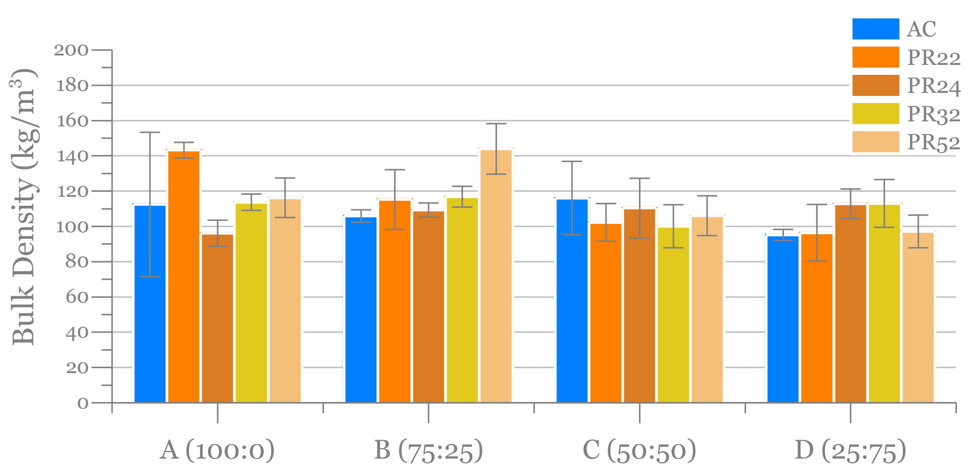

Table 10-6: Bulk Density Comparison

Ref.	Bulk Density (kg/m^3)	Aerogel Type
Chen et al. (2012)	90 – 170	Ammonium alginate & Na-MMT (Polymer: clay = 0-15%:5%)
Gawryla (2009)	80 – 150	Casein & Na-MMT (Polymer: clay = 0-15%:10%)
Mehling et al. (2009)	100 – 160	Sodium alginate (polymer – 2%)
(Chen et al., 2013b)	47 – 129	Ammonium alginate & whey protein isolate & clay (polymer: clay = 5-15%:5%)
This Study	90– 150	Sodium Alginate & bentonite (polymer: clay = 0-10%:0-10%)

10.2.1.3. Compressive Strength at Yield

Images of the samples before and after testing can be found in Figure 10-46 showing the apparent buckling of the cylinders after the test. An example of one of the specimens which was taken beyond the 20% level of compression is also shown for comparison. The resulting stress-strain plots for the aerogels are also shown in Figure 10-41 to Figure 10-45, highlighting the variation between specimens prepared using different alginate types. The profiles were similar to that of elastomeric foams with an initial linear portion followed by a visible yield point and sustained plateau due to cell collapse (Gibson and Ashby, 1999). In all cases failure occurred quickly and at low levels of strain similar to observations by Nussinovitch et al. (1993). The stress-strain plot for the sample taken beyond 20% compression (Figure 10-46) shows the apparent densification of the specimen as the cells are compressed with the increased loading causing the cylinder to deform further into a flat disc.

Figure 10-40: Aerogel Specimens before and after compression

Before test | After test (20% compression) | After 70% compression

Figure 10-41: Stress-strain plots (AC)

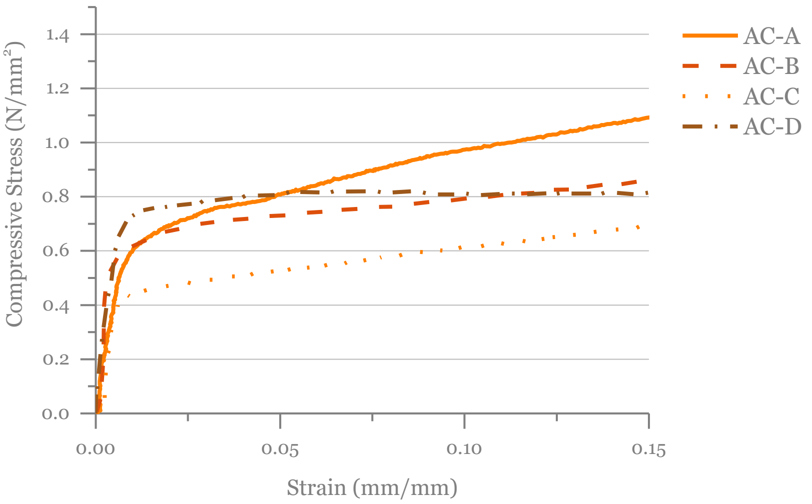

Figure 10-42: Stress-strain plots (PR22)

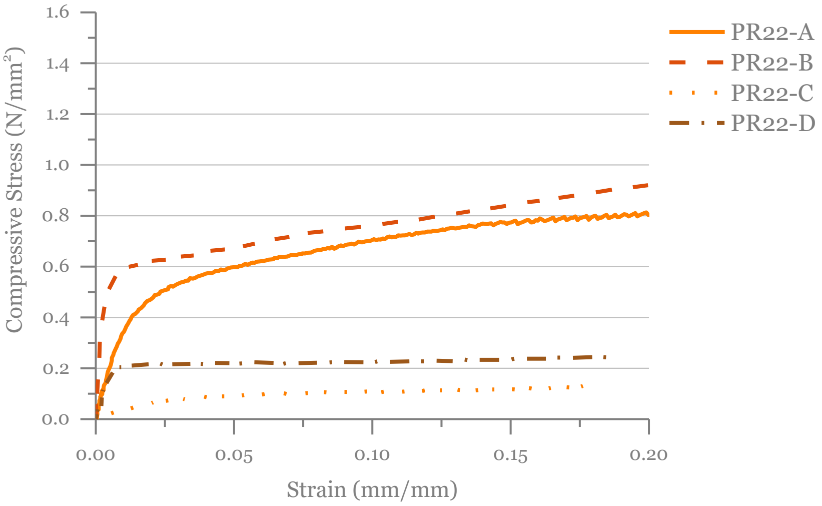

Figure 10-43: Stress-strain plots (PR24)

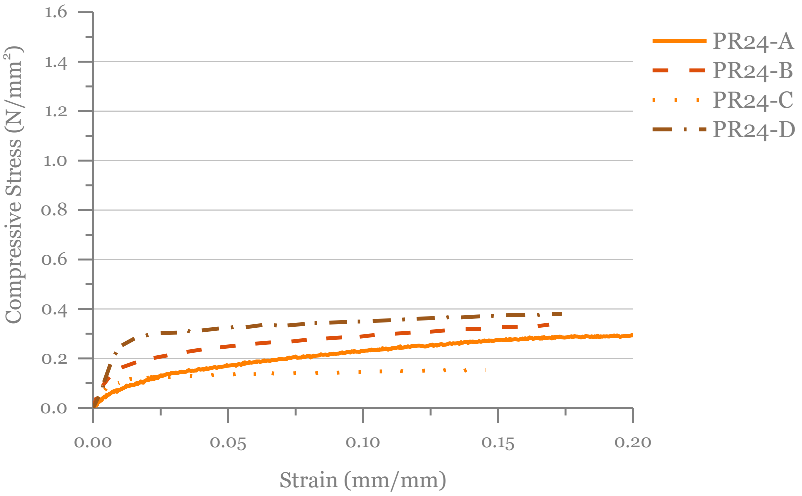

Figure 10-44: Stress-strain plots (PR32)

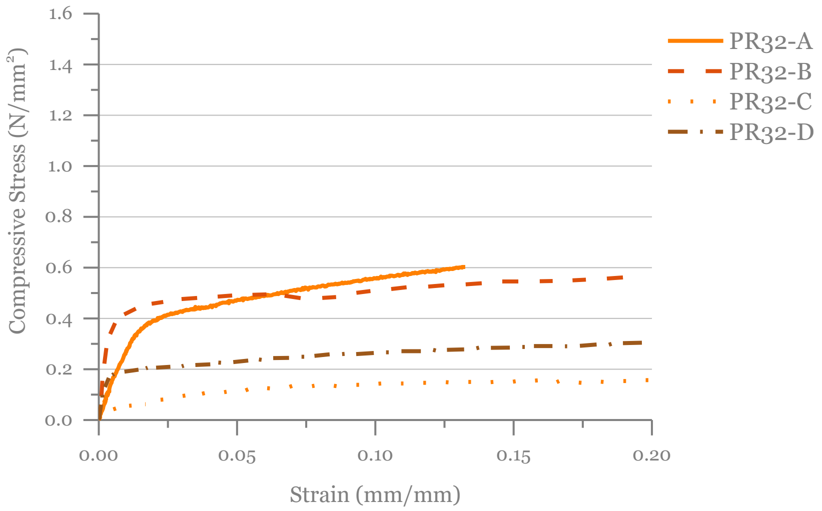

Figure 10-45: Stress-strain plots (PR52)

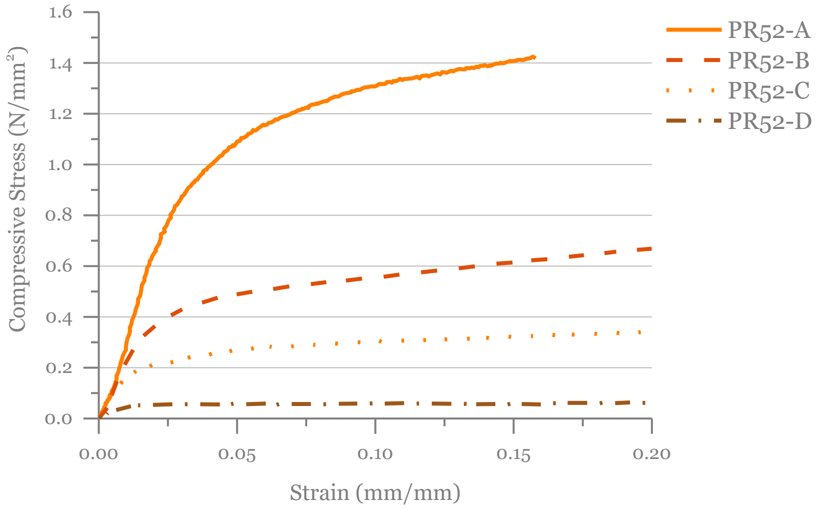

Figure 10-46: Stress-strain plots (Densification)

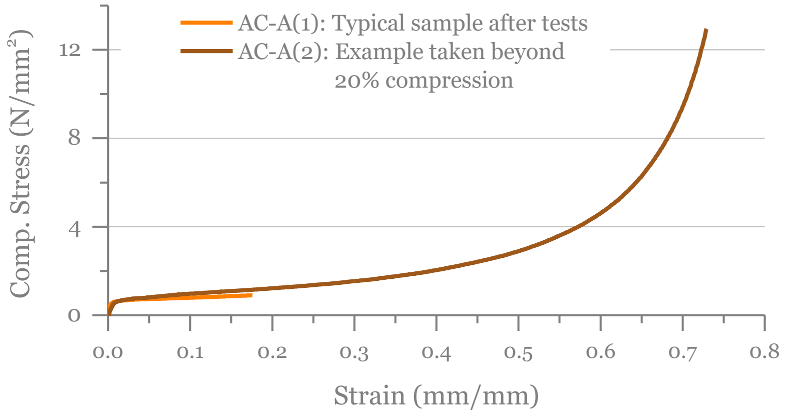

As shown in Figure 10-47, the resulting values for the compressive strength at yield vary quite considerably with results ranging from 0.06 to 0.9 N/mm^2. The strength-to-weight ratios (specific strength) were also found to vary between 0.5 and 7 (Appendix E). Only 11 out of the 20 specimens had a compressive strength within the range of 0.3 – 1.7 N/mm^2 for low density rigid polymer foams (Ashby et al., 2013) with AC-A offering the highest mean compressive strength value. In fact the AC samples demonstrated statistically significant improvements over all of the other alginate types at polymer contents of 100%, 75% and 50%, with the exception of PR22-A and PR52-A where the strength were still lower than for AC but the difference was insignificant. For AC, a statistically significant reduction in compressive strength was found when the clay content was increased to 50% with the C sample resulting in lower mean value than for A and B. Interestingly, the D sample which contained only 25% alginate, achieved similar results to the 50:50 mix.

PR22 follows a similar pattern to AC with the neat alginate sample offering the highest strength with smaller values observed for the lower polymer contents. Although the lowest polymer content offers a slight increase over the 50:50 mix, the difference between the mean values is not found to be statistically significant. For PR24, although the A, B and D mix ratios demonstrate quite similar compressive strengths, a significant decrease in strength is observed for the C samples. Indeed this is the only alginate type for which the 25% alginate content sample offers a significant improvement over the 50% mix. The relatively low strength of the A and B samples in this case, in comparison to the other alginate types, is most likely due to the fact that the high viscosity of the PR24 samples resulted in poorer mixing during sample preparation for high polymer contents. This also explains the defects observed in PR24-A and PR24-B. For PR32, mix ratios A and B were again similar with significantly lower results observed for both the B and C samples. Similar observations were also made for PR52, although in this case the neat alginate sample was found to be significantly greater than all of the clay containing samples. Sample D was found to have a much lower strength than for the higher polymer contents.

Figure 10-47: Variable 1 - Compressive Strength

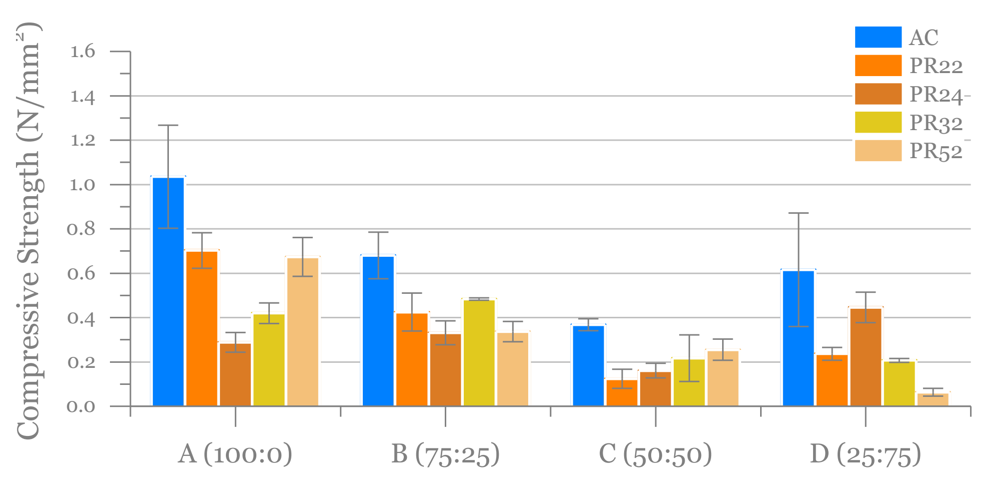

Overall the compressive strength results indicate that whilst the addition of alginate leads to improvements over the clay only samples, since these samples are too fragile to even be handled, the most effective alginate dosage is dependent upon the source. In considering ratios B, C and D, for the highest viscosity alginates (AC and PR24) an alginate content of only 25% provides sufficient improvements. However for the lower viscosity alginates (PR22, PR32 and PR52), better results are achieved with 75% alginate. Furthermore, in terms of alginate composition, PR24 has a much greater G content than the other products which suggests a greater capacity for crosslinking with calcium. PR24 may therefore perform better when there is a greater quantity of clay present due to the additional availability of calcium. The strength values achieved by most of the other D samples further support the idea that an increase in available calcium may enhance clay-polymer interactions leading to similar, or indeed improved, results compared to the 50:50 mixes. Ohta and Nakazawa (1995) reported increasing strength values with increasing polymer content which is generally in line with the results presented here with the exceptions of AC and PR24 where in fact the D samples offered greater strengths than some of the higher polymer contents. Overall the compressive strength values for the 50:50 mixes were generally lower than for the comparable starch-clay aerogel described by Ohta and Nakazawa (1995) which achieved a value of 0.5 N/mm^2.

10.2.1.4. Modulus of Elasticity

The modulus of elasticity calculated for each of the aerogels is summarised in Figure 10-48. In comparing the mean values, again results vary depending on the alginate type and dosage with results ranging between 3 - 33 N/mm^2. This is slightly lower than the range for typical polymer foams (23 – 80 N/mm^2) and more comparable to a natural material like cork (13 – 50 N/mm^2) as quoted by Ashby et al. (2013). However the results for the C (50:50) samples which fall within the 3 – 10 N/mm^2 range are similar to the modulus of ~6 N/mm^2 reported a for a 50:50 clay-alginate aerogel (Chen et al., 2012). Chen et al's. (2012) results also showed a general increase in modulus with increasing alginate content. In this case for AC, while all of the clay containing samples are found to be significantly lower that the alginate only sample, and a general decrease in mean modulus values with decreasing polymer content was observed, differences between the B and C or C and D mix ratios were not statistically significant.

In considering the MBL samples, for PR22 a statistically significant difference between the A and C samples was observed while the modulus values for the other mix ratios were found to be relatively similar. For PR32 and PR52, the mean values again decreased with decreasing alginate content with statistically significant differences being observed between the A and D samples. A slightly different trend was observed for PR24 where the lowest alginate content (D) was found to have a significantly greater modulus of elasticity than the higher polymer contents (B and C). Again it is possible that the high viscosity of alginate and presence of air voids is leading to poorer rigidity in the high polymer content samples. The particularly high value exhibited by PR24-D compared to the other alginates further highlights the importance of the G content when sufficient quantities of clay are present.

Figure 10-48: Variable 1 – Modulus of Elasticity

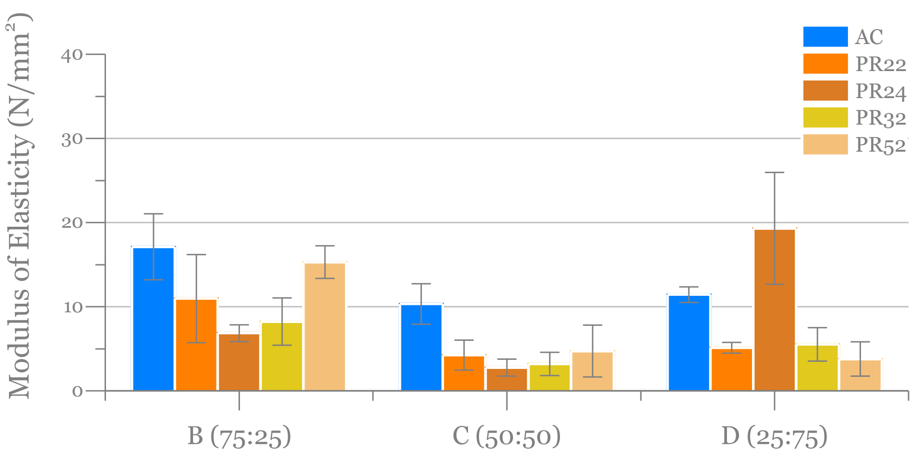

10.2.1.5. Microstructure

For the microstructural analysis, cross-sections were cut from the aerogel cylinders and coated in goldas per the brick specimens (Figure 10-49). Samples images from the SEM analysis are displayed Figure 10-50 to Figure 10-55, showing the porous structures obtained as a result of the sublimation of the ice crystals. It should be pointed out that while the images presented aim to be representative, most of the samples were highly heterogeneous across the fracture surface highlighting that the overall microstructure was not uniform. This can be partly explained by the freezing process since the cell morphology is largely governed by the ice crystal growth which is in turn dependent on the freezing temperature, rate and direction of heat flow (O'Brien et al., 2004; Wang et al., 2013). In this case while the same flash freezing method was adopted for all samples, there is still limited control of the kinetics of ice crystal growth. Indeed it would be expected that while there would be a general bottom up solidification process, simultaneous nucleation of ice crystals on the vials of the wall growing horizontally towards the centre would also be occuring (Gawryla, 2009). Therefore while attempts have been made to obtain images of the cross-sections of the resulting pores (i.e. perpendicular to the main solidification direction) this could not always be guaranteed. Furthermore, despite repeated attempts with multiple samples, some of the images were also poorer in quality than others due to charging and possible edge effects. It is therefore difficult to make definitive conclusions from some of the resulting images in terms of quantitative analysis (e.g. mean cell dimensions and cell wall thickness). Nevertheless, some general qualitative observations are offered.

Figure 10-49: Gold coated specimens - aerogels

In firstly considering, the neat alginate samples (A), for all of the polymers the structures are fairly disordered consisting of parallel sheets with relatively thick cell walls. In contrast, the neat clay sample (Figure 10-55) displays a distinct lamellar structure, similar to the linear pore structure observed by Nakazawa et al. (1987) for 10 wt% bentonite aerogels.

Figure 10-50: Variable 1 - SEM Images (AC)

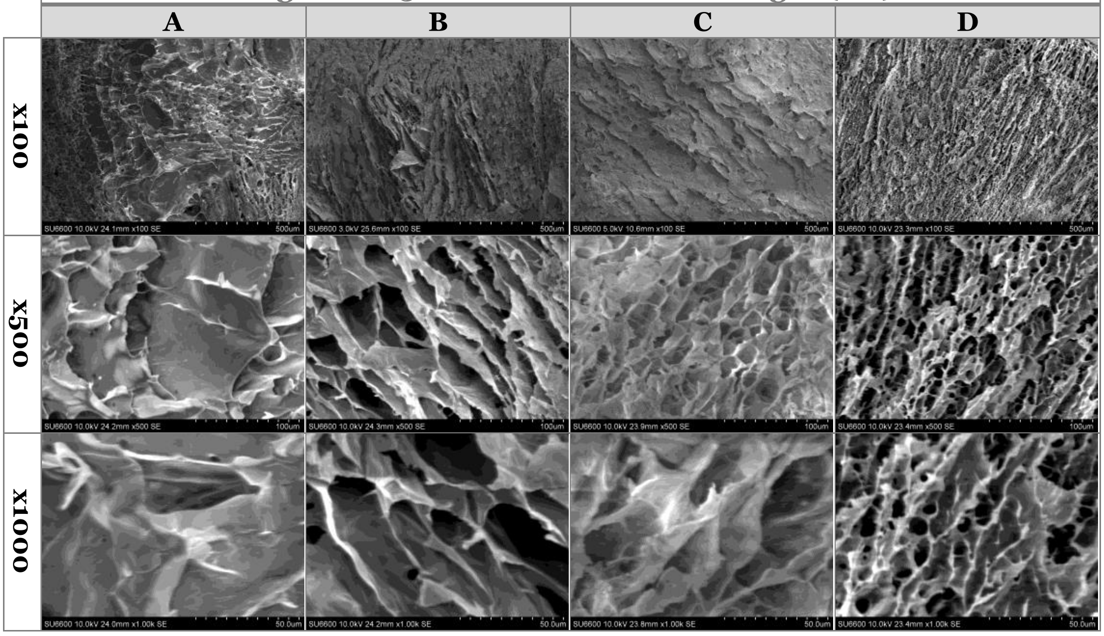

Figure 10-51: Variable 1 - SEM Images (PR22)

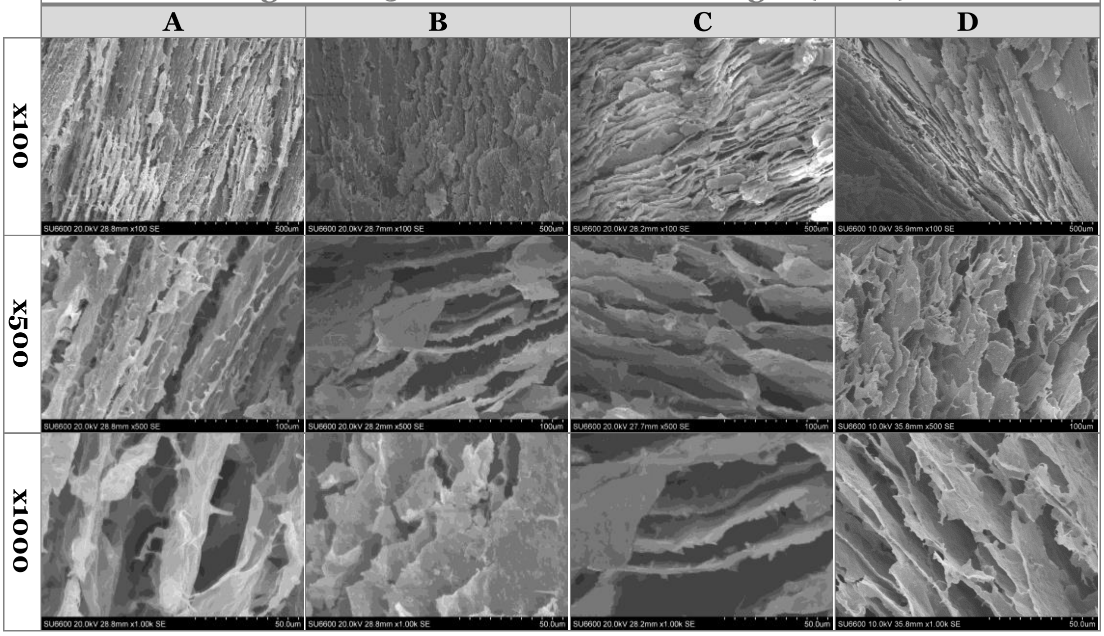

Figure 10-52: Variable 1 - SEM Images (PR24)

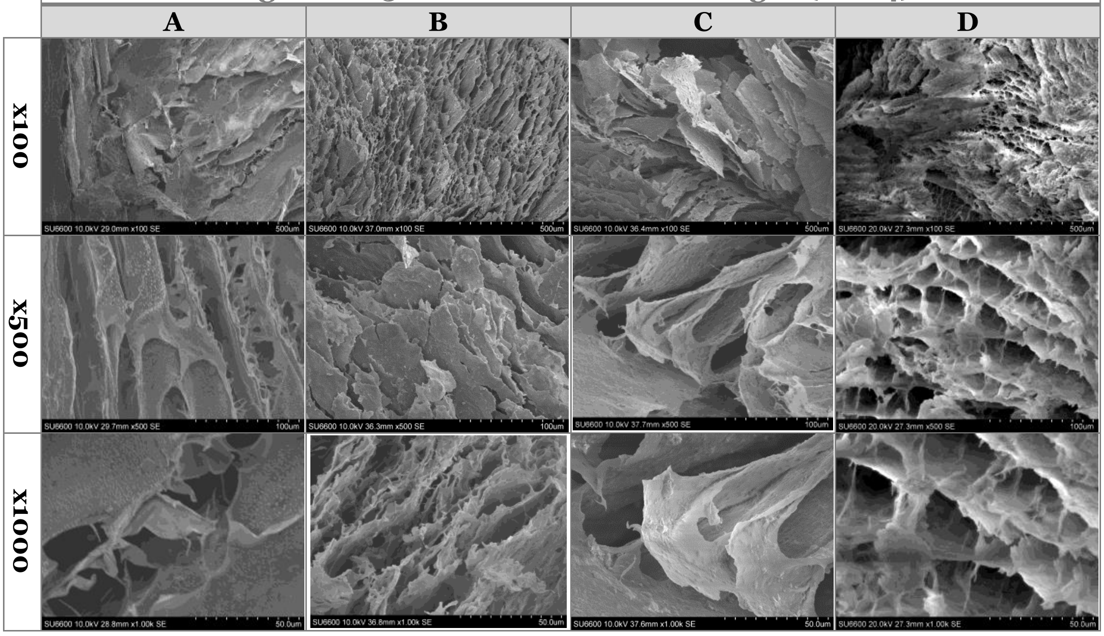

Figure 10-53: Variable 1 - SEM Images (PR32)

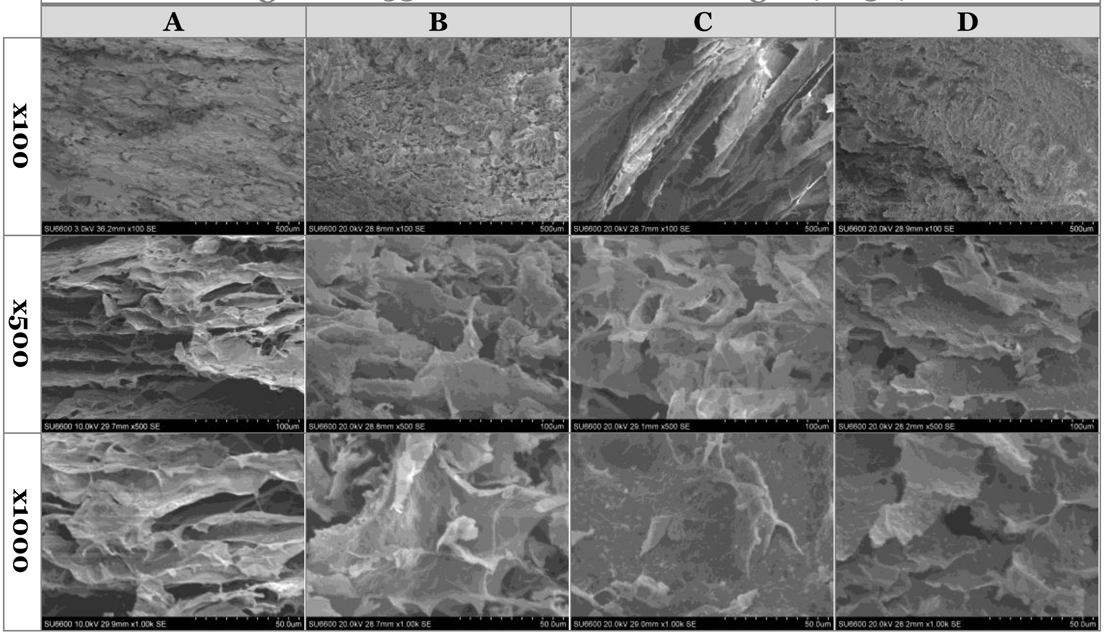

Figure 10-54: Variable 1 - SEM Images (PR52)

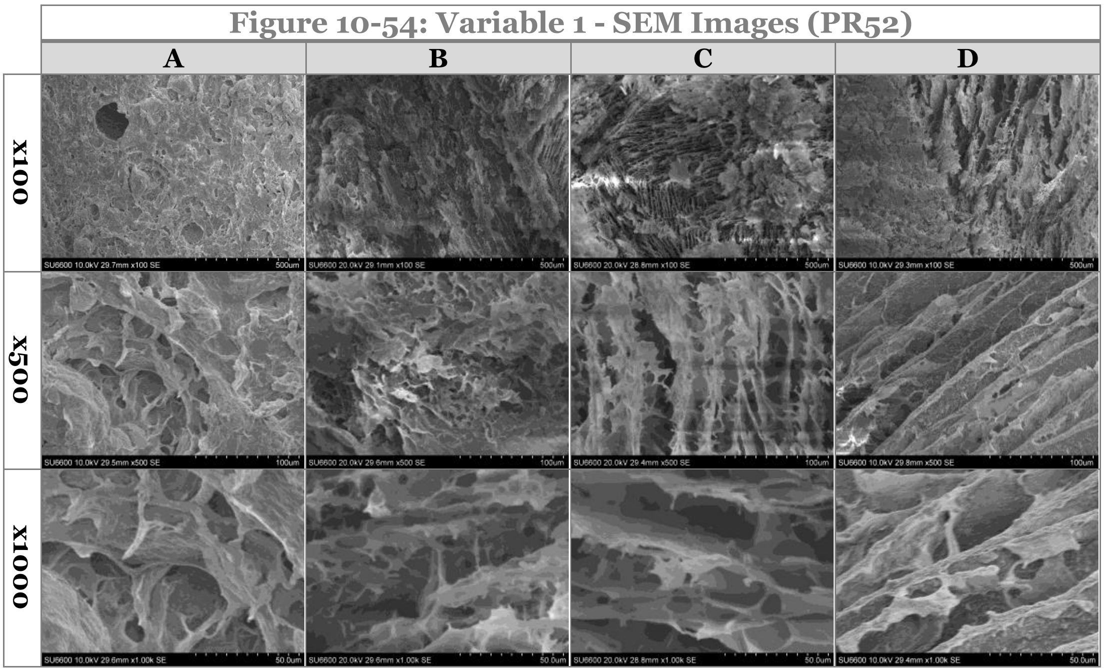

Figure 10-55: Variable 1 - SEM Images (E)

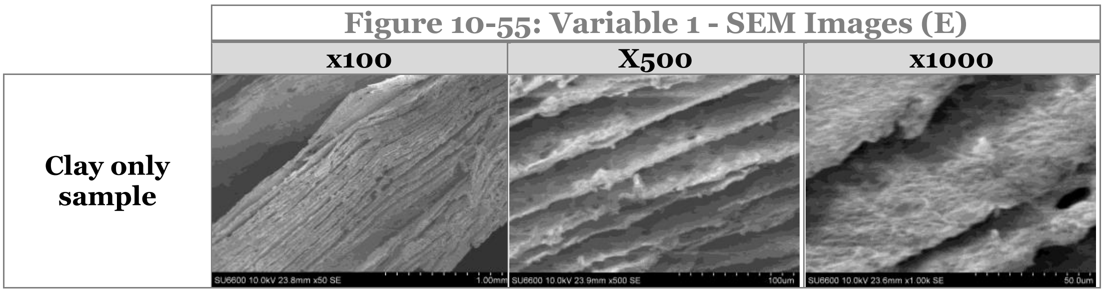

It has been reported that an increase in viscosity can also retard crystal growth meaning that a higher molecular weight polymer, increased polymer concentration or increased level of cross-linking could increase the liklehood of a cellular, network structure rather than lamellar morphology (Gawryla et al., 2008; Chen et al. 2012). From the images presented here for the composite materials (mix ratios B, C & D), both types of structure are visible. In relating these observations to the results of the mechanical testing, the formation of a network structure with small cells helps to reduced local stress and can therefore be linked to higher compressive strengths and higher modulus values (Svagan et al., 2011; Wang, 2015). Given that this type of structure is particularly apparent in AC-C, AC-D and PR22-D and, this may explain the relatively good strength characteristics of these samples despite their low polymer content. These observations also support work by Chen et al. (2012) where the addition of montmorillonite clay was also found transform the distinct layered morphology of an alginate aerogel to a co-continuous network which consequently improved the mechanical properties. Gawryla et al. (2008) also describe this shift in casein-clay aerogels whereby the separated layers change to a network structure whereby the layers are connected by a polymer web. This web-like structure reportedly helps to increase the isotropy of the material, meaning that it its less influenced by the size or direction the ice crystal growth.

On the other hand, as described by Pojanavaraphan et al. (2010), the system viscosity can also have detrimental effect on the aerogel microstructure with high molecular weight or high polymer concentrations hindering the mobility of the clay particles and consequently leading to disordered morphologies. This can lead to the entrapment of air resulting in the formation of spherical voids within the internal structure as observed in SEM analysis of other clay-biopolymer aerogels (Gawryla et al., 2008). For the alginate-clay aerogels, in addition to the macroscopic air bubbles highlighted as part of the visual observations, evidence of these types of defects were also found in the SEM micrographs (Figure 10-56. It should be acknowledged that the links between the complex variables involved in the ice-templating process and the resulting morphologies, which are in turn linked to the distribution of local stresses and mechanical response, are still not fully understood (Svagan et al., 2011 ;Li et al., 2012; Deville et al., 2016). However these structural defects will clearly have an impact on the structural properties and may explain the high variations in compressive strength and modulus reported earlier in the chapter.

Figure 10-56: Variable 1 - SEM Images (Defects)

		AC (x50)	**PR22A** (x50)	**PR52A** (x100)
Clay only sample	**E**	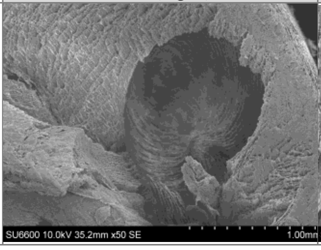	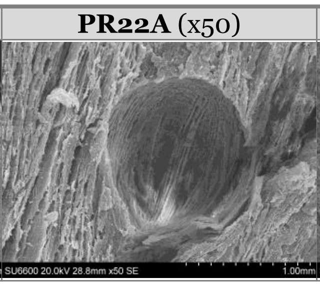	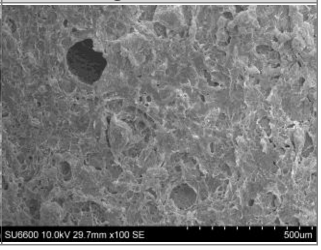

10.2.2. Aerogel Specimens - Variable 2: pH

As discussed in the literature review, and as observed in the rheology tests, a reduction in pH can help to reduce the electrostatic repulsion between the polymer chains. In order to make an initial assessment of the role of pH on the properties of the aerogels, the gels were modified using HCl to give an approximate pH of 4. This was based on the pH at which the maximum viscosity was observed during Phase 1. These samples were then compared against the unmodified samples (~pH 8). In order to focus on the behaviour of the two components together, rather than the effect of pH modification on the polymer or clay alone, only the alginate-clay mix ratios of 75:25, 50:50 and 25:75 were studied. Given that pH modification was found to have a limited effect on PR32 and PR52 during Phase 1, only the commercial product (AC) and 2 of the MBL products (PR22 and PR24) were included.

10.2.2.1. Visual Observations

From the visual observations it was found that for the neat clay samples (E), pH modification did not appear to improve the stability of the aerogels as these were still very friable (Figure 10-57). The pH modified AC samples however had relatively good homogeneity and stability whilst the MBL alginate samples (PR22 and PR24) had several defects as shown in Figure 10-57. Interestingly the 50:50 mix for AC (pH

4) appeared to have the least defects whilst for the MBL samples, the 50:50 ratio samples were much poorer in quality. A summary of these observations is presented in Table 10-7.

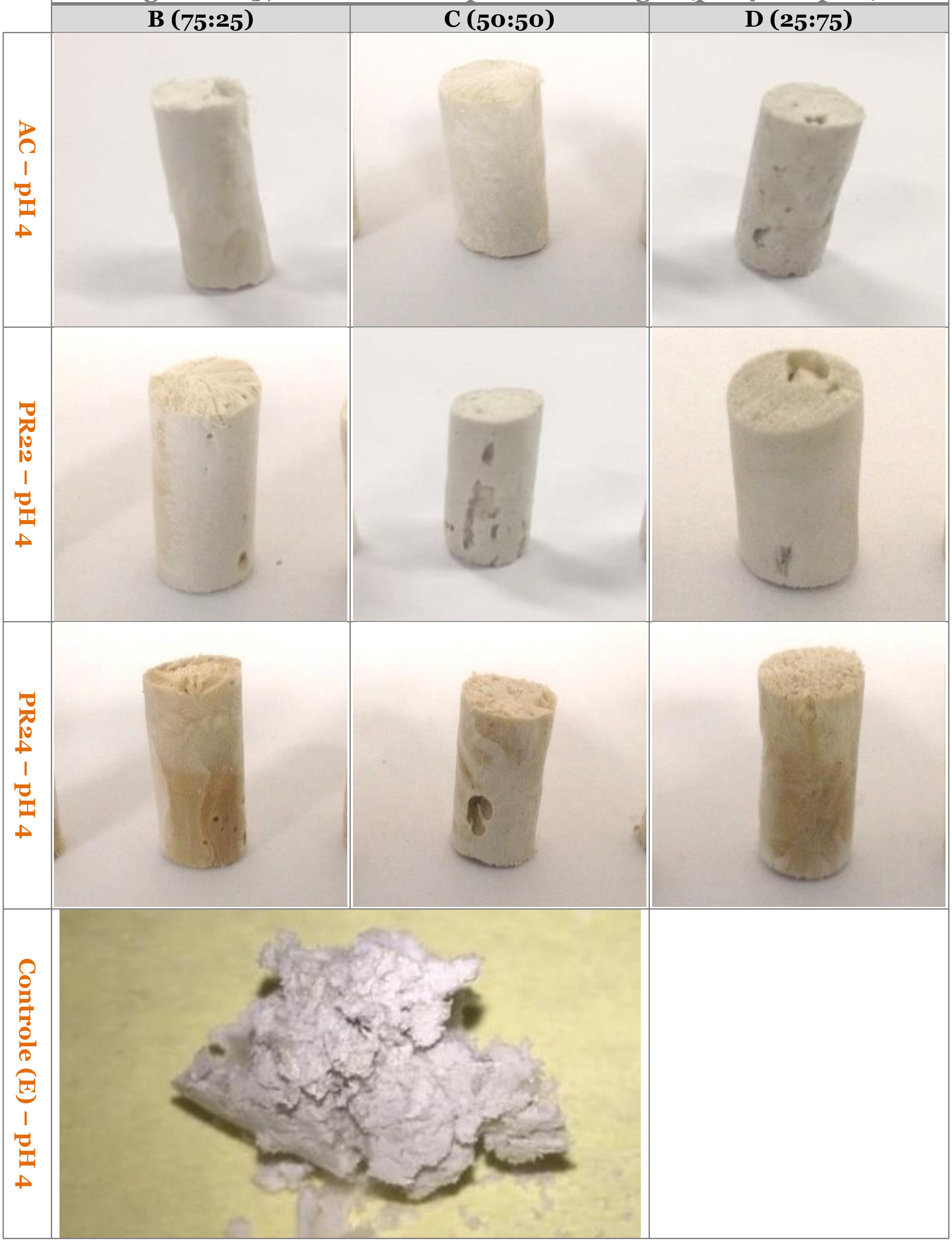
Figure 10-57: Variable 2 - Specimen Images (pH 4 samples)

Table 10-7: Variable 2 - Specimens Homogeneity

	75:25	50:50	25:75	0:100
AC pH 4	Mod.	Good	Mod.	Poor
PR22 pH 4	Poor	Poor	Mod.	-
PR24 pH 4	Mod.	Poor	Mod.	-

10.2.2.2. Dimensions, mass and bulk density

In terms of bulk density, the values achieved for the pH 8 and pH 4 specimens were relatively similar, ranging between 90 and 130 kg/m^3 (Figure 10-58). The only statistically significant change in density due to pH modification occurred for AC-D where an increase was observed for the lower pH sample.

Figure 10-58: Variable 2 - Bulk Density

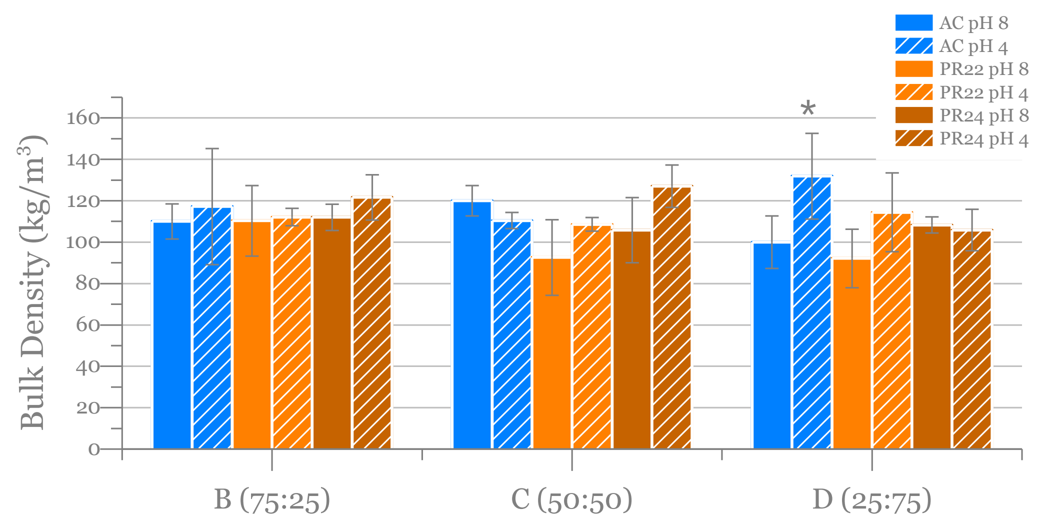

10.2.2.3. Compressive Strength at Yield

In comparing the behaviour of the pH modified samples, typical stress-strain plots are shown in Figure 10-59 to Figure 10-61, whilst a summary of the mean values are shown in Figure 10-62. The resulting compressive strength values range from 0.1 to 1.35 N/mm^2. For the commercial alginate (AC), the compressive strength values for mix ratios B and D are relatively similar however the C sample shows a significant increase in strength in acidic conditions. Indeed the strength of the pH 4 sample was found to be over 4 times that of the pH 8 sample. On the other hand, for PR22 there is a statistically significant reduction in strength for the pH 4 sample at the highest alginate concentration (B) whilst the strength shows a significant increase for the lowest alginate concentration (D). Furthermore, at the 50:50 mix ratio there is no significant difference between the pH 8 and pH 4 samples. For the PR24 samples, the only significant difference is observed for the highest polymer content (B) where the pH modification is found to reduce strength as per the observations for PR22.

Figure 10-59: Stress-strain plots (AC – pH 4 & pH 8)

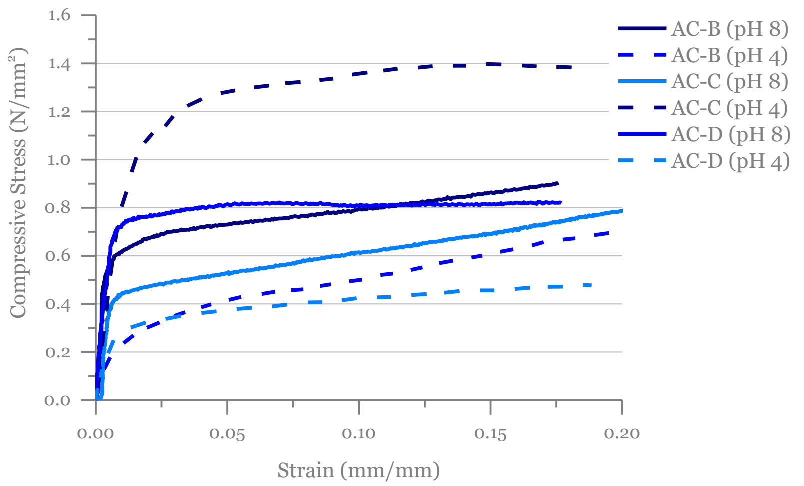

Figure 10-60: Stress-strain plots (PR22 – pH 4 & pH 8)

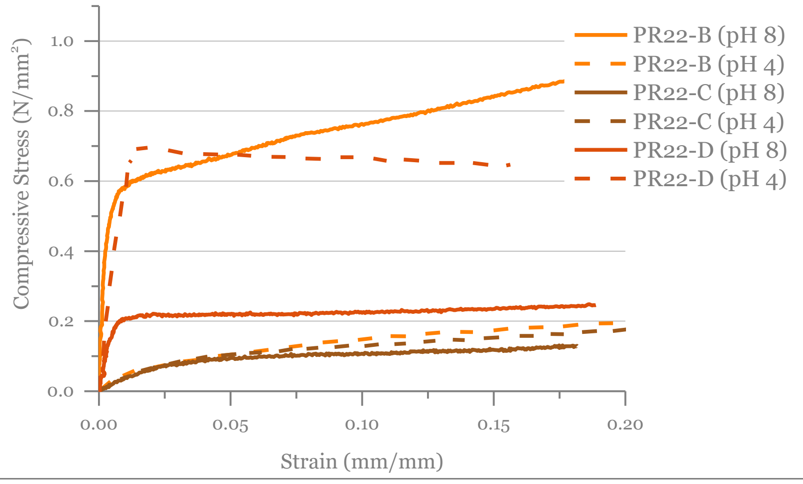

Figure 10-61: Stress-strain plots (PR24 – pH 4 & pH 8)

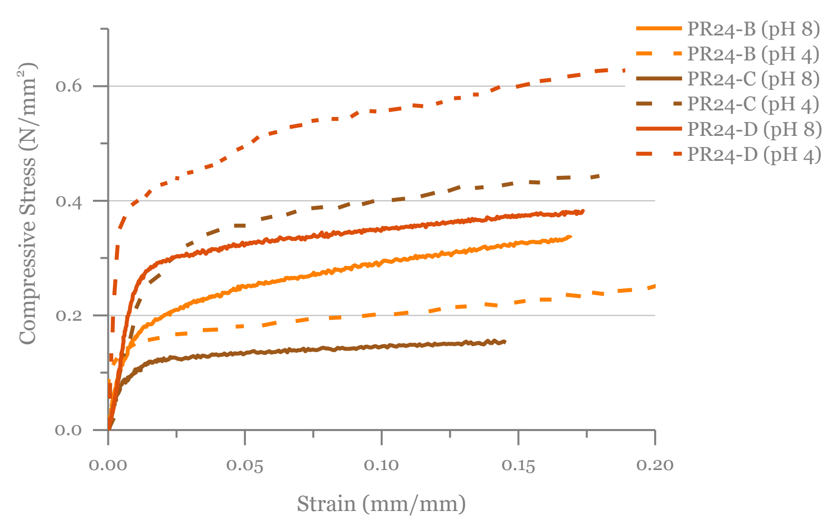

Figure 10-62: Variable 2 – Compressive Strength

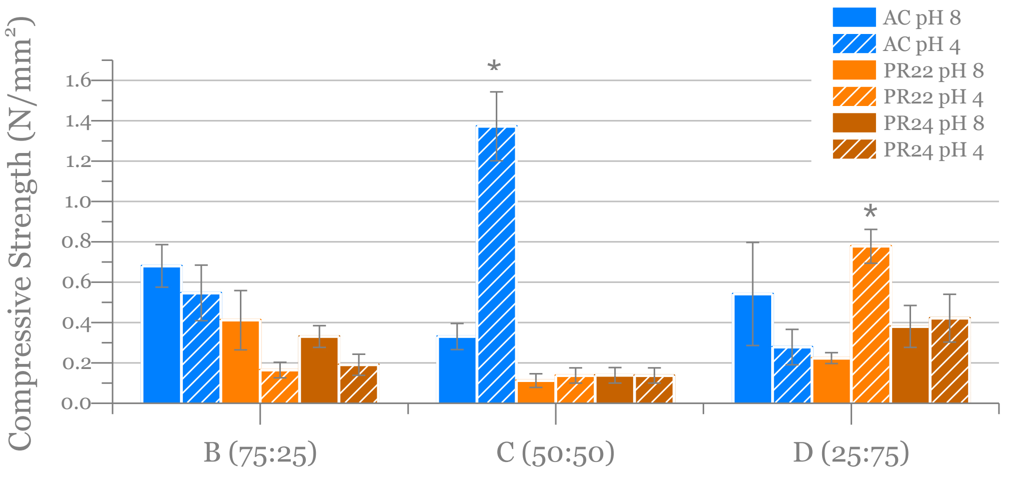

Overall, these results suggest that the mechanical strength of the aerogels can be improved through modification of pH given the significant increases in strength observed for the AC-C and PR22-D samples. However, given that this effect is not apparent for all of the alginate types, nor for all of the mix ratios studied, there are clearly other contributing factors. Indeed in a few cases, where there is a high alginate content, pH modification appears to have a negative impact on the strength of the samples. This may be due to the fact that in strongly acidic conditions (e.g.

below pH 4), where the H^+ ions are added directly, the alginate may form a precipitate leading to a reduced viscosity and weaker gel formation. A further investigation using a more controlled modification method and wider pH range would therefore be required for more defined conclusions to be made.

10.2.2.4. Modulus of Elasticity

In relation to the modulus of elasticity, the mean values for Variable 2 are shown in Figure 10-63. Again specific modulus values are not included given the relatively similar densities of these samples. For the AC samples a significant increase in stiffness can be seen at the 50:50 ratio when the pH is reduced from 8 to 4 whilst the modulus values for mix ratios B and D do not show any significant changes upon pH modification. These results follow a similar pattern to the observed changes in compressive strength. For the MBL samples, there is no significant change in modulus for the 50:50 ratios. For PR22 there is however a significant increase observed from the lowest polymer content (D). This again reflects the compressive strength results. For PR24, while a reduction in modulus is observed for mix ratio B upon reduction of pH, no significant difference was found for the other ratios.

Figure 10-63: Variable 2 – Modulus of Elasticity

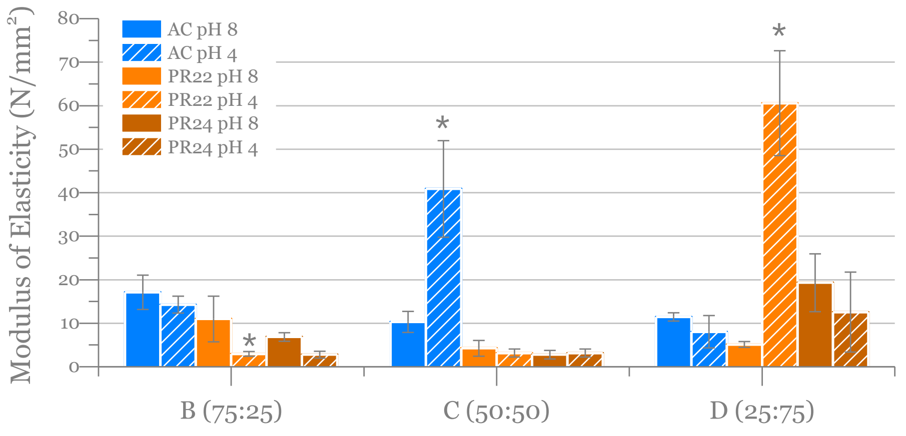

10.2.2.5. Microstructure

In considering the microstructure of the pH modified samples, SEM images for the pH 4 samples are shown in Figure 10-64 to Figure 10-66. Again there were inhomogeneous areas across most of the fracture surfaces due to the non-uniform freezing. For the AC samples, the images for the C sample show a more ordered structure with more clearly defined and finer grained cells compared to the B and D samples. In linking these observations with the mechanical strength tests, it is interesting that sample C, which displays the smaller cell sizes, also exhibited the highest strength. This therefore reinforces the hypothesis that smaller pores sizes can reduce local stresses and therefore improve the overall strength of the material. These findings are further supported by the rheology observations given that for AC the pH 4 sample offered a much greater viscosity than the pH 8 sample and that viscosity is known to be an important factor in reducing the pore sizes by retarding ice crystal growth during the freezing process (Gutiérrez et al., 2007).

Figure 10-64: Variable 2 - SEM Images (AC pH 4)

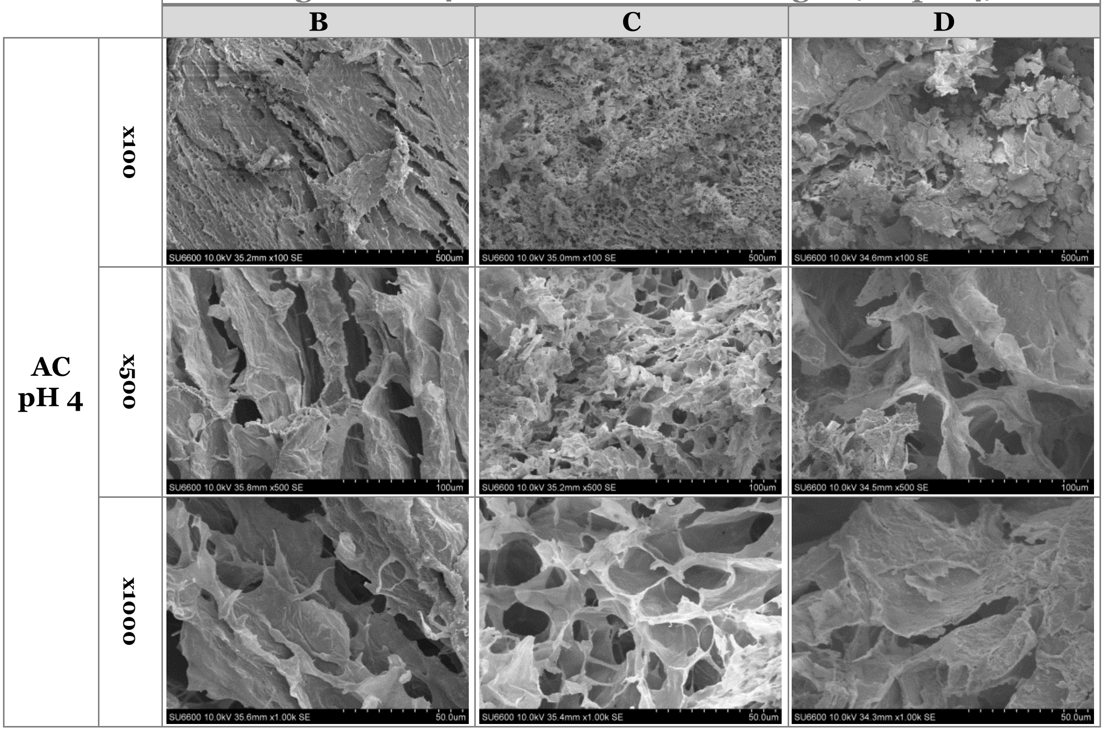

Figure 10-65: Variable 2 - SEM Images (PR22 pH 4)

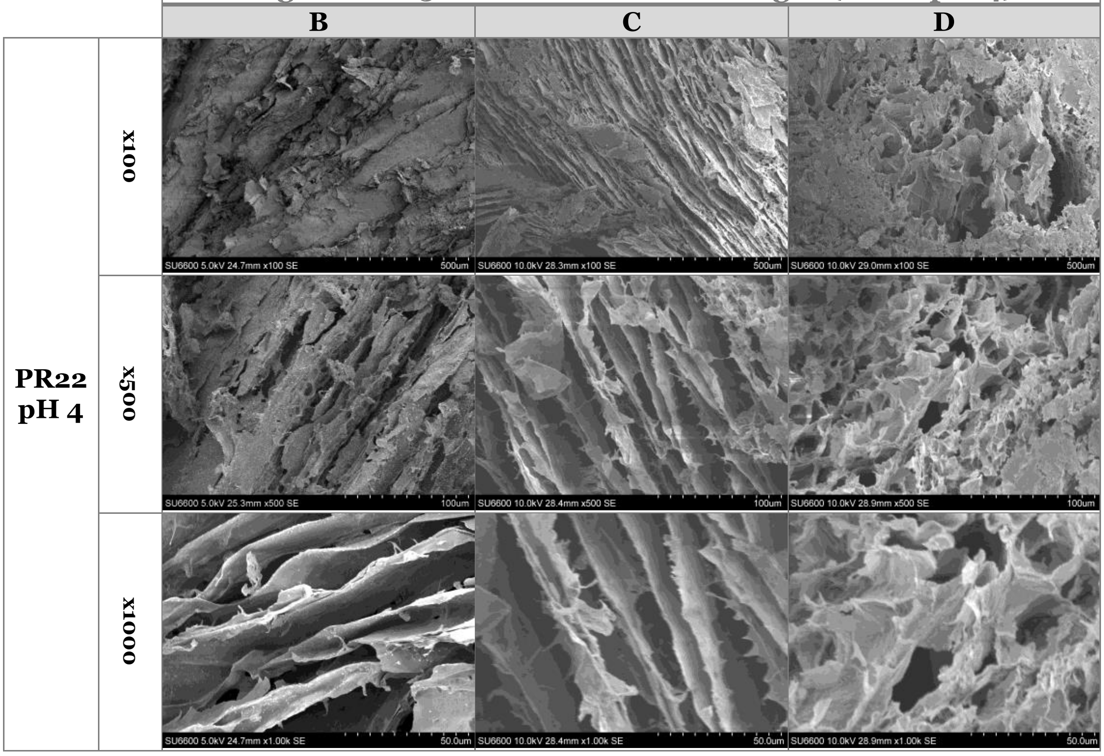

Figure 10-66: Variable 2 - SEM Images (PR24 pH 4)

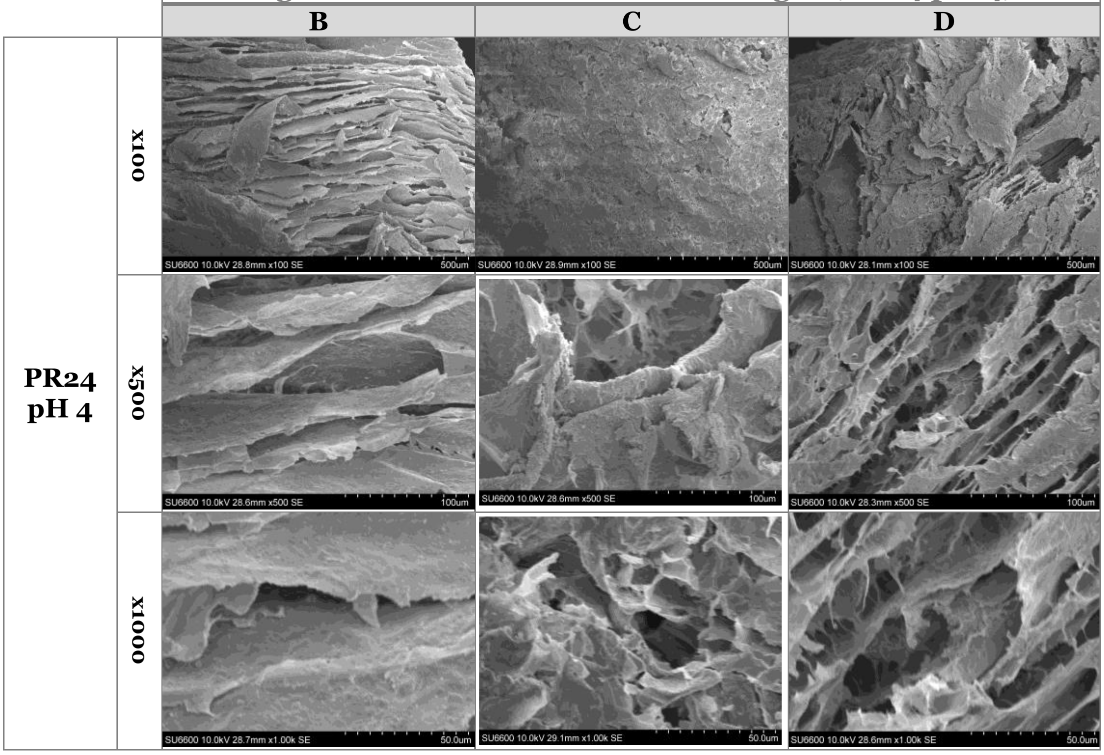

By comparison, for the MBL samples the C samples do not show this same cellular structure which may explain why the compressive strengths of these samples are much lower than the AC sample. However, a more visible cellular structure is observed for PR22D. This particular sample also offers a significant increase in compressive strength compared to the pH 8 sample, although the increase is less dramatic compared to the ACC sample. Again it is possible that the reduction in pH is helping to retard ice crystal growth by increasing the system viscosity. While there is some evidence of this for PR24, the cellar structure appears more disordered. Furthermore, even without pH modification the PR24D sample offers a network structure, possibly due to the high viscosity of this particular polymer. This may explain why the pH 4 sample offers only a small increase in strength compared to the pH 8 sample.

10.2.3. Aerogel Specimens - Variable 3: Clay Type

The third variable to be tested was the type of clay used in the clay-alginate composite. As discussed in the literature review, the clay mineralogy and the presence of different crosslinking ions can both have an effect on the aerogel properties. In order to investigate the role of these variables on the properties of an alginate aerogel, the commercial alginate (AC) was used to provide a comparison between three different clay types – an unmodified bentonite, a calcium saturated bentonite and kaolinite. Due to limited availability of the MBL samples, only the unmodified and calcium saturated bentonite were compared for PR22 and PR24. A summary of the samples tested is presented in Table 10-8.

Table 10-8: Variable 3 - Specimens Tested

	100:0	75:25	50:50	25:75	0:100
AC Ca-Bentonite	-	CBB	CBC	CBD	CBE
AC Kaolinite	-	KB	KC	KD	KE
PR22 Ca-Bentonite	-	CB22B	CB22C	CB22D	-
PR24 Ca-Bentonite	-	CB24B	CB24C	CB24D	-

10.2.3.1. Visual Observations

A summary of the visual observations is presented in Table 10-9. In all cases the alginate containing samples were more stable than the neat clay samples show in Figure 10-67. It was found that for AC, in comparison to the unmodified bentonite samples, the Ca-bentonite and kaolinite samples appeared to be much poorer in quality with several visible defects (Figure 10-68 to Figure 10-70). For the Ca-bentonite, the D mix ratio samples were also found to be rather fragile and disintegrated upon handling. Similar behaviour was also noted for the PR22 and PR24 samples.

Table 10-9: Variable 3 - Specimen Homogeneity

	75:25	50:50	25:75	0:100
AC Ca-Bentonite	Moderate	Poor	Poor	Poor
AC Kaolinite	Moderate	Moderate	Moderate	Poor
PR22 Ca-Bentonite	Moderate	Good	Poor	-
PR24 Ca-Bentonite	Moderate	Good	Poor	-

Figure 10-67: Variable 3 – Specimen Images (E)

	Ca-Bentonite	Kaolinite
Control (E)		

Figure 10-68: Variable 3 - Specimen Images (AC - CaB)

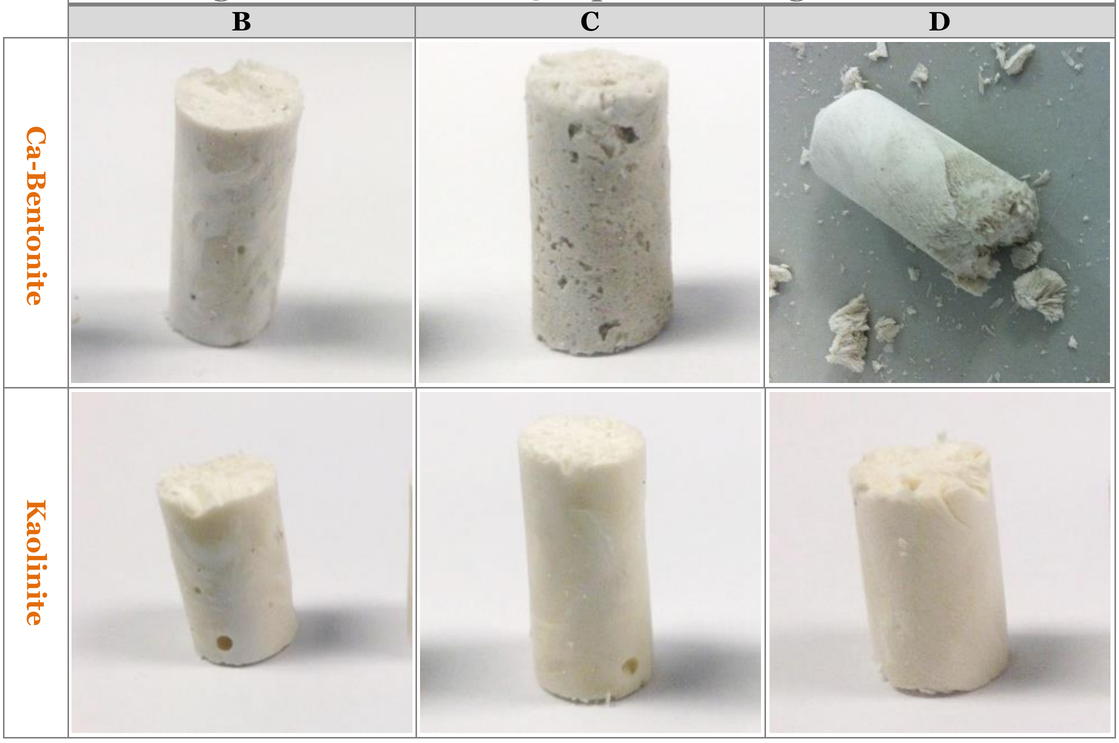

Figure 10-69: Variable 3 - Specimen Images (PR22)

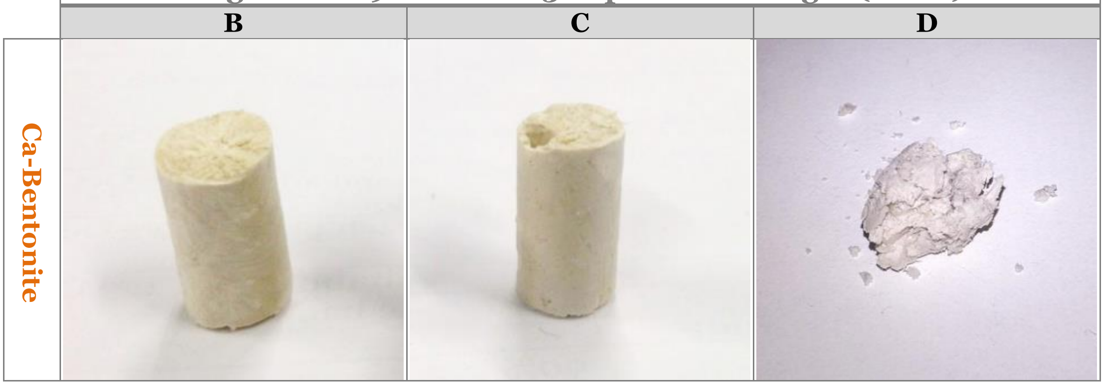

Figure 10-70: Variable 3 - Specimen Images (PR24)

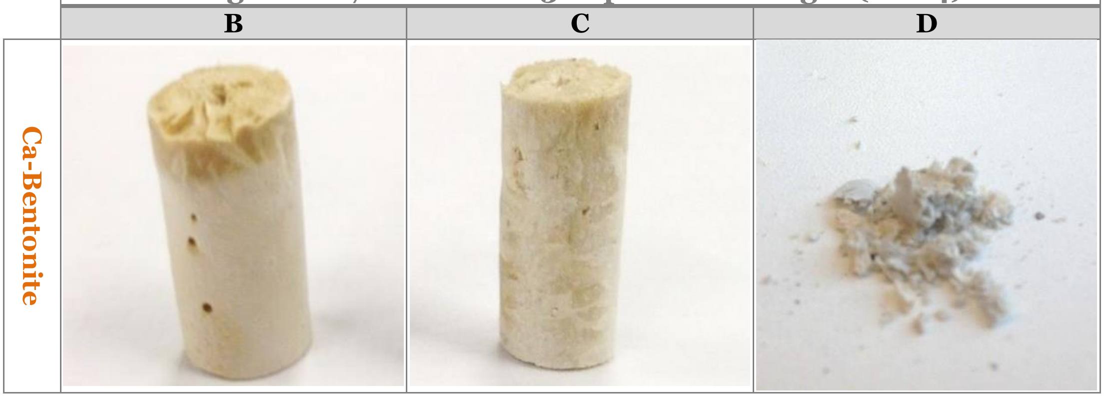

10.2.3.2. Dimensions, mass and bulk density

In terms of bulk density (Figure 10-71), the values achieved for the Ca-bentonite and kaolinite samples were relatively similar, ranging between 90 and 140 kg/m³. For the AC samples, at mix ratio B the greatest value was obtained for the kaolinite sample which had a significantly higher bulk density than both of the bentonite samples. There was no significant difference in density at mix ratio C while a slight increase in mean density values for mix ratio D was observed for the kaolinite sample compared to the bentonite sample. For the MBL samples, no significant differences were observed between clay types for PR22 while for PR24 a significant difference was observed for mix ratio B only (Figure 10-72).

Figure 10-71: Variable 3 - Bulk Density (AC)

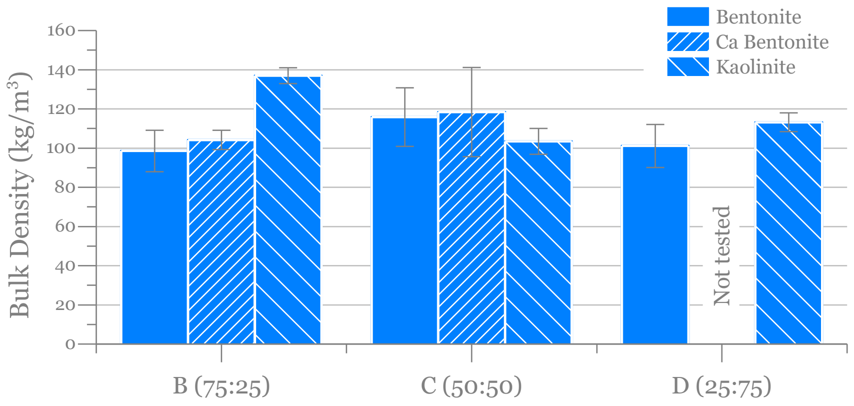

Figure 10-72: Variable 3 - Bulk Density (PR22 & PR24)

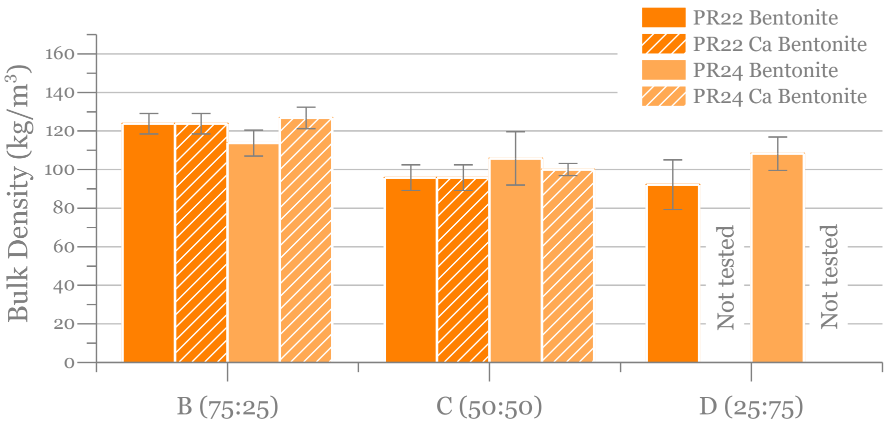

10.2.3.3. Compressive Strength at Yield

In considering the compressive strength behaviour of samples produced using different clay types, representative stress-strain plots for the commercial alginate (AC) and the MBL samples are shown in Figure 10-73 and Figure 10-74, respectively.

Figure 10-73: Stress-strain plots (ACC)

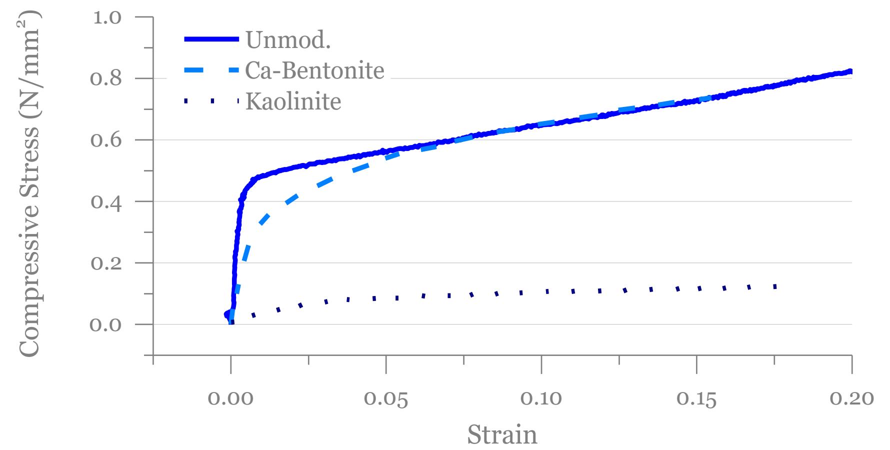

Figure 10-74: Stress-strain plots (PR22C & PR24C)

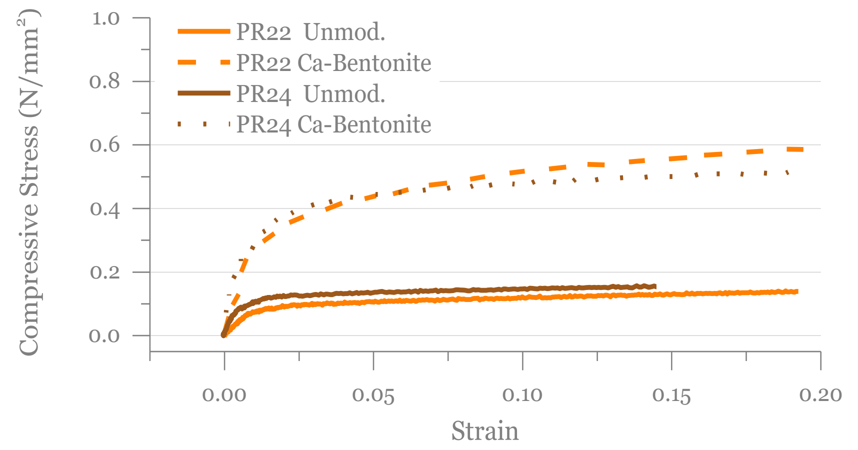

For the commercial alginate (AC), differences between the mean compressive strengths of the B (75:25) samples were not significant due to the high standard deviations (Figure 10-75). For the C (50:50) sample, calcium modification of the bentonite appeared to have a positive effect on the compressive strength compared to the unmodified bentonite but again the increase was not significant. The kaolinite sample was found to have a lower value than both bentonite types. For the D (25:75) mix ratio, the calcium modified sample was too fragile to be tested whilst the kaolinite sample again had a much lower compressive strength than the bentonite. For the MBL samples, as illustrated in Figure 10-76, for mix ratio B (75:25) the calcium bentonite was found to have a lower compressive strength than the unmodified sample. For the C (50:50) samples, both PR22 and PR24 demonstrated a significant increase in compressive strength upon modification with calcium however. In this case the improvements witnessed are much greater than those observed for AC. The D (25:75) samples for the MBL samples were also unsuitable for mechanical testing and are therefore omitted from the results.

Figure 10-75: Variable 3 – Compressive Strength (AC)

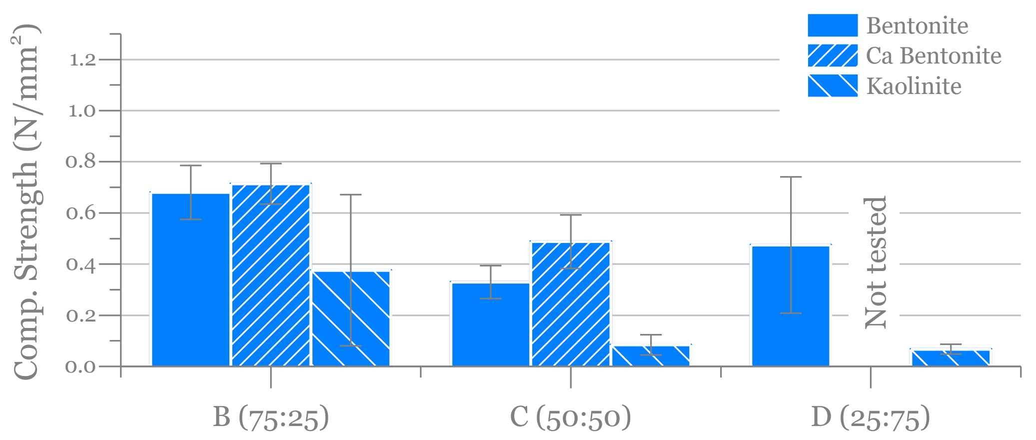

Figure 10-76: Variable 3 – Compressive Strength (PR22 & PR24)

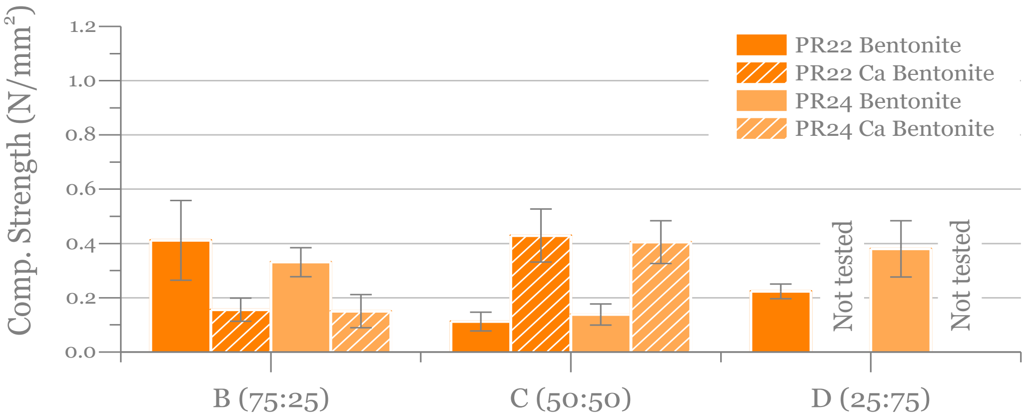

Overall these results demonstrate that significant improvements in strength can be achieved when the calcium saturated clay is used over a natural bentonite but only when a 50:50 mix of clay and alginate is used. This suggests that for this particular ratio, the addition of calcium ions helps to promote crosslinking with alginate hence leading to a stronger network structure. However when the clay content is increased to 75% or decreased to 25%, the addition of calcium ions appears to have a negative impact on the strength of the samples. For the high clay content sample (D) it is possible that there is an insufficient alginate content for this crosslinking effect to occur. For the high polymer content (B), calcium modification of the clay may not have a significant impact due to the lower clay and hence lower calcium content. These samples were also noted to have considerable defects which have contributed to the overall lower strength.

10.2.3.4. Modulus of Elasticity

Figure 10-77 shows the mean modulus of elasticity values for the AC samples. While no significant difference was found between the different clay types at the B mix ratio, at the C mix ratio the kaolinite samples were found to be significantly lower than both of the bentonite samples. For the highest clay content, the kaolinite sample was again found to have a much lower modulus compared to the bentonite. As per the compressive strength results, a comparable modulus for the Ca-Bentonite could not be determined since these samples were not tested. For the MBL samples (Figure 10-78), while a statistically significant reduction in modulus is observed for the B mix ratio when the Ca-Bentonite clay is used, a significant increase in the modulus values is observed for the C mix ratios, reflecting the increase in compressive strength observed for these samples.

Figure 10-77: Variable 3 – Modulus of Elasticity (AC)

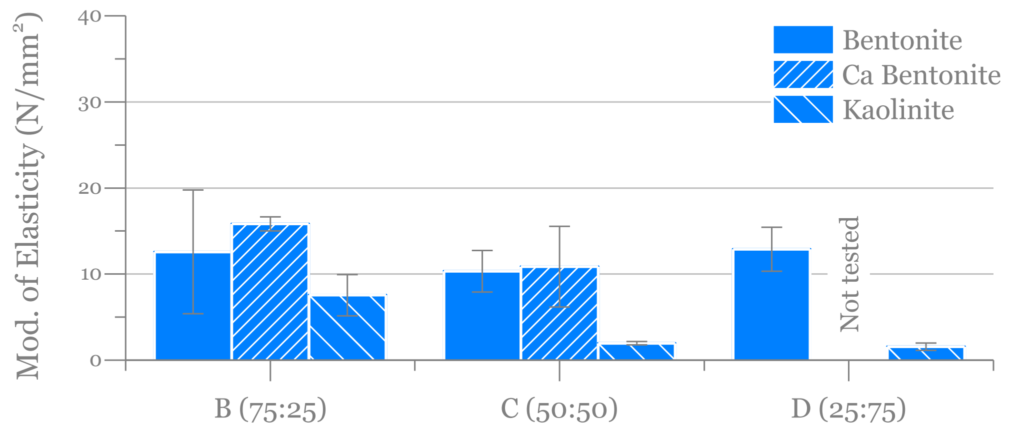

Figure 10-78: Variable 3 - Modulus of Elasticity (PR22 & PR24)

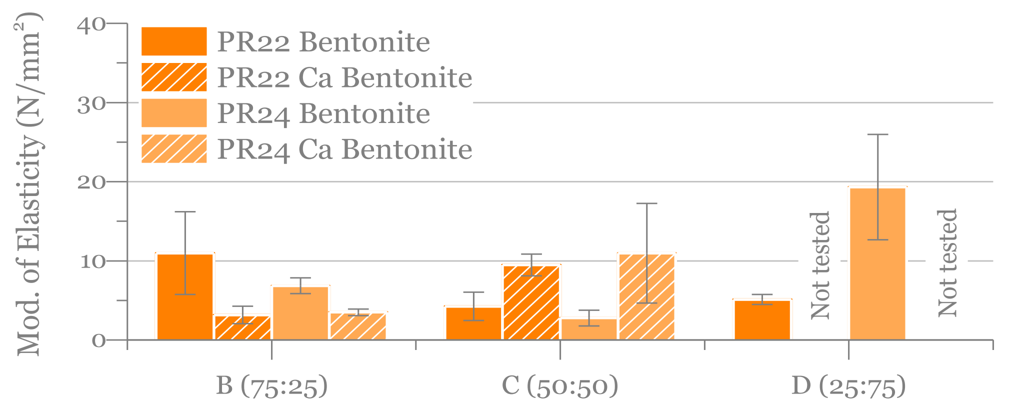

10.2.3.5. Microstructure

In terms of microstructural characteristics, SEM images for the different clay types are shown in Figure 10-79 to Figure 10-81. As discussed previously by Cheng et al. (2012), the addition of calcium as a crosslinking ion in an alginate aerogel can alter the microstructure due to the increase in system viscosity. A study by Gawryla (2009) described that the strong interactions between another biopolymer (pectin) and the calcium ions present in a Ca-MMT clay mean that the polymer and clay come out of solution simultaneously thereby creating a smooth surface on the SEM micrograph. By comparison, a PVOH polymer which is not as strongly bound with the clay resulted in a rougher surface creating by the polymer interacting with the ice crystal.

Figure 10-79: Variable 3 - SEM Images (Ca-Bentonite AC)

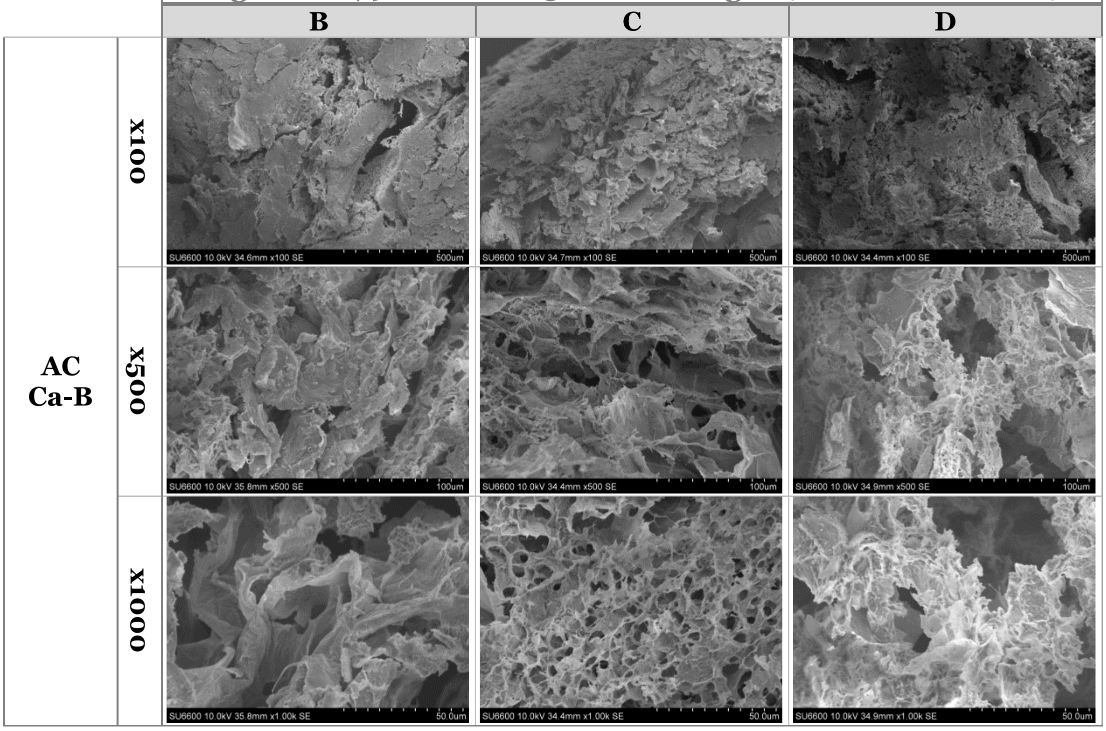

Figure 10-80: Variable 3 - SEM Images (Ca-Bentonite PR22)

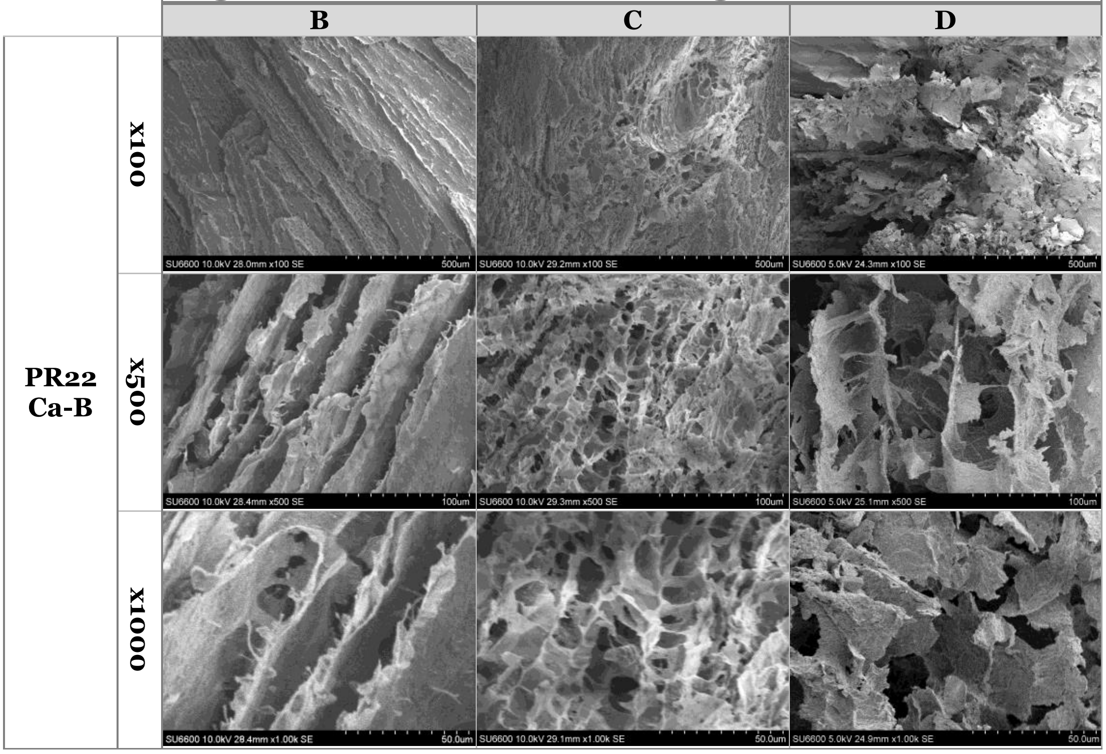

Figure 10-81: Variable 3 - SEM Images (Ca-Bentonite PR24)

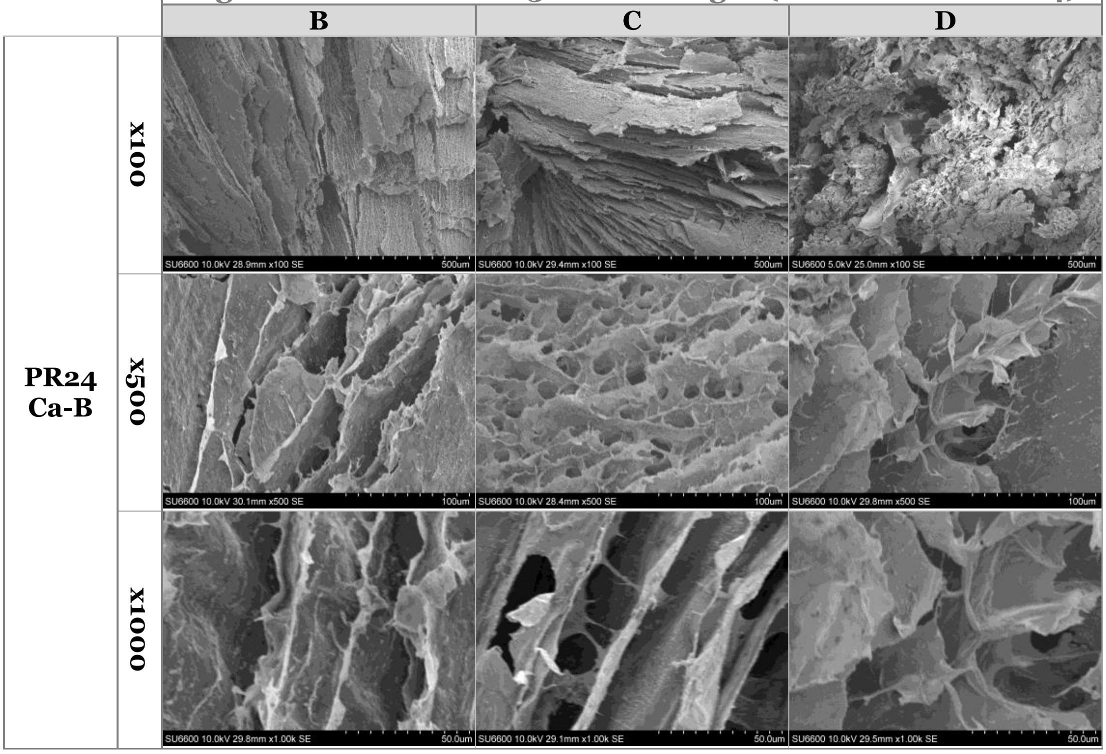

In considering the alginate and clay composites, this smoothing effect is not apparent given the similarities between the images presented for the unmodified clay and Ca-modified clay. For all 3 alginate products the C samples do appear to show a fine grained network rather than the lamellar arrangement observed for the higher polymer content. However the affect is arguably just as pronounced for the natural bentonite samples shown in Figure 10-50, Figure 10-51 and Figure 10-52. It is therefore difficult to verify whether the additional calcium is what causes the change in structure. Furthermore for the D samples, the Ca-bentonite samples appear to be more disordered than the equivalent unmodified samples which offer a more ordered cellular structures. This may explain why the calcium modified samples were much poorer in strength. While the rheology observations presented earlier in this chapter confirmed that the presence of calcium ions would increase the system viscosity, for this particular mix ratio (25:75) the increase in viscosity does not appear retard ice crystal growth as observed for other samples. Indeed for the AC sample, for the highest calcium/clay content (D) there is also some evidence of aggregation and possible flocculation of the clay platelets with combination of fac- to-face and edge-to-edge to orientation. This is likely due to the fact that for calcium bentonites the individual clay plates are more likely to associate resulting in aggregates which are 3 to 4 times thicker than an equivalent sodium bentonite (van Olphen, 1967). It is therefore possible that the introduction of calcium ions modifies the microstructure and arrangement of the clay particles in a manner which produces a less stable structure that the unmodified bentonite.

For the kaolinite samples which were tested only with the commercial alginate, as shown in Figure 10-82, all of the samples appear to retain a lamellar formation which supports the findings of the compressive strength tests where the strength of the kaolinite samples was found to be very low.

Figure 10-82: Variable 3 - SEM Images (Kaolinite AC)

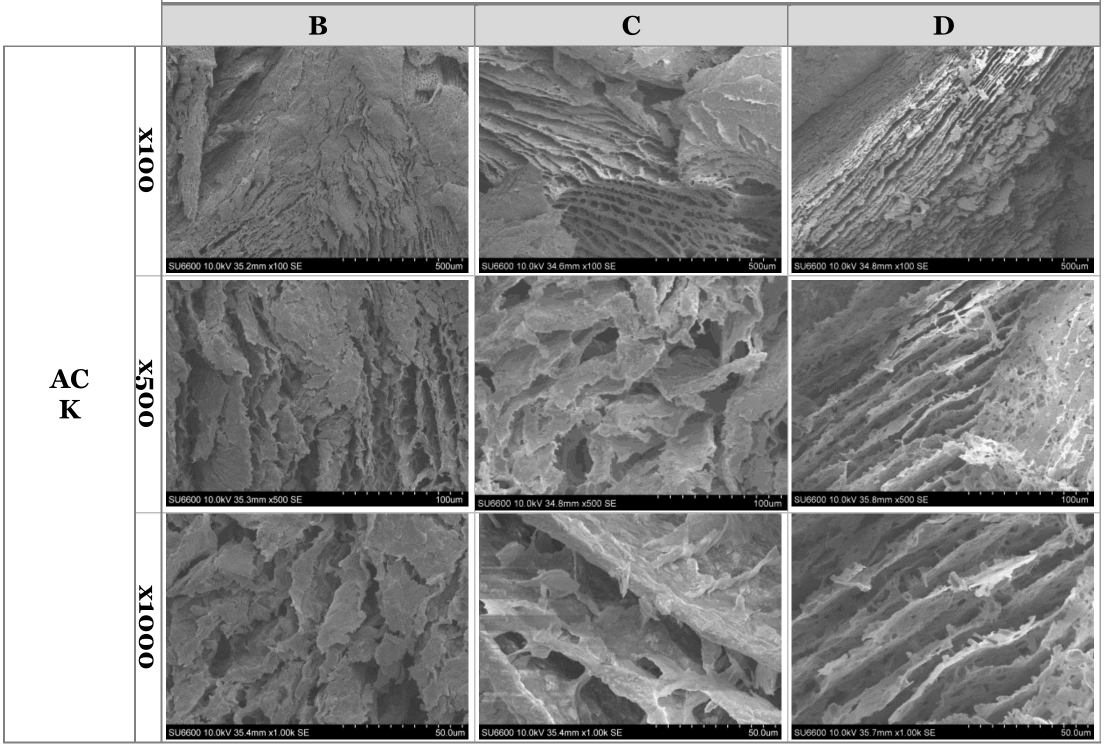

10.3. Phase 3 – Aerogel Specimens: Upscaling

In considering the upscaling trial using a larger 8 x 8 x 4cm steel mould, a single specimen was successfully produced. This larger sample was prepared using the commercial alginate (AC) mixed with unmodified bentonite at a 50:50 mix ratio. Images of the frozen specimen in the freeze-dryer and after drying are shown in Figure 10-83. The sample was a stable monolith which was easy to handle and had an estimated bulk density of 100 kg/m^3. Although this sample was not subjected to further testing, the upscaling trial demonstrated that a larger scale sample could be successfully produced. The next stage of development would therefore be to conduct additional characterisation tests such as compressive strength flexural strength, thermal conductivity and water absorption tests on these larger samples.

Figure 10-83: Large Scale Aerogel Specimen

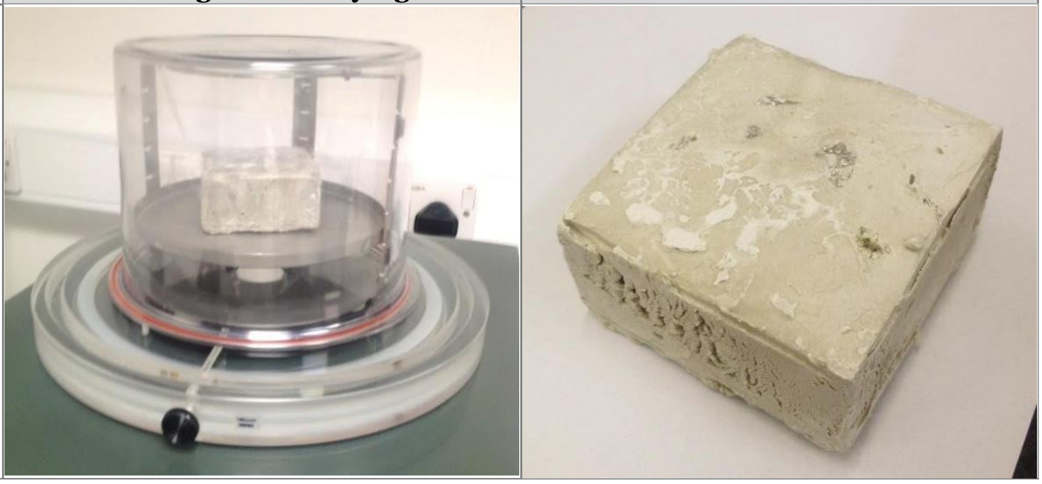

During Freeze-drying

After removal

Trial Sample

For commercial production it would be assumed that larger samples would be prepared and that larger, more efficient practices would be adopted. In current practice for silica aerogel blankets, a typical schematic of the production process is shown in Figure 10-84. In the case of a clay-alginate aerogel, as illustrated in Figure

10-85, the principal parts of the process include mixing, gelation, flash freezing and the freeze-drying. Industrial freezers and freeze-dryers are used commonly for large scale drying of various substances including biological materials, pharmaceuticals and various food products (Mujumdar, 2014). In the case of freezing, large scale air blast freezers, plate freezers and immersion freezers are available (Johnston et al., 1994). In the latter case, the product is submerged in a liquid refrigerant, such as liquid nitrogen, as per the laboratory scale production in this study. Freeze dryers also come in various forms including tunnel, vacuum spray and continuous freeze-dryer which allow for large batches of material to be produced in one drying cycle.

Figure 10-84: Industrial Silica Aerogel Production

Source: Adapted from Aspen Aerogels (http://www.aerogel.org/?p=1058)

Figure 10-85: Lab Scale Process - Aerogels

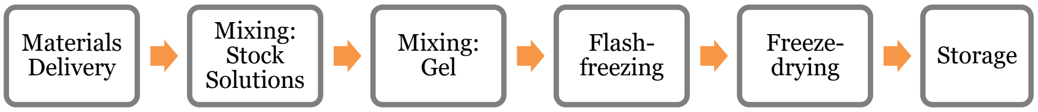

10.4. Phase 4 – Aerogels: Commercial Feasibility

10.4.1. Economic Potential

The results from the cost modelling calculations, based on estimated material and production costs from the aerogel prototypes, are presented in Table 10-10. Further details of these calculations can also be found in Appendix F. It should be noted that these costs are based on lab-scale production for prototype samples with production volume of approximately 100 cm^3. The costs are also based purely on the basic cost of consumables and electricity meaning that the costs associated with equipment, labour and overheads have not been included at this stage.

Table 10-10: Cost Estimations - Aerogels

		75:25 (a:c)	**50:50 (a:c)**	**25:75 (a:c)**
		Estimated cost £/100 cm^3	**Estimated cost** £/100 cm^3	**Estimated cost** £/100 cm^3
AN	*Materials*	£1.62	£1.65	£1.68
	Processing	£1.46	£1.46	£1.46
	Total	**£3.08**	**£3.11**	**£3.14**
LH	*Materials*	£1.64	£1.67	£1.69
	Processing	£1.46	£1.46	£1.46
	Total	**£3.10**	**£3.13**	**£3.15**

As shown, the material costs are dependent upon the mix ratio used and based on these estimates, the higher costs of clay (£20/kg) mean that the 75:25 (alginate: clay) option offers a marginally cheaper option. In terms of production, the greatest cost is associated with the freeze-drying and the electricity consumed during this process, however these costs are small in comparison to the material costs. In total this gives estimated production costs of approximately £3 per 100 cm^3 sample.

These cost calculations are based on laboratory scale equipment however it would be assumed that for commercial production, larger and more cost efficient practices would be adopted. As illustrated in Table 10-11, simply extrapolating the costs of the small samples gives a figure of £308 - 315 per kg or £616 - 630 per m^2 based on a 20mm thick panel. For larger scale production, as discussed by Smith (2011), the capital costs of immersion type freezers are relatively low and freezing of large volumes can be achieved rapidly. However the main disadvantage is the high cost of the liquid nitrogen since the mass of liquid nitrogen required can equate to over 3 times the mass of the material being frozen (Smith, 2011).

Table 10-11: Cost Estimations – Aerogels (upscaling)

	Totals	**75:25 (a:c)**	**50:50 (a:c)**	**25:75 (a:c)**
Upscaling	**Estimated cost per lab scale batch** (£/100 cm^3)	**£3.08-3.10**	**£3.11-£3.13**	**£3.14 - 3.15**
	Estimated costs per kg* (£/kg) Lab scale x 100	**£308 - 310**	**£311-313**	**£314 - 315**
	Estimated costs per m^3* (£/m^3) Lab scale x 10000	**£30,800 - 310,000**	**£31,100 - 31,300**	**£31,400 - 31,500**
	Estimated costs per m^2** (£/m^2) m^3 value x 0.02	**£616 - 620**	**£622 - 626**	**£628 - 630**

*Assuming density of 100 kg/m^3, 1kg = 10,000 cm^3
** Based on 20mm thick panel

In terms of drying, again assuming the use of an industrial scale freeze-dryer such as those used within the food industry, it would be anticipated that cost savings could be achieved compared to the laboratory scale dryer. In general the fixed costs for freeze-drying equipment tends to exceed the running costs by a factor of approximately 1.5 to 2.5 (Mellor, 1978). Although when compared with air-drying, the cost of freeze-drying can be 4-8 times more expensive (Ratti, 2001), there are on-going efforts to increase the efficiency and energy demands of the freeze-drying process which should help to reduce costs in future (Y. Liu et al., 2008). Furthermore other studies regarding clay-based aerogels have reported that it is the use of freeze-drying as an alternative to the relatively expensive solvent exchange and autoclave drying required for silica aerogels which helps to keep the manufacturing costs low (Schiraldi et al., 2010). Indeed Dalton et al. (2010) give an estimated cost of £200 per m^3 for their clay-polymer product which uses a similar production process to the aerogels produced in this study. If these production costs could be achieved, as shown in Figure 10-86, on a m^2 basis a clay-polymer aerogel would therefore be much less than for silica aerogel. Indeed , although it is has been predicted that by 2050 the production costs of silica aerogels will decrease, the estimated costs are still likely to be around £500/m^3 (Cuce et al., 2014a). The estimated costs for the clay-polymer aerogel would also be more comparable to conventional insulations discussed previously in the literature review (based on 20 mm thickness and equivalent thermal performance to silica aerogel blanket).

Figure 10-86: Estimated Insulation Costs per m^2

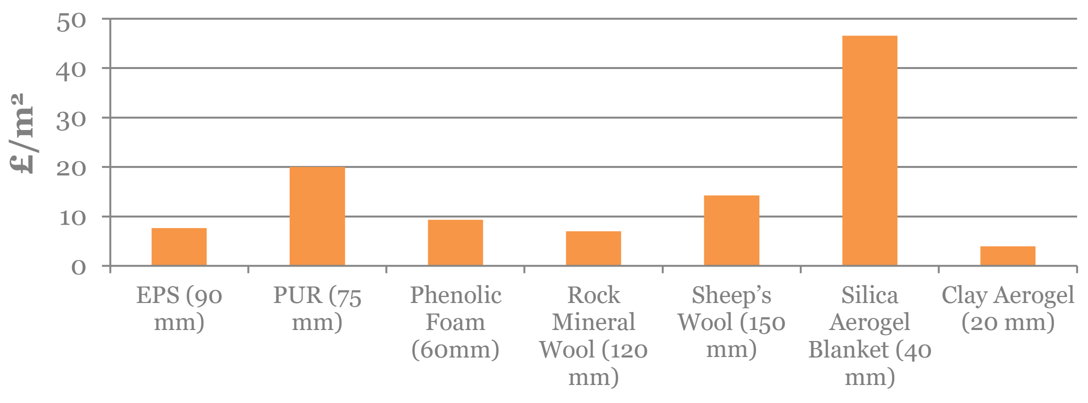

Source: BRE (2016) and Dalton et al. (2010)

10.4.2. Environmental Analysis

In considering the environmental analysis of the aerogels, as discussed in Part I the embodied energy of the alginate, based data from MBL, equates to 6.57 and 8.39 MJ/kg of dry alginate product for the AN and LH products respectively. Compared to other polymers which are typically used in clay-polymer aerogels, PVOH for example, which is used in the aerogels described by Bandi and Schiraldi (2006) and Hostler et al. (2009), is reported to have an embodied energy of 60 to 100 MJ per kg (Patel et al., 2003). Other polymers used in clay aerogels include natural rubber (Pojanavaraphan et al., 2010b) and epoxy resins (Arndt et al., 2007) which have an embodied energy of 73 MJ/kg and 137 MJ/kg respectively (Hammond and Jones, 2011). Provided that the rest of the production process is the identical, an alginate –

based aerogel would have less of an environmental impact than these other clay-polymer aerogels.

In considering aspects other than the alginate, for the clay component, the process for obtaining this material typically involves either hydraulic mining or open pit extraction followed by purifying, drying, milling, packaging and transport (Heath et al., 2014). EE and EC values quoted for bentonite, such as those used by Brandt (2015), are 0.4 MJ/kg and 0.031 kg CO_2/kg. These are not dissimilar to the equivalent values for other quarried materials like soil, perlite and vermiculite (Hammond and Jones, 2011).

Aside from the environmental impacts of the material, the energy requirements associated with parts of the production process must also be considered. In considering firstly the freezing process, as per the cost modelling, one of the key aspects to consider is the use of liquid nitrogen (N_2) as significant amounts of energy are required in its production. Pušavec et al. (2009) for example quote a value of 1.8 MJ per kg. Water is also used during the production of liquid nitrogen as a cooling fluid although it is not physically consumed and can therefore be recycled/returned to the environment (Pušavec et al., 2009). Waste outputs are however minimal as the cooling water is non-toxic and no CO or SO is produced. It should also be pointed out that according to Ratti (2001), in terms of the overall freeze-drying process, the freezing stage equates to only 4% of the total energy consumption whilst the sublimation element accounts for around 45%. Overall the energy required to remove 1 kg of water by way of freeze-drying is nearly double of that required using conventional drying methods (Y. Liu et al., 2008). Nonetheless compared to other supercritical drying methods, such as those involving CO_2, it has been argued that freeze-drying offers a more environmentally benign alternative (Schiraldi et al., 2010). There is however currently a lack of evidence to support this since a comprehensive LCA for freeze-dried aerogels has yet to be conducted. In fact, according to a recent study regarding drying methods for foodstuffs (Hofland, 2014), supercritical drying with CO_2 was shown to consume less energy than freeze-drying. Lower EC values of 5 kg CO_2 /kg dried product were also reported for the CO_2 methods compared to of 30 kg CO_2 /kg for freeze-drying (Hofland, 2014).

Based on the production processes used in this study, estimates regarding the energy inputs for the laboratory scale prototypes are illustrated in Table 10-12. These are also converted to embodied CO_2 values in Table 10-13 using the DECC conversion factors (Hill et al., 2013; DECC, 2016). Further details of these calculations are provided in Appendix G. As expected, the greatest energy input is that of the drying phase which constitutes over 90% of the total, meaning that differences between mix ratios are considered minor. The resulting EE estimate of 54 MJ per 100cm^3 batch of material is similar to the value of 29 MJ per 40cm^3 calculated by Dowson et al. (2012) for a high-temperature supercitically dried aerogel and lower than that of a low-temperature supercritically dried materials (63 MJ per 40cm^3 batch). The estimated EC value of 6.7 kg CO_2 per 100cm^3 is also higher than that of a high temperature supercritically dried silica aerogel (0.73 kg CO_2 per 40cm^3) but lower than the value of 6.63 kg CO_2 per 40cm^3 quoted for a low temperature supercritically dried silica aerogel.

Table 10-12: Embodied Energy - Aerogels				
	Product	**75:25 (a:c)**	**50:50 (a:c)**	**25:75 (a:c)**
		MJ/100 cm^3	MJ/100 cm^3	MJ/100 cm^3
Material	Alginate	0.049 – 0.063	0.033 – 0.042	0.016 – 0.021
	Bentonite	0.001	0.002	0.003
	Liquid N^2	1.80	1.80	1.80
	Water	0.001	0.001	0.001
Process	Mixing *(4 hours x 45W)*	0.65	0.65	0.65
	Freeze-drying *(24 hours x 600W)*	51.84	51.84	51.84
	Total	**54.3 – 54.4**	**54.3 – 54.3**	**54.3 – 54.3**
	Total (MJ/kg)	**5430 - 5440**	**5430**	**5430**
	Total (MJ/m^3)	**543,000 – 544,400**	**543, 000**	**543, 000**

Table 10-13: Embodied CO_2 - Aerogels				
		75:25 (a:c)	**50:50 (a:c)**	**25:75 (a:c)**
		kg CO_2 e/100 cm^3	kg CO_2 e/100 cm^3	kg CO_2 e/100 cm^3
Material	Alginate	0.0028 – 0.0038	0.0019 – 0.0026	0.0009 – 0.0013
	Bentonite	0.0001	0.0002	0.0002
	Liquid N^2	-	-	-
	Water	0.0001	0.0001	0.0001
Process	Mixing *(4 hours x 45W)*	0.0832	0.0832	0.0832
	Freeze-drying *(24 hours x 600W)*	6.655	6.655	6.655
	Total	**6.74**	**6.74**	**6.74**
	Total (kg CO_2 e/kg)	**674**	**674**	**674**
	Total (kg CO_2 e/m^3)	**67,400**	**67,400**	**67,400**

However, extrapolating these results to a larger mass of material gives an EE value of 5395 - 5399 MJ/kg and an EC value of 674 kg CO_2/kg which is still considerably higher than values quoted for other insulation materials. The estimated EE figure is also much higher than the 53 MJ/kg quoted by Aspen Aerogels (2011) for their Spaceloft product although it should be noted that their calculation is per kg of the final composite blanket rather than the pure aerogel. The calculations for the alginate-clay prototypes are also based on laboratory scale equipment and so energy-efficiency savings would be expected for larger scale production. Indeed Dowson et al. (2012) demonstrated that scaling revisions between laboratory scale samples and industrial production involving larger batches could lead to an EE reduction of around two thirds with a similar reduction on the CO_2 burden. Assuming that similar savings could be achieved for the clay-aerogel samples, this would give approximate values of below 1800 MJ/kg and 225 kg CO_2/kg. While these are relatively high, it should also be noted that these estimations are also related to the embodied energy per kg rather than the equivalent amount of material required in order to achieve a given U-value. Assuming that the thermal conductivity of the alginate-clay aerogel would be similar to that of the clay-polymer aerogels described by Dalton et al. (2010), a 20mm thickness would therefore give a comparable performance to a silica aerogel blanket. Comparison of the embodied energy and CO_2 values at this m^2 rate is therefore shown in Figure 10-87.

Figure 10-87: Embodied Energy/CO_2 Estimations per m^2

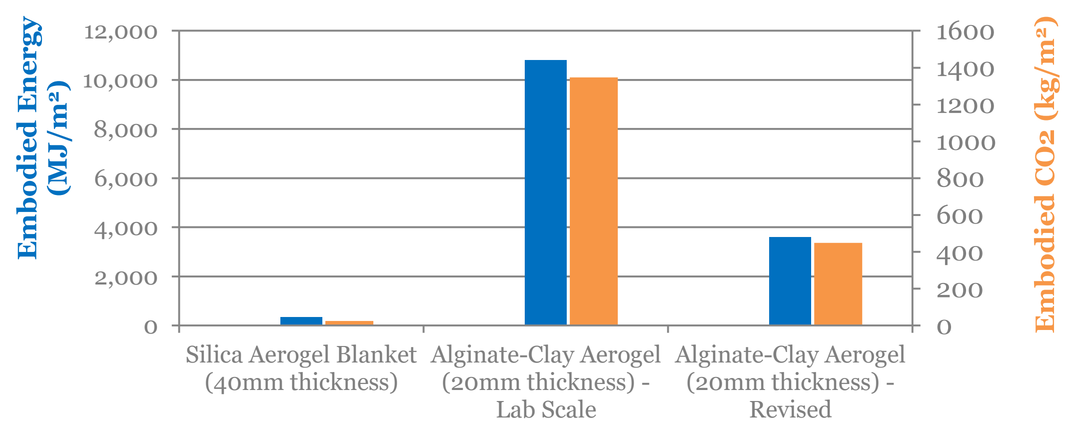

The values for the proposed alginate-clay aerogel are much higher than that of the Spacetherm product. Even assuming the aforementioned scaling revisions are applied, the embodied energy of the aerogel product is still over 10 times greater than the industry standard. Given that that these comparisons are based on extrapolated values and estimated thermal properties, a more detailed analysis involving the specific thermal conductivity values and more accurate production data would shed further light on the environmental performance.

10.4.3. Market comparison

As discussed in the literature review, the market for insulation products is expected grow in future years due to increasing energy efficiency targets and the need to improve the energy performance of both new and existing buildings. While aerogels currently form only a minor part of this market, it has been argued that this will increase in future due to the predicted improvements in the production cost-efficiency of aerogels as well as the increased demand for high performance insulation products (Business Innovation Observatory, 2015). A summary of the typical properties of commercially available and some developing aerogel products, which are noted to be suitable for construction applications, is provided in Table 10-14. Further details of the specific products can be found in Appendix H.

Table 10-14: Market Comparison

	Bulk Density	**Comp. Strength**	**Thermal Conductivity**	**Approx. Cost**	**EE**
Units:	kg/m^3	N/mm^2	W/mK	£	MJ/m$_2$
Silica aerogel granules	40 – 400	0.02 – 2.29	0.018	-	-
Silica Aerogel Blanket	70 – 160	0.05 – 0.08	0.014 – 0.025	24 – 174 per m^2	53
VIP (silica aerogel core)	180 – 210	≥ 0.15	0.007	100 per m^2	-
Silica Aerogel tiles	1 – 1000	2 -14	0.018 – 0.035	-	-
Clay-polymer Aerogels	30 - 200	0.01 – 20	0.01 – 0.03	200 per m^3	-
Insulating plaster (aerogel granules)	220	-	0.028	-	-
PU Aerogel	120	>3	0.017	-	-
Clay -alginate-Aerogel	**90 – 150**	**0.02 – 1.35**	**-**	**200 per m^3**	**~500**

It should be noted that whilst the alginate-clay specimens have been produced only as small cylinders and the one larger block, it is assumed that the alginate-clay mix could be processed in a similar manner to other clay-polymer aerogels in order to form powders, granules, larger boards and fibre-reinforced blankets (see Appendix H). The can also potentially be used as fillers for insulating plasters or the inner core of VIPs. Nonetheless, in comparing the physical properties of the alginate-clay prototypes with other pure aerogels, the bulk densities are close to the values reported for silica aerogels and other clay-polymer aerogels. Compressive strengths, although highly variable in this study depending on the exact composition, are also within the range quoted for other aerogel products. Although thermal conductivity has not been measured in this study, based on the properties of similar materials a target value of 0.01 - 0.03 W/m-K would be required in order to compete with existing products. Finally in cost terms, if a production cost of ~£200 per m^3 could be achieved, as described for other clay-polymer products, this would give an equivalent m^2 cost which would be much less than existing silica aerogel blanket products and VIP products. On the other hand, given that the initial motivation of the project was to develop a material which would be more environmentally friendly than existing products on the market, there are still significant energy inputs required for the clay-alginate product despite the fact that it created from natural, renewable raw materials. The energy demand would therefore need to be reduced in order to justify the production of such a material and to offer a clear benefit over existing insulation products.

11. PART II CONCLUSIONS

In concluding Part II of thesis, this element of the study set out to investigate the use of alginate in a composite aerogel which could potentially be used as a building insulation product. A review of the current insulation market has highlighted the fact that research into aerogels has been increasing in recent years. This is linked to a general increase in the demand for high performance insulation materials driven by rising fuel costs, global targets for reducing CO2 emissions and increasingly stringent building regulations. While aerogels offer a potential solution to reducing heat losses in buildings, the relatively high costs and poor environmental performance of aerogel based insulations currently hinder their widespread use in construction. Consequently, strategies to reduce the processing costs, including the use of lower cost raw materials, will likely make aerogels more affordable in the future and hence increase the commercial viability of using such materials in bulk applications like building insulation.

In responses to these issues, aerogels produced using biopolymers and clays have been proposed as a potential alternative to the more commonly produced silica aerogels. The empirical investigations of Part II therefore set out to develop aerogel materials using locally sourced alginate, in combination with a natural clay. A testing programme was developed and a series of experiments conducted, the objectives of which were to characterise the aerogel prototypes, produced using MBL's alginate products, and investigate the role of the alginate type and other potential variables.

In returning to the key questions posed for Part II, a number of conclusions relating to the role of alginate variables can be made from the results of rheological observations, mechanical testing and microstructural observations Firstly from the rheology studies it was confirmed that that the addition of alginate to a bentonite clay, even at polymer dosages rates of ≤1%, facilitated a visible shift from near Newtonian behavior to pseudo-plastic behavior with the exception of the PR32 sample. This effect was also found to be more pronounced in the commercial alginate sample than in the MBL samples. The results from the flow curves therefore confirmed that the flow behavior of the alginate-clay hydrogels was largely dictated by the viscosity of the alginate polymer. However it was also found that the sample with the greatest G content (PR24) also exhibited the greatest degree of thixotrophy and highest yield stress. Given that this behavior is usually associated with cross-linking and that cross-linking typically takes place at G sites on the polymer chain, these rheology observations also point towards the importance of alginate composition. In addition to alginate type, it was also confirmed that pH modification could be used to increase the system viscosity with significant increases in viscosity found for AC, PR22 and PR24 upon the reduction of pH, with the most dramatic changes in flow behavior observed at pH 4-5. These observations were also supported by the findings of the creep compliance tests where a shift from linear viscous fluid behavior to viscoelastic solid behavior was also found for these samples upon modification from the natural pH (~pH 8) to mildly acidic conditions. Results from the ζ -potential tests also demonstrated that the level of electrostatic repulsion between clay and alginate (AC sample only) was also lowest at pH 4. A final finding from the rheology tests was that by saturating the bentonite clay with calcium ions prior to mixing with the alginates, an increase in viscosity, thixotrophy and resistance to deformation could be achieved. This increase in viscosity was particularly apparent for the high G sample (PR24), again highlighting the importance the alginate composition in determining the degree of Ca^{2+} crosslinking.

XRD analysis also confirmed that all of the clay-alginate composites were of the phase separated type, given that no signs of intercalation or exfoliation were observed.

The second set of findings was related to the prototype aerogel samples. It was first of all demonstrated that composite aerogels prepared using the alginate and clay materials discussed in the rheology tests, could be produced using laboratory scale freeze-drying equipment. Furthermore, it was found that the addition of alginate to a clay based aerogel, even at a 25:75 (alginate: clay) mix ratio, allowed the production of a composite monolith which was rigid enough to be handled. Indeed samples prepared without the polymer were much more friable are formed a powder rather than a monolith material. It should however be noted that while the homogeneity and stability of the samples was generally found to be improved by the addition of alginate, samples with a high polymer contents or high viscosity products did increase the chances of defects being formed. For example evidence of air voids, which are not uncommon in biopolymer-clay aerogels, was found during visual inspections and microstructure observations meaning that the quality of the samples were found to be highly variable. The samples were also small in size (~9mm diameter and 15mm in height) meaning that even small defects could have a significant impact on the mechanical response. It has however been demonstrated that larger scale samples (8 x 8 x 4cm), which may help to improve the accuracy of results, can be produced using the same equipment.

For the mechanical strength tests, despite that fact that multiple samples were tested for each batch, the disparities in specimen quality also meant that considerable variation in compressive strength was found amongst samples produced using the same alginate and clay compositions. Consequently, differences between batches were not always statistically significant. Microstructural observations also highlighted the heterogeneity of the internal morphologies. Nonetheless, some key conclusions regarding the influence of the different compositional variables on mechanical strength can be made. Firstly it was confirmed that all of the samples exhibited stress-strain behaviour similar to that of elastomeric foams with an initial linear portion followed by a visible yield point which occurred at relatively low levels of strain. Secondly, it was found that the alginate type had an influence the compressive strength of the samples given the differences in strength observed for the five alginate types tested. For example, for the majority of samples with a polymer content above 25%, the AC samples were found to offer significantly higher mean compressive strengths than the MBL samples. It was also found that highest compressive strength achieved for each of the alginate types was dependent of the mix ratio adopted. For example, in considering the composite samples (mix ratio B, C & D), for the high viscosity alginates (AC and PR24) an alginate content of only 25% was found to offer the highest compressive strength whereas for the other samples (PR22, PR32 & PR52), the highest strength values were achieved with a 75% polymer content. These results were again linked to the fact that for the combination of a high viscosity polymer and a high polymer content increased the likelihood of defects in the sample.

In response to the second key question for Part II, which required an investigation of other potential variables, it was first of all found that reducing the pH of the bentonite clay from pH 8 to pH 4 was found to have a significant effect on the mechanical strength of particular samples (e.g. AC-C and PR22-D). For the commercial alginate (AC), while the compressive strength values for mix ratios B and D were found to relatively similar, the C sample showed a significant increase in strength in acidic conditions. Indeed the strength of the pH 4 sample was found to be over 4 times that of the pH 8 sample. A similar increase was also observed for PR22-D but was not observed for any of the MBL samples. While these results indicate that pH modification can certainly have an impact on compressive strength, the findings are not consistent with the rheology tests. For example pH modification did not appear to increase the compressive strength of the PR24 samples, despite the clear shift to a gel network at this pH in the flow curves. Again this could be due to the high viscosity leading to defects within the sample.

With respect to the role of the clay type, more stable samples were produced using the smectite type clay compared to the kaolinite. Further increases in strength were also achieved however when the natural bentonite was substituted for a calcium saturated bentonite. For example, a statistically significant improvements were found for PR22-C and PR24-C demonstrating that where equal parts of alginate and clay were used, the addition of calcium ions had a positive effect on compressive strength, supporting the hypothesis that an increased level of crosslinking increases the aerogel strength. There were however inconsistent results for the other mix ratios given that for the MBL samples there was a significant decrease in the strength of the 75:25 (B) samples and the 25:75 (D) samples were in fact too fragile to be subjected to mechanical testing. Again these results are at odds with the rheology tests where the significant increase in viscosity and resistance to deformation, which was indicative of a stronger gel network following the addition of calcium, was apparent even at low polymer contents. Consequently, the rheology tests which describe the behavior of the hydrogel system, cannot be assumed to be a good predictor of the aerogel properties. Comparison of the given variables was easier for direct viscosity measurements as opposed to the compressive strength measurements of the aerogels since these were somewhat masked by other factors (e.g. defects due to freezing variations & the formation of air bubbles).

Finally, in considering the properties of the prototypes and how these compare with other similar materials, alginate-clay aerogels with basic physical properties (e.g. bulk density, compressive strength and modulus of elasticity) which were within the ranges expected for other polymer foams were produced. Direct comparison with other aerogel materials demonstrated that some existing products demonstrate slightly lower bulk densities as well as higher compressive strengths. For other factors such as cost, while extrapolation of the costs associated with the prototypes resulted in very expensive production figures (~£370/kg), estimates based on other similar clay-polymer aerogels produced using the freeze-drying method suggest that costs comparable to and in some cases lower than existing insulation products could be achieved.

On the other hand, a basic environmental assessment also illustrated that the production of the proposed material still resulted in relatively high embodied energy and embodied CO_2 burdens compared to other insulation materials. This finding highlights the fact that although many authors cite good environmental performance and low cost as key drivers in the development freeze-dried biopolymer-clay aerogels, very few studies provide evidence to support these supposed benefits. Indeed the estimations of energy use produced for the prototypes produced in this study highlight the fact that use of a natural materials (i.e. alginate and clay) does not guarantee superior environmental performance compared to supercritically-dried silica products. It was however established that the majority of the both the financial and environmental cost are associated with the freeze-drying element rather than the alginate, or indeed clay, component. Given that the original ambition of this research was to investigate composite building products which incorporate natural, renewable materials but which also help to enhance the energy performance of the building envelope, at this stage the processing energy requirements would have to be reduced before the use of this material as an insulator could be justified. Increased economies of scale or more efficient drying methods could however help to minimise these impacts.

11.1. Contribution to knowledge

In summarising the contributions to knowledge contained within Part II, an empirical study into to the use of alginate biopolymers in a composite aerogel is presented. Similar to Part I, this new investigation builds upon existing academic research by testing a wider range of alginate products than offered in previous publications and therefore provides additional evidence on the role of alginate variables. The experimental data presented in Chapter 10 demonstrates the differences in the quality of specimens produced using alginate from different sources. Again this emphasises the importance of the alginate source in determining the physical properties of the prototype composites. As a final contribution, the investigation also includes a cost and environmental assessment of the proposed aerogel product.

12. FUTURE WORK

In considering recommendations for future work, in light of the findings described in Chapter 7 and Chapter 11 some comments are common to both elements of the study while others are more specific to each product. The proposals for further investigations are therefore presented firstly as general recommendations followed by more specific recommendations for Part I and II.

12.1. General Recommendations

For both Part I and Part II of the study, the experimental work was centered around investigating products supplied in-kind by MBL. While this meant that a range of locally sourced products could be studied, there were also limitations to the material supply which had an impact on the scope of both Part I and II. Firstly, there were general limitations to the quantities of each alginate which MBL were able to provide. This was partly due to delays with the development of MBL's pilot plant and issues with batch continuity. MBL were developing various products throughout the project and while this resulted in a very broad range of alginate materials, most were produced in trial batches meaning that the quantities of alginate available for producing both the brick products and aerogels were much smaller than had originally been anticipated. This meant that the number of samples produced, both in terms of the number of variables tested and the number of replicates, was adapted during project to suit these reduced quantities. Similar issues of material supply were also encountered with regards to the soils used. Therefore a general recommendation for future work is that larger batches of different alginate types are sourced. This would allow for increased sample sizes in order to improve the statistical accuracy of results as well as allowing for additional tests to be performed.

A further limitation, which was applicable to both parts of the project, was the size of the prototypes produced. This was not only linked to the aforementioned issues with material supply but was also constrained by the equipment available. The brick prototypes for instance were produced using mortar prism moulds (160 x 40 x 40 mm) and so the natural next step would be to move towards full scale brick specimens (215 x 102.5 x 65 mm). The aerogels were also produced in 2ml vials but as discussed in Chapter 10, this could be up-scaled to much larger specimens if the samples were produced as individual blocks.

12.2. Part I

In considering specific recommendations for Part I, the main priority for any further development for the unfired clay bricks should involve strategies to improve the overall strength characteristics. This could comprise investigation of further process variables, including a study of different moulding water contents or alternative compaction methods. For example the use of either a manual press or a mechanical extruder would ensure better control of the compactive effort applied to the material, thereby improving overall specimen quality, as well as increasing the overall density and compressive strength. These methods would also potentially allow for a lower moulding water content which could again be beneficial for improving the mechanical properties. Furthermore, using an industrial press or extruder would allow for larger specimens, more comparable to traditional bricks and blocks to studied, rather than the small scale prototypes used in this study.

In additional to these process variables, a study of further material variables would also help to provide additional information on the optimum mix compositions as well as potentially allowing for greater strength increase that those witnessed in this study. This could include a more controlled studied of soil variables by using a base soil with measured modifications in pH, calcium content and grading. Such a study would allow for a less ambiguous analysis of the importance of these individual properties. Furthermore, the effect of the different alginate types in combination with other additives such as an additional calcium source (in order increase ionic crosslinking potential), natural fibres (to improve flexural strength and shrinkage) or protective coatings (to improve moisture sensitivity) could also be useful. As mentioned, an investigation of different solid: water ratios would also be informative, not only from a moulding and processing point of view, but the hydration of the system may also influence the mobility of the alginate.

In addition to modifications of the specimens to help further improve the strength, in order to further investigate the suitability of the material as a masonry product for commercial use, more advanced material characterisation tests would also be required. This could include testing of properties such as porosity in order to gain a deeper understand the compaction behaviour and internal structure of the material. A more detailed study of hygro-thermal behaviour including water vapour transfer and thermal storage properties would also be beneficial. Another area of study which would need to be investigated is the long term durability of the bricks. Due to the time-constraints of this project the specimens were tested 2 weeks after the initial manufacturing. A staged study comparing the mechanical strengths of specimens after 6, 12 and 24 months for example would confirm whether there are any significant changes in strength over time. A similar study by Chang et al. (2015) for example has been performed on xanthan gum earth blocks where results demonstrated that despite being a biodegradable polymer, there was no significant loss in strength, even after a period of two years. It would therefore be interesting to compare this behaviour with the long term stability of the alginate. Known methods for accelerated erosion tests such as those discussed by Walker (1995), would likely be too harsh for the specimens in this projects and so a more suitable method of assessing long term durability would also have to be developed. In developing the prototypes for use in construction, the next stage would also be to move beyond the testing of individual units and alternatively investigate the full masonry system. This would allow investigations of characteristics strength, including a study of different mortars, by testing masonry prisms rather than individual units.

Finally, given that the specimens in this study demonstrated relatively low strength values, more comparable with mortars or plasters, it may be more suitable for the material to be considered for these alterative applications where compressive strength values are of less importance. In this case however it would need to be demonstrated that the addition of alginate would offer an improvement over a standard clay mortar or other conventional mortars in terms of properties like workability (e.g. workable life and correction time), shrinkage, water vapour permeability, adhesive strength and compatibility with substrates (Hendry, 2001).

12.3. Part II

For Part II, the first recommendation for future work would be to investigate alternative drying methods which could help to reduce the overall energy consumption and thereby make the material more attractive as an environmentally friendly alternative to silica based aerogels. Furthermore, given the size limitations of the cylindrical specimens produced within this study, production of larger scale samples would facilitate more accurate testing of physical properties like density and mechanical behaviour. Larger samples would also be required in order to perform other tests usually associated with insulation materials such as assessments of flammability and combustion behaviour, moisture absorption and vapour permeability testing as well as an investigation into thermal and acoustic performance. An evaluation of the long term stability and durability of the materials would also need to be performed in order to confirm whether the structural integrity of the products would be suitable for the proposed life-span of the building.

In addition, although this study describes some basic compositional variables for the alginate-clay mix, from the results presented here it is clear that there are many other variables which it would be useful to study in future. For example, improved control of the gelation process through the use of additional sequestering agents could help to create more uniform and homogenous aerogels. Furthermore, the use of additional calcium sources in addition to the calcium contained with the clay could improve the feeding ratio of calcium ions to G-blocks on the alginate chain thereby helping to promote cross-linking. While a bentonite clay was used in this study for the purposes of minimising cost, future studies could use a pure montmorillonite clay to eliminate the effects of any impurities. A further investigation of the role of pH, including a wider pH range would also be required in order to fully explain the observations and to determine the optimum pH for each alginate type. It should also be noted that only sodium alginate samples were included in this study and so it would be worthwhile comparing these results with other alginate salts such as potassium or ammonium alginate. Polymer blends could also be investigated to give more tailored properties. Other components such as fibrous materials could also be incorporated into the material in order to improve properties like flexural strength.

Bibliography

Aaltonen, O., Jauhiainen, O., 2009. The preparation of lignocellulosic aerogels from ionic liquid solutions. Carbohydr. Polym. 75, 125–129. doi:10.1016/j.carbpol.2008.07.008

Abu-Jdayil, B., 2011. Rheology of sodium and calcium bentonite–water dispersions: Effect of electrolytes and aging time. Int. J. Miner. Process. 98, 208–213.

Achenza, M., Fenu, L., 2006. On Earth Stabilization with Natural Polymers for Earth Masonry Construction. Mater. Struct. 39, 21–27. doi:10.1617/s11527-005-9000-0

Adam, E., Agib, A., 2001. Compressed stabilised earth block manufacture in Sudan. Fr. Paris Print. Graphoprint UNESCO.

Aerogel Technologies, 2016. Airloy Ultramaterials [WWW Document]. URL http://www.airloy.com/category/properties/ (accessed 3.25.16).

Agarwal, A., 1981. Mud, mud: the potential of earth-based materials for third world housing. Earthscan.

Akther, S., Hwang, J., Lee, H., 2008. Sedimentation characteristics of two commercial bentonites in aqueous suspensions. Clay Miner. 43, 449–457.

Alam, M., Singh, H., Limbachiya, M.C., 2011. Vacuum Insulation Panels (VIPs) for building construction industry – A review of the contemporary developments and future directions. Appl. Energy 88, 3592–3602. doi:10.1016/j.apenergy.2011.04.040

Alemán, J., Chadwick, A.V., He, J., Hess, M., Horie, K., Jones, R.G., Kratochvíl, P., Meisel, I., Mita, I., Moad, G., 2007. Definitions of terms relating to the structure and processing of sols, gels, networks, and inorganic-organic hybrid materials (IUPAC Recommendations 2007). Pure Appl. Chem. 79, 1801–1829.

Alexandre, M., Dubois, P., 2000. Polymer-layered silicate nanocomposites: preparation, properties and uses of a new class of materials. Mater. Sci. Eng. R Rep. 28, 1–63.

Alhassan, S.M., Qutubuddin, S., Schiraldi, D., 2010. Influence of electrolyte and polymer loadings on mechanical properties of clay aerogels. Langmuir 26, 12198–12202.

Al-Homoud, D.M.S., 2005. Performance characteristics and practical applications of common building thermal insulation materials. Build. Environ. 40, 353–366. doi:10.1016/j.buildenv.2004.05.013

AMA Research, 2015. 6% growth forecast for the UK building insulation market in 2015 [WWW Document]. Build. Constr. Des. URL http://www.buildingconstructiondesign.co.uk/news/6-growth-forecast-for-the-uk-building-insulation-market-in-2015/

Andresen, I.-L., Skipnes, O., Smidsrod, O., Ostgaard, K., Hemmer, P., 1977. Some biological functions of matrix components in benthic algae in relation to their chemistry and the composition of seawater. Presented at the ACS Symposium Series-American Chemical Society (USA).

Anifowose, A.Y.B., 2000. Stabilisation of lateritic soils as a raw material for building blocks. Bull. Eng. Geol. Environ. 58, 151–157. doi:10.1007/s100640050009

Appleton, E.V., Rose, R.C., Plesch, P.H., Cefoil Ltd, 1946. Improvements in or relating to the Manufacture of Cellular Materials of Low Density. Patent No. 574,382.

Arndt, E.M., Gawryla, M.D., Schiraldi, D.A., 2007. Elastic, low density epoxy/clay aerogel composites. J. Mater. Chem. 17, 3525–3529.

Arumala, J.O., Gondal, T., 2007. Compressed Earth Building Blocks For Affordable Housing, in: The Construction and Building Research Conference of the Royal Institution of Chartered Surveyors. Presented at the COBRA 2007, RICS, Georgia Tech, Atlanta USA.

Ashby, M.F., Shercliff, H., Cebon, D., 2013. Materials: engineering, science, processing and design, 3rd ed. Butterworth-Heinemann, Oxford.

Ashton, R.S., Banerjee, A., Punyani, S., Schaffer, D.V., Kane, R.S., 2007. Scaffolds based on degradable alginate hydrogels and poly(lactide-co-glycolide) microspheres for stem cell culture. Biomaterials 28, 5518–5525. doi:10.1016/j.biomaterials.2007.08.038

Aspen Aerogels, 2011. Datasheet Spaceloft® High Performance Insulation for Building Envelopes [WWW Document]. URL http://www.tcnano-norge.no/Spaceloft_10_A2_REV1.pdf (accessed 6.29.15).

Aspinall, G.O., 2014. The polysaccharides. Academic Press Inc., New York.

ASTM, 2013. ASTM E1461 - 13 Standard Test Method for Thermal Diffusivity by the Flash Method. ASTM International.

ASTM, 2012. ASTM E1050 - 12 Standard Test Method for Impedance and Absorption of Acoustical Materials Using a Tube, Two Microphones and a Digital Frequency Analysis System. ASTM International.

ASTM, 2011. Standard Practice for Classification of Soils for Engineering Purposes (Unified Soil Classification System) (No. ASTM D2487-11).

ASTM, 2010a. ASTM C1498 – 04a Standard Test Method for Hygroscopic Sorption Isotherms of Building Materials.

ASTM, 2010b. ASTM E2392/E2392M-10e1 Standard Guide for Design of Earthen Wall Building Systems. ASTM International.

Atterberg, A., 1911. Die plastizität der tone. Int. Mitteilungen Für Bodenkd. 1, 10–43.

Attou, F., Bruand, A., Bissonnais, Y. le, 1998. Effect of clay content and silt—clay fabric on stability of artificial aggregates. Eur. J. Soil Sci. 49, 569–577.

Atzeni, C., Pia, G., Sanna, U., Spanu, N., 2008. Surface wear resistance of chemically or thermally stabilized earth-based materials. Mater. Struct. 41, 751–758.

Au, P.-I., Leong, Y.-K., 2013. Rheological and zeta potential behaviour of kaolin and bentonite composite slurries. Colloids Surf. Physicochem. Eng. Asp. 436, 530–541. doi:10.1016/j.colsurfa.2013.06.039

Aubert, J.E., Fabbri, A., Morel, J.C., Maillard, P., 2013. An earth block with a compressive strength higher than 45 MPa! Constr. Build. Mater. 47, 366–369. doi:10.1016/j.conbuildmat.2013.05.068

Aubert, J.E., Maillard, P., Morel, J.C., Al Rafii, M., 2015. Towards a simple compressive strength test for earth bricks? Mater. Struct. 1–14. doi:10.1617/s11527-015-0601-y

Auhim, H.S., Hassan, S.S., 2013. Production and characterization of alginate from Azotobacter vinellandii A3. Int J Adv Pharm Biol Chem 2.

Aymerich, F., Fenu, L., Meloni, P., 2012. Effect of reinforcing wool fibres on fracture and energy absorption properties of an earthen material. Constr. Build. Mater. 27, 66–72.

Baetens, R., Jelle, B.P., Gustavsen, A., 2011. Aerogel insulation for building applications: A state-of-the-art review. Energy Build. 43, 761–769. doi:10.1016/j.enbuild.2010.12.012

Baetens, R., Jelle, B.P., Gustavsen, A., Grynning, S., 2010. Gas-filled panels for building applications: A state-of-the-art review. Energy Build. 42, 1969–1975. doi:10.1016/j.enbuild.2010.06.019

Bailey, J., 1998. Seaweed Processing in the West of Scotland. Ayrsh. Notes No. 1.

Bak, M., Yimmou, B.M., Csupor, K., Németh, R., Csóka, L., 2012. Enhancing the durability of wood against wood destroying fungi using nano-zinc. Presented at the International Scientific Conference on Sustainable Development & Ecological Footprint.

Baker, P., 2011. U-values and traditional buildings: in situ measurements and their comparisons to calculated values (No. Technical Paper 10). Historic Scotland Conservation Group.

Bal, H., Jannot, Y., Quenette, N., Chenu, A., Gaye, S., 2012. Water content dependence of the porosity, density and thermal capacity of laterite based bricks with millet waste additive. Constr. Build. Mater. 31, 144–150.

Balakrishnan, B., Mohanty, M., Umashankar, P., Jayakrishnan, A., 2005. Evaluation of an in situ forming hydrogel wound dressing based on oxidized alginate and gelatin. Biomaterials 26, 6335–6342.

Balo, F., Yucel, H.L., 2013. Assessment of Thermal Performance of Green Building Materials Produced with Plant Oils. Int. J. Mater. Sci. 3.

Balo, F., Yucel, H.L., Ucar, A., 2010. Determination of the thermal and mechanical properties for materials containing epoxidised palm oil, clay and fly ash. Int. J. Sustain. Eng. 3, 47–57.

Bandeira, L.C., Calefi, P.S., Ciuffi, K.J., de Faria, E.H., Nassar, E.J., Vicente, M.A., Trujillano, R., 2012. Preparation of composites of laponite with alginate and alginic acid polysaccharides. Polym. Int. 61, 1170–1176. doi:10.1002/pi.4196

Bandi, S., Bell, M., Schiraldi, D.A., 2005. Temperature-responsive clay aerogel-polymer composites. Macromolecules 38, 9216–9220.

Bandi, S., Schiraldi, D.A., 2006. Glass transition behavior of clay aerogel/poly (vinyl alcohol) composites. Macromolecules 39, 6537–6545.

Barbetta, A., Barigelli, E., Dentini, M., 2009. Porous Alginate Hydrogels: Synthetic Methods for Tailoring the Porous Texture. Biomacromolecules 10, 2328–2337. doi:10.1021/bm900517q

Barker, K., 2004. Review of housing supply: Delivering stability: Securing our future housing needs. HM Government, London.

Barker, T.C., Dickinson, R., Hardie, D., 1956. The origins of the synthetic alkali industry in Britain. Economica 23, 158–171.

Barnes, H.A., 1997. Thixotropy—a review. J. Non-Newton. Fluid Mech. 70, 1–33.

BASF, 2016. Slentite® A Panel for All Climates [WWW Document]. URL http://www.polyurethanes.basf.de/pu/solutions/en/function/conversions:/publish/content/group/News_und_Medien/Polyurethan/Slentite_EN.pdf

Beas, M.I.G., 1991. Traditional architectural renders on earthen surfaces (MSc Thesis). University of Pennsylvania.

Bei, G., Papayianni, I., 2003. Compressive strength of compressed earth block masonry. Trans. Built Environ., WIT Press 66.

BeMiller, J.N., 2000. Carbohydrates, in: Kirk-Othmer Encyclopedia of Chemical Technology. John Wiley & Sons, Inc.

Benchabane, A., Bekkour, K., 2006. Effects of anionic additives on the rheological behavior of aqueous calcium montmorillonite suspensions. Rheol. Acta 45, 425–434.

Benhelal, E., Zahedi, G., Shamsaei, E., Bahadori, A., 2013. Global strategies and potentials to curb CO2 emissions in cement industry. J. Clean. Prod. 51, 142–161. doi:10.1016/j.jclepro.2012.10.049

Benli, B., Boylu, F., Can, M.F., Karakaş, F., Çinku, K., Ersever, G., 2011. Rheological, electrokinetic, and morphological characterization of alginate–bentonite biocomposites. J. Appl. Polym. Sci. 122, 19–28. doi:10.1002/app.33627

Berevoescu, L., Stoian, V., Dan, D., 2009. Aerogel–a performant Nanomaterial for sustainable buildings. Presented at the 11th WSEAS International Conference on Sustainability in Science Engineering, pp. 457–462.

Bergna, H.E., Roberts, W.O., 2005. Colloidal silica: fundamentals and applications. CRC Press, London.

Bernu, C.J., Bachman, J.L., Werler, P.F., 2010. Soil Stabilization Compositions. Patent No. US 20110113983 A1.

Billong, N., Melo, U., Louvet, F., Njopwouo, D., 2009. Properties of compressed lateritic soil stabilized with a burnt clay–lime binder: effect of mixture components. Constr. Build. Mater. 23, 2457–2460.

Binici, H., Aksogan, O., Bakbak, D., Kaplan, H., Isik, B., 2009. Sound insulation of fibre reinforced mud brick walls. Constr. Build. Mater. 23, 1035–1041.

Binici, H., Aksogan, O., Shah, T., 2005. Investigation of fibre reinforced mud brick as a building material. Constr. Build. Mater. 19, 313–318.

Binz, A., Moosmann, A., Steinke, G., Schonhardt, U., Fregnan, F., Simmer, H., Brunner, S., Ghazi, K., Bundi, R., Heinemann, U., 2005. Vacuum insulation in the building sector: Systems and applications. IEAECBCS Annex 39.

BioMara, 2014. The importance of seaweed across the ages [WWW Document]. URL http://www.biomara.org/understanding-seaweed/the-importance-of-seaweed-across-the-ages (accessed 10.24.14).

Bishop, M.D., Ward, O.G., Gray, L.A., McNickle, E.W., 2000. Clay composition containing a tannin and a method for producing bricks therefrom. Patent No. US 6159886 A.

Bisson, A., Rigacci, A., Lecomte, D., Rodier, E., Achard, P., 2003. Drying of Silica Gels to Obtain Aerogels:Phenomenology and Basic Techniques. Dry. Technol. 21, 593–628. doi:10.1081/DRT-120019055

Bixler, H.J., Porse, H., 2011. A decade of change in the seaweed hydrocolloids industry. J. Appl. Phycol. 23, 321–335.

Bloodworth, A.J., Cowley, J.F., Highley, D.E., Britain, G., 2001. Brick Clay: Issues for Planning. British Geological Survey.

Borer, P., Harris, C., 1998. The Whole House Book:cological Building Design and Materials. Centre for Alternative Technology Publications.

Bourdinaud, M., Cheze, J.B., Thevenin, J.C., 1976. Use of silica aerogel for Cherenkov radiation counter. Nucl. Instrum. Methods 136, 99–103. doi:10.1016/0029-554X(76)90401-8

Boyle, C.A., 2005. Sustainable buildings. Proc. ICE-Eng. Sustain. 158, 41–48.

Brandon, T.L., Brown, J.J., Daniels, W.L., DeFazio, T.L., Filz, G.M., Mitchell, J.K., Musselman, J., Forsha, C., 2009. Rapid Stabilization/Polymerization of Wet Clay Soils; Literature Review. DTIC Document.

Brandt, A.R., 2015. Embodied Energy and GHG Emissions from Material Use in Conventional and Unconventional Oil and Gas Operations. Environ. Sci. Technol. 49, 13059–13066. doi:10.1021/acs.est.5b03540

BRE, 2016. Rethinking refurbishment: Todmorden and Nelson [WWW Document]. URL http://www.bre.co.uk/filelibrary/victorian_terrace/pdfs/BRE5776Elevate&Calder-e.pdf (accessed 6.1.16).

BRE, 2008. BRE Global Methodology for Environmental Profiles of Construction Products. (No. SD6050). Building Research Establishment, Watford, UK.

Bribián, I.Z., Capilla, A.V., Usón, A.A., 2011. Life cycle assessment of building materials: Comparative analysis of energy and environmental impacts and evaluation of the eco-efficiency improvement potential. Build. Environ. 46, 1133–1140. doi:10.1016/j.buildenv.2010.12.002

Brick Development Association, 2012. Sustainability Strategy Progress Report 2012. BDA.

Brick Development Association, 2001. A Sustainability Strategy for the Brick Industry. BDA.

Brindley, G., MacEwan, D., 1953. Structural aspects of the mineralogy of clays and related silicates. 15–59. Presented at the Green, AT, and Stewart, GH Ceramics—A symposium. The British Ceramic Society Stoke-on-Trent, UK.

British Geological Survey, 2007. Brick Clay, Geology and Mineral Planning Factsheet. Scottish Executive.

Broderick, G., Daniel, D., 1990. Stabilizing Compacted Clay against Chemical Attack. J. Geotech. Eng. 116, 1549–1567. doi:10.1061/(ASCE)0733-9410(1990)116:10(1549)

Browne, G., 2009. Stabilised interlocking rammed earth blocks: alternatives to cement stabilisation. Southampton Solent University.

Brundtland, G.H., 1985. World commission on environment and development. Environ. Policy Law 14, 26–30.

BSI, 2014. BS EN ISO 12571:2014 Hygrothermal performance of building materials and products. Determination of hygroscopic sorption properties. British Standards Institution.

BSI, 2013a. BS EN 933-9:2009+A1:2013 Tests for geometrical properties of aggregates. Assessment of fines. Methylene blue test. British Standards Institution.

BSI, 2013b. BS EN 826:2013 Thermal insulating products for building applications. Determination of compression behaviour. British Standards Institution.

BSI, 2012a. BS EN 15804:2012+A1:2013 Sustainability of construction works — Environmental product declarations — Core rules for the product category of construction products. British Standards Institution.

BSI, 2012b. BS EN 15935:2012 Sludge, treated biowaste, soil and waste. Determination of loss on ignition. British Standards Institution.

BSI, 2012c. BS EN 15933:2012 Sludge, treated biowaste and soil. Determination of pH. British Standards Institution.

BSI, 2012d. BS EN 1996-1-1:2005+A1:2012 Eurocode 6. Design of masonry structures. General rules for reinforced and unreinforced masonry structures. British Standards Institution.

BSI, 2011a. BS EN 772-1:2011 Methods of test for masonry units. Determination of compressive strength. British Standards Institution.

BSI, 2011b. BS EN 771-1:2011 Specification for masonry units: Clay masonry units. British Standards Institution.

BSI, 2010. BS EN ISO 10140-2:2010 Acoustics. Laboratory measurement of sound insulation of building elements. Measurement of airborne sound insulation. British Standards Institution.

BSI, 2002. BS EN 1015-18:2002 Methods of test for mortar for masonry. Determination of water absorption coefficient due to capillary action of hardened mortar. British Standards Institution.

BSI, 2001a. BS EN 12664:2001 Thermal performance of building materials and products. Determination of thermal resistance by means of guarded hot plate and heat flow meter methods. Dry and moist products of medium and low thermal resistance. British Standards Institution.

BSI, 2001b. BS EN ISO 10534-2:2001 Acoustics. Determination of sound absorption coefficient and impedance in impedance tubes. Transfer-function method. British Standards Institution.

BSI, 1999. BS EN 1015-11:1999 Methods of test for mortar for masonry. Determination of flexural and compressive strength of hardened mortar. British Standards Institution.

BSI, 1997a. BS EN 1351:1997 Determination of flexural strength of autoclaved aerated concrete. British Standards Institution.

BSI, 1997b. BS EN 821-2:1997 Advanced technical ceramics. Monolithic ceramics. Thermo-physical properties. Determination of thermal diffusivity by the laser flash (or heat pulse) method. British Standards Institution.

BSI, 1990a. BS 1377-4:1990 Methods of test for soils for civil engineering purposes. Compaction-related tests. British Standards Institution.

BSI, 1990b. BS 1377-2:1990 Methods of test for soils for civil engineering purposes: Classification tests. British Standards Institution.

BSI, 1990c. BS 1924-2:1900 Stabilized materials for civil engineering purposes — Part 2: Methods of test for cement-stabilized and lime-stabilized materials. British Standards Institution.

BSI, 1987. BS 476-20:1987. Fire tests on building materials and structures. Method for determination of the fire resistance of elements of construction (general principles). British Standards Institution.

Buchholz, C.M., Krause, G., Buck, B.H., 2012. Seaweed and man, in: Seaweed Biology. Springer, pp. 471–493.

Building Standards Division, 2010. The Small Buildings Structural Guidance. Scottish Government.

Buratti, C., Moretti, E., Belloni, E., Agosti, F., 2014. Development of Innovative Aerogel Based Plasters: Preliminary Thermal and Acoustic Performance Evaluation. Sustainability 6, 5839–5852.

Burey, P., Bhandari, B.R., Howes, T., Gidley, M.J., 2008. Hydrocolloid Gel Particles: Formation, Characterization, and Application. Crit. Rev. Food Sci. Nutr. 48, 361–377. doi:10.1080/10408390701347801

Burroughs, S., 2008. Soil property criteria for rammed earth stabilization. J. Mater. Civ. Eng. 20, 264–273.

Burrows, M.T., Macleod, M., Orr, K., 2010. Mapping the intertidal seaweed resources of the Outer Hebrides (No. Scottish Association for Marine Science Internal Report No. 269). S.A.M.S & Hebridean Seaweed Company.

Business Innovation Observatory, 2015. Advanced Materials: Aerogels, getting their second wind (No. Case study 56. 190/PP/ENT/CIP/12/C/N03C01). European Comission.

Buson, M., Lopes, N., Varum, H., Sposto, R.M., Real, P.V., 2012. Evaluation of performance under fire of compressed earth blocks. Presented at the 15th International Conference on Experimental Mechanics (ICEM15).

Cabot Corporation, 2013. Thermal Wrap TM Datasheet [WWW Document]. URL file:///C:/Users/Owner/Downloads/Datasheet-ThermalWrap-TW800pdf.pdf

Call, F., 1953. Preparation of Dry Clay-Gels by Freeze-drying. Nature 172, 126–126. doi:10.1038/172126a0

Camões, A., Eires, R., Jalali, S., 2012. Old materials and techniques to improve the durability of earth buildings. University of Minho.

Campbell, L., Na, B., Ko, E., 1992. Synthesis and characterization of titania aerogels. Chem. Mater. 4, 1329–1333.

Carbon Trust, 2010. Industrial Energy Efficiency Accelerator: A Guide to the Brick Industry (No. CTG043).

Carlson, G., Lewis, D., McKinley, K., Richardson, J., Tillotson, T., 1995. Aerogel commercialization: technology, markets and costs. J. Non-Cryst. Solids 186, 372–379.

Carroll, D., 1959. Ion Exchange in Clays and Other Minerals. Geol. Soc. Am. Bull. 70, 749–779. doi:10.1130/0016-7606(1959)70[749:IEICAO]2.0.CO;2

Carty, L., Garnier, C., Williamson, J.B., Currie, J., 2013. New thin aerogel for high performance internal wall insulation of existing solid wall buildings, in: Rehab 2014. Green Lines Institute.

Casagrande, A., 1932. Research on the Atterberg limits of soils. Public Roads 13, 121–136.

CBA, 2014. CBA Update - Supporting the Concrete Block Industry (No. spring 2014). Concrete Block Association.

Cha, Y.-C., Yoon, J.-S., Lee, J., Hwang, H.-J., Moon, J.-W., 2008. Ambient Pressure Dried Silica Aerogel Thin Film from Water Glass. J. Korean Ceram. Soc. 45, 87–89.

Chan, C.-M., 2011. Effect of Natural Fibres Inclusion in Clay Bricks: Physico-Mechanical Properties. Int. J. Civ. Environ. Eng. 3, 51–57.

Chan, R.W., Ho, P.N., Chan, E.P., 1999. Report on concrete admixtures for waterproofing construction. Structural Engineering Branch, Architectural Services Department.

Chang, I., Cho, G.-C., 2012. Strengthening of Korean residual soil with β-1,3/1,6-glucan biopolymer. Constr. Build. Mater. 30, 30–35. doi:10.1016/j.conbuildmat.2011.11.030

Chang, I., Im, J., Prasidhi, A.K., Cho, G.-C., 2015. Effects of Xanthan gum biopolymer on soil strengthening. Constr. Build. Mater. 74, 65–72. doi:10.1016/j.conbuildmat.2014.10.026

Chapman, A.D., 2009. Numbers of living species in Australia and the world, 2nd ed. Australian Biological Resources Study, Canberra.

Chen, H., Wang, Y., Sánchez-Soto, M., Schiraldi, D., 2012. Low flammability, foam-like materials based on ammonium alginate and sodium montmorillonite clay. Polymer 53, 5825–5831. doi:http://dx.doi.org/10.1016/j.polymer.2012.10.029

Chen, H.-B., Chiou, B.-S., Wang, Y.-Z., Schiraldi, D.A., 2013a. Biodegradable pectin/clay aerogels. ACS Appl. Mater. Interfaces 5, 1715–1721.

Chen, H.-B., Wang, Y.-Z., Schiraldi, D.A., 2013b. Foam-like materials based on whey protein isolate. Eur. Polym. J. 49, 3387–3391. doi:10.1016/j.eurpolymj.2013.07.019

Cheng, Y., Lu, L., Zhang, W., Shi, J., Cao, Y., 2012. Reinforced low density alginate-based aerogels: Preparation, hydrophobic modification and characterization. Carbohydr. Polym. 88, 1093–1099. doi:10.1016/j.carbpol.2012.01.075

Chindaprasirt, P., Pimraksa, K., 2008. A study of fly ash–lime granule unfired brick. Powder Technol. 182, 33–41. doi:10.1016/j.powtec.2007.05.001

Chopin, T., 2012. Seaweed aquaculture provides diversified products, key ecosystem functions. Part II Recent Evol. Seaweed Ind. Glob. Aquac. Advocate 14, 24–27.

Chorom, M., Rengasamy, P., 1995. Dispersion and zeta potential of pure clays as related to net particle charge under varying pH, electrolyte concentration and cation type. Eur. J. Soil Sci. 46, 657–665. doi:10.1111/j.1365-2389.1995.tb01362.x

Christian, S., Billington, S., 2009. Sustainable Biocomposites for Construction. Presented at the ACMA Composites & Polycom Conference (January 15-17, 2009), Tampa, Florida.

Chukwudi, B., Eng, M., Uche, R., 2008. Flocculation of Kaolinite Clay using Natural Polymer. Pac. J. Sci. Technol. 9, 495–501.

CIB, 1999. Agenda 21 for Sustainable Construction (No. Report Publication 237). International Council for Research and Innovation in Building and Construction, Rotterdam, The Netherlads.

Cid-Falceto, J., Mazarrón, F.R., Cañas, I., 2012a. Assessment of compressed earth blocks made in Spain: International durability tests. Non Destr. Tech. Assess. Concr. 37, 738–745. doi:10.1016/j.conbuildmat.2012.08.019

Cid-Falceto, J., Mazarrón, F.R., Cañas, I., 2012b. Assessment of compressed earth blocks made in Spain: International durability tests. Constr. Build. Mater. 37, 738–745.

Clark, A.Q., Herrington, T.M., Petzold, J.C., 1990. The flocculation of kaolin suspensions with anionic polyacrylamides of varying molar mass and anionic character. Colloids Surf. 44, 247–261. doi:10.1016/0166-6622(90)80200-N

Clark, D.E., Gibsen, K.F., Steiner, A.B., 1946. Algin-bitumen composition and its method of preparation. Patent No. 2,393,022.

Cokca, E., Birand, A., 1993. Determination of Cation Exchange Capacity of Clayey Soils by the Methylene Blue Test. Geotech. Test. J. 16, 518–524. doi:10.1520/GTJ10291J

Compadre, 2014. Aeroclay [WWW Document]. URL http://www.aeroclay.com/

Competition Commission, 2007. Wienerberger / Baggeridge Merger Inquiry: Provisional Findings Report.

Construction Resources, 2015. Claytec light unfired clay bricks (No. Uniclass L32119).

Cook, W., 1986a. Alginate dental impression materials: chemistry, structure, and properties. J. Biomed. Mater. Res. 20, 1–24.

Cook, W., 1986b. Alginate dental impression materials: Chemistry, structure, and properties. J. Biomed. Mater. Res. 20, 1–24. doi:10.1002/jbm.820200103

Corwin, D., Lesch, S., 2005. Apparent soil electrical conductivity measurements in agriculture. Comput. Electron. Agric. 46, 11–43.

Costa, A., Keane, M.M., Torrens, J.I., Corry, E., 2013. Building operation and energy performance: Monitoring, analysis and optimisation toolkit. Appl. Energy 101, 310–316.

Cotter, M., 2012. Could Bricks Made of Animal Blood Be the Future of Construction? [WWW Document]. Inhabitat. URL http://inhabitat.com/could-bricks-made-of-animal-blood-be-the-future-of-construction/

Craig, R., 1988. Review of dental impression materials. Adv. Dent. Res. 2, 51–64.

Craig, R.F., 2004. Craig's soil mechanics, 7th ed. CRC Press, London.

Critchley, R., Gilbertson, J., Grimsley, M., Green, G., Warm Front Study Group, 2007. Living in cold homes after heating improvements: evidence from Warm-Front, England's Home Energy Efficiency Scheme. Appl. Energy 84, 147–158.

Cuce, E., Cuce, P.M., Wood, C.J., Riffat, S.B., 2014a. Toward aerogel based thermal superinsulation in buildings: A comprehensive review. Renew. Sustain. Energy Rev. 34, 273–299.

Cuce, E., Cuce, P.M., Wood, C.J., Riffat, S.B., 2014b. Optimizing insulation thickness and analysing environmental impacts of aerogel-based thermal superinsulation in buildings. Energy Build. 77, 28–39.

Dalton, J.C., Brase, A., Kuo, N., Marzano, M., 2010. Evacuated Panels Utilizing Clay-Polymer Aerogel Composites for Improved Housing Insulation. Case Western Reserve University.

Darling, E.K., Cros, C.J., Wargocki, P., Kolarik, J., Morrison, G.C., Corsi, R.L., 2012. Impacts of a clay plaster on indoor air quality assessed using chemical and sensory measurements. Build. Environ. 57, 370–376. doi:10.1016/j.buildenv.2012.06.004

Davis, M., 1994. How to Make Low-cost Building Blocks: Stabilized Soil Block Technology. Intermediate Technology Publications.

Davis, T.A., Llanes, F., Volesky, B., Diaz-Pulido, G., McCook, L., Mucci, A., 2003. 1H-NMR study of Na alginates extracted from Sargassum spp. in relation to metal biosorption. Appl. Biochem. Biotechnol. 110, 75–90.

Day, M., Wiles, D., 1978. Combustibility of loose fiber fill cellulose insulation: The role of borax and boric acid. J. Build. Phys. 2, 30–39.

DBERR, 2008. Strategy for Sustainable Construction (No. Pub 8731/2k/6/08/NP URN 08/973). Department for Business, Enterprise & Regulatory Reform., HM Government & Strategic Forum for Construction.

Deboucha, S., Hashim, R., 2011. A review on bricks and stabilized compressed earth blocks. Sci. Res. Essays 6, 499–506.

DeBrouse, D.R., 2013. Alginate-based building materials. Patent No. US 8246733 B2.

DECC, 2016a. UK Government GHG Conversion Factors for Company Reporting.

DECC, 2016b. Prices of fuels purchased by non-domestic consumers in the United Kingdom excluding/including CCL.

DECC, 2013a. Estimates of Home Insulation Levels in Great Britain: July 2013 (No. 19 September 2013), STATISTICAL RELEASE: EXPERIMENTAL STATISTICS. Department of Energy & Climate Change, London.

DECC, 2013b. Estimated impacts of energy and climate change policies on energy prices and bills (No. URN 12D/390). Department of Energy and Climate Change, London.

Degirmenci, N., 2008. The using of waste phosphogypsum and natural gypsum in adobe stabilization. Constr. Build. Mater. 22, 1220–1224. doi:10.1016/j.conbuildmat.2007.01.027

Delgado, M., Guerrero, I.C., 2006. Earth building in Spain. Constr. Build. Mater. 20, 679–690.

Demir, I., 2008. Effect of organic residues addition on the technological properties of clay bricks. Waste Manag. 28, 622–627. doi:10.1016/j.wasman.2007.03.019

Demir, I., 2006. An investigation on the production of construction brick with processed waste tea. Build. Environ. 41, 1274–1278.

Densley-Tingley, D., Hathway, A., Davison, B., 2015. An environmental impact comparison of external wall insulation types. Build. Environ. 85, 182–189. doi:10.1016/j.buildenv.2014.11.021

Derjaguin, B., Landau, L., 1941. Theory of the stability of strongly charged lyophobic sols and of the adhesion of strongly charged particles in solutions of electrolytes. Acta Physicochim URSS 14, 633–662.

DESA, U., 2015. World Population Prospects: The 2015 Revision, Key Findings and Advance Tables. Working Paper No ESA/P/WP. 241, United Nations, Department of Economic and Social Affairs, Population Division, New York.

Deville, S., Meille, S., Seuba, J., 2016. A meta-analysis of the mechanical properties of ice-templated ceramics and metals. Sci. Technol. Adv. Mater.

Deze, E.G., Papageorgiou, S.K., Favvas, E.P., Katsaros, F.K., 2012. Porous alginate aerogel beads for effective and rapid heavy metal sorption from aqueous solutions: Effect of porosity in Cu2+ and Cd2+ ion sorption. Chem. Eng. J. 209, 537–546. doi:10.1016/j.cej.2012.07.133

DIN, 1998. Standard DIN 4102-1 Fire behaviour of building materials and building components - Part 1: Building materials; concepts, requirements and tests.

Donati, I., Asaro, F., Paoletti, S., 2009. Experimental Evidence of Counterion Affinity in Alginates: The Case of Nongelling Ion Mg2+. J. Phys. Chem. B 113, 12877–12886. doi:10.1021/jp902912m

Donati, I., Paoletti, S., 2009. Material properties of alginates, in: Alginates: Biology and Applications. Springer, pp. 1–53.

Dove, C.A., 2012. Material Metabolisms (M. Arch Thesis). University of Strathclyde, Glasgow.

Dowson, M., Grogan, M., Birks, T., Harrison, D., Craig, S., 2012. Streamlined life cycle assessment of transparent silica aerogel made by supercritical drying. Appl. Energy 97, 396–404.

Dowson, M., Harrison, D., Dehouche, Z., 2014. Trombe walls with nanoporous aerogel insulation applied to UK housing refurbishments. Int. J. Smart Nano Mater. 5, 283–303. doi:10.1080/19475411.2014.999730

Draget, K., Phillips, G., Williams, P., 2009. Alginates. Handb. Hydrocoll. 807–828.

Draget, K.I., Skjåk-Bræk, G., Stokke, B.T., 2006. Similarities and differences between alginic acid gels and ionically crosslinked alginate gels. 7th Int. Hydrocoll. Conf. 20, 170–175. doi:10.1016/j.foodhyd.2004.03.009

Draget, K.I., Smidsrød, O., Skjåk-Bræk, G., 2005. Alginates from algae. Biopolym. Online 6. doi:10.1002/3527600035.bpol6008

Draget, K.I., Steinsvåg, K., Onsøyen, E., Smidsrød, O., 1998. Na- and K-alginate; effect on Ca2+-gelation. Carbohydr. Polym. 35, 1–6. doi:10.1016/S0144-8617(97)00237-3

Draget, K.I., Taylor, C., 2011. Chemical, physical and biological properties of alginates and their biomedical implications. Diet. Fibre Bioact. Polysacch. 25, 251–256. doi:10.1016/j.foodhyd.2009.10.007

Duer, K., Svendsen, S., 1998. Monolithic silica aerogel in superinsulating glazings. Sol. Energy 63, 259–267. doi:10.1016/S0038-092X(98)00063-2

Durán, J.D.G., Ramos-Tejada, M.M., Arroyo, F.J., González-Caballero, F., 2000. Rheological and Electrokinetic Properties of Sodium Montmorillonite Suspensions: I. Rheological Properties and Interparticle Energy of Interaction. J. Colloid Interface Sci. 229, 107–117. doi:10.1006/jcis.2000.6956

Edwin, G.M., 1949. Process of molding compositions comprising alginates. Patent No. US 2488135.

Ekström, A., Gustafsson, O., Kvarned, A., Löf-Nilsson, E., Proper, S., Sköld, M., Snögren, P., Ullsten, O., 2014. Mechanical properties dependence on microstructure in aerogel-like Quartzene® (No. TVE 14 003 Maj). Uppsala University.

El Kadib, A., Bousmina, M., 2012. Chitosan Bio-Based Organic–Inorganic Hybrid Aerogel Microspheres. Chem.- Eur. J. 18, 8264–8277.

Elimelech, M., Gregory, J., Jia, X., 2013. Particle deposition and aggregation: measurement, modelling and simulation. Butterworth-Heinemann.

Ely, A., Baudu, M., Kankou, M.O.S.O., Basly, J.-P., 2011. Copper and nitrophenol removal by low cost alginate/Mauritanian clay composite beads. Chem. Eng. J. 178, 168–174. doi:10.1016/j.cej.2011.10.040

Emerson, W., 1956. Synthetic soil conditioners. J Agric Sci 47, 7–121.

Enokela, O., Alada, P., 2012. Strength Analysis of Coconut Fiber Stabilized Earth for Farm Structures. Int. J. Adv. Res. Technol. Vol 1 No 2 P 5-11 1, 5–11.

Erdahl, B., 1922. Process of rendering concrete resistant to waters charged with soluble compounds and product thereof. Patent No. US1415324 A.

European Commission, 2010. Europe 2020: a strategy for smart, sustainable and inclusive growth. Bruss. Eur. Comm.

Fairhurst, D., 2013. An Overview of the Zeta Potential Part 3: Uses and Applications. Part. Sci. Inc.

FAO, 2011. World Aquaculture 2010 (No. 500/1). Food and Agriculture Organisation of the United Nations, Rome.

Fickler, S., Milow, B., Ratke, L., Schnellenbach-Held, M., Welsch, T., 2015. Development of High Performance Aerogel Concrete. Energy Procedia 78, 406–411.

Field, C.B., Behrenfeld, M.J., Randerson, J.T., Falkowski, P., 1998. Primary production of the biosphere: integrating terrestrial and oceanic components. Science 281, 237–240.

Finlay, K., Gawryla, M.D., Schiraldi, D.A., 2007. Biologically Based Fiber-Reinforced/Clay Aerogel Composites. Ind. Eng. Chem. Res. 47, 615–619. doi:10.1021/ie0705406

Fixit, 2013. Aerogel Insulating Plaster System [WWW Document]. URL http://www.fixit.ch/aerogel/pdf/Fixit_222_Aerogel_Verarbeitungsrichtlinien_A4_EN.pdf

Fleurence, J., 1999. Seaweed proteins: biochemical, nutritional aspects and potential uses. Trends Food Sci. Technol. 10, 25–28.

Forsythe, W., 2006. The archaeology of the kelp industry in the northern islands of Ireland. Int. J. Naut. Archaeol. 35, 218–229.

Forth, J., Zoorob, S., 2006. Non-traditional binders for construction materials. Presented at the Proceedings of the IABSE Henderson Colloquium, Cambridge, UK, pp. 10–12.

Fouquet, M., Levasseur, A., Margni, M., Lebert, A., Lasvaux, S., Souyri, B., Buhé, C., Woloszyn, M., 2015. Methodological challenges and developments in LCA of low energy buildings: Application to biogenic carbon and global warming assessment. Build. Environ. 90, 51–59. doi:10.1016/j.buildenv.2015.03.022

Francese, D., Mensitieri, G., Iannace, S., Balestra, C., 2013. New Materials for Ecological Building Products, in: Öchsner, A., Silva, L.F.M., Altenbach, H. (Eds.), Characterization and Development of Biosystems and Biomaterials, Advanced Structured Materials. Springer Berlin Heidelberg, pp. 203–215.

Fricke, J., 1985. Proceedings of the First International Symposium September 23–25, 1985. Springer-Verlag Berlin Heidelberg, Würzburg, Fed. Rep. of Germany. doi:10.1007/978-3-642-93313-4

Fricke, J., Heinemann, U., Ebert, H.P., 2008. Vacuum insulation panels—From research to market. World Energy Crisis Part 2 Some More Vac.-Based Solut. 82, 680–690. doi:10.1016/j.vacuum.2007.10.014

Fricke, J., Tillotson, T., 1997. Aerogels: production, characterization, and applications. Thin Solid Films 297, 212–223.

Fuerst, F., McAllister, P., Nanda, A., Wyatt, P., 2015. Does energy efficiency matter to home-buyers? An investigation of EPC ratings and transaction prices in England. Energy Econ. 48, 145–156.

Funami, T., Fang, Y., Noda, S., Ishihara, S., Nakauma, M., Draget, K.I., Nishinari, K., Phillips, G.O., 2009. Rheological properties of sodium alginate in an aqueous system during gelation in relation to supermolecular structures and Ca2+ binding. Food Hydrocoll. 23, 1746–1755. doi:10.1016/j.foodhyd.2009.02.014

Gacesa, P., 1998. Bacterial alginate biosynthesis-recent progress and future prospects. Microbiology 144, 1133–1143.

Galán-Marín, C., Rivera-Gómez, C., Bradley, F., 2013. Ultrasonic, Molecular and Mechanical Testing Diagnostics in Natural Fibre Reinforced, Polymer-Stabilized Earth Blocks. Int. J. Polym. Sci. 2013.

Galan-Marin, C., Rivera-Gomez, C., Bradley, F., 2012. A combination of SEM and EDX studies on a clay-based natural composite with animal fibre and its mechanical implications. EECM15.

Galán-Marín, C., Rivera-Gómez, C., García-Martínez, A., 2015. Embodied energy of conventional load-bearing walls versus natural stabilized earth blocks. Energy Build. 97, 146–154. doi:10.1016/j.enbuild.2015.03.054

Galán-Marín, C., Rivera-Gómez, C., Petric, J., 2010. Clay-based composite stabilized with natural polymer and fibre. Constr. Build. Mater. 24, 1462–1468. doi:10.1016/j.conbuildmat.2010.01.008

Galimberti, M., 2012. Chapter 4: Rubber Clay Nanocomposites, in: Boczkowska, A. (Ed.), Advanced Elastomers - Technology, Properties and Applications.

Gao, T., Jelle, B.P., Gustavsen, A., Jacobsen, S., 2014. Aerogel-incorporated concrete: An experimental study. Constr. Build. Mater. 52, 130–136.

García-González, C.A., Alnaief, M., Smirnova, I., 2011. Polysaccharide-based aerogels—Promising biodegradable carriers for drug delivery systems. Carbohydr. Polym. 86, 1425–1438. doi:10.1016/j.carbpol.2011.06.066

Garner, W., 1945. Thermal insulation material made from fibrous substances. Patent No. 2,381,214.

Gawryla, M.D., 2009. Low density materials through freeze-drying: Clay aerogels and beyond. (PhD Thesis). AA (Case Western Reserve University).

Gawryla, M.D., Nezamzadeh, M., Schiraldi, D.A., 2008. Foam-like materials produced from abundant natural resources. Green Chem. 10, 1078–1081.

Gawryla, M.D., van den Berg, O., Weder, C., Schiraldi, D.A., 2009. Clay aerogel/cellulose whisker nanocomposites: a nanoscale wattle and daub. J. Mater. Chem. 19, 2118–2124.

GEAT, 2016. Green Earth Aerogels [WWW Document]. URL http://www.green-earth-aerogel.com/geat/index.html

Genevieve, M.R., Francois, P.-L.J., 1959. Fireproofing textiles and the like. Patent No. 2,907,683.

Gensel, P.G., 2008. The earliest land plants. Annu. Rev. Ecol. Evol. Syst. 459–477.

Gibiat, V., Lefeuvre, O., Woignier, T., Pelous, J., Phalippou, J., 1995. Acoustic properties and potential applications of silica aerogels. Proc. Fourth Int. Symp. AEROGELS 186, 244–255. doi:10.1016/0022-3093(95)00049-6

Gibson, L.J., Ashby, M.F., 1999. Cellular solids: structure and properties. Cambridge University Press, Cambridge.

Glenn, G., Miller, R., Orts, W., 1998. Moderate strength lightweight concrete from organic aquagel mixtures. Ind. Crops Prod. 8, 123–132.

Goodhew, S., Griffiths, R., 2005. Sustainable earth walls to meet the building regulations. Energy Build. 37, 451–459.

Gooding, D., Thomas, T., 1995. The potential of cement-stabilised building blocks as an urban building material in developing countries. ODA Rep. Sch. Eng. UK Univ. Warwick.

Government of New Mexico, 2009. 2009 New Mexico Earthen Building Materials Code (No. NMAC 14.7.4).

Grant, G.T., Morris, E.R., Rees, D.A., Smith, P.J.C., Thom, D., 1973. Biological interactions between polysaccharides and divalent cations: The egg-box model. FEBS Lett. 32, 195–198. doi:10.1016/0014-5793(73)80770-7

Grasdalen, H., Larsen, B., Smidsrød, O., 1979. A p.m.r. study of the composition and sequence of uronate residues in alginates. Carbohydr. Res. 68, 23–31. doi:10.1016/S0008-6215(00)84051-3

Green, V.S., Stott, D., 1999. Polyacrylamide: A review of the use, effectiveness, and cost of a soil erosion control amendment. Presented at the The 10th International Soil Conservation Organization Meeting, pp. 384–389.

GreenSpec, 2015a. Blocks [WWW Document]. URL http://www.greenspec.co.uk/green-products/blocks/

GreenSpec, 2015b. Building insulation materials 4: Oil - based polymers [WWW Document]. URL http://www.greenspec.co.uk/building-design/insulation-oil-derived/ (accessed 3.6.15).

Gu, B., Doner, H.E., 1992. The interaction of polysaccharides with Silver Hill illite. Clays Clay Miner. 40, 151–156.

Gu, B., Schmitt, J., Chen, Z., Liang, L., McCarthy, J.F., 1994. Adsorption and desorption of natural organic matter on iron oxide: mechanisms and models. Environ. Sci. Technol. 28, 38–46. doi:10.1021/es00050a007

Guettala, A., Abibsi, A., Houari, H., 2006. Durability study of stabilized earth concrete under both laboratory and climatic conditions exposure. Constr. Build. Mater. 20, 119–127. doi:10.1016/j.conbuildmat.2005.02.001

Gutiérrez, M.C., García-Carvajal, Z.Y., Jobbágy, M., Rubio, F., Yuste, L., Rojo, F., Ferrer, M.L., del Monte, F., 2007. Poly (vinyl alcohol) scaffolds with tailored morphologies for drug delivery and controlled release. Adv. Funct. Mater. 17, 3505–3513.

Habert, G., d'Espinose de Lacaillerie, J., Roussel, N., 2011. An environmental evaluation of geopolymer based concrete production: reviewing current research trends. J. Clean. Prod. 19, 1229–1238.

Hairstanes, R., Kermani, A., 2007. Briefing: Structural insulated panels in modern construction. Proc. ICE-Constr. Mater. 160, 91–94.

Hall, M., Swaney, B., 2005. Stabilised rammed earth (SRE) wall construction- now available in the UK. Build. Eng. 80, 12–15.

Hall, M.R., Lindsay, R., Krayenhoff, M., 2012. Modern earth buildings: Materials, engineering, constructions and applications. Elsevier, Cambridge.

Hammond, G., Jones, C., 2011. Inventory of Carbon & Energy Version 2.0 (ICE V2. 0). Dep. Mech. Eng. Univ. Bath Bath UK.

Hammond, G., Jones, C., 2008. Inventory of Carbon & Energy: ICE. Sustainable Energy Research Team, Department of Mechanical Engineering, University of Bath.

Hammond, G.P., Jones, C.I., 2008. Embodied energy and carbon in construction materials. Proc. Inst. Civ. Eng.-Energy 161, 87–98.

Hansen, K.K., Hansen, M., 2002. Unfired clay bricks-moisture properties and compressive strength. Presented at the Proceedings of the 6th Symposium on Building Physics in the Nordic Countries, Norwegian University of Science and Technology, Trondheim, Norway.

Harris, J., Rumack, B., Aldrich, F., 1981. Toxicology of urea formaldehyde and polyurethane foam insulation. JAMA 245, 243–246. doi:10.1001/jama.1981.03310280019020

Harris, W., White, G.N., 2008. X-ray diffraction techniques for soil mineral identification. Methods Soil Anal. Part 81–116.

Harrison, J., 1968. Reducing checking in timber by use of alginates. Aust. Timber J. Build. Prod. Merch. 34, 24–25.

Hasanbeigi, A., 2013. Emerging Energy-efficiency and CO2 Emission-reduction Technologies for Cement and Concrete Production.

Hatakeyama, H., Hatakeyama, T., 2005. Environmentally Compatible Hybrid-Type Polyurethane Foams Containing Saccharide and Lignin Components. Macromol. Symp. 224, 219–226. doi:10.1002/masy.200550619

Haug, A., Smidsrod, O., 1962. Determination of intrinsic viscosity of alginates. Acta Chem Scand 16, 3.

Hay, I.D., Rehman, Z.U., Moradali, M.F., Wang, Y., Rehm, B.H., 2013. Microbial alginate production, modification and its applications. Microb. Biotechnol. 6, 637–650.

Heath, A., 2015. Unfired clay bricks [WWW Document]. GreenSpec. URL http://www.greenspec.co.uk/building-design/unfired-clay-bricks/

Heath, A., Maskell, D., Walker, P., Lawrence, M., Fourie, C., 2012a. Modern earth masonry: structural properties and structural design. Struct. Eng. 90, 38–44.

Heath, A., Paine, K., McManus, M., 2014. Minimising the global warming potential of clay based geopolymers. J. Clean. Prod. 78, 75–83.

Heath, A., Walker, P., Fourie, C., Lawrence, M., 2009. Compressive strength of extruded unfired clay masonry units. Proc. ICE-Constr. Mater. 162, 105–112.

Heath, A., Walker, P., Jaquin, P., Lawrence, M., 2012b. Render-induced cracking of earth masonry. Proc. ICE-Struct. Build. 165, 435–442.

Heathcote, K., 1995. Durability of earthwall buildings. Constr. Build. Mater. 9, 185–189.

Heathcote, K., Jankulovski, E., 1992. Aspect ratio correction factors for soilcrete blocks. Trans. Inst. Eng. Aust. Civ. Eng. 34, 309–312.

Heathcote, K.A., 2002. An investigation into the erodibility of earth wall units (PhD Thesis). University of Technology, Sydney.

Heaton, T., Sammon, C., Ault, J., Black, L., Forth, J.P., 2014. Masonry units bound with waste vegetable oil – Chemical analysis and evaluation of engineering properties. Constr. Build. Mater. 64, 460–472. doi:10.1016/j.conbuildmat.2014.04.079

Hendry, E.A.., 2001. Masonry walls: materials and construction. Constr. Build. Mater. 15, 323–330. doi:10.1016/S0950-0618(01)00019-8

Herrmann, G., Iden, R., Mielke, M., Teich, F., Ziegler, B., 1995. On the way to commercial production of silica aerogel. J. Non-Cryst. Solids 186, 380–387.

Hill, N., Venfield, H., Dun, C., James, K., 2013. Government GHG conversion factors for company reporting: methodology paper for emission factors. DEFRA DECC.

Hill, R.C., Bowen, P.A., 1997. Sustainable construction: principles and a framework for attainment. Constr. Manag. Econ. 15, 223–239.

HM Government, 2010. Approved Document E (Resistance to the passage of sound), Building Regulations (2010). NBS & RIBA.

Hoefer, D., Schnepf, J.K., Hammer, T.R., Fischer, M., Marquardt, C., 2015. Biotechnologically produced microbial alginate dressings show enhanced gel forming capacity compared to commercial alginate dressings of marine origin. J. Mater. Sci. Mater. Med. 26, 1–9.

Hofland, G., 2014. Preserving Raw materials Into Excellent and Sustainable End Products While Remaining Fresh (No. 245280).

Horga, R., Di Renzo, F., Quignard, F., 2007. Ionotropic alginate aerogels as precursors of dispersed oxide phases. Nucleation Growth Microstruct. Matrices Creat. Nano-Dispersed Redox Oxide Catal. Oxid. Catal. Dedic. Dr Jean-Claude Volta 325, 251–255. doi:10.1016/j.apcata.2007.02.042

Hostler, S.R., Abramson, A.R., Gawryla, M.D., Bandi, S.A., Schiraldi, D.A., 2009. Thermal conductivity of a clay-based aerogel. Int. J. Heat Mass Transf. 52, 665–669. doi:10.1016/j.ijheatmasstransfer.2008.07.002

Houben, H., Guillaud, H., 1994. Earth construction: a comprehensive guide. Intermediate Technology Publications, London.

Houben, H., Rigassi, V., Garnier, P., 1994. Compressed earth blocks: production equipment. CDI and CRATere-Eag.

Howard, N., 2000. Sustainable construction-the data (No. CR258/99). Centre for Sustainable Construction & Building Research Establishment, Watford, UK.

Hrubesh, L.W., 1998. Aerogel applications. J. Non-Cryst. Solids 225, 335–342. doi:10.1016/S0022-3093(98)00135-5

Hughes, J., Maul, P.L., 1979. Brick composition and method therefor. Patent No. US 4,148,662.

Huntzinger, D.N., Eatmon, T.D., 2009. A life-cycle assessment of Portland cement manufacturing: comparing the traditional process with alternative technologies. Present Anticip. Demands Nat. Resour. Sci. Technol. Polit. Econ. Ethical Approaches Sustain. Manag. 17, 668–675. doi:10.1016/j.jclepro.2008.04.007

Hyun, S.H., Kim, T.Y., Kim, G.S., Park, H.H., 2000. Synthesis of low-k porous silica films via freeze drying. J. Mater. Sci. Lett. 19, 1863–1866. doi:10.1023/A:1006775213914

IBSTOCK, 2014. Ideas Into Action: Ecoterre™ Earth Bricks [WWW Document]. URL http://www.ibstock.com/pdfs/ecoterre/Ecoterre.pdf (accessed 10.24.14).

ICECLAY, 2014. Periodic Report Summary 1 - ICECLAY (Highly efficient production of ultra-lightweight clay-aerogel materials and their integrated composites for building insulation).

Indergaard, M., Minsaas, J., 1991. Animal and human nutrition, in: Seaweed Resources in Europe : Uses and Potential. John Wiley & Sons, Chichester, UK.

İşçi, S., Ünlü, C., Atici, O., Güngör, N., 2006. Rheology and structure of aqueous bentonite-polyvinyl alcohol dispersions. Bull. Mater. Sci. 29, 449–456.

ISO, 2006. ISO 14040: 2006 - ISO Environmental management–Life cycle assessment–Principles and framework. International Organization for Standardization.

Israel, A., Einav, R., Seckbach, J., 2010. Seaweeds and their role in Globally Changing Environments. Springer Science & Business Media.

Jelle, B.P., 2011. Traditional, state-of-the-art and future thermal building insulation materials and solutions – Properties, requirements and possibilities. Energy Build. 43, 2549–2563. doi:10.1016/j.enbuild.2011.05.015

Jenkins, M., 2012. Refurbishment Case Study 4: Sword Street, Glasgow - Internal wall insulation to six tenement flats. Historic Scotland.

Jensen, K.I., Schultz, J.M., Kristiansen, F.H., 2004. Development of windows based on highly insulating aerogel glazings. Aerogels 7 Proc. 7th Int. Symp. Aerogels 7th Int. Symp. Aerogels 350, 351–357. doi:10.1016/j.jnoncrysol.2004.06.047

Jiménez Delgado, M.C., Guerrero, I.C., 2007. The selection of soils for unstabilised earth building: A normative review. Constr. Build. Mater. 21, 237–251. doi:10.1016/j.conbuildmat.2005.08.006

Johansson, P., 2012. Vacuum Insulation Panels in Buildings: Literature Review. Chalmers University of Technology.

John, B.S., Norman, H.C., 1946. Production of fabrics from alginic materials. Patent No. US 2,409,319.

John, R.P., Anisha, G., Nampoothiri, K.M., Pandey, A., 2011. Micro and macroalgal biomass: a renewable source for bioethanol. Bioresour. Technol. 102, 186–193.

Johnson III, J.R., Spikowski, J., Schiraldi, D.A., 2009. Mineralization of clay/polymer aerogels: a bioinspired approach to composite reinforcement. ACS Appl. Mater. Interfaces 1, 1305–1309.

Johnson, J.R., Schiraldi, D.A., 2012. Improving the mechanical properties of clay/polymer aerogels by a simple dip-coating procedure. J. Appl. Polym. Sci. 126, 2004–2009. doi:10.1002/app.36632

Johnston, W., Nicholson, F., Roger, A., Stroud, D., 1994. Freezing and refrigerated storage in fisheries (No. Technical Report 340). Food & Agriculture Organisation of the United Nations, Rome.

Jones, S., 2006. Aerogel: Space exploration applications. J. Sol-Gel Sci. Technol. 40, 351–357. doi:10.1007/s10971-006-7762-7

Joyce, M., Gilbert, R., Khan, S.A., 1996. Effect of Ca++ ions on the water retention of alginate in paper coatings. J. Pulp Pap. Sci. 22, J126–J130.

Jubran, B., Habali, S., Hamdan, M., Zaid, A.I., 1988. Some mechanical and thermal properties of clay bricks for the Jordan valley region. Mater. Struct. 21, 364–369.

Julie Sandeen, 2010. Soil texture triangular plot diagram. CK-12 Earth Science (p331).

Kalwall, 2011. Kalwall with Lumira Aerogel [WWW Document]. URL http://www.kalwall.com/wp-content/uploads/2015/03/Kalwall-plus-aerogel.pdf

Kamang, E., 1998. Strength Properties of Compressed Earth Bricks (CEB) with Earthworm Cast as Stabilizer. J. Environ. Sci. 1, 65–70.

Kaya, A., Ören, A.H., Yükselen, Y., 2006. Settling of kaolinite in different aqueous environment. Mar. Georesources Geotechnol. 24, 203–218.

Kaygusuz, H., Uysal, M., Adımcılar, V., Erim, F.B., 2015. Natural alginate biopolymer montmorillonite clay composites for vitamin B2 delivery. J. Bioact. Compat. Polym. Biomed. Appl. 30, 48–56.

Keil, R., Mayer, L., 2013. Mineral matrices and organic matter, in: Treatise on Geochemistry. Elsevier, Oxford, UK.

Kelly, L., Collier, L., Costello, M.J., Diver, M., McGarvey, S., Kraan, S., Morrissey, J., Giury, M., 2001. Impact assessment of hand and mechanical harvesting of Ascophyllum nodosum on regeneration and biodiversity (No. No. 19), Marine Resource Series. Marine Fisheries Services Division, Dublin.

Kenicer, G., Bridgewater, S., Milliken, W., 2000. The ebb and flow of Scottish seaweed use. Bot. J. Scotl. 52, 119–148.

Khaleel, A., Kapoor, P.N., Klabunde, K.J., 1999. Nanocrystalline metal oxides as new adsorbents for air purification. Nanostructured Mater. 11, 459–468.

Khater, H., 2011. Utilization of demolished concrete, grog, hydrated lime and cement kiln dust in building materials. J. Mech. Eng. Res. 3, 279–285.

Kibert, C.J., 1994. Sustainable Construction: Proceedings of the First International Conference of CIB TG 16, November 6-9, 1994, Tampa, Florida, USA. University of Florida, Center for Construction & Environment.

Kim, G.-S., Hyun, S.-H., 2003. Synthesis of window glazing coated with silica aerogel films via ambient drying. J. Non-Cryst. Solids 320, 125–132.

King, S., See, H., Thomas, G., Swain, M., 2008. Determining the complex modulus of alginate irreversible hydrocolloid dental material. Dent. Mater. 24, 1545–1548.

Kingspan, 2013. Optim-r External Wall System [WWW Document]. URL http://www.kingspaninsulation.co.uk/kins_cms/media/media.global/Optim-R-Ext-Wall-System-1st-Issue-July-13.pdf

Kiss, B., Manchón, C.G., Neij, L., 2013. The role of policy instruments in supporting the development of mineral wool insulation in Germany, Sweden and the United Kingdom. Environ. Manag. Sustain. Univ. EMSU 2010 Eur. Roundtable Sustain. Consum. Prod. ERSCP 2010 48, 187–199. doi:10.1016/j.jclepro.2012.12.016

Kistler, S.S., 1934. The Relation between Heat Conductivity and Structure in Silica Aerogel. J. Phys. Chem. 39, 79–86. doi:10.1021/j150361a006

Kistler, S.S., 1932. Coherent Expanded Aerogels. J. Phys. Chem. 36, 52–64.

Kistler, S.S., 1931. Coherent Expanded Aerogels and Jellies. Nature 127, 741.

Kistler, S.S., Caldwell, A.G., 1934. Thermal Conductivity of Silica Aërogel. Ind. Eng. Chem. 26, 658–662. doi:10.1021/ie50294a016

Klamer, M., Morsing, E., Husemoen, T., 2004. Fungal growth on different insulation materials exposed to different moisture regimes. Int. Biodeterior. Biodegrad. 54, 277–282. doi:10.1016/j.ibiod.2004.03.016

Knirsch, M., Penschke, A., Krebs, S., Russ, W., Mörtel, H., Mayer, W., Meyer-Pittroff, R., 1998. Application of brewery wastes in the production of bricks. Tile Brick Int. 14, 93–101.

Kogel, J.E., Trivedi, N.C., Barker, J.M. (Eds.), 2006. Industrial minerals & rocks: commodities, markets, and uses. Society for Mining Metallurgy & Exploration, Colorado, USA.

Kong, Q., Wang, B., Ji, Q., Xia, Y., Guo, Z., Yu, J., 2009. Thermal degradation and flame retardancy of calcium alginate fibers. Chin. J. Polym. Sci. 27, 807–812.

Korjenic, A., Petránek, V., Zach, J., Hroudová, J., 2011. Development and performance evaluation of natural thermal-insulation materials composed of renewable resources. Energy Build. 43, 2518–2523. doi:10.1016/j.enbuild.2011.06.012

Kouakou, C.H., Morel, J.C., 2009. Strength and elasto-plastic properties of non-industrial building materials manufactured with clay as a natural binder. Appl. Clay Sci. 44, 27–34. doi:10.1016/j.clay.2008.12.019

Kumar, A., Walia, B.S., Bajaj, A., 2007. Influence of fly ash, lime, and polyester fibers on compaction and strength properties of expansive soil. J. Mater. Civ. Eng. 19, 242–248.

Kuo, C.K., Ma, P.X., 2001. Ionically crosslinked alginate hydrogels as scaffolds for tissue engineering: Part 1. Structure, gelation rate and mechanical properties. Biomaterials 22, 511–521. doi:10.1016/S0142-9612(00)00201-5

Langlois, J., Sassi, J., Jard, G., Steyer, J., Delgenes, J., Hélias, A., 2012. Life cycle assessment of biomethane from offshore-cultivated seaweed. Biofuels Bioprod. Biorefining 6, 387–404.

Law, D.C.-F., Sandoval, C.P., Garcia, R.G., 1998. Perlite-based insulation board. Patent No. US5749954 A.

Lawrence, M., Heath, A., Walker, P., 2010. Development of a novel binder for mortar for unfired clay bricks. Presented at the Proceeding of second international conference on sustainable construction materials and technologies, Ancona, Italy, pp. 28–30.

Lawrence, R., Heath, A.C., Walker, P., 2008. Mortars for thin unfired clay masonry walls. Presented at the Proceedings of LEHM 5th International conference on Building with Earth, Koblenz, Germany, pp. 66–73.

Lawrence, S., Page, A., Trenerry, J., 2013. TBA 06 - Design of Clay Masonry for Compression. Think Brick Australia.

Lazko, J., Landercy, N., Laoutid, F., Dangreau, L., Huguet, M.H., Talon, O., 2013. Flame retardant treatments of insulating agro-materials from flax short fibres. Polym. Degrad. Stab. 98, 1043–1051. doi:10.1016/j.polymdegradstab.2013.02.002

Lee, B.J., Schlautman, M.A., Toorman, E., Fettweis, M., 2012. Competition between kaolinite flocculation and stabilization in divalent cation solutions dosed with anionic polyacrylamides. Water Res. 46, 5696–5706.

Lee, K.-C., Her, J.-H., Kwon, S.-K., 2008. Red clay composites reinforced with polymeric binders. Constr. Build. Mater. 22, 2292–2298.

Lehm, D., 2002. Lehmbau-Regeln: Begriffe - Baustoffe - Bauteile. Vieweg, Wiesbaden.

Lehre Seip, K., 1980. A computational model for growth and harvesting of the marine alga Ascophyllum nodosum. Ecol. Model. 8, 189–199. doi:10.1016/0304-3800(80)90037-X

Lenci, S., Piattoni, Q., Clementi, F., Sadowski, T., 2011. An Experimental Study On Damage Evolution of Unfired Dry Earth Under Compression. Int. J. Fract. 172, 193–200.

Lencina, M.S., Andreucetti, N.A., Gómez, C.G., Villar, M.A., 2013. Recent Studies on Alginates Based Blends, Composites, and Nanocomposites, in: Advances in Natural Polymers. Springer, pp. 193–254.

Lertwattanaruk, P., Choksiriwanna, J., 2011. The physical and thermal properties of adobe brick containing bagasse for earth construction. J. Archit. Res. Stud. 5, 187–199.

Li, W., Lu, K., Walz, J., 2012. Freeze casting of porous materials: review of critical factors in microstructure evolution. Int. Mater. Rev. 57, 37–60.

Liibert, L., Treu, A., Meier, P., 2011. The Fixation of new alternative wood protection systems by means of oil treatment. Mater. Sci. 17, 402–406.

Lim, F., Sun, A.M., 1980. Microencapsulated islets as bioartificial endocrine pancreas. Science 210, 908–910.

Lime Technology, 2015. Hemcrete® Structural Block Information Sheet [WWW Document]. URL http://www.limetech.info/upload/documents/1194950699_hemcrete_structural_block_information_sheet.pdf

Lincoln, J., Tettenhorst, R., 1971. Freeze-dried and thawed clays. Clays Clay Min. 19, 103–107.

Lindsey Zemke-White, W., Ohno, M., 1999. World seaweed utilisation: An end-of-century summary. J. Appl. Phycol. 11, 369–376. doi:10.1023/A:1008197610793

Little, B., Morton, T., Scottish Executive, 2001. Building with earth in Scotland: Innovative design and sustainability. Scottish Executive Central Research Unit Edinburgh, UK.

Liu, F., Carlos, L.D., Ferreira, R.A.S., Rocha, J., Gaudino, M.C., Robitzer, M., Quignard, F., 2008. Photoluminescent Porous Alginate Hybrid Materials Containing Lanthanide Ions. Biomacromolecules 9, 1945–1950. doi:10.1021/bm8002122

Liu, X., Qian, L., Shu, T., Tong, Z., 2003. Rheology characterization of sol–gel transition in aqueous alginate solutions induced by calcium cations through in situ release. Polymer 44, 407–412. doi:10.1016/S0032-3861(02)00771-1

Liu, Y., Zhao, Y., Feng, X., 2008. Exergy analysis for a freeze-drying process. Appl. Therm. Eng. 28, 675–690. doi:10.1016/j.applthermaleng.2007.06.004

Liuzzi, S., Hall, M.R., Stefanizzi, P., Casey, S.P., 2013. Hygrothermal behaviour and relative humidity buffering of unfired and hydrated lime-stabilised clay composites in a Mediterranean climate. Build. Environ. 61, 82–92. doi:10.1016/j.buildenv.2012.12.006

Longo, S., Mauro, M., Daniel, C., Galimberti, M., Guerra, G., 2013. Clay exfoliation and polymer/clay aerogels by supercritical carbon dioxide. Front. Chem. 1. doi:10.3389/fchem.2013.00028

Lovell, H., Smith, S.J., 2010. Agencement in housing markets: The case of the UK construction industry. Geoforum 41, 457–468. doi:10.1016/j.geoforum.2009.11.015

Lu, L., Liu, X., Tong, Z., 2006. Critical exponents for sol–gel transition in aqueous alginate solutions induced by cupric cations. Carbohydr. Polym. 65, 544–551. doi:10.1016/j.carbpol.2006.02.010

Lu, X., Nilsson, O., Fricke, J., Pekala, R.W., 1993. Thermal and electrical conductivity of monolithic carbon aerogels. J. Appl. Phys. 73, 581–584.

Luckham, P.F., Rossi, S., 1999. The colloidal and rheological properties of bentonite suspensions. Adv. Colloid Interface Sci. 82, 43–92.

Lützow, M. v, Kögel-Knabner, I., Ekschmitt, K., Matzner, E., Guggenberger, G., Marschner, B., Flessa, H., 2006. Stabilization of organic matter in temperate soils: mechanisms and their relevance under different soil conditions–a review. Eur. J. Soil Sci. 57, 426–445.

Ma, X., Bruckard, W.J., 2010. The effect of pH and ionic strength on starch–kaolinite interactions. Int. J. Miner. Process. 94, 111–114. doi:10.1016/j.minpro.2010.01.004

MacKenzie, F., Mackenzie, F., 2010. Energy Efficiency in New and Existing Buildings: Comparative Costs and CO2 Savings. BRE Press.

Mackenzie, R.C., 1953. Clay - Water Relationships. Nature 171, 681–683. doi:10.1038/171681a0

Madyan, O.A., Fan, M., Feo, L., Hui, D., 2016. Physical properties of clay aerogel composites: An overview. Compos. Part B Eng. 102, 29–37. doi:10.1016/j.compositesb.2016.06.057

Magwood, C., 2014. Making Better Buildings: A Comparative Guide to Sustainable Construction for Homeowners and Contractors. New Society Publishers, Canada.

Malhotra, S., Tehri, S., 1996. Development of bricks from granulated blast furnace slag. Constr. Build. Mater. 10, 191–193.

Mallepally, R.R., McHugh, M.A., Ward, K.R., 2012. Superabsorbent Alginate Aerogels. J. Supercrit. Fluids 79, 202–208.

Man, C.K., Yeung, H.S., 1997. The effects of using pulverized fuel ash as partial substitute for cement in concrete. Sci. Total Environ. 196, 171–176. doi:10.1016/S0048-9697(96)05418-6

Martins, M., Barros, A.A., Quraishi, S., Gurikov, P., Raman, S.P., Smirnova, I., Duarte, A.R.C., Reis, R.L., 2015. Preparation of macroporous alginate-based aerogels for biomedical applications. J. Supercrit. Fluids. doi:10.1016/j.supflu.2015.05.010

Martinsen, A., Skjåk-Bræk, G., Smidsrød, O., 1989. Alginate as immobilization material: I. Correlation between chemical and physical properties of alginate gel beads. Biotechnol. Bioeng. 33, 79–89.

Marx, E., Hart, J.M., Stevens, R.G., 1996. Soil test interpretation guide. Oregon State University Extension Service Oregon.

Maskell, D., 2013. Development of stabilised extruded earth masonry units (PhD Thesis). University of Bath, UK.

Maskell, D., Heath, A., Walker, P., 2015. Appropriate structural unfired earth masonry units. Proc. Inst. Civ. Eng. Constr. Mater. 1–10.

Maskell, D., Heath, A., Walker, P., 2013. Laboratory scale testing of extruded earth masonry units. Mater. Des. 45, 359–364.

Maskell, D., Walker, P., Heath, A., 2012. The compressive strength of lignosulphonate stabilised extruded earth masonry units. Presented at the Terra 2012: 11th International Conference on the Study and Conservation of Earthen Architecture Heritage, University of Bath.

McFarlane, A., Bremmell, K., Addai-Mensah, J., 2006. Improved dewatering behavior of clay minerals dispersions via interfacial chemistry and particle interactions optimization. J. Colloid Interface Sci. 293, 116–127. doi:10.1016/j.jcis.2005.06.034

McGregor, F., Heath, A., Fodde, E., Shea, A., 2014a. Conditions affecting the moisture buffering measurement performed on compressed earth blocks. Build. Environ. 75, 11–18. doi:10.1016/j.buildenv.2014.01.009

McGregor, F., Heath, A., Shea, A., Lawrence, M., 2014b. The moisture buffering capacity of unfired clay masonry. Build. Environ. 82, 599–607. doi:10.1016/j.buildenv.2014.09.027

McHugh, D.J., 2003. A Guide to the Seaweed Industry. Food and Agriculture Organization of the United Nations, Rome.

McHugh, D.J., 1987. Production and utilization of products from commercial seaweeds. FAO.

McLeod, R., Mead, K., Standen, M., 2011. Passivhaus Primer: Designer's Guide: A Guide for the Design Team and Local Authorities. BRE Trust, Watford, UK.

McLeod, R.S., Hopfe, C.J., Rezgui, Y., 2012. An investigation into recent proposals for a revised definition of zero carbon homes in the UK. Energy Policy 46, 25–35. doi:10.1016/j.enpol.2012.02.066

McMullan, R., 2007. Environmental science in building. Basingstoke: Palgrave Macmillan.

Meena, A.K., Mishra, G., Rai, P., Rajagopal, C., Nagar, P., 2005. Removal of heavy metal ions from aqueous solutions using carbon aerogel as an adsorbent. J. Hazard. Mater. 122, 161–170.

Mehling, T., Smirnova, I., Guenther, U., Neubert, R.H.H., 2009. Polysaccharide-based aerogels as drug carriers. J. Non-Cryst. Solids 355, 2472–2479. doi:10.1016/j.jnoncrysol.2009.08.038

Mekhamer, W.K., Al Andis, N., El Shabanat, M., 2009. Kinetic study on the sedimentation behavior of Na- and Ca-kaolinite suspension in the presence of polyethyleneimine. J. King Saud Univ. - Sci. 21, 125–132. doi:10.1016/j.jksus.2009.07.005

Melaku, S., Dams, R., Moens, L., 2005. Determination of trace elements in agricultural soil samples by inductively coupled plasma-mass spectrometry: microwave acid digestion versus aqua regia extraction. Anal. Chim. Acta 543, 117–123.

Mellor, J.D., 1978. Fundamentals of freeze-drying. Academic Press Inc. Ltd., London.

Merton, R.R., 1964. Improvements in or relating to Construction Materials. Patent No. 963, 503.

Mesbah, A., Morel, J., Walker, P., Ghavami, K., 2004. Development of a Direct Tensile Test for Compacted Earth Blocks Reinforced with Natural Fibers. J. Mater. Civ. Eng. 16, 95–98. doi:10.1061/(ASCE)0899-1561(2004)16:1(95)

Mesbah, A., Morel, J.C., Olivier, M., 1999. Comportement des sols fins argileux pendant un essai de compactage statique: détermination des paramètres pertinents. Mater. Struct. 32, 687–694. doi:10.1007/BF02481707

Miano, F., Rabaioli, M., 1994. Rheological scaling of montmorillonite suspensions: the effect of electrolytes and polyelectrolytes. Colloids Surf. Physicochem. Eng. Asp. 84, 229–237.

Michaels, A.S., Bolger, J.C., 1962. Settling Rates and Sediment Volumes of Flocculated Kaolin Suspensions. Ind. Eng. Chem. Fundam. 1, 24–33. doi:10.1021/i160001a004

Milledge, J.J., Smith, B., Dyer, P.W., Harvey, P., 2014. Macroalgae-derived biofuel: a review of methods of energy extraction from seaweed biomass. Energies 7, 7194–7222.

Milliken, W., Bridgewater, S., 2001. Flora Celtica: sustainable development of Scottish plants. Scottish Executive Central Research Unit.

Millogo, Y., Morel, J.-C., 2012. Microstructural characterization and mechanical properties of cement stabilised adobes. Mater. Struct. 45, 1311–1318.

Minke, G., 2006. Building with earth. Birkhäuser, Basel.

Miqueleiz, L., Ramirez, F., Oti, J.E., Seco, A., Kinuthia, J.M., Oreja, I., Urmeneta, P., 2013. Alumina filler waste as clay replacement material for unfired brick production. Eng. Geol. 163, 68–74. doi:10.1016/j.enggeo.2013.05.006

Mitchell, J., 1993. Fundamentals of Soil Behavior. John Wiley and Sons, Inc., New York.

Mitchell, J.K., Soga, K., 2005. Fundamentals of soil behavior.

MMC, 1979. FMC Corporation, Merck & Co. Inc., Alginate Industries Limited: a report on the proposed mergers (No. 0102175802). Monopolies and Mergers Commission, London.

Moayedi, H., Huat, B.B., Moayedi, F., Asadi, A., Parsaie, A., 2011. Effect of sodium silicate on unconfined compressive strength of soft clay. Electron. J Geotechn Eng 16, 289–295.

Monsanto, 1954. SANTOCEL... Can this remarkable silica aerogel improve YOUR processing or products? Chem. Eng. News Arch. 32, 4179. doi:10.1021/cen-v032n042.p4179

Moore, D.M., Reynolds Jr, R.C., 1989. X-ray Diffraction and the Identification and Analysis of Clay Minerals. Oxford University Press (OUP).

Moquin, M., 1996. Ancient solutions for future sustainability: Building with adobe, rammed earth, and mud. Earth Build. Cob Revival Read. 3, 7–12.

Morel, J., Pkla, A., 2002. A model to measure compressive strength of compressed earth blocks with the “3 points bending test.” Constr. Build. Mater. 16, 303–310.

Morel, J.-C., Pkla, A., Walker, P., 2007. Compressive strength testing of compressed earth blocks. Constr. Build. Mater. 21, 303–309.

Morton, T., 2008. Earth masonry: Design and construction guidelines. IHS BRE Press, Watford, UK.

Morton, T., 2005. Unfired Earth Brick Building. Build. Future Autumn 2005, 24–27.

Morton, T., Stevenson, F., Taylor, B., Smith, N.C., 2005. Low Cost Earth Brick Construction. Arc Chart. Archit. Fife.

Mosquera, P., Cañas, I., Cid-Falceto, J., Marcos, F., 2014. Determination of the Thermal Conductivity in Adobe With Several Models. J. Heat Transf. 136, 031303.

Mpofu, P., Addai-Mensah, J., Ralston, J., 2004. Flocculation and dewatering behaviour of smectite dispersions: effect of polymer structure type. Miner. Eng. 17, 411–423.

Mpofu, P., Addai-Mensah, J., Ralston, J., 2003. Investigation of the effect of polymer structure type on flocculation, rheology and dewatering behaviour of kaolinite dispersions. Int. J. Miner. Process. 71, 247–268. doi:10.1016/S0301-7516(03)00062-0

Mueller, A., Sokolova, S.N., Vereshagin, V.I., 2008. Characteristics of lightweight aggregates from primary and recycled raw materials. Constr. Build. Mater. 22, 703–712. doi:10.1016/j.conbuildmat.2007.06.009

Mujumdar, A.S., 2014. Handbook of industrial drying, 4th ed. CRC Press, London.

Mukhopadhyay, T.K., Ghosh, S., Chakraborti, S., Ghatak, S., 2005. Effect of sodium silicate on the durability of common building bricks. Interceram 54, 262–267.

Munsell, A., 2000. Munsell Soil Color Charts. Gretag Macbeth, NewWindsor, New York.

Muntohar, A.S., 2011. Engineering characteristics of the compressed-stabilized earth brick. Constr. Build. Mater. 25, 4215–4220.

Murillo, C.G., Walker, P.J., Ansell, M.P., 2005. Henequen fibres for reinforcement of unfired earth blocks.

Murray, J., Frost, J., Wang, Y., 2000. Behavior of a sandy silt reinforced with discontinuous recycled fiber inclusions. Transp. Res. Rec. J. Transp. Res. Board 1714, 9–17.

Naeini, S.A., Naderinia, B., Izadi, E., 2012. Unconfined compressive strength of clayey soils stabilized with waterborne polymer. KSCE J. Civ. Eng. 16, 943–949.

Nakazawa, H., Yamada, H., Fujita, T., Ito, Y., 1987. Texture control of clay-aerogel through the crystallization process of ice. Clay Sci. 6, 269–276.

National Records of Scotland, 2012. National Statistics: Household Projections for Scotland (2010) [WWW Document]. URL http://www.gro-scotland.gov.uk/files2/stats/household-projections/2010-based/2010-based-household-proj-publication.pdf

Ng, S., Sandberg, L.I.C., Jelle, B.P., 2015. Insulating and Strength Properties of an Aerogel-Incorporated Mortar Based an UHPC Formulations. Presented at the Key Engineering Materials, Trans Tech Publ, pp. 43–48.

Nguyen, M.H., Dao, L.H., 1998. Effects of processing variable on melamine–formaldehyde aerogel formation. J. Non-Cryst. Solids 225, 51–57.

Ni, C., 2013. Scanning Electron Microscopy (SEM), in: Wang, Q.J., Chung, Y.-W. (Eds.), Encyclopedia of Tribology. Springer US, Boston, MA, pp. 2977–2982.

Niazi, A., Dai, J.S., Balabani, S., Seneviratne, L., 2005. Product Cost Estimation: Technique Classification and Methodology Review. J. Manuf. Sci. Eng. 128, 563–575. doi:10.1115/1.2137750

Nokhodchi, A., Tailor, A., 2004. In situ cross-linking of sodium alginate with calcium and aluminum ions to sustain the release of theophylline from polymeric matrices. Il Farm. 59, 999–1004. doi:10.1016/j.farmac.2004.08.006

Nordby, A.S., Shea, A.D., 2013. Building Materials in the Operational Phase. J. Ind. Ecol. n/a-n/a. doi:10.1111/jiec.12046

Norrish, K., Rausell-Colom, J., 1962. Effect of freezing on the swelling of clay minerals. Clay Min. Bull 5, 9–16.

Nugent, R.A., Zhang, G., Gambrell, R.P., 2009. Effect of exopolymers on the liquid limit of clays and its engineering implications. Transp. Res. Rec. J. Transp. Res. Board 2101, 34–43.

Nussinovitch, A., 1997. Hydrocolloid applications: gum technology in the food and other industries. Springer.

Nussinovitch, A., Velez-Silvestre, R., Peleg, M., 1993. Compressive characteristics of freeze-dried agar and alginate gel sponges. Biotechnol. Prog. 9, 101–104. doi:10.1021/bp00019a015

Nussinovitch, A., Zvitov-Marabi, R., 2008. Unique shape, surface and porosity of dried electrified alginate gels. Food Hydrocoll. 22, 364–372. doi:10.1016/j.foodhyd.2006.12.002

O'Brien, F.J., Harley, B.A., Yannas, I.V., Gibson, L., 2004. Influence of freezing rate on pore structure in freeze-dried collagen-GAG scaffolds. Biomaterials 25, 1077–1086.

Official Journal of the European Union, 2011. EU Regulation No 305/2011 of the European Parliament and of the Council of 9 March 2011 laying down harmonised conditions for the marketing of construction products and repealing Council Directive 89/106.

Official Journal of the European Union, 1996. Council Directive 96/61/EC of 24 September 1996 concerning integrated pollution prevention and control, 96/61/EC.

Official Journal of the European Union, 1989. 89/106/EEC of December 21, 1988 concerning construction products.

Ogacho, A., Aduda, B., Nyongesa, F., 2003. Thermal conductivity of a kaolinite refractory: effect of a plant-derived organic binder. J. Mater. Sci. 38, 2293–2297.

Ogunye, F., Boussabaine, H., 2002. Diagnosis of assessment methods for weatherability of stabilised compressed soil blocks. Constr. Build. Mater. 16, 163–172.

Oh, S.-T., Kim, W.-R., Kim, S.-H., Chung, Y.-C., Park, J.-S., 2011. The preparation of polyurethane foam combined with pH-sensitive alginate/bentonite hydrogel for wound dressings. Fibers Polym. 12, 159–165. doi:10.1007/s12221-011-0159-4

Ohta, S., Nakazawa, H., 1995. Porous clay-organic composites: Potential substitutes for polystyrene foam. Appl. Clay Sci. 9, 425–431. doi:10.1016/0169-1317(95)00003-M

Olaoye, G.S., Anigbogu, N.A., 2000. Properties of compressed earth bricks stabilised with termite mound materials. Niger. J. Constr. Technol. Manag. 3, 150–156.

Oldham, J.C., Eaves, R.C., White Jr, D.W., 1977. Materials evaluated as potential soil stabilizers. DTIC Document.

Olivier, M., Mesbah, A., El Gharbi, Z., Morel, J., 1997. Test method for strength tests on blocks of compressed earth. Mater. Struct. 30, 515–517.

ONS, 2015. Building materials and components statistics: July 2015. Office for National Statistics.

Orts, W., Roa-Espinosa, A., Sojka, R., Glenn, G., Imam, S., Erlacher, K., Pedersen, J., 2007. Use of Synthetic Polymers and Biopolymers for Soil Stabilization in Agricultural, Construction, and Military Applications. J. Mater. Civ. Eng. 19, 58–66. doi:10.1061/(ASCE)0899-1561(2007)19:1(58)

Osanyintola, O.F., Simonson, C.J., 2006. Moisture buffering capacity of hygroscopic building materials: Experimental facilities and energy impact. Energy Build. 38, 1270–1282. doi:10.1016/j.enbuild.2006.03.026

Osula, D.O.A., 1996. A comparative evaluation of cement and lime modification of laterite. Eng. Geol. 42, 71–81. doi:10.1016/0013-7952(95)00067-4

Oti, J., Kinuthia, J., Bai, J., 2010a. Design thermal values for unfired clay bricks. Mater. Des. 31, 104–112.

Oti, J., Kinuthia, J., Bai, J., 2010b. Unfired clay masonry bricks incorporating slate waste. Proc. ICE-Waste Resour. Manag. 163, 17–27.

Oti, J.E., Kinuthia, J.M., Bai, J., 2009. Unfired clay bricks: from laboratory to industrial production. Proc. ICE-Eng. Sustain. 162, 229–237.

Oti, J.E., Kinuthia, J.M., Bai, J., 2008. Developing unfired stabilised building materials in the UK. Proc. ICE - Eng. Sustain. 161, 211–218(7).

Pacheco-Torgal, F., Jalali, S., 2012. Earth construction: Lessons from the past for future eco-efficient construction. Constr. Build. Mater. 29, 512–519. doi:10.1016/j.conbuildmat.2011.10.054

Pacheco-Torgal, F., Labrincha, J., 2014. Biotechnologies and bioinspired materials for the construction industry: an overview. Int. J. Sustain. Eng. 7, 235–244.

Padfield, T., 1998. The role of absorbent building materials in moderating changes of relative humidity. Dep. Struct. Eng. Mater. Lyngby Tech. Univ. Den. 150.

Padfield, T., Jensen, L.A., 2011. Humidity buffering of building interiors by absorbent materials. Presented at the Proceedings of the 9th Nordic Symposium on Building Physics, Tampere, Finland, pp. 475–482.

Palomino, A.M., Santamarina, J.C., 2005. Fabric map for kaolinite: effects of pH and ionic concentration on behavior. Clays Clay Miner. 53, 211–223.

Pan, W., Gibb, A.G., Dainty, A.R., 2007. Perspectives of UK housebuilders on the use of offsite modern methods of construction. Constr. Manag. Econ. 25, 183–194.

Panda, R.K., Dhal, J.P., Mishra, S.C., 2012. Effect of sodium silicate on strengthening behaviour of fly ash compacts. Int. J.

Papadopoulos, A.M., 2005. State of the art in thermal insulation materials and aims for future developments. Energy Build. 37, 77–86. doi:10.1016/j.enbuild.2004.05.006

Pappu, A., Saxena, M., Asolekar, S.R., 2007. Solid wastes generation in India and their recycling potential in building materials. Build. Environ. 42, 2311–2320. doi:10.1016/j.buildenv.2006.04.015

Park, S.-S., 2009. Effect of fiber reinforcement and distribution on unconfined compressive strength of fiber-reinforced cemented sand. Geotext. Geomembr. 27, 162–166.

Parliament of the United Kingdom, 2000. Finance Act, 2000 c 17.

Patel, M., Bastioli, C., Marini, L., Würdinger, E., 2005. Life-cycle Assessment of Bio-based Polymers and Natural Fiber Composites, in: Biopolymers Online. Wiley-VCH Verlag GmbH & Co. KGaA.

Patel, M., Bastioli, C., Marini, L., Würdinger, E., 2003. Environmental assessment of bio-based polymers and natural fibres. Life-Cycle Assess. Bio-Based Polym. Nat. Fibres Chapter "biopolymers 10.

Patil, P., Chavanke, D., Wagh, M., 2012. A review on ionotropic gelation method: novel approach for controlled gastroretentive gelispheres. Int. J. Pharm. Pharm. Sci. 4, 27–32.

Pekala, R., Alviso, C., Lu, X., Gross, J., Fricke, J., 1995. New organic aerogels based upon a phenolic-furfural reaction. J. Non-Cryst. Solids 188, 34–40.

Pekala, R.W., 1989. Organic aerogels from the polycondensation of resorcinol with formaldehyde. J. Mater. Sci. 24, 3221–3227. doi:10.1007/BF01139044

Pekala, R.W., Farmer, J.C., Alviso, C.T., Tran, T.D., Mayer, S.T., Miller, J.M., Dunn, B., 1998. Carbon aerogels for electrochemical applications. J. Non-Cryst. Solids 225, 74–80. doi:10.1016/S0022-3093(98)00011-8

Pekmezci, B.Y., Kafescioglu, R., Agahzadeh, E., 2012. Improved performance of earth structures by lime and gypsum addition. METU JFA 2, 205.

Petraitis, P.S., Dudgeon, S.R., 2004. Detection of alternative stable states in marine communities. J. Exp. Mar. Biol. Ecol. 300, 343–371.

Piattoni, Q., Quagliarini, E., Lenci, S., 2011. Experimental analysis and modelling of the mechanical behaviour of earthen bricks. Constr. Build. Mater. 25, 2067–2075.

Pierre, A.C., Pajonk, G.M., 2002. Chemistry of aerogels and their applications. Chem. Rev.-Columb. 102, 4243–4266.

Pirard, R., Blacher, S., Brouers, F., Pirard, J., 1995. Interpretation of mercury porosimetry applied to aerogels. J. Mater. Res. 10, 2114–2119.

Place, E.S., Rojo, L., Gentleman, E., Sardinha, J.P., Stevens, M.M., 2011. Strontium- and zinc-alginate hydrogels for bone tissue engineering. Tissue Eng. Part A 17, 2713–2722.

Plank, J., 2005. Applications of Biopolymers in Construction Engineering, in: Biopolymers Online. Wiley-VCH Verlag GmbH & Co. KGaA.

Plesch, P.H., Cefoil Ltd., 1947. Improvements in or relating to the Manufacture of Low Density Alginic Materials. Patent No. 584,140.

Pojanavaraphan, T., Magaraphan, R., Chiou, B.-S., Schiraldi, D.A., 2010a. Development of Biodegradable Foamlike Materials Based on Casein and Sodium Montmorillonite Clay. Biomacromolecules 11, 2640–2646. doi:10.1021/bm100615a

Pojanavaraphan, T., Schiraldi, D.A., Magaraphan, R., 2010b. Mechanical, rheological, and swelling behavior of natural rubber/montmorillonite aerogels prepared by freeze-drying. Appl. Clay Sci. 50, 271–279. doi:10.1016/j.clay.2010.08.020

Pongjanyakul, T., 2009. Alginate–magnesium aluminum silicate films: Importance of alginate block structures. Int. J. Pharm. 365, 100–108. doi:10.1016/j.ijpharm.2008.08.025

Pongjanyakul, T., Puttipipatkhachorn, S., 2007. Sodium alginate-magnesium aluminum silicate composite gels: Characterization of flow behavior, microviscosity, and drug diffusivity. AAPS PharmSciTech 8, E158–E165. doi:10.1208/pt0803072

Poon, C., Kou, S., Lam, L., 2002. Use of recycled aggregates in molded concrete bricks and blocks. Constr. Build. Mater. 16, 281–289.

Poppe, L.J., Paskevich, V.F., Hathaway, J.C., Blackwood, D.S., 2001. A Laboratory Manual for X-Ray Powder Diffraction (No. U. S. Geological Survey Open-File Report 01-041). U.S. Department of the Interior, U.S. Geological Survey, Woods Hole, MA.

POST, 2012. PostNote 403: Low Carbon Technologies for Energy-Intensive Industries. The Parliamentary Office of Science and Technology, London.

Proctor Group, 2015. Datasheet Spacetherm® Thermal Insulation [WWW Document]. URL http://www.proctorgroup.com/images/downloads/Thermal-Insulation/Spacetherm/Proctors%20-%20Spacetherm%20Datasheet.pdf (accessed 6.29.15).

Pusavec, F., Krajnik, P., Kopac, J., 2010. Transitioning to sustainable production–Part I: application on machining technologies. J. Clean. Prod. 18, 174–184.

Pušavec, F., Stoić, A., Kopač, J., 2009. The role of cryogenics in machining processes. Teh. Vjesn. 16, 3–9.

Quagliarini, E., Lenci, S., 2010. The influence of natural stabilizers and natural fibres on the mechanical properties of ancient Roman adobe bricks. J. Cult. Herit. 11, 309–314. doi:10.1016/j.culher.2009.11.012

Quastel, J., Webley, D., 1947. The effects of the addition to soil of alginic acid and other forms of organic matter on soil aeration. J Agric Sci 37, 257–266.

Quignard, F., Valentin, R., Di Renzo, F., 2008. Aerogel materials from marine polysaccharides. New J. Chem. 32, 1300–1310.

Quraishi, S., Martins, M., Barros, A.A., Gurikov, P., Raman, S., Smirnova, I., Duarte, A.R.C., Reis, R.L., 2015. Novel non-cytotoxic alginate-lignin hybrid aerogels as scaffolds for tissue engineering. J. Supercrit. Fluids 105, 1–8.

Rassis, D., Nussinovitch, A., Saguy, I.S., 2003. Tailor-made porous solid foods. Int. J. Food Sci. Technol. 32, 271–278.

Ratti, C., 2001. Hot air and freeze-drying of high-value foods: a review. J. Food Eng. 49, 311–319.

Rauch, A., Harmon, J., Katz, L., Liljestrand, H., 2002. Measured effects of liquid soil stabilizers on engineering properties of clay. Transp. Res. Rec. J. Transp. Res. Board 33–41.

Reddy, B.V., Kumar, P.P., 2010. Embodied energy in cement stabilised rammed earth walls. Energy Build. 42, 380–385.

Reddy, B.V.V., Lokras, S.S., 1998. Steam-cured stabilised soil blocks for masonry construction. Energy Build. 29, 29–33. doi:10.1016/S0378-7788(98)00033-4

Rees, D.A., Welsh, E.J., 1977. Secondary and tertiary structure of polysaccharides in solutions and gels. Angew. Chem. Int. Ed. Engl. 16, 214–224.

Rehm, B. (Ed.), 2009. Alginates: Biology and applications, Microbiology Monographs. Springer, London.

Reim, M., Beck, A., Körner, W., Petricevic, R., Glora, M., Weth, M., Schliermann, T., Fricke, J., Schmidt, C., Pötter, F.., 2002. Highly insulating aerogel glazing for solar energy usage. Sol. Energy 72, 21–29. doi:10.1016/S0038-092X(01)00086-X

Resurreccion, E.P., Colosi, L.M., White, M.A., Clarens, A.F., 2012. Comparison of algae cultivation methods for bioenergy production using a combined life cycle assessment and life cycle costing approach. Adv. Biol. Waste Treat. Bioconversion Technol. 126, 298–306. doi:10.1016/j.biortech.2012.09.038

Rezende, R., Bártolo, P., Mendes, A., Filho, R.M., 2007. Experimental Characterisation of the Alginate Gelation Process for Rapid Prototyping. Chem. Eng. 11.

Rhoades, J., Chanduvi, F., Lesch, S., 1999. Soil salinity assessment: Methods and interpretation of electrical conductivity measurements, FAO Irrigation and Drainage Paper. Food and Agriculture Organization of the United Nations, Rome.

Rice, R.M., Wengert, E.M., Schroeder, J., 1988. The potential for check reduction using surface coatings. For. Prod. J. 39, 17–23.

Riffat, S.B., Qiu, G., 2013. A review of state-of-the-art aerogel applications in buildings. Int. J. Low-Carbon Technol. 8, 1–6.

Rigacci, A., Marechal, J., Repoux, M., Moreno, M., Achard, P., 2004. Preparation of polyurethane-based aerogels and xerogels for thermal superinsulation. J. Non-Cryst. Solids 350, 372–378.

Rigassi, V., 1995. Compressed earth blocks: Manual of production, A publication of Deutsches Zentrum für Entwicklungstechnologien - GATE, a division of the Deutsche Gesellschaft für Technische Zusammenarbeit (GTZ) GmbH in coordination with the Building Advisory Service and Information. Vieweg, CRATerre-EAG.

Rivera-Gómez, C., Galán-Marín, C., Bradley, F., 2014. Analysis of the Influence of the Fiber Type in Polymer Matrix/Fiber Bond Using Natural Organic Polymer Stabilizer. Polymers 6, 977–994.

Riza, F.V., Rahman, I.A., Zaidi, A.M.A., 2010. A Brief Review of Compressed Stabilized Earth Brick (CSEB). Presented at the Science and Social Research (CSSR), 2010 International Conference on, IEEE, pp. 999–1004.

Robert-Hughes, R., Fox, W., Scott-Marshall, A., 2011. The case for space: The size of England's new homes. RIBA, London.

Robertson, G.P., Coleman, D.C., Bledsoe, C.S., Sollins, P. (Eds.), 1999. Standard soil methods for long-term ecological research. Oxford University Press, New York.

Robitzer, M., David, L., Rochas, C., Renzo, F.D., Quignard, F., 2008. Nanostructure of Calcium Alginate Aerogels Obtained from Multistep Solvent Exchange Route. Langmuir 24, 12547–12552. doi:10.1021/la802103t

Rode, C., Peuhkuri, R.H., Mortensen, L.H., Hansen, K.K., Time, B., Gustavsen, A., Ojanen, T., Ahonen, J., Svennberg, K., Arfvidsson, J., 2005. Moisture buffering of building materials (No. 8778771951). Department of Civil Engineering, Technical University of Denmark.

Rogatzki, P., 2015. The development of in-situ and prefabricated masonry processes using high performance mortars. (PhD Thesis). University of Surrey, UK.

Röhlen, U., Ziegert, C., 2011. Earth Building Practice: Planning-Design-Building. Beuth Verlag, Berlin.

Rosenow, J., Platt, R., Flanagan, B., 2013. Fuel poverty and energy efficiency obligations–A critical assessment of the supplier obligation in the UK. Energy Policy 62, 1194–1203.

Ross, D.S., Ketterings, Q., 1995. Recommended methods for determining soil cation exchange capacity, in: Newark: College of Agriculture, University of Delaware.

Ross, K., 2002. Non-traditional Housing in the UK: A Brief Review.

Rothe, J., Hays, D., Benemann, J., 2012. New Fuels: Macroalgae, Future Transportation Fuels Study, National Petroleum Council, Working Document of the NPC Future Transportation Fuels Study.

Roux, H.J., 1958. Waterproof fiberboard. Patent No. 2,825,660.

Rowley, J.A., Madlambayan, G., Mooney, D.J., 1999. Alginate hydrogels as synthetic extracellular matrix materials. Biomaterials 20, 45–53.

RSC, 2014. Making aircraft from seaweed! [WWW Document]. R. Soc. Chem. URL http://www.rsc.org/learn-chemistry/content/filerepository/CMP/00/000/029/Making_aircraft_from_seaweed.pdf (accessed 10.24.14).

Ruskulis, O., 2002a. Additives to Clay: Mineral and Synthetic Additives (Technical Brief). Practical Action.

Ruskulis, O., 2002b. Additives to Clay: Organic Additives (Technical Brief). Practical Action.

Santamarina, J., Klein, K., Wang, Y., Prencke, E., 2002. Specific surface: determination and relevance. Can. Geotech. J. 39, 233–241.

Santoni, R.L., Tingle, J.S., Webster, S.L., 2002. Stabilization of silty sand with nontraditional additives. Transp. Res. Rec. J. Transp. Res. Board 1787, 61–70.

Sartori, I., Hestnes, A.G., 2007. Energy use in the life cycle of conventional and low-energy buildings: A review article. Energy Build. 39, 249–257. doi:10.1016/j.enbuild.2006.07.001

Scherer, G.W., 1998. Characterization of aerogels. Adv. Colloid Interface Sci. 76–77, 321–339. doi:10.1016/S0001-8686(98)00051-7

Schiraldi, D.A., Bandi, S.A., Gawryla, M.D., 2006. Progress in clay aerogel/polymer composite materials. Polym. Prepr. 47, 313.

Schiraldi, D.A., Gawryla, M.D., Alhassan, S., 2010. Clay Aerogel Composite Materials. Adv. Sci. Technol. 63, 147–151.

Schiraldi, D.A., Gawyrla, M.D., Bandi, S.A., 2007. Clay aerogel-based polymer composites, materials and methods. Patent No. US20070208124 A1.

Schneider, G.L., 1977. Method of stabilizing soils. Patent No. US4022633 A.

Scholen, D.E., 1992. Non-standard stabilizers. U.S. Dept. of Transportation, Federal Highway Administration, Office of Direct Federal Programs, Washington, D.C.

Scottish Government, 2015. Technical Handbook - Domestic: Section 5 - Noise. Scottish Government, Edinburgh.

Scottish Government, 2014. Home Energy Efficiency Programmes for Scotland: Summary Delivery Report 2013/14. Edinburgh.

Scottish Government, 2013. Draft Seaweed Policy Statement - Consultation Document (No. DPPAS14668). Edinburgh.

Sharma, B., Bora, P.K., 2003. Plastic limit, liquid limit and undrained shear strength of soil-reappraisal. J. Geotech. Geoenvironmental Eng. 129, 774–777.

Sharp, G., 1987. Growth and production in wild and cultured stocks of Chondrus crispus. Presented at the Twelfth International Seaweed Symposium, Springer, pp. 349–354.

Shchipunov, Y.A., Karpenko, T.Y., 2004. Hybrid Polysaccharide–Silica Nanocomposites Prepared by the Sol–Gel Technique. Langmuir 20, 3882–3887. doi:10.1021/la0356912

Shukla, A., Tiwari, G.N., Sodha, M.S., 2009. Embodied energy analysis of adobe house. Renew. Energy 34, 755–761. doi:10.1016/j.renene.2008.04.002

Silva, B., Correia, J., Nunes, F., Tavares, P., Varum, H., Pinto, J., 2010. Bird nest construction-Lessons for building with earth. WSEAS Trans. Environ. Dev. 6, 95–104.

Smith, A.S., Bingel, P., Bown, A., 2009. Sustainability of masonry in construction, in: Sustainability of Construction Materials. Woodhead Publishing, UK.

Smith, C., n.d. Help to Buy boom leads to brick shortage in Scotland, 15 July 2014 [WWW Document]. BBC News. URL http://www.bbc.co.uk/news/uk-scotland-28303482

Smith, D.M., Deshpande, R., Jeffrey Brinke, C., 1992. Preparation of low-density aerogels at ambient pressure. Presented at the MRS Proceedings, Cambridge Univ Press, p. 567.

Smith, D.S., Wood, J.B., Mackenzie, R., 2006. Housing and Sound Insulation: Improving existing attached dwellings and designing for conversions. Scottish Government, Edinburgh.

Smith, E.W., Austin, G.S., 1989. Adobe, pressed-earth, and rammed-earth industries in New Mexico. New Mexico Bureau of Mines & Mineral Resources.

Smith, P.G., 2011. An Introduction to Food Process Engineering, 2nd ed, Food Science Text. Springer, USA.

Solomon, D., Rossetti, M., 1996. Foamed glass manufacture. Patent No. US5516351 A.

Somlai, L.S., Bandi, S.A., Schiraldi, D.A., Mathias, L.J., 2006. Facile processing of clays into organically-modified aerogels. AIChE J. 52, 1162–1168. doi:10.1002/aic.10710

Sorgho, B., Zerbo, L., Keita, I., Dembele, C., Plea, M., Sol, V., Gomina, M., Blanchart, P., 2014. Strength and creep behavior of geomaterials for building with tannin addition. Mater. Struct. 47, 937–946. doi:10.1617/s11527-013-0104-7

Stahl, T., Brunner, S., Zimmermann, M., Ghazi Wakili, K., 2012. Thermo-hygric properties of a newly developed aerogel based insulation rendering for both exterior and interior applications. Energy Build. 44, 114–117. doi:10.1016/j.enbuild.2011.09.041

Standards New Zealand, 1998. NZS 4297 (1998): Engineering design of earth buildings [Building Code Compliance Documents B1 (VM1), B2 (AS1)].

Stanford, E.C.C., 1886. Algin and other useful components. Patent No. US349760 A.

Stec, A.A., Hull, T.R., 2011. Assessment of the fire toxicity of building insulation materials. Energy Build. 43, 498–506. doi:10.1016/j.enbuild.2010.10.015

Stokke, B.T., Draget, K.I., Smidsrød, O., Yuguchi, Y., Urakawa, H., Kajiwara, K., 2000. Small-angle X-ray scattering and rheological characterization of alginate gels. 1. Ca-alginate gels. Macromolecules 33, 1853–1863.

Straatmann, A., Borchard, W., 2003. Phase separation in calcium alginate gels. Eur. Biophys. J. 32, 412–417.

Su, L.F., Miao, L., Tanemura, S., Xu, G., 2012. Low-cost and fast synthesis of nanoporous silica cryogels for thermal insulation applications. Sci. Technol. Adv. Mater. 13, 035003.

Sung Ho Kim, 2008. Polyacrylamine Treated Kaolinite: A Fabric Study (Masters Thesis). Pennsylvania State University.

Sutton, Andy, Black, D., Walker, P., 2011. Infromation Paper (IP 16/11) Unfired Clay Masonry - An introduction to low-impact building materials.

Sutton, A, Black, D., Walker, P., 2011. Natural Fibre Insulation: An introduction to low-impact building materials (Information Paper No. (IP 18/11)). BRE Ltd.

Svagan, A.J., Berglund, L.A., Jensen, P., 2011. Cellulose Nanocomposite Biopolymer Foam: Hierarchical Structure Effects on Energy Absorption. ACS Appl. Mater. Interfaces 3, 1411–1417.

Tan, W., Takeuchi, S., 2007. Monodisperse alginate hydrogel microbeads for cell encapsulation. Adv. Mater. 19, 2696–2701.

Taytak, B., Pulat, H.F., Yukselen-Aksoy, Y., 2012. Improvement of engineering properties of soils by biopolymer additives. Presented at the 3rd International Conference on New Developments in Soil Mechanics and Geotechnical Engineering, 28-30 June 2012, Near East University, Nicosia, North Cyprus.

Technavio, 2015. Global Aerogel Market 2015-2019 [WWW Document]. URL http://www.technavio.com/report/aerogel-market-2015-2019-global-trends-forecasts-vendor-analysis

Tenpierik, M.J., Hasselaar, E., 2013. Reflective multi-foil insulations for buildings: A review. Energy Build. 56, 233–243. doi:10.1016/j.enbuild.2012.10.003

TenWolde, A., Pilon, C.L., 2007. The effect of indoor humidity on water vapor release in homes, in: 30 Years of Research Proceedings Thermal Performance of the Exterior Envelopes of Whole Buildings X. Presented at the Buildings X Conference, Clearwater Beach, Florida December, 2-7, 2007, American Society for Heating, Refrigerating, and Air-Conditioning Engineers, Inc.

Tewari, P.H., Hunt, A.J., Lofftus, K.D., 1985. Ambient-temperature supercritical drying of transparent silica aerogels. Mater. Lett. 3, 363–367. doi:10.1016/0167-577X(85)90077-1

Tezcan, F., Günister, E., Özen, G., Erim, F.B., 2012. Biocomposite films based on alginate and organically modified clay. Int. J. Biol. Macromol. 50, 1165–1168. doi:10.1016/j.ijbiomac.2012.01.006

Theng, B.K.G., 2012a. Chapter 11 - Polysaccharides, in: B.K.G. Theng (Ed.), Developments in Clay Science. Elsevier, pp. 351–390.

Theng, B.K.G., 2012b. Chapter 4 - Negatively Charged Polymers (Polyanions), in: B.K.G. Theng (Ed.), Developments in Clay Science. Elsevier, pp. 111–127.

Theng, B.K.G., 1972. Formation, properties, and practical applications of clay—organic complexes. J. R. Soc. N. Z. 2, 437–457. doi:10.1080/03036758.1972.10423293

Thermablok, 2015. Thermablok Aerogel Insulation Blanket [WWW Document]. URL http://www.thermablok.co.uk/wp/wp-content/uploads/2015/11/thermablokaerogelblanketdatasheet2.pdf

Thormark, C., 2002. A low energy building in a life cycle—its embodied energy, energy need for operation and recycling potential. Build. Environ. 37, 429–435. doi:10.1016/S0360-1323(01)00033-6

Thu, B., Bruheim, P., Espevik, T., Smidsrød, O., Soon-Shiong, P., Skjåk-Bræk, G., 1996. Alginate polycation microcapsules: I. Interaction between alginate and polycation. Biomaterials 17, 1031–1040.

Tingle, J.S., Newman, J.K., Larson, S.L., Weiss, C.A., Rushing, J.F., 2007. Stabilization mechanisms of nontraditional additives. Transp. Res. Rec. J. Transp. Res. Board 1989, 59–67.

Tiraferri, A., Borkovec, M., 2015. Probing effects of polymer adsorption in colloidal particle suspensions by light scattering as relevant for the aquatic environment: An overview. Spec. Issue Eng. Nanoparticles Soils Waters 535, 131–140. doi:10.1016/j.scitotenv.2014.11.063

Topuz, F., Henke, A., Richtering, W., Groll, J., 2012. Magnesium ions and alginate do form hydrogels: a rheological study. Soft Matter 8, 4877–4881.

Trens, P., Valentin, R., Quignard, F., 2007. Cation enhanced hydrophilic character of textured alginate gel beads. Colloids Surf. Physicochem. Eng. Asp. 296, 230–237. doi:10.1016/j.colsurfa.2006.09.049

Tunç, S., Duman, O., 2008. The effect of different molecular weight of poly(ethylene glycol) on the electrokinetic and rheological properties of Na-bentonite suspensions. Colloids Surf. Physicochem. Eng. Asp. 317, 93–99. doi:10.1016/j.colsurfa.2007.09.039

Turgut, P., 2012. Manufacturing of building bricks without Portland cement. J. Clean. Prod. 37, 361–367.

Tyler, P., 1994. Ascophyllum Harvesting in the Outer Hebrides (MSc Thesis). Heriott Watt University, Edinburgh.

UK Government, 2007. The Energy Performance of Buildings (Certificates and Inspections) (England and Wales) Regulations 2007 (Statutory Instruments 2007 No. No. 991). The Stationary Office, London.

UN, 1997. Kyoto protocol to the united nations framework convention on climate change (No. CM5379), Miscellaneous Series No. 1 (2002). Crown Copyright.

Valentin, R., Molvinger, K., Quignard, F., Di Renzo, F., 2005. Methods to Analyse the Texture of Alginate Aerogel Microspheres. Macromol. Symp. 222, 93–102. doi:10.1002/masy.200550410

van Olphen, H., 1967. Polyelectrolyte reinforced aerogels of clays - Application as chromatographic absorbents. Clays Clay Miner. 15, 423–435. doi:10.1346/CCMN.1967.0150142

Van Olphen, H., 1965. Process for preparing physically strong aerogels. Patent No. US3203903 A.

Van Olphen, H., 1964. Internal mutual flocculation in clay suspensions. J. Colloid Sci. 19, 313–322.

Van Wyk, L., Mapiravana, J., Ampofo-Anti, N., 2012. Sustainable materials in building and architecture, in: Materials for a Sustainable Future. Royal Society of Chemistry, London.

Venkatarama Reddy, B., Jagadish, K., 2003. Embodied energy of common and alternative building materials and technologies. Energy Build. 35, 129–137.

Verwey, E., Overbeek, J.T.G., 1955. Theory of the stability of lyophobic colloids. J. Colloid Sci. 10, 224–225.

Vieira, M., Klemm, D., Einfeldt, L., Albrecht, G., 2005. Dispersing agents for cement based on modified polysaccharides. Cem. Concr. Res. 35, 883–890.

Viggiano, R.P., Gawryla, M.D., Schiraldi, D.A., 2014. Foam-like polymer/clay aerogels which incorporate air bubbles. J. Appl. Polym. Sci. 131.

Viggiano, R.P., Schiraldi, D.A., 2014. Fabrication and mechanical characterization of lignin-based aerogels. Green Mater. 2, 153–158.

Vilane, B., 2010. Assessment of stabilisation of adobes by confined compression tests. Biosyst. Eng. 106, 551–558.

Vilaplana, F., Strömberg, E., Karlsson, S., 2010. Environmental and resource aspects of sustainable biocomposites. Polym. Degrad. Stab. 95, 2147–2161.

Vinod, J., Indraratna, B., Mahamud, M.A., 2010. Stabilisation of an erodible soil using a chemical admixture.

Virdi, S., 2012. Construction science and materials. John Wiley & Sons, Oxford.

Vroomen, R., 2007. Gypsum stabilised Earth-Research on the Properties of cast Gypsum-stabilised Earth and its Suitability for Low Cost Housing

Construction in Developing Countries (Final thesis for MSc Architecture, Building & Planning). Eindhoven University of Technology, The Netherlands.

Vu, H.M., Forth, J.P., 2014. Mechanisms of strength development in masonry units using blended organic binders. Constr. Build. Mater. 52, 294–305. doi:10.1016/j.conbuildmat.2013.11.053

Wagh, P., Begag, R., Pajonk, G., Rao, A.V., Haranath, D., 1999. Comparison of some physical properties of silica aerogel monoliths synthesized by different precursors. Mater. Chem. Phys. 57, 214–218.

Walker, F., 1954. Distribution of Laminariaceae around Scotland. J. Cons. 20, 160–166.

Walker, F.T., 1947. Sublittoral Seaweed Surveys. J. Ecol. Vol. 35, No. 1/2, 166–185.

Walker, P., 2002. The Australian earth building handbook.

Walker, P., 1999. Bond characteristics of earth block masonry. J. Mater. Civ. Eng. 11, 249–256.

Walker, P., Stace, T., 1997. Properties of some cement stabilised compressed earth blocks and mortars. Mater. Struct. 30, 545–551.

Walker, P.J., 2004. Strength and erosion characteristics of earth blocks and earth block masonry. J. Mater. Civ. Eng. 16, 497–506.

Walker, P.J., 1995. Strength, durability and shrinkage characteristics of cement stabilised soil blocks. Cem. Concr. Compos. 17, 301–310. doi:10.1016/0958-9465(95)00019-9

Wallis, N.K., 1970. Australian Timber Handbook, 3rd ed. Timber Development Association, Sydney.

Wang, L., 2015. Aerogels based on biodegradable polymers and clay (PhD Thesis). Universitat Politècnica de Catalunya, Barcelona.

Wang, L., Schiraldi, D.A., Sanchez-Soto, M., 2014. Foamlike Xanthan Gum/Clay Aerogel Composites and Tailoring Properties by Blending with Agar. Ind. Eng. Chem. Res. 53, 7680–7687.

Wang, Yuxin, Gawryla, M.D., Schiraldi, D.A., 2013. Effects of freezing conditions on the morphology and mechanical properties of clay and polymer/clay aerogels. J. Appl. Polym. Sci. 129, 1637–1641. doi:10.1002/app.39143

Wang, Yizhe, Wang, W., Shi, X., Wang, A., 2013. A superabsorbent nanocomposite based on sodium alginate and illite/smectite mixed-layer clay. J. Appl. Polym. Sci. 130, 161–167. doi:10.1002/app.39141

Ward, D.A., Ko, E.I., 1993. Synthesis and structural transformation of zirconia aerogels. Chem. Mater. 5, 956–969.

Watson, R., Downey, O., 2008. The Little Red Book of Acoustics: A Practical Guide, 2nd ed. Blue Tree Acoustics.

Wei, T., Chang, T., Lu, S., Chang, Y., 2007. Preparation of monolithic silica aerogel of low thermal conductivity by ambient pressure drying. J. Am. Ceram. Soc. 90, 2003–2007.

Wernick, I.K., Ausubel, J.H., 1995. National materials flows and the environment. Annu. Rev. Energy Environ. 20, 463–492.

Wilcox, H.A., 1975. Hothouse earth, US Dept. of Defense, Navy's Ocean Farm Project. Praeger, New York.

Williams, C., Goodhew, S., Griffiths, R., 2011. The flexural strength of earth-block masonry for sustainable walling. Struct. Surv. 29, 46–62.

Williams, C., Goodhew, S., Griffiths, R., Watson, L., 2010. The feasibility of earth block masonry for building sustainable walling in the United Kingdom. J. Build. Apprais. 6, 99–108.

Wilson, M.J., 1987. A handbook of determinative methods in clay mineralogy. Blackie. Chapman and Hall.

Woodward, F.N., 1951. The Scottish Seaweed Research Association. J. Mar. Biol. Assoc. U. K. 29. doi:10.1017/S0025315400052899

Worrell, E., Price, L., Martin, N., Hendriks, C., Meida, L.O., 2001. Carbon Dioxide Emissions from the Global Cement Industry. Annu. Rev. Energy Environ. 26, 303–329. doi:10.1146/annurev.energy.26.1.303

WRAP, 2013. Unfired earth clay brick, Exemplars: Resource Efficiency in Construction Products. Waste & Resource Action Programme.

Wu, D., Fu, R., Sun, Z., Yu, Z., 2005. Low-density organic and carbon aerogels from the sol–gel polymerization of phenol with formaldehyde. J. Non-Cryst. Solids 351, 915–921.

Yalçın, T., Alemdar, A., Ece, Ö.I., Güngör, N., 2002. The viscosity and zeta potential of bentonite dispersions in presence of anionic surfactants. Mater. Lett. 57, 420–424.

Yalley, P.P.-K., Manu, D., 2013. Strength and Durability Properties of Cow Dung Stabilised Earth Brick. Civ. Environ. Res. 3, 117–125.

Yang, J., Li, Z., Du, Q., 2012. An experimental study on material and structural properties of structural insulated panels (SIPs). Presented at the Applied Mechanics and Materials, Trans Tech Publ, pp. 127–131.

Yang, L., Liang, G., Zhang, Z., He, S., Wang, J., 2009. Sodium alginate/Na+-rectorite composite films: Preparation, characterization, and properties. J. Appl. Polym. Sci. 114, 1235–1240. doi:10.1002/app.30521

Yesilata, B., Turgut, P., 2007. A simple dynamic measurement technique for comparing thermal insulation performances of anisotropic building materials. Energy Build. 39, 1027–1034.

Yttrup, P., Diviny, K., Sottile, F., 1981. Development of a drip test for the erodibility of mud bricks. Deakin University, School of Architecture, Geelong, Australia.

Yuguchi, Y., Urakawa, H., Kajiwara, K., Draget, K.I., Stokke, B.T., 2000. Small-angle X-ray scattering and rheological characterization of alginate gels. 2. Time-resolved studies on ionotropic gels. J. Mol. Struct. 554, 21–34. doi:10.1016/S0022-2860(00)00556-1

Yukselen, Y., Kaya, A., 2008. Suitability of the methylene blue test for surface area, cation exchange capacity and swell potential determination of clayey soils. Eng. Geol. 102, 38–45.

Zami, M.S., Lee, A., 2010. Economic benefits of contemporary earth construction in low-cost urban housing–State-of-the-art review. J. Build. Apprais. 5, 259–271.

Zhang, B., Su, H., Gu, X., Huang, X., Wang, H., 2013. Effect of structure and charge of polysaccharide flocculants on their flocculation performance for bentonite suspensions. Colloids Surf. Physicochem. Eng. Asp. 436, 443–449. doi:10.1016/j.colsurfa.2013.07.017

Zhang, L., 2013. Production of bricks from waste materials–A review. Constr. Build. Mater. 47, 643–655.

Zhang, S., Zhao, D., 2012. Aerospace Materials Handbook. CRC Press, Boca Raton.

Zimmermann, H., Wählisch, F., Baier, C., Westhoff, M., Reuss, R., Zimmermann, D., Behringer, M., Ehrhart, F., Katsen-Globa, A., Giese, C., Marx, U., Sukhorukov, V.L., Vásquez, J.A., Jakob, P., Shirley, S.G., Zimmermann, U., 2007. Physical and biological properties of barium cross-linked alginate membranes. Biomaterials 28, 1327–1345. doi:10.1016/j.biomaterials.2006.11.032

Zukowski, M., Haese, G., 2010. Experimental and numerical investigation of a hollow brick filled with perlite insulation. Energy Build. 42, 1402–1408. doi:10.1016/j.enbuild.2010.03.009

Appendix A: MBL Cost & Energy Data

Table A 1: Processing Cost Breakdown (LH Stem)

A - Harvesting Costs[b]	**Annual Working Hours**[a]	**Fuel Usage** (L per hour)	**Annual Fuel Usage** (L)	**Fuel Costs** (£/L)	**Annual Fuel Cost** Cost x usage
Transport from harvest site to dock	666	80	666 x 80 = 53280	0.66	53280 x 0.66 = £35,164.80
Cutting	8094	5	8094 x 5 = 40470	0.66	40470 x 0.66 = £26,710.20
a - Based on maximum of 200 harvesting days b - Based on 20,000 tonnes per year (100 tonnes per day) and yield for LH Stem (29.41)				**Total =**	**£61,875.00**
				Total = (per tonne of alginate)	(£61,875.00 ÷ 20,000) x 29.41 = **£90.99**

B - Processing & Energy Costs[c]	**Annual Energy Consumption** (MWh)	**Energy Costs** (£ per MWh)	**Annual Processing Costs** Cost x consumption
Electrical Energy	4940	85.00	£419,905.44
Latent Heat (Fluid Bed Dryer)	20348	23.53 [d]	£478,785.06
Sensible Heat	8090	35 [e]	£283,157.41
c - Based on 1500T Capacity plant based at Barcaldine d -Based on Wood Chip fuel source e - Based on using a Heat Pump		**Total =**	**£1,181,847.90**
		Total = (per tonne of alginate)	£1,181,847.90 ÷ 1500 = **£787.90**

C - Chemical Costs[c]	**Cost** (£/t)	**Usage** (t/t alginate)	**Chemical Costs** Cost x usage
Catalyst	8000	0.0020	£16.00
Sequestrant	10000	0.0040	£40.00
Hydrochloric Acid (Conc HCl)	199	0.2770	£55.12
Sodium Carbonate (Na_2CO_3)	299	0.9230	£275.98
Sodium Hydroxide (NaOH)	615	0.0740	£45.51
Formaldehyde (HCHO)	500	0.0170	£8.50
Hydrogen Peroxide (H_2O_2)	397	0.0440	£17.47
Calcium chloride ($CaCl_2$)	195	0.9100	£177.45
Delivery Transport costs	5.04	2.2510	11.35
		Total = (per tonne of alginate)	**£647.37**

D – Water Usage[c]	**Water Cost** (£/m^3)	**Usage per Tonne of Alginate** (m^3)	**Water Costs** Cost x usage
	£0.20	293.17	**£58.63**
		Total Cost per tonne of alginate (Excluding overheads, staff, capital expenditure etc)	**£1,584.89**
		Proposed Retail Cost per kg of alginate (from MBL figures)	**£11.00**

Table A 2: Processing Cost Breakdown (AN)

A - Harvesting Costs[b]	**Annual Working Hours**[a]	**Fuel Usage** (L per hour)	**Annual Fuel Usage** (L)	**Fuel Costs** (£/L)	**Annual Fuel Cost** Cost x usage
Transport from harvest site to dock	666	80	53280	0.66	53280 x 0.66 = £35,164.80
Cutting	8094	5	40470	0.66	40470 x 0.66 = £26,710.20
a - Based on maximum of 200 harvesting days b - Based on 20,000 tonnes per year (100 tonnes per day) and yield for AN (19.61)				**Total =**	**£61,875.00**
				Total = (per tonne of alginate)	(£61,875.00 ÷ 20,000) x 19.61 = **£60.67**

B - Processing & Energy Costs[c]	**Annual Energy Consumption** (MWh)	**Energy Costs** (£ per MWh)	**Annual Processing Costs** Cost x consumption
Electrical Energy	4940	85.00	£419,905.44
Latent Heat (Fluid Bed Dryer)	20348	23.53 [d]	£478,785.06
Sensible Heat	8090	35 [e]	£283,157.41
c - Based on 1500T Capacity plant based at Barcaldine d -Based on Wood Chip fuel source e - Based on using a Heat Pump		**Total =**	**£1,181,847.90**
		Total = (per tonne of alginate)	£1,181,847.90 ÷ 1500 = **£787.90**

C - Chemical Costs[c]	**Cost** (£/t)	**Usage** (t/t alginate)	**Chemical Costs** Cost x usage
Catalyst	8000	0.0020	16.00
Sequestrant	10000	0.0040	50.00
Hydrochloric Acid (Conc HCl)	199	0.2770	62.09
Sodium Carbonate (Na_2CO_3)	299	0.9230	305.58
Sodium Hydroxide (NaOH)	615	0.0740	51.05
Formaldehyde (HCHO)	500	0.0170	98.00
Hydrogen Peroxide (H_2O_2)	397	0.0440	13.62
Calcium chloride ($CaCl_2$)	195	0.9100	198.90
Delivery Transport costs	5.04	2.6743	13.48
		Total = (per tonne of alginate)	**£808.71**

D – Water Usage[c]	**Water Cost** (£/m^3)	**Usage per Tonne of Alginate** (m^3)	**Water Costs** Cost x usage
	£0.20	293.17	**£58.63**
		Total Cost per tonne of alginate (Excluding overheads, staff, capital expenditure etc)	**£1,715.91**
		Proposed Retail Cost per kg of alginate (from MBL figures)	**£8.50**

Table A 3: MBL Production Cost Data – Summary

		Dry Alginate Product Produced (tonnes per tonne of wet seaweed)	**Basic Processing Cost per tonne** (Excluding overheads, staff, capital expenditure etc)	**Proposed Cost £/kg** (Final Product)
Product	**Sodium Alginate** (AN)	0.051	£1,716	£8.50
	Sodium Alginate (LH Stem)	0.034	£1,585	£11.00
	Sodium Alginate (LH Frond)	0.026	£1,597	£11.00
	Residue	n/a	n/a	£0.20
	Milled Seaweed	n/a	£3	£0.04

Table A 4: Processing Energy Breakdown (LH Stem)

A - Harvesting Energy [b]	**Embodied Energy – Fuel** (kWh/L)	**Fuel Use** (L/tonne of alginate)	**Energy Use** (kWh/t)	**Embodied Energy** (MJ/kg)
	Diesel oil[a]	MBL figures[b]	EE x Fuel Use	$\frac{EE}{1000} \times 3.6$
Transport from harvest site to dock	11[a]	78.35	11 x 78.35 = 861.85	3.10
Cutting	11[a]	59.51	11 x 59.51 = 654.61	2.36
a – Based on figures from DECC (2016) b - Based on 20,000 tonnes per year (100 tonnes per day) and yield for LH Stem			**Total =**	3.10 + 2.36 = **5.46**

B - Processing & Energy Costs [c]	**Annual Energy Consumption** (kWh)	**Energy Use** (kWh/ tonne of alginate)	**Embodied Energy** (MJ/kg)
	MBL figures[b]	MBL figures[c]	$\frac{\text{Energy Use}}{1000} \times 3.6$
Electrical Energy	4,940	4,940 ÷ 1,500 = 3.29	0.01
Latent Heat (Fluid Bed Dryer)	20,348[d]	20,348 ÷ 1500 = 13. 57	0.05
Sensible Heat	8,090[e]	8,090 ÷ 1500 = 5.39	0.02
c - Based on 1500T Capacity plant based at Barcaldine d -Based on Wood Chip fuel source e - Based on using a Heat Pump		**Total =**	**0.08**

D – Water Usage [c]	**Embodied Energy - Water** (MJ/kg)	**Water Use** (kg per tonne of Alginate)	**Embodied Energy** (MJ/kg)
	Water - Hammond and Jones (2011)	MBL figures	$\frac{\text{EE x Water Use}}{1000}$
Water required for washing/processing	0.01	293,166.70	**2.93**
		Total EE per kg of alginate (MJ/kg)	**8.47**

Table A 5: Processing Energy Breakdown (AN)

A - Harvesting Energy [b]	**Embodied Energy – Fuel** (kWh/L)	**Fuel Use** (L/tonne of alginate)	**Energy Use** (kWh/t)	**Embodied Energy** (MJ/kg)
	Diesel oil[a]	MBL figures[b]	EE x Fuel Use	$\frac{EE}{1000} \times 3.6$
Transport from harvest site to dock	11[a]	52.24	11 x 52.24= 574.64	2.07
Cutting	11[a]	39.68	11 x 39.68= 426.48	1.57
a – Based on figures from DECC (2016) b - Based on 20,000 tonnes per year (100 tonnes per day) and yield for AN			**Total =**	2.07 + 1.57 = **3.64**

B - Processing & Energy Costs [c]	**Annual Energy Consumption** (kWh)	**Energy Use** (kWh/ tonne of alginate)	**Embodied Energy** (MJ/kg)
	MBL figures[b]	MBL figures[c]	$\frac{\text{Energy Use}}{1000} \times 3.6$
Electrical Energy	4,940	4,940 ÷ 1,500 = 3.29	0.01
Latent Heat (Fluid Bed Dryer)	20,348[d]	20,348 ÷ 1500 = 13. 57	0.05
Sensible Heat	8,090[e]	8,090 ÷ 1500 = 5.39	0.02
c - Based on 1500T Capacity plant based at Barcaldine d -Based on Wood Chip fuel source e - Based on using a Heat Pump		**Total =**	**0.08**

D – Water Usage[c]	**Embodied Energy - Water** (MJ/kg)	**Water Use** (kg per tonne of Alginate)	**Embodied Energy** (MJ/kg)
	Water - Hammond and Jones (2011)	MBL figures	$\frac{\text{EE x Water Use}}{1000}$
Water required for washing/processing	0.01	293,166.70	**2.93**
		Total EE per kg of alginate (MJ/kg)	**6.65**

Table A 6: Embodied Carbon Estimates (LH Stem)

	Energy Use per tonne of alginate (kWh/t)	**Conversion Factor** (kg CO_2e/kWh)	**Embodied CO_2** Energy Use x Conversion Factor (kg CO_2e/tonne)
A - Harvesting Energy	Transport = 861.85 Cutting = 654.61 **Total = 1516.46**	0.27[a]	1516.46 x 0.27 = 409.44
B - Processing & Energy Cost	Electricity = 3.29	0.41[b]	3.29 x 0.41 = 1.35
	Latent Heat = 1.36	0.01[c]	1.36 x 0.01 = 0.01
	Sensible Heat = 5.39	0.41[b]	5.39 x 0.41 = 2.21
	Water Use per tonne of alginate (m^3/t)	**Conversion Factor** (kg Co2e/m^3)	**Embodied CO_2** Water Use x Conversion Factor (kg CO_2e/tonne)
D – Water Usage	293.17	0.344[d]	293.17 x 0.344 = 100.85
a – Diesel (100% mineral diesel) b – Electricity c – Biomass d – Mains Water (all from DECC (2016))		**Total =**	**513.86**
		Total EC per kg of alginate (kg CO_2e /kg)	**0.51**

Table A 7: Embodied Carbon Estimates (AN)

	Energy Use per tonne of alginate (kWh/t)	**Conversion Factor** (kg CO_2e/kWh)	**Embodied CO_2** Energy Use x Conversion Factor (kg CO_2e/tonne)
A - Harvesting Energy	Transport = 574.64 Cutting = 436.48 **Total = 1011.12**	0.27[a]	1011.12 x 0.27 = 273.00
B - Processing & Energy Cost (Electricity)	Electricity = 3.29	0.41[b]	3.29 x 0.41 = 1.35
	Latent Heat = 1.36	0.01[c]	1.36 x 0.01 = 0.01
	Sensible Heat = 5.39	0.41[b]	5.39 x 0.41 = 2.21
	Water Use per tonne of alginate (m^3/t)	**Conversion Factor** (kg Co2e/m^3)	**Embodied CO_2** Water Use x Conversion Factor (kg CO_2e/tonne)
D – Water Usage	293.17	0.344[d]	293.17 x 0.344 = 100.85
a – Diesel (100% mineral diesel) b – Electricity c – Biomass d – Mains Water (all from DECC (2016))		**Total =**	**377.42**
		Total EC per kg of alginate (kg CO_2e /kg)	**0.38**

Appendix B: Soil Characterisation Tests

Soil Sources

Figure B 1: Quarry Locations

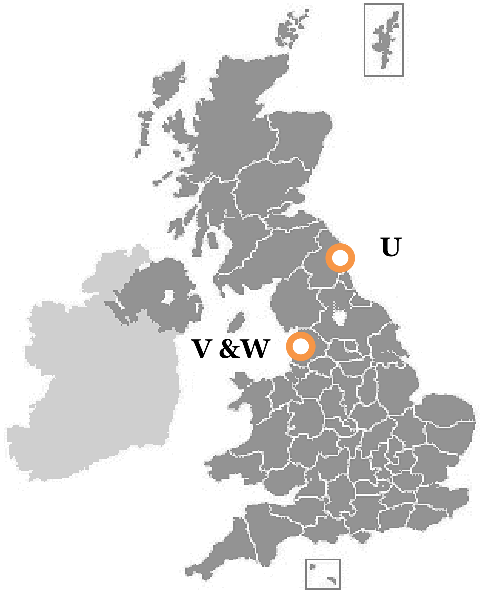	**U**	*Throckley, Newcastle upon Tyne (Ibstock)*
	V	*Ravenhead, Skelmerdale, Lancashire (Ibstock)*
	W	*Ravenhead, Skelmerdale, Lancashire (Ibstock)*

Particle size distribution

The particle size distribution testing was based on the procedures outlines in BS 1377-2 (BSI, 1990b) and consisted of two key parts: seive analysis and sedimentation anaylsis. The seive analysis was firstly used to determine the distribution of course particles (63µm to 75mm) by passing the material through seives of different mesh sizes and calculating the weight of the material retained on each. In this case, the soils were found to retain less than 5% of particles on the 2mm test sieve (Table B 1).

Table B 1: Sieve Analysis

	U	V	W
Initial Weight Sample (g)	108.61	111.89	105.0
Weight retained on 2mm sieve (g)	4.39	3.21	2.52
% > 2mm	4.0%	2.9%	2.4%

For sedminentation analysis, the most commonly used method is the hydrometer method which involves measuing the density of a soil suspension over time. This test is based on Stokes Law (Equation B1) which relates the velocity (v) of spherical particles in a liquid as they settle with the particle diameter (d), the acceleration due to gravity (g), the viscosity of the liquid (η) and the particle and liquid densities (ρ_p and ρ_l). The particle density value for soils usually ranges between 2.6 and 2.7 Mg/cm^3 and so 2.65 Mg/cm^3 was used as the typical value.

$$v = \frac{d^2\ g\ (\rho_p - \rho_l)}{18\eta}$$

Equation B1

As per the methods of BS 1377-2 (BSI, 1990b), the soil samples were mixed with a dispersant (sodium hexametaphosphate , 2g/L) and DI water for a minumim of four hours. The soil slurry was then placed in a 1L sedimentation cylinder and topped up with DI water to the 1000mL graduation line. The cyclinder was then turned end over end for a period of 1 minute and placed into a water bath. A hydrometer (Figure B 3) was inserted into the cylinder and readings taken at specified time intervals (t) along with temperature (T) measurements. The true hydrometer reading (R_h) was obtained by adding the observed reading (R_h') to the meniscus correction value (C_m).

Figure B 2: Sedimentation cylinder	**Figure B 3: Hydrometer**
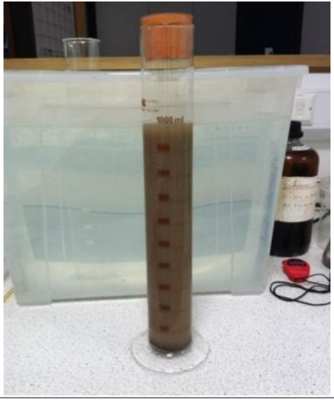	

The equivalent particle diameter (D) can then be caculated using Equation B2 .

$$D = 0.005531\sqrt{\frac{\eta H_r}{(\rho_p - 1)t}}$$

Equation B2

The results were plotted as a semi-logarithmic PSD curve as shown in Table B 2 to Table B 4. The soil texture classifications are also shown in Figure B 4.

Table B 2: Particle Size Distribution – Soil U

Elapsed *t* (min)	*T* (°C)	R_h'	$R_h = R_h' + C_m$	H_r (mm)	η (mPa s)	*D* (μm)	$R_d = R_h' - R_o'$	**% finer than D**
1	22	22.5	23	116.6	0.979	46.0	23	74.7
1.5	22	22	22.5	118.6	0.979	37.9	22.5	73.1
2	22	21	21.5	122.4	0.979	33.3	21.5	69.8
3	22	20.5	21	124.3	0.979	27.4	21	68.2
4	22	19.5	20	128.2	0.979	24.1	20	65.0
6	22	18.5	19	132.1	0.979	20.0	19	61.7
8	22	18	18.5	134.0	0.979	17.4	18.5	60.1
16	22	16.5	17	139.8	0.979	12.6	17	55.2
32	22	15.5	16	143.6	0.979	9.0	16	52.0
65	22	13.5	14	151.4	0.979	6.5	14	45.5
120	22	12.5	13	155.2	0.979	4.8	13	42.2
251	22	11	11.5	161.0	0.979	3.4	11.5	37.4
1158	22	8.5	9	170.7	0.979	1.6	9	29.2
1689	22	7.5	8	174.5	0.979	1.4	8	26.0
2913	22	7	7.5	176.5	0.979	1.0	7.5	24.4
7149	22	6	6.5	180.3	0.979	0.7	6.5	21.1
8843	22	6	6.5	180.3	0.979	0.6	6.5	21.1

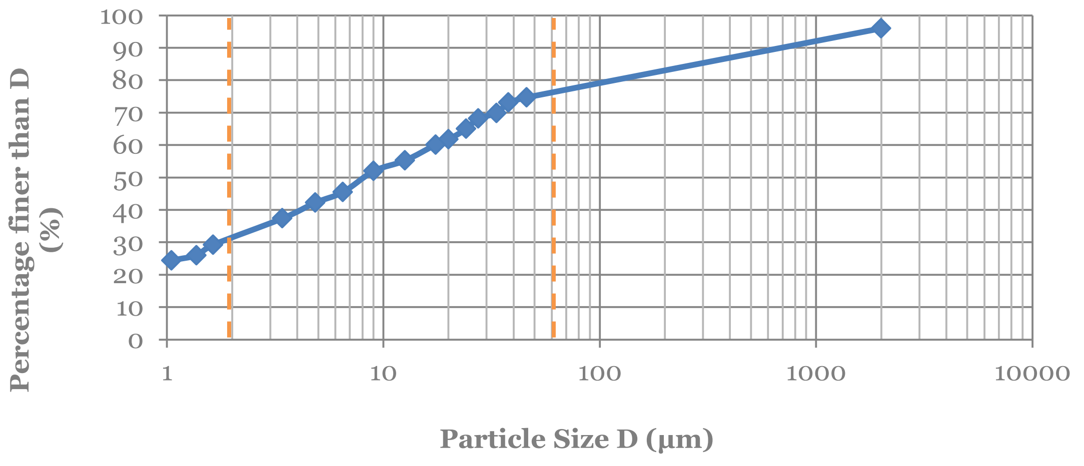

Table B 3: Particle Size Distribution – Soil V

Elapsed ***t*** (min)	***T*** (°C)	R_h'	$R_h = R_h' + C_m$	H_r (mm)	η (mPa s)	D (μm)	$R_d = R_h' - R_o'$	**% finer than D**
0.5	22	22	22.5	118.6	0.979	65.6	22.5	73.1
1	22	21	21.5	122.4	0.979	47.1	21.5	69.9
1.5	22	20	20.5	126.3	0.979	39.1	20.5	66.6
2	22	19.5	20	128.2	0.979	34.1	20	65.0
3	22	19	19.5	130.1	0.979	28.1	19.5	63.4
4	22	18.5	19	132.1	0.979	24.5	19	61.7
8	22	17	17.5	137.9	0.979	17.7	17.5	56.9
16	22	15.5	16	143.6	0.979	12.8	16	52.0
32	22	14	14.5	149.4	0.979	9.2	14.5	47.1
60	22	12.5	13	155.2	0.979	6.9	13	42.2
120	22	11	11.5	161.0	0.979	4.9	11.5	37.4
160	22	10.5	11	162.9	0.979	4.3	11	35.7
1061	22	8	8.5	172.6	0.979	1.7	8.5	27.6
1314	22	7.5	8	174.5	0.979	1.6	8	26.0
1450	22	7	7.5	176.5	0.979	1.5	7.5	24.4
1948	22	6.5	7	178.4	0.979	1.3	7	22.7
3020	22	6	6.5	180.3	0.979	1.0	6.5	21.1
4278	22	6	6.5	180.3	0.979	0.9	6.5	21.1
8478	22	5.5	6	182.2	0.979	0.6	6	19.5
10172	22	5	5.5	184.2	0.979	0.6	5.5	17.9

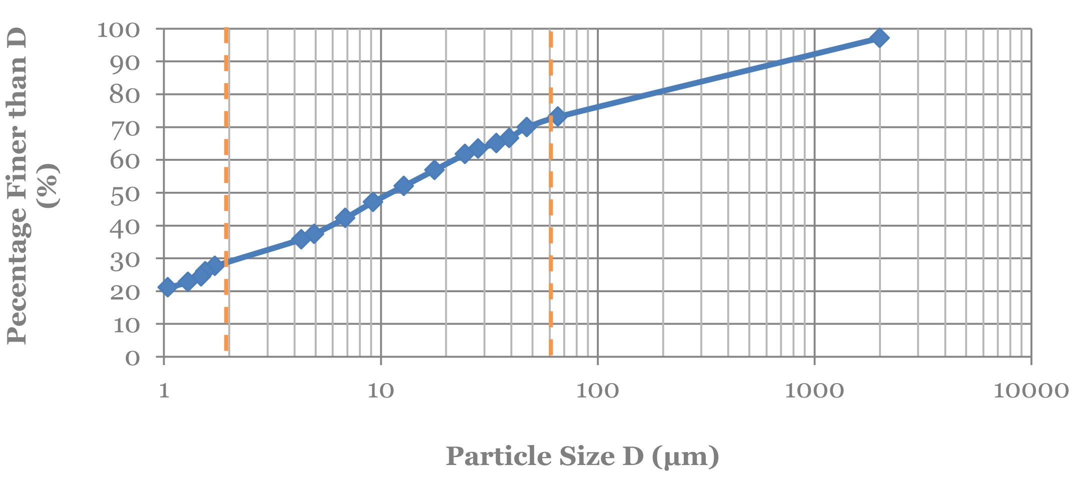

Table B 4: Particle Size Distribution – Soil W

Elapsed *t* (min)	*T* (°C)	R_h'	$R_h = R_h' + C_m$	H_r (mm)	η (mPa s)	*D* (µm)	$R_d = R_h' - R_o'$	% finer than D
0.5	21	27.5	28	78.9	0.979	53.5	24	76.9
1	21	26.5	27	83.2	0.979	38.9	23	73.7
2	21	25.5	26	87.5	0.979	28.2	22	70.5
4	21	24	24.5	93.9	0.979	20.6	20.5	65.7
8.5	21	21.5	22	104.6	0.979	14.9	18	57.7
17.5	21	19	19.5	115.4	0.979	10.9	15.5	49.6
30	21	17	17.5	123.9	0.979	8.7	13.5	43.2
60	21	15	15.5	132.5	0.979	6.3	11.5	36.8
90	21	13.5	14	138.9	0.979	5.3	10	32.0
1045	21	8	8.5	162.5	0.979	1.7	4.5	14.4
1521	21	7	7.5	166.8	0.979	1.4	3.5	11.2
2661	21	6	6.5	171.1	0.979	1.1	2.5	8.0
0.5	21	27.5	28	78.9	0.979	0.5	24	76.9

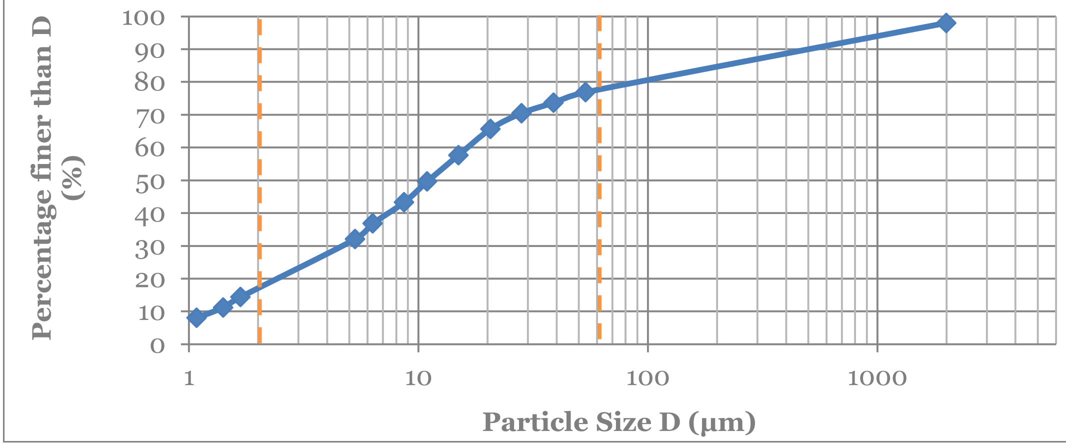

Figure B 4: Soil Texture Classification

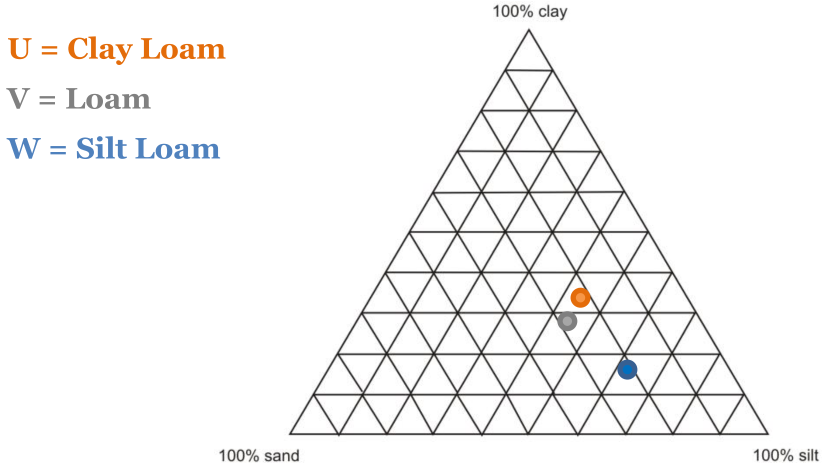

Sources: Adapted from Sandeen (2010)

Further analysis of the curves produced can be achieved by comparing the Coefficient of Uniformity (C_U) and Coefficient of Curvature (C_Z), which can be calculated from Equation B 3 and Equation B 4, where D_{60} is th particle size at 60% finer , D_{30} is the particle size at 30% finer and D_{10} is the particle size at 10% finer (ASTM, 2011). C_U describes the uniformity of the particle size while while C_Z provides a measure of the shape of the curve between the 60% passing and 10% passing segment. A C_U value of greater than 4 and C_Z value of between 1 and 4 is indicative of a well graded soil.

$$\boldsymbol{C_U = \frac{D_{60}}{D_{10}}}$$

Equation B 3

$$\boldsymbol{C_Z = \frac{D_{30}^2}{D_{60}D_{10}}}$$

Equation B 4

Table B 5: Curve Coefficients

	U	**V**	**W**
Coefficient of Uniformity *(C_U)*	175	220	12
Coefficient of Curvature *(C_Z)*	1.9	2	1.2
Grading	Well Graded	Well Graded	Well Graded

Atterberg limits

The plasticity of soils is commonly determined using a series of tests devised in the early 1900s by Atterberg (1911) and developed further by Casagrande (1932). These limits relate to the property changes witnessed in fine grained soils upon the addition of water. Depending on the quantity of water added, the soil can be described as being in one of the following states: solid, semi-solid, plastic and liquid. Each state will display a different consistency and behaviour and the boundaries between each stage, shrinkage limit (SL), plastic limit (PL) and liquid limit (LL), are known collectively as the Atterberg limits. They are routinely determined using the procedures outlined in in BS 1377-2 (BSI, 1990b).

For the purpose of this study, the aim was to test both the PL and LL in order to determine the PI. For the plastic limit test, a 20g soil sample was mixed with water until cohesive enough to be moulded into a ball. This material was subsequently divided into two 10g samples which could then be further divided into four equal parts (Figure B 5). Each of these sub-samples was then rolled by hand into a thread of approximately 3mm diameter and then reformed into a ball. Examples of the soil threads are shown in Figure B 6. This process was repeated until the thread could no longer be formed due to the material drying out and crumbling. This point was defined as the plastic limit of the material. The procedure was repeated for the other 3 subsamples and the resulting material transferred to a container and its moisture content determined. The same process was then replicated for the other 10g sample and the results compared to confirm that there was no more than a 1% variance.

Figure B 5: Equipment for PL test	**Figure B 6: Soil Thread**
	

For the liquid limit test, the cone penetrometer is the most commonly used method. In this case a 300g sample of the soil was used and mixed with water until a thick, homogenous paste was formed. This material was placed into a metal cup, ensuring that a level suface was achieved on top. This filled cup was then placed under the penetrometer with the tip of the cone just touching the soil surface. The cone was released for a period of 5 seconds and locked into position allowing penetration distance to be be calculated. The soil was then removed from the cup and its moisture content determined. This processs was repeated for at least two additional moisture contents, allowing the moisture content corresponding to a target penetration distance of 20mm to be calculated.

Figure B 7: Equipment for LL test	**Figure B 8: Tip of cone touching soil surface for initial Reading**
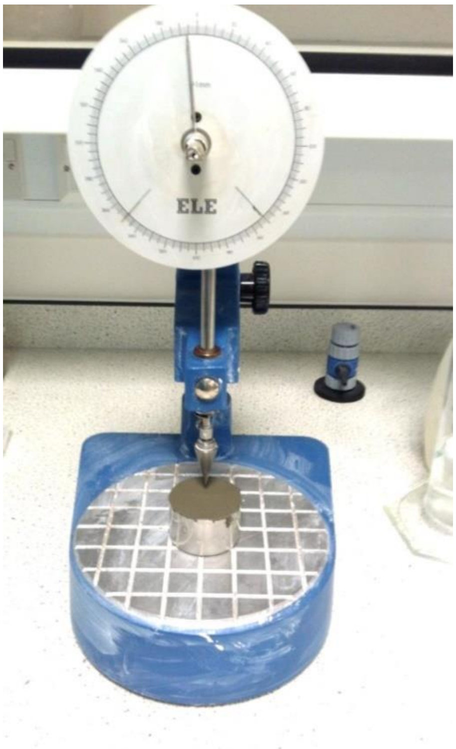 	

Table B 6: Atterberg Limits (Soil U)

Plastic Limit:	**1st 10g sample**	**2nd 10g sample**
Mass of wet soil (g)	7.246	9.758
Mass of dry soil (g)	6.112	8.173
Moisture Content (%)	**15.7%**	**16.3%**

Liquid Limit:	**Moisture Content 1**			**Moisture Content 2**			**Moisture Content 3**			**Moisture Content 4**		
Initial Gauge Reading (mm)	0.0	0.0	0.0	0.0	0.0	0.0	0.0	0.0	0.0	0.0	0.0	0.0
Final Gauge Reading (mm)	12.3	10.2	11.0	25.8	12.3	12.6	19.9	17.8	18.2	25.9	25.8	24.2
Average Reading (mm)	**11.2**			**12.9**			**18.6**			**25.1**		
Mass of wet soil (g)	2.23			1.46g			1.97g			2.66g		
Mass of dry soil (g)	1.72			1.11			1.45			1.87		
Moisture Content (%)	**22.9%**			**24.0%**			**26.4%**			**30.0%**		

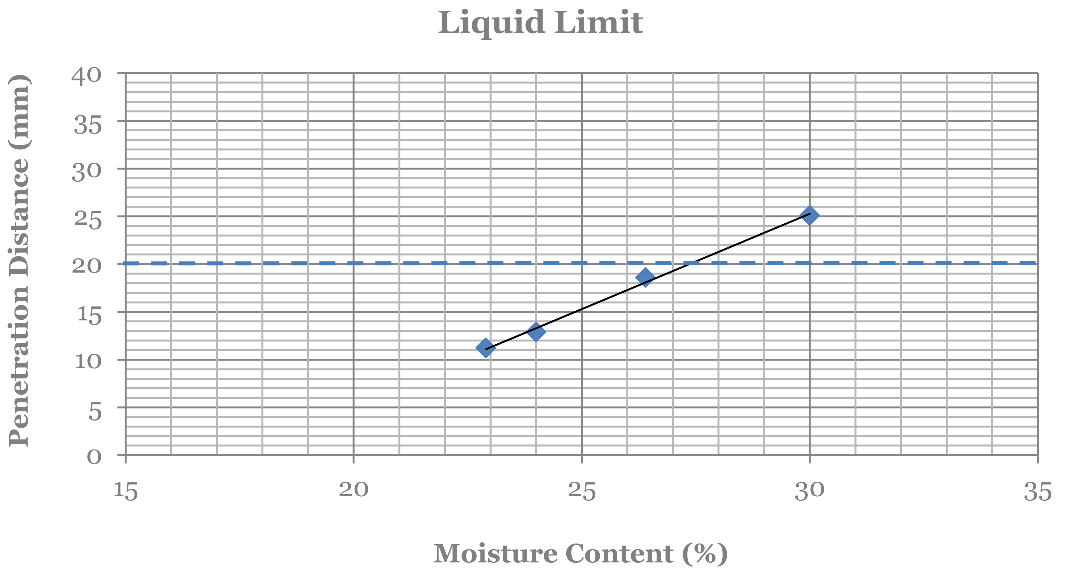

LL = Moisture Content at 20mm	**27.3%**
PL (Average)	**16.0%**
PI (LL – PL) =	27.3% - 16.0% = **11.3%**

Table B 7: Atterberg Limits (Soil V)

Plastic Limit:	**1st 10g sample**						**2nd 10g sample**					
Mass of wet soil (g)	6.719						9.234					
Mass of dry soil (g)	5.771						7.850					
Moisture Content (%)	**14.1%**						**15.0%**					
Liquid Limit:	**Moisture Content 1**			**Moisture Content 2**			**Moisture Content 3**			**Moisture Content 4**		
Initial Gauge Reading (mm)	0.0	0.0	0.0	0.0	0.0	0.0	0.0	0.0	0.0	0.0	0.0	0.0
Final Gauge Reading (mm)	8.4	9.1	8.4	11.4	13.3	11.2	13.1	14.0	14.6	21.3	18.7	21.5
Average Reading (mm)	8.6			12.0			13.8			20.8		
Mass of wet soil (g)	4.80			3.25			3.95			2.29		
Mass of dry soil (g)	3.74			2.44			2.94			1.66		
Moisture Content (%)	**22.0%**			**24.9%**			**25.6%**			**27.5%**		

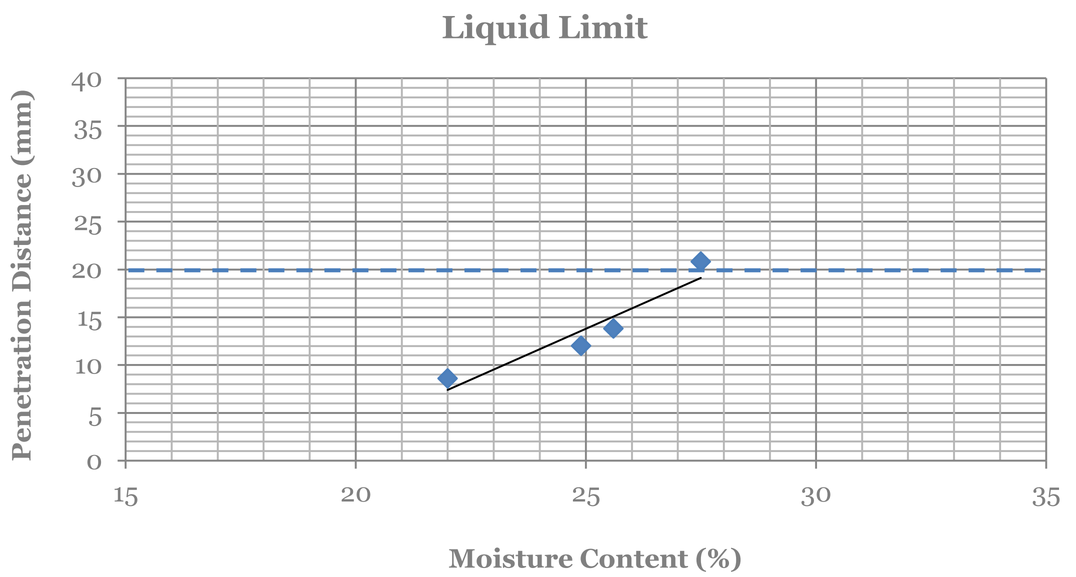

LL = Moisture Content at 20mm	**27.9%**
PL (Average)	**14.6%**
PI (LL – PL) =	27.9% - 14.6% = **13.3%**

Table B 8: Atterberg Limits (Soil W)

Plastic Limit:	**1st 10g sample**	**2nd 10g sample**
Mass of wet soil (g)	8.50	11.65
Mass of dry soil (g)	7.16	10.14
Moisture Content (%)	**15.8%**	**14.8**

Liquid Limit:	**Moisture Content 1**			**Moisture Content 2**			**Moisture Content 3**			**Moisture Content 4**		
Initial Gauge Reading (mm)	10.4	9.9	10.0	10.4	9.1	8.5	8.7	8.6	-	11.8	11.0	-
Final Gauge Reading (mm)	13.9	12.9	13.2	20.1	19.1	18.3	35.4	35.5	-	42.9	42.9	-
Average Reading (mm)	**3.2**			**9.8**			**26.8**			**31.5**		
Mass of wet soil (g)	8.88			6.47			6.13			10.55		
Mass of dry soil (g)	7.22			5.08			4.40			7.45		
Moisture Content (%)	**18.7%**			**21.5%**			**28.2%**			**29.4%**		

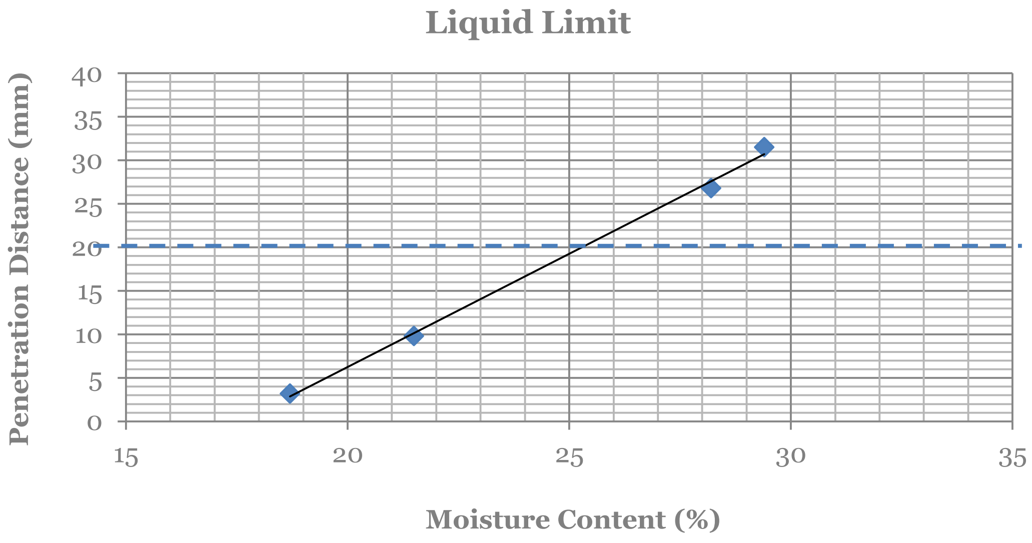

LL = Moisture Content at 20mm	**25.4%**
PL (Average)	**15.3%**
PI (LL – PL) =	25.4 - 15.3% = **10.1%**

Compaction Behaviour

The moisture content of earthen materials has an important influence on its behaviour, including the workability and plasticity of the soil mixture, the maximum dry density which can be achieved during compaction and the degree of shrinkage observed upon drying. If too little water is added during moulding, the material will be very dry, stiff and often difficult to mix homogenously as well as limiting the cohesiveness between the soil particles. If too much water is added, then the material may exceed its liquid limit and compaction will become difficult if the material begins to behave more like a liquid. The optimum moisture content (OMC) which corresponds to the maximum dry density value, varies depending not only on the soil's characteristics (e.g. particle size distribution) and the compactive effort which is applied to the soil (Craig, 2004). The aim of compaction is to pack the individual soil particles closer together, reducing the volume of air and increasing the density of the soil. This can be achieved through number of methods, either static, vibro-static or dynamic, and can involve either manual or mechanical techniques. As such the OMC will be dependent not only on the soil type but also on the specific manufacturing technique used.

Typically the OMC (w_{opt}) value is obtained through the Proctor test, or modified Proctor test, as outlined in BS 1377-4 (BSI, 1990a). This method involves compacting the soil in a metal cylindrical mould, of a known volume, using a metal rammer to deliver a standard compactive effort to the material and then calculating the bulk density (ρ) from the soil mass (m) and the mould volume (V). The process is repeated over a range of different moisture contents with results plotted as a graph showing the relationship between dry density (ρ_d) and moisture content (w) using

Equation B5. The maximum ρ_d value and corresponding w_{opt} value can then be obtained from the maximum point on the best fit curve.

$$\boldsymbol{\rho_d} = \frac{100\rho}{100 + w}$$

Equation B5

Whilst the Proctor test is the most common method for use in most civil engineering applications, some authors have argued that the w_{opt} value obtained from this method is not always equal to the optimum moulding water content required for brick production (Kouakou and Morel, 2009). This is because the compaction effort utilised in the Proctor test is not always representative of the compaction achieved during the brick moulding process. For example, a traditional adobe brick generally requires a moulding moisture content (w_m) which is higher than the w_{opt} in order to assist in pouring the material into the mould. Similarly Maskell et al. (2013) has demonstrated that earth bricks produced using an extrusion method also required a moulding water content which was slightly greater than the w_{opt} obtained from the modified Proctor test, otherwise surface cracks became visible on the bricks. On the other hand, CEB systems tend to use low moisture content which are much closer to the w_{opt}. Kouakou and Morel (2009) divide these different systems into two categories: dry moulding and wet moulding techniques which have w_m values of 8-15% and 16-35% respectively. Therefore the OMC should ideally be calculated in relation to the particular compactive effort used in manufacturing the brick.

In this study, the optimum moulding water content for each of the different soils was measured using the same compaction technique and mould as proposed for the brick prototypes. This involved filling the brick mould (40 x 40 x 160mm) with soil in three layers, with each layer being compacted using 25 strokes of the hammer/tamper. The rest of the test procedure was as previously described for the Proctor method. The results are shown in Tables B9 to B11.

Table B 9: Compaction Behaviour (Soil U)

Mould volume *(cm^3)*	256				
Mass of soil, m_1 *(g)*	478.7	529.9	540.2	535.0	517.1
Mass of wet sample, m_2 *(g)*	0.746	0.769	0.729	0.391	0.506
Mass of dry sample, m_3 *(g)*	0.659	0.668	0.629	0.334	0.425
w *(%)*	**13.2**	**15.1**	**15.9**	**17.1**	**19.1**
Bulk density, ρ *(kg/m^3)*	187	2070	2110	2090	2020
Dry density, ρ_d *(kg/m^3)*	**1650**	**1800**	**1820**	**1790**	**1700**
w_{opt} (%)	**16.2%**	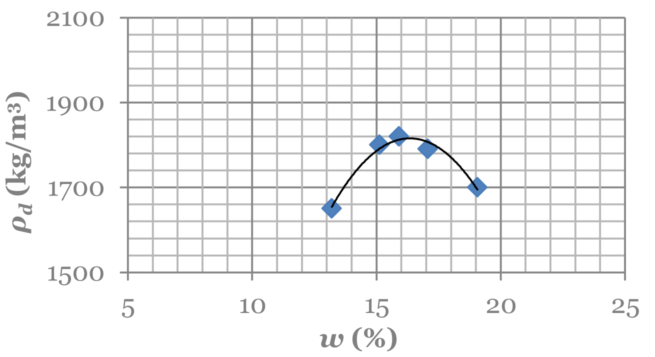			
Max dry density, ρ_d *(kg/m^3)*	**1820**				

Table B 10: Compaction Behaviour (Soil V)

Mould volume *(cm^3)*	256				
Mass of soil, m_1 *(g)*	492	571	596	604	548
Mass of wet sample, m_2 *(g)*	3.99	8.61	6.36	3.78	4.46
Mass of dry sample, m_3 *(g)*	3.56	7.46	5.38	3.14	3.62
w *(%)*	**12.1**	**15.4**	**18.2**	**20.4**	**23.2**
Bulk density, ρ *(kg/m^3)*	1920	2230	2330	2360	2140
Dry density, ρ_d *(kg/m^3)*	**1710**	**1930**	**1970**	**1960**	**1740**
w_{opt} (%)	**17.8%**	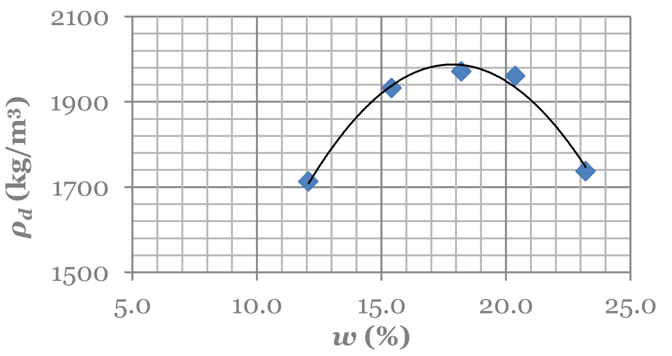			
Max dry density, ρ_d *(kg/m^3)*	**1980**				

Table B 11: Compaction Behaviour (Soil W)

Mould volume (*cm*^{3})	256				
Mass of soil, m_1 (*g*)	484	520	568	553	512
Mass of wet sample, m_2 (*g*)	0.386	0.622	1.943	1.23	1.193
Mass of dry sample, m_3 (*g*)	0.357	0.56	1.71	1.036	0.979
w (%)	**8.1**	**11.1**	**13.6**	**18.7**	**21.9**
Bulk density, **ρ** (*kg/m*^{3})	1.89	2.03	2.22	2.16	2.00
Dry density, ρ_d (*kg/m*^{3})	**1750**	**1830**	**1950**	**1820**	**1640**
w_{opt} (%)	**14.4%**	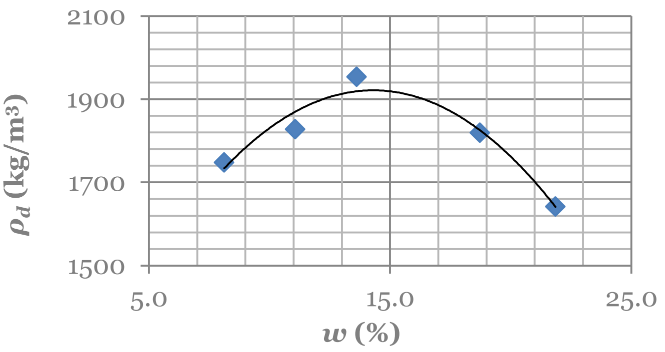			
Max dry density, ρ_d (*kg/m*^{3})	**1920**				

Electrical Conductivity

The electrical conductivity of a soil is a measure of the ions present in a soil solution and hence is commonly used as an indicator of soil salinity (Rhoades et al., 1999). As the minerals in soils weather they release salts. Upon the addition of water, these salts will disassociate and form an ionic solution. The electrical conductivity of the soil therefore increases with number of ions, or salts, which are present in the soil. Electrical conductivity is therefore commonly used to provide a numerical value for the total dissolved salts is an aqueous sample. The electrical conductivity test does not identify which salts are present and simply indicates the overall concentration of salts. The apparent soil electrical conductivity is also affected by other factors including the soil's clay content and mineralogy, the water content, the organic matter content, the soils bulk density and temperature (Corwin and Lesch, 2005). These factors must therefore be taken into account when conducting measurements.

In this study electrical conductivity was measured using a handheld HM Digital EC-3 meter which consists of two metal electrodes across which a constant voltage is applied. This induces the flow of an electric current through the solution which will vary depending on the concentration of dissolved ions. The meter was first of all calibrated using a KCl solution (1413 µS). A soil slurry consisting of 2 parts DI water and 1 part soil was mixed using a magnetic stirrer and then left to stand for 30 minutes. The soil was gently stirred prior to inserting the electrodes and a reading taken once the measurement had stabilised. Since EC is also temperature dependent, a temperature controlled water bath was used in order to maintain a temperature of 25 ±1°C. The meter was removed and the electrodes cleaned prior to the next test. Results were recorded in microSiemens per centimeter (µS/cm) and calculated as an average of 3 readings as shown in Table B 1.

Table B 12: Electrical Conductivity (25°C)

	U	V	W
Electrical Conductivity (µS/cm)	**640** (±2)	**115** (±3)	**169** (±2)

Cation Exchange Capacity (CEC)

Another property which measures the behaviour of ions in a soil solution is the cation exchange capacity (CEC). Ion exchange in soils is a process which occurs principally due to the exchange of ions at the clay mineral surfaces and ions in a solution which come into contact with the clay mineral. These ions, known as exchangeable ions, are present in clay minerals due to unbalanced electrical charges. This is a reversible chemical reaction which can involve either positively charged ions or negatively charged ions. The CEC measures the exchanges of positively charged ions which occur at negatively charged sites on the clay (Brindley and

MacEwan, 1953). The most commonly found cations in clay minerals are calcium, magnesium, sodium and potassium. In acidic conditions H+ ions can also replace metallic ions. Divalent ions such as Ca^{2+} and Mg^{2+} are more likely to occupy exchange sites over univalent ions like Na^{+} (Carroll, 1959).

In considering the CEC of a soil sample rather than a pure clay, since CEC is largely governed by the clay-sized fraction, the overall PSD of the soil will influence the quantity of available exchange sites. The CEC will also be influenced by the type of clay minerals present. For example, in the case of kaolinite, which has a neutral 1:1 structure, negatively charged sites are only present as a result of unsatisfied bonds the edges of the crystal structure (Theng, 1972). Kaolinite therefore has a relatively low CEC value (3 – 15 meq/100g). However, smectitie clays such as montmorillonite are known as high activity clays with CEC values of 70 -100 meq/100g. This is primarily due to the 2:1 structure which requires the presence of exchangeable ions between the structural unit as well as the smaller crystal size which provides a greater surface area for ions to be absorbed.

An estimation of overall CEC can be obtained from the Methylene Blue tests. Other methods which allow a more detailed analysis of the different exchangeable cations require that soil exchange sites are first forced into solution (Robertson et al., 1999). This can be achieved using various soil extractants which can extract either multiple elements or elements of particular interest (Ross and Ketterings, 1995). The elements present are then determined using techniques such as flame atomic absorption spectrometry (FAAS) or inductively coupled plasma (ICP). In this case the Methlyene Blue (MB) test was first of all performed on all of the soils using the methods outlined in BS EN 933-9 (BSI, 2013a) . A soil slurry was first prepared using a known mass of soil (0 to 2mm fraction) and 500ml DI water. This was mixed using a magnetic mixer for a period of 5 minutes. Under continued mixing, MB solution (10g/L) was then added dropwise to the soil using a burette. After each addition of the dye, a pipette was then used to remove a drop of the mixture and transfer this to filter paper. The this process was then repeated for each addition of dye until a visible 'blue halo' was formed around the material on the filter paper as shown in Figure B 9 and Figure B 10. The final volume of methylene blue (V_1) required to form a permanent halo was then recorded for each soil type.

Figure B 9: MB test - No halo	**Figure B 10: MB test - Halo present**
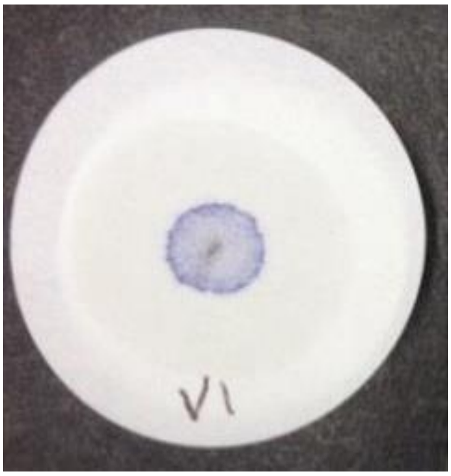	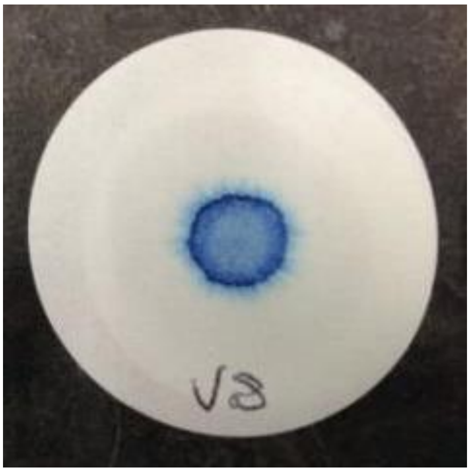

The methylene blue value (MB) was calculated using Equation B 6 where m_1 is the dry mass of the initial soil sample. The results are shown in Table B 13.

$$MB = \frac{V_1}{m_1} X\, 10$$

Equation B 6

The CEC can be calculated form the MB values using Equation B 7 (Cokca and Birand, 1993) where N_{mb} is the normality of the MB which in this case is 0.031 meq/L.

$$CEC = \frac{100}{m_1} V_1 N_{mb}$$

Equation B 7

The Specific Surface Area (SSA) can also be determined from the MB value using Equation B 8 where A_v is Avogadro's number (6.02 x 10^{23}/mol) and A_{MB} is the area covered by an individual MB molecule, which is estimated to be 130 $Å^2$ (Santamarina et al., 2002; Yukselen and Kaya, 2008).

$$\boldsymbol{SSA = \frac{1}{319.87}\frac{1}{200}V_1 A_V A_{MB}\frac{1}{10}}$$

Equation B 8

The resulting CEC and SSA values for each soil type are also shown in Table B 13. From this test method the CEC values of the 3 soil types are relatively similar and comparable to that of a low clay content soil.

Table B 13: MB Test

	U	V	W
Soil dry weight, m_1 (g)	4	5	4
MB Volume, V_1 (ml)	5	8	7
MB (g/kg)	12.5	16	17.5
Cation Exchange Capacity, CEC (meq/100 g clay)	3.9	5.0	5.4
Specific Surface Area, SSA (m^2/g)	6.1	9.8	8.6

In addition to the MB test, further analysis of the exchangeable cations was performed using the ICP method in order to obtain more detailed information on the quantities of the elements of interest present. Two types of analysis were performed, one of which used the aqua regia soil extract method (Melaku et al., 2005) to analyse the total elemental content of Ca, Mg, Na and K, while the other analysed DI water extracts in order to determine the effective CEC. All samples were analysed in triplicate by the Dept. of Chemistry at the University of Strathclyde using an Agilent 7700 ICP-MS. The results are summarised in Table B 14.

Table B 14: ICP Results

Aqua Regia Extract	**U**	**V**	**W**
Na (mg/kg)	2,761 (±100)	2,181 (±251)	1,894 (±215)
Mg (mg/kg)	11,440 (±1,483)	34,410 (±3,333)	42,577 (±788)
K (mg/kg)	29,129 (±5,744)	36,620 (±2,420)	43,370 (±22,065)
Ca (mg/kg)	1,665 (±103)	3,383 (±1,042)	3,464 (±649)
DI Water extract	**U**	**V**	**W**
Na (mg/kg)	22 (±4)	Nil/trace	Nil/trace
Mg (mg/kg)	558 (±20)	1,459 (±58)	997 (±106)
K (mg/kg)	268 (±9)	286 (±6)	358 (±39)
Ca (mg/kg)	751 (±33)	2,300 (±52)	1,734 (±121)

The mg/kg value, which is equivalent to parts per million (ppm) can also be convert into a meq/100g values by dividing by the appropriate conversion factors for each element (Na = 230, Mg = 121, K = 391 and Ca = 200) (Marx et al., 1996). These converted values, along with the estimated CEC values which are calculated by adding the values for each of the elements, are shown in Table B 15. Since the ICP analysis was conducted only on the fine clay fraction, the results for the DI water extract are slightly higher than that of the MB tests which are performed on the 0 to 2mm fraction. The values are within the ranges expected for kaolinite (3 -1 5 meq/100g) or illite (10-40 meq/100g) (Carroll, 1959).

Table B 15: ICP Results - Converted

Aqua Regia Extract	**U**	**V**	**W**
Na (meq/100g)	12 (±0.4)	7 (±1.1)	8 (±0.9)
Mg (meq/100g)	95 (±12.3)	227 (±27.5)	352 (±6.5)
K (meq/100g)	74 (±14.7)	76 (±6.2)	111 (±56.4)
Ca (meq/100g)	8 (±0.5)	17 (±5.2)	17 (±3.2)
Total (meq/100g)	**189**	**328**	**488**
DI Water extract	**U**	**V**	**W**
Na (meq/100g)	0.1 (±0.0)	Nil/trace	Nil/trace
Mg (meq/100g)	5 (±0.1)	12 (±0.5)	8 (±0.9)
K (meq/100g)	1 (±0.0)	1 (±0.0)	1 (±0.1)
Ca (meq/100g)	4 (±0.2)	11 (±0.3)	9 (±0.6)
Total (meq/100g)	**9**	**24**	**18**

Elemental Analysis (EDS)

In addition to the analysis of exchangeable cations, an overall elemental analysis was also performed using Scanning Electron Microscope - Energy Dispersive X-ray Spectroscopy (SEM-EDS). The principal behind this method is that a focused beam of electrons is directed towards the sample. The backscattered electron images in the SEM then produce compositional contrasts resulting from different atomic number elements allowing for a localised elemental analysis to be performed. The soil samples were mounted and then sputter coated in gold to create a conducting surface before being placed in the SEM chamber (HITACHI S-3700 SW). The samples were then analysed under vacuum with Oxford's INCA system which was used to generate X-ray spectra and relative weight percentages of the elements found in each sample (Table B 16). The resulting EDS spectra are also shown in Figure B 11 to Figure B 13.

Table B 16: Soil Composition

Element	**Oxide**	**U** – Weight %	**V** – Weight %	**W** – Weight %
Carbon	CO_2	12.15	10.49	16.66
Oxygen	**-**	59.29	61.14	52.83
Sodium	Na_2O	-	0.25	0.38
Magnesium	MgO	0.39	0.63	0.76
Aluminium	Al_2O_3	9.70	7.84	7.27
Silicon	SiO_2	14.77	14.76	16.27
Potassium	K_2O	1.35	1.69	2.01
Titanium	TiO_2	0.60	0.43	0.45
Iron	Fe_2O_3	1.76	2.77	3.37

Figure B 11: EDS Spectra – Soil U

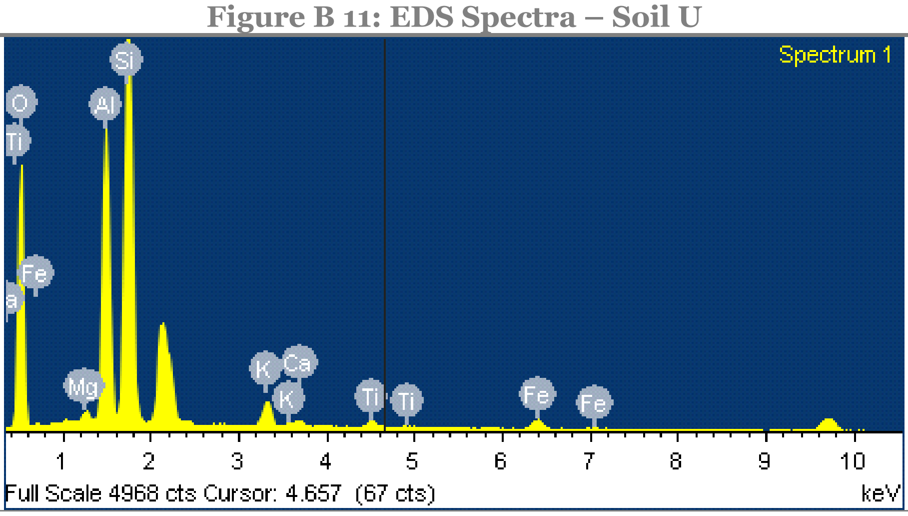

Figure B 12: EDS Spectra – Soil V

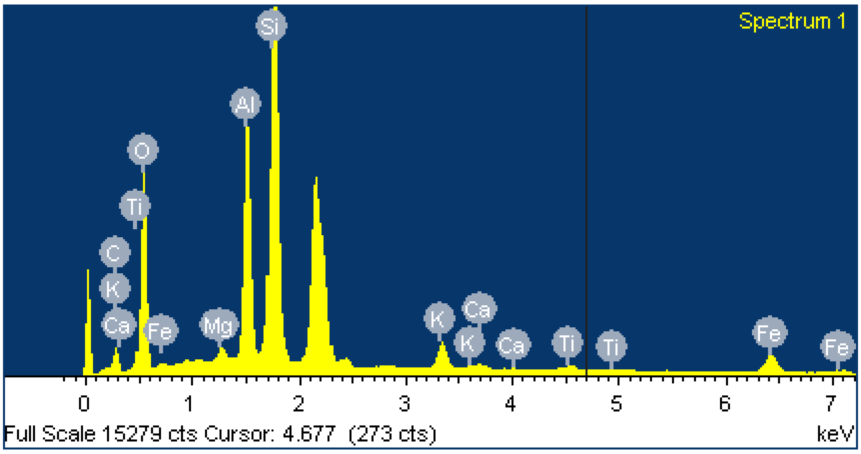

Figure B 13: EDS Spectra – Soil W

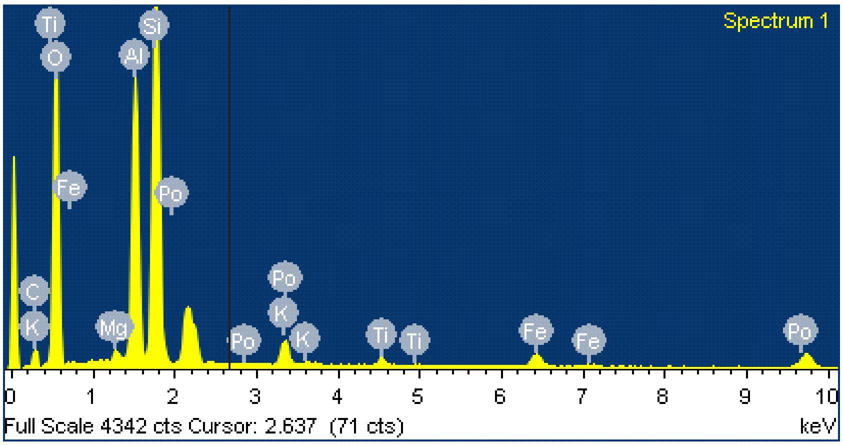

Mineralogy (XRD)

As discussed in Chapter 3, the mineralogy of the soils was analysed using XRD which allows detailed information about the structure of crystalline materials to be obtained (Harris and White, 2008). This form of non-destructive analysis relies on the use of X-rays (the part of the electromagnetic spectrum with a wavelength between 10^{-3} and 10 nm) which are produced by releasing high velocity electrons from a cathode and then colliding those electrons with a metal target. An X-ray diffractor will therefore normally consist of an X-ray tube containing a filament electron source, and a target, also known as the anode. The main principle of XRD involves X-rays of a fixed wavelength being produced and aimed at the sample with the intensity of the reflected radiation then being recorded using a goniometer.

In this study, the clay minerals present in the soil were determined using the orientated aggregate mount method (Poppe et al., 2001). This involved firstly separating the clay fraction of the soil and then transferring this material to a glass slide. A 5g soil sample was first mixed with a dispersant (0.25g of sodium hexametaphosphate) and then centrifuged for 6 minutes at 500 RPM to remove the clay fraction. The clay fraction was then decanted into another centrifuge tube and rinsed 3 times in DI water, with the supernatant being removed after each rinse following 30 minutes in the centrifuge at 2500 RPM. The resulting clay suspension was then mounted onto a clean glass microscope slide using a pipette and dried overnight in an oven at 50°C. Additional treatments were also performed on samples to provide further information for mineral identification. For example, selected samples were prepared on heat resistant glass slides allowing for heat treatments (350°C and 550°C) to be conducted in a Carbolite muffle furnace with a temperature dwell time of 30 minutes. In the case of the ethyl glycol (EG) treatments, a glass dessicator was filled with EG to a depth of approximately 1cm. The glass slides were then placed on the upper shelf and the sealed dessicator placed in an oven at 60°C for at least 4 hours (Poppe et al., 2001).

Once prepared, each sample was then carefully loaded into the diffractometer (Bruker D8 Advance) and X-ray diffraction pattern was recorded using a Cu Kα X-ray radiation at a range of 3° to 40°. This range was deemed suitable to provide enough peaks to identify the minerals most commonly found in soils. The diffractometer then measures the intensity of the diffracted beam at specific angles across this range. A wavelength of 1.54060 was used for all samples. The y-axis on the patterns produced is a measure of the peak intensity measured as the number of counts and the x-axis records the diffraction 2θ angles. Using Bragg's Law (Equation B 9), values for the interplanar spacings (*d*) were then obtained used to identify the specific minerals present by comparison with existing references.

$$n\lambda = 2d\ \sin\theta$$

Equation B 9

Figure B 14: Bragg's Law Schematic

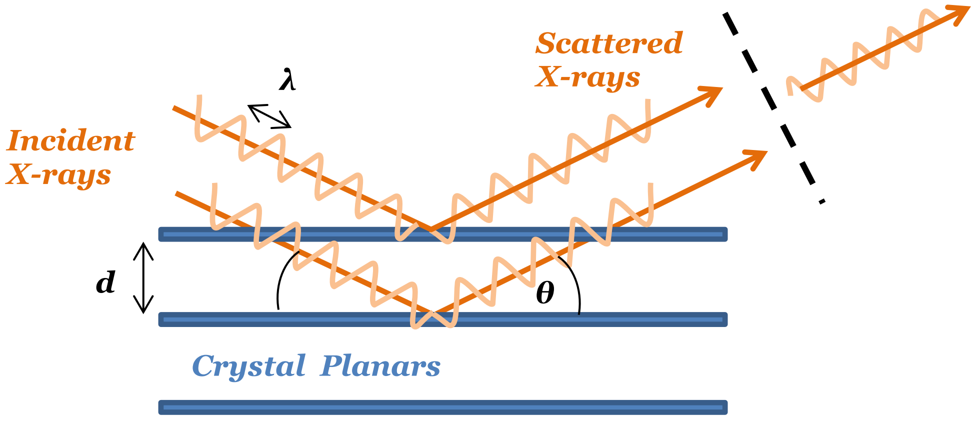

Source: Adapted from Mitchell and Soga (2005)

The diffractograms are shown in Figure B 15 to Figure B 17 where a is the untreated sample, *b* has been heated to 350°C, *c* has been heated to 550°C and *d* is the Ethyl Glycol (EG) treated sample. A semi-quantitative summary of the proportions of the minerals present is also shown in Table B 17.

Figure B 15: XRD – Soil U

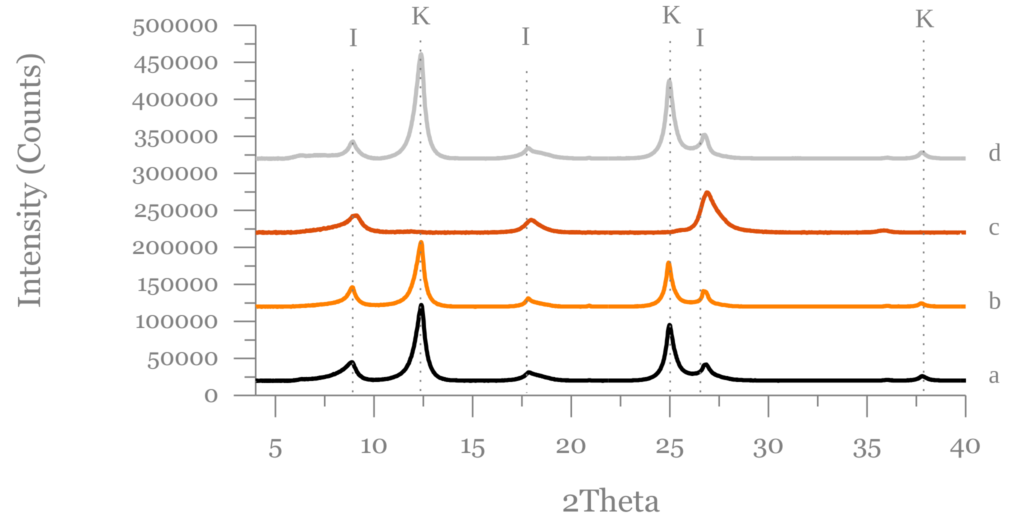

Figure B 16: XRD – Soil V

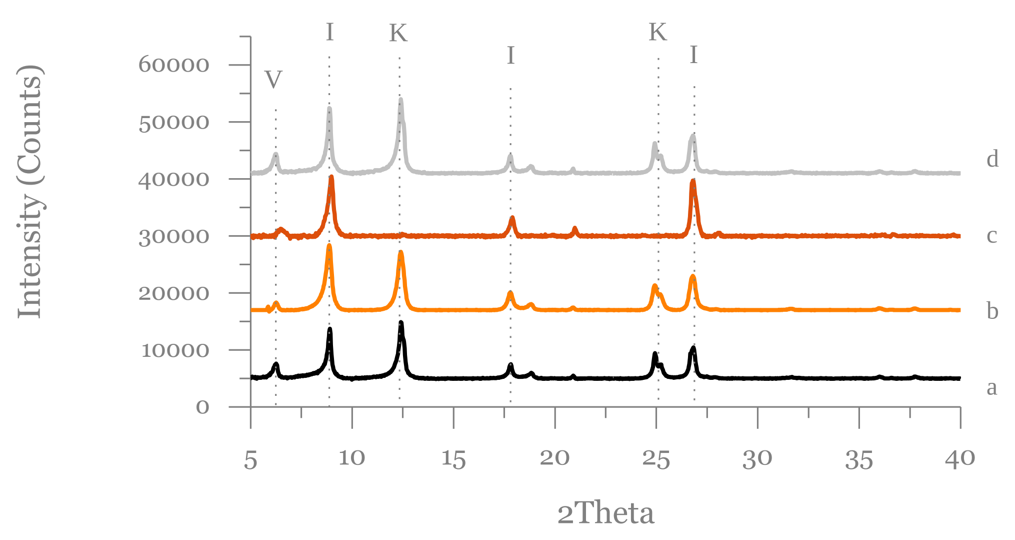

Figure B 17: XRD – Soil W

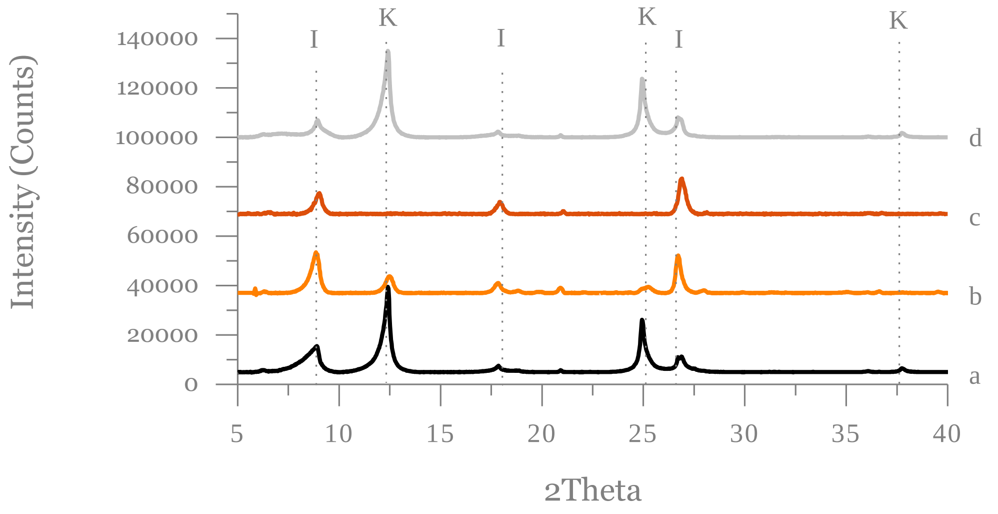

Table B 17: XRD Mineralogy

	U	V	W
Kaolinite	**	**	**
Illite	*	**	*
Muscovite	-	**	*
Montmorillonite	tr	tr	tr
Illite/montmorillonite	*	-	-
Vermiculite	tr	-	-
Chlorite	*	*	*

Dominant (***), major (**), minor (*) and trace (tr).

Appendix C: Trial Study

Prior to the manufacturing of the prototypes, an initial trial study was conducted in order to optimise the production process and make some initial observations regarding the plasticity and cohesiveness of the alginate-soil mixes.

Alginate Preparation

During the initial trial, dissolution of the MBL sodium alginate products took approximately 4 hours using a magnetic mixer using a mixing speed of ~200 RPM. The commercial alginate product (AC) dissolved slightly quicker owing to the smaller particle size. A standard mixing time of 4 hours was therefore deemed adequate for all samples. The milled seaweed and residue products were also mixed with the required amount of DI water to achieve the desired moisture content. For the dental alginate products, as per the methods of Rivera-Gómez et al. (2014), the dry powder was added directly to the soil with no prior dissolution.

Mixing

Mixing trials were conducted using both hand mixing and mechanical mixing techniques. While achieving a homogenous mix was possible by hand, the process was labour intensive and time consuming. On the other hand, mixing a batch of material equivalent to 3 bricks took only 2-3 mins using a mechanical mortar mixer with a rotation speed of 140 RPM. This was therefore selected as the preferred mixing method.

Mix ratios

Trial mixes, consisting of between 0.1 and 2% alginate by weight of the dry soil, were also prepared in order to define appropriate mix ratios. It was observed during this study that dosages of above 1% resulted in a highly viscous, unworkable material which was very difficult to mix with the available equipment. This material was found to form small aggregates coated by the polymer, as shown in Figure C 1, rather than a cohesive mass as observed for the lower dosages. The inadequate mixing for the 1% samples also resulted in poor quality, inhomogeneous brick specimens most of which had severe desiccation cracks. Dosages above 1% were therefore not included in the main study.

Water Content and Compaction

In terms of moulding water content, specimens were also prepared at various ratios with observations made regarding mixing and compaction. Generally, moisture contents below 13% were too dry to form to form a cohesive mix while those above 18% hindered the compaction of the material, in some cases leading to significant air entrapment. These observations were in general agreement with Kouakou and Morel (2009) who describe 15 -22% as the optimum moisture content for pressed adobe blocks which are an intermediate between dry systems like CEB and wet systems like adobe.

Drying

Finally, in terms of drying methods, specimens were dried using three different techniques: natural drying at ambient temperature, oven-drying at 50°C and oven drying at 105°C. For natural drying, the specimens were unable to be removed from mould for at least 3 days while for both of the oven-drying techniques, a 24 hour drying period was sufficient to produce a semi-dry material which could be handled easily. For these specimens, constant mass was achieved following a further 72 hours air-drying after removal from the mould. In comparing the two drying temperatures, at 105°C visible desiccation cracks were apparent in most specimens due to the faster drying rate. The 50°C procedure was therefore adopted as this not only allowed for relatively quick drying times without sacrificing specimen quality, but also allowed direct comparison with Galán-Marín et al. (2010) who also opted for this drying method.

Figure C 1: Trial brick samples

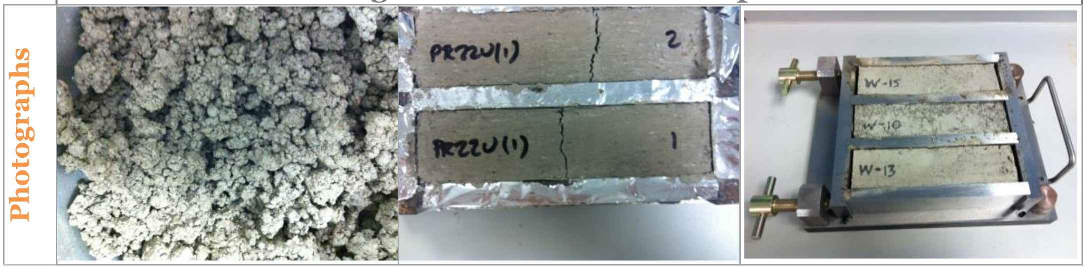

Abrasive Strength

Abrasive strength tests provide a measure of how well a material can withstand the impacts of mechanical erosion to its surface. Abrasive strength is therefore a useful indicator of durability. Some trial tests were conducted on the brick samples in order to give an initial estimation of this property. The test involved applying a given number of strokes to the material surface using a wire brush and measuring the difference in mass before and after brushing (Adam and Agib, 2001). For the purposes of this study, a wooden brush with metal bristles and a 2kg weight attached was used. After weighing the initial mass of the specimen (m_1), the brush was then used to abrade the surface of the sample using a standard procedure of 60 strokes.

After brushing, any loose material was removed and the specimen was reweighed (m_2).The abrasive strength coefficient (C_a) in cm^2 /g was then calculated, taking into account the length of the specimen (l) and the width of the brush (b):

$$C_a = \frac{l\ x\ b}{m_1 - m_2}$$

(Equation D1)

Figure C 2: Abrasive Strength Test

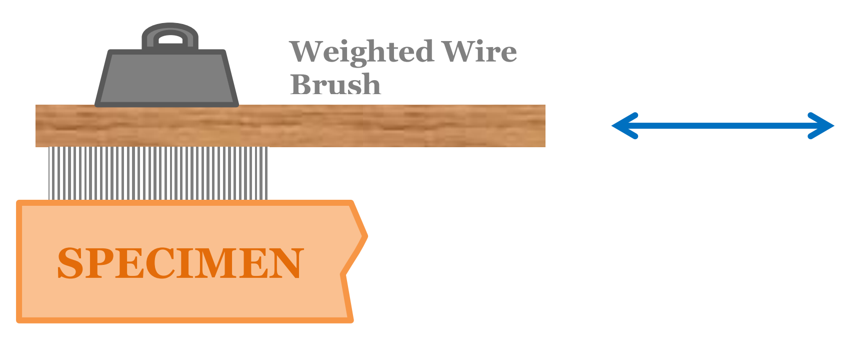

The abrasive strength test results are shown in Figure C 2 with statistical significant differences indicated by an asterix. Specimens which demonstrated an increase in abrasive strength coefficient compared to the relevant control sample include 4 of the soil U specimens (PR22U, PR32U, PR52U and ACU) and one of the soil W specimens (PR22W). For soil V, although there is an indication of conservative improvements with some products, high variability within the results means that these changes are not statistically significant. Indeed the only statistically significant results for soil V are for LHV and DAV where the abrasive strength in fact appears to be reduced. For the soil V specimens, abrading the surface with the brush resulted in larger chunks of material being removed compared to the other soils. The resulting values for the abrasive strength coefficient were found to vary between 8 and 47 cm^2/g. This equates to overall mass losses of between 0.2 and 1.2%. This is slightly lower than the figures reported by Yalley and Manu (2013) for unfired bricks stabilised with cow dung (1.5 - 3.5%). Although three of the samples (PR22, PR44 and PR52) did offer a statistically significant improvement over the control, there was high variability in all of the results. Therefore while in a few cases it does appear that a larger brushing area is required to remove a given amount of material from the brick surface, in general most of the additives did not significantly improve the abrasive strength.

Figure C 3: Variable 2 – Abrasive Strength Coefficient

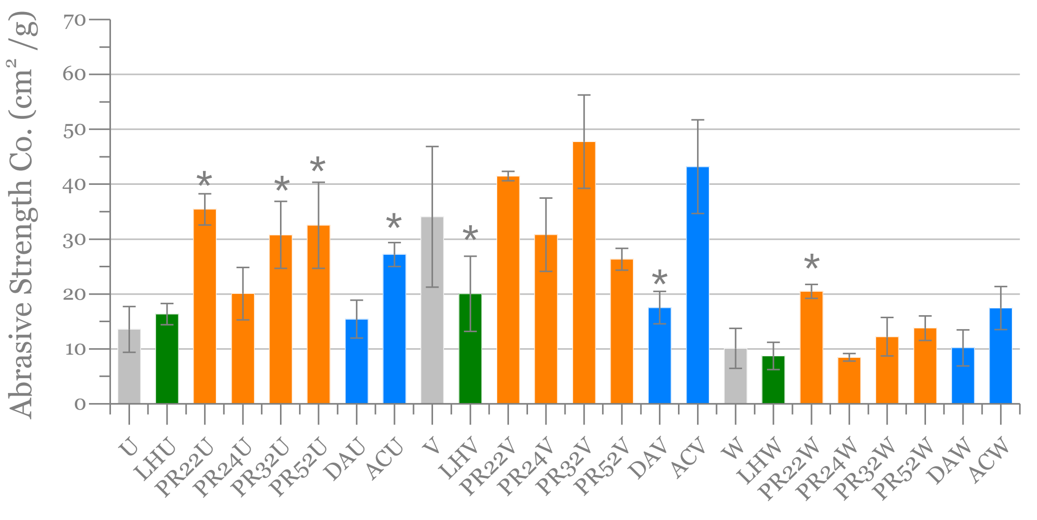

Overall, in relating the results of the abrasive strength tests to those observed in the flexural and compressive strength, PR22 performs particularly well for soils U and W in all three tests. This suggests that this particular additive does impart additional cohesion between the soil particles, particularly for soil W where the greatest relative improvements are observed. While specimens such as PR32U, PR52U and ACU appear to offer an improvement in particle bonding at the surface level, these do not translate to improvements in the overall specimen strength. Furthermore, the DA specimens, which offer improvements in compressive strength for Soil U and W, do not result in significant increases in abrasive strength.

Water Stability

Another trial study was also conducted in order to provide an intial, comparative assessment of the water sensitivy of the samples. Assessment of the water stability of earth masonry materials in generally achieved by comparing the dry compressive strength with the 'wet' compressive strength after the specimens have been submerged in water (Heathcote, 1995)). In the case of unfired materials which are to be used in protected applications, these tests are unsuitable since the material generally disintegrates when fully immersed in water. Other accelerated erosion tests, such as spray or drip tests, aim to simulate the effects of driving rainfall (Heathcote, 2002;Walker, 2004). For those involving a pressurised spray or shower, again this is not representative of the type of conditions which are likely to be experienced internally and would also require much larger samples than the small scale prototypes prepared in this study. A trial study of the drip test method, similar to that described by Yttrup et al. (1981), also highlighted the difficulties is making precise measurements of the resulting pitting depths. This method was therefore also deemed unsuitable since it was not possible to determine accurate differences between the samples.

A simplified test was therefore devised using an adapted verison of the capilliary absorption tests (*BS EN 1015-18:2002* or B*S EN 772-11:2011*) typically used for masonry (BSI, 2002), which offers a less severe method than those which involve full submersion in water. Normally this test is used to determine the initial rate of absorption (C_{wi}) and is useful in determining the most appropriate mortars to be used with a particular masonry unit. In this case, however, it was used to compare the behaviour of the specimens upon exposure to moisture on one surface. The test procedure involved firstly drying the specimens to constant mass in the oven overnight. The dimensions of the face which is to be immersed in water was then measured using a digital caliper. A large tray was filled with DI water, including a supporting mesh material to ensure that the specimens did not touch the base of the container but allowed 5 mm ± 1 mm of the specimen to be immersed in water (Figure C 4). An immersion period of 60s was used for each sample and the water level was kept at the same level for the test duration.

Figure C 4: Water Stability Test

After immersion, the samples were again oven dried for 24 hours allowing the difference in unit mass before (m_1) and after testing (m_1) to be calculated. This was then used to compare the percentage of material lost during the controlled exposure to water for each sample.

$$\text{Mass loss (\%)} = \frac{m_1 - m_2}{m_1} \text{ x } 100$$

Equation D2

In considering firstly the water stability tests, the overall mass loss for the samples upon exposure to water for a period of 60s is shown in Figure C 5. Although only a few statistically significant results were observed in comparison to the control samples (PR24V and ACV), the test highlights the overall sensitivity of the samples, with and without the alginate, when the surface is directly exposed to moisture.

Indeed all of the samples were found to lose between ~0.5 – 2.5% of their total mass due to the submerged portion of material disintegrating at the surface.

While it may be argued that this issue may be mitigated through appropriate detailing (Morton, 2008), this still limits the use of the material to internal, protected applications. This also does not completely eradicate the risk of wetting and remains a concern for load-bearing walls (Heath et al., 2012a). Furthermore, unlike other conventional stabilisers, the addition of alginate does not render the material impervious to water. Therefore, despite some indications of a minor decrease in overall mass loss, the alginate bricks do not appear to offer a major advantage, in water stability over non-stabilised earth and additional protection measures would need to be applied.

Figure C 5: Water Stability – selected samples

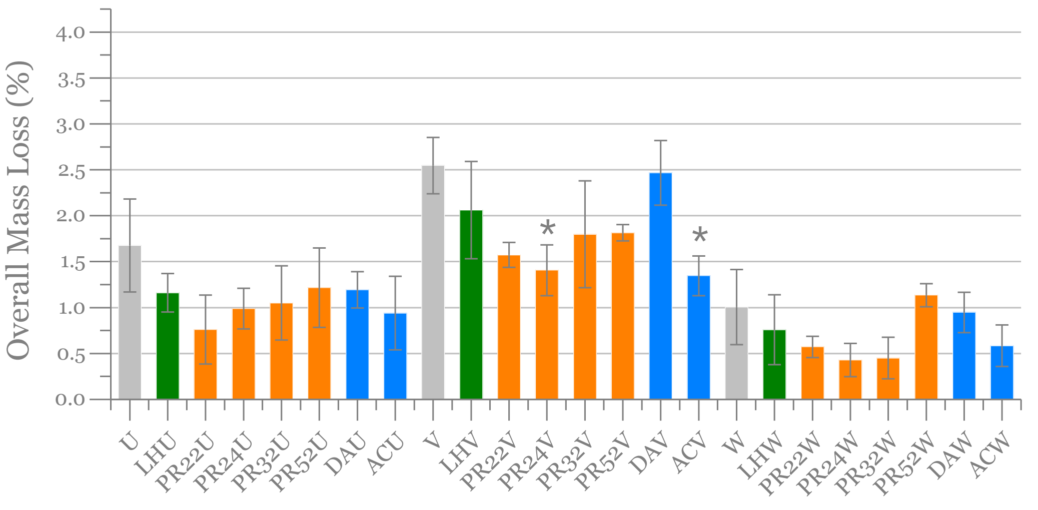

Appendix D: Clay Characteristics

Atterberg limits

Table D 1: Atterberg Limits (Bentonite)

Plastic Limit:	**1st 10g sample**	**2nd 10g sample**
Mass of wet soil (g)	13.7	12.9
Mass of dry soil (g)	8.9	8.6
Moisture Content (%)	**35.0%**	**33.3%**

Liquid Limit:	**Moisture Content 1**			**Moisture Content 2**			**Moisture Content 3**			**Moisture Content 4**		
Initial Gauge Reading (mm)	0	0	0	0	0	0	0	0	0	0	0	0
Final Gauge Reading (mm)	7.1	7.2	8	12	13	10.5	15	14.8	16.4	26.4	26.8	26.9
Average Reading (mm)	7.4			11.8			15.4			26.7		
Mass of wet soil (g)	1.123			1.161			1.153			0.905		
Mass of dry soil (g)	0.467			0.361			0.27			0.194		
Moisture Content (%)	**58.4**			**68.9**			**76.6**			**78.6**		

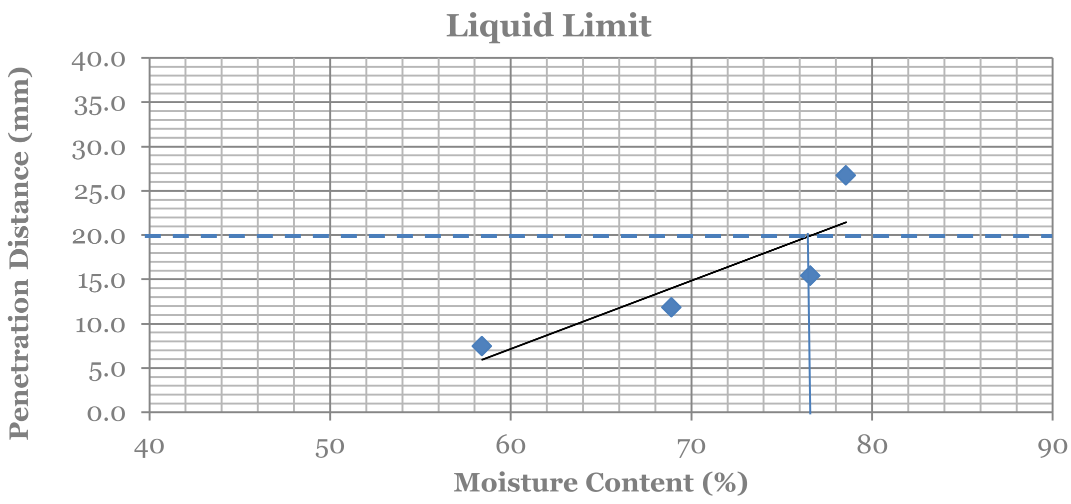

LL = Moisture Content at 20mm	**76.7%**
PL (Average)	**34.2%**
PI (LL – PL) =	76.7% - 34.2% = **42.5%**

Table D 2: Atterberg Limits (Kaolinite)

Plastic Limit:	**1st 10g sample**						**2nd 10g sample**					
Mass of wet soil (g)	9.78						8.57					
Mass of dry soil (g)	7.62						6.49					
Moisture Content (%)	**22.1%**						**24.3%**					
Liquid Limit:	**Moisture Content 1**			**Moisture Content 2**			**Moisture Content 3**			**Moisture Content 4**		
Initial Gauge Reading (mm)	0	0	0	0	0	0	0	0	0	0	0	0
Final Gauge Reading (mm)	14.5	15.1	14.4	17	17.5	17.8	29.6	30.7	32.2	20.9	20.5	18.9
Average Reading (mm)	14.7			17.4			30.8			20.1		
Mass of wet soil (g)	0.675			0.501			0.759			1.101		
Mass of dry soil (g)	0.481			0.335			0.452			0.711		
Moisture Content (%)	**28.7**			**33.1**			**40.4**			**35.4**		

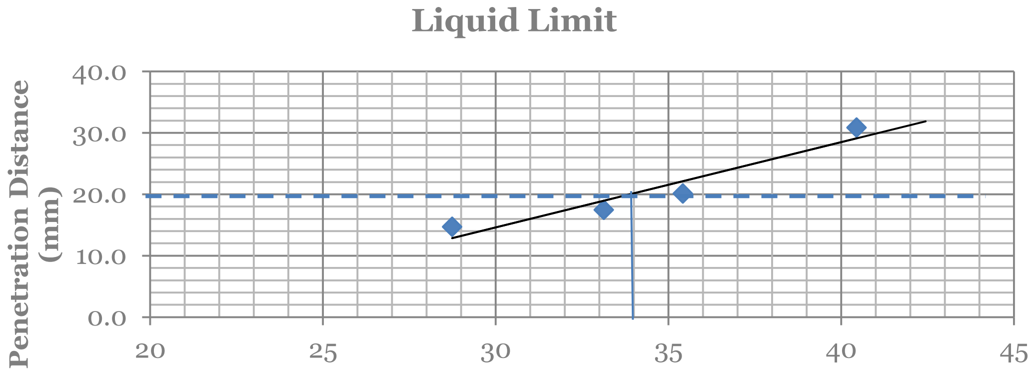

LL = Moisture Content at 20mm	**34.0%**
PL (Average)	**23.2%**
PI (LL – PL) =	34.0% - 23.2% = **10.8%**

Cation Exchange Capacity (CEC)

Table D 3: MB Test

	Bentonite	Kaolinite
Soil dry weight, m_1 (g)	1.0	4.9
MB Volume, V_1 (ml)	21	7
MB (g/kg)	210.0	14.3
Cation Exchange Capacity, CEC (meq/100 g clay)	65.1	4.4
Specific Surface Area, SSA (m^2/g)	52.9	17.6

Clay XRD

Figure D 1: XRD – Bentonite

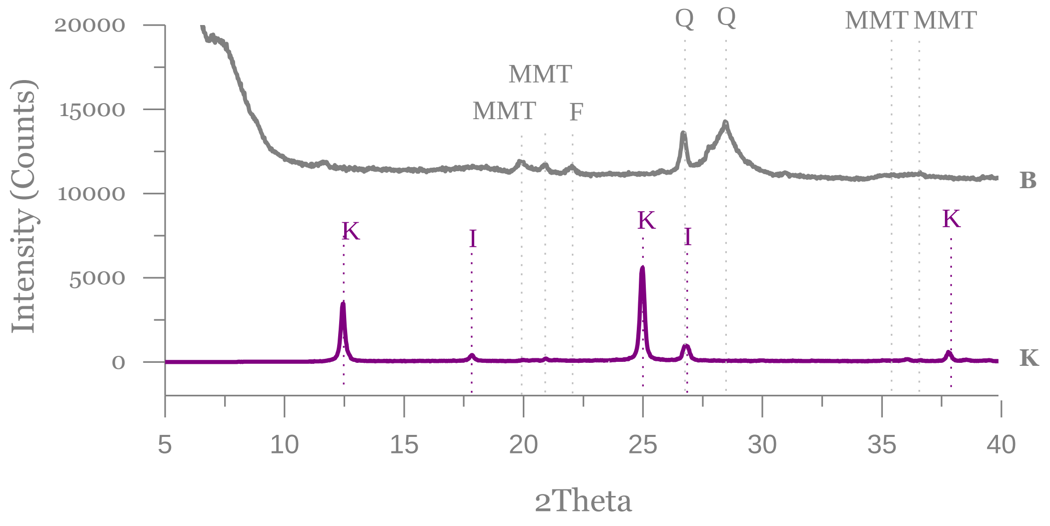

MMT = Montorillonite, K = Kaolinite, I = Illite, Q = Quartz, F = Feldspar

Table D 4: ICP Results - Bentonite

Aqua Regia Extract	(mg/kg)	(meq/100g)
Na	61,459	267
Mg	42,408	350
K	4,410	11
Ca	9,734	49
DI Water extract		
Na	8,955	
Mg	1,012	8
K	271	1
Ca	4,228	21

Appendix E: Aerogel Specimens

Specimen Stability

Table E 1: Specimen Stability

	100:0	75:25	50:50	25:75	0:100
AC	Monolith	Monolith	Monolith	Monolith	Fragile monolith
PR22	Monolith	Monolith	Monolith	Monolith	Fragile monolith
PR24	Monolith	Monolith	Monolith	Monolith	Fragile monolith
PR32	Monolith	Monolith	Monolith	Monolith	Fragile monolith
PR52	Monolith	Monolith	Monolith	Monolith	Fragile monolith
AC pH 8	Monolith	Monolith	Monolith	Monolith	Powder
AC pH 4	-	Monolith	Monolith	Monolith	Fragile monolith
PR22 pH 8	Monolith	Monolith	Monolith	Monolith	-
PR22 pH 4	-	Monolith	Monolith	Monolith	-
PR24 pH 8	Monolith	Monolith	Monolith	Monolith	-
PR24 pH 4	-	Monolith	Monolith	Monolith	-
AC Ca-Bentonite	Monolith	Monolith	Fragile Monolith	Powder	Dense flakes
AC Kaolinite	Monolith	Monolith	Monolith	Powder	Powder
PR22 Ca-Bentonite	Monolith	Monolith	Fragile Monolith	Powder	Dense flakes
PR24 Ca-Bentonite	Monolith	Monolith	Fragile Monolith	Powder	Dense flakes

Sample images

Figure E 1: Variable 1 - Specimen Images

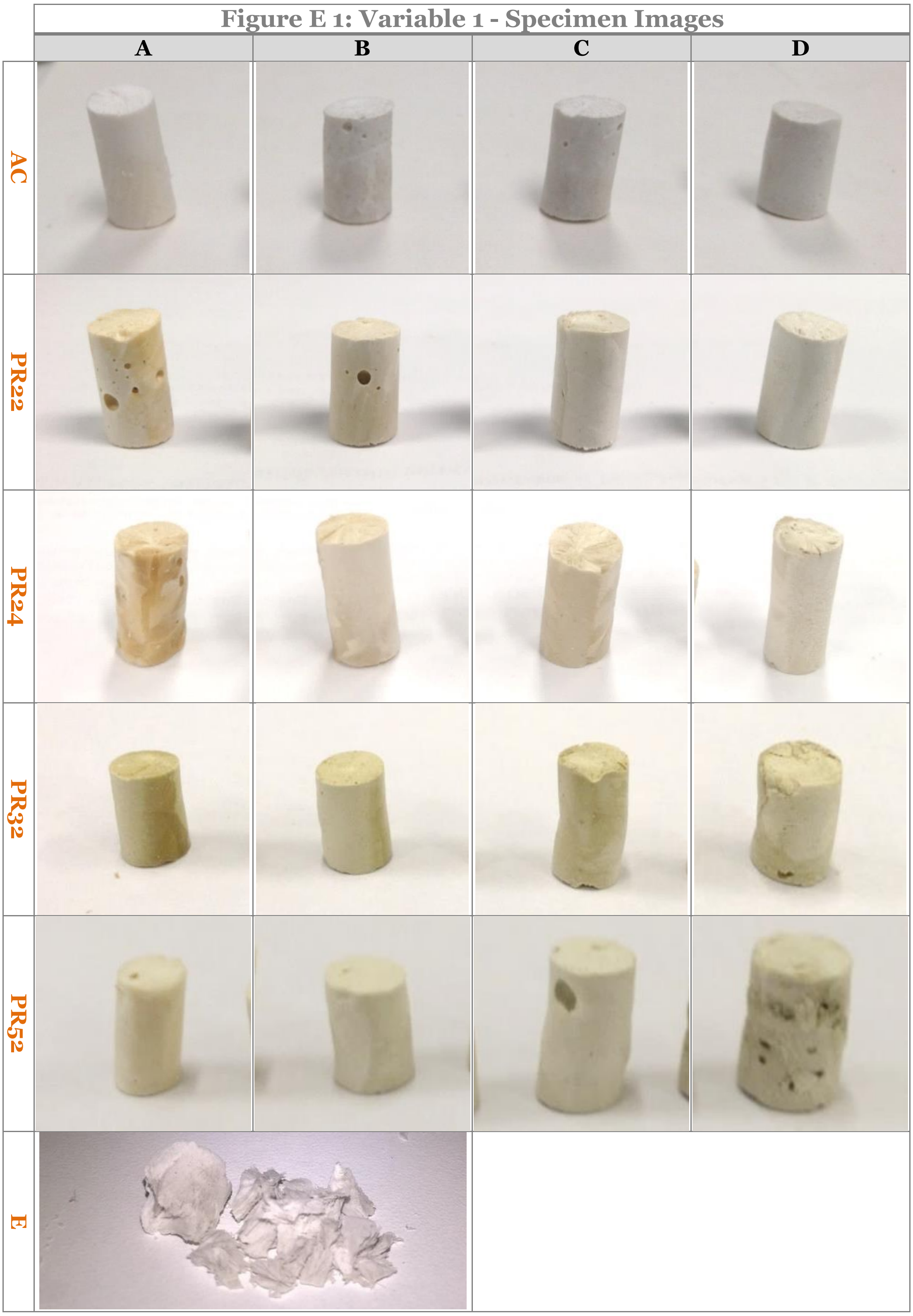

Specific Strength and Specific Modulus of Elasticity

Specific strength was calculated by dividing the compressive strength (σ_m) by the bulk density (ρ). The mean specific strength values are shown in Figure E 2 to Figure E 5. The resulting strength-to-weight ratios, which account for variations in density, were found to range between 0.5 and 12.5. The majority of the samples however fall within the range expected for a material like cork (1 -3) whilst the higher strength to weight ratios observed for AC-A, AC-B, PR22-A and PR52A are more comparable to the range of 4.3 – 45 expected for low density polymer foams (Ashby et al., 2013). Overall, the pattern of results is relatively similar to the compressive strength results given the similarity of the bulk densities.

Figure E 2: Variable 1 - Specific Strength

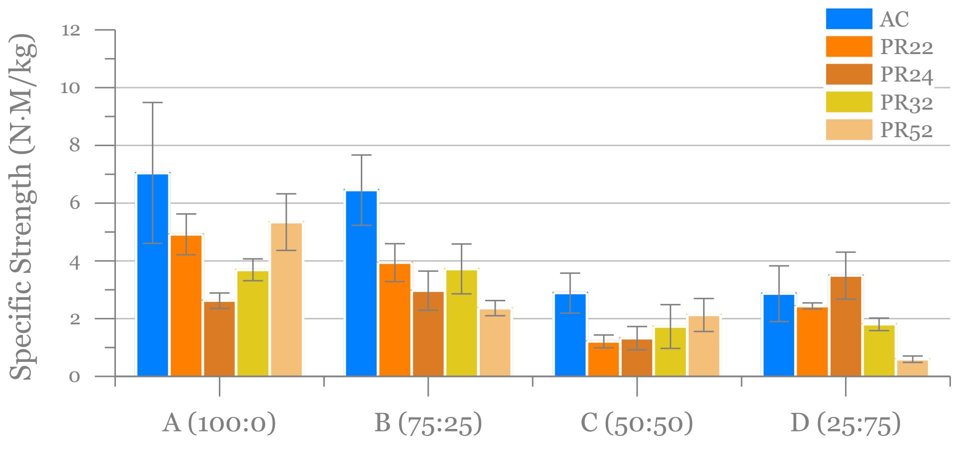

Figure E 3: Variable 2 - Specific Strength

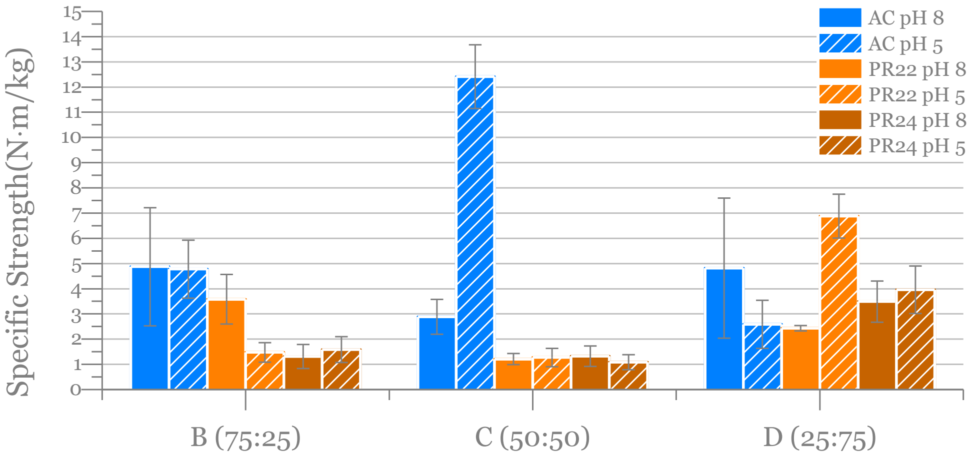

Figure E 4: Variable 3 - Specific Strength (AC)

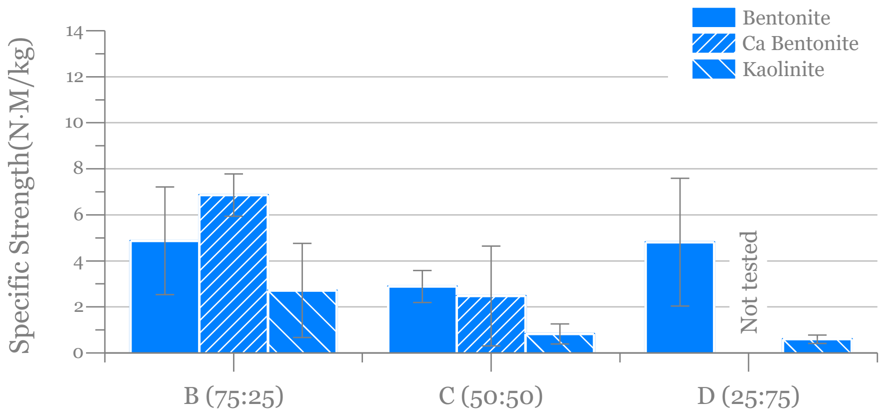

Figure E 5: Variable 3 - Specific Strength (MBL)

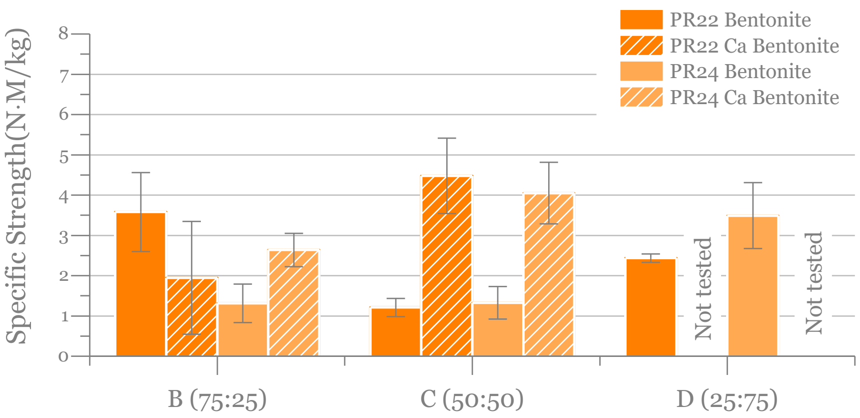

The average specific modulus of elasticity values are also summarised in Figure E 6 to Figure E 9. Again the pattern of results is similar to the modulus of elasticity values given the relatively similar bulk densities of the specimens. In comparing to Chen et al. (2012) where a specific modulus of 0.07 N/mm^2 (m^3/kg) is reported for the 50:50 mix, values for AC-C, PR22-C, PR24-C, PR32-C and PR52-C are within the 0.03-0.09 N/mm^2 (m^3/kg) range.

Figure E 6: Variable 1 - Specific Modulus

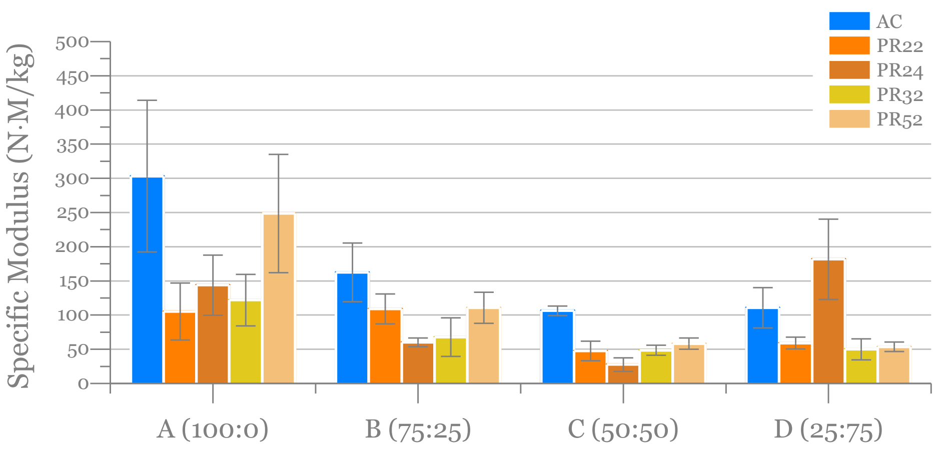

Figure E 7: Variable 2 - Specific Modulus

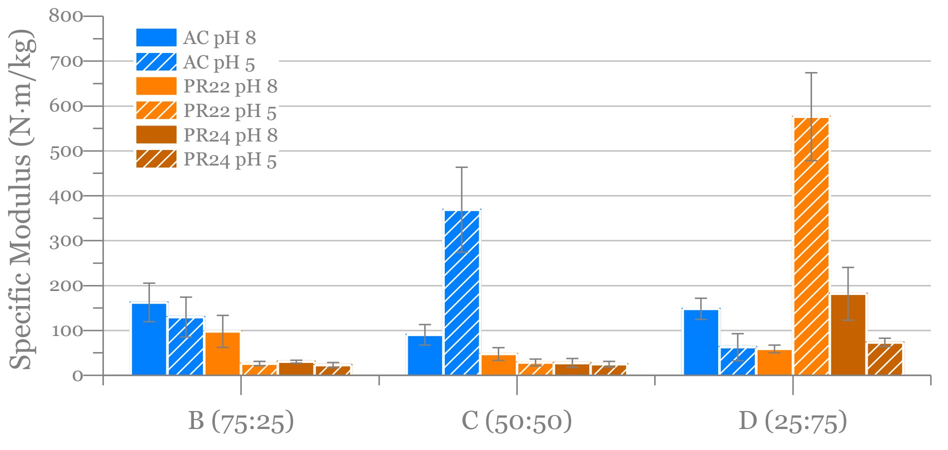

Figure E 8: Variable 3 - Specific Modulus (AC)

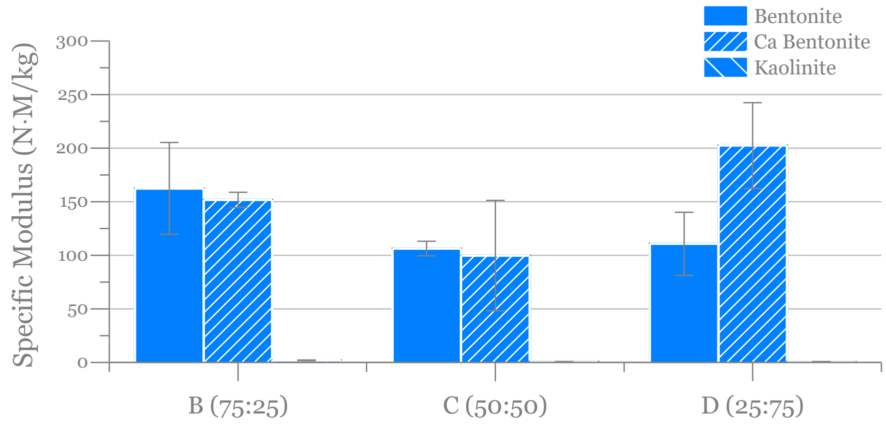

Figure E 9: Variable 3 - Specific Modulus (MBL)

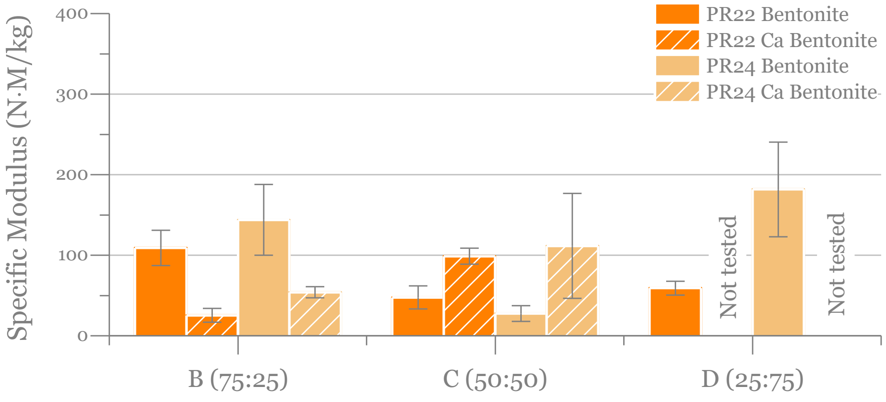

Porosity

Porosity is defined as a measure of the void spaces within a solid and is an important property, particularly for insulation materials, since the size, shape and volume of the pores have an important influence on transport properties such as and thermal conductivity and vapour permeability as well as mechanical strength. There are a number of experimental techniques which can be used to characterise porous materials however image analysis (SEM or TEM), Nitrogen Adsorption/Desorption (NAD) and Mercury Intrusion Porosimetry (MIP) are the most common methods. There are however some limitations to these methods. Image analysis is firstly limited in that it measures only the 2D structure (Pirard et al., 1995). The latter two techniques are also limited in the range of pore sizes which can be analysed since the NAD technique is unable to detect large pores (greater than 50nm) while MIP is only valid for meso- and macro-pores. Aerogels are likely to have a wide pore size distribution and therefore a single technique may not be sufficient to capture the true porosity (Bergna and Roberts, 2005). Secondly these measurement techniques can transform the aerogel structure during measurement by exerting pressure onto the sample thereby leading to false measurements (Scherer, 1998). Since aerogels and other low density foams are typically compressible, there are general difficulties in obtaining accurate porosity data. Many studies which discuss clay-polymer aerogels do not actually measure porosity, even where the thermal behavior of the porous structure is measured (Hostler et al., 2009; Chen et al., 2012; Viggiano et al., 2014). The study by Ohta and Nakazawa (1995) for example simply makes the assumption that porosity will be equal to the water content of the sample.

For this study, the aim was therefore to observe the comparative effects of porisimetry measurement on the prototype samples and determine to what extent the measured porosity differed from the theoretical porosity. Selected samples were analysed through MIP using a Quantachrome Poremaster 60 which measures pores within the 3.5nm to 900 μm range. This technique involves injecting mercury into the specimen over a range of different pressures. The pore diameter (D) can then be determined from the pressure required to inject the mercury into the pores (P) using the Washburn equation (Equation E1) where γ is the surface tension (0.48 J/m^2) and θ is the contact angle (140°).

$$D = \frac{-4\gamma \cos\theta}{P}$$

Equation E1

The MIP results were then compared with the theoretical porosity as determined using Equation E2, as per the methods of Rassis et al. (2003), Longo et al. (2013) and Wang et al. (2014), where ρ_p is the bulk density of the sample and ρ_p is the overall particle density calculated based on the mass fraction of each component and particle density estimates of 2.5 g/cm^3 for bentonite (Kogel et al., 2006) and 1.59 for alginate (Aspinall, 2014).

$$P = (1 - \frac{\rho_p}{\rho_p})\, x\ 100\%$$

Equation E2

Results

The results from the MIP tests for the commercial alginate (AC) are shown in Figure E 10 alongside summary values in Table E 2. It should be noted that only one sample was tested for each of the mix ratios in order to give initial indications of the behavior of the samples during the mercury intrusion process. In considering firstly the pore size distributions obtained, it would appear that macropores greater than 600 nm are present in all samples, with the majority of apparent pore diameters falling around 1000 nm. While the pressures involved for these larger pores are relatively low (greater than 1000 nm = less than 1.4 MPa), based on the linear compressive stress-strain plots of the AC samples (Chapter 10) it is likely that there is still an element of compression taking place at this pressure meaning that the size of even these larger pores maybe underestimated. Nonetheless the results confirm the presence of large macropores as observed visually and from the SEM micrographs. For the smaller pore diameters, although the pore size distribution curves appear to show pores within the 5 to 10 nm range, given that the pressures of over 140 MPa are required within this measurement range, it is likely that these are in fact larger pores which have been compressed during the measurement. Given that no pores smaller than 600 nm are displayed for AC-B and AC-C it is possible that these samples are compressed to greater extent than the other samples. Consequently the measured total porosity values for these samples are also very low (4% and 8% respectively). Given that the air pores in the aerogel samples are created from the ice crystals formed during the freezing process, it would be expected that the porosity of the aerogels would be dependent on the volume of the water component. Since all of the samples consist of 10 wt% solids, the total theoretical porosity should be close to 90%. The results presented here for the measured porosity are however much lower, confirming the lack of sensitivity of the MIP method. For the calculated porosities, which are based on the sample weights and volumes, the values range from 93% to 96%. These values are much closer to the calculated porosities for other polymer-clay aerogels produced using the same solids content. For example Wang (2015) quotes a porosity value of around 94% for PVOH-clay aerogels while Longo et al. (2013) describe values of close to 90% for PS-clay composites.

Figure E 10: Pore Size Distribution (Alginate Dosage)

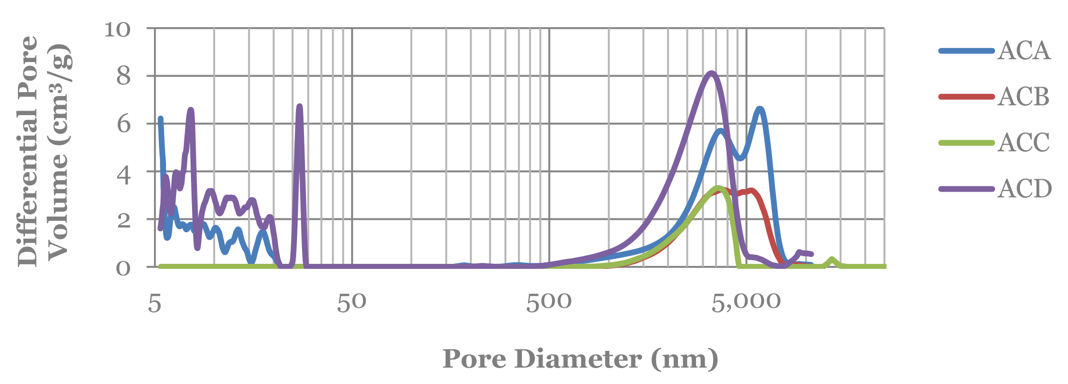

Table E 2: MIP Results – Alginate Dosage

	AC-A	AC-B	AC-C	AC-D
Total Porosity (measured)	**33.9%**	**4.1%**	**8.1%**	**48.4%**
Bulk Density (kg/m^3)	97.3	97.0	75.9	103.5
Alginate particle density (Mg/m^3)	1.59	1.1925	0.795	0.3975
Bentonite particle density (Mg/m^3)	0	0.625	1.25	1.875
Total Porosity (calculated)	**92.7%**	**94.6%**	**94.3%**	**95.6%**

For the MBL samples, the apparent pore size distributions for the 50:50 (C) samples are illustrated in Figure E 11 alongside the AC-C sample. Very large pores (greater than 6000 nm) are observed for PR52-C which is indicative of the presence of large voids within this particular sample. For the other alginate types the distribution curves are relatively similar with the presence of large macopores (600 – 6000 nm) and some mesopores, although again the size of these is likely underestimated due to the compressive effects. The resulting total porosity values for the MBL samples are again much lower than expected with the exception of PR52-C where the measured porosity is higher due to the aforementioned defects (Table E 3). The calculated porosity values also fall within the 94% to 98% range. The high value of the PR24-C is attributed to the very low bulk density value of the sample used (30 kg/m^3) which is lower than the average for this batch (100±10 kg/m^3).

Figure E 11: Pore Size Distribution (Alginate Type)

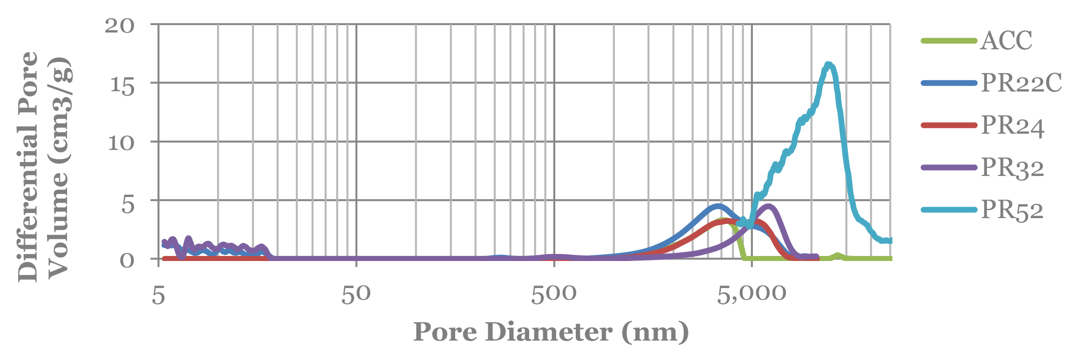

Table E 3: MIP Results – Alginate Type

	AC-C	PR22-C	PR24-C	PR32-C	PR52-C
Total Porosity (measured)	**8.1%**	**19.5%**	**5.2%**	**20.6%**	**88.6%**
Bulk Density (kg/m^3)	75.9	85.1	34.9	119.3	130.9
Alginate particle density (Mg/m^3)	0.795	0.795	0.795	0.795	0.795
Bentonite particle density (Mg/m^3)	1.25	1.25	1.25	1.25	1.25
Total Porosity (calculated)	**94.3%**	**95.8%**	**98.3%**	**94.2%**	**93.6%**

As a further comparison, the estimated porosities calculated from the average bulk density of each batch and the mass fractions of the clay and alginate components are shown in Figure E 12. As expected the porosity decreases with increasing density. The values for all of the batches included within the study are also found to vary between 92% and 96% which again within the range of 80-99.8%described in other studies of composite clay aerogels (Madyan et al., 2016).

Figure E 12: Estimated Porosity (all samples)

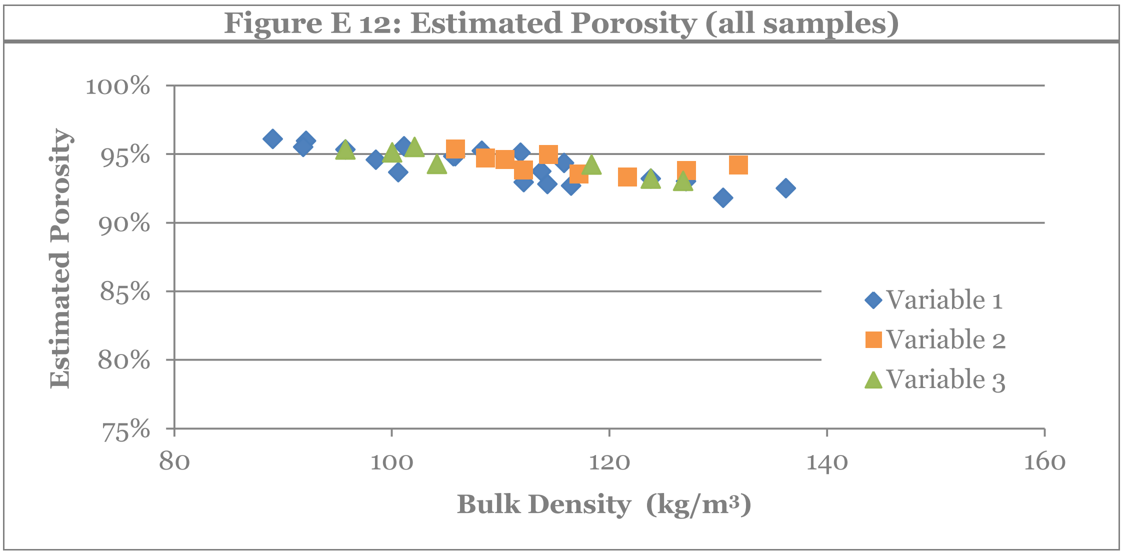

Appendix F: Cost Calculations

Table F 1: Cost Estimations - Bricks

		Alginate Dosage = 0.1 wt%	**Alginate Dosage = 0.5 wt%**	**Alginate Dosage = 1.0 wt%**
LH	**Alginate Content per Volume*** (kg per m^3)	2	10	20
	Alginate Cost per Volume (£/m^3) £11 per kg	2 x £11 = £22	10 x £11 = £110	20 x £11 = £220
	Alginate Cost per Area** (£/m^2)	£22÷100 = **£0.21**	£110÷100 = **£1.10**	£222÷100 = **£2.20**
AN	**Alginate Content per Volume*** (kg per m^3)	2	10	20
	Alginate Cost per Volume (£/m^3) £8.50 per kg	2 x £8.5 = £17	10 x £8.5 = £85	20 x £8.5 = £170
	Alginate Cost per Area** (£/m^2)	**£0.17**	**£0.85**	**£1.70**

*Based 2000 kg/m^3 unit
** Based on 100mm thick wall

Table F 2: Cost Estimations – Bricks (LH)

	Unit Type* (based on a 100mm thick wall)	**Standard Unit**	**Standard Unit + 0.1% alginate**	**Standard Unit + 0.5% alginate**	**Standard Unit + 1.0% alginate**
		Equivalent cost (£/m^2)	**Equivalent cost** (£/m^2)	**Equivalent cost** (£/m^2)	**Equivalent cost** (£/m^2)
Bricks	**UK Industrial Mass-Produced Earth Bricks**	10.40- 11.05	**+0.21 =** 10.61 – 11.26	**+ 1.10 =** 11.50 – 12.15	**+2.20** = 12.60 – 13.25
	UK Small-scale Mass-Produced Earth Bricks	28.45 – 60.46	**+0.21 =** 28.66 – 62.80	**+ 1.10 =** 29.52 – 61.53	**+2.20** = 30.65 – 62.66
	One-off Hand-made Earth Bricks	108.23 – 162.34	**+0.21 =** 108.44 – 162.55	**+ 1.10 =** 109.33 + 163.44	**+2.20** = 110.43 – 164.54
Blocks	**UK Large-scale mass-produced Earth Blocks**	4.78	**+0.21 =** 4.99	**+ 1.10 =** 5.88	**+2.20** = 6.98
	UK Small-scale mass-produced Earth Blocks	22.14 - 41.51	**+0.21 =** 22.35 – 41.72 0.5 - 0.9%	**+ 1.10 =** 23.24 – 42.61	**+2.20** = 24.34 – 43.71
	One-off Hand Moulded Earth Blocks	108.23 - 162.34	**+0.21 =** 108.44 – 162.55 0.2% - 0.1%	**+ 1.10 =** 109.33 – 163.44	**+2.20** = 110.43 – 164.54

*Assumes 2000 kg/m^3 units

Table F 3: Cost Estimations – Bricks (AN)

	Unit Type* (based on a 100mm thick wall)	Standard Unit	Standard Unit + 0.1% alginate	Standard Unit + 0.5% alginate	Standard Unit + 1.0% alginate
		Equivalent cost (£/m^2)	**Equivalent cost** (£/m^2)	**Equivalent cost** (£/m^2)	**Equivalent cost** (£/m^2)
Bricks	**UK Industrial Mass-Produced Earth Bricks**	10.40- 11.05	**+0.17 =** 10.57 – 11.2	**+0.85 =** 11.25 – 11.90	**+1.70 =** 12.10 – 12.75
	UK Small-scale Mass-Produced Earth Bricks	28.45 – 60.46	**+0.17 =** 28.62 – 60.63	**+0.85 =** 29.30 – 61.31	**+1.70 =** 30.15 – 62.16
	One-off Hand-made Earth Bricks	108.23 – 162.34	**+0.17 =** 108.4	**+0.83 =** 109.08 – 163.19	**+1.70 =** 109.93 – 164.04
Blocks	**UK Large-scale mass-produced Earth Blocks**	4.78	**+0.17 =** 4.95	**+0.85 =** 5.62	**+1.70 =** 6.48
	UK Small-scale mass-produced Earth Blocks	22.14 - 41.51	**+0.17 =** 22.31 – 41.68	**+0.85 =** 22.99 – 42.36	**+1.70 =** 23.84 – 43.21
	One-off Hand Moulded Earth Blocks	108.23 - 162.34	**+0.17 =** 108.4 – 162.51	**+0.83 =** 109.08 – 163.19	**+1.70 =** 109.93 – 164.04

*Assumes 2000 kg/m^3 units
All standard unit costs taken from Morton (2008)

Table F 4: Cost Estimations - Aerogels

			75:25 (a:c)		50:50 (a:c)		25:75(a:c)	
		Cost	**Quantity**	**Cost**	**Quantity**	**Cost**	**Quantity**	**Cost**
		£	(per 100 cm^3 batch)	(£/100 cm^3)	(per 100 cm^3 batch)	(£/100 cm^3)	(per 100 cm^3 batch)	(£/100 cm^3)
Materials	Alginate	£8.50 - £11 per kg[a]	0.0075 kg	**£0.06 -0.08**	0.005 kg	**£0.04-0.06**	0.0025 kg	**£0.02 - 0.03**
	Clay *(Bentonite)*	£20 per kg[b]	0.0025 kg	**£0.05**	0.005 kg	**£0.10**	0.0075 kg	**£0.15**
	Liquid N^2	£1 per L[c]	1 L	**£1.00**	1 L	**£1.00**	1 L	**£1.00**
	Isopentane	£25.40 per L[d]	0.02 L	**£0.51**	0.02 L	**£0.51**	0.02 L	**£0.51**
	Water	£0.20 /1000 L[e]	0.9 L	**£0.00**	0.9 L	**£0.00**	0.9 L	**£0.00**
	Materials Total		**= 1.62 – 1.64**		**= 1.62 – 1.64**		**= £1.68 – 1.69**	
Processing	Electricity: Mixing	£0.10 per kWh[f]	*4 h x 45W=* 0.18 kWh	**£0.02**	0.18 kWh	**£0.02**	*4 h x 45W=* 0.18 kWh	**£0.02**
	Electricity: Freeze-drying	£0. 10 per kWh[f]	*24h x 600W* =14.4 kWh	**£1.44**	14.4 kWh	**£1.44**	*24h x 600W* =14.4 kWh	**£1.44**
	Processing Total		**£1.46**		**£1.46**		**£1.46**	
	Totals		**£3.08-3.10**		**£3.11-£3.13**		**£3.14-3.15**	

a – from Table 3-2 (MBL data)
b – based on purchase price from Acros organics (2015)
c – based on purchase price from University of Strathclyde chemical store
d – based on purchase price from Acros organics (2015)
e – from MBL data
f – Based on average non-domestic electricity rates (DECC. 2016b). Excludes standing charges.

Appendix G: Embodied Energy and CO_2 Calculations

Table G 1: EE & EC Estimations – Bricks						
		Standard Unit (MJ/kg)	**Alginate (LH)** (MJ/kg)	**Standard Unit + 0.1% alginate**	**Standard Unit + 0.5% alginate**	**Standard Unit + 1.0% alginate**
EE MJ/kg	**Standard CEB**	0.53[a]	8.47[c]	(0.999 x 0.53) + (0.001 x 8.47) = **0.54**	(0.995 x0.53) + (0.005 x 8.47) = **0.57**	(0.99 x 0.53) + (0.01 x 8.47) = **0.61**
EC kgCO2/kg	**Standard CEB**	0.04[b]	0.51[d]	(0.999 x 0.04) + (0.001 x 0.51) = **0.04**	(0.995 x 0.04) + (0.005 x 0.51) = **0.04**	(0.99 x 0.04) + (0.01 x 0.51) = **0.04**
		Standard Unit (MJ/kg)	**Alginate (AN)** (MJ/kg)	**Standard Unit + 0.1% alginate**	**Standard Unit + 0.5% alginate**	**Standard Unit + 1.0% alginate**
EE MJ/kg	**Standard CEB** Morton et al. (2005)	0.53[a]	6.65[e]	(0.999 x 0.53) + (0.001 x 6.65) = **0.54**	(0.995 x0.53) + (0.005 x 6.65) = **0.56**	(0.99 x 0.53) + (0.01 x 6.65) = **0.59**
EC kgCO2/kg	**Standard CEB** Morton et al. (2005)	0.04[a]	0.38[f]	(0.999 x 0.04)+ (0.001 x 0.38) = **0.04**	(0.995 x 0.04) + (0.005 x 0.38) = **0.04**	(0.99 x 0.04) + (0.01 x 0.38) = **0.04**
	a - from Morton et al. (2005), b - from Morton et al. (2005) c - from Table A4, d - from Table A6 e - from Table A5, f - from Table A7					

Table G 2: EE Estimations - Aerogels								
			75:25 (a:c)		**50:50 (a:c)**		**25:75 (a:c)**	
		EE	**Quantity**	**Total EE** = EE x Quantity	**Quantity**	**Total EE** = EE x Quantity	**Quantity**	**Total EE** = EE x Quantity
		MJ/kg	kg/ kg	MJ/kg	kg/ kg	MJ/kg	kg/ kg	MJ/kg
Materials	Alginate	6.65 – 8.47[a]	0.75	**4.99 – 6.35**	0.5	**3.33 – 4.24**	0.25	**1.66 – 2.12**
	Bentonite	0.4[b]	0.25	**0.10**	0.5	**0.20**	0.75	**0.30**
	Liquid N^2	1.8[c]	100	**180.0**	100	**180.0**	100	**180.0**
	Water	0.01[d]	9	**0.09**	10	**0.09**	10	**0.09**
	Materials Total (MJ/kg)		**= 185.18 – 186.54**		**= 183.62 – 184.53**		**= 182.05 – 182.51**	
Processing	Electricity: Mixing (MJ/kg)		*100cm³ batch = 4h x 45W* = 0.18 kWh 1kg batch = 0.18 kWh x 100 = 18 kWh/kg 18 kWh/kg x 3.6* = **64.8**					
	Electricity: Freeze-drying (MJ/kg)		*100cm³ batch = 24h x 600W* = 14.4 kWh 1kg batch = 14.4 kWh x 100 = 1440 kWh/kg 1440 kWh/kg x 3.6* = **5184**					
	Processing Total (MJ/kg)		64.8 + 5148 = **5212.8**					
	Totals		**5397.92 - 5399.28 MJ/kg**		**5396.38 - 5397.29 MJ/kg**		**5394.83 - 5395.31 MJ/kg**	
	a - from Table A4 & A5, b – from Ecoinvent (Brandt, 2015), c –from Pusavec et al. (2010) d - from Hammond and Jones (2011), *conversion factor from kWh to MJ							

Table G 3: EC Estimations - Aerogels

			75:25 (a:c)		**50:50 (a:c)**		**25:75 (a:c)**	
		EC	**Quantity**	**Total EC** = EC x Quantity	**Quantity**	**Total EC** = EC x Quantity	**Quantity**	**Total EE** = EC x Quantity
		kg CO_2e/ kg	kg/ kg	kg CO_2e/ kg	kg/ kg	kg CO_2e/ kg	kg/ kg	kg CO_2e/ kg
Materials	Alginate	0.37 – 0.51[a]	0.25	**0.09 – 0.13**	0.5	**0.19 – 0.26**	0.75	**0.28 – 0.38**
	Bentonite	0.03[b]	0.75	**0.02**	0.5	**0.02**	0.25	**0.01**
	Liquid N^2	0.21[c]	100	**210**	100	**210**	100	**210**
	Water	0.001[d]	9	**0.009**	9	**0.009**	9	**0.009**
	Materials Total		**= 210.12 – 210.16**		**= 210.22 – 210.29**		**= 210.30 – 210.40**	
Processing	Electricity: Mixing (kg CO2e /kg)		18 kWh/kg x 0.46219[d] = **8.32**					
	Electricity: Freeze-drying (kg CO2e /kg)		1440 kWh/kg x 0.46219[d] = **665.55 kg CO2e /kg**					
	Processing Total		8.32 + 665.55 = **673.78 kg CO2e /kg**					
	Totals		**884.06 - 883.94 kg CO2e /kg**		**884.00 – 884.07 kg CO2e /kg**		**884.08 – 884.18 kg CO2e /kg**	

a - from Table A6 & A7, b – from Ecoinvent (Brandt, 2015)
c – Assuming energy figure from Pusavec et al. (2010) is for electricity consumption only. (1.8 MJ/kg = 0.5 kWh/kg = 0.5 x 0.41 kg CO_2e/kWh (electricity conversion factor) = 0.21 kg CO_2e / kg
d - from Hammond and Jones (2011)

Table G 4: EE Estimations – Aerogels (upscaling)

	Totals	**75:25 (a:c)**	**50:50 (a:c)**	**25:75 (a:c)**
Upscaling	**Estimated cost per lab scale batch** (MJ/100 cm^3)	**53.98 – 53.99**	**53.96 – 53.97**	**53.95**
	Estimated EE per kg* (MJ/kg)	5398 - 5399	5396-5397	5395
	Estimated EE per m^3* (MJ/m^3)	**539,800 – 539,900**	**539, 600 – 539,700**	**539,500**
	Estimated EE per m^2** (MJ/m^2)	**10, 796 – 10, 798** (m^3 value x 0.02)	**10, 792 – 10, 794** (m^3 value x 0.02)	**10, 790** (m^3 value x 0.02)

*Assuming density of 100 kg/m^3, 1kg = 10,000 cm3
** Based on 20mm thick panel

Appendix H: Product Comparisons

Table H 1: Product Comparison – Unfired Clay Bricks

Product		[This image has been removed by the author of this thesis for copyright reasons]	[This image has been removed by the author of this thesis for copyright reasons]
	Product Name	**Ecoterre Brick**	**Ecoterre Block**
	Manufacturer	Ibstock Ltd.	Ibstock Ltd.
	Materials	Recycled clay (unfired)	Recycled clay (unfired)
	Commercial Status	Commercially available	Commercially available
	Applications	Internal Walls	Internal Walls
	Bulk density	1940 kg/m^3	1940 kg/m^3
	Thermal Conductivity	1.04 W/m-K	1.04 W/m-K
	Comp. Strength	3.8 N/mm2	2.9 N/mm2
	Reference	http://www.ibstock.com/	
Product		[This image has been removed by the author of this thesis for copyright reasons]	[This image has been removed by the author of this thesis for copyright reasons]
	Product Name	**Claytec compressed unfired clay bricks**	**Claytec light clay bricks**
	Manufacturer	Claytec	Claytec
	Materials	Clay (unfired)	Clay, sand and straw (unfired)
	Commercial Status	Commercially available	Commercially available
	Applications	Non-loadbearing Internal Walls	Non-loadbearing Internal Walls
	Bulk density	1500 kg/m^3	700 kg/m^3
	Thermal Conductivity	0.95 W/m-K	0.21 W/m-K
	Comp. Strength	-	-
	Reference	http://www.constructionresources.com/	

Table H 2: Product Comparison – Aerogels (Commercial)

Product		[This image has been removed by the author of this thesis for copyright reasons]	[This image has been removed by the author of this thesis for copyright reasons]
	Product Name	**Spacetherm® Blanket**	**Aspen Aerogel Spaceloft®**
	Manufacturer	Proctor Group	Aspen Aerogels
	Aerogel Type	Silica	Silica
	Commercial Status	Commercially available	Commercially available
	Applications	Wall/floor/roof insulation	Wall/floor/roof insulation
	Bulk density	150 kg/m^3	160 kg/m^3
	Thermal Conductivity	0.015 W/m-K	0.017 W/m-K
	Comp. Strength	0.08 N/mm^2	0.055 N/mm^2
	Cost	£24 – 174 per m^2	£24 – 174 per m^2
	Reference	(Proctor Group, 2015) http://www.proctorgroup.com/	(Aspen Aerogels, 2011) http://www.aerogel.com/
Product		[This image has been removed by the author of this thesis for copyright reasons]	[This image has been removed by the author of this thesis for copyright reasons]
	Product Name	**Lumira Thermal Wrap ™ Aerogel Blanket**	**Thermablok® Aerogel Blanket**
	Manufacturer	Cabot Corporation	Thermablock
	Aerogel Type	Silica	Silica
	Commercial Status	Commercially available	Commercially available
	Applications	Wall/floor/roof insulation	Wall/floor/roof insulation
	Bulk density	70 kg/m^3	150 kg/m^3
	Thermal Conductivity	0.020 – 0.025 W/m-K	0.014 W/m-K
	Comp. Strength	-	0.08 N/mm^2
	Cost	£24 – 174 per m^2	£24 – 174 per m^2
	Reference	(Cabot Corporation, 2013) http://www.buyaerogel.com/product/thermal-wrap-8-mm/	(Thermablok, 2015) http://www.thermablok.co.uk/

Product		[This image has been removed by the author of this thesis for copyright reasons]	[This image has been removed by the author of this thesis for copyright reasons]
	Product Name	**Spacetherm® Boards** (bonded to plywood, chipboard, plaster board etc.)	**Spacetherm® Cold Bridge Strips**
	Manufacturer	Proctor Group	Proctor Group
	Aerogel Type	Silica	Silica
	Commercial Status	Commercially available	Commercially available
	Applications	Internal Lining	Lining for Steel/timber frames
	Bulk density	150 kg/m^3	150 kg/m^3
	Thermal Conductivity	0.015 W/m-K	0.015 W/m-K
	Comp. Strength	-	-
	Cost	-	-
	Reference	(Proctor Group, 2015) http://www.proctorgroup.com/	(Proctor Group, 2015) http://www.proctorgroup.com/
Product		[This image has been removed by the author of this thesis for copyright reasons]	[This image has been removed by the author of this thesis for copyright reasons]
	Product Name	**OPTIM-R ®**	**Kalwall® + Lumira Aerogel**
	Manufacturer	Kingspan, UK	Cabot Corporation, USA
	Aerogel Type	Silica aerogel core in VIP	Silica aerogel granules within panel system
	Commercial Status	Commercially available	Commercially available
	Applications	Wall/floor/roof insulation	Translucent Walling/rooflights
	Bulk density	180 – 210 kg/m^3	70 – 100 kg/m^3
	Thermal Conductivity	0.007 W/m-K	0.018 W/m-K
	Comp. Strength	$\geq$ 0.15 N/mm^2	-
	Cost	£100 per m^2	-
	Reference	(Kingspan, 2013) http://www.kingspaninsulation.co.uk/	(Kalwall, 2011) http://www.kalwall.com/

Product		[This image has been removed by the author of this thesis for copyright reasons]	[This image has been removed by the author of this thesis for copyright reasons]
	Product Name	**Fixit 222 Aerogel insulating plaster**	**Airloy™ Aerogel Tiles**
	Manufacturer	Fixit Gruppe , Switzerland	Aerogel Technologies, USA
	Aerogel Type	Silica granules	Silica monolith
	Commercial Status	Commercially available	Commercially available
	Applications	Internal Plaster	Insulation tiles/panels
	Bulk density	220 kg/m^3	10 – 1000 kg/m^3
	Thermal Conductivity	0.028 W/m-K	0.018 – 0.035 W/m-K
	Comp. Strength	-	2 -14 N/mm^2
	Cost	-	-
	Reference	(Fixit, 2013) http://www.fixit.ch/	(Aerogel Technologies, 2016) http://www.aerogeltechnologies.com/

Product and Properties		[This image has been removed by the author of this thesis for copyright reasons]	[This image has been removed by the author of this thesis for copyright reasons]
	Product Name	**Green Earth Aerogel Blocks**	**Green Earth Aerogel Granules**
	Manufacturer	Green Earth Aerogel Technology, Spain	Green Earth Aerogel Technology, Spain
	Aerogel Type	Silica (from rice husk and rice residues)	Silica (from rice husk and rice residues)
	Commercial Status	In development	In development
	Applications	Insulation boards/panels	Filler for translucent walls, additive for paints
	Bulk density	50 kg/m^3	50 kg/m^3
	Reference	(GEAT, 2016)	(GEAT, 2016)

Product		[This image has been removed by the author of this thesis for copyright reasons]	[This image has been removed by the author of this thesis for copyright reasons]
	Product Name	**Quartzene®**	**Aeroclay**
	Manufacturer	Svenska Aerogel AB, Sweden	Aeroclay Inc/ Compadre, USA
	Aerogel Type	Silica	Clay and polymer
	Commercial Status	Powder/pellets in production (insulation board/blanket still in development)	Prototype stage – in development
	Applications	Thermal insulation board/blanket, paints/coatings	Thermal insulation board, internal core for VIPs
Properties	*Bulk density*	40 to 400 kg/m^3	50 -200 kg/m^3
	Thermal Conductivity	-	~0.01 W/m-K
	Comp. Strength	0.02 – 2.29 N/mm^2	1 – 20 N/mm^2
	Cost	-	£200 per m^3 (£4 per m^2 – 20mm)
	Reference	(Ekström et al., 2014)	(Compadre, 2014)(Dalton et al., 2010)(Schiraldi et al., 2007)
Product		[This image has been removed by the author of this thesis for copyright reasons]	[This image has been removed by the author of this thesis for copyright reasons]
	Product Name	**ICECLAY Panels**	**ICECLAY Powder/granules**
	Manufacturer	Active Aerogels, Portugal	Active Aerogels, Portugal
	Aerogel Type	Clay/polymer	Clay/polymer
	Commercial Status	Prototype (in development)	Prototype (in development)
	Applications	Wall/roof insulation boards, panels and strips	Thermal enhancing filler materials
	Bulk density	30 kg/m^3	30 kg/m^3
	Thermal Conductivity	0.03 W/m-K	0.03 W/m-K
	Compressive Strength	0.007 - 0.075 N/mm^2	-
	Reference	(ICECLAY, 2014) http://iceclay-fp7.eu/index.php/overview	(ICECLAY, 2014) http://iceclay-fp7.eu/index.php/overview

Product		[This image has been removed by the author of this thesis for copyright reasons]	[This image has been removed by the author of this thesis for copyright reasons]
	Product Name	**Aerogel Incorporated Concrete**	**Slentite®**
	Manufacturer	Norwegian University of Science and Technology, Norway	BASF, Germany
	Aerogel Type	Silica aerogel granules (60% volume in concrete)	Polyurethane Aerogel
	Commercial Status	In development	Pilot production
	Applications	Concrete walling/flooring	Thermal insulation board, internal core for VIPs
	Bulk density	100 kg/m^3	120 kg/m^3
	Thermal Conductivity	~0.26 W/m-K	0.017 W/m-K
	Compressive Strength	~8.3 N/mm^2	>3 N/mm^2
	Reference	(Gao et al., 2014)	(BASF, 2016) http://www.polyurethanes.basf.de/